

DESIGN OF FIBRE COMPOSITE STRUCTURES

FOR LARGE WATER VALVES

Farid Mahmoud Hasan Bizzari B.Sc., M.Sc.

A thesis submitted for the degree of

Doctor of Philosophy

in the University of London

Department of Mechanical Engineering

Imperial College of Science and Technology

London S.W.7

July 1980

TO FADWA

S U M M A R Y

A brief introduction to the types of problem occurring in the stress analysis of Water Valves of the butterfly type is given to show the need for developing a design method for these structures.

The analytical work which has been undertaken for establishing a closed form solution to the problem is given, with comments.

A description of the anisotropic characteristics of the fibre composite material is presented in the form needed to allow the use of matrix algebra and practical examples of these materials are given.

A general finite element is derived in detail to show how it represents the structure in a plate or shell shape made of Isotropic, Orthotropic or Anisotropic material. Also a finite element method is suggested to investigate the structural strength and behaviour of different types of blades made of different materials and the advantages of the method are shown.

A method for the optimal design of fibre composite structures is suggested and recommendations for future work are given.

The computer program and the numerical results are presented.

CONTENTS

	Page No.
SUMMARY	3.
ACKNOWLEDGEMENTS	8.
LIST OF FIGURES	9.
LIST OF TABLES	17.
NOTATIONS	19.
CHAPTER ONE INTRODUCTION	22.
1.1. General	23.
1.2. Description of the structure of main interest.	27.
1.2.1. The disk or blade	28.
1.2.2. The shaft	34.
1.2.3. The body	34.
1.2.4. Seating seals	36.
1.2.5. Operating equipment	37.
1.3. Review.	37.
1.4. Materials	39.
1.5. Limitation and scope of study.	40.
CHAPTER TWO ANALYTICAL PROCEDURE FOR THE STRUCTURAL ANALYSIS OF THE BLADES OF ORDINARY BUTTERFLY VALVES.	41.
2.1. The governing differential equation for circular plates.	42.
2.2. The general solution of the governing differential equation.	47.
2.3. The solution for stresses and deflections in a circular plate of uniform thickness subjected to a uniform normal pressure and supported at two points at opposite ends of a diameter.	49.
2.3.1. Analytical work	49.
2.3.2. Finite element analysis	68.

CHAPTER TWO	2.4. The solution for stresses and deflections in a circular plate of uniform thickness subjected to a uniform normal pressure and supported at two short lengths of arcs at opposite ends of a diameter.	77.
	2.4.1. Introduction	77.
	2.4.2. Analytical work	77.
	2.4.3. Finite element analysis	82.
	2.5. Experimental Work.	88.
	2.5.1. Introduction	88.
	2.5.2. 4-Point bend testing of a perspex beam	96.
	2.5.3. The testing equipment	106.
	2.5.4. Testing a 12" diameter disk supported on two clamped short arcs subjected to a uniform pressure.	121.
	2.5.5. Testing a 12" diameter disk supported on two clamped short arcs subjected to a point load.	122.
	2.5.6. Testing a 12" diameter disk supported on two clamped short arcs and two short lengths of the diameter subjected to a uniform pressure.	123.
CHAPTER THREE	RELEVANT PARTS OF THE THEORY OF ANISOTROPIC ELASTICITY	196.
	3.1. Introduction	197.
	3.2. The generalised Hooke's law for anisotropy.	199.
	3.3. Elastic symmetry and orthotropic case.	202.
	3.4. Transformation rules for an orthotropic body.	207.

	Page No.	
CHAPTER THREE	3.4.1. Stress transformation	207.
	3.4.2. Strain transformation	210.
	3.4.3. Constants of elasticity	211.
CHAPTER FOUR	FINITE ELEMENT MODEL AND SOLUTION	213.
	4.1. Introduction	214.
	4.2. Geometry representation	214.
	4.3. Displacement field	216.
	4.4. Strain-displacement relations	220.
	4.5. Stress-strain relations	222.
	4.6. Derivation of the stiffness matrix.	223.
	4.7. Flow chart of solid finite element computer programme	225.
CHAPTER FIVE	IDEALIZATION OF FINITE ELEMENTS FOR STRUCTURAL DESIGN, NUMERICAL AND EXPERIMENTAL RESULTS.	227.
	5.1. Introduction	228.
	5.2. Cast iron blade of ordinary butterfly valve.	231.
	5.3. Test samples of composite materials.	233.
	5.3.1. Introduction	233.
	5.3.2. Preparation of test specimens, testing equipment and procedure.	240.
	5.3.3. Elastic constants of the specimens.	270.
	5.3.4. Finite element idealization of G.R.P. test beam.	271.
	5.3.5. Experimental work on G.R.P. test beam.	273.
	5.4. G.R.P. blade of ordinary butterfly valve.	291.

CHAPTER SIX	CONCLUSIONS AND RECOMMENDATIONS FOR FURTHER WORK.	304.
	6.1. The analysis of ordinary blades	305.
	6.1.1. Conclusions	305.
	6.1.2. Further work	306.
	6.2. Fibre composite blades	307.
	6.2.1. Approach for optimal design.	307.
	6.2.2. Further work	308.
REFERENCES		311.
APPENDICES	APPENDIX 1	319.
	APPENDIX 2	338.
	APPENDIX 3	357.
	APPENDIX 4	373.
	APPENDIX 5	376.

ACKNOWLEDGEMENTS

The author wishes to express his sincere thanks to Professor J.M. Alexander for his valuable advice and kind encouragement while supervising this work.

He also wishes to thank the following, who have assisted with the experimental work and computing facilities. The staff of the University of London Computer Centre, especially the Advisory Department. The technicians and laboratory staff of the Dept. of Mechanical Engineering, University College Swansea. The librarian of the Dept. of Mechanical Engineering, Imperial College. Mr. M. Stone and Mr. J.M. Griffiths of Boving & Co. Ltd. Mr. R. Lovell of Tods of Weymouth. Dr. S.A. Abi-Shaheen and Mr. D. Lo of Stemmos Ltd.

Finally, I would like to thank my wife Fadwa for her encouragement and patience throughout the whole period of the work and Mrs. Mary Aldridge for typing the whole text.

LIST OF FIGURES

	Page No.
1.1. Optimum approach to design with composites	25.
1.2. A disk of constant thickness	29.
1.3a. A tapered disk	30.
1.3b. A hollow tapered disk	31.
1.4. Shaft through the disk	32.
1.5. Two shafts fitted in humps	32.
1.6. Shafts as integral casting of the disk	32.
1.7. Components of butterfly valve	33.
1.8. Single flange body	35.
1.9. "U" flangeless body	35.
1.10. Double flanged body	35.
1.11. Flangeless body	35.
2.1. Expressions for bending moments and transverse shear in cartesian coordinates.	44.
2.2. Polar coordinates.	44.
2.3. Plate element in polar coordinates	46.
2.4. Circular plates supported at two points	50.
2.5. Pure bending on circular plate supported at two points.	52.
2.6. Quadratic plate finite element	52.
2.7. Finite element mesh	69.
2.8a. Plate simply supported on two arcs.	78.
2.8b. Reactive forces on plate simply supported on two arcs and subjected to uniform pressure.	78.
2.8c. Plate supported on two clamped arcs.	78.

2.9.	Plate supported on two short lengths of arc and short lengths of diameter.	89.
2.10.	Analysis of pure bending of a beam.	98.
2.11.	4-Point bend testing of a perspex beam.	98.
2.12.	4-Point bend testing equipment.	99.
2.13.	4-Point bend testing of a perspex beam.	99.
2.14.	A plot of total load vs central deflection.	101.
2.15.	A plot of strain vs deflection at the centre.	104.
2.16	Testing equipment.	107.
2.17.	Sample flange.	108.
2.18.	Testing equipment and control panel.	107.
2.19.	Perspex blade sample.	111.
2.20.	Sample blade with strain gauges connected fitted in testing flange.	111.
2.21.	Short flange for clamping.	112.
2.22.	Testing rig.	112.
2.23.	Dial gauges during testing.	113.
2.24.	Dial gauges frame.	113.
2.25.	Point load cell.	114.
2.26.	Point load cell attached to testing rig.	114.
2.27.	Point load testing	115.
2.28.	Line support.	115.
2.29.	Line support uniform pressure testing.	116.
2.30.	Dummy gauges.	116.
2.31.	Complete testing equipment.	117.
2.32.	Location of strain gauges.	118.
2.33.	U.V. Recorder output scale.	119.

2.34.	Full scale U.V. strain output.	119.
2.35	Strain circle of a rosette.	120.
2.36a.	Dial gauge locations.	125.
2.36b	Dial gauge locations.	126.
2.37.	Comparison of deflections due to uniform distributed pressure along x & y axis - 5 psi	127.
2.38.	Comparison of deflections due to uniform distributed pressure along x & y axis - 10 psi.	128.
2.39.	Location of strain gauges on finite element mesh	129.
2.40.	Comparison of principal stresses - Gauge 1.	143.
2.41.	Comparison of principal stresses - Gauge 2.	144.
2.42.	Comparison of principal stresses - Gauge 3 & 7.	145.
2.43.	Comparison of principal stresses - Gauge 4.	146.
2.44.	Comparison of principal stresses - Gauge 5.	147.
2.45.	Comparison of principal stresses - Gauge 8.	148.
2.46.	Comparison of principal stresses - Gauge 9.	149.
2.47.	Dial gauge and point load locations.	150.
2.48.	Comparison of deflections due to point load at Node 6 along x-axis.	162.
2.49.	Comparison of deflections due to point load at Node 6 along x-axis.	163.
2.50a.	Comparison of deflections due to point load at Node 6 along y-axis.	164.
2.50b.	Comparison of deflections due to point load at Node 6 along y-axis.	164.
2.51.	Comparison of principal stresses - Gauge 1.	165.
2.52.	Comparison of principal stresses - Gauge 2.	165.
2.53.	Comparison of principal stresses - Gauge 4.	166.
2.54.	Comparison of principal stresses - Gauge 5.	167.
2.55.	Comparison of principal stresses - Gauge 7.	168.

	Page No.
2.56. Comparison of principal stresses - Gauge 8.	169.
2.57. Comparison of principal stresses - Gauge 9.	170.
2.58. Dial gauge locations	171.
2.59. Comparison of deflections due to uniform distributed pressure along x-axis. - 5 psi.	172.
2.60. Comparison of deflections due to uniform distributed pressure along y-axis. - 10 psi.	172.
2.61. Comparison of principal stresses - Gauge 1.	188.
2.62. Comparison of principal stresses - Gauge 2.	189.
2.63. Comparison of principal stresses - Gauge 3.	190.
2.64. Comparison of principal stresses - Gauge 4.	191.
2.65. Comparison of principal stresses - Gauge 5.	192.
2.66. Comparison of principal stresses - Gauge 7.	193.
2.67. Comparison of principal stresses - Gauge 8.	194.
2.68. Comparison of principal stresses - Gauge 9.	195.
3.1. A 3-dimensional solid of fibres embedded in matrix	198.
3.2. Illustration of an orthotropic material in its laminated and lamina forms.	198.
3.3. 3-Dimensional state of stress	204.
3.4. 3-Dimensional element	204.
4.1. 8-Node first order hexahedron	217.
4.2. 16-Node element	217.
4.3a.)	
4.3b.) General elements (natural coordinates.	217.
4.3c.)	
4.4. 20-Node quadratic hexahedron	218.

	Page No.
5.1a. Blades of throughflow valves	229.
5.1b. Blades of throughflow valves	229.
5.2. A 72" dia. Cast iron butterfly valve - blade	232.
5.3a. Finite element mesh of the cast iron blade	234.
5.3b. Finite element mesh of the cast iron blade	234.
5.3c. Finite element mesh of the cast iron blade	235.
5.4a. Deflection test of the cast iron blade	236.
5.4b. Deflection test of the cast iron blade	236.
5.4c. Deflection test of the cast iron blade	236.
5.5a. Actual dimensions of composite deep beam No. D1	241.
5.5b. Composite deep beam specimen	241.
5.6a. Composite deep beam specimen	242.
5.6b. Composite deep beam specimen	242.
5.7. Layout of multi G.R.P. layer samples.	243.
5.8. Woven roving and unidirectional woven glass layers	244.
5.9. Individual layer specimens	244.
5.10. Individual layer specimens	245.
5.11. Individual layer specimens	245.
5.12. Individual layer specimens	246.
5.13. 4-Point testing of G.R.P. beam specimen	248.
5.14. 4-Point testing of G.R.P. beam specimen	248.
5.15. Load vs. deflection in direction 1 - Layer A	249.
5.16. Load vs. deflection in direction 2 - Layer A	250.
5.17. Load vs. deflection in direction 1 - Layer B	251.
5.18. Load vs. deflection in direction 2 - Layer B	252.
5.19. Load vs. deflection in direction 1 - Layer C	253.
5.20. Load vs. deflection in direction 2 - Layer C	254.

	Page No.
5.21. Longitudinal & transverse strain vs. deflection direction 1 - Layer A.	255. 255.
5.22. Longitudinal & transverse strain vs. deflection direction 2 - Layer A.	256.
5.23. Longitudinal & transverse strain vs. deflection direction 1 - Layer B.	257.
5.24. Longitudinal & transverse strain vs. deflection direction 2 - Layer B.	258.
5.25. Longitudinal & transverse strain vs. deflection direction 1 - Layer C.	259.
5.26. Longitudinal & transverse strain vs. deflection direction 2 - Layer C.	260.
5.27. 4-Point bend testing of G.R.P. beam for v_{13} & v_{23}	261.
5.28. 4-Point bend testing of G.R.P. beam for v_{13} & v_{23}	261.
5.29. 4-Point bend testing of G.R.P. beam for v_{13} & v_{23}	262.
5.30. Actual size specimen.	262.
5.31. Longitudinal vs. vertical strains in direction 1 - Layer A.	263.
5.32. Longitudinal vs. vertical strains in direction 2 - Layer A.	264.
5.33. Longitudinal vs. vertical strains in direction 1 - Layer B.	265.
5.34. Longitudinal vs. vertical strains in direction 2 - Layer B.	266.
5.35. Longitudinal vs. vertical strains in direction 1 - Layer C.	267.
5.36. Longitudinal vs. vertical strains in direction 2 - Layer C.	268.
5.37. Minimum set of specimens.	269.
5.38. Apparatus used for 4-Point bend testing of beams.	269.
5.39. Finite element idealization of G.R.P. test beam.	272.

Page No.

5.40a.)	Location and numbers of strain gauges.	274.
5.40b.)		
5.41.	Experiment arrangement of G.R.P. test beam.	275.
5.42.	Experiment arrangement of G.R.P. test beam.	276.
5.43.	Experiment arrangement of G.R.P. test beam.	276.
5.44.	Gauge locations on the finite element mesh.	277.
5.45.	Comparison of stresses in direction 1 at Node 203	279.
5.46.	Comparison of stresses in direction 2 at Node 203	280.
5.47.	Comparison of stresses in direction 2 at Node 210	281.
5.48.	Comparison of stresses in direction 3 at Node 210	282.
5.49.	Comparison of stresses in direction 2 at Node 215	283.
5.50.	Comparison of stresses in direction 3 at Node 215	284.
5.51.	Comparison of stresses in direction 1 at Node 218	285.
5.52.	Comparison of stresses in direction 2 at Node 218	286.
5.53.	Comparison of stresses in direction 2 at Node 211	287.
5.54.	Comparison of stresses in direction 3 at Node 211	288.
5.55.	Comparison of stresses in direction 2 at Node 206	289.
5.56.	Comparison of stresses in direction 3 at Node 206	290.
5.57.	Load vs. deflections in direction 3 at Node 1	292.
5.58.	Load vs. deflections in direction 3 at Node 45	293.
5.59.	Load vs. deflections in direction 1 at Node 30	294.
5.60.	G.R.P. butterfly blade	295.
5.61.	G.R.P. butterfly blade	296.
5.62.	G.R.P. butterfly blade	296.
5.63.	G.R.P. butterfly blade	297.
5.64a.	Finite element idealization of G.R.P. blade	299.
5.64b.	Finite element idealization of G.R.P. blade	300.

	Page No.
5.65a. Strain gauge locations on G.R.P. blade	301.
5.65b. Strain gauge locations on G.R.P. blade	302
5.66. Testing arrangement for deflections in G.R.P. blade.	303
A4.1. Global, local and principal directions for thin shell element	375. <i>Draft</i>
A5.1. Three dimensional para//el/o piped	378. <i>hh</i>

LIST OF TABLES

Page No.

- 2.1. Deflections and moments in a circular plate simply supported around the periphery and subjected to a uniform pressure. 70.
- 2.2. Moments design coefficients for circular plate simply supported on two points at opposite ends of a diameter and subjected to a uniform pressure obtained from finite element method. 72.
- 2.3. Comparison of deflection coefficients obtained by the 'closed-form' equation and finite element in circular plate simply supported on two points at opposite ends of a diameter and subjected to a uniform pressure. 73.
- 2.4. Comparison of moments coefficients obtained by the 'closed-form' equation and finite element in circular plate simply supported on two points at opposite ends of a diameter and subjected to a uniform pressure. 76.
- 2.5. Comparison of deflection coefficients obtained by 'closed-form' equation and finite element in circular plates simply supported on two short lengths of arcs at opposite ends of a diameter and subjected to a uniform pressure. 83.
- 2.6. Moments design coefficients for circular plate simply supported on two short lengths of arcs at opposite ends of a diameter and subjected to uniform pressure obtained from finite element method. 84.
- 2.7. Comparison of moments coefficients obtained by the 'closed-form' equation and finite element in circular plate simply supported on two short lengths of arcs at opposite ends of a diameter and subjected to a uniform pressure. 85.

✓

- 2.8a. Coefficients for deflections in circular plates simply supported on two short lengths of arcs at opposite ends of a diameter due to point load at the shown location. 86.
- 2.8b. Coefficients for moments in circular plates simply supported on two short lengths of arcs at opposite ends of a diameter due to point load at the shown location. 87.
- 2.9. Coefficients for deflections in circular plates clamped on two short lengths of arcs at opposite ends of a diameter due to point load at the shown location. 90.
- 2.10. Coefficients for deflections in circular plate supported on two clamped short lengths of arc at opposite ends of a diameter and subjected to a uniform pressure. 91.
- 2.11. Coefficients for moments in circular plate supported on two clamped short lengths of arc at opposite ends of a diameter and subjected to a uniform pressure. 92.
- 2.12a. Coefficients for deflections in circular plates supported on two clamped arcs at the end of the diameter and two short lengths of the diameter as shown and subjected to uniform pressure. 93.
- 2.12b. Coefficients for moments in circular plates supported on two clamped arcs at the end of the diameter and two short lengths of the diameter as shown and subjected to uniform pressure. 94.
- 2.12c. Coefficients for deflections in circular plates supported on two clamped arcs at the end of the diameter and two short length of the diameter as shown due to point load at the shown location. 95.
- 3.1. Direction cosines between two sets of coordinates 209.
- 5.1. Material properties as given by manufacturers.
Ref. (67). 237.

NOTATIONS

w	w_p , w_c	Deflections, load during tests
a		Radius of a circle
r		Radial distance of a point
θ		Polar angle
p		Point loads
c_i		Constants, coefficients
∇		Differential operator as defined in Equation (2.8).
$x, y, z.$		Cartesian coordinates
ρ, θ, z		Polar coordinates
$1, 2, 3.$		Material coordinates
M_x , M_y , M_{xy}		Moments and twisting moments in cartesian coordinates per unit length.
M_r , M_t , M_{rt}		Moments and twisting moments in polar coordinates per unit length
ν		Poisson's ratio for an isotropic material
ν_{ij}		Poisson's ratio for an isotropic material giving the strain in the j direction caused by the strain in the i direction.
E		Young's modulus of elasticity.
E_x , E_y , E_z		Young's moduli of elasticity along x, y, z direction.
E_1 , E_2 , E_3		Young's moduli of elasticity along $1, 2, 3$ the natural axis of material.
∂		Variation
q		Uniformly distributed load on pressure
D		Flexural rigidity
Q		Shear forces per unit length
t		Plate thickness

I	Second moments of area or integration value
F_i^n	Functions of n
n	Harmonic number
π	= 3.141592654
R	Reaction force
d, d'	Variations as defined in Equation (2.29)
$\beta .$	Constant as defined in Equation (2.32), angle
α	Angle of arc support
A_i^n, B_i^n	Constant
V_r	Kirchhoff shear
K	As defined in Equation (2.43a).
σ, ϵ	Stresses and strain respectively
$\sigma_{ij}, \epsilon_{ij}$	(i,j = 1,2,3) Stress and strain components in material natural axis. (i,j = x,y,z) Stress and strain components in global cartesian coordinates.
τ_{ij}, γ_{ij}	(i,j = 1,2,3) Shear stresses and strains in material axis. (i,j = x,y,z) Shear stresses and strain in global cartesian coordinates.
G_{ij}	(i,j = 1,2,3) Shear moduli associated with the material natural axis. (i,j = x,y,z) Shear moduli material associated with global axis.
$C_{ij kl}$	(i,j = 1,3 and k,l = 1,9) Elastic constants of material.
$[C]$	Compliance or flexibility matrix
$[D], [D]$	Elasticity matrices related to global and natural axis respectively.
Ω	Strain energy per unit volume.
l_i, m_j, n_k	(i,j,k = 1,2,3) Direction cosines.
$[R]$	Stress transformation matrix
$[R_\epsilon]$	Strain transformation matrix

$[I]$	Unit matrix
f_i	($i = 1,2$) Interpolation functions
N_i	($i = 1,20$) Shape function
ξ, η, ζ	Isoparametric coordinates
a_i	($i = 1,20$) Constants
u, v, w	Displacement components in the global x, y, z directions respectively.
u_i, v_i, w_i	($i = 1,20$) Nodal displacements along the natural axis.
$[J]$	Jacobian matrix
$[B]$	Elasticity matrix
$[B^*]$	Defined in Equation (4.16)
$\{\sigma'\}, \{\epsilon'\}$	Stress and strain vectors in material coordinates respectively.
$[k]$	Element stiffness matrix

CHAPTER ONE

INTRODUCTION

CHAPTER ONE

INTRODUCTION

1.1. General

The butterfly valve constitutes a very special case for structural analysis due to its geometrical shape which is determined by complex loading and boundary conditions during operation Ref. (1) which are very difficult to model mathematically.

In addition to this, its main function is as an engineering structure for sealing pipes, where deflections play an important role in defining the criteria for its efficient operation and possible failure.

Existing methods of analysis and design are based generally on approximate idealized "closed form" mathematical models for circular plates.

A long history of empirical formulae and experimental studies of butterfly valves exists, but as sizes of valves and industrial installations became larger with higher pressures, the desirable closing characteristic of the butterfly valve and new sealing methods led to its taking a greater share of the valve market and its replacing other types of valve. Ref. (2) (3) .

Due to the traditional methods of design which did not give confidence either to the buyers or to the manufacturers, very strict standards were demanded. Ref. (4) (5) (6) (7) . These specified minimum thicknesses for blades, bodies and shafts and required test pressures that seldom occur in practice.

As a consequence of this, very expensive test procedures had to be carried out in the manufacturing workshops rather than in the actual installations.

The use of butterfly valves in cooling systems employing sea water introduced corrosion as another major parameter to be considered in their design. This led to the use of coatings and linings and although this was satisfactory in temperate climates such as are found on European and North American coasts where sea water temperatures are low, it proved unsatisfactory in warm sea water Ref. (8) . In such environments the use of materials that provide good corrosion resistance, such as 18/8 3% molybdenum stainless steel, aluminium bronze or ni-resist cast iron becomes mandatory if metals are to be considered.

Fibre composite materials should therefore be seriously considered as alternatives, from the point of view of offering both corrosion resistance and cost savings.

Since such materials do not possess isotropic properties, analytical analysis becomes very complicated. More and more alternative combinations of fibre and matrix materials possessing high strength, high modulus and desirable corrosion properties (such as glass fibre reinforced plastic (G.R.P.), boron-epoxy, graphite-epoxy and boron-aluminium) have become available. Ref. (9) .

In contrast to the engineer who has traditionally designed a structure from a designated metal, in the field of composites the designer has freedom to design both the material and the structure as illustrated in Fig.(1.1)Ref. (10) .

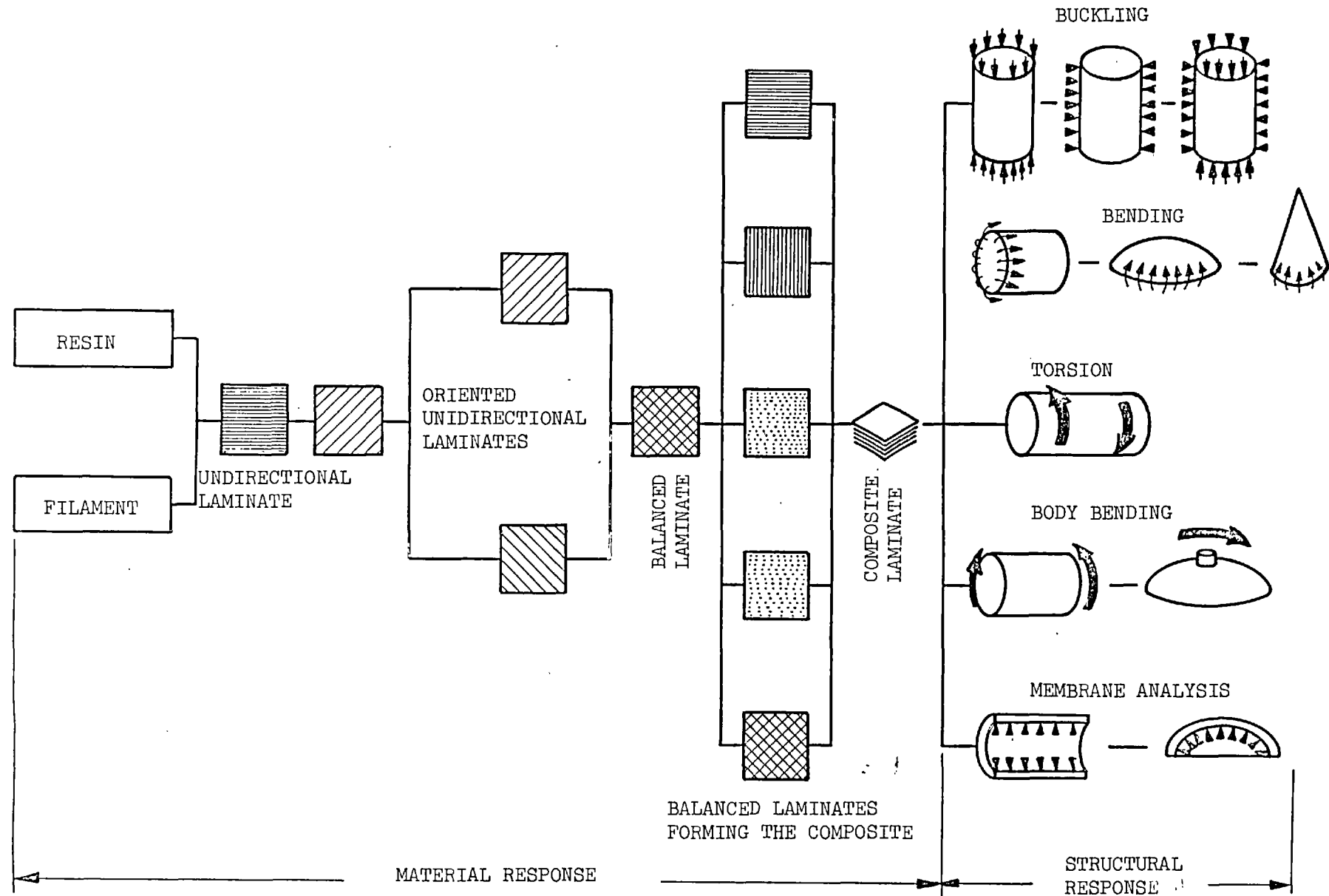


Fig. 1.1. Optimum Approach to Design with Composites

The need for numerical methods of analysis using modern computers to aid the design function becomes inevitable and the finite element method as applied in this study gives great confidence in such techniques. These techniques provide the necessary expertise and confidence to designers and their governing manufacturers, who have to take responsibility for guaranteeing efficient operation of their products, to promote and guarantee the application of butterfly valves in such applications. The overall concepts of product design and structural proportions have thereby been redefined and reviewed for the valve components and the possibility of using working stresses much closer to the yield point of the material, as in modern methods of designing other structures. This has consequently reduced the cross-sectional dimensions and weights of valves eventually. The reduction in size of the structural proportions of valve components is seen in the valve industry as the greatest single factor which can tilt the balance in favour of a better market share for products designed in this way. Ref. (11) .

1.2. Description of the Structure of Main Interest.

The butterfly valve essentially comprises a disk or blade which can rotate at right angles in a wing-like structure, about a diametrical axis within a pipe section body. A 90° rotation of the disk opens or closes the valve.

This basic simplicity provides a compact structure which has the least amount of body metal of any valve type, having few component parts (disk, shaft, body, seating seals and operating equipment).

Fully open the valve disk is the only obstruction which occupies the minimum amount of flow line space and causes very little head loss across the valve Ref. (18).

The valves are usually either resilient or metal to metal seated; the resilient seating may be in the body or attached to the periphery of the disk.

Butterfly valves are available in diameters from 2.5 cm to 10 m and even larger sizes are presently being considered for tidal and ocean thermal energy conversion schemes Ref. (2) for pressures that range from vacuum to 300 psi full differential, depending on the valve size.

The 90° turn offers quick opening or closing with ease of operation and the pressure shut-off capabilities require modest actuator power compared to other types of valves, since the butterfly valve is balanced in the closed position against upstream and downstream line pressures. Dynamic flow torque does not reach a maximum until somewhere between 30° to 75° open. Thus the peak dynamic flow torque does not occur at the same time as the higher torque which is required to unseat the valve. Ref. (19).

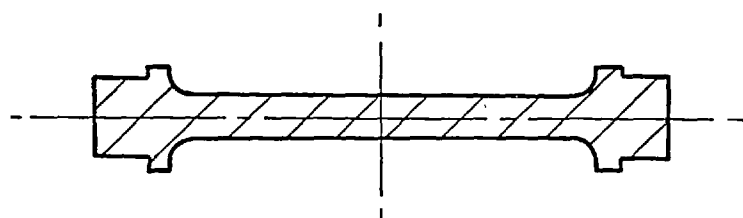
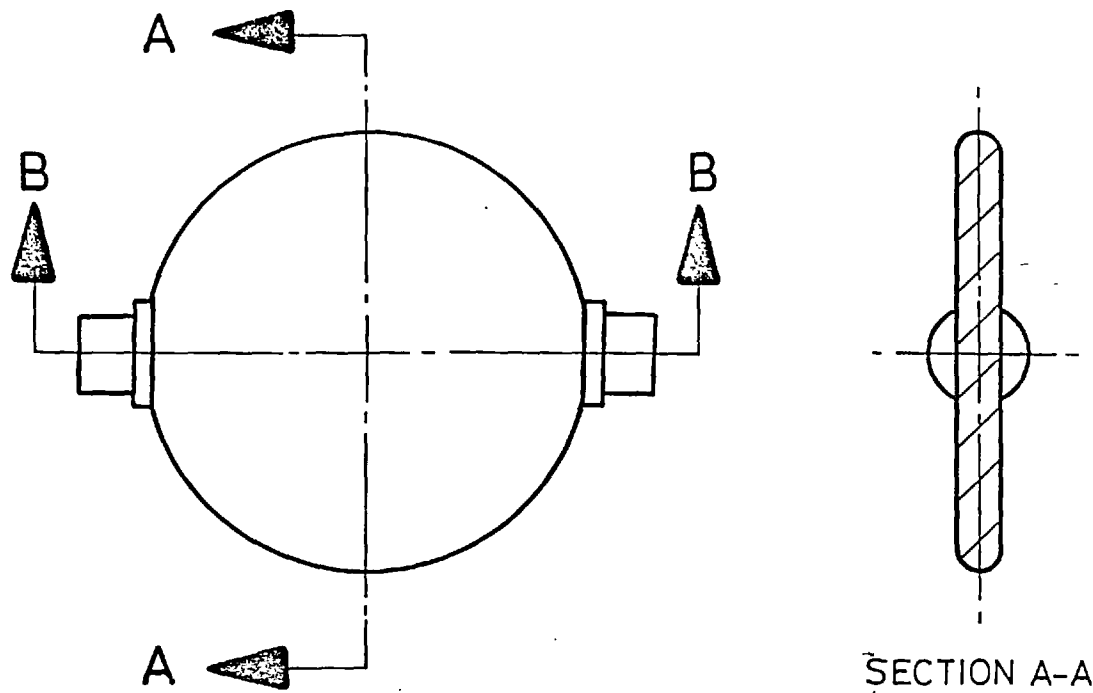
Butterfly valves can be installed in systems with constant-head sources such as nearby reservoirs or in pumping systems where pressure falls off with valve opening. During the closing movement the rate of cut-off of the flow diminishes as the disk moves towards the closed position, making the valve well suited for flow regulation purposes, (e.g. throttling).

1.2.1. The Disk or Blade

The disk or blade of the valve is the most important component of the valve, as its configuration has the greatest effect on:-

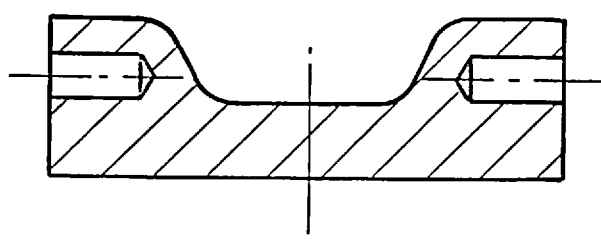
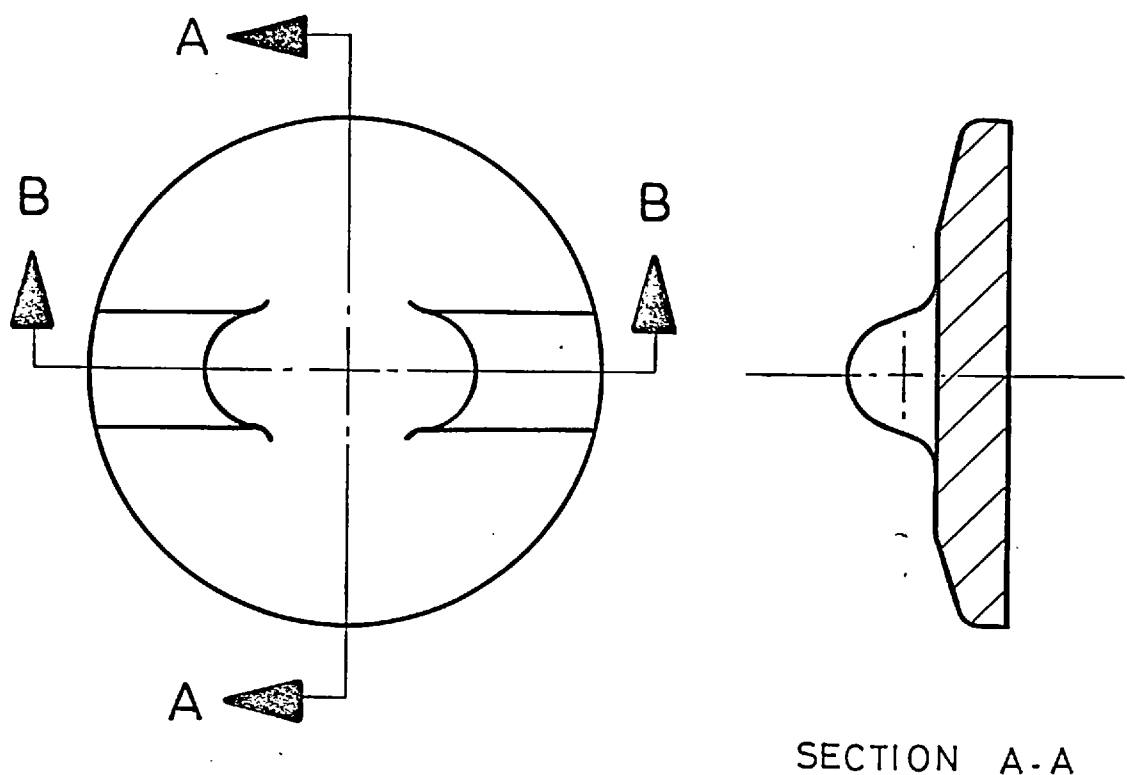
- (i) the head loss across the valve,
- (ii) the torque applied on the shafts,
- (iii) cavitation of the system,
- (iv) the sealing efficiency,
- (v) the noise.

The blade could be a simple flat disk of constant thickness Fig. (1.2) A Disk, or a solid or hollow tapered disk, Fig. (1.3) A Tapered Disk, or a lattice supported disk. As the size of the shaft varies according to the torque applied, the connection between the shaft and the blade varies from; shaft through the disk, Fig. (1.4), two shafts fitted in humps on the disk Fig. (1.5), and shafts as integral casting of the disk Fig. (1.6) and (1.7).



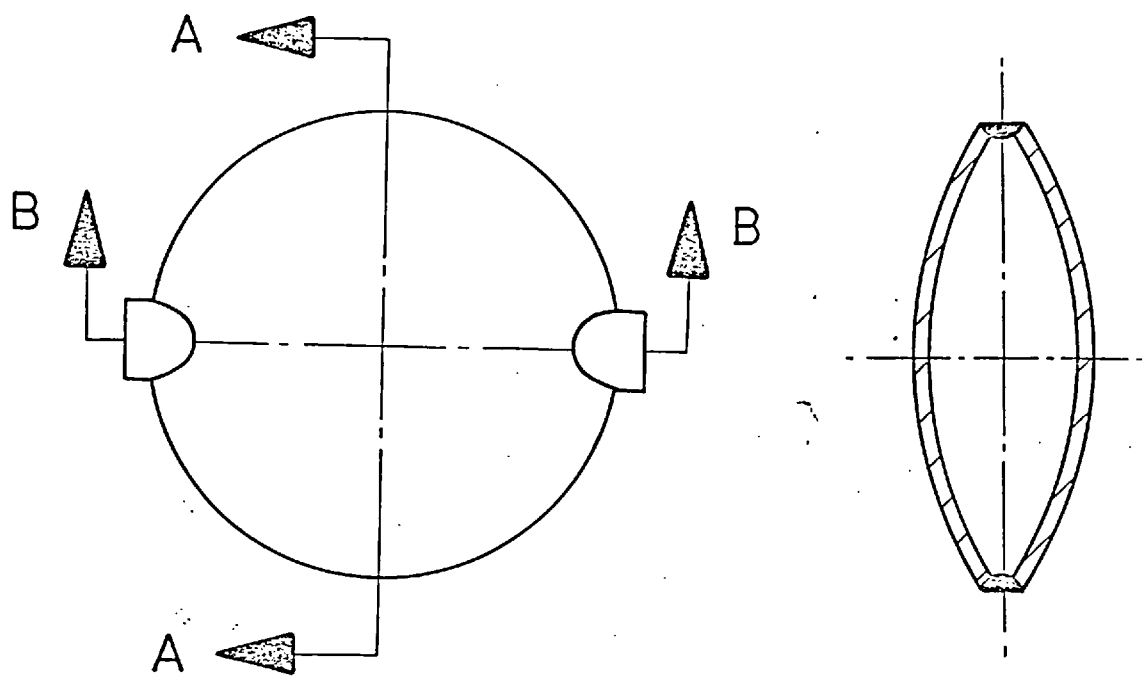
SECTION B-B

Fig. 1.2. A Disk of Constant Thickness

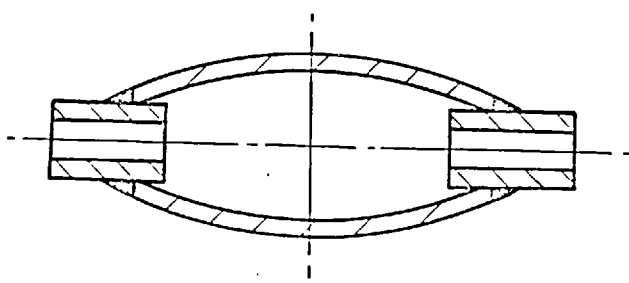


SECTION B-B

Fig. 1.3a. A Tapered Disk



SECTION A-A



SECTION B-B

Fig. 1.3b. A Hollow Tapered Disk

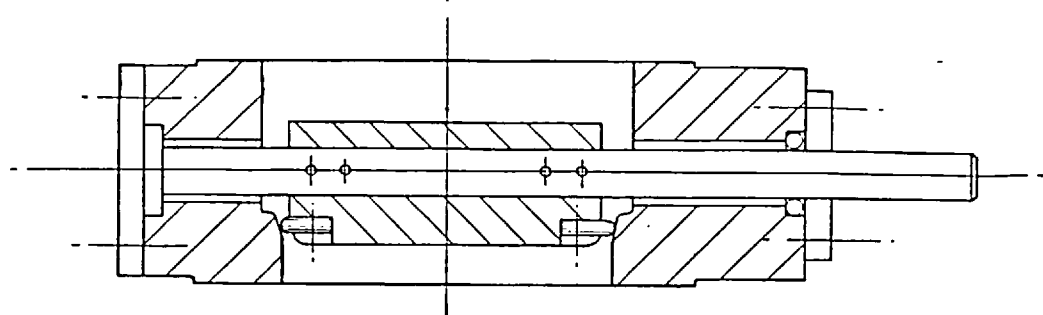


Fig. 1.4: Shaft through the disk

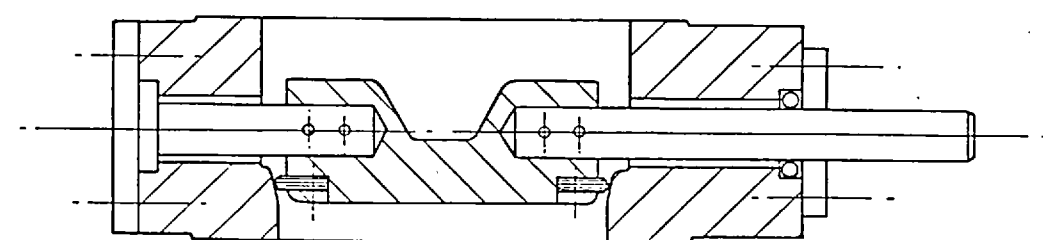


Fig. 1.5: Two shafts fitted in humps

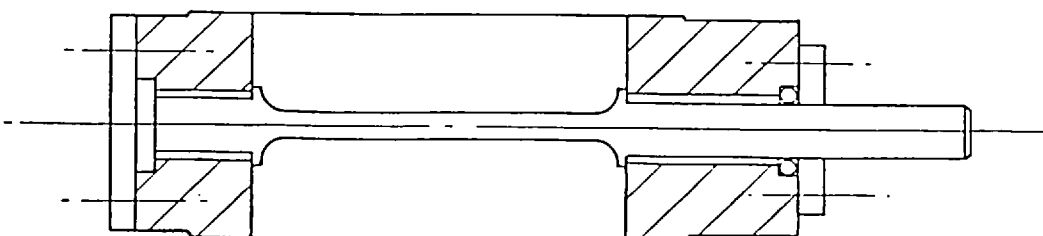


Fig. 1.6: Shafts as integral casting of the disk

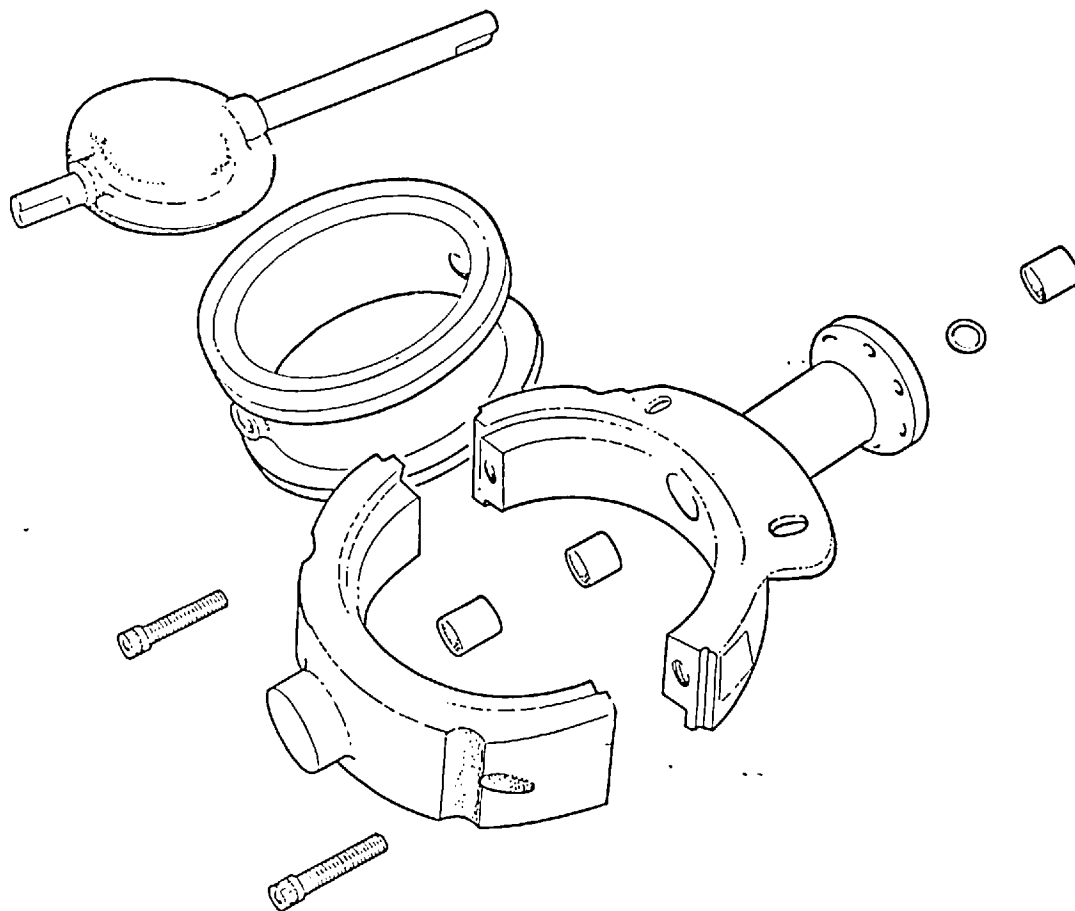


Fig. 1.7: Components of butterfly valve

1.2.2. The Shaft

The governing factor in the design of the shaft is the torque applied to it. The torque analysis of butterfly valves is a major subject which has received a fair amount of research and development in the past and has therefore not been tackled in this work.

One of the most significant observations in this study is the effect of the type of connection between shaft and blade or shaft and body, on the structural behaviour of the blade. No attempt to establish a criterion is made but it is left to the designer to assume the most suitable idealisation for the connection because this depends on working practices, allowable clearances, bearing arrangements and materials and empirical assumptions established by different design methods.

1.2.3. The Body

The body is the second most important component of the valve and it divides the valves mainly into two categories Ref. (2) .

Wafer: this is a valve for clamping between pipe flanges, using through bolting. The body may be single flange, flangeless or "U" section, as illustrated in Figs. (1.8), (1.9) and (1.11) respectively.

Double flanged: this is a valve having flanged ends for connection to pipe flanges by individual bolting Fig.(1.10). A wafer type with "U" section body will also come within this category if it is suitable for the

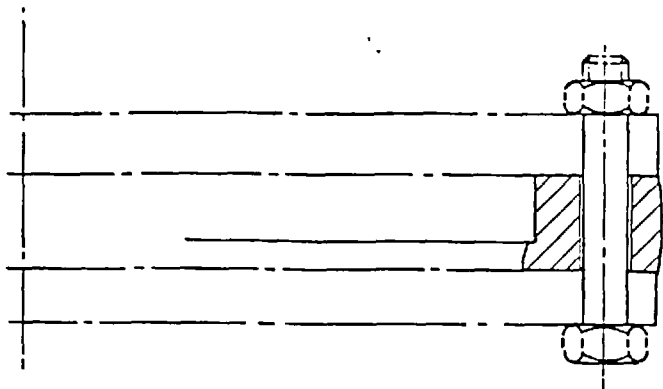


Fig. 1.8: Single flange body

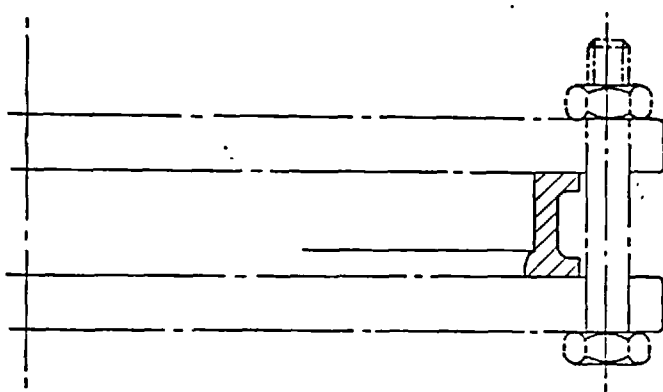


Fig. 1.9: U''U flangeless body

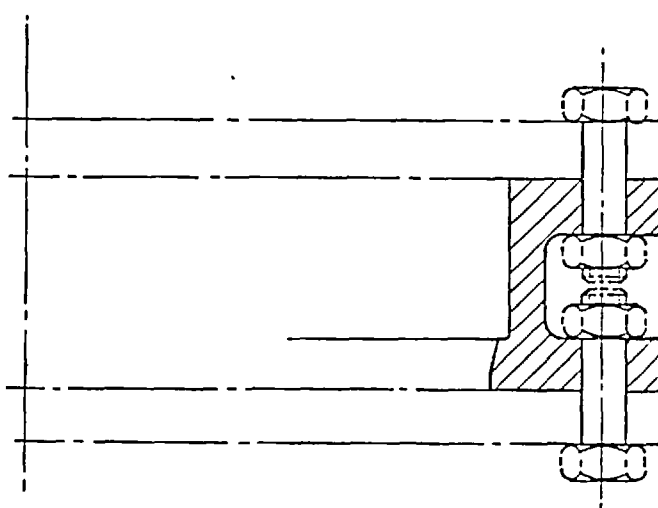


Fig. 1.10: Double flanged body

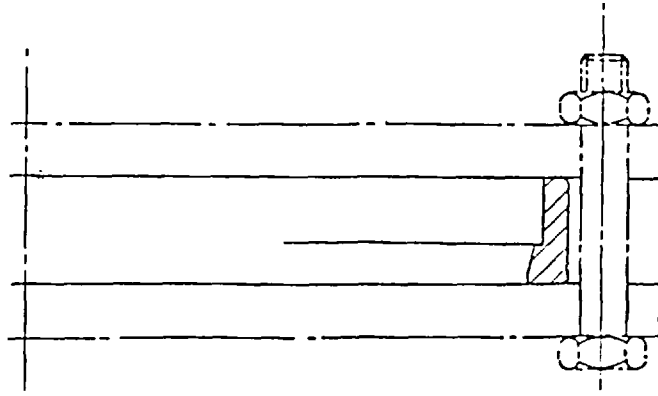


Fig. 1.11: Flangeless body

individual bolting of each flange to the pipework.

In smaller valves the body could be in two sections.

Fig. (1.7).

An unconventional body is the body of a 4-way butterfly valve which is the intersection of two pipes with an elliptical blade. The design of the body is governed by the piping system and the flange design. It is mainly a ring with two holes where a concentrated load causing shear, with or without correct installation and alignment, is another design factor to ensure non-interference between the blade and the piping system

Ref. (19) . The design of the body is not part of this work.

1.2.4. Seating Seals

These are either resilient or metal to metal seated.

The latter will normally provide longer life than resilient seated designs but are more difficult to make completely leak-tight. They are better suited for higher temperature duties as they do not have the temperature restrictions imposed by resilient seatings.

Regarding the former, an extensive range of synthetic elastomer and plastic materials for use as resilient seatings have been developed. Positive shut-off with repeatability of performance is assured and the wide choice of seating materials provides the butterfly valve with a comprehensive range of service applications.

The mechanical interference between the metal and the elastomeric seat requires a torque to unseat the valve. This depends on the type of seat material, the seat shape and the shape of the disk edge profile. Without the interference, of course, the valve could not be made leak-tight against high line pressure. The design of seats for sealing is not part of this study.

1.2.5. Operating Equipments

These generally comprise a gear box connected to the shaft of the blade at one end (or both ends) coupled with a manual and/or electrical/hydraulic actuator. These equipments are very important, especially in large installations, for the safety and control of any process. They can be controlled from a console in the hall of the plant and at the moment are undergoing great developments, introducing microelectronics processors as detectors and remote control systems, which will make a great change in this field. Such developments are not covered by this study.

1.3 Review

Engineering literature in the English language on the topic under discussion is very sparse. There is only one book Ref. (12) , on the design of valves, to the knowledge of the writer and this does not mention butterfly valves at all.

Hydraulic handbooks Ref. (13), (14), (15), & (16), contain a few brief references to the butterfly valve, describing its geometrical shape, the characteristics of special installations and methods of operating the valve. They make no reference at all to the structural design of such valves.

Again the butterfly valve is described in most handbooks Refs. (2), (3) & (17), on choosing valves in a minor way with no mention at all of structural analysis.

Reviewing existing books on the design of turbines, pumps and piping systems, Ref. (15), it may be observed that the valve is considered mainly in respect of its hydraulic characteristics with very brief guidance to methods of calculating torque on shafts and no guidance is given about structural analysis or design.

The British Hydromechanics Research Association have published, Ref.(20) for their members a bibliography on butterfly valves, covering the period from 1929 to 1966. This has been reviewed by the present writer, who subsequently extended the bibliography to cover the years from 1967 to the end of 1979, covering all known relevant engineering publications in this field.

Nowhere in all that literature is there to be found any study about the structural analysis of the valve components generally or on the blade or disc of the valve, which is the component whose dimensions and strength are of most importance in the overall design of the valve.

Reviewing structural analysis handbooks for the analysis of rings, circular, and other plates, Ref. (33), (34), it became evident that there is a great need to develop a body of knowledge with which to guide designers and structural analysts devoted to this task. Such a body of knowledge has been developed by the writer and is described in Chapter 2.

In considering new anisotropic materials and the more complex shapes of butterfly valve disc now required, the need to develop finite element programs for the purpose became evident. This has not been done before and has therefore been developed by the writer, as described in Chapters 3, 4, 5 and 6.

1.4. Materials

Valves are manufactured from a wide range of materials chosen to meet different operating requirements such as high or low temperature, corrosion, impact of particles carried in the flow, vibration characteristics, etc., subject to their availability. The materials to be discussed in this thesis are metallic alloys, glass reinforced plastic and perspex (for the experimental work). It is known that blades are made of polymers and fibres other than glass for the reinforcement of the matrix material with the result that Young's Modulus and Poisson's ratio can have virtually any value. In the analytical work (to be discussed in Chapter 2) Poisson's ratio has been varied from 0.05 to 0.5 to allow the designer to consider all possible alternative materials. In glass reinforced plastic Poisson's ratio is in the vicinity of 0.1, for polymers it is 0.35 - 0.4 and for metals it is 0.25 - 0.35.

1.5. Limitations and Scope of Study

The study is concerned with the structural analysis of the blades of butterfly valves, simulation of the loading applied and all possible boundary conditions occurring at the supports. It does not cover the very important subjects listed below since there is already an extensive literature in existence covering them.

1. Hydraulic analysis.
2. Torque analysis and design of shafts. Ref. (21) & (22).
3. Cavitation analysis. Ref. (23) & (24).
4. Analysis and design of the valve body. Ref. (25).
5. Noise analysis. Ref. (2) & (26).
6. Design of sealing, interference provisions and methods of installation and alignment. Ref. (27).
7. Vibration analysis. Ref. (28).
8. Temperature effects. Ref. (29).

CHAPTER TWO

ANALYTICAL PROCEDURE FOR THE STRUCTURAL ANALYSIS
OF THE BLADES OF ORDINARY BUTTERFLY VALVES

CHAPTER TWO

ANALYTICAL PROCEDURE FOR THE STRUCTURAL ANALYSIS OF THE BLADES OF ORDINARY BUTTERFLY VALVES

The search of an approximate "closed-form" solution for estimating the deflections and stresses in such blades is based on the general solution Equation (2.9) given by Clebsch Ref. (1) to be derived later. Now:

$$w(r, \theta) = w_p + w_c \quad 2.9$$

in the governing differential equation of a circular plate, namely:

$$\nabla^4 w = \frac{q(r, \theta)}{D} \quad 2.8$$

which has to be solved with suitably defined boundary conditions and loading.

In Equation (2.9) w_p represents a known particular integral solution of the governing differential equation which is added to a complementary function w_c which is the solution of the simple (Poisson) homogeneous equation

$$\nabla^4 w_c = 0 \quad 2.10$$

to satisfy the case under consideration.

The procedure is developed in detail as follows

2.1 The Governing Differential Equation for Circular Plates

To obtain the differential equation of a circular plate the starting point is to use the expressions for bending moment and transverse shear which are known for a cartesian system of co-ordinates, as illustrated in Fig. (2.1) (from Szilard Ref. (31)).

$$M_x = -D \left(\frac{\partial^2 w}{\partial x^2} + \nu \frac{\partial^2 w}{\partial y^2} \right) \quad 2.1a$$

$$M_y = -D \left(\frac{\partial^2 w}{\partial y^2} + \nu \frac{\partial^2 w}{\partial x^2} \right) \quad 2.1b$$

$$M_{xy} = M_{yx} = - (1-\nu) D \frac{\partial^2 w}{\partial x \partial y} \quad 2.1c$$

$$Q_x = \frac{\partial M_x}{\partial x} + \frac{\partial M_{xy}}{\partial y} \quad 2.1d$$

$$Q_y = \frac{\partial M_y}{\partial y} + \frac{\partial M_{xy}}{\partial x} \quad 2.1e$$

In the polar co-ordinates system shown in Fig. (2.2) the .

relationships between cartesian and polar co-ordinates are as follows:-

$$x = r \cos \theta \quad 2.2a$$

$$y = r \sin \theta \quad 2.2b$$

$$r = \sqrt{x^2 + y^2} \quad 2.2.c$$

$$\theta = \tan^{-1}(\frac{y}{x}) \quad 2.2d$$

The derivatives of $w(r, \theta)$ with respect to x can be derived

from the derivatives with respect to r & θ as follows:-

$$\frac{\partial w}{\partial x} = \frac{\partial w}{\partial r} \frac{\partial r}{\partial x} + \frac{\partial w}{\partial \theta} \frac{\partial \theta}{\partial x} \quad 2.3$$

$$\frac{\partial r}{\partial x} = \cos \theta \quad \text{and} \quad \frac{\partial \theta}{\partial x} = -\frac{1}{r} \sin \theta \quad 2.4$$

$$\frac{\partial r}{\partial y} = \sin \theta \quad \text{and} \quad \frac{\partial \theta}{\partial y} = +\frac{1}{r} \cos \theta \quad 2.5$$

The expressions for internal moments and shear forces in Equation (2.1) can be converted into polar co-ordinates using Equations (2.2, 2.3, 2.4 & 2.5) thus,

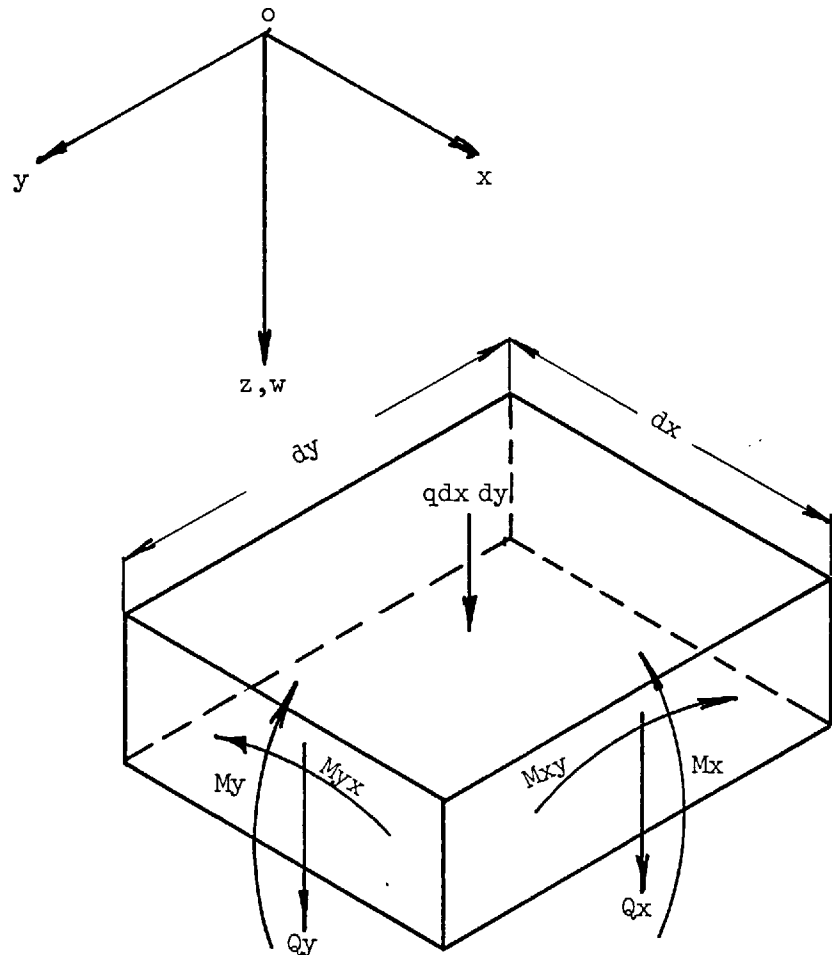


Fig. 2.1: Expressions for bending moments and transverse shear in cartesian coordinates.

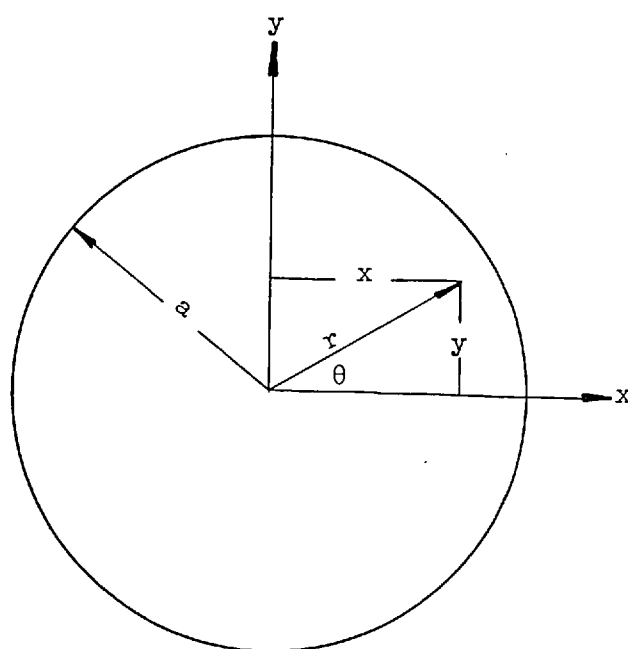


Fig. 2.2: Polar coordinates

$$M_r = -D \left[\frac{\partial^2 w}{\partial r^2} + \nu \left(\frac{1}{r^2} \frac{\partial^2 w}{\partial \theta^2} + \frac{1}{r} \frac{\partial w}{\partial r} \right) \right] \quad 2.6a$$

$$M_\theta = -D \left[\frac{1}{r} \frac{\partial w}{\partial r} + \frac{1}{r^2} \frac{\partial^2 w}{\partial \theta^2} + \nu \frac{\partial^2 w}{\partial r^2} \right] \quad 2.6b$$

$$M_{rt} = M_{\theta r} = -(1-\nu) D \left[\frac{1}{r} \frac{\partial^2 w}{\partial r \partial \theta} - \frac{1}{r^2} \frac{\partial w}{\partial \theta} \right] \quad 2.6c$$

$$Q_r = -D \frac{\partial}{\partial r} \nabla_r^2 w \quad 2.6d$$

$$Q_\theta = -D \frac{1}{r} \frac{\partial}{\partial \theta} \nabla_r^2 w \quad 2.6e$$

Considering an infinitesimally small plate element in the polar co-ordinates of Fig. (2.3) summing the moments (with correct signs) and neglecting moments due to the external load on the element as small quantities of higher order, we obtain the equilibrium equation in the 'r' direction of the element as:-

$$\begin{aligned} & \left(M_r + \frac{\partial M_r}{\partial r} dr \right) (r + dr) d\theta - M_r r d\theta - M_\theta dr d\theta \\ & + Q_r r d\theta dr = 0 \end{aligned} \quad 2.7a$$

hence

$$M_r + \frac{\partial M_r}{\partial r} r - M_\theta + Q_r = 0 \quad 2.7b$$

Substituting Equation (2.6) for $M_r - M_\theta$ and Q_r and taking the derivatives with respect to r , Equation (2.7b) becomes

$$\nabla_r^2 (\nabla_r^2 w) = \frac{q(r, \theta)}{D} \quad 2.8$$

where

$$q(r, \theta) = \frac{\partial Q_r}{\partial r}$$

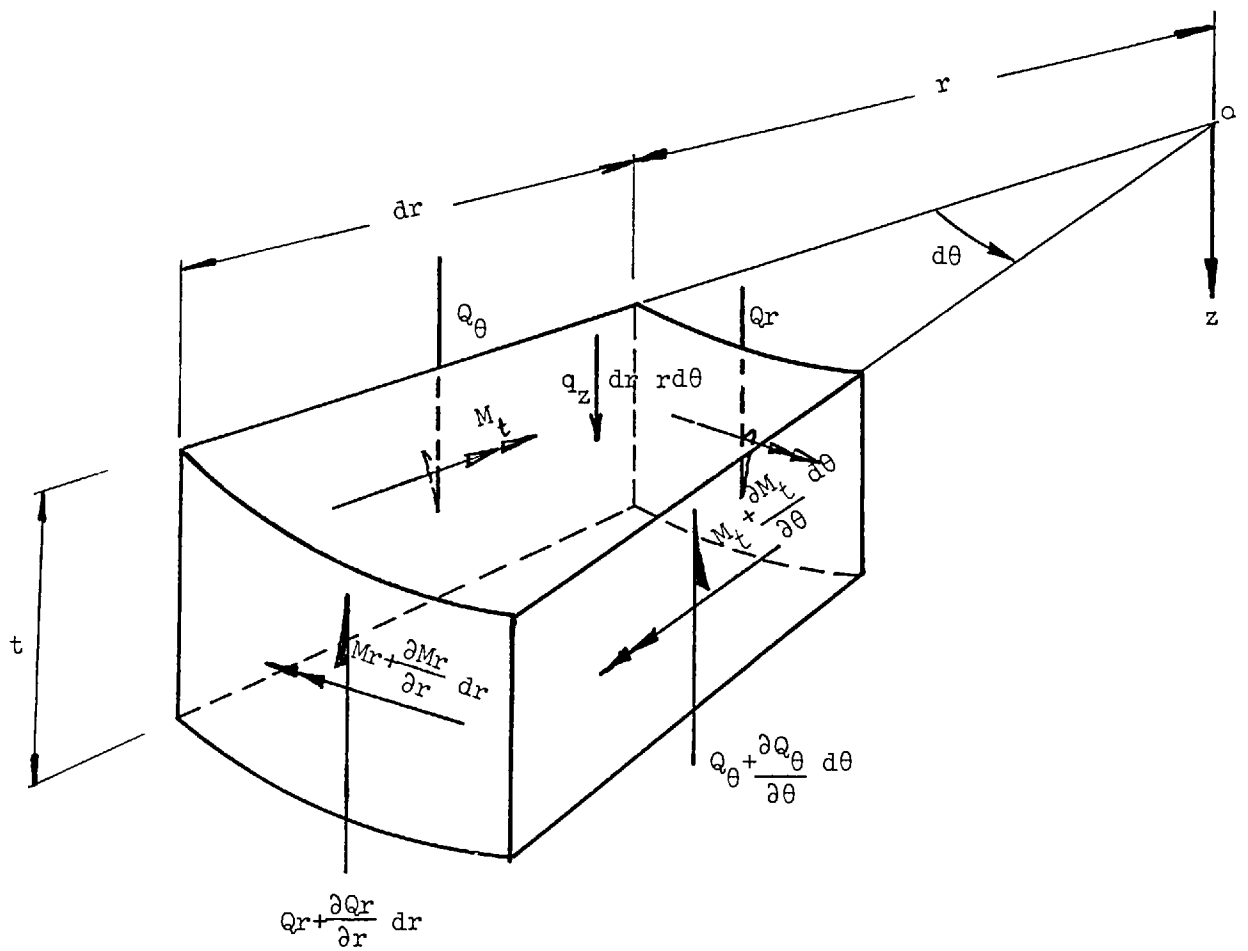


Fig. 2.3: Plate element in polar coordinates

and

$$\nabla_r^2 w = \frac{\partial^2}{\partial r^2} + \frac{1}{r} \frac{\partial}{\partial r} + \frac{1}{r^2} \frac{\partial^2}{\partial \theta^2}$$

Equation (2.8) is the governing differential equation for a thin circular plate of isotropic material.

2.2. The General Solution of the Governing Differential Equation

The general solution of this biharmonic equation

$$\nabla_r^4 w = \frac{q(r, \theta)}{D} \quad 2.8$$

can be taken as the sum of the two functions on the right-hand side of this equation:-

$$w(r, \theta) = w_p + w_c \quad 2.9$$

in which w_p is a known particular integral solution of Equation (2.8) and w_c is a complementary function which is the solution of the homogeneous equation

$$\nabla_r^4 w_c = 0 \quad 2.10$$

The solution of Equation (2.10) for a circular plate was obtained by Clebsch Ref. (30) in the form of the following series:

$$w_c = F_0 + \sum_{n=1}^{\infty} F_n \cos n\theta + \sum_{n=1}^{\infty} F'_n \sin n\theta \quad 2.11$$

Where each term of the series is a harmonic of order n .

Each summation is for a particular value of n and extends over as many terms as are necessary for a proper representation of the loading.

The $F_1, F_2 \dots F_n$ are functions of r only, which is the radial distance to any point on the disc Fig. (2.2), and they represent the symmetric components of the loading system. The $F'_1, F'_2 \dots F'_n$ are functions of r only and apply to the antisymmetric components of the loading system. F_0 is a function of r only and is completely independant of the angle θ unlike the other functions which are symmetric or antisymmetric. Substituting these series into Equation (2.10) leads for each of these functions to an ordinary differential equation of the following kind.

$$\left(\frac{\partial^2}{\partial r^2} + \frac{1}{r} \frac{\partial}{\partial r} - \frac{n^2}{r^2} \right) \left(\frac{\partial^2 F_n}{\partial r^2} + \frac{1}{r} \frac{\partial F_n}{\partial r} - \frac{n^2 F_n}{r^2} \right) = 0 \quad 2.12$$

the solutions of which are:

$$F_0 = C_{10} + C_{20} r^2 + C_{30} \ln \frac{r}{a} + C_{40} r^2 \ln \frac{r}{a} \quad (\text{for } n = 0)$$

$$F_1 = C_{11} r + C_{21} r^3 + C_{31} r^{-1} + C_{41} r \ln \frac{r}{a} \quad (\text{for } n = 1) \quad 2.13$$

- - - - - - - - - - - -

- - - - - - - - - - - -

- - - - - - - - - - - -

The general solution of $n > 1$ is therefore

$$F_n = C_{1n} r^n + C_{2n} r^{2+n} + C_{3n} r^{-n} + C_{4n} r^{-n+2}$$

Similar expressions can be written for the functions F'_n .

Substituting these expressions for the functions F_n and F'_n into the series Equation (2.11) we obtain the general solution of Equation (2.10). The constants C_{1n}, C_{2n}, C_{3n} and C_{4n} in each particular case must be determined so as to satisfy the given boundary conditions.

2.3. The Solution for Stresses and Deflections in a Circular Plate of Uniform Thickness Subjected to a Uniform Normal Pressure and Supported at two points at Opposite ends of a Diameter.

2.3.1. Analytical Work

In this case a circular disc of uniform thickness "t" is assumed, subjected to a uniform normal pressure "q" and supported at two points at opposite ends of a diameter.

The reaction of this loading, which develops at each of the support points (trunnions in the case of a valve blade), depends on the degree of fixity of the shafts, as will be discussed later.

If the support reaction is simulated in this analysis by a triangularly distributed load (illustrated in Fig. (2.4a)) which is replaced by a reaction R acting at the centroid of the triangle so that the point of simple support is assumed to be at a distance $a + a'$ from the centre of the disc Fig. (2.4b).

This system of loading can then be replaced by two systems, the effects of which are added together, as follows:

- (i) Two diametrically opposed moments as illustrated in Fig. (2.4c) with

$$M = R a'$$

2.14

(These moments act in a plane perpendicular to the disc and pass through the points of support).

- (ii) A uniformly distributed load of intensity q acting all over the area of one face of the circular disc, supported by two diametrically opposed equal reactions R acting at the periphery of the disc Fig. (2.4d) where

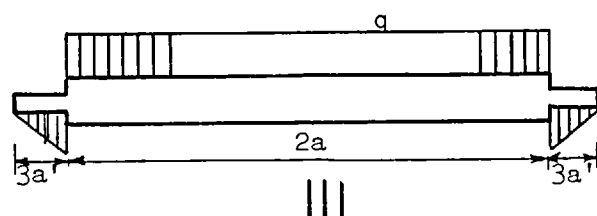
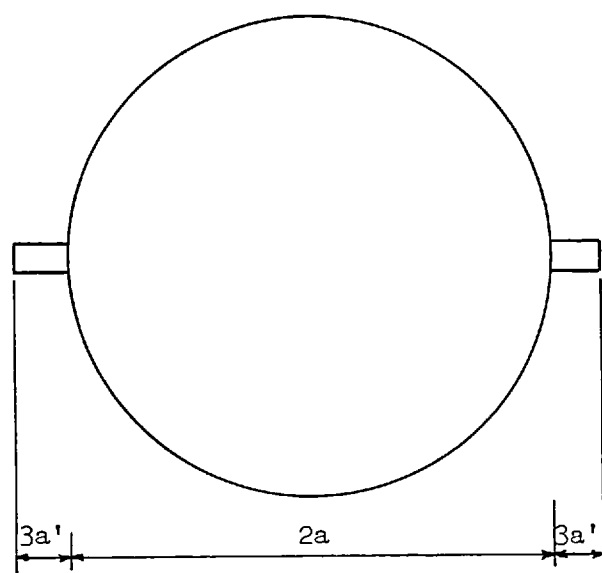


Fig. 2.4a

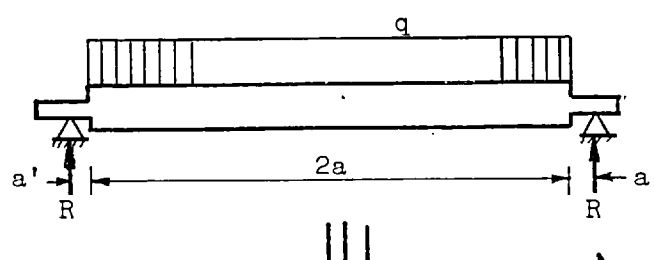


Fig. 2.4b

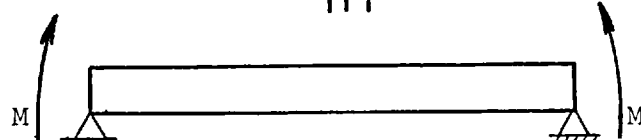


Fig. 2.4c

+

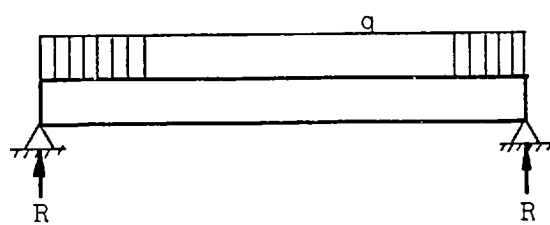


Fig. 2.4d

Fig. 2.4: Circular plates supported at two points

$$R = q \frac{\pi a^2}{2}$$

2.15

This loading occurs only when the valve is totally closed of course.

The effect of the first case of loading (pure bending) on a plate of non-uniform section Fig. (2.5) will now be considered.

The radial moment per unit length of any section can be obtained by dividing M (given by Equation (2.14)) by the appropriate chord length. The deflections along the diameter between the supports can be found as follows:-

$$\frac{\partial^2 w}{\partial x^2} = - \frac{M}{EI} \quad (\text{as given by Szilard Ref. (31)}) \quad 2.16$$

where

$$I = \frac{2yt^3}{12(1-\nu^2)} \quad 2.17$$

Substituting Equation (2.17) in Equation (2.16) gives:

$$\frac{\partial^2 w}{\partial x^2} = \frac{-6(1-\nu^2)}{Et^3} \frac{M}{y} \quad 2.18$$

Since $x = a \cos \theta$ and $y = a \sin \theta$, (from Equations (2.2a) and (2.2b)).

$$dx = -a \sin \theta d\theta.$$

Integrating Equation (2.18) with respect to x leads to

$$\begin{aligned} \int \frac{\partial^2 w}{\partial x^2} dx &= C_1 + \frac{6(1-\nu^2)M}{Et^3} \int_{\frac{\pi}{2}}^{\theta} \frac{a \sin \theta d\theta}{a \sin \theta} \\ \frac{\partial w}{\partial x} &= C_1 + \frac{6(1-\nu^2)M}{Et^3} \int_{\frac{\pi}{2}}^{\theta} d\theta \\ &= C_1 - \frac{6(1-\nu^2)M}{Et^3} \left(\frac{\pi}{2} - \theta \right) \end{aligned} \quad 2.19$$

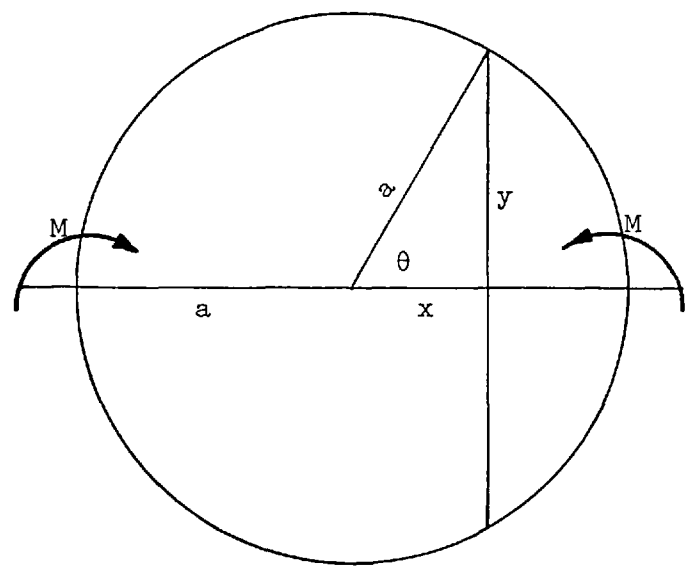


Fig. 2.5: Pure bending on circular plate supported at two points

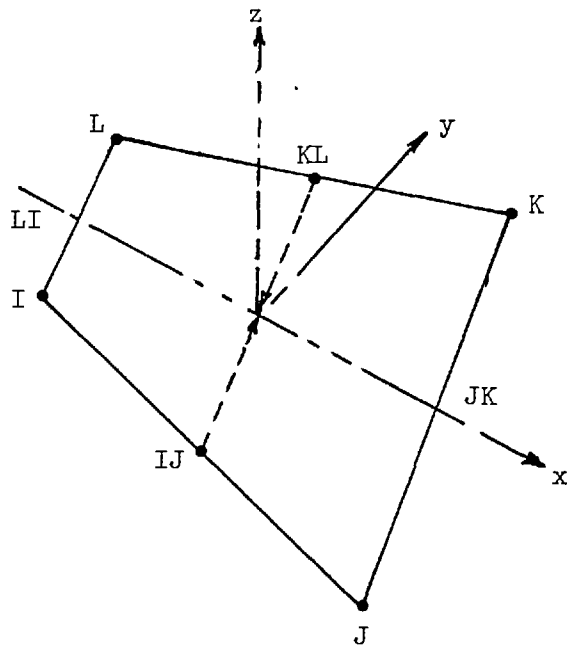


Fig. 2.6: Quadratic plate finite element

At $\theta = \frac{\pi}{2}$, $\frac{\partial w}{\partial x} = 0$ so C_1 must be zero

Integrating Equation (2.19) along x,

$$\begin{aligned}
 w &= C_2 + \frac{6(1-v^2)M}{Et^3} a \int_{\frac{\pi}{2}}^{\theta} \left(\frac{\pi}{2} - \theta \right) \sin \theta d\theta \\
 &= C_2 + \frac{6aM(1-v^2)}{Et^3} \left[\left(-\frac{\pi}{2} \cos \theta + \theta \cos \theta - \sin \theta \right) \right]_{\frac{\pi}{2}}^{\theta} \\
 &= C_2 - \frac{6aM(1-v^2)}{Et^3} \left[-1 + \left(\frac{\pi}{2} - \theta \right) \cos \theta + \sin \theta \right] \quad 2.20
 \end{aligned}$$

At $\theta = 0$, $w = 0$ thus

$$C_2 = \frac{6aM(1-v^2)}{Et^3} \left(\frac{\pi}{2} - 1 \right) = \frac{Ma}{2D} \left(\frac{\pi}{2} - 1 \right)$$

and

$$w = \frac{Ma}{2D} \left[\frac{\pi}{2} - \left(\frac{\pi}{2} - \theta \right) \cos \theta - \sin \theta \right] \quad 2.21$$

Maximum w occurs at $\theta = \frac{\pi}{2}$ so that

$$w_{\max} = \frac{Ma}{2D} \left(\frac{\pi}{2} - 1 \right) = 0.28548 \frac{Ma}{D} \quad 2.22$$

The deflection of the disc at any point due to the second case of loading, Fig (2.4d) can be determined as the sum of the deflection of the disc simply supported along its entire periphery (as a particular solution) and the deflection due to a system of forces distributed along it periphery to satisfy the loading of Fig (2.4d) with the boundary conditions of the disc being also fulfilled.

In what follows the complementary function and the particular integral have been solved together and dealt with in the various derivations as the single function w of Equation (2.8).

In Equation (2.9) w_p (the particular integral solution for the deflection of a disc simply supported along its entire periphery) given by Timoshenko et al. Ref. (32) as

$$w_p = \frac{qa^4}{64D} (1-\rho^2) \left(\frac{5+v}{1+v} - \rho^2 \right) \quad 2.23$$

where

$$\rho = \frac{r}{a} \quad 2.24$$

This is a symmetrical case of loading and deflections are measured from the diameter on which the two supports are positioned, i.e. the condition of geometrical symmetry is satisfied so that sin terms of the series Equation (2.11) may be omitted and the complimentary function may be written as

$$w_c = F_0 + \sum_{n=1}^{\infty} F_n \cos n\theta \quad 2.25$$

Substituting Equation (2.25) into Equation (2.10) and solving we obtain Equation (2.13) which must be satisfied by the constants C_{1n} , C_{2n} , C_{3n} and C_{4n} for this case. Since, at the centre of the plate the deflection, the slope and the internal moment are finite, at $r = 0$

$$\begin{aligned} C_{30} &= C_{40} = 0 \\ C_{31} &= C_{41} = 0 \\ - &- - \\ - &- - \\ C_{3n} &= C_{4n} = 0 \end{aligned} \quad 2.26$$

and Equation (2.13) can be written as

$$F_n = (C_{1n} r^n + C_{2n} r^{2+n}). \quad 2.27$$

Using Equation (2.25) and multiplying the first part by

$\frac{a^n}{a^n}$ and the second part by $\frac{a^{n+2}}{a^{n+2}}$ there results the equation

$$F_n = (C_{1n}^1 + C_{2n}^1 \rho^2) \rho^n$$

where

$$C_{1n}^1 = a^n C_{1n} \text{ (a new constant)}$$

and

$$C_{2n}^1 = a^{n+2} C_{2n} \text{ (a new constant)}$$

Substituting these into Equation (2.25) and multiplying by

$\frac{D}{qa^4}$ gives:

$$\frac{D}{qa^4} w_c = \sum_{n=0}^{\infty} (A_n + B_n \rho^2) \rho^n \cos n\theta \quad 2.28$$

where A_n and B_n are constants and $\rho = r/a$

At the boundary of the disc the radial bending moment is zero. Assuming the following relationships:-

$$d = a \frac{\partial}{\partial r}$$

$$\frac{\partial}{\partial r} = \frac{d}{a} \quad 2.29a$$

$$\frac{\partial^2}{\partial r^2} = \frac{d^2}{a^2}$$

and from Equation (2.25) $r = a\rho$

$$\frac{1}{r} \frac{\partial}{\partial r} = \frac{1}{r} \frac{d}{a} = \frac{1}{a\rho} \frac{d}{\frac{d}{a}} = \frac{d}{a^2\rho} \quad 2.29b$$

$$d' = \frac{\partial}{\partial \theta} \quad 2.29c$$

and using Equation (2.29) with Equation (2.6a) gives:

$$\begin{aligned} M_r_{\rho=1} &= -D \left[\frac{\partial^2}{\partial r^2} + \nu \left(\frac{1}{r^2} \frac{\partial^2}{\partial \theta^2} + \frac{1}{r} \frac{\partial}{\partial r} \right) \right] (w)_{\rho=1} + 0 \\ &= -D \left[\frac{d^2}{a^2} + \nu \left(\frac{1}{a^2 \rho^2} d'^2 + \frac{1}{a \rho} \frac{d}{a} \right) \right] (w)_{\rho=1} = 0 \end{aligned}$$

hence

$$M_r_{\rho=1} = \frac{-D}{a^2} \left[d^2 + \nu \left(\frac{d}{\rho} + \frac{d'^2}{\rho^2} \right) \right] (w)_{\rho=1} = 0 \quad 2.30$$

Applying Equation (2.30) with Equation (2.23) gives zeros

for w_p and applying Equation (2.30) with Equation (2.28)

for w_c gives:

$$B_0 = B_1 = 0 \quad 2.31$$

and

$$n(n-1) A_n + (n+1) \left(\frac{n+2}{\beta} \right) B_n = 0 \quad 2.32$$

$$\cdot \quad n > 1$$

where

$$\beta = \frac{1 - \nu}{1 + \nu}$$

At the supports the deflections are zero, i.e. $w_p = 0$

At $\rho = 1$ for $\theta = 0$ & π

Putting $\theta = 0$, $\rho = 1$ and using Equation (2.31) in

Equation (2.28) there results:

$$0 = \sum_{n=2,3}^{\infty} A_n + B_n$$

or

$$A_0 + A_1 + \sum_{n=2,3}^{\infty} (A_n + B_n) = 0 \quad 2.33$$

Putting $\theta = \pi$, $\rho = 1$ and using Equation (2.31) with Equation (2.28) results in

$$A_0 + A_1 + \sum_{n=2,3}^{\infty} (A_n + B_n) \cos n\pi = 0 \quad 2.34$$

Solving Equation (2.22) and Equation (2.34) with

$$\cos n\pi = +1 \quad (\text{for even } n)$$

$$\cos n\pi = -1 \quad (\text{for odd } n)$$

gives

$$A_0 = - \sum_{n=2,4}^{\infty} (A_n + B_n) \quad 2.35$$

and

$$A_1 = - \sum_{n=3,5}^{\infty} (A_n + B_n) \quad 2.36$$

The reactions R at the supports can be found from the Equations:

$$\frac{R}{\pi a} \left(\frac{1}{2} + \sum_{n=1}^{\infty} \cos n\theta \right) \quad 2.37$$

and

$$\frac{R}{\pi a} \left(\frac{1}{2} + \sum_{n=1}^{\infty} \cos n(\theta-\pi) \right)$$

as given by Timoshenko et al. Ref (32).

The value of the intensity of the vertical reaction at the boundary is the sum of these expressions

$$(V_r)_{\rho=1} = \frac{-R}{\pi a} \left[\frac{1}{2} + \sum_{n=1}^{\infty} \cos n\theta + \frac{1}{2} + \sum_{n=1}^{\infty} \cos n(\theta-\pi) \right] \quad 2.38$$

since $\cos n(\theta-\pi) = \cos n\theta \cos n\pi$

$$= \cos n\theta \quad (\text{for even } n)$$

$$= -\cos n\theta \quad (\text{for odd } n)$$

$$(V_r)_{\rho=1} = \frac{-R}{\pi a} \left(1 + 2 \sum_{n=2,4}^{\infty} \cos n\theta \right) \quad 2.39$$

The differential equation for V_r as given by Timoshenko et al. Ref. (32) (p.284) is

$$(V_r)_{\rho=1} = (Q_r - \frac{\partial}{r} \frac{M_{r\theta}}{\partial \theta})_{\rho=1} = 0 \quad 2.40$$

Using Equation (2.29a)

$$(V_r)_{\rho=1} = (Q_r - \frac{1}{\rho a} d' M_{r\theta})_{\rho=1} = 0$$

From Equation (2.6d) we get

$$Q_r = -D \frac{\partial}{\partial r} \left(\frac{\partial}{\partial r^2} + \frac{1}{r} \frac{\partial}{\partial r} + \frac{1}{r^2} \frac{\partial^2}{\partial \theta^2} \right) (w)_{\rho=1}$$

$$Q_r = -D \left(\frac{\partial^3}{\partial r^3} + \frac{1}{r} \frac{\partial^2}{\partial r^2} - \frac{1}{r^2} \frac{\partial}{\partial r} + \frac{1}{r^2} \frac{\partial^2}{\partial \theta^2} \frac{\partial}{\partial r} - 2 \frac{1}{r^3} \frac{\partial^2}{\partial \theta^2} \right) (w)_{\rho=1}$$

Using Equation (2.29a)

$$Q_r = \frac{-D}{a^3} \left(d^3 + \frac{d^2}{\rho} - \frac{d}{\rho^2} + \frac{dd'^2}{\rho^2} - 2 \frac{d'^2}{\rho^3} \right) \quad 2.41$$

From Equation (2.6c)

$$-\frac{1}{\rho a} d' M_{r\theta} = -\frac{D}{a^3} \left[\frac{(1-v)}{\rho^2} dd'^2 - \frac{(1-v)}{\rho^3} d'^2 \right] \quad 2.42$$

Substituting Equation (2.41) and Equation (2.42) into

Equation (2.40) gives:

$$(V_r)_{\rho=1} = \frac{-D}{a^3} \left[d^3 + \frac{d^2}{\rho} - \frac{d}{\rho^2} + \frac{(2-v)}{\rho^2} dd'^2 + \frac{(v-3)}{\rho^3} d'^2 \right] (w)_{\rho=1}$$

$$\text{as } w = w_p + w_c \quad 2.43$$

To carry the solution further we have to obtain the differentiation of w_p and w_c from Equations (2.23) and (2.28)

Assuming $\frac{qa^4}{D}$ is a constant = k, then

$$\frac{qa^4}{D} = k \quad 2.43a$$

$$\begin{aligned}
d(w_p) &= a \frac{\partial}{\partial r} (w_p) = a \frac{k}{64} \frac{\partial}{\partial r} \left[(1 - \frac{r^2}{a^2}) (\frac{5+v}{1+v} - \frac{r^2}{a^2}) \right] \\
&= \frac{ak}{64} \left[(1 - \frac{r^2}{a^2}) (-\frac{2r}{a^2}) + (\frac{5+v}{1+v} - \frac{r^2}{a^2}) (\frac{-2r}{a^2}) \right] \\
&= (\frac{ak}{64}) (\frac{-2r}{a^2}) \left[(1 - \rho^2) (\frac{5+v}{1+v} - \rho^2) \right] \\
&= \frac{-kp}{32} (1 + \frac{5+v}{1+v} - 2\rho^2) \\
&= \frac{-kp}{32} (\frac{1+v+5+v}{1+v} - 2\rho^2) \\
&= \frac{-kp}{32} (\frac{6+2v}{1+v} - 2\rho^2)
\end{aligned}$$

and

$$d(w_p) = \frac{-kp}{16} (\frac{3+v}{1+v} - \rho^2) \quad 2.44$$

$$\begin{aligned}
d^2(w_p) &= a \frac{\partial}{\partial r} \frac{k}{16} \frac{r}{a} (\frac{3+v}{1+v} - \frac{r^2}{a^2}) \\
&= \frac{k}{16} \frac{\partial}{\partial r} \left[(\frac{3+v}{1+v}) r - \frac{r^3}{a^2} \right] \\
&= \frac{k}{16} (\frac{3+v}{1+v} - 3\rho^2) \quad 2.45
\end{aligned}$$

$$d^3(w_p) = a \frac{\partial}{\partial r} \frac{k}{16} (\frac{3+v}{1+v} - 3\frac{r^2}{a^2})$$

$$d^3(w_p) = \frac{k}{16} (- 6 \frac{r}{a}) = \frac{3k}{8} \rho \quad 2.46$$

and

$$\begin{aligned}
d'(w_p) &= d'^2(w_p) = dd'(w_p) = dd'^2(w_p) = d^2d'(w_p) \\
&= d'^3(w_p) = 0 \quad 2.47
\end{aligned}$$

Similarly, for ($n=2, 4, \dots, \infty$) we get

$$d(w_c) = k \sum \left[n A_n + (n+2) B_n \rho^2 \right] \rho^{n-1} \cos n\theta \quad 2.48$$

$$d^2(w_c) = k \sum \left[n(n-1) A_n + (n+2)(n+1) B_n \rho^2 \right] \rho^{n-2} \cos n\theta \quad 2.49$$

$$d^3(w_c) = k \sum \left[n(n-1) A_n + (n+2)(n+1)n B_n \rho^2 \right] \rho^{n-3} \cos n\theta \quad 2.50$$

and

$$d'(w_c) = -k \sum (n A_n + n B_n \rho^2) \rho^n \sin n\theta \quad 2.51$$

$$d'^2(w_c) = -k \sum (n^2 A_n + n^2 B_n \rho^2) \rho^n \cos n\theta \quad 2.52$$

$$d'^3(w_c) = k \sum (n^3 A_n + n^3 B_n \rho^2) \rho^n \sin \theta \quad 2.53$$

$$dd'(w_c) = -k \sum \left[n^2 A_n + n(n+2) B_n \rho^2 \right] \rho^{n-1} \sin n\theta \quad 2.54$$

$$dd'^2(w_c) = -k \sum \left[n^3 A_n + n^2(n+2) B_n \rho^2 \right] \rho^{n-1} \cos n\theta \quad 2.55$$

$$d^2 d'(w_c) = -k \sum \left[n^2 (n-1) A_n + n(n+2)(n+1) B_n \rho^2 \right] \rho^{n-2} \sin n\theta \quad 2.56$$

Using Equations (2.44 to 2.56) in Equation (2.43) for

$(w_p + w_c) = 1$ and using Equation (2.31) for B_0, B_1 we get

$$\begin{aligned} (v_r)_{\rho=1} &= \frac{-D}{a^3} k \left\langle \frac{3}{8} \rho - \frac{1}{16} \left(\frac{3+v}{1+v} - 3\rho^2 \right) \frac{1}{\rho} + \frac{1}{16} \left(\frac{3+v}{1+v} - \rho^2 \right) \frac{1}{\rho} \right. \\ &\quad \left. + \sum_{n=2,3}^{\infty} \left\{ \left[n(n-1)(n-2) + n(n-1) - n - (2-v)n^3 \right. \right. \right. \\ &\quad \left. \left. - (v-3)n^2 \right] A_n + \left[(n+2)(n+1)n + (n+2)(n+1) - (n+2) \right. \right. \\ &\quad \left. \left. - (2-v)n^2 (n+2) - (v-3)n^2 \right] B_n \rho^2 \right\} \rho^{n-3} \cos n\theta \right\rangle_{\rho=1} \quad 2.57 \end{aligned}$$

$$(v_r)_{\rho=1} = \frac{-D}{a^3} k \left\langle \frac{1}{2} + \sum_{n=2,3}^{\infty} \left\{ -n^2(n-1)(1-v) A_n + n(n+1) \left[\frac{1}{4-n(1-v)} \right] B_n \rho^2 \right\} \rho^{n-3} \cos n\theta \right\rangle_{\rho=1} \quad 2.58$$

$$(v_r)_{\rho=1} = \frac{-D}{a^3} k \left\langle \frac{1}{2} + \sum_{n=2,3}^{\infty} \left\{ -n^2(n-1)(1-v) A_n + n(n+1) \left[\frac{1}{4-n(1-v)} \right] B_n \right\} \cos n\theta \right\rangle_{\rho=1}$$

From Equation (2.15) we have $2R = \pi a^2 q$ and $k = \frac{qa^4}{D}$

so

$$\frac{-D}{a^3} k = - \frac{qa^4}{D} \frac{D}{a^3} = - \frac{2R}{\pi a}$$

Using this in Equation (2.58) leads to

$$(v_r)_{\rho=1} = \frac{-R}{\pi a} \left[1 + 2 \sum_{n=2,3}^{\infty} \left\{ -n^2(n-1)(1-v) A_n + n(n+1) \left[\frac{1}{4-n(1-v)} \right] B_n \right\} \cos n\theta \right]_{\rho=1} \quad 2.59$$

The coefficients of $\cos n\theta$ in Equations (2.59) and (2.39)

should be equal, thus

$$-n^2(n-1)(1-v) A_n + n(n+1) \left[\frac{1}{4-n(1-v)} \right] B_n = 1 \quad 2.60$$

for $n = 2, 4, 6\dots$

and

$$-n^2(n-1)(1-v) A_n + n(n+1) \left[\frac{1}{4-n(1-v)} \right] B_n = 0 \quad 2.61$$

for $n = 3, 5, 7\dots$

Solving Equations (2.32) and (2.61) gives

$$A_n = B_n = 0 \quad \text{for } n = 3, 5, 7\dots \quad 2.62$$

Hence from Equation (2.36) we get

$$A_1 = 0$$

Solving Equations (2.32) and (2.60) gives

$$A_n = \frac{-(n+2/\beta)}{2n^2(n-1)(3+\nu)} \quad 2.62a$$

or as

$$A_n = \frac{-1}{2(3+\nu)} \left[\frac{1}{n(n-1)} + \frac{1}{\beta n^2(n-1)} \right] \quad 2.62b$$

Also,

$$B_n = \frac{1}{2n(n+1)(3+\nu)} \quad 2.63$$

Therefore,

$$A_n + B_n = \frac{-1}{3+\nu} \left[\frac{1}{n(n^2-1)} + \frac{1}{\beta n^2(n-1)} \right] \quad 2.64$$

Equations (2.62a, 2.62b, 2.63 and 2.64) are for

$$n = 2, 4, 6, \dots \text{etc.}$$

Using Equation (2.64) in Equation (2.35) gives

$$A_0 = \frac{1}{3+\nu} \sum_{n=2,4} \left[\frac{1}{n(n^2-1)} + \frac{1}{\beta n^2(n-1)} \right]$$

Considering ln series,

$$A_0 = \frac{1}{3+\nu} (\ln 2 - \frac{1}{2}) + \frac{1}{\beta} (\ln 2 - \frac{\pi^2}{24})$$

or

$$A_0 = \frac{1}{3+\nu} \left[\frac{2 \ln 2}{1-\nu} - \frac{\pi^2}{24\beta} - \frac{1}{2} \right] \quad 2.65$$

Hence, Equation (2.28) since $A_1 = B_0 = B_1 = 0$ can be written as

$$\frac{D}{qa^4} w_c = A_0 + \sum_{n=2,4}^{\infty} (A_n + B_n \rho^2) \rho^n \cos n\theta \quad (2.28)$$

Using Equations (2.62b) and (2.65) gives

$$\frac{D}{qa^4} w_c = \frac{1}{3+v} \left[\left\{ \frac{2 \ln 2}{1-v} - \frac{\pi^2}{24} - \frac{1}{2} \right\} - \frac{1}{2} \sum_{n=2,4}^{\infty} \left\{ \frac{1}{n(n-1)} \right. \right. \\ \left. \left. + \frac{2}{\beta n^2(n-1)} - \frac{\rho^2}{n(n+1)} \right\} \rho^n \cos n\theta \right] \quad 2.66$$

and for the complete expression of deflection

$$w = w_p + w_c \quad 2.69$$

$$w = \frac{qa^4}{D} \frac{1}{64} (1-\rho^2) \left(\frac{5+v}{1+v} - \rho^2 \right) + \frac{qa^4}{D} \frac{1}{2(3+v)} \\ \left[\left\{ \frac{4 \ln 2}{1-v} - \frac{\pi^2}{12\beta} - 1 \right\} - \sum_{n=2,4}^{\infty} \left\{ \frac{1}{n(n-1)} + \right. \right. \\ \left. \left. \frac{2}{\beta n^2(n-1)} - \frac{\rho^2}{n(n+1)} \right\} \rho^n \cos n\theta \right] \quad 2.67$$

or

$$\frac{wD}{qa^4} = \left(\frac{1-\rho^2}{64} \right) \left(\frac{5+v}{1+v} - \rho^2 \right) + \frac{1}{2(3+v)} \left\{ 2 \ln 2 - 1 \right. \\ \left. + \left(\frac{1+v}{1-v} \right) \left(2 \ln 2 - \frac{\pi^2}{12} \right) - \sum_{n=2,4}^{\infty} \left[\frac{1}{n(n-1)} \right. \right. \\ \left. \left. + \frac{2(1+v)}{(1-v)(n-1)n^2} - \frac{\rho^2}{n(n+1)} \right] \rho^n \cos n\theta \right\} \quad 2.68$$

which is the complete solution.

The expression for the radial moment M_r , using

Equations (2.44 to 2.56) with Equation (2.30) is

$$M_r = -k \frac{D}{a^2} \left\langle \left[\frac{-1}{16} \left(\frac{3+v}{1+v} - 3\rho^2 \right) - \frac{v}{16} \left(\frac{3+v}{1+v} - \rho^2 \right) \right] \right. \\ \left. + \sum_{n=2,4}^{\infty} \left\{ \left[n(n-1) + v(n-n^2) \right] A_n + \left[(n+2)(n+1) \right. \right. \right. \\ \left. \left. \left. + v(n+2) - vn^2 \right] B_n \rho^2 \right\} \rho^{n-2} \cos n\theta \right\rangle$$

$$= \frac{-Dk}{a^2} \left[\frac{-(3+v)}{16} (1-\rho^2) + \sum_{n=2,4}^{\infty} \left\{ n(n-1)(1-v) A_n + n(n+1) \left[(1-v) + \frac{2}{n} (1+v) \right] B_n \rho^2 \right\} \rho^{n-2} \cos n\theta \right] \quad 2.69$$

Substituting for k , A_n & B_n from Equations (2.42a), (2.62b) and (2.63) leads to

$$\frac{M_r}{a^2 q} = \frac{1}{16} (3+v)(1-\rho^2) + \frac{1}{2} \left(\frac{1+v}{3+v} \right) \sum_{n=2,4}^{\infty} \left(\beta + \frac{2}{n} \right) (1-\rho^2) \rho^{n-2} \cos n\theta \quad 2.70$$

The expression for the tangential moment M_t , using Equation (2.43) to (2.52), Equation (2.29) and Equation (2.6b) is

$$M_t = -k \frac{D}{a^2} \left\langle \left[\frac{-1}{16} \left(\frac{3+v}{1+v} - \rho^2 \right) - \frac{v}{16} \left(\frac{3+v}{1+v} - 3\rho^2 \right) \right] + \sum_{n=2,4}^{\infty} \left\{ \left[n-n^2 + vn(n-1) \right] A_n + \left[(n+2) - n^2 + v(n+2)(n+1) \right] B_n \rho^2 \right\} \rho^{n-2} \cos n\theta \right\rangle$$

or

$$M_t = -k \frac{D}{a^3} \left[\frac{-1}{16} (3+v) - (1+3v)\rho^2 \right] + \sum_{n=2,4}^{\infty} \left\{ n(n-1)(1-v) A_n + n(n+1) \left[(1-v) \frac{-2}{n} (1+v) \right] B_n \rho^2 \right\} \rho^{n-2} \cos n\theta \quad 2.71$$

Substituting k , A_n & B_n from Equations (2.42a, 2.61b and 2.62) leads to

$$\frac{M_t}{a^2 q} = \frac{1}{16} \left[(3+v) - (1+3v)\rho^2 \right] - \frac{1}{2} \left(\frac{1+v}{3+v} \right) \sum_{n=2,4}^{\infty} \left\{ \beta(1-\rho^2) + \frac{2}{n} (1+\rho^2) \right\} \rho^{n-2} \cos n\theta \quad 2.72$$

The expression for the twisting moment $M_{r\theta}$, using Equations (2.43) to (2.52), Equation (2.29) and Equation (2.6c)

$$\begin{aligned} M_{rt} &= k \frac{D}{a^2} (1-\nu) \sum_{n=2,4}^{\infty} \left\{ (-n^2+n) A_n + \right. \\ &\quad \left. \left[-n(n+2)+n \right] B_n \rho^2 \right\} \rho^{n-2} \sin n\theta \\ &= k \frac{D}{a^2} (1-\nu) \sum_{n=2,4}^{\infty} \left\{ -n(n-1) A_n - \right. \\ &\quad \left. n(n+1) B_n \rho^2 \right\} \rho^{n-2} \sin n\theta \end{aligned} \quad 2.73$$

Substituting for k , A_n & B_n from Equations (2.42a, 2.61b and 2.62) leads to

$$\frac{M_{rt}}{a^2 q} = \frac{1}{2} \left(\frac{1+\nu}{3+\nu} \right) \sum_{n=2,4}^{\infty} \left\{ \beta (1-\rho^2) + \frac{2}{n} \right\} \rho^{n-2} \sin n\theta \quad 2.74$$

The expression for the radial shear Q_r , using Equations (2.43) to (2.52), Equation (2.29) and Equation (2.6d)

$$\begin{aligned} Q_r &= -k \frac{D}{a^3} \left\langle \frac{3}{8} \rho - \frac{1}{16} \left(\frac{3+\nu}{1+\nu} - 3\rho^2 \right) \frac{1}{\rho} + \frac{1}{16} \right. \\ &\quad \left. \left(\frac{3+\nu}{1+\nu} - \rho^2 \right) \frac{1}{\rho} + \sum_{n=2,4}^{\infty} \left[\begin{aligned} &n(n-1)(n-2) + \\ &n(n-1) - n - n^3 + 2n^2 \end{aligned} \right] A_n + \left[\begin{aligned} &(n+2)(n+1)n \\ &+ (n+2)(n+1) - (n+2) - n^2(n+2) + 2n^2 \end{aligned} \right] B_n \rho^2 \right\rangle \rho^{n-3} \cos n\theta \\ Q_r &= -k \frac{D}{a^3} \left[\frac{\rho}{2} + 4 \sum_{n=2,4}^{\infty} n(n+1) B_n \rho^{n-1} \cos n\theta \right] \end{aligned} \quad 2.75$$

$$\frac{Q_r}{qa} = \frac{-1}{2} - \frac{2}{(3+\nu)} \sum_{n=2,4}^{\infty} \rho^{n-1} \cos n\theta \quad 2.76$$

The expression for the tangential shear Q_t , using Equations (2.43) to (2.52), Equation (2.29) and Equation (2.6e)

$$Q_t = -k \frac{D}{a^3} \sum_{n=2,4}^{\infty} \left[-n^2(n-1) - n^2 + n^3 \right] A_n + \left[-n(n+2)(n+1) - n(n+2) + n^3 \right] B_n \rho^2 \rho^{n-3} \sin n\theta$$

$$Q_t = -k \frac{D}{a^3} 4 \sum_{n=2,4}^{\infty} -n(n+1) B_n \rho^{n-1} \sin n\theta \quad 2.77$$

$$\frac{Q_t}{qa} = \frac{2}{(3+v)} \sum_{n=2,4}^{\infty} \rho^{n-1} \sin n\theta \quad 2.78$$

In Equation (2.68) the right-hand side would give a constant coefficient for a defined Poisson's ratio v at a defined location (ρ, θ) on the plate. This coefficient can be converted into a deflection due to the uniformly distributed load by multiplying it by

$$\frac{qa^4}{D}$$

This further lends itself to the development of a hand table of coefficients which is shown in Appendix (1). In Equations (2.70, 2.72 and 2.74) the right-hand side would give a constant coefficient for a defined Poisson's ratio v at a defined location (ρ, θ) on the plate. This coefficient can be converted into stresses due to the moments by multiplying it by

$$\pm 6q \left(\frac{a}{t}\right)^2$$

as the value of the moments acting in the radial and tangential directions, taken with respect to the centre of the plate, are calculated per unit length. Thus in the radial and tangential directions along sections described by $\theta = 0^\circ$ and $\theta = 90^\circ$ this procedure produces stresses in the principal directions whilst the radial and tangential moments acting along any other section, as described by $0^\circ < \theta < 90^\circ$, produce only stresses in the given directions, the twisting moment $M_{r\theta}$ not being zero. Along $\theta = 0^\circ$ and $\theta = 90^\circ$ the stresses caused by the couples in Fig. (2.4c) should be added directly to the stresses acting in the radial and tangential direction as appropriate.

In Equations (2.76) and (2.78) the right-hand side would give a constant coefficient for a defined Poisson's ratio at a defined location (ρ, θ) on the plate. These coefficients can be converted into shear stresses by multiplying by

$$qa$$

Equations (2.68, 2.70, 2.72, 2.74, 2.76 and 2.78) were written in two small computer programs.

- (i) To produce a complete hand table of coefficients for deflections, moment and shears as shown in Appendix (1). A FORTRAN listing of the program is in Appendix (2.A).
- (ii) To suit a top desk microcomputer Ref. (36) where the designer interacts directly through the computer screen, feeding in t , a , E , v , ρ , θ and q

in a free format and immediately obtaining the deflection at the point and all the stresses due to moments and shears.

A FORTRAN IV listing of the program is given in Appendix (2.B) This completes the analytical work of this case.

2.3.2. Finite Element Analysis

The first step was the analysis of a circular plate simply supported around the periphery and subjected to a uniformly distributed load which is a well documented case in many texts such as Ref. (31), (32) & (35).

An existing finite element program for the analysis of plates was used, Ref. (38). It employs a quadratic plate element as shown in Fig. (2.6).

A sufficiently fine mesh, as determined by convergence criteria consisting of 160 elements, 184 nodal points per half circular plate was adopted as adequate for this study as shown later and illustrated in Fig. (2.7). The degree of symmetry in this case calls for quarter of a circle but lesser degrees of symmetry, called for later in this work, required the use of half a circle.

A comparison of results for a typical example of this simply supported case is shown in Table (2.1). This leads to the conclusion that the finite element model is adequate and useful for predicting the deflections and stresses in circular plates.

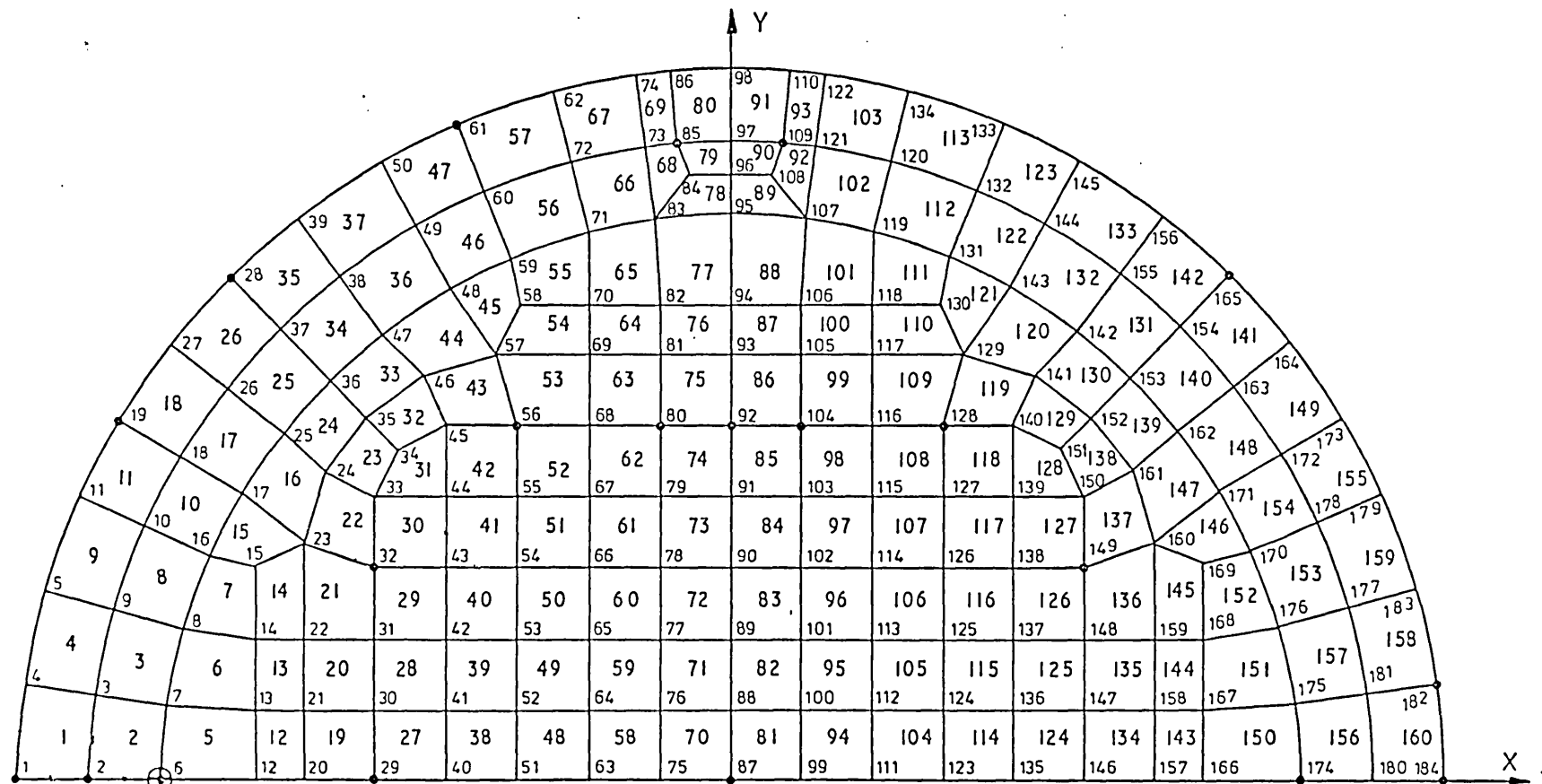


Fig. 2.7. Finite element mesh.

LOCATION		CENTRE POINT	$\rho = 0.5$
DEFLECTION	FINITE ELEMENT	$0.06544 \frac{qa^4}{D}$	$0.046147 \frac{qa^4}{D}$
	CLOSED FORM SOLUTION EQUATION	$0.065622 \frac{qa^4}{D}$	$0.04628 \frac{qa^4}{D}$
M_x, M_r	FINITE ELEMENT	$0.2014 q a^2$	$0.1586 q a^2$
	CLOSED FORM SOLUTION EQUATION	$0.203125 q a^2$	$0.1523 q a^2$
M_y, M_θ	FINITE ELEMENT	$0.2014 q a^2$	$0.17545 q a^2$
	CLOSED FORM SOLUTION EQUATION	$0.203125 q a^2$	$0.17578 q a^2$

Dimensions of example used for the finite element solution:

$$a = 100, \quad t = 5, \quad E = 2 \times 10^6, \quad v = 0.25, \quad q = 2.$$

Table 2.1. Deflections and moments in a circular plate simply supported around the periphery and subjected to a uniform pressure.

The second step was to adopt a boundary condition representing the case in hand, i.e. simply supported at two points at opposite ends of a diameter. Using the finite element results provides an independent method from the "closed form" theoretical solutions of 2.3.1. and also allows the production of design coefficient tables.

The use of these coefficients is valid when the plate is to be considered as a stiff plate which is also a thin plate, i.e. $t/2a < 1/8$ with flexural rigidity, carrying loads two-dimensionally mostly by internal (bending and torsional) moments and by transverse shears, as in Fig. (2.1).

Deflections can be assumed to be a function of the uniformly distributed load q , the flexural rigidity of the plate per unit length being expressed in the usual notation by

$$D = \frac{Et^3}{12(1-\nu^2)} \quad 2.79$$

and a^4 (a being the radius) in the following form:-

$$w = C_1 \frac{qa^4}{D} \quad 2.80$$

Similarly the bending moments per unit length can be written as:-

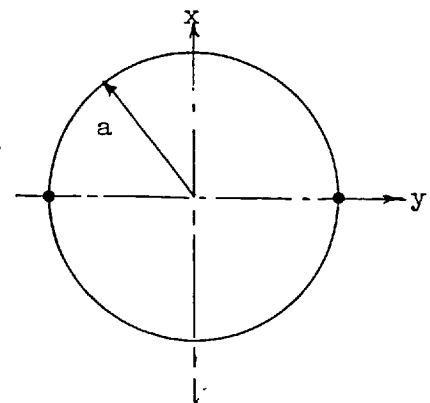
$$M_x = C_2 q a^2 \quad 2.81$$

$$M_y = C_3 q a^2 \quad 2.82$$

$$M_{xy} = C_4 q a^2 \quad 2.83$$

A table of coefficients C_1 to C_4 at the 12 locations as indicated in Tables (2.2) and (2.3) can then be produced.

Element No.	Location		C_2	C_3	C_4
	x.a	y.a			
1	0.95	0.062	+0.0004	-0.3667	+0.0142
2	0.85	0.055	+0.0014	-0.3882	+0.0165
18	0.788	0.527	-0.2835	+0.0018	-0.1280
22	0.495	0.3675	+0.0351	-0.3835	+0.1088
27	0.45	0.05	+0.0422	-0.4649	-0.0076
35	0.5998	0.7128	-0.1228	-0.0745	-0.25
53	0.252	0.55	+0.1743	-0.3905	-0.0767
57	0.30475	0.8977	+0.1154	-0.0424	-0.2522
70	0.05	0.05	+0.0844	-0.5031	-0.0011
75	0.05	0.55	+0.2335	-0.4087	-0.0174
79	0.025	0.875	+0.6334	-0.2192	-0.0724



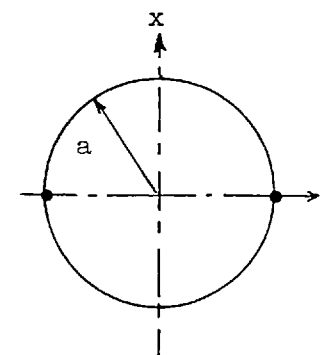
Symmetrical around x & y

$$v = 0.378$$

$$M = C q a^2$$

Table: 2.2. Moments design coefficients for circular plate simply supported on two points at opposite ends of a diameter and subjected to a uniform pressure obtained from finite element method.

F.E. Node No.	Location		C_1	C_1
	x/a	y/a	From F.E.	From Equat.
1	1.0	0.0	0.43767	0.43948
2	0.9	0.0	0.41438	0.41596
6	0.8	0.0	0.39277	0.39420
19	0.866	0.5	0.35216	0.35346
28	0.707	0.707	0.2582	0.25786
29	0.5	0.0	0.3395	0.35638
32	0.5	0.3	0.3150	0.322487
56	0.3	0.5	0.2427	0.22729
80	1.0	0.5	0.2265	0.226427
85	0.0588	0.898	0.0585	0.06
87	0.0	0.0	0.30195	0.30245
92	0.0	0.5	0.2245	0.224809



Symmetrical around
x & y

$$v = 0.378$$

$$w = C_1 \frac{qa^4}{D}$$

Table: 2.3. Comparison of deflection coefficients obtained by the 'closed-form' equation and finite element in circular plate simply supported on two points at opposite ends of a diameter and subjected to a uniform pressure.

The accuracy of the coefficients is directly dependent on the degree of refinement of the finite element mesh, i.e. the number of degrees of freedom in the considered plate. For this purpose, a number of meshes were used with increasing numbers of degrees of freedom until no significant change occurred to the resulting coefficients. This asymptotic convergence is an established procedure in finite element solutions.

Thus in the solution E is extracted from the answers through the flexural rigidity D as described above. The deflections and bending moments (M_x , M_y , M_{xy}) can be worked out using the coefficients for a specific value of say ν_1 . Then the effects of another Poisson's ratio ν_2 can be estimated from:- Szilard Ref. (31).

$$w_2(x,y) \approx \frac{1-\nu_2^2}{1-\nu_1^2} w_1(x,y) \quad 2.84$$

$$(M_x)_2 \approx \frac{1}{1-\nu_1^2} \left[(1-\nu_1\nu_2)(M_x)_1 + (\nu_2-\nu_1)(M_y)_1 \right] \quad 2.85$$

$$(M_y)_2 \approx \frac{1}{1-\nu_1^2} \left[(\nu_2-\nu_1)(M_x)_1 + (1-\nu_1\nu_2)(M_y)_1 \right] \quad 2.86$$

$$(M_{xy})_2 = \frac{1-\nu_2^2}{1-\nu_1^2} (M_{xy})_1 \quad 2.87$$

This case was run using a typical plate having values of $E = 0.46 \times 10^6$ lb/in² and $\nu = 0.378$, $a = 12$ in. The coefficients for deflections at twelve nodes are compared with the coefficients from Appendix (1) in Table (2.3). The coefficients for moments are compared in Table (2.4), the conversion from local x-y coordinates of the finite element mesh to global polar coordinates being described in Appendix (4).

The practical application of these coefficients is in day-to-day work, since they provide a reliable and simple technique for calculating deflections. In fact, they can predict to within 10% the measured deflections obtained in testing valves. However, it is not a good method for calculating the stresses especially in the vicinity of the support, because in reality the point support is a hypothetical point and can not be simulated in tests. Mathematically the coefficients obtained from the finite element solution would be a more accurate simulation of a point support for the stresses.

Element No.	Location		C_2 F.E.	C_2 Equ.	C_3 F.E.	C_3 Equ.	C_4 F.E.	C_4 Equ.
	x/a	y/a						
1	0.946	0.054	+0.0004	+0.000	-0.3667	0.39	+0.0142	0.00
2	0.846	0.056	+0.0014	+0.004	-0.3882	-0.40	+0.0165	0.00
18	0.788	0.527	-0.2835	-0.32	+0.0018	0.0018	-0.1280	-0.10
27	0.450	0.050	+0.0422	0.043	-0.4649	-0.467	-0.0076	-0.033
70	0.05	0.05	0.294	0.21	0.294	0.21	0.252	0.2935
75	0.05	0.55	+0.2334	0.24	-0.4087	-0.4087	-0.0174	0.0

Table: 2.4. Comparison of moments coefficients obtained by the 'closed-form' equation and finite element in circular plate simply supported on two points at opposite ends of a diameter and subjected to a uniform pressure.

2.4. The Solution for Stresses and Deflections in a Circular Plate of Uniform Thickness subjected to a Uniform Normal Pressure and supported along two short lengths of Arc at two opposite ends of a Diameter.

2.4.1. Introduction

This idealisation, shown in Fig. (2.8a), is a more practical one as the shafts occupy a short length of the periphery of any blade. This becomes significant when the valve is used for regulating the flow and the torque loads are significant. This removes the singularity at the support of 2.3. and enables the calculation of the stresses and deflections at any point, including the points of attachment.

2.4.2. Analytical Work

The same analytical work done in 2.3.1. applies, from Figs. (2.8a) and (2.8b). The boundary conditions would be:

- (i) At the boundary of the disc the radial bending moment is zero. Thus the work up to Equation (2.32) is applicable.
- (ii) At the supports the deflections are zero at two points given by:-

$$\theta = \alpha \text{ and } \theta = \pi - \alpha$$

Putting $\theta = \alpha$, $\rho = 1$ and using Equation (2.31) in Equation (2.28) there results:-

$$A_0 + A_1 \cos \alpha + \sum_{n=2,3}^{\infty} (A_n + B_n) \cos n\theta = 0 \quad 2.88$$

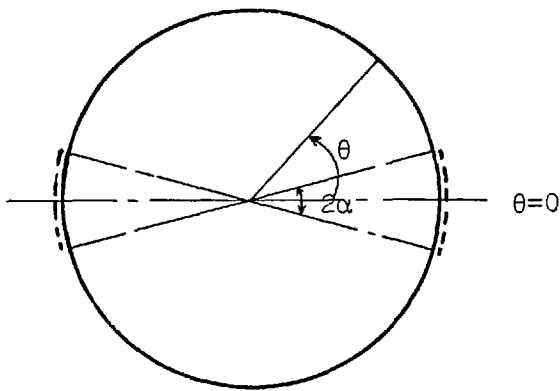


Fig. 2.8a. Plate simply supported on two arcs.

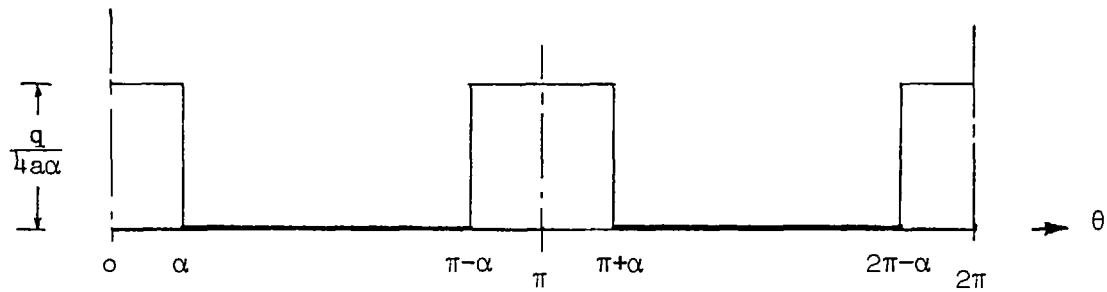


Fig. 2.8b. Reactive forces on plate simply supported on two arcs and subjected to uniform pressure.

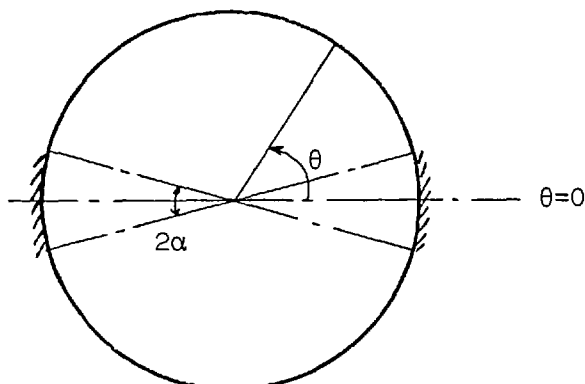


Fig. 2.8c. Plate supported on two clamped arcs.

Putting $\theta = \pi - \alpha$, $\rho = 1$ and using Equation (2.31)

with Equation (2.28) gives:-

$$A_0 = A_1 \cos \alpha + \sum_{n=2,3}^{\infty} (A_n + B_n) \cos n\alpha \cos n\pi = 0 \quad 2.89$$

Solving Equation (2.22) and Equation (2.93) with

$$\cos n\pi = +1 \text{ (for even } n\text{)}$$

$$\cos n\pi = -1 \text{ (for odd } n\text{)}$$

gives

$$A_0 = - \sum_{n=2,4}^{\infty} (A_n + B_n) \cos n\alpha \quad 2.90$$

And

$$A_1 \cos n\alpha = - \sum_{n=3,5}^{\infty} (A_n + B_n) \cos n\alpha \quad 2.91$$

- (iii) The intensity of the reactive forces on the boundary
can be expressed by a fourier expansion, see Fig. (2.8b)

$$\begin{aligned} (v_r)_{\rho=1} &= \frac{-R}{a} \left[\frac{1}{2} + \sum_{n=2,4}^{\infty} \left(\frac{\sin n\alpha}{n\alpha} \right) \cos n\theta \right] \\ &= -qa \left[\frac{1}{2} + \sum_{n=2,4}^{\infty} \left(\frac{\sin n\alpha}{n\alpha} \right) \cos n\theta \right] \end{aligned} \quad 2.92$$

This is equal to Equation (2.39) and proceeding
similarly using Equations (2.40) to (2.56) leads to:

$$\begin{aligned} (v_r)_{\rho=1} &= -qa \left\langle \frac{1}{2} + \sum_{n=2,3}^{\infty} \left\{ \begin{array}{l} -n^2(n-1)(1-v) A_n \\ + n(n+1) [(4-n)(1-v)] B_n \end{array} \right\} \cos n\theta \right\rangle_{\rho=1} \end{aligned} \quad 2.93$$

Equating the coefficients of $\cos n\theta$ in Equation (2.91)
and Equation (2.97) gives:

$$-n^2(n-1)(1-v) A_n + n(n+1) \left[\frac{1}{4-n} (1-v) \right] B_n = \frac{\sin n\alpha}{n\alpha} \quad \text{for } n = 2, 4, \dots \quad 2.94$$

$$-n^2(n-1)(1-v) A_n + n(n+1) \left[\frac{1}{4-n} (1-v) \right] B_n = 0 \quad \text{for } n = 3, 5 \quad 2.95$$

The constants A_n & B_n are determined, as follows:-

Solving Equation (2.32) and Equation (2.95) gives

$$A_n = B_n = 0 \quad \text{for } n = 3, 5, 7$$

Applying this in Equation (2.91) leads to

$$A_1 = 0$$

Solving Equation (2.32) and Equation (2.94) gives:

$$A_n = \frac{-(n+2/\beta) (\sin n\alpha/n\alpha)}{2n^2(n-1) (3+v)} \quad 2.96$$

$$B_n = \frac{\sin n\alpha/n\alpha}{2n(n+1) (3+v)} \quad 2.97$$

$$A_n + B_n = \frac{-\sin n\alpha}{2(3+v)n\alpha} \left[\frac{1}{n(n^2-1)} + \frac{2}{\beta n^2(n-1)} - \frac{1}{n(n+1)} \right] \quad 2.98$$

Equations (2.96, 2.97, 2.98) are for $n = 2, 4, 6, \dots$ etc

Using Equation (2.98) in Equation (2.90) gives

$$A_0 = \frac{1}{2(3+v)} \sum_{n=2,4}^{\infty} \left(\frac{\sin n\alpha}{n\alpha} \right) \left\{ \frac{1}{n(n-1)} + \frac{2}{\beta n^2(n+1)} - \frac{1}{n(n+1)} \right\} \cos n\alpha \quad 2.99$$

Proceeding with the solution as in 2.3.1 we obtain similar equations as follows:

$$W = \frac{qa^4}{64D} \left\langle (1-\rho^2) \left(\frac{5+v}{1+v} - \rho^2 \right) + \frac{1}{2\alpha(3+v)} \left[\sum_{n=2,4}^{\infty} \left(\frac{\sin n\alpha}{n} \right) \right. \right. \\ \left. \left. \left\{ \frac{1}{n(n-1)} + \frac{2}{\beta n^2(n-1)} - \frac{1}{n(n+1)} \right\} \cos n\alpha - \sum_{n=2,4}^{\infty} \left(\frac{\sin n\alpha}{n} \right) \right. \right. \\ \left. \left. \left\{ \frac{1}{n(n-1)} + \frac{2}{\beta n^2(n-1)} - \frac{\rho^2}{n(n+1)} \right\} \rho^n \cos n\theta \right] \right\rangle \quad 2.100$$

$$M_r = qa^2 \left\langle \frac{1}{16} (3+v)(1-\rho^2) + \frac{1}{2\alpha} \left(\frac{1+v}{3+v} \right) \sum_{n=2,4}^{\infty} \left(\frac{\sin n\alpha}{n} \right) \right. \\ \left. (\beta + \frac{2}{n})(1-\rho^2) \rho^{n-2} \cos n\theta \right\rangle \quad 2.101$$

$$M_t = qa^2 \left\langle \frac{1}{16} \left[(3+v) - (1+3v)\rho^2 \right] - \frac{1}{2\alpha} \left(\frac{1+v}{3+v} \right) \sum_{n=2,4}^{\infty} \left(\frac{\sin n\alpha}{n} \right) \right. \\ \left. \left\{ \beta(1-\rho^2) + \frac{2}{n}(1+\rho^2) \right\} \rho^{n-2} \cos n\theta \right\rangle \quad 2.102$$

$$M_{rt} = \frac{qa^2}{2\alpha} \left(\frac{1+v}{3+v} \right) \sum_{n=2,4}^{\infty} \left(\frac{\sin n\alpha}{n} \right) \left\{ \beta(1-\rho^2) + \frac{2}{n} \right\} \rho^{n-2} \sin n \quad 2.103$$

These equations were written in two small computer programs similar to those of 2.3.1. to produce hand tables of coefficients for deflections and moments. The program for the generation of the tables is listed in Appendix (2.C) and the relevant parts of the tables are given as a sample in Appendix (3).

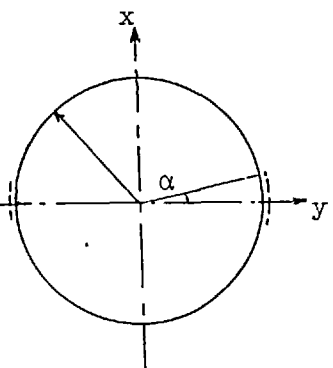
2.4.3. Finite Element Analysis

The same mesh as used in 2.3.2. of Fig. (2.7) was used to simulate a boundary condition of simply supported arc of angle $\alpha = 7.5^\circ$ by restraining nodes nos. 74, 86, 98, 110 and 122 in the z direction only and following the same procedure adopted in 2.3.2.. Similar coefficients were obtained. The coefficients for deflections at 12 locations are given in Table (2.5) compared with the equivalent ones obtained from Appendix (3). The coefficients for moments were obtained at 11 locations and are shown in Table (2.6). The coefficients for moments are compared with the equivalent ones obtained from Appendix (3) in Table (2.7). For comparing more coefficients the conversion from local x,y coordinates of the finite element mesh to the global polar coordinates must be observed as described in Appendix (4).

From this a method of simulating real boundary conditions and providing a more accurate value for the deflections and stresses is clearly possible using the finite element model. In this way coefficients can be obtained for cases which are very difficult or impossible to simulate mathematically such as:-

- (i) Plates simply supported on two short lengths of arc and subjected to point load acting at a specified point. Table (2.8a).and (2.8b).
- (ii) Plates which are clamped on a short length of arc at two opposite ends of a diameter Fig. (2.8c). and subjected to:

F.E. Note No.	Location		C_1 From F.E.	C_1 From Equat.
	x/a	y/a		
1	1.0	0.0	0.3715	0.403225
2	0.9	0.0	0.3509	0.381545
6	0.8	0.0	0.3318	0.361462
19	0.866	0.5	0.2915	0.320969
28	0.707	0.707	0.2043	0.229868
29	0.5	0.0	0.2856	0.311838
32	0.5	0.3	0.2625	0.290845
56	0.3	0.5	0.1976	0.212901
80	1.0	0.5	0.185	0.201193
85	0.0588	0.898	0.0415	0.045
87	0.0	0.0	0.2535	0.28376
92	0.0	0.5	0.1834	0.21253



Symmetrical around
x & y

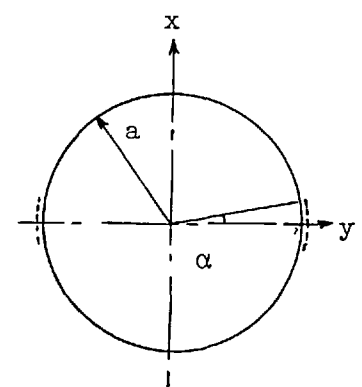
$$\alpha = 7.5^\circ$$

$$v = 0.378$$

$$w = C_1 \frac{qa^4}{D}$$

Table: 2.5. Comparison of deflection coefficients obtained by 'closed-form' equation and finite element in circular plates simply supported on two short lengths of arcs at opposite ends of a diameter and subjected to a uniform pressure.

F.E. Node No.	Location		C_2	C_3	C_4
	x/a	y/a			
1	0.95	0.062	-0.0002	-0.3543	+0.0141
2	0.85	0.055	-0.0008	-0.3745	+0.0163
18	0.7865	0.527	-0.2667	+0.0007	-0.1215
22	0.495	0.3675	+0.0229	-0.3607	+0.1097
27	0.45	0.05	+0.0261	-0.4416	0.0057
35	0.5988	0.7128	-0.0877	-0.0710	-0.2468
53	0.252	0.55	+0.1468	-0.3534	-0.0392
57	0.30475	0.8977	+0.2498	-0.0694	-0.2234
70	0.05	0.05	+0.0515	-0.4697	-0.0007
75	0.05	0.55	+0.1480	-0.3536	-0.0048
79	0.025	0.875	+0.0760	-0.0544	+0.0482



Symmetrical around
x & y

$$\alpha = 0.75^\circ$$

$$v = 0.378$$

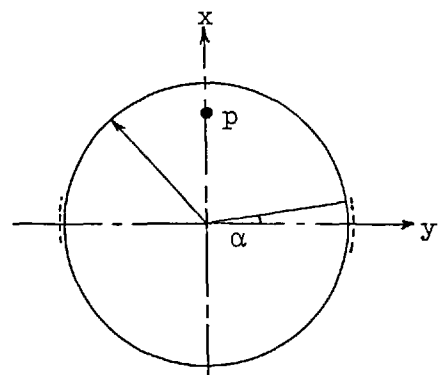
$$M = C q a^2$$

Table: 2.6. Moments design coefficients for circular plate simply supported on two short lengths of arcs at opposite ends of a diameter and subjected to uniform pressure obtained from finite element method.

Element No.	Location		C_2 F.E.	C_2 Equ.	C_3 F.E.	C_3 Equ.	C_4 F.E.	C_4 Equ.
	x/a	y/a						
1	0.946	0.054	0.003	0.008	-0.35	-0.658	0.03	0.0
18	0.788	0.527	0.031	0.03	0.294	0.0861	0.179	0.190
27	0.45	0.05	0.434	0.401	-0.02	-0.149	0.057	0.003
41	0.35	0.35	0.133	0.123	0.2044	0.233	0.240	0.264
70	0.05	0.05	0.211	0.2064	0.211	0.209	0.261	0.295
75	0.05	0.55	-0.153	-0.0279	0.323	0.449	0.050	0.0

Table: 2.7. Comparison of moments coefficients obtained by the 'closed-form' equation and finite element in circular plate simply supported on two short lengths of arcs at opposite ends of a diameter and subjected to a uniform pressure.

F.E. Node No.	Location		C_1
	x/a	y/a	
1	- 1.0	0.0	- 0.47975
2	- 0.9	0.0	- 0.43435
6	- 0.8	0.0	- 0.39045
19	- 0.866	0.5	- 0.3605
29	- 0.5	0.0	- 0.2668
32	- 0.5	0.3	- 0.2471
56	- 0.3	0.5	- 0.15095
85	- 0.0588	0.898	- 2.117
87	- 0.0	0.0	- 0.11275
109	0.0588	0.898	- 0.01485
128	0.3	0.5	- 0.0291
146	0.5	0.0	- 0.01175
149	0.5	0.3	- 0.06735
174	0.8	0.0	0.0372
182	0.9914	0.13	0.0671
184	1.0	0.0	0.0679



Symmetrical around x-axis

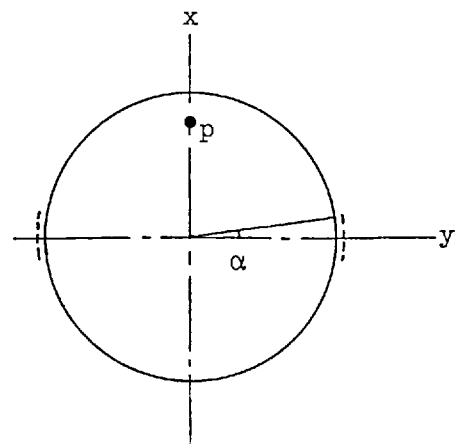
p at 0.8a

$\alpha = 7.5^\circ$

$$W = C_1 \frac{qa^4}{D}$$

Table: 2.8a. Coefficients for deflections in circular plates simply supported on two short lengths of arcs at opposite ends of a diameter due to point load at the shown location.

Element No.	Location		C_2	C_3	C_4
	x/a	y/a			
1	0.95	0.062	-0.0256	-0.473	+0.0196
2	0.85	0.055	-0.1086	-0.5193	+0.0057
18	0.788	0.527	-0.1058	+0.0021	-0.1446
22	0.495	0.3675	+0.0555	-0.1814	+0.1636
27	0.45	0.05	+0.2304	-0.3278	+0.0112
35	0.5998	0.7128	+0.1522	-0.0363	-0.1994
53	0.252	0.55	+0.2503	-0.1719	+0.1005
57	0.3047	0.8977	+0.4888	-0.0688	-0.1348
70	0.05	0.05	+0.1263	-0.1979	+0.0121
75	0.05	0.55	+0.1641	-0.1335	+0.1449
79	0.025	0.875	+0.1338	-0.0011	+0.3485
90	-0.025	0.875	-0.0185	-0.0068	+0.301
124	-0.45	0.05	+0.0391	-0.0924	+0.0068
137	-0.495	0.3675	+0.0272	-0.0784	+0.0014
142	-0.5998	0.7128	-0.0261	-0.0594	-0.0371
160	-0.95	0.062	+0.0161	-0.051	-0.0008



Symmetrical around x-axis

p at $0.8a$

$\alpha = 7.5^\circ$

$M = C_p$

Table: 2.8b. Coefficients for moments in circular plates simply supported on two short lengths of arcs at opposite ends of a diameter due to point load at the shown location.

- (a) Hydrostatic load (which is a very important case occurring during the use of the valve for throttling in large valves).
 - (b) Point load acting at a point perpendicular to the shaft line (which is used to unseat the valve with a screw) an example being given in Table (2.9).
 - (c) The all important uniform pressure. Table (2.10) and (2.11).
- (iii) Plates which are supported on clamped or simply supported arcs plus short length of the diameter in simple or clamped manner as shown in Fig. (2.9) subjected to loading conditions (a), (b) & (c) above. A sample is given in Table (2.12a), (2.12b) and (2.12c).
- (iv) Plates which have a non-circular configuration generally, in this application the elliptical blades of butterfly valves.

2.5. Experimental Work

Although the two theoretical approaches which have been discussed are sound, since the problem has been solved independently by closed-form mathematical solutions and by finite element methods, it was felt that experimental work was necessary as a confirmation especially in the cases where it was not possible to check the finite element solutions by "closed-form" mathematical solutions. A number of experiments was carried out and this section which follows is to describe the procedure and give a sample result for a plate supported on two short arcs at opposite ends of a diameter.

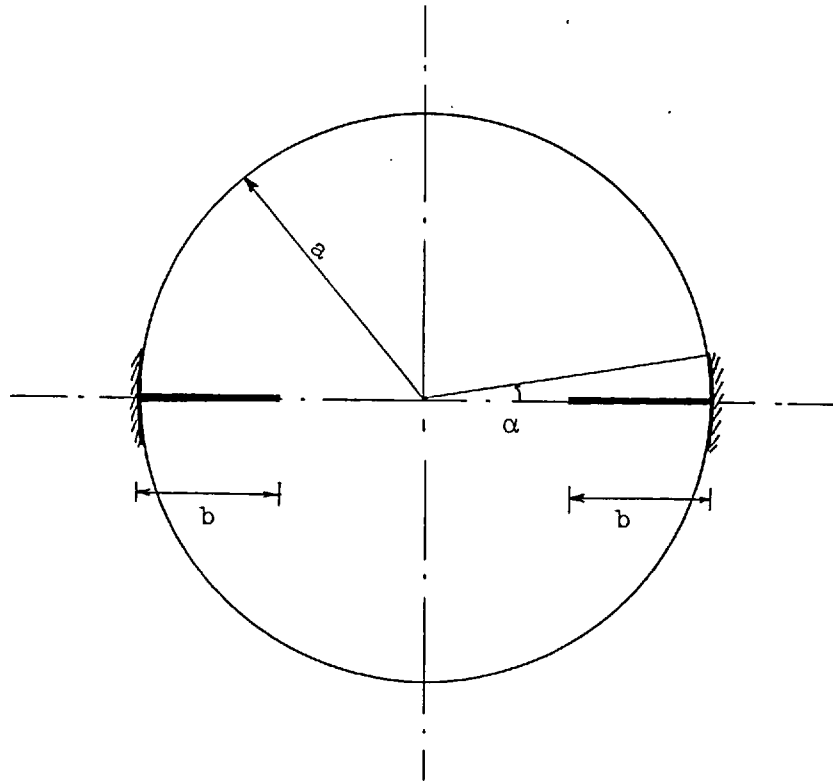
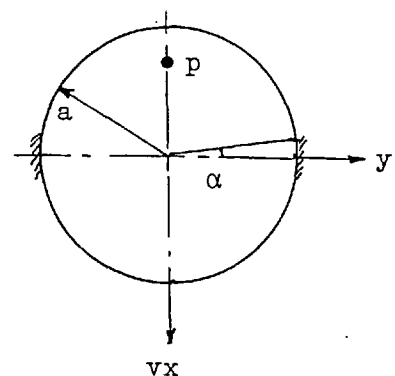


Fig. 2.9. Plate supported on two short lengths of arc and short lengths of diameter

F.E. Node No.	Location		C_1
	x/a	y/a	
1	- 1.0	0.0	0.33
2	- 0.9	0.0	0.294
6	- 0.8	0.0	0.2592
19	- 0.866	0.5	0.2362
29	- 0.5	0.0	0.16045
32	- 0.5	0.3	0.14615
56	- 0.3	0.5	0.0753
85	- 0.0588	0.898	0.00025
87	- 0.0	0.0	0.04155
109	0.0588	0.898	0.0001
128	0.3	0.5	- 0.00965
146	0.5	0.0	- 0.03055
149	0.5	0.3	- 0.0309
174	0.8	0.0	- 0.0661
182	0.9914	0.13	- 0.08825
184	1.0	0.0	- 0.08945



Symmetrical around x

$$w = C_1 \frac{Pa^2}{D}$$

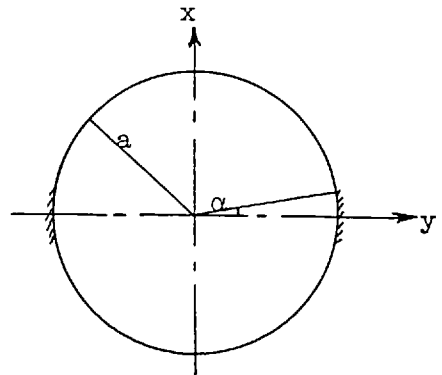
$$\alpha = 7.5^\circ$$

$$v = 0.378$$

$$p \text{ at } 0.8a$$

Table: 2.9. Coefficients for deflection in circular plates clamped on two short lengths of arcs at opposite ends of a diameter due to point load at the shown location.

F.E. Node No.	Location		C_1
	x/a	y/a	
1	1.0	0.0	0.1744
2	0.9	0.0	0.1606
6	0.8	0.0	0.1475
19	0.866	0.5	0.1300
28	0.707	0.707	0.0834
29	0.5	0.0	0.1143
32	0.5	0.3	0.1029
56	0.3	0.5	0.0659
80	1.0	0.5	0.0560
85	0.0588	0.898	0.0041
87	0.0	0.0	0.0896
92	0.0	0.5	0.5474



Symmetrical around
x & y axies.

$$W = C_1 \frac{qa^4}{D}$$

$$\alpha = 7.5^\circ$$

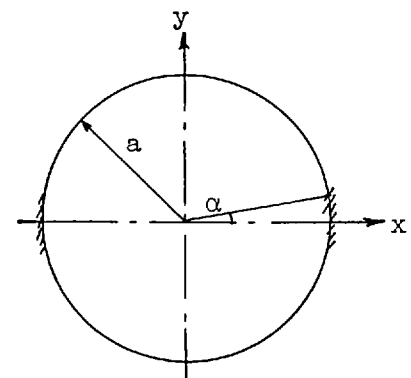
$$v = 0.378$$

Table: 2.10 Coefficients for the deflection in circular plate supported on two clamped short lengths of arc at opposite ends of a diameter and subjected to a uniform pressure.

Element No.	Location		C_2	C_3	C_4
	x/a	y/a			
1	0.95	0.062	-0.0003	-0.1789	+0.0077
2	0.85	0.055	+0.0007	-0.1873	+0.0086
18	0.788	0.527	-0.1002	+0.0011	-0.0597
22	0.495	0.3675	+0.0413	-0.1413	+0.0528
27	0.45	0.05	+0.0494	-0.2092	-0.0036
35	0.5988	0.7128	+0.0516	+0.0031	-0.0855
53	0.252	0.55	+0.1676	-0.0425	-0.0223
57	0.30475	0.8977	+0.3230	+0.0882	+0.0669
70	0.05	0.05	+0.1014	-0.2176	-0.0006
75	0.05	0.55	+0.2264	-0.0128	-0.0056
79	0.025	0.875	+0.3475	+0.5795	+0.0275

$$M_x = C_2 q a^2, \quad M_y = C_3 q a^2, \quad M_{xy} = C_4 q a^2$$

Table: 2.11. Coefficients for moments in circular plate supported on two clamped short lengths of arc at opposite ends of a diameter and subjected to a uniform pressure.

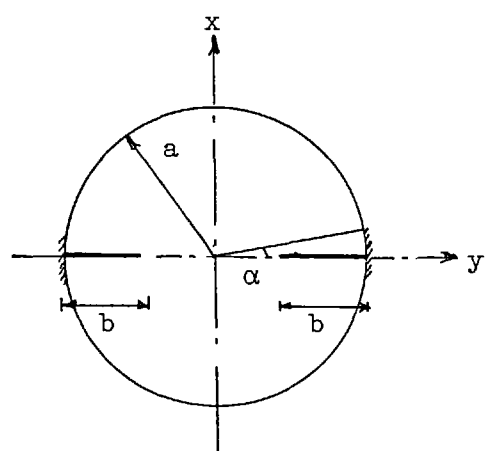


Symmetrical around
x & y axis

$$\alpha = 7.5^\circ$$

$$v = 0.378$$

F.E. Node No.	Location		C_1
	x/a	y/a	
1	1.0	0.0	- 0.1084
2	0.9	0.0	- 0.0963
6	0.8	0.0	- 0.0845
19	0.866	0.5	- 0.0299
28	0.707	0.707	- 0.0505
29	0.5	0.0	- 0.0528
32	0.5	0.3	- 0.0473
56	0.3	0.5	- 0.0213
80	1.0	0.5	- 0.0096
85	0.0588	0.898	- 0.0000
87	0.0	0.0	- 0.0266
92	0.0	0.5	- 0.0079



Symmetrical around x & y

$$b = \frac{2a}{3}$$

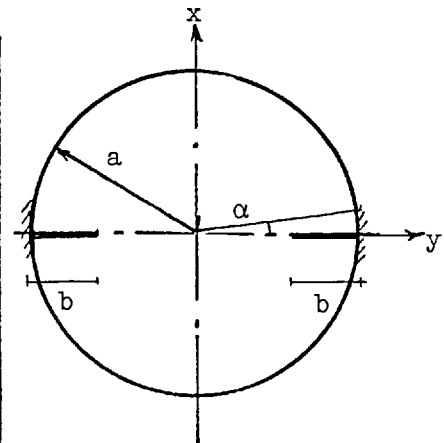
$$\nu = 0.378$$

$$\alpha = 7.5^\circ$$

$$w = C_1 \frac{qa^4}{D}$$

Table: 2.12a. Coefficients for deflections in circular plates supported on two clamped arcs at the end of the diameter and two short lengths of the diameter as shown and subjected to uniform pressure.

F.E. Node No.	Location		C_2	C_3	C_4
	x	y			
1	0.95	0.062	-0.0002	-0.0879	+0.0044
2	0.85	0.055	+0.0022	-0.09	+0.0047
18	0.788	0.527	-0.0248	+0.0012	-0.0311
22	0.495	0.3675	+0.0497	-0.0323	+0.0261
27	0.45	0.05	+0.075	-0.0847	-0.0032
35	0.5988	0.7128	+0.0863	+0.0143	-0.0302
53	0.252	0.55	+0.1772	+0.1190	-0.0053
57	0.30475	0.8977	+0.21	+0.0146	+0.0247
70	0.05	0.05	+0.1736	-0.0838	-0.0011
75	0.05	0.55	+0.4250	+0.2617	-0.0323
79	0.025	0.875	+0.0753	+0.0318	+0.0319



$$b = \frac{2a}{3}$$

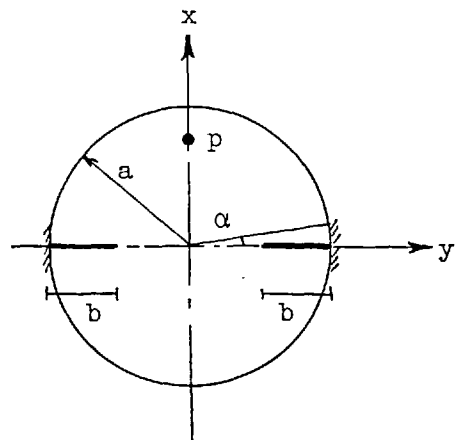
$$\nu = 0.378$$

$$\alpha = 7.5^\circ$$

$$M_x = C_2 qa^2, \quad M_y = C_3 qa^2, \quad M_{xy} = C_4 qa^2$$

Table: 2.12b. Coefficients for moments in circular plates supported on two clamped arcs at the end of the diameter and two short lengths of the diameter as shown and subjected to uniform pressure.

F.E. Node No.	Location		C_1
	x/a	y/a	
1	- 1.0	0.0	- 0.30065
2	- 0.9	0.0	- 0.2654
6	- 0.8	0.0	- 0.23115
19	- 0.866	0.5	- 0.2139
29	- 0.5	0.0	- 0.13305
32	- 0.5	0.3	- 0.12145
56	- 0.3	0.5	- 0.05545
85	- 0.0588	0.898	- 0.00095
87	- 0.0	0.0	- 0.01355
109	0.0588	0.898	0.00085
128	0.3	0.5	0.02945
146	0.5	0.0	0.05795
149	0.5	0.3	0.0556
174	0.8	0.0	0.0941
182	0.9914	0.13	0.11715
184	1.0	0.0	0.11875



Symmetrical around x-axis

$$b = \frac{2a}{3}$$

$$\alpha = 7.5^\circ$$

$$\nu = 0.378$$

$$P \text{ at } 0.8a$$

$$w = C_1 pa^2$$

Table: 2.12c. Coefficients for deflections in circular plates supported on two clamped arcs at the end of the diameter and two short lengths of the diameter as shown due to point load at the shown location.

2.5.1. Introduction

As the number of experimental tests required in this programme of checking was large, a great deal of consideration went into the design of the test arrangements, so as to simulate as many cases of loading as possible with minimum delays and maximum flexibility, to give as many cases of supporting conditions within the time available without damaging or replacing many samples.

A one inch thick 'perspex'* sheet simulating the blade was used because of ease of handling, availability and economy.

2.5.2. Four Point Bend Testing of a Perspex Beam

i Aims

- i.1 To determine the Young's modulus of perspex and Poisson's ratio.
- i.2 To examine the effect of creep on the properties of perspex.
- i.3 To assess the reliability of using strain gauges to measure strains in perspex.
- i.4 To determine the effect of low strain rates on the behaviour of perspex and to see whether it is possible to simulate the behaviour of a metal using perspex.

* 'Perspex' is a trade name for polymethylmethacrylate (p.m.m.a.)

ii The Test Beam

The dimensions of the perspex bar were as shown in Fig. (2.11) This was machined from a large sheet of 1 in. thick perspex and the rest of the sheet is being used to machine a circular diaphragm which will be used to simulate the blade of a large butterfly valve. (Fig. (2.19)).

All dimensions of the beam were accurate to within $\pm 1.0\%$

iii The Testing Equipment

The beam was supported on two mild steel rollers which were 10 ins. apart as shown in Fig. (2.13). These rollers were screwed on to a mild steel plate to prevent them from slipping. The load was applied to the beam through a load cell and another pair of rollers to give 4-point loading with a constant bending moment.

Two strain gauges (PL-10 made by Tokyo Sokki Kenkyoso Co. Ltd. (T.S.K. Ltd.) gauge resistance $120 \pm 0.3\Omega$, gauge length 10mm) were stuck longitudinally and another two perpendicular gauges to measure the transverse strain were stuck to each face of the centre of the beam as also shown in Fig. (2.12).

The adhesive used was CN Adhesive made by T.M.L. Ltd. of T.S.K. Ltd.

The load cell was used solely for applying the load to the metal plate. The load readings were obtained from the scale of the 60,000 lb. maximum capacity Avery testing machine used for the experiments. The scale used for these experiments was 0-3,000 lbs. with each small division being equal to 5-lbs.

The two longitudinal strain gauges were arranged in a half bridge and fed with 3.V through a Brüel and Kjaer strain gauge amplifier, type 1526. The output was fed back to the amplifier which indicated the total strain in 'micro strains'*

* Note:- 1 microstrain = 1×10^{-6} strain

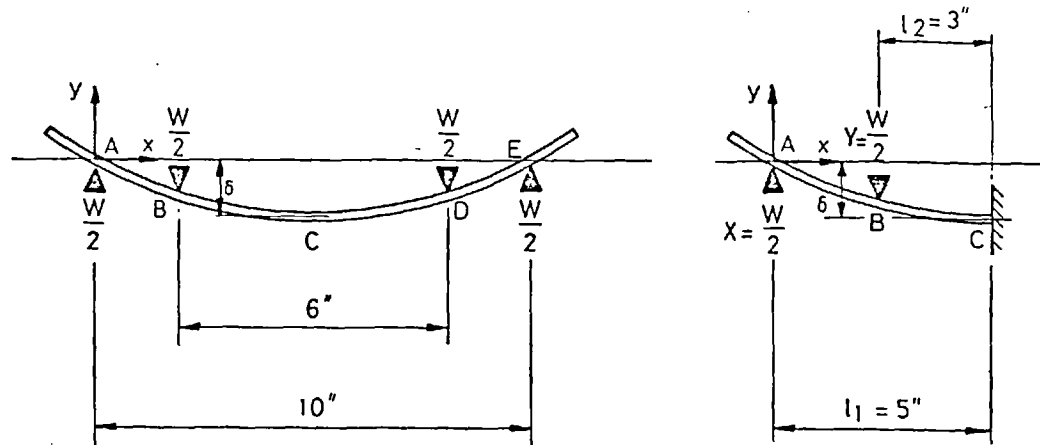


Fig. 2.10: Analysis of pure bending of a beam

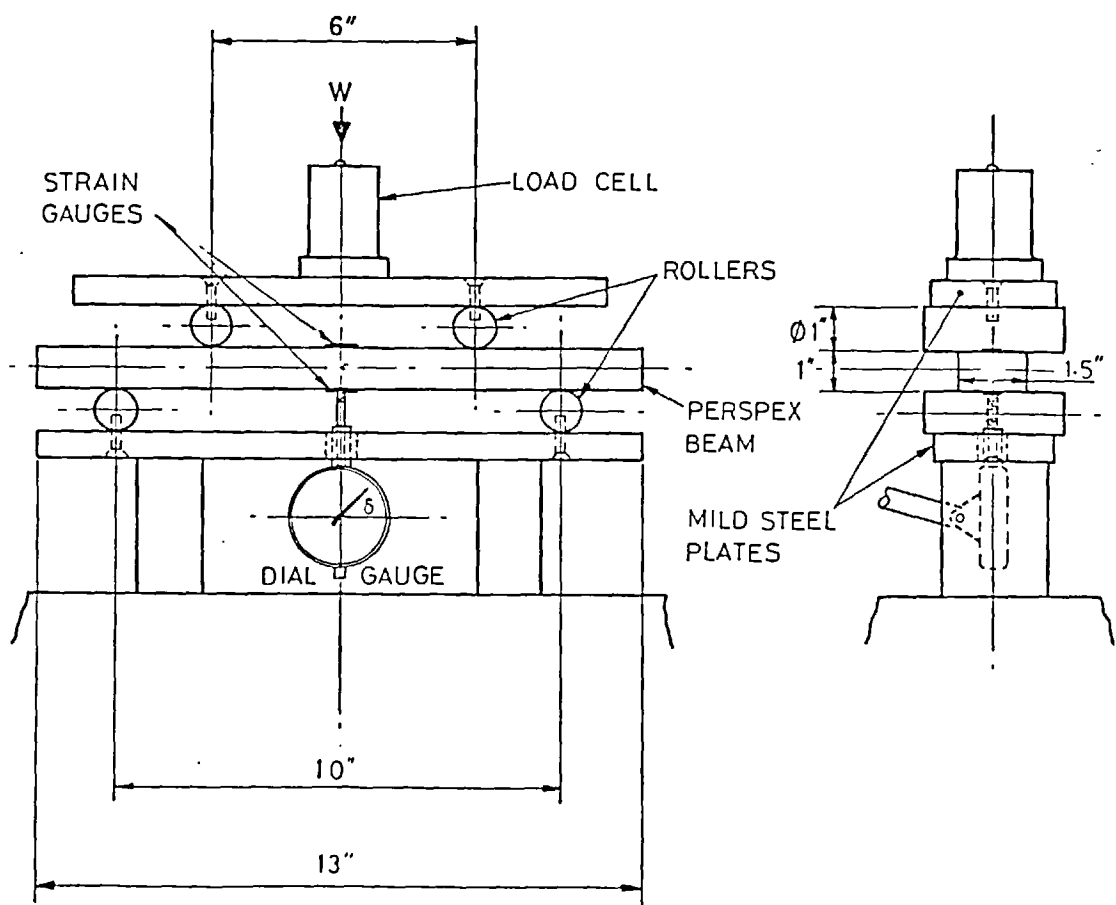


Fig. 2.11: 4-Point bend testing of a perspex beam



Fig. 2.12. 4-Point bend testing equipment

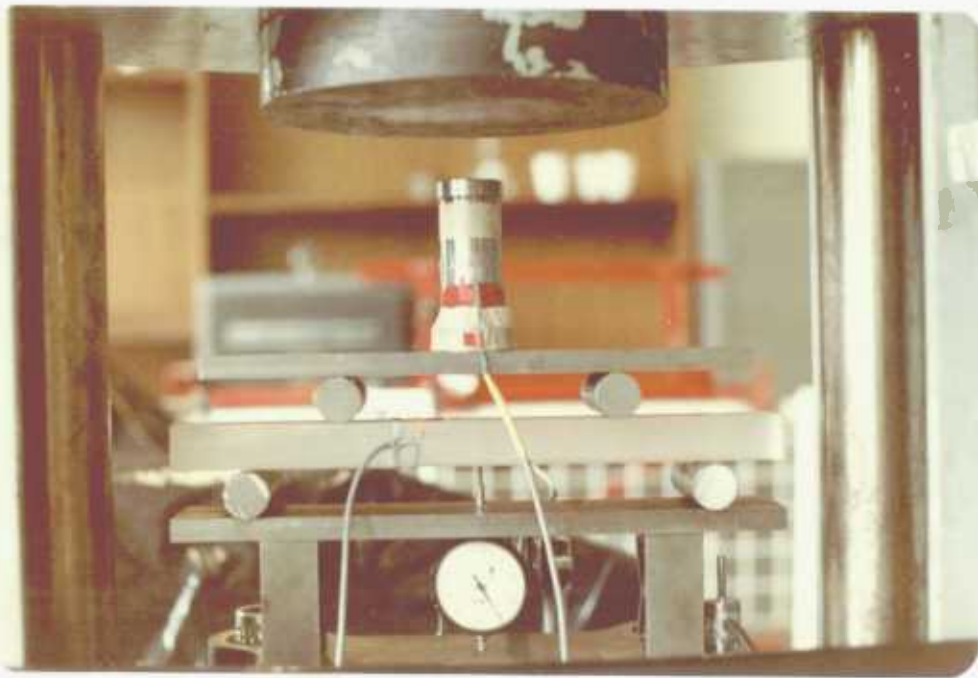


Fig. 2.13. 4-Point bend testing of a perspex beam

in a L.E.D. (Light Emitting Diode) display. (Although the gauge factor quoted by the manufacturer was 2.07, it was found that to obtain the theoretically correct readings on the display unit the gauge factor on the amplifier had to be set at 1.84 with the same arrangement for the two transverse strain gauges).

The deflection of the beam was measured by means of a 0.0001 in. smallest division dial gauge placed directly underneath the centre of the beam, as shown in Fig. (2.14).

iv Theory

From Fig. (2.10) it can be seen that the loading of the beam is equivalent to a cantilever subjected to two point loads. This similarity can be used to calculate the central deflection of the beam (δ) when it is subjected to a total load of W .

Therefore,

$$\begin{aligned} \delta &= \left[\frac{\frac{W}{2} x \frac{\ell^3}{1}}{3EI} \right] - \left[\frac{\frac{W}{2} x \frac{\ell^3}{2}}{3EI} + \frac{\frac{W}{2} \ell^2}{2EI} (\ell_1 - \ell_2) \right] \\ &= \frac{W}{EI} \left[\frac{\ell_1^3}{6} - \frac{\ell_2^3}{6} - \frac{\ell_2^2}{4} (\ell_1 - \ell_2) \right] \end{aligned} \quad 2.104$$

However, $\ell_1 = 5$ in. and $\ell_2 = 3$ in.

Therefore,

$$\delta = \frac{W}{EI} \left[\frac{125}{6} - \frac{27}{6} - \frac{18}{4} \right]$$

and

$$W = \frac{6EI}{71} \delta \quad 2.105$$

Referring to Fig. (2.10) the bending moment in the region BD is constant and is equal to $\frac{W}{2}$. $(\ell_1 - \ell_2)$ which is equal to W , if ℓ_1 and ℓ_2 are measured in inches.

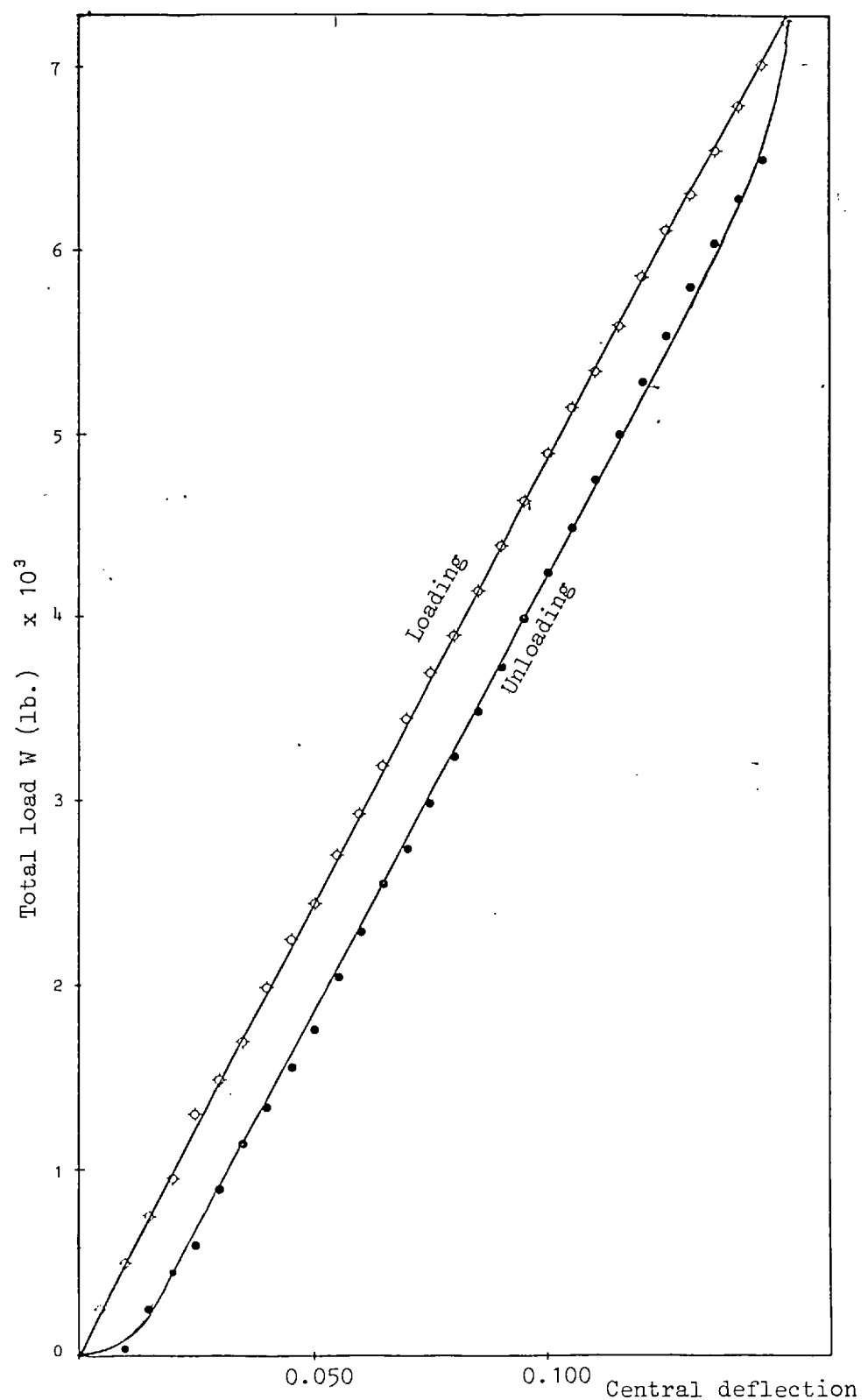


Fig. 2.14. A plot of total load vs central deflection

$$M = \frac{W}{2} (\ell_1 - \ell_2) = W \text{ (lbf.in. if } W \text{ is in lbf. for example)} \quad 2.106$$

Using

$$\frac{M}{I} = \frac{E}{R} = \frac{\sigma}{y} \quad 2.107$$

Where y is the distance from the neutral axis.

thus

$$\frac{W}{I} = \frac{E}{R} = \frac{\sigma_{\max}}{\frac{d}{2}}, \quad 2.108$$

at the surface of the beam where d is the depth of the beam.

$$\text{Therefore } \sigma_{\max} = \frac{Wd}{2\ell}$$

$$\text{However, } \epsilon_{\max} = \frac{\sigma_{\max}}{E}$$

$$\text{Therefore } \epsilon_{\max} = \frac{Wd}{2EI}$$

Substituting for $\frac{W}{EI}$ using Equation (2.105)

$$\epsilon_{\max} = \frac{3}{71} \delta \cdot d$$

However, $d = 1$ in.

$$\text{Therefore } \epsilon_{\max} = \frac{3\delta}{71} \text{ (if } \delta \text{ is in inches).} \quad 2.109$$

For the beam

$$I = \frac{1}{12} \times b \times d^3 \text{ in}^4 \quad 2.110$$

where b is the width and equals 1.5 ins. Hence

$$I = \frac{1}{12} \times 1.5 \times 1^3 \text{ in}^4 = 0.125 \text{ in}^4$$

v Experimental Procedure

The beam was loaded to a maximum deflection of 0.150 in. (assuming $\sigma_{\text{allowable}} = \sigma_{\text{yield}}$ for perspex is 3000 lbf./in² and E for perspex is 0.4×10^6 lbf./in²), $\epsilon_{\text{allowable}} = 0.0075$. Therefore δ_{max} , using Equation (2.109) is approximately 0.180 in. All tests were carried out at the very low speed of 12.5×10^{-3} in. central deflection/min. to avoid strain-rate effects (approximately equal to 500 μ -strain/min.). The load and the total strain were recorded at 0.005 in. intervals of the central deflection. Then, the beam was unloaded at the same speed and similar readings were taken. Figs. (2.14) and (2.15) show the results obtained.

The experiments were repeated at different speeds up to strain rates of .002/min., but no significant difference was observed. However, these results are not valid for suddenly applied loads. The error in such a case can be about $\pm 5\%$.

vi Calculations

Using the gradient of Fig. (2.14)

$$\frac{W}{\delta} = \frac{6EI}{71} = \frac{6}{71} E \times 0.125 = 4850$$

Therefore

$$E = 0.459 \times 10^6 \text{ lbf./in}^2$$

$$\text{The gradient of Fig. (2.15)} = \frac{\epsilon_{\text{max}}}{\delta} = 0.0424 \frac{1}{\text{in.}}$$

The theoretically correct gradient (from 2.109)

$$= \frac{3}{71} \frac{1}{\text{in.}} = 0.0423 \frac{1}{\text{in.}}$$

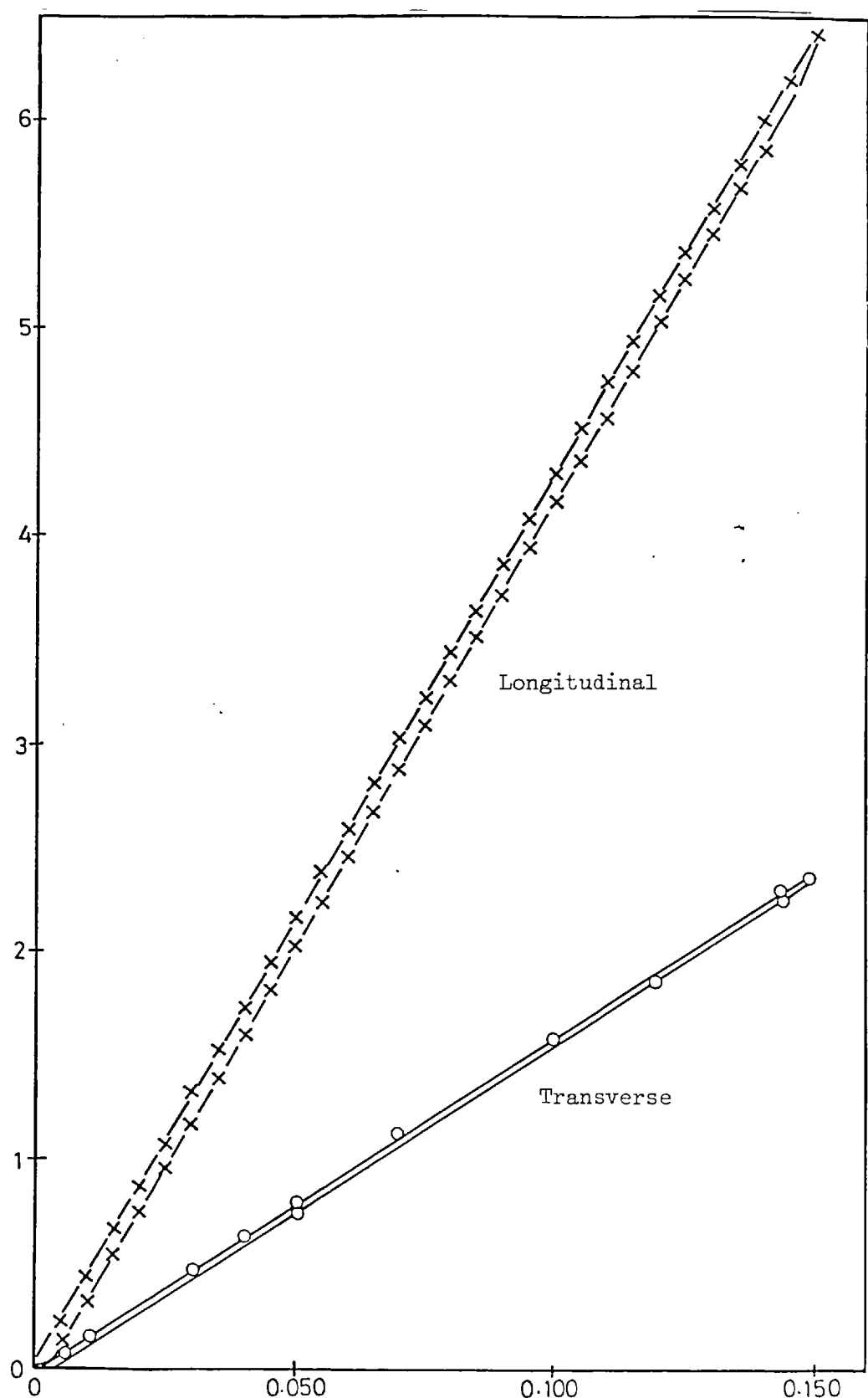


Fig. 2.15. A plot of strain vs. deflection at the centre.

Therefore the gauge factor should be set at 1.84.

The ratio between the transverse and longitudinal strains is Poisson's ratio and this was measured by taking the ratio of the gradients shown in Fig. (2.15).

vii Discussion and Conclusions

- (1) The Young's modulus of perspex is approximately 0.46×10^6 lbf./in².
- (2) The Poisson's ratio of perspex is approximately 0.378.
- (3) The experiments have shown that perspex creeps at room temperature.

Therefore, for comparing experimental results the readings have to be taken either instantaneously or after fixed time delays.

Provided this is remembered, perspex can be used to simulate metals or other elastic materials.

- (4) It is possible to stick strain gauges on perspex and obtain reliable results.
- (5) Perspex is not seriously affected by low strain rates - i.e. up to about .002/min. -. However, unlike metals, the sudden application of a load can lead to unreliable results, even if sufficient time is given to reach steady state conditions.

2.5.3. The Testing Equipment

To simulate a uniformly distributed pressure a $6\frac{3}{4}$ " length of 12" diameter pipe with 3/8" wall thickness was used as the basic pressure container. A $\frac{3}{4}$ " thick plate at the bottom and a $\frac{3}{4}$ ", 18" nominal diameter flange were welded to the pipe with a rubber O ring fitted at the upper side. Small pipes were welded to the bottom for air bleed, water drain, water or air inlet and a connection to the pressure gauge Fig. (2.16) and (2.28).

A 1" thick, 18" nominal diameter and 12" diameter flange was machined to fit on top of the pipe flange Fig. (2.17) and (2.20). Two short lengths of flange were provided to clamp the supports of the specimen in location as shown in Fig. (2.17) and (2.21). The whole assembly was bolted to a table 30" x 30" wide and 30" high from the ground, which can be levelled by screws fitted to its legs.

The frame was made up of $1\frac{1}{2}$ " steel angles and the top was made of 30" x 30" x $\frac{1}{2}$ " steel plate bolted to the angles. A 4" diameter hole was provided at the centre of the plate for the small pipes which come from the panel attached to the table. The panel carries a pressure gauge, air and water valves and regulator for the air supply Fig. (2.18) and (2.22).

The dial gauges (with 0.0001 in. division) could be placed over the sample to measure the deflection by fixing them to a three-legged frame which can stand above the diaphragm Fig. (2.22), (2.23) and (2.24). As the relative strength of the steel to the

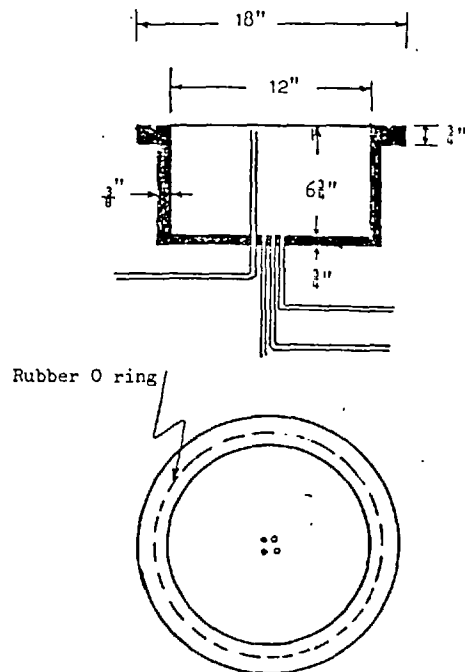


Fig. 2.16 Testing Equipment

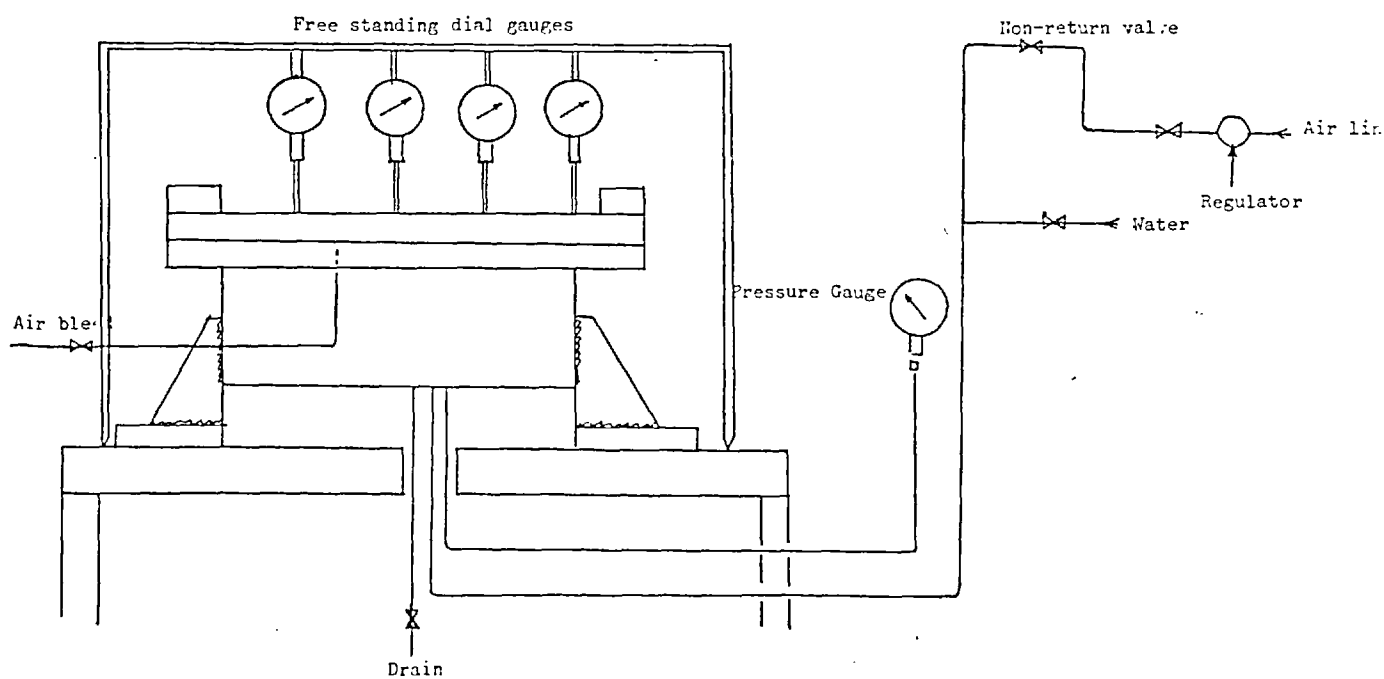


Fig. 2.18. Testing equipment and control panel

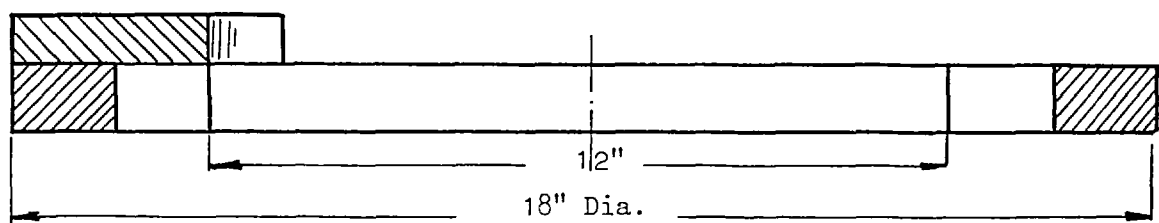
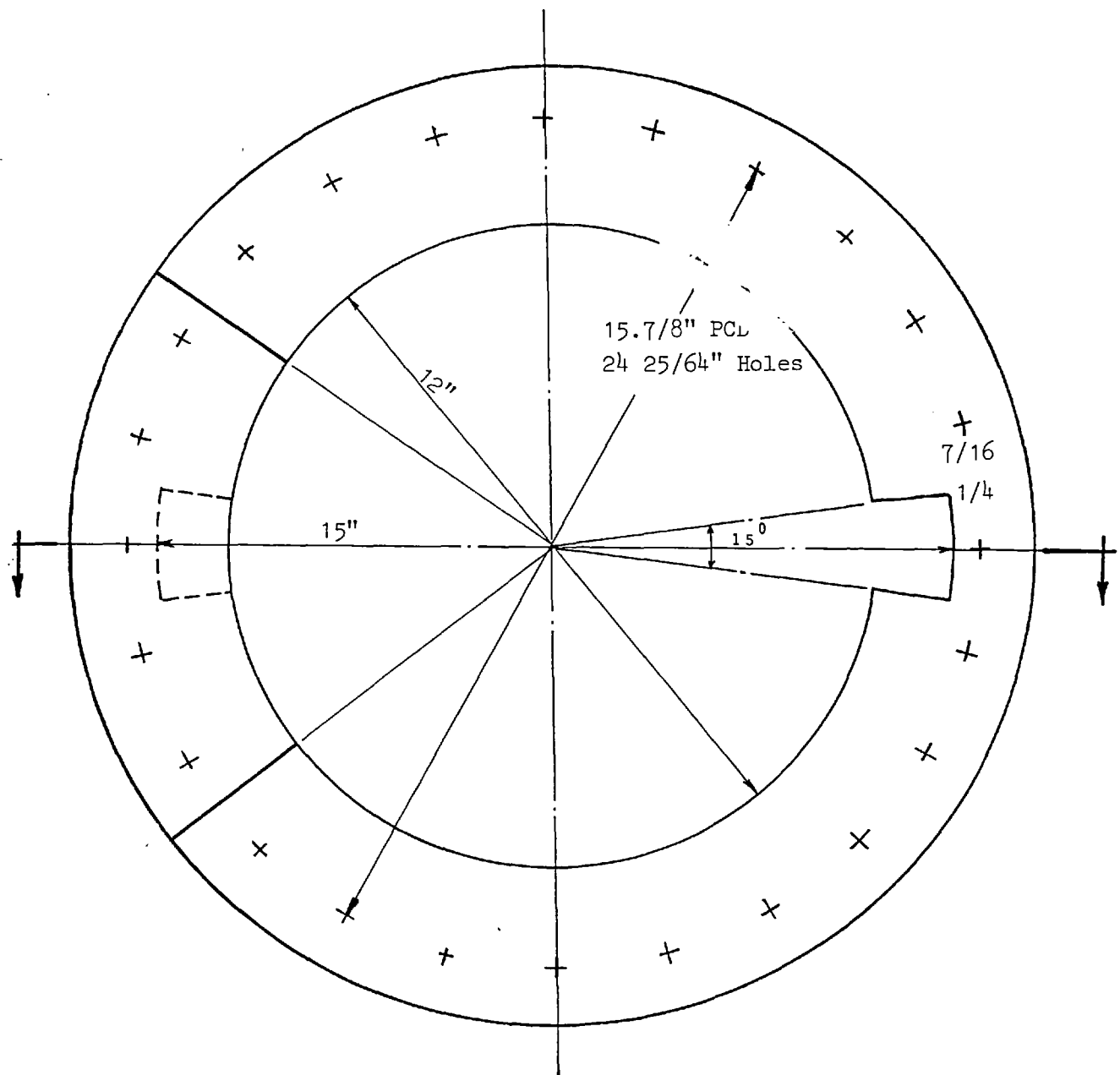


Fig. 2.17: Sample flange

perspex is high, there was no need to measure the uplift of the flange due to the pressure as it would be insignificant. This is not the case if the body and blade of a real valve are made from the same material.

The point load is applied through a calibrated load cell by turning a screw when it is attached to a frame which can be fixed to the flange of the rig as in Fig. (2.25), (2.26) and (2.27). The location of the load can be changed by turning the frame or using different holes in it.

The line support for a circular plate is provided by two short sharp-edged pieces of metal of known lengths attached to a plate which can be fitted to the two clamps at the support. The contact between the supports and the surface of the specimen can be controlled by the screws shown in Figs. (2.28) and (2.29).

Nine rosette strain gauges type FRA-6-11 made by T.S.K. Ltd. Gauge resistance $120 \pm 0.5 \Omega$, gauge length 6mm were stuck to the upper surface of the perspex plate as shown in Figs. (2.20) and (2.32). Another nine dummy gauges of the same type were stuck to a beam of perspex from the same sheet. Fig. (2.30). Each gauge and the corresponding dummy gauge was connected to a channel of two Brueiland and Kjaer switching units. An automatic selector, type 1542, which can switch from one gauge to the other at varying speeds down to 0.5 second and a twenty point panel type 1543 was connected to the other Fig. (2.31). This arrangement made it possible to read the 27 gauges in 13.5 seconds (to avoid creep effects).

The active gauge and the dummy one were arranged in a half bridge and fed with 3.0V. through a Brueiland and Kjaer strain gauge amplifier, type 1526. The output was fed back to the amplifier which indicated the total strain in micro strains on a L.E.D. display. Because of the speed of switching this had to be fed in to S & P twelve-twelve U.V. recorder. Fig. (2.33) shows a plot at two known strains which was obtained at the beginning to provide the scale. Fig. (2.34) shows a typical full-scale result. All gauges were balanced within ± 50 micro strains at the beginning of every experiment and a 'no-load' plot was obtained for corrections as shown on page

The results were converted into maximum and minimum principal stresses using the Mohr strain circle principle as in Fig. (2.35) where:-

$$x = \frac{\epsilon_x + \epsilon_y}{2}$$

$$y = \frac{\epsilon_x - \epsilon_y}{2}$$

$$z = x - \epsilon_{45}$$

$$R = \sqrt{y^2 + z^2}$$

$$\epsilon_1 = x + R$$

$$\epsilon_2 = x - R$$

and the principal stresses

$$\sigma_1 = \frac{E}{1-\nu^2} (\epsilon_1 + \nu \epsilon_2)$$

$$\sigma_2 = \frac{E}{1-\nu^2} (\epsilon_2 + \nu \epsilon_1)$$

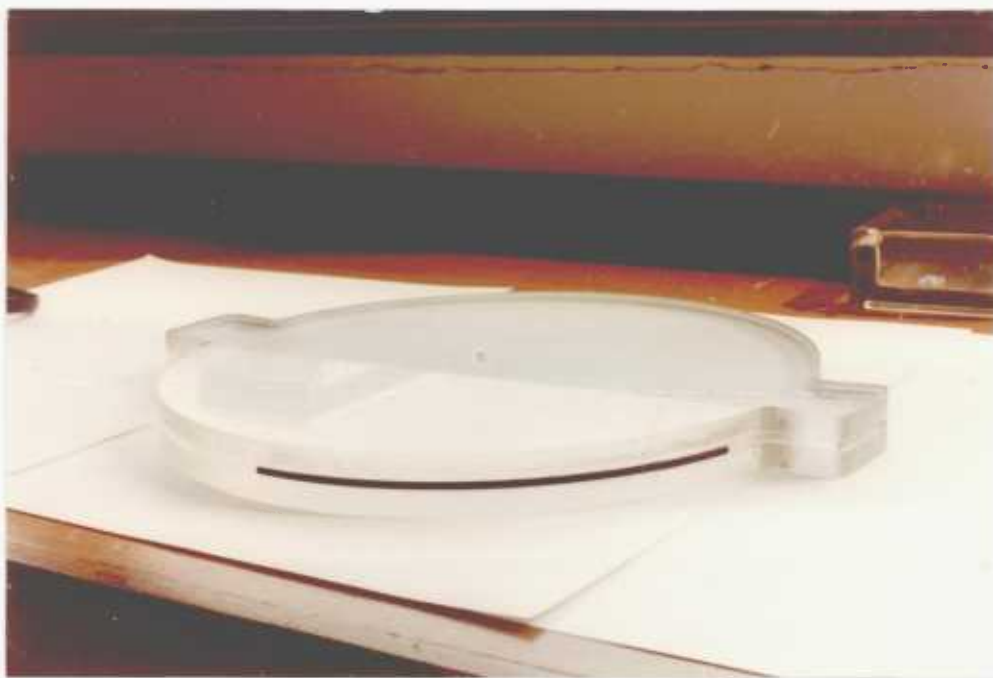


Fig. 2.19. Perspex blade sample

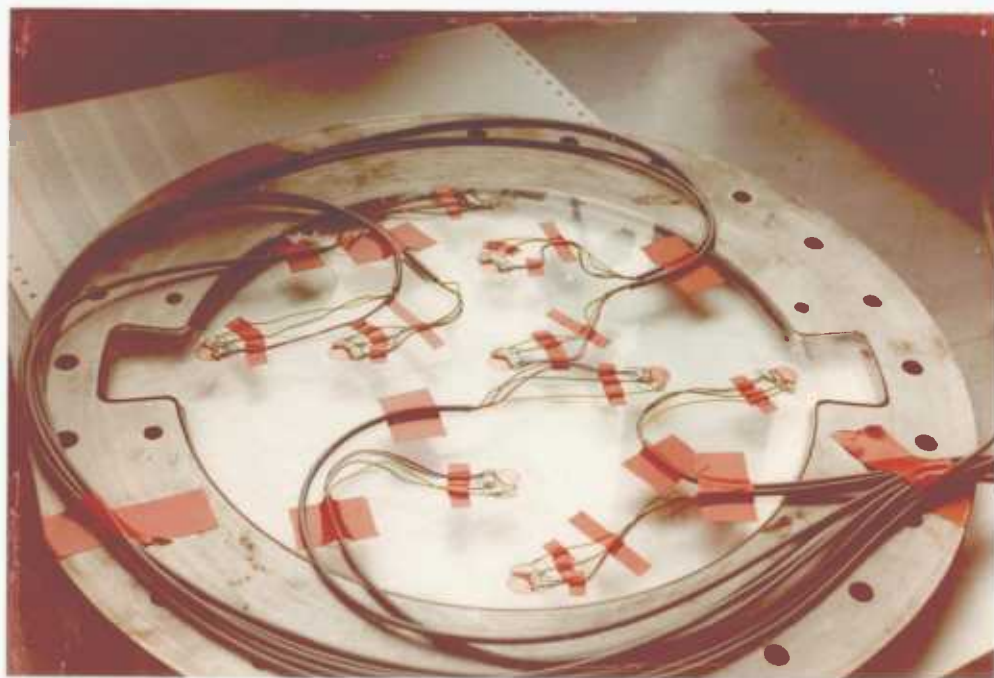


Fig. 2.20. Sample blade with strain gauges connected
fitted in testing flange

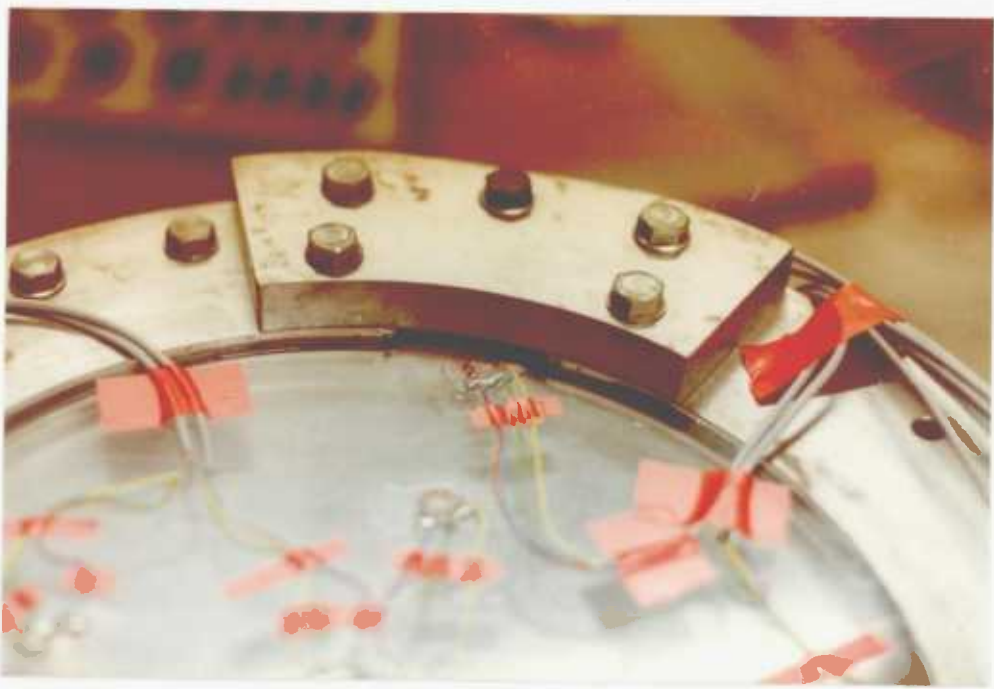


Fig. 2.21. Short flange for clamping

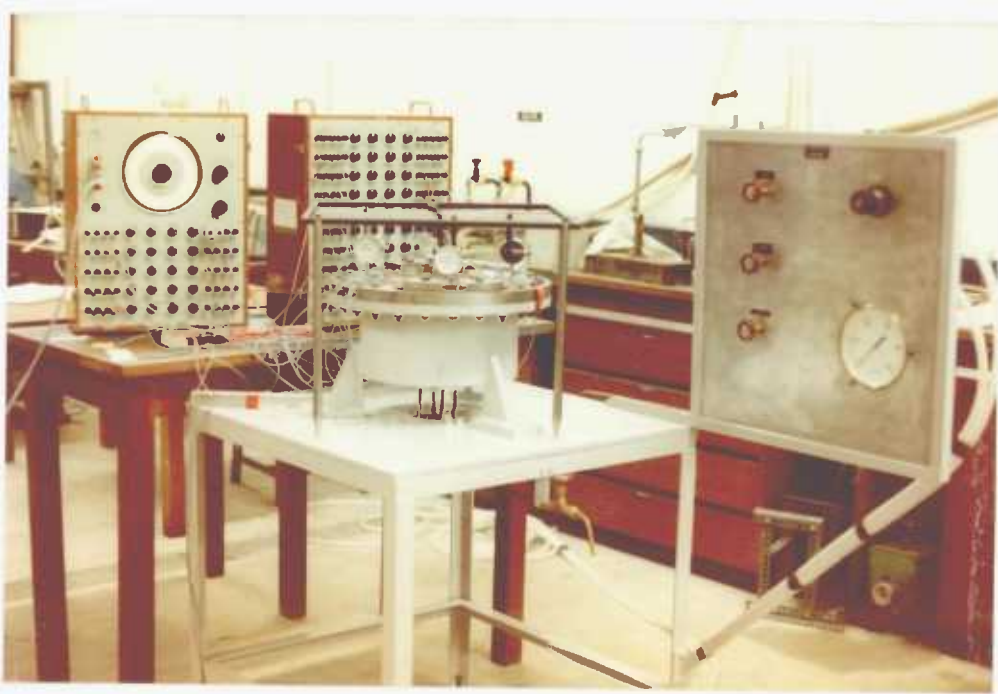


Fig. 2.22. Testing rig.

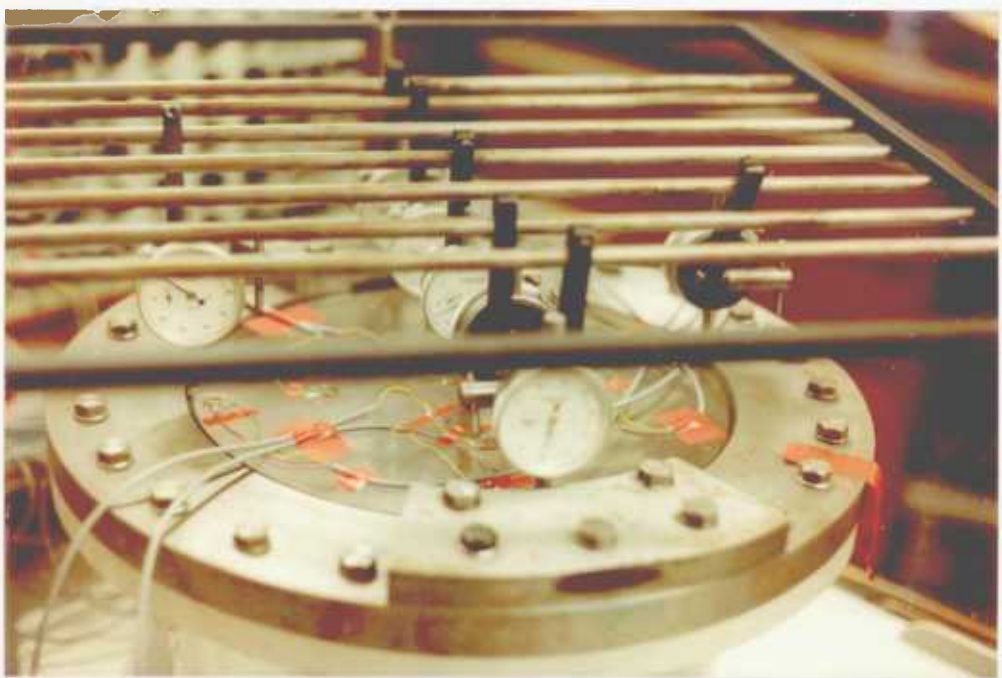


Fig. 2.23: Dial gauges during testing

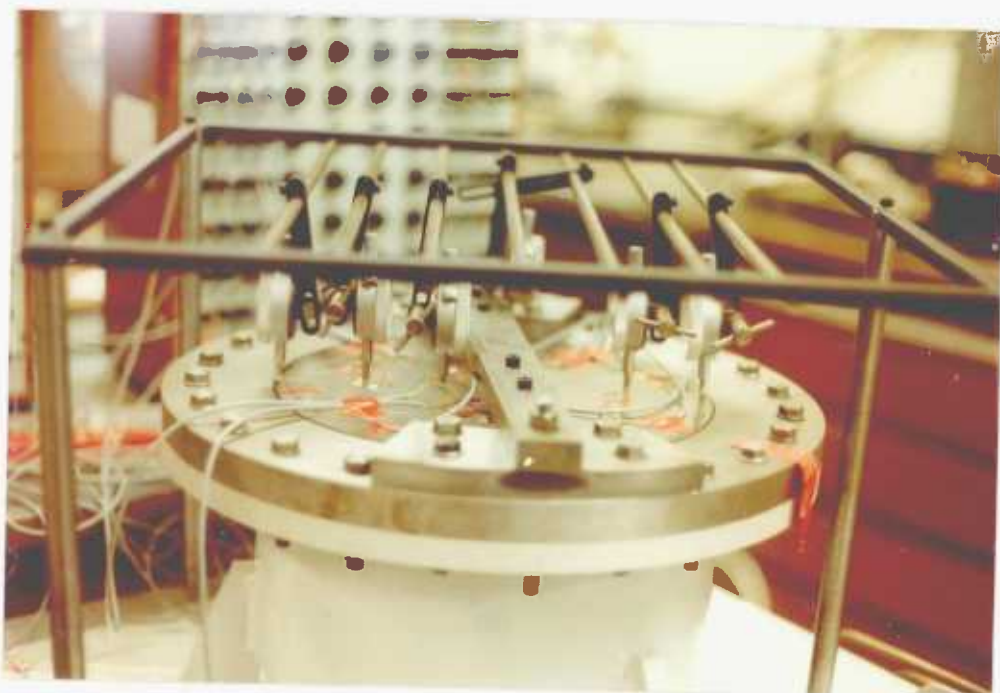


Fig. 2.24: Dial gauges frame

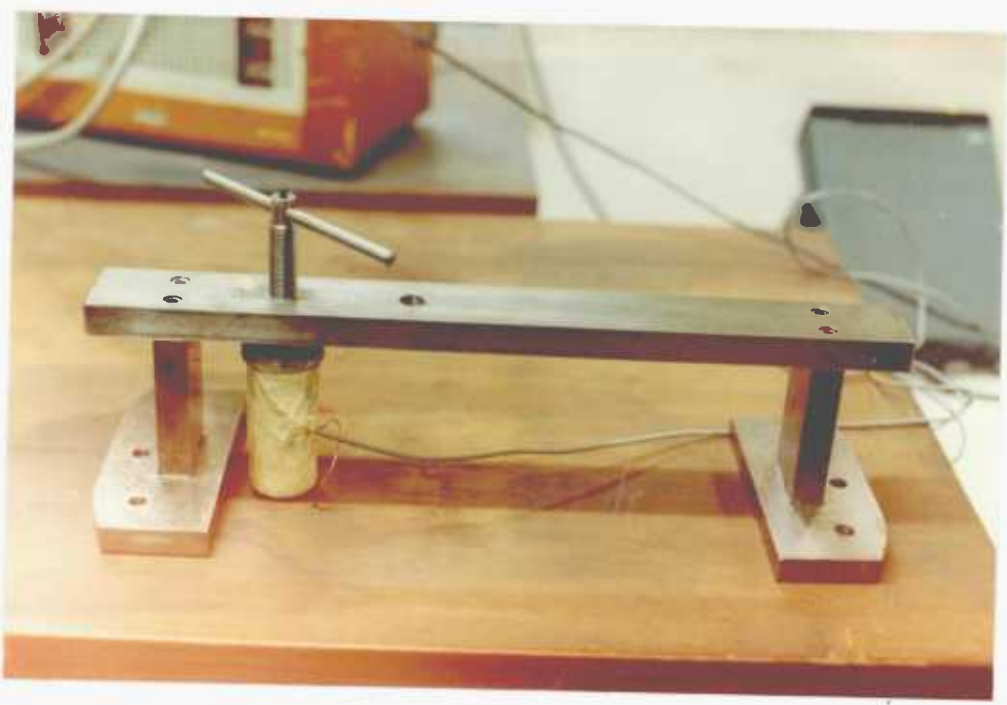


Fig. 2.25. Point load cell



Fig. 2.26. Point load cell attached to testing rig.

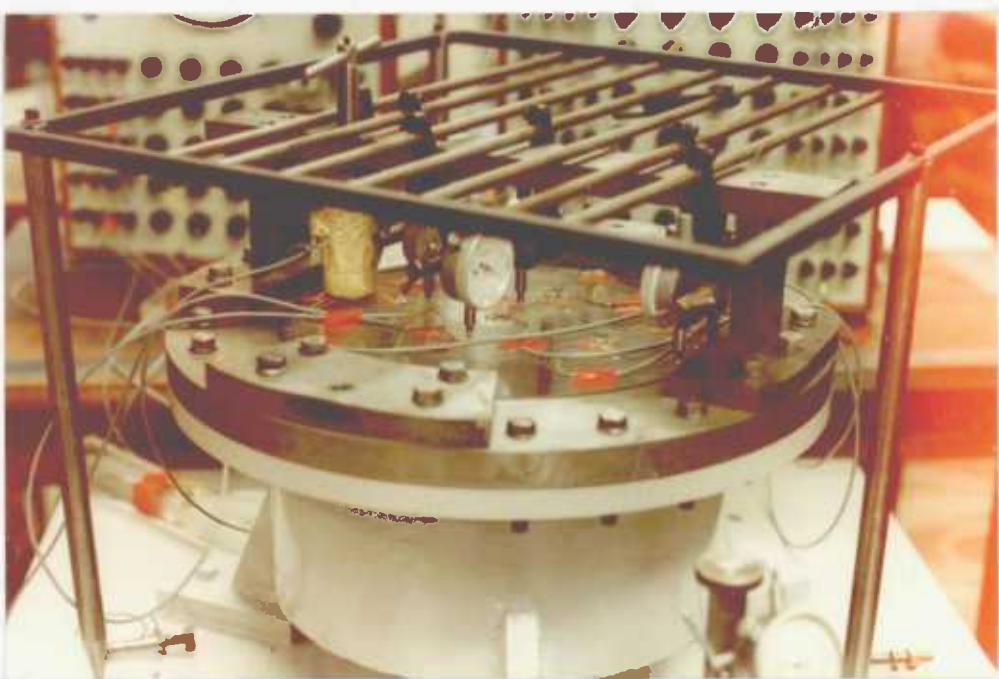


Fig. 2.27. Point load testing.



Fig. 2.28. Line support

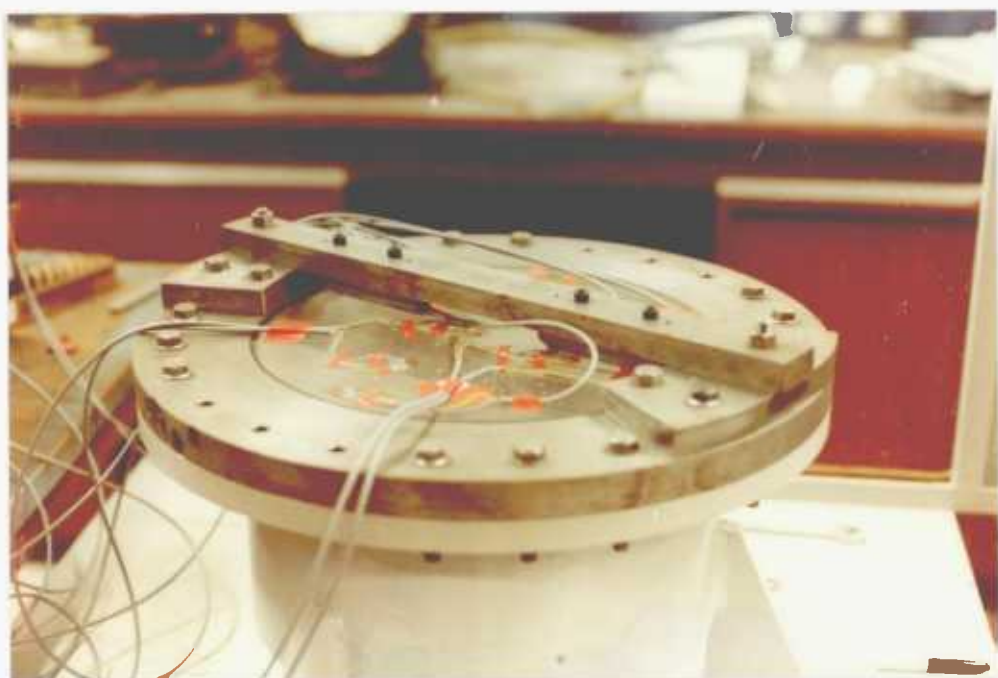


Fig. 2.29. Line support uniform pressure testing

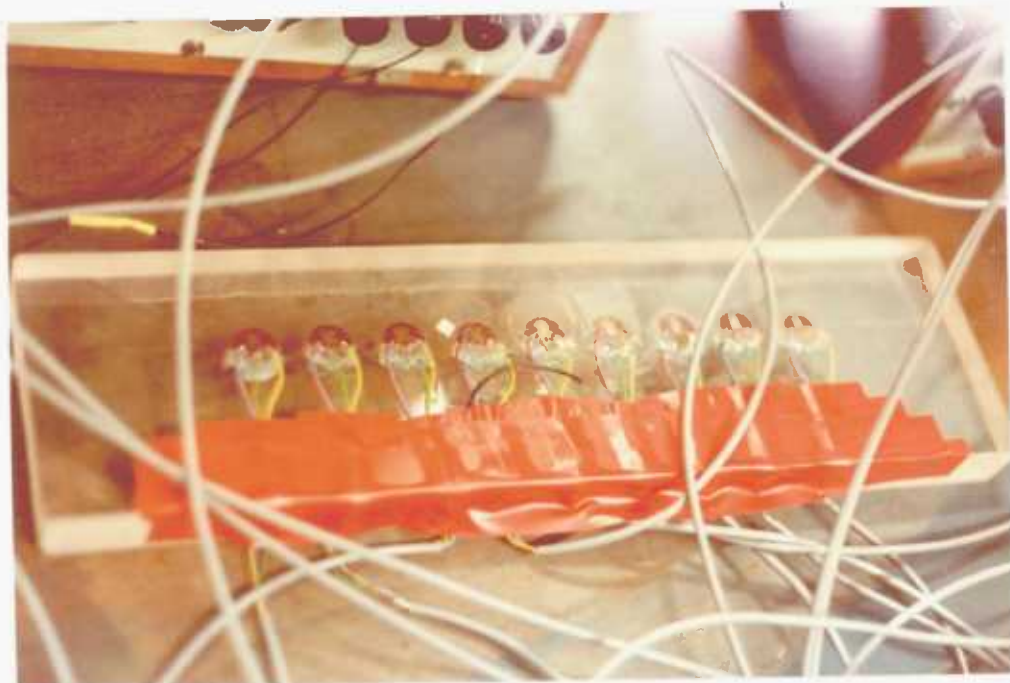


Fig. 2.30. Dummy gauges

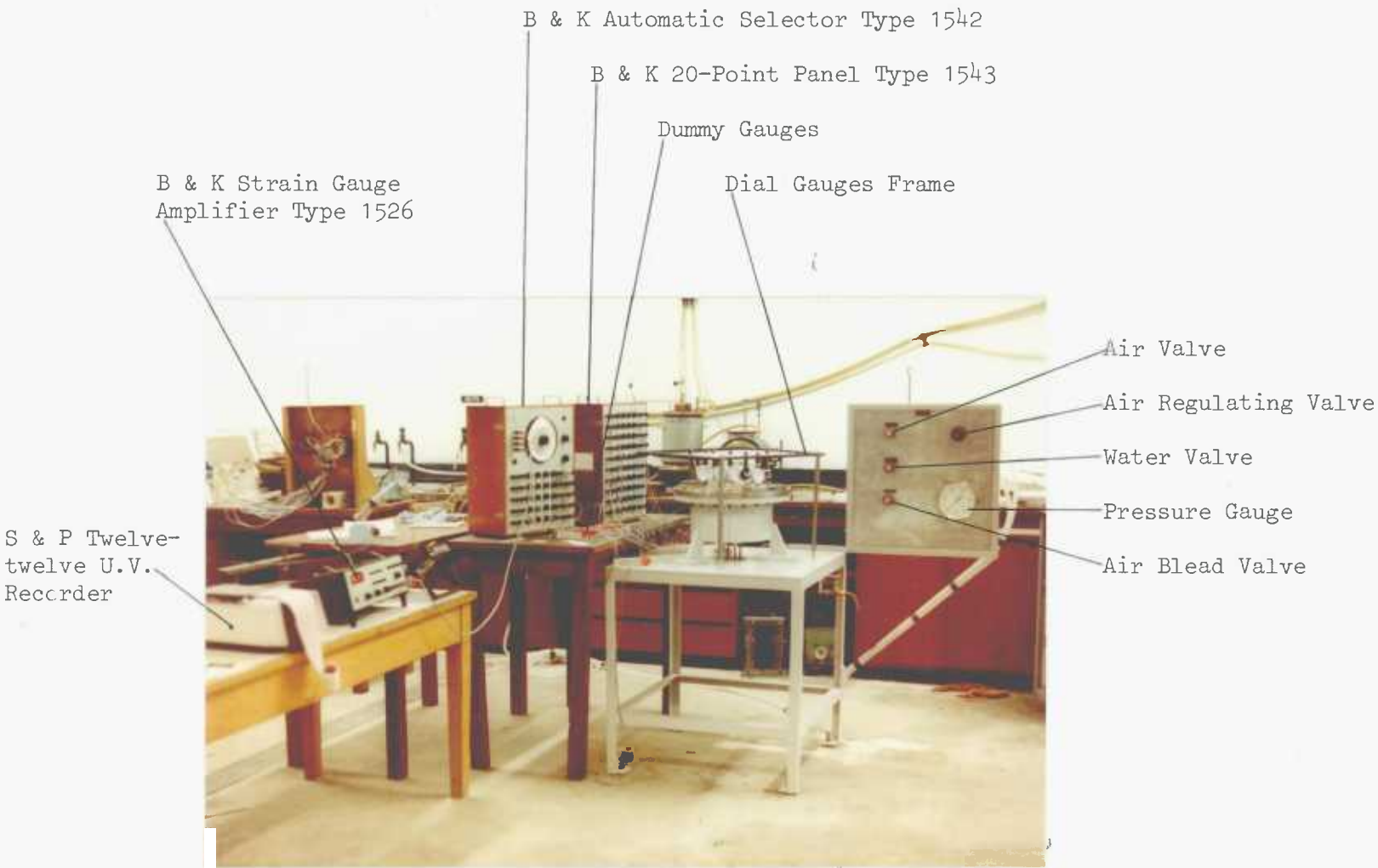


Fig. 2.31: Complete testing equipment

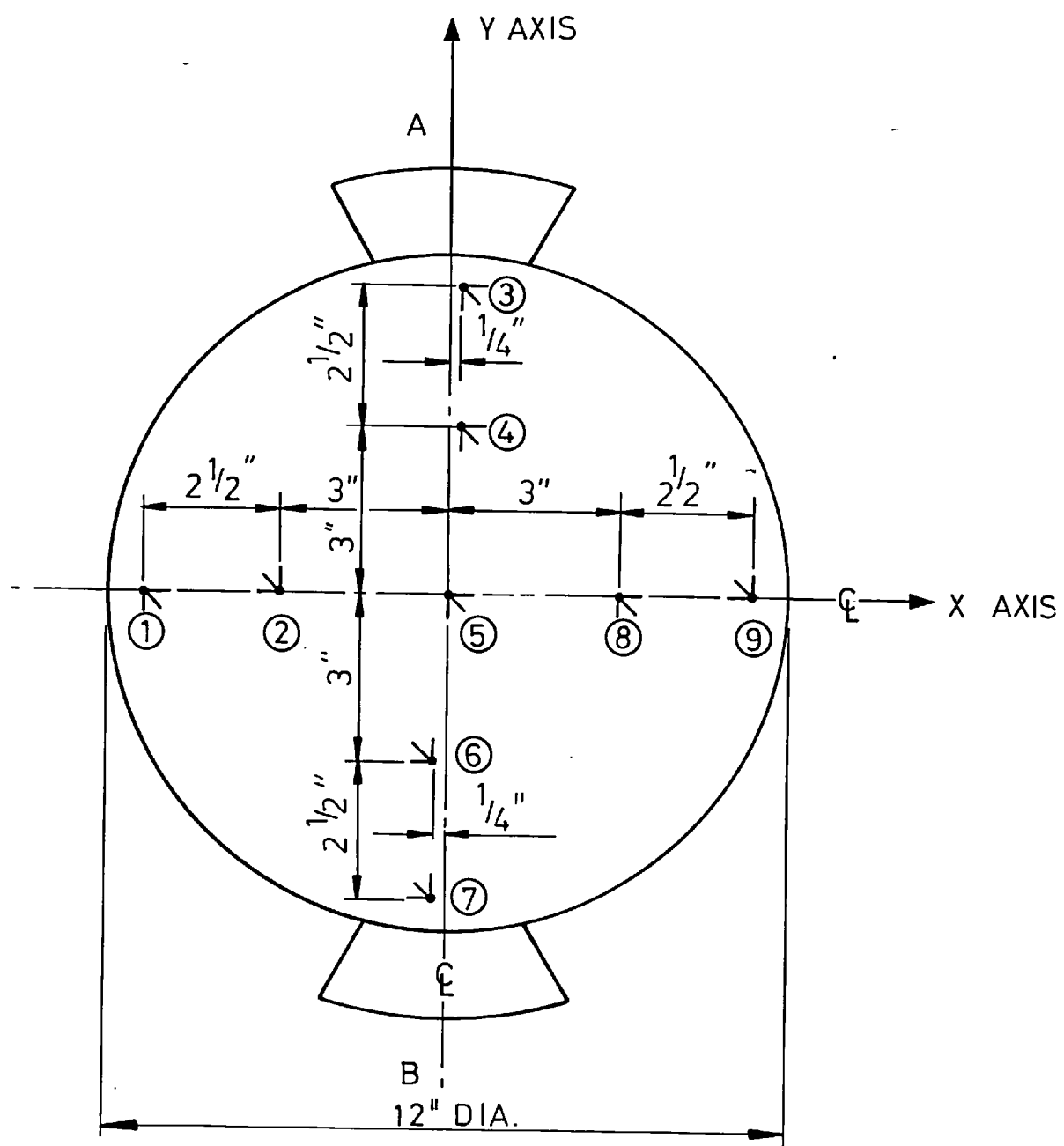


Fig. 2.32. Location of strain gauges.

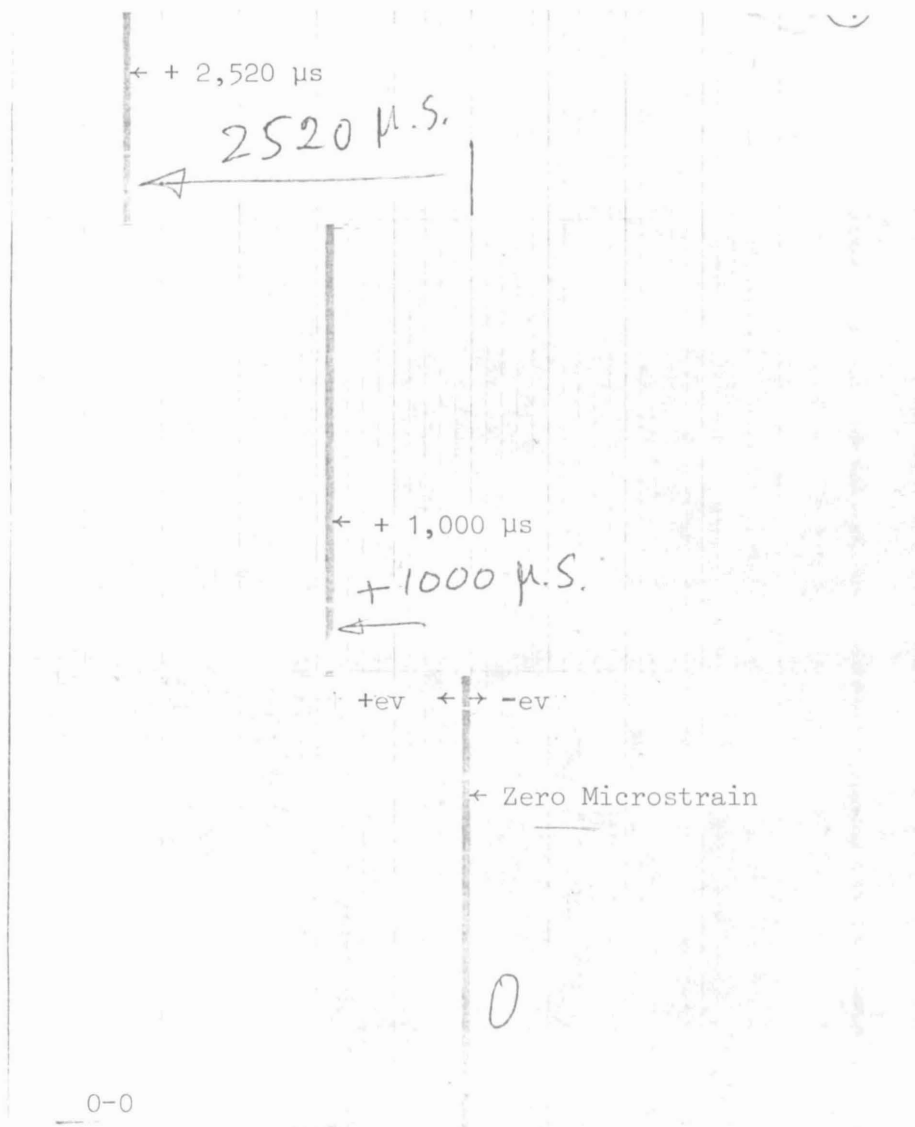


Fig. 2.33. U.V. recorder output

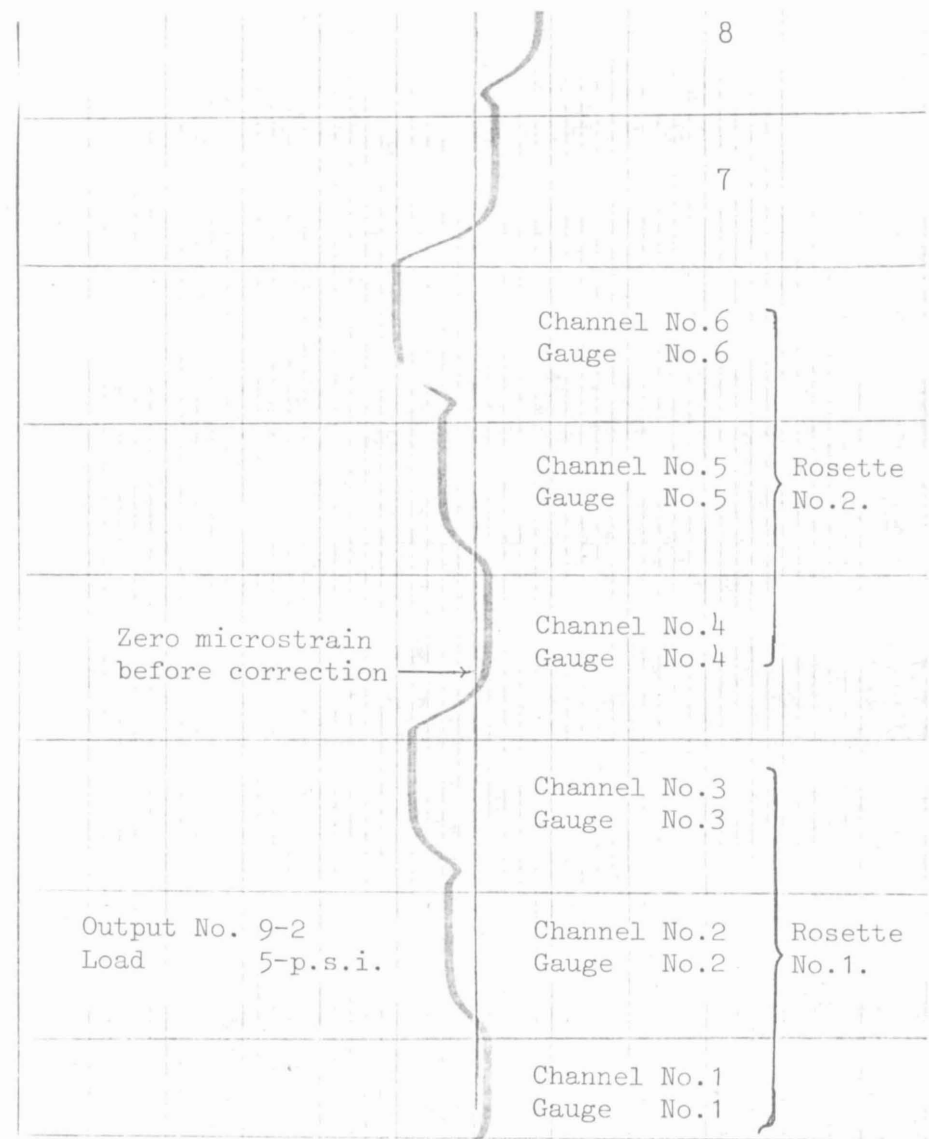


Fig. 2.34. Full-scale u.v. strain output

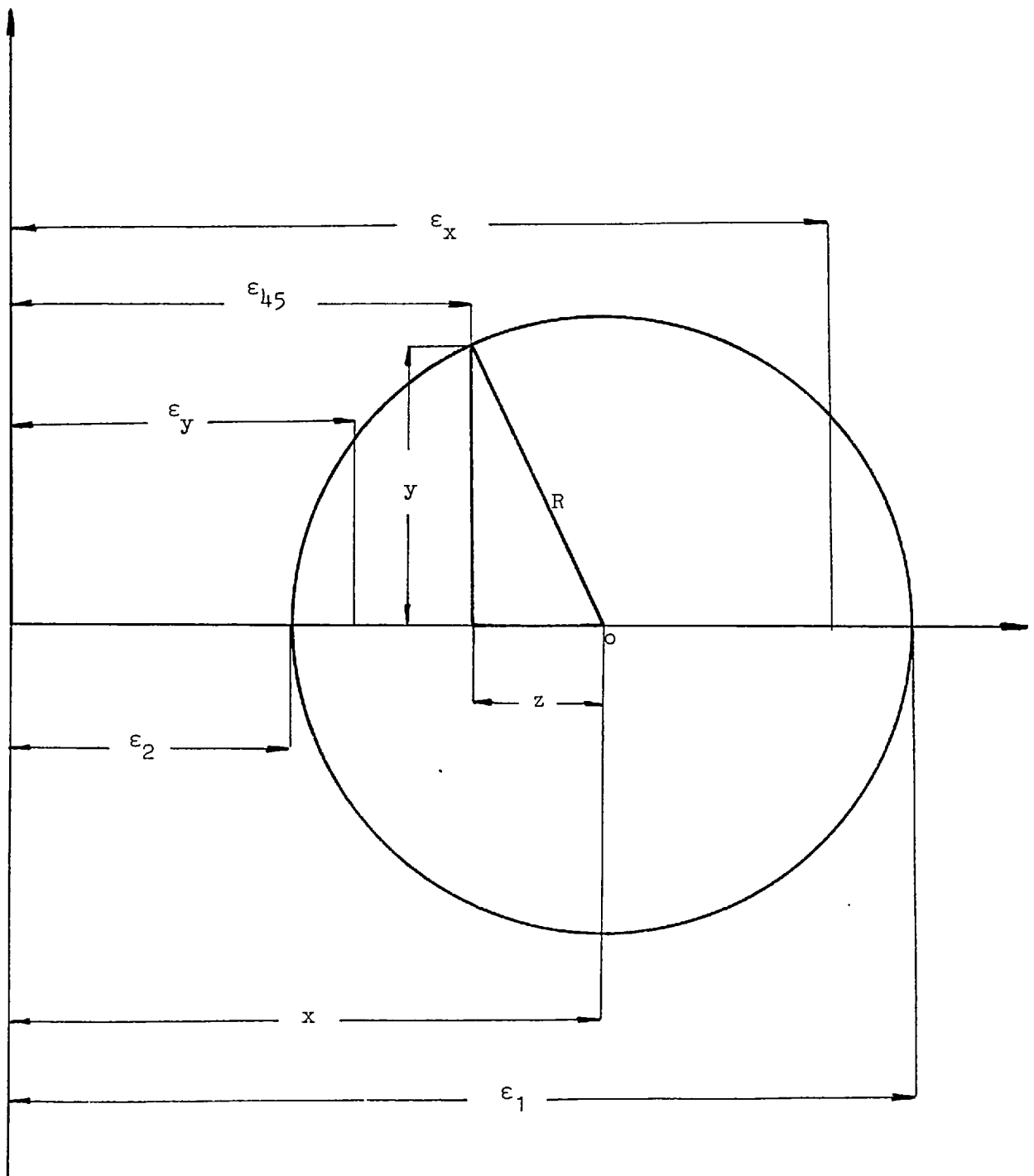


Fig. 2.35: Strain circle of a rosette

Where ϵ_x , ϵ_y , ϵ_{45} are the strains read from the plottings to the nearest 0.25mm multiplied by the scale of the u.v. recorder and fed into a small computer program listed in Appendix (2.D) which converted them from micro strains to strains and prints out the rosette number, the strains, the maximum and minimum strains ϵ_1 and ϵ_2 and the principal stresses σ_1 and σ_2 .

2.5.4. Testing a 12" Diameter Disc supported on two clamped short arcs subjected to a uniform pressure.

(i) Deflections

Measuring the deflections at five locations as shown in Fig. (2.36) and (2.23) initial loading and unloading readings were taken and the results plotted on Fig. (2.37) and (2.38) against a plot of the deflections obtained from the finite element solution for a clamped and simply supported arc. The similarity between the two results is clear and satisfactory.

(ii) Stresses

The strain gauges were read in 13.5 seconds after the load was reached to avoid the creep effect on the reading. The creep would stop in 5 to 6 hours if the load was kept constant but this proved to be an impractical procedure.

The results plotted on the u.v. recorder are given on pages 130 to 136 reduced photographically. A full scale copy of the beginning of these records is shown in Fig. (2.34). The computer outputs for the principal stresses at the rosette locations is given on pages 137 to 142. The maximum stresses are plotted for each gauge against

the maximum principal stresses obtained from the finite element solution for clamped arc support and simply supported arc. The program provides the principal stresses at the centre of the elements. The location of the strain gauges on the finite element mesh is shown in Fig. (2.39). Gauges 3 and 4 are shown on the equivalent location due to the symmetry. This case is symmetrical around x axes and y axes.

The results in Figs. (2.40), (2.41), (2.42), (2.43), (2.44), (2.45) and (2.46) show good agreement with the finite element solution and therefore with the solution based on the coefficients derived from it.

As in real valves it can be seen that the support was not 100% clamped. The degree of fixity is a major quality control problem in the clearances between the shaft and the body and the type of bearing used.

2.5.5. Testing a 12" Diameter Disc supported on two Clamped short arcs subjected to a point load.

Increasing loads of 200, 400 and 500 lbs. were applied through the pressure cell and then reduced similarly. The location of the applied load is shown in Fig. (2.47) and (2.26).

(i) Deflections

The deflections were measured at six locations as shown in Fig. (2.47) and (2.27). The results are plotted on Fig. (2.48) . (2.49), (2.50a) and (2.50b) against a plot of the deflections obtained from the finite element solution for a clamped and a simply supported arc. The similarity between the two is clear and satisfactory.

(ii) Stresses

The strains were read in the same manner as before, the results plotted on the u.v. recorder are given on pages 151 to 156.

The computer outputs for the principal stresses at the rosette locations is given on pages 157 to 161.

The maximum stresses are plotted for each gauge against the maximum principal stresses obtained from the finite element solution for clamped arc support and simply supported arc, as shown in Figs. (2.51), (2.52), (2.53), (2.54), (2.55), (2.56) and (2.57).

The results show good agreement in the vicinity of the applied load and give higher stresses than expected by the finite element solution. This is considered satisfactory because in practice this load is small in comparison with the uniformly distributed pressure on the valves.

2.5.6. Testing 12" Diameter Disc supported on two clamped short arcs and two short lengths of the diameter subjected to a uniform pressure.

(i) Deflections

The deflections were measured at the locations shown in Fig. (2.58). The results are plotted on Figs. (2.59) and (2.60) against the finite element solution. The results are self-explanatory. From the finite element solution it can be seen that the deflections are governed by the diameter support and the effect of the arc being clamped or simply supported is insignificant

(ii) Stresses

The strains were read in the same manner as before, the results plotted on the u.v. recorder are given on pages 173 to 180.

The computer outputs for the principal stresses at the rosette locations is given on pages 181 to 187.

The maximum stresses are plotted for each gauge against the maximum principal stresses obtained from the finite element solution for clamped and simply supported arcs. This is shown in Figs. (2.61), (2.62), (2.63), (2.64) (2.65), (2.66), (2.67) and (2.68).

The results show good agreement with the finite element solution and therefore with the solution based on the coefficients derived from it.

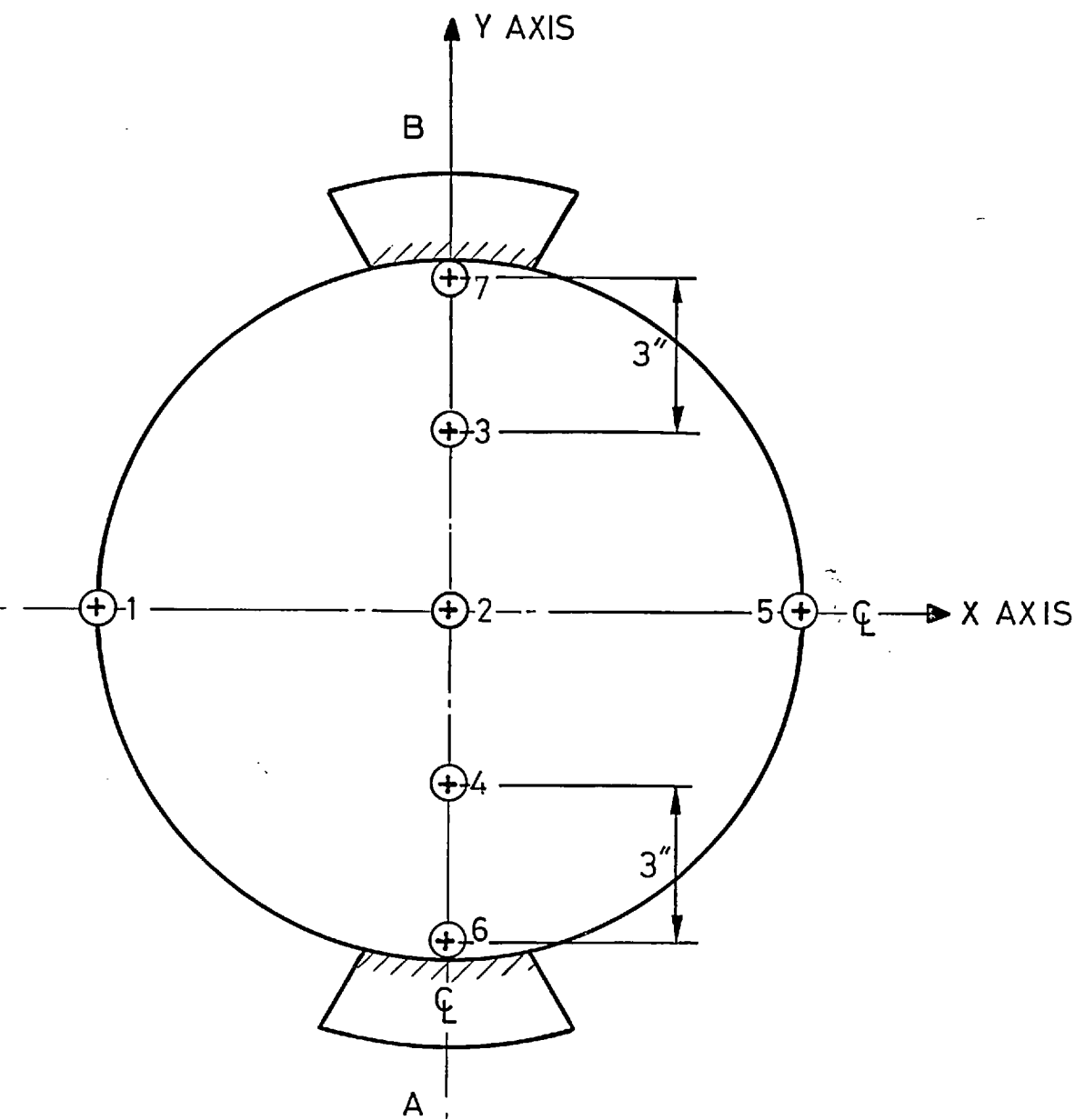


Fig. 2.36a Dial Gauge Locations

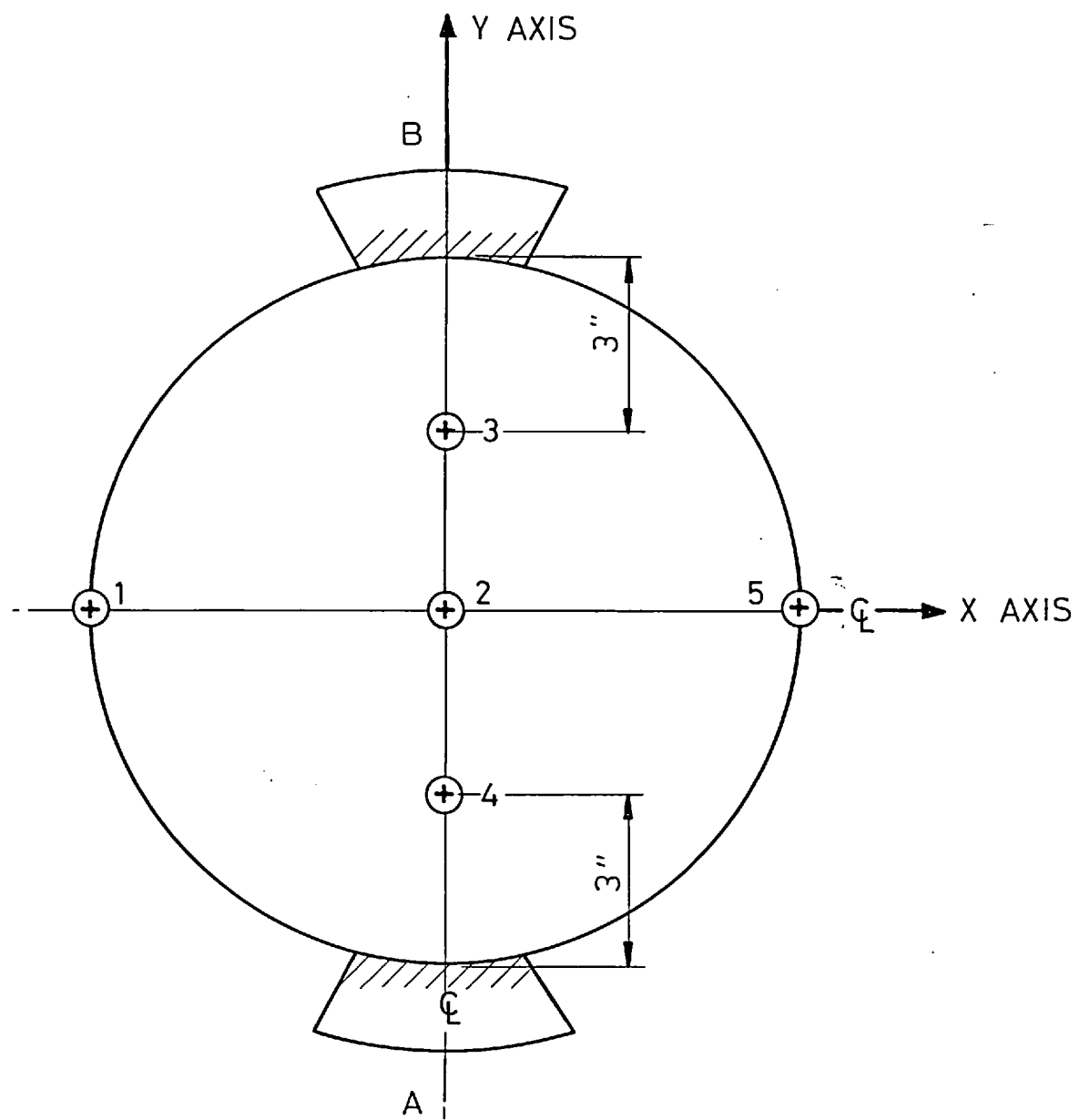


Fig. 2.36b : Dial gauge locations

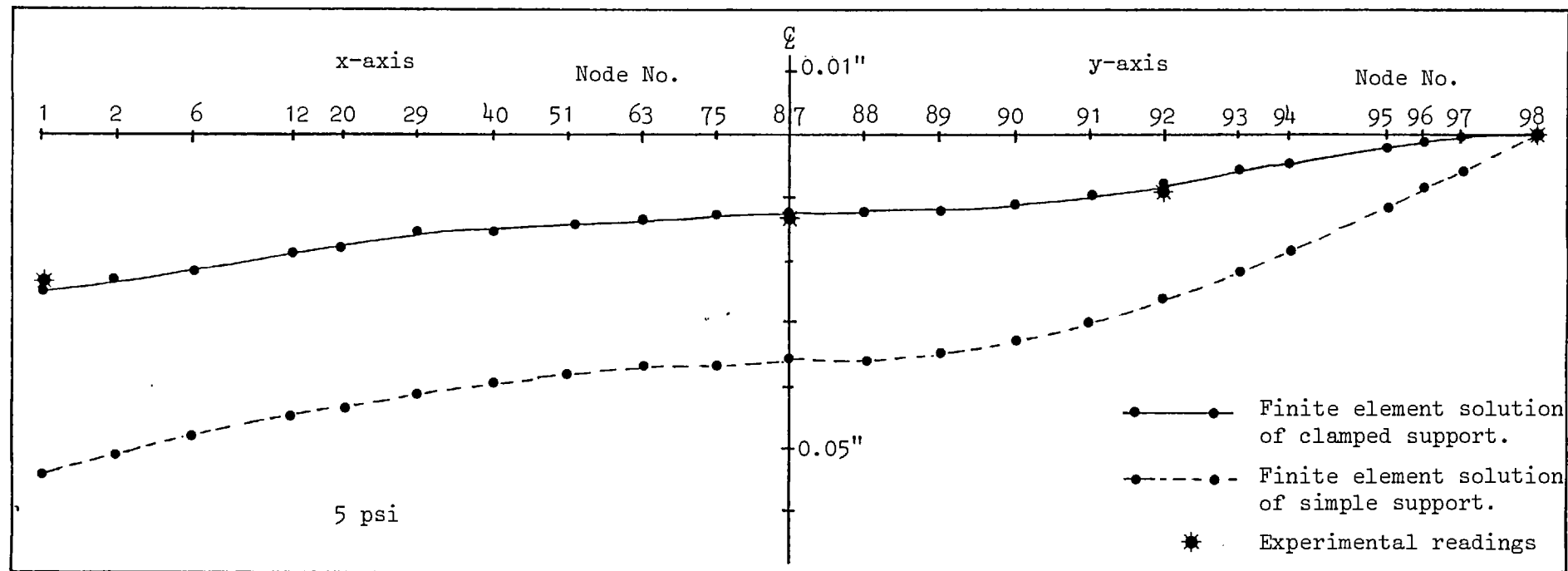


Fig. 2.37. Comparison of deflections due to uniform distributed pressure along x & y-axis.

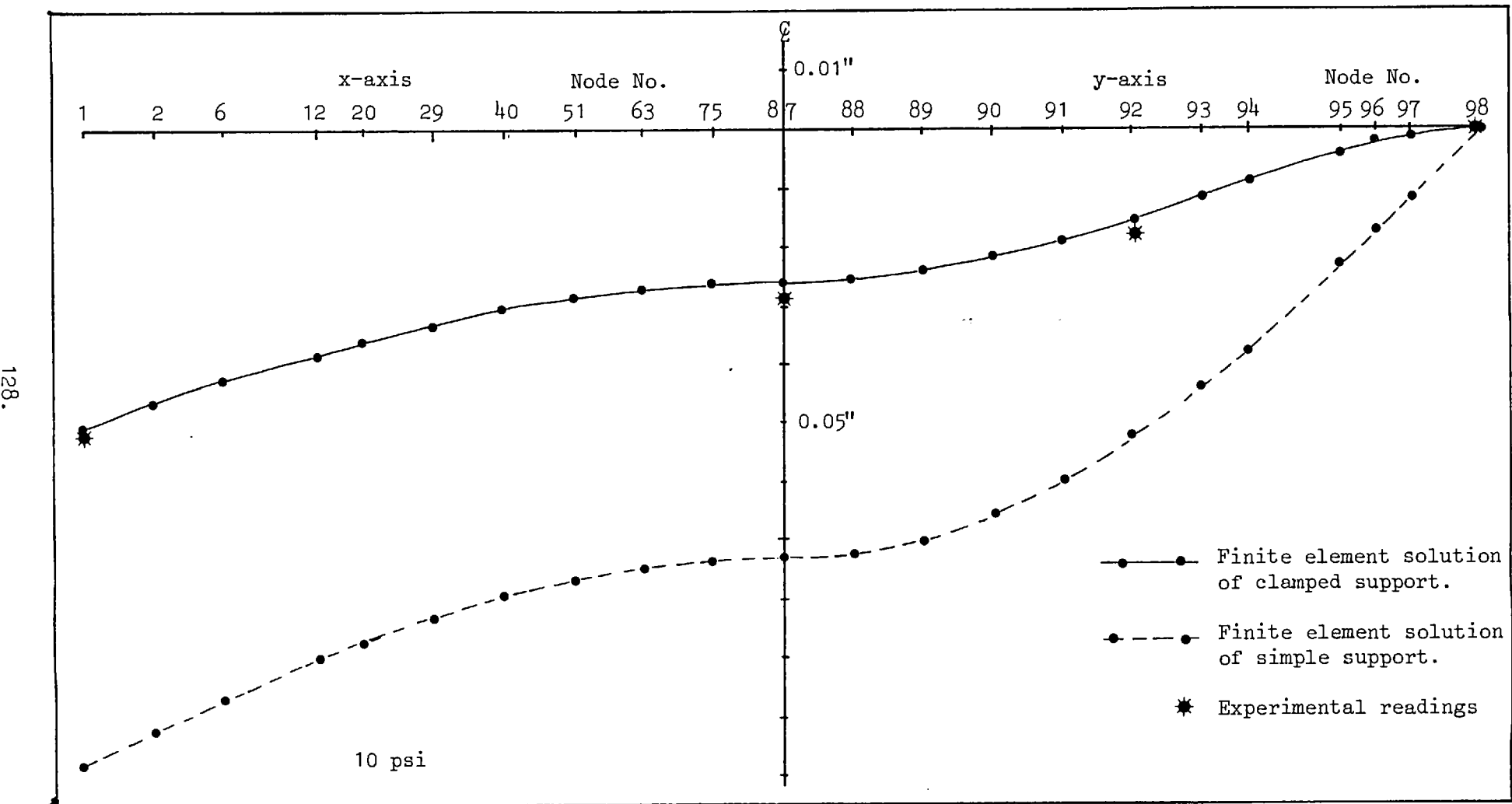


Fig. 2.38. Comparison of deflections due to uniform distributed pressure along x & y-axis

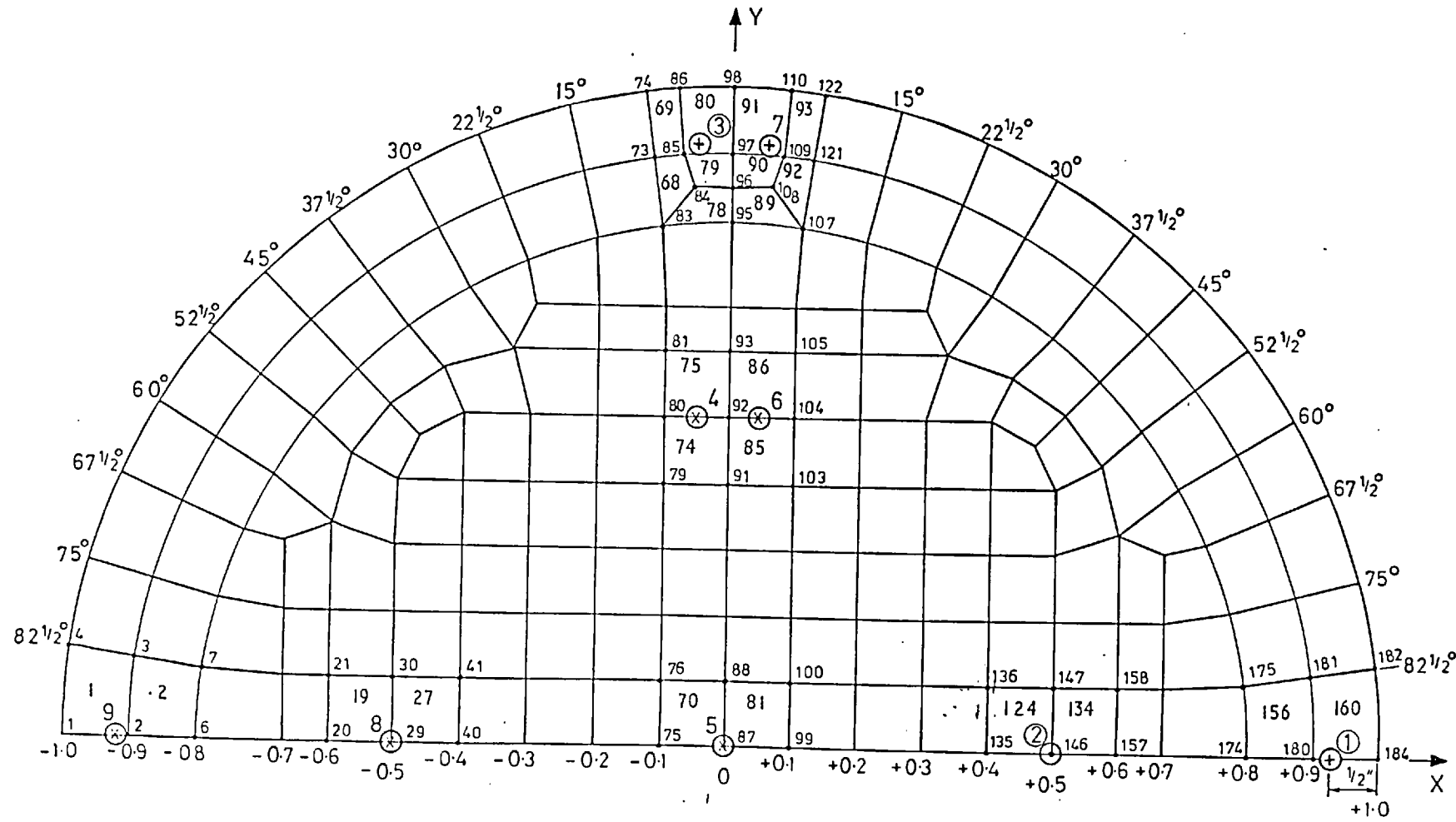
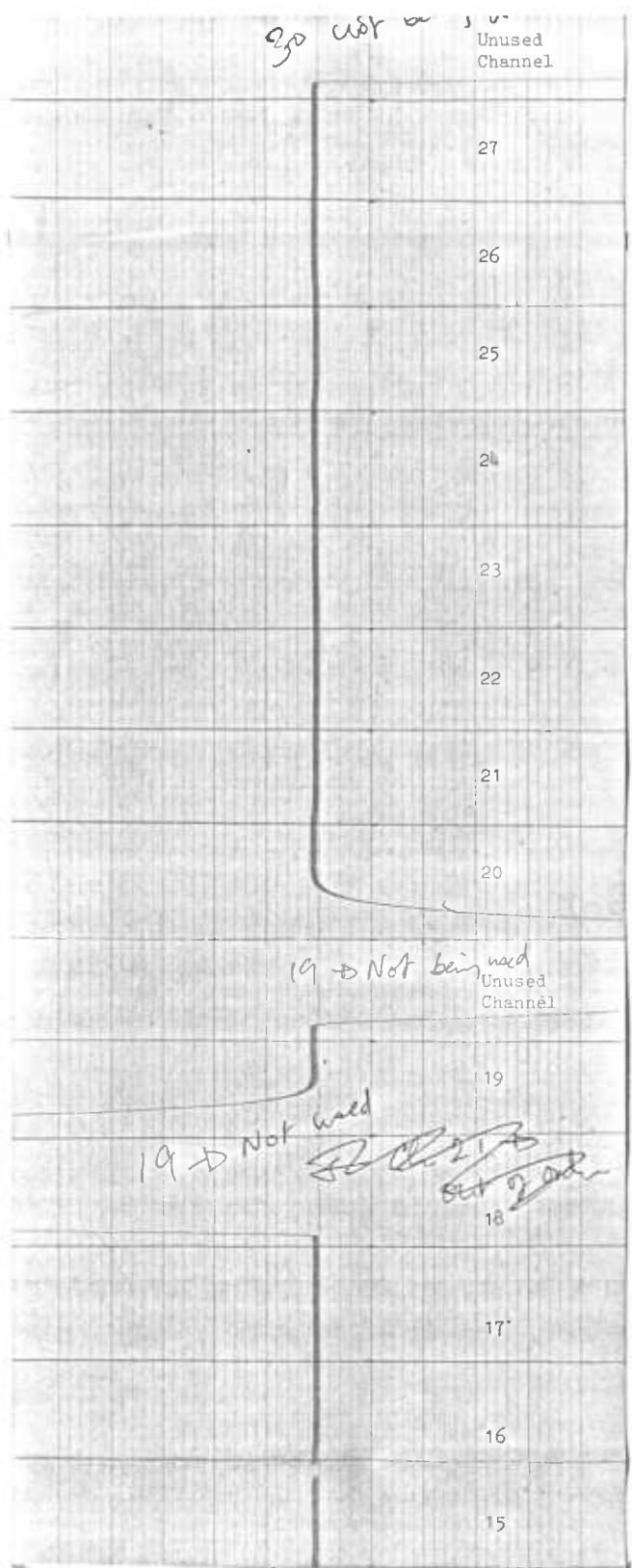
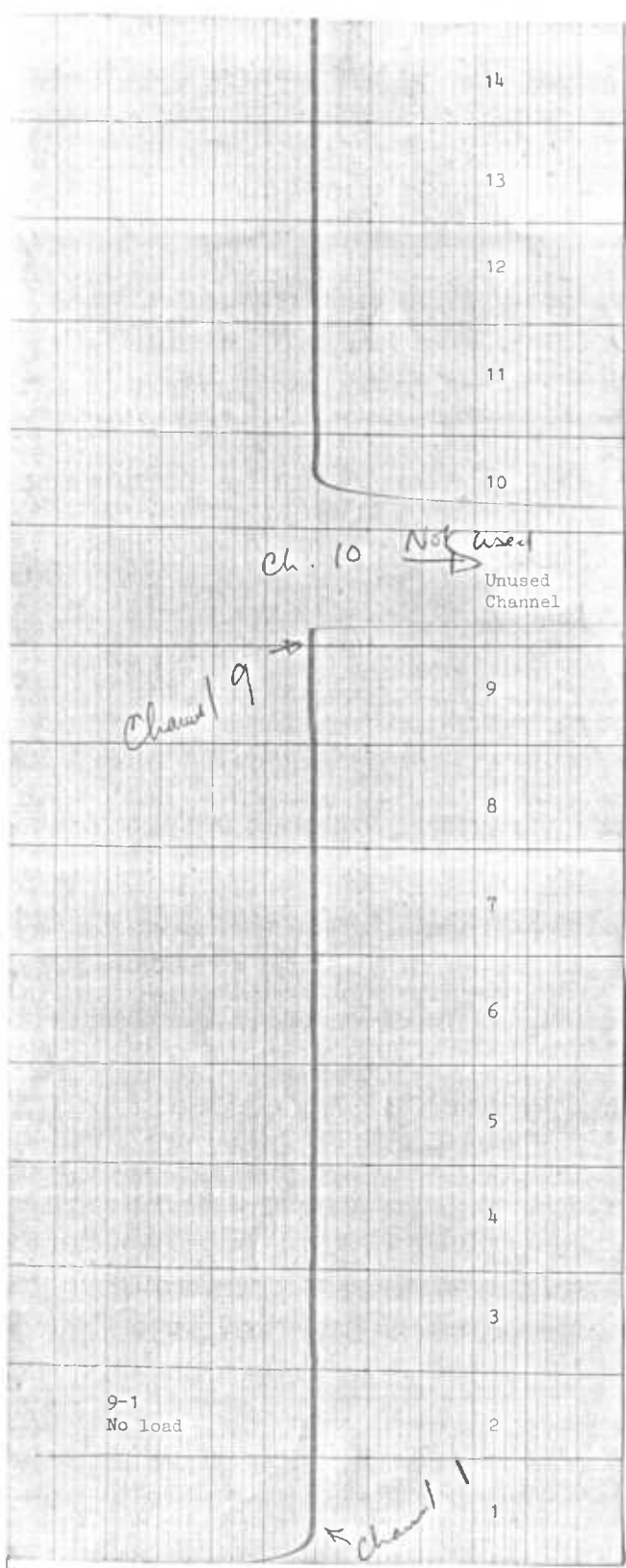
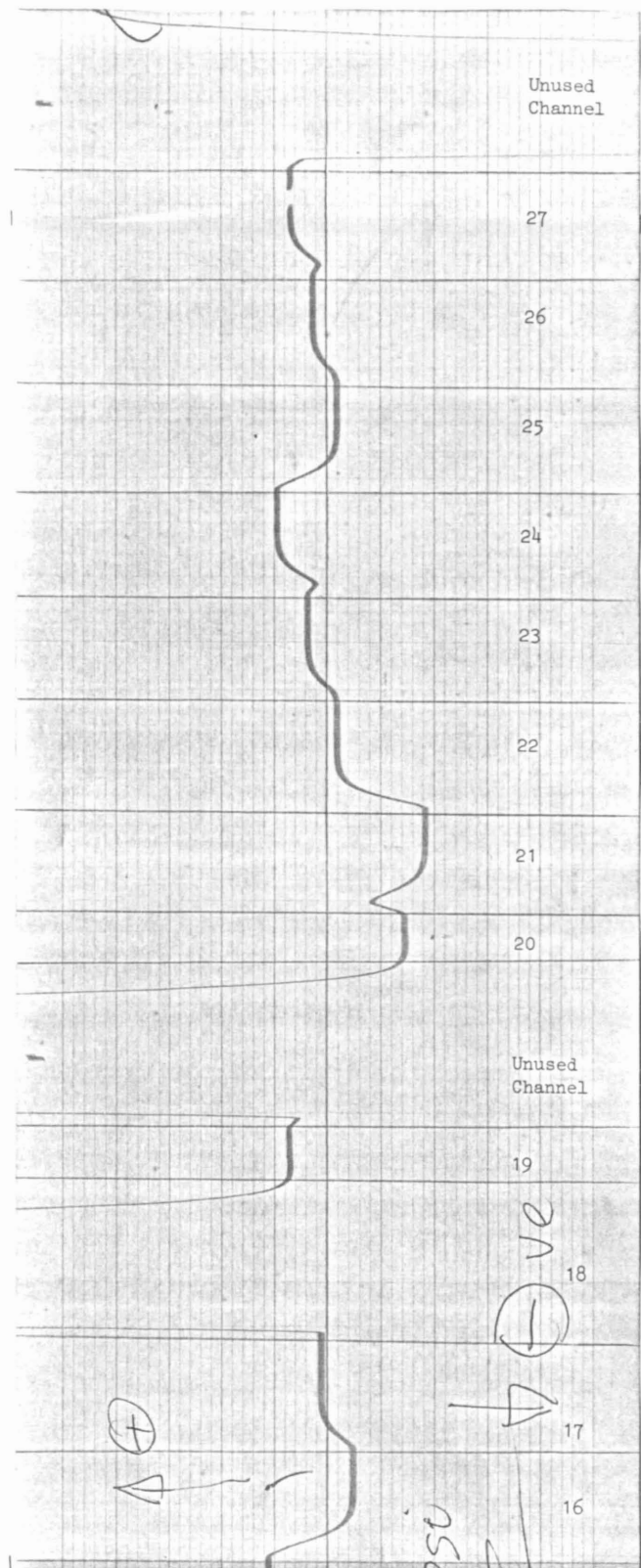
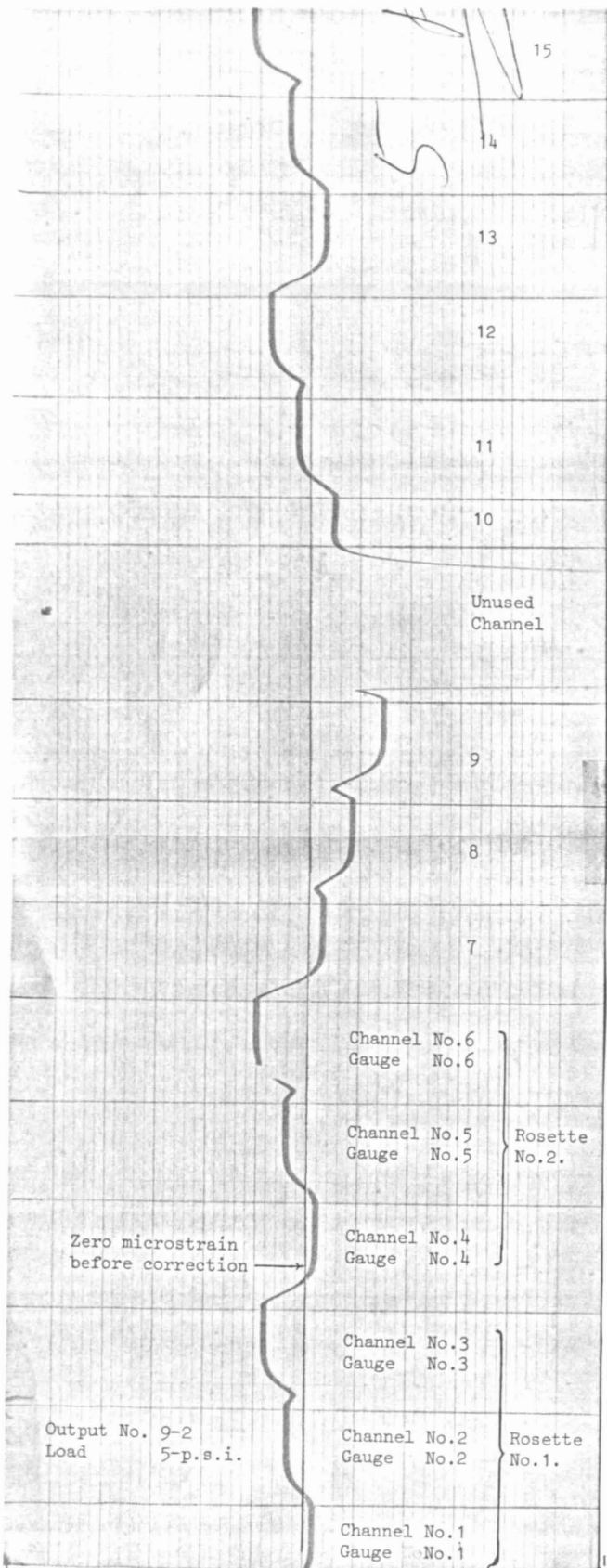
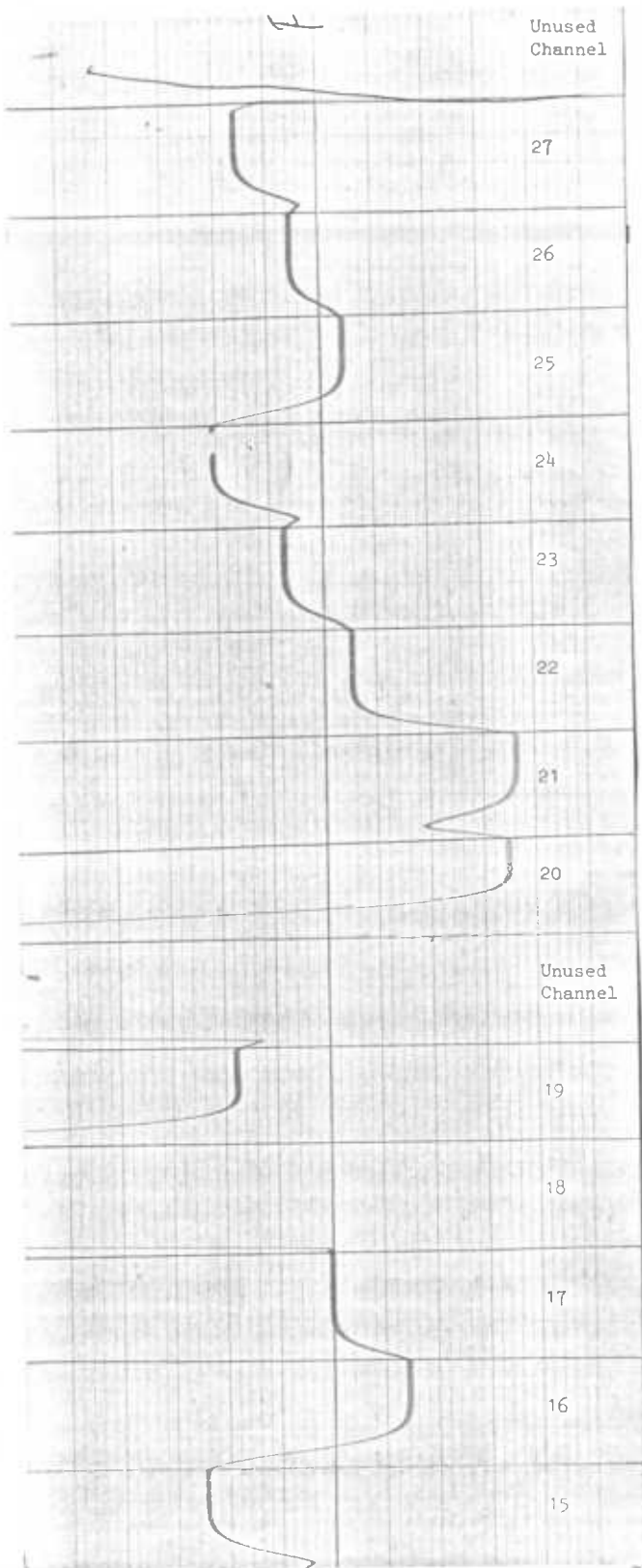
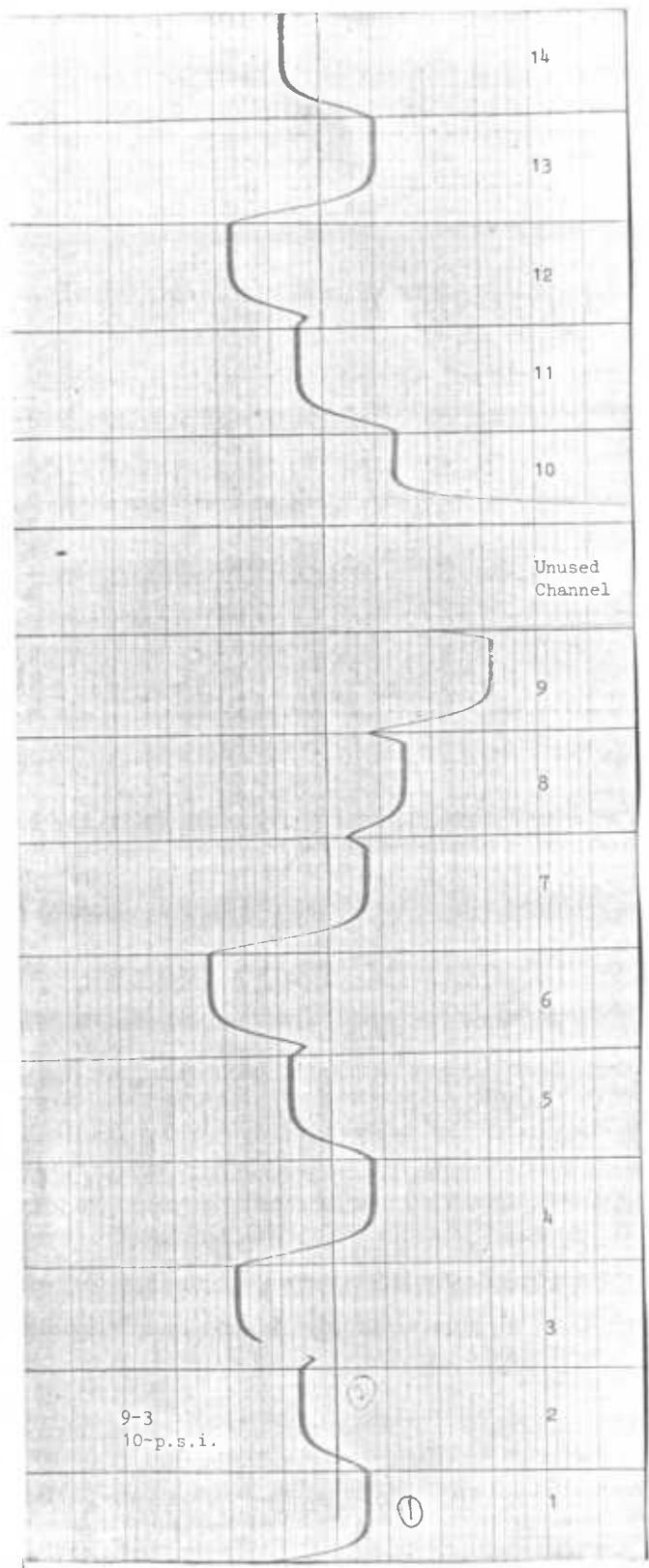
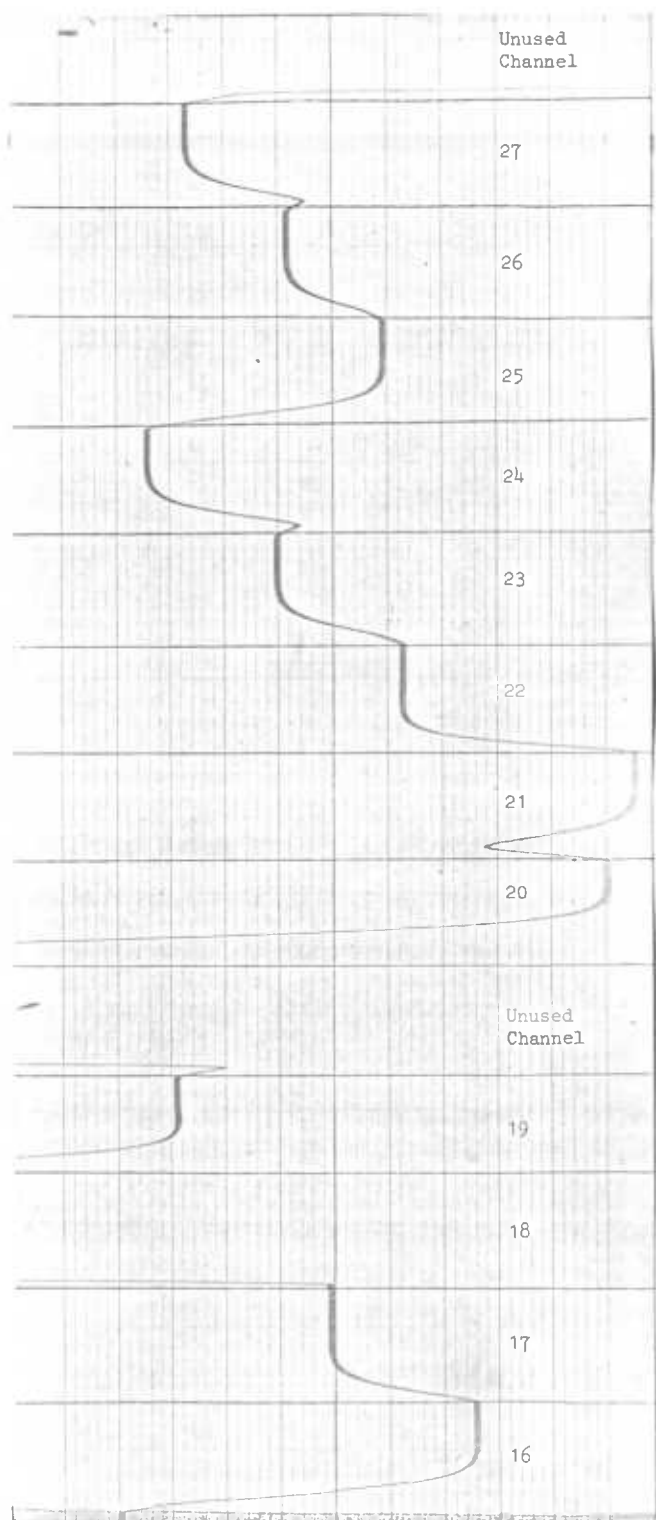
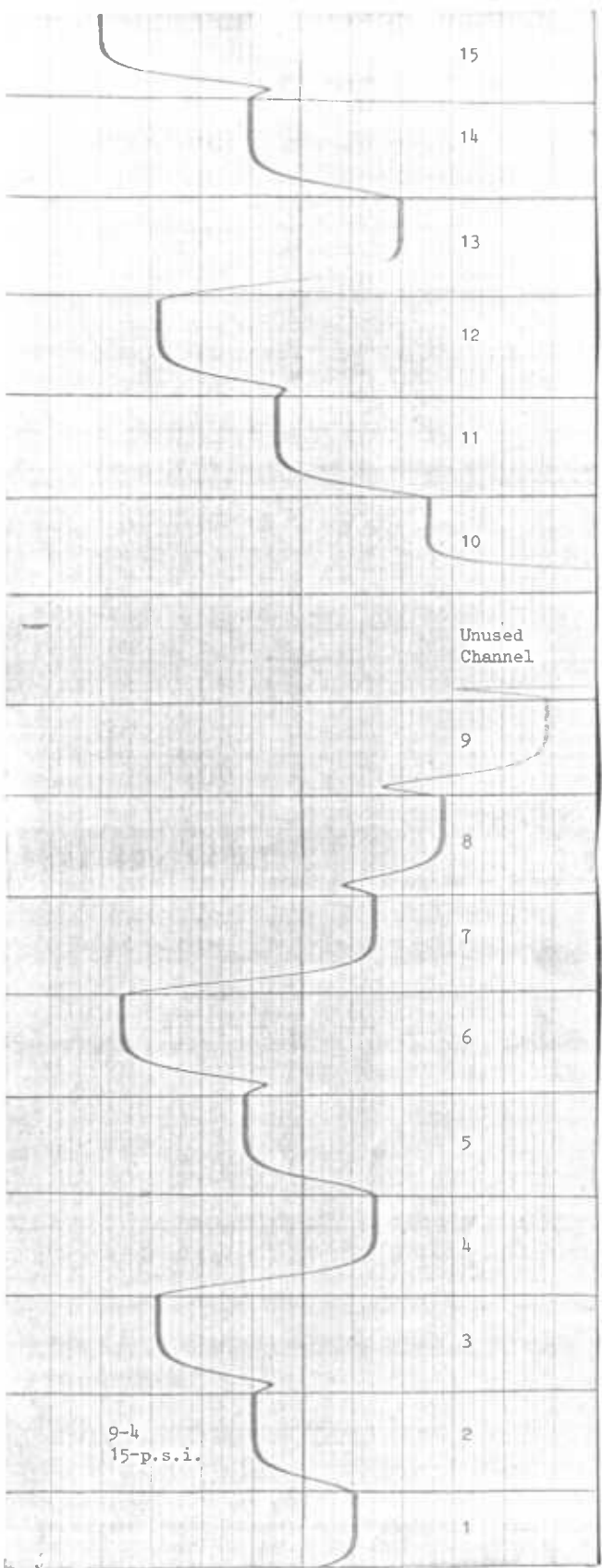


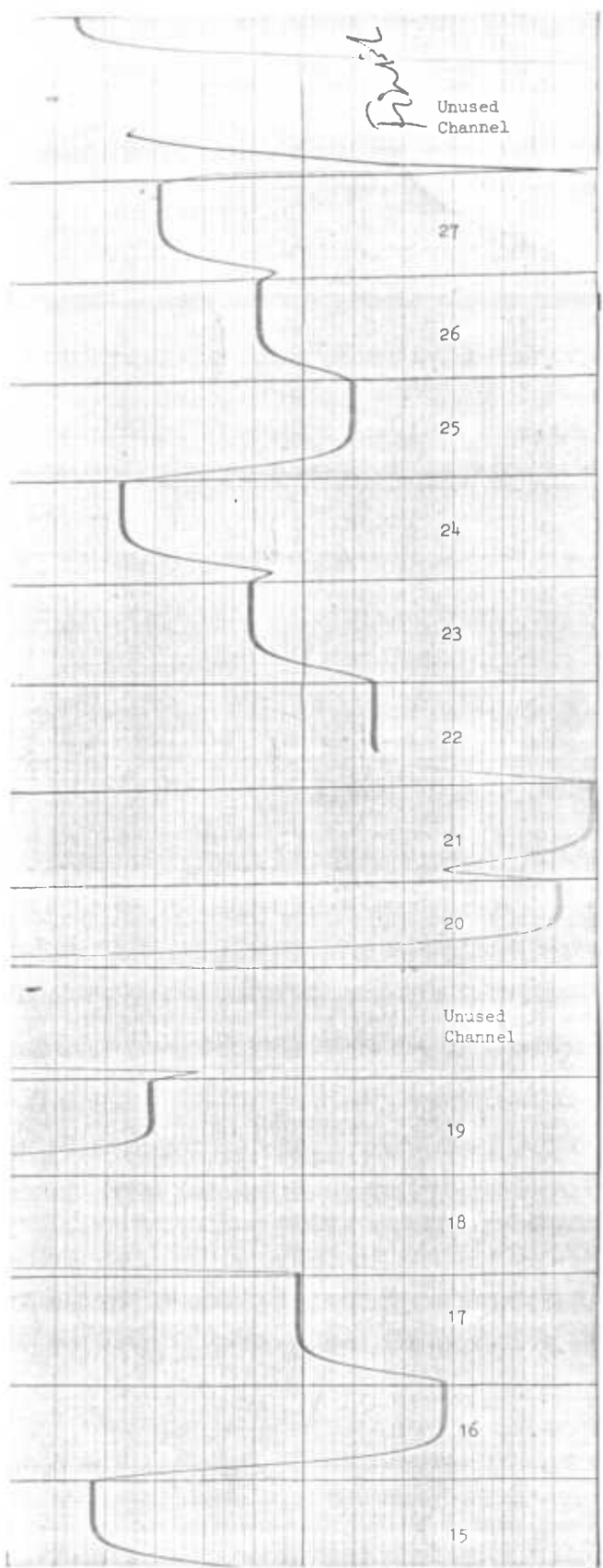
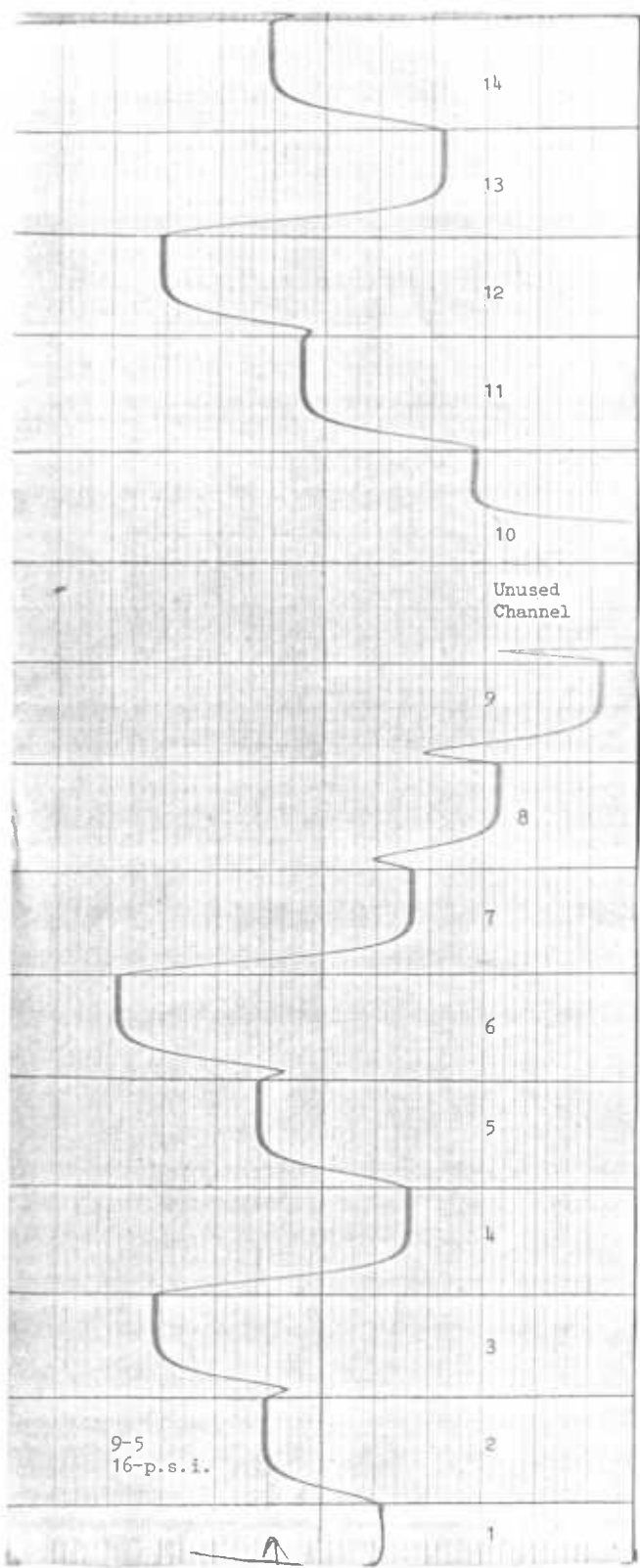
Fig. 2.39. LOCATION OF STRAIN GAUGES ON F. E. MESH.

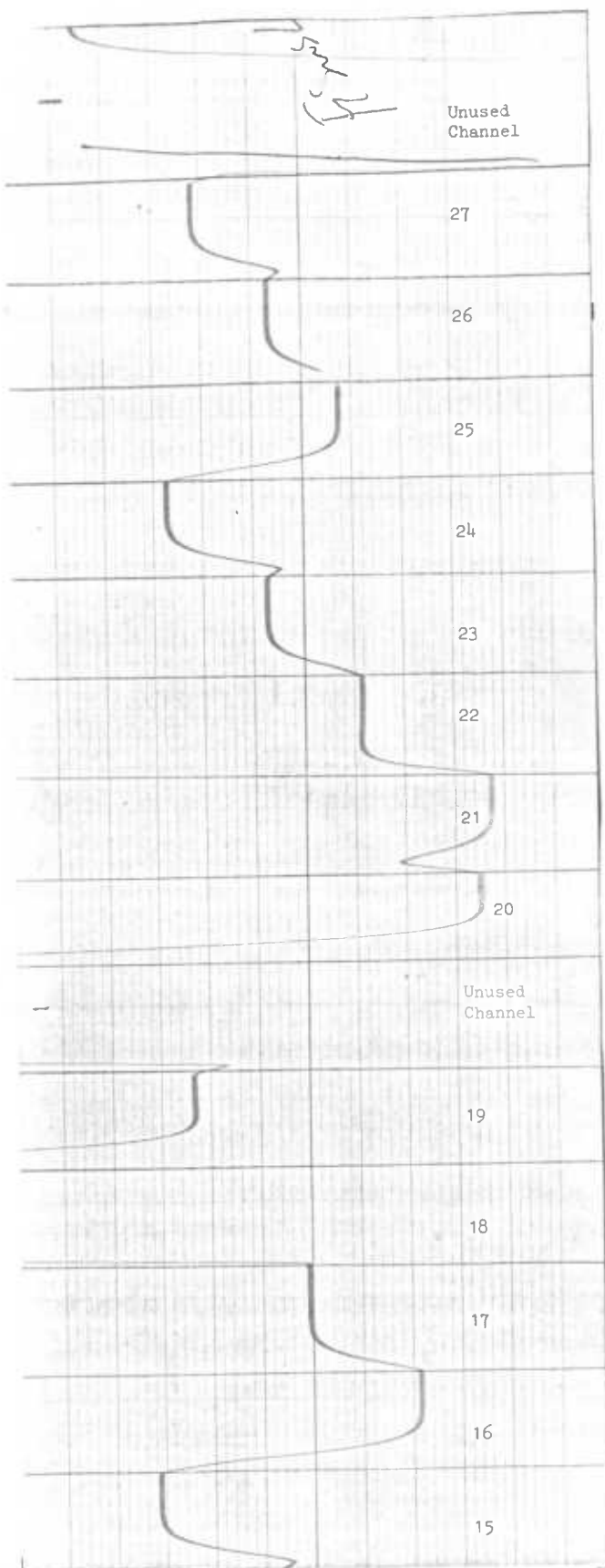
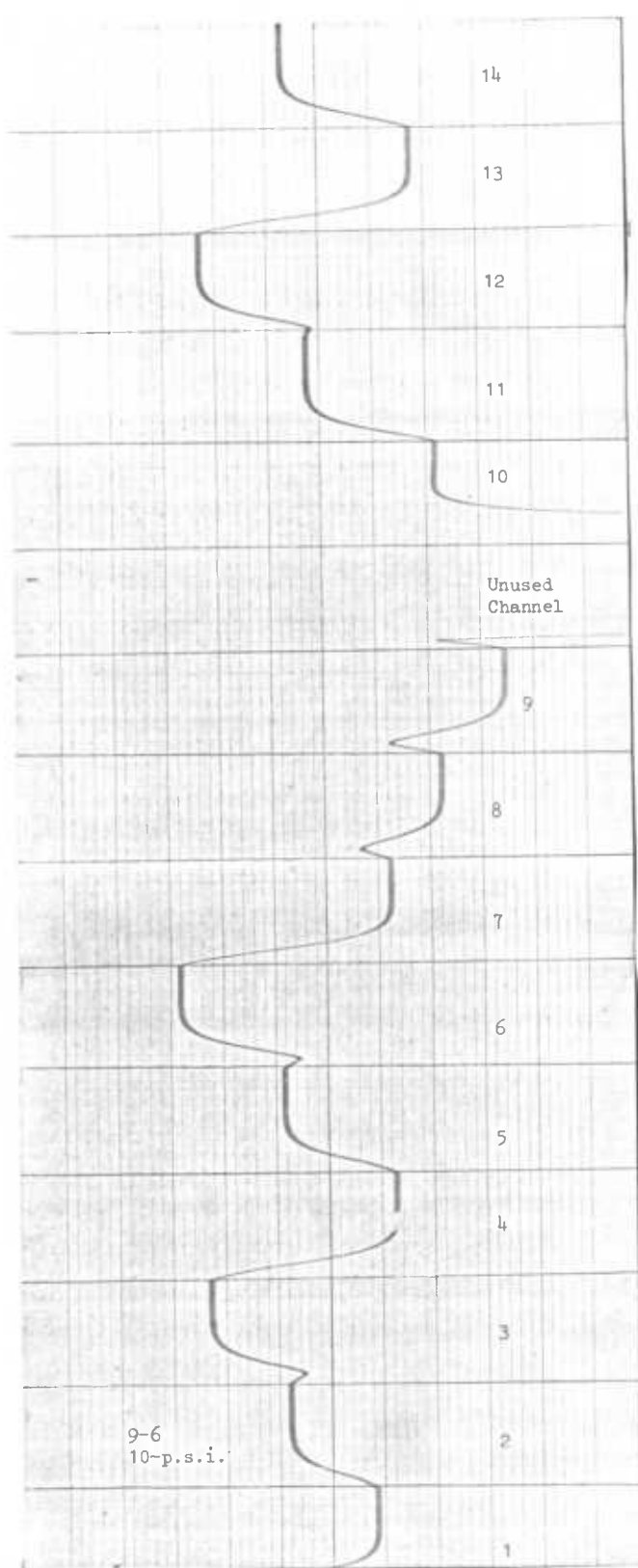


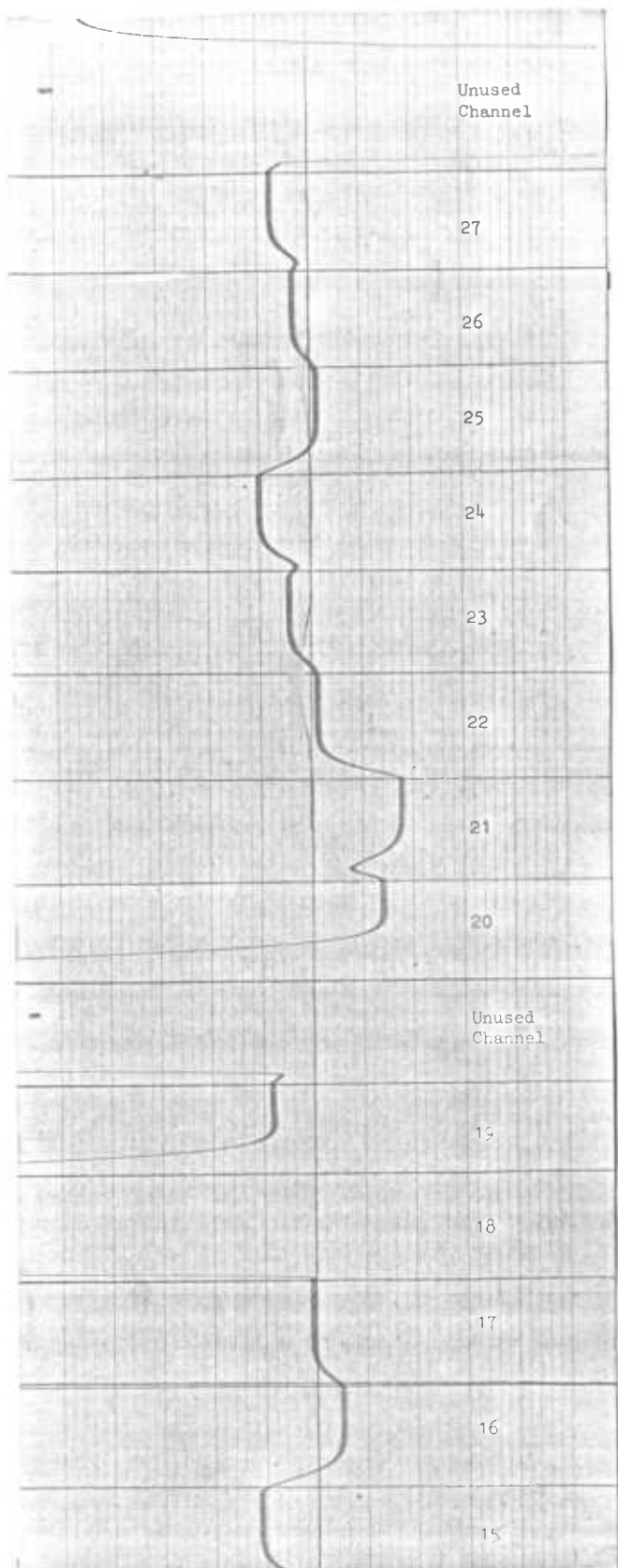
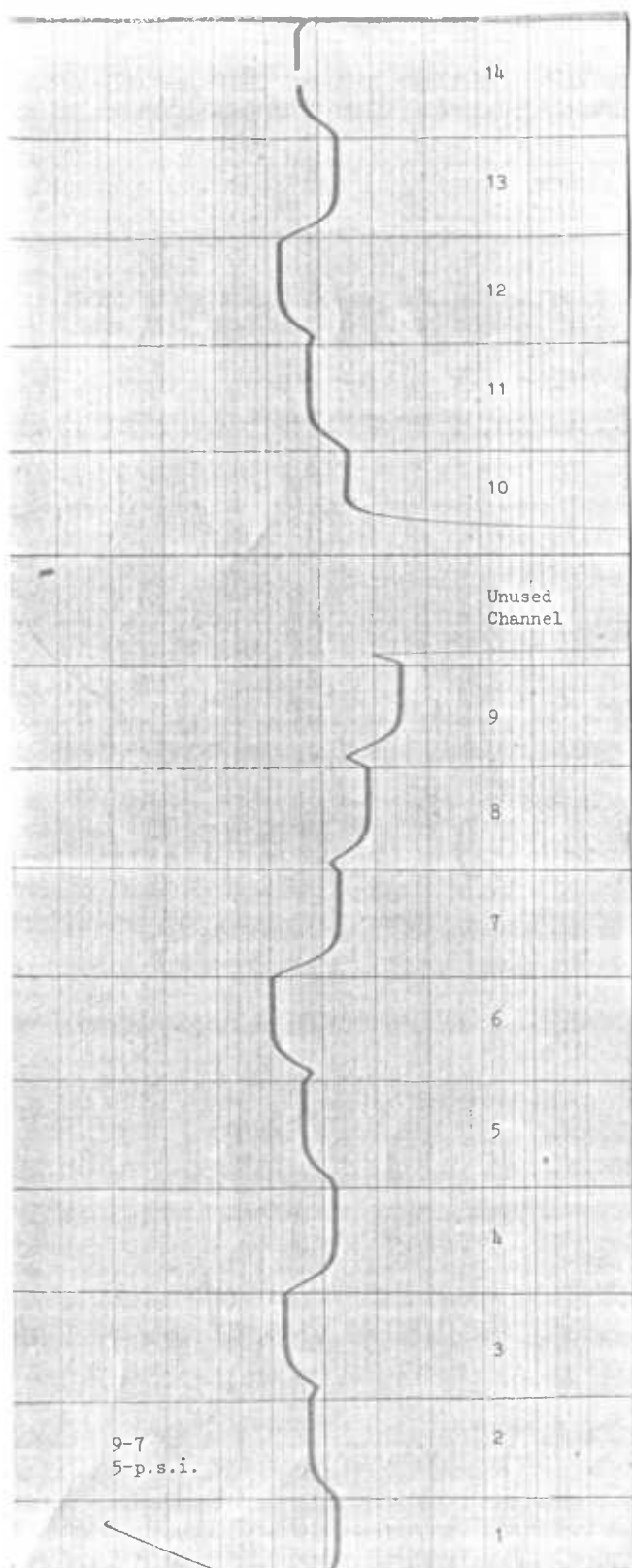












STRESS
9

THE TOTAL NUMBER OF READINGS = 9

INPUT THE STRAINS OF READING NO. 1
-83.43, 208.57, 458.87

1 - .00008343 .00020857 .00045887 .00048491-.00035977 187.26 -94.71

INPUT THE STRAINS OF READING NO. 2
-111.24, 236.39, 570.11

2 - .00011124 .00023639 .00057011 .00059905-.00047390 225.36 -132.81

INPUT THE STRAINS OF READING NO. 3
-139.05, -472.77, -889.92

3 - .00013905-.00047277-.00088992 .00030147-.00091329 -23.48 -428.99

INPUT THE STRAINS OF READING NO. 4
-278.10, 152.96, 458.87

4 - .00027810 .00015296 .00045887 .00050166-.00062680 142.08 -234.62

INPUT THE STRAINS OF READING NO. 5
-166.86, 236.39, 639.63

5 - .00016686 .00023639 .00063963 .00067235-.00060282 238.55 -187.13

INPUT THE STRAINS OF READING NO. 6
0.0, 0.0, 0.0

6 0.000000000.000000000.000000000.000000000.000000000 0.00 0.00

INPUT THE STRAINS OF READING NO. 7
347.63, -876.01, -1056.78

7 - .00034763-.00087601-.00105678 .00073707-.00126545 138.86 -529.62

INPUT THE STRAINS OF READING NO. 8
-111.24, 208.57, 542.30

8 - .00011124 .00020857 .00054230 .00056755-.00047022 209.20 -137.22

INPUT THE STRAINS OF READING NO. 9
-111.24, 152.96, 403.25

9 - .00011124 .00015296 .00040325 .00042542-.00039370 150.48 -119.62

STOP

>STRESS
9

THE TOTAL NUMBER OF READINGS = 9

INPUT THE STRAINS OF READING NO. 1
-333.72, 375.44, 1020.63

1 - .00033372 .00037544 .00102063 .00108165-.00103993 369.54 -338.68

INPUT THE STRAINS OF READING NO. 2
-444.96, 444.96, 1279.27

2 - .00044496 .00044496 .00127927 .00135445-.00135445 452.14 -452.14

INPUT THE STRAINS OF READING NO. 3
-403.25, -834.30, -1863.27

3 - .00040325-.00083430-.00186327 .00064424-.00188179 -36.00 -879.23

INPUT THE STRAINS OF READING NO. 4
-792.59, 278.10, 973.35

4 - .00079259 .00027810 .00097335 .00108475-.00159924 257.74 -638.23

INPUT THE STRAINS OF READING NO. 5
-597.92, 411.59, 1404.41

5 - .00059792 .00041159 .00140441 .00148719-.00167352 458.65 -596.45

INPUT THE STRAINS OF READING NO. 6
0.0, 0.0, 0.0,

6 0.000000000.000000000.000000000.000000000.00000000 0.00 0.00

INPUT THE STRAINS OF READING NO. 7
973.35, -2016.22, -2057.94

7 .00097335-.00201622-.00205794 .00162221-.00266508 329.96 -1101.21

INPUT THE STRAINS OF READING NO. 8
-305.91, 444.96, 1181.93

8 - .00030591 .00044496 .00118193 .00124358-.00110453 443.34 -340.50

INPUT THE STRAINS OF READING NO. 9
-250.29, 305.92, 903.83

9 - .00025029 .00030592 .00090383 .00094691-.00089128 327.38 -284.24

STOP

>STRESS

9

THE TOTAL NUMBER OF READINGS = 9

INPUT THE STRAINS OF READING NO. 1

-584.01, 556.20, 1612.99

1 -.00058401 .00055620 .00161299 .00170999-.00173780 565.18 -585.75

INPUT THE STRAINS OF READING NO. 2

-806.49, 653.54, 2030.14

2 -.00080649 .00065354 .00203014 .00215304-.00230599 687.69 -800.81

INPUT THE STRAINS OF READING NO. 3

-806.49, -1585.17, -2808.81

3 -.00080649-.00158517-.00280881 .00046347-.00285513 -330.47 -1438.28

INPUT THE STRAINS OF READING NO. 4

-1446.12, 278.10, 1612.98

4 -.00144612 .00027810 .00161298 .00177607-.00294409 355.93 -1219.74

INPUT THE STRAINS OF READING NO. 5

-1140.21, -556.20, -2252.61

5 -.00114021-.00055620-.00225261 .00058624-.00228265 -148.45 -1106.13

INPUT THE STRAINS OF READING NO. 6

0.0, 0.0, 0.0

6 0.000000000.000000000.000000000.000000000.00000000 0.00 0.00

INPUT THE STRAINS OF READING NO. 7

1585.17, -2892.24, -3142.53

7 .00158517-.00289224-.00314253 .00269414-.00400121 634.19 -1600.83

INPUT THE STRAINS OF READING NO. 8

-736.97, 584.01, 1654.70

8 -.00073697 .00058401 .00165470 .00177642-.00192938 561.97 -675.09

INPUT THE STRAINS OF READING NO. 9

-528.39, 458.87, 1529.55

9 -.00052839 .00045887 .00152955 .00160559-.00167511 521.87 -573.28

STOP

>STRESS

9

THE TOTAL NUMBER OF READINGS = 9

INPUT THE STRAINS OF READING NO. 1

-625.73, 611.82, 1765.94

1 -.00062573 .00061182 .00176594 .00187082-.00188473 621.69 -681.98

INPUT THE STRAINS OF READING NO. 2

-917.73, 681.35, 2155.28

2 -.00091773 .00068135 .00215528 .00229177-.00252815 717.08 -891.89

INPUT THE STRAINS OF READING NO. 3

-945.54, -1863.27, -3003.48

3 -.00094554-.00186327-.00300348 .00025920-.00306801 -483.29 -1593.97

INPUT THE STRAINS OF READING NO. 4

-1599.08, 286.39, 1752.03

4 -.00159908 .00023639 .00175203 .00191934-.00328203 364.26 -1372.04

INPUT THE STRAINS OF READING NO. 5

-1268.14, 645.19, 2419.47

5 -.00126814 .00064519 ,00241947 .00258218-.00320513 735.60 -1196.30

INPUT THE STRAINS OF READING NO. 6

0.0, 0.0, 0.0

6 0.000000000.000000000.000000000.000000000.000000000 0.00 0.00

INPUT THE STRAINS OF READING NO. 7

1710.32, -2933.95, -3267.68

7 .00171032-.00293395-.00326768 .00291606-.00413969 725.20 -1630.13

INPUT THE STRAINS OF READING NO. 8

-806.49, 611.82, 2071.85

8 -.00080649 .00061182 .00207185 .00218483-.00237950 689.84 -833.81

INPUT THE STRAINS OF READING NO. 9

-556.20, 500.59, 1646.35

9 -.00055620 .00050059 .00164635 .00172776-.00178337 565.47 -606.60

STOP

>STRESS
9

THE TOTAL NUMBER OF READINGS = 9

INPUT THE STRAINS OF READING NO. 1

-486.68, 444.96, 1279.27

1 -.00048668 .00044496 .00127927 .00136020-.00140192 445.59 -476.45

INPUT THE STRAINS OF READING NO. 2

-723.06, 472.77, 1571.27

2 -.00072306 .00047277 .00157127 .00167356-.00192385 507.89 -692.99

INPUT THE STRAINS OF READING NO. 3

-695.25, -1251.45, -2002.32

3 -.00069525-.00125145-.00200232 .00009254-.00203924 -364.03 -1075.65

INPUT THE STRAINS OF READING NO. 4

-1223.64, 139.05, 1307.07

4 -.00122364 .00013905 .00130707 .00142859-.00251318 256.86 -1058.97

INPUT THE STRAINS OF READING NO. 5

-1001.16, 389.34, 1779.84

5 -.00100116 .00038934 .00177984 .00189266-.00250448 507.69 -960.16

INPUT THE STRAINS OF READING NO. 6

0.0, 0.0, 0.0,

6 0.000000000.000000000.000000000.000000000.00000000 0.00 0.00

INPUT THE STRAINS OF READING NO. 7

1265.36, -2016.22, -2113.56

7 .00126536-.00201622-.00211356 .00201482-.00276568 520.26 -1075.56

INPUT THE STRAINS OF READING NO. 8

-667.44, 431.06, 1557.37

8 -.00066744 .00043106 .00155737 .00164510-.00188148 501.21 -676.02

INPUT THE STRAINS OF READING NO. 9

-417.15, 375.44, 1237.55

9 -.00041715 .00037544 .00123755 .00129848-.00134019 424.99 -455.84

STOP

>STRESS
9

THE TOTAL NUMBER OF READINGS = 9

INPUT THE STRAINS OF READING NO. 1
-125.15, 166.86, 403.25

1 - .00012515 .00016686 .00040325 .00043018-.00038847 152.06 -121.21

INPUT THE STRAINS OF READING NO. 2
-139.05, 208.58, 528.40

2 - .00013905 .00020858 .00052840 .00055811-.00048858 200.41 -148.99

INPUT THE STRAINS OF READING NO. 3
-180.77, -500.58, -903.83

3 - .00018077-.00050058-.00090383 .00024474-.00092609 -56.52 -447.37

INPUT THE STRAINS OF READING NO. 4
-305.91, 125.15, 431.06

4 - .00030591 .00012515 .00043106 .00047385-.00065461 121.51 -255.19

INPUT THE STRAINS OF READING NO. 5
-194.67, 208.58, 639.63

5 - .00019467 .00020858 .00063963 .00067098-.00065707 226.81 -216.52

INPUT THE STRAINS OF READING NO. 6
0.0, 0.0, 0.0

6 0.000000000.000000000.000000000.000000000.000000000 0.00 0.00

INPUT THE STRAINS OF READING NO. 7
417.15, -848.20, -1001.16

7 .00041715-.00084820-.00100116 .00079319-.00122424 177.33 -496.12

INPUT THE STRAINS OF READING NO. 8
-69.52, 250.29, 570.11

8 - .00006952 .00025029 .00057011 .00059606-.00041529 235.65 -101.96

INPUT THE STRAINS OF READING NO. 9
-83.43, 166.87, 431.06

9 - .00008343 .00016687 .00043106 .00045068-.00036724 167.37 -105.66

STOP

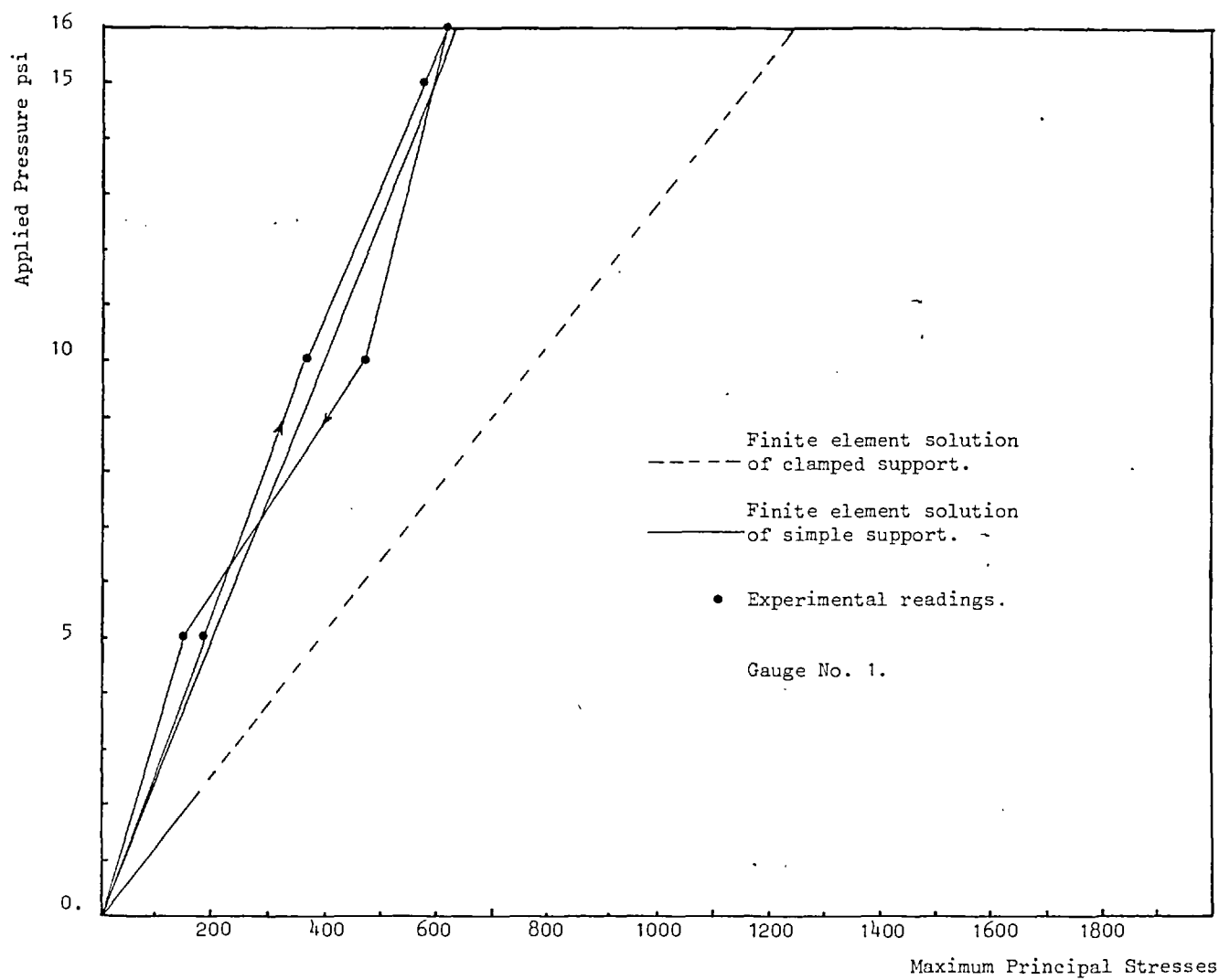


Fig. 2.40. Comparison of principal stresses.

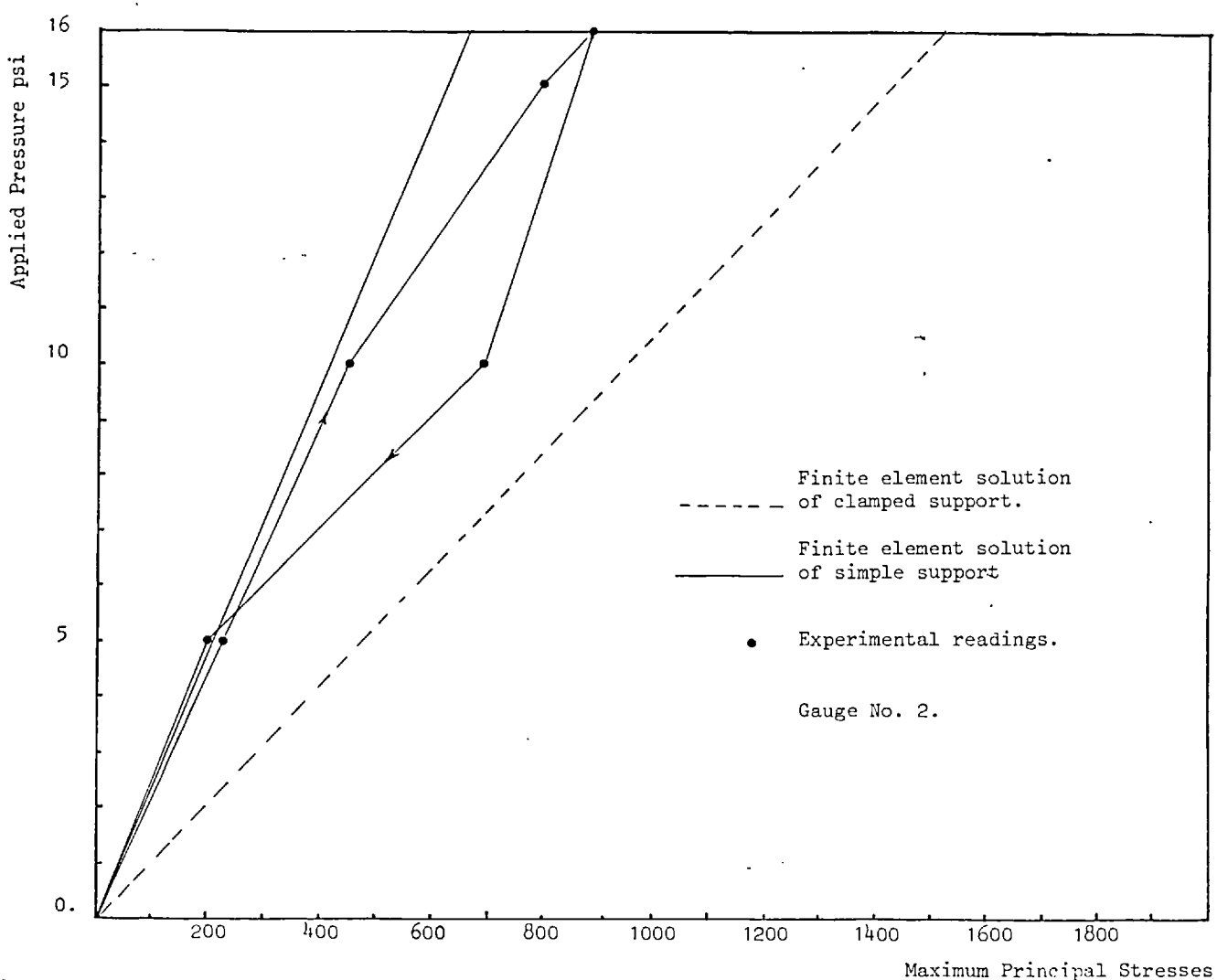


Fig. 2.41. Comparison of principal stresses.

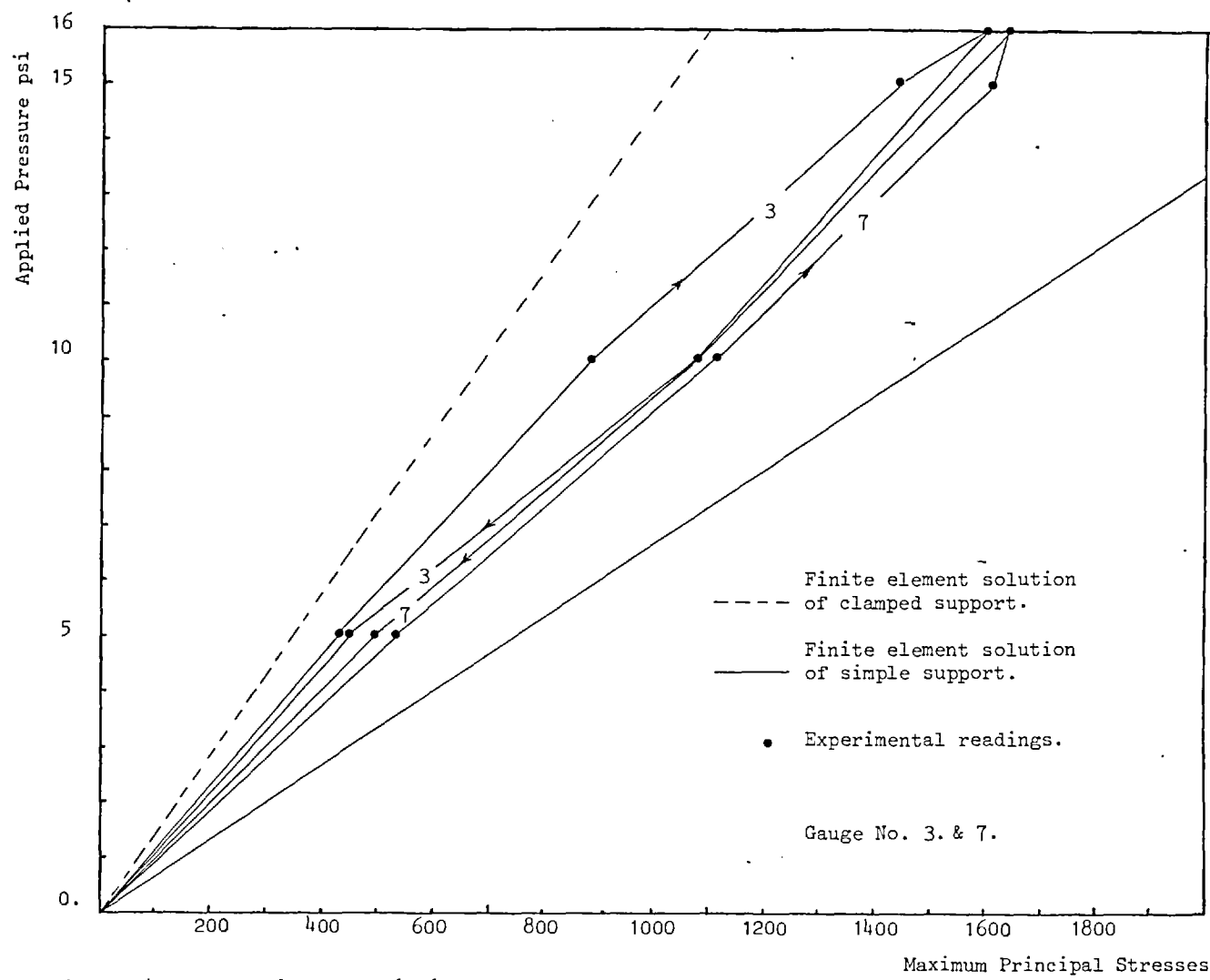


Fig. 2.42. Comparison of principal stresses.

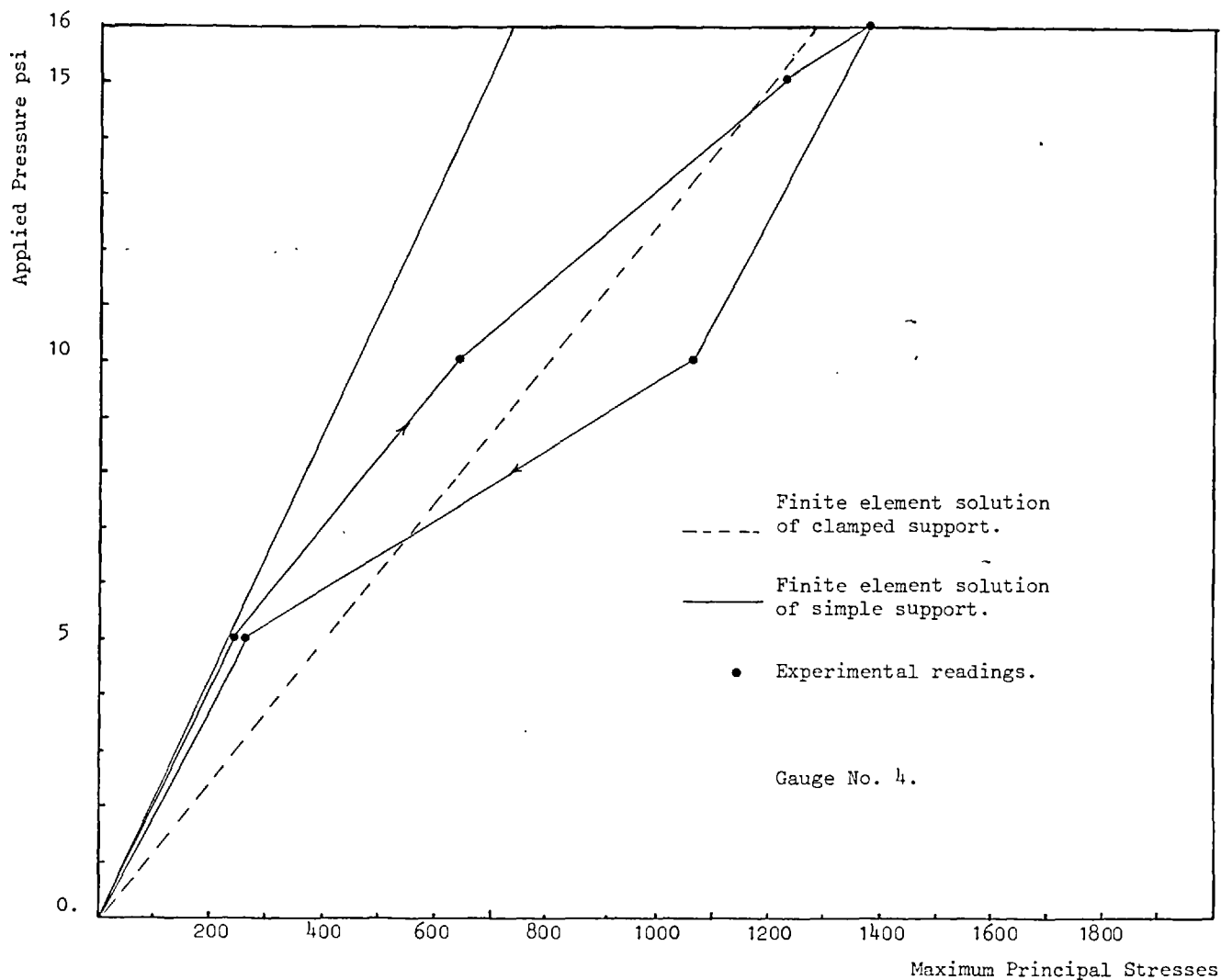


Fig. 2.43. Comparison of principal stresses.

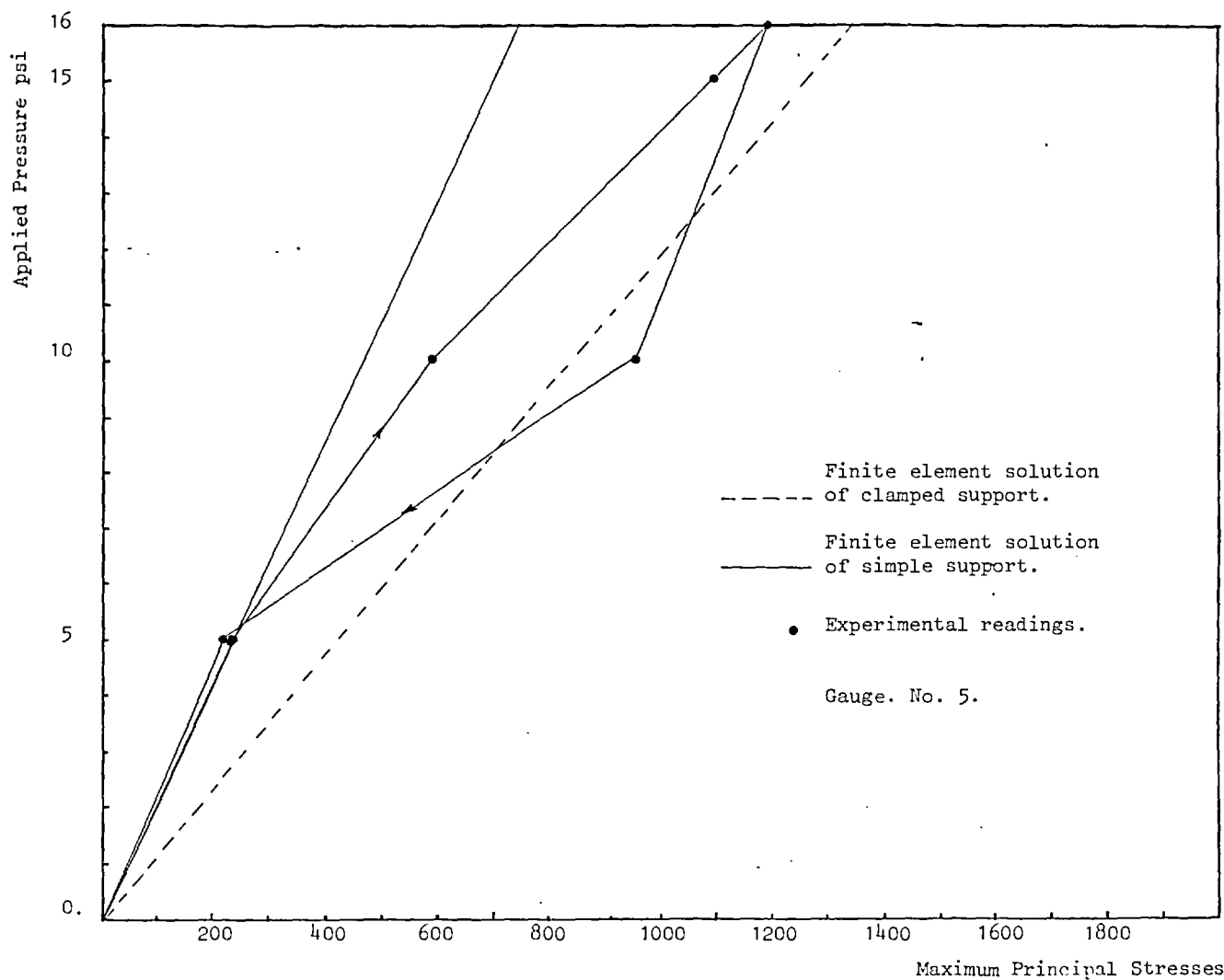


Fig. 2.44. Comparison of principal stresses

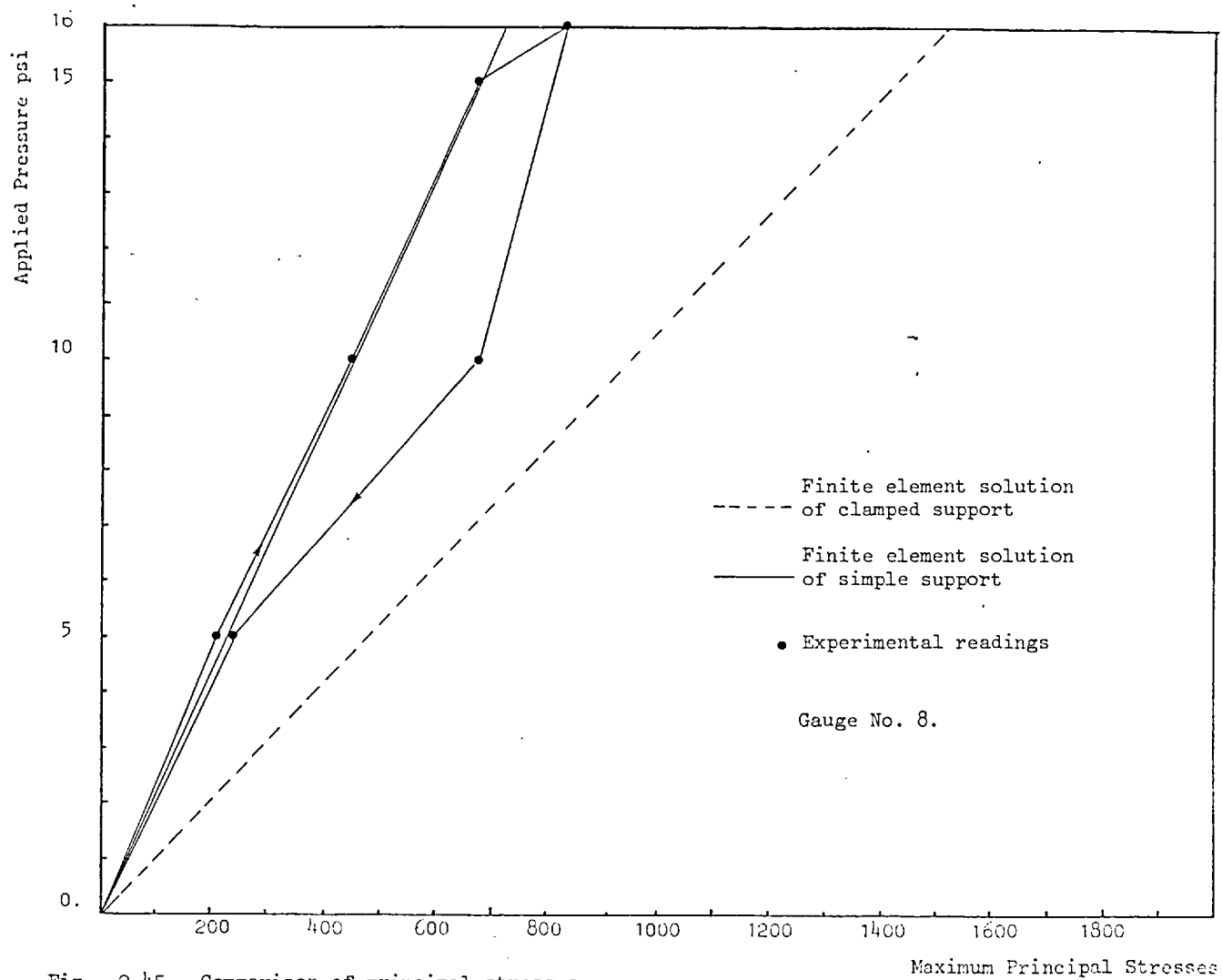


Fig. 2.45. Comparison of principal stresses

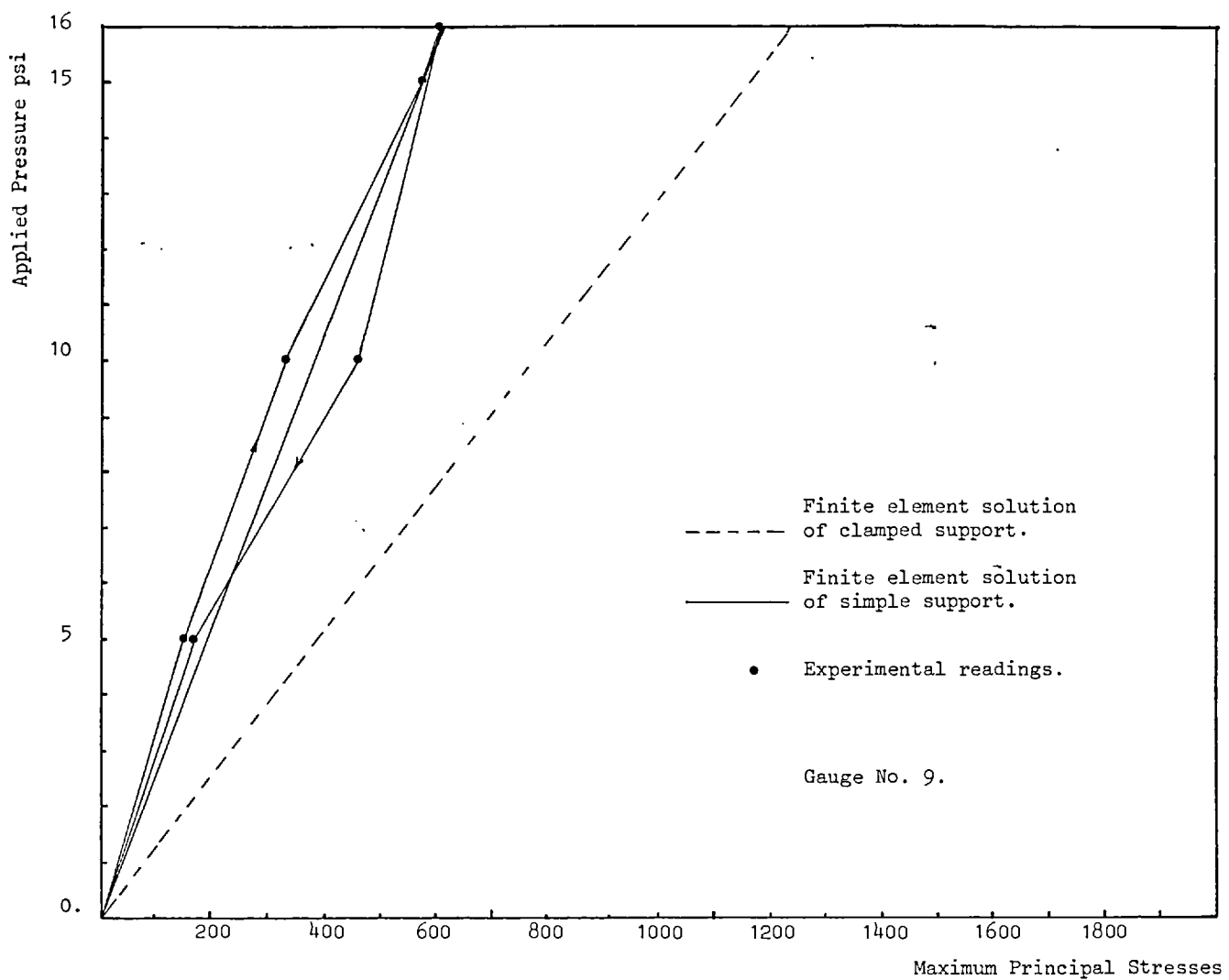


Fig. 2.46. Comparison of principal stresses

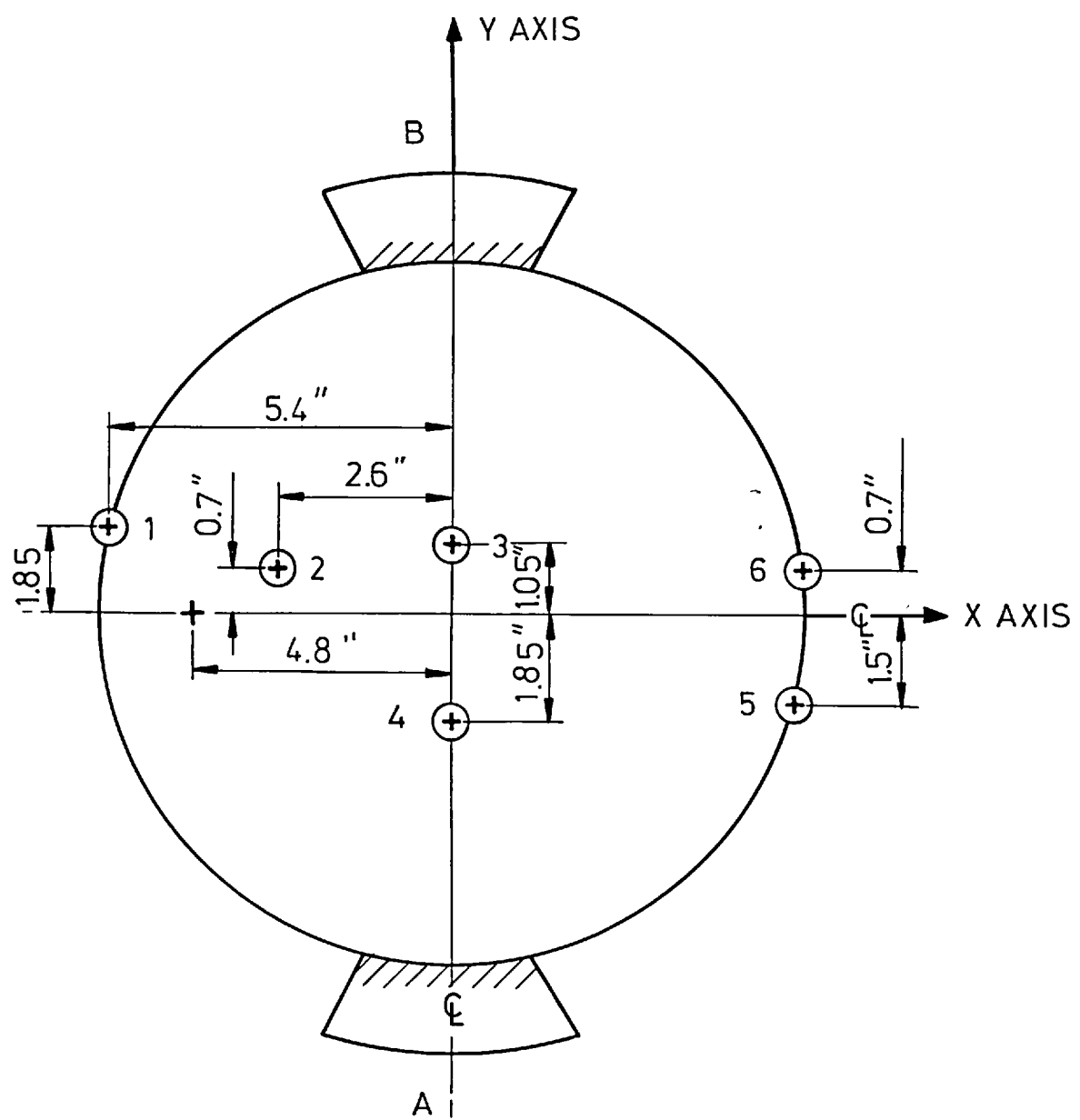
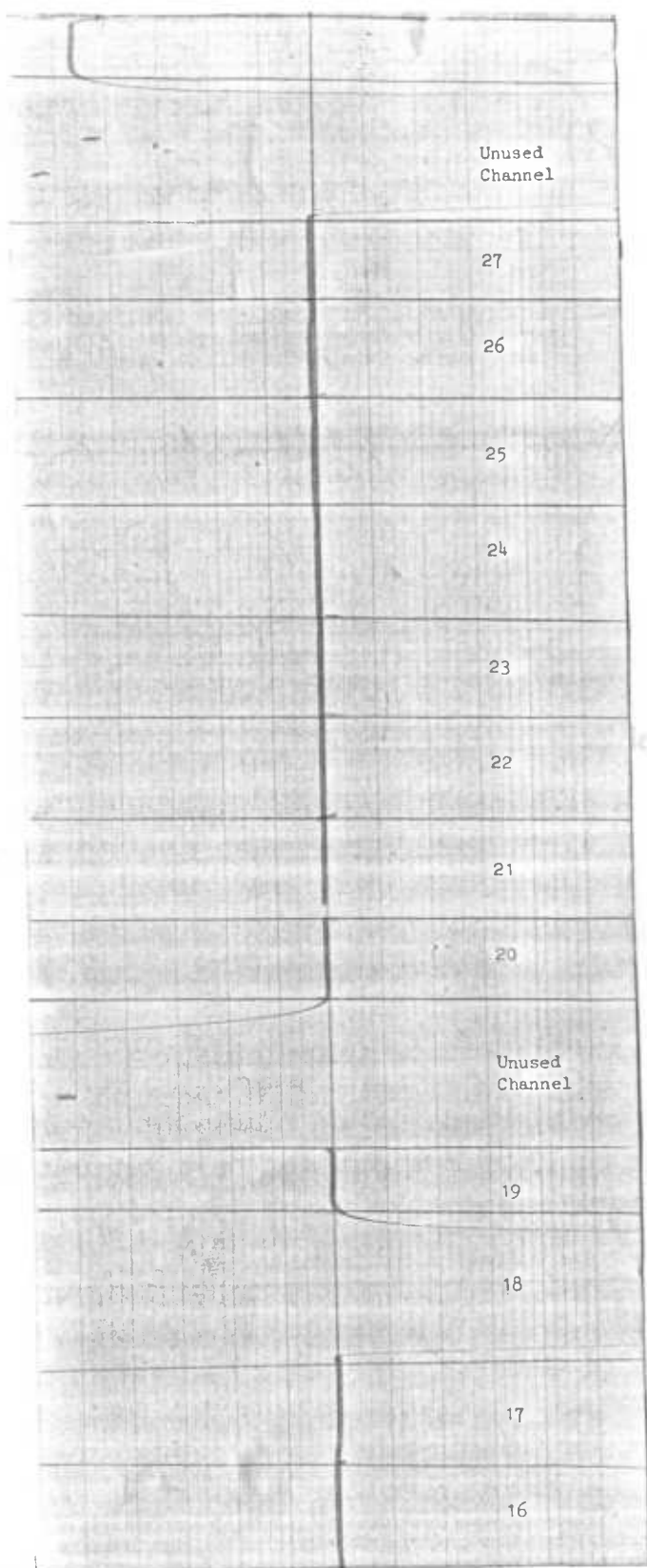
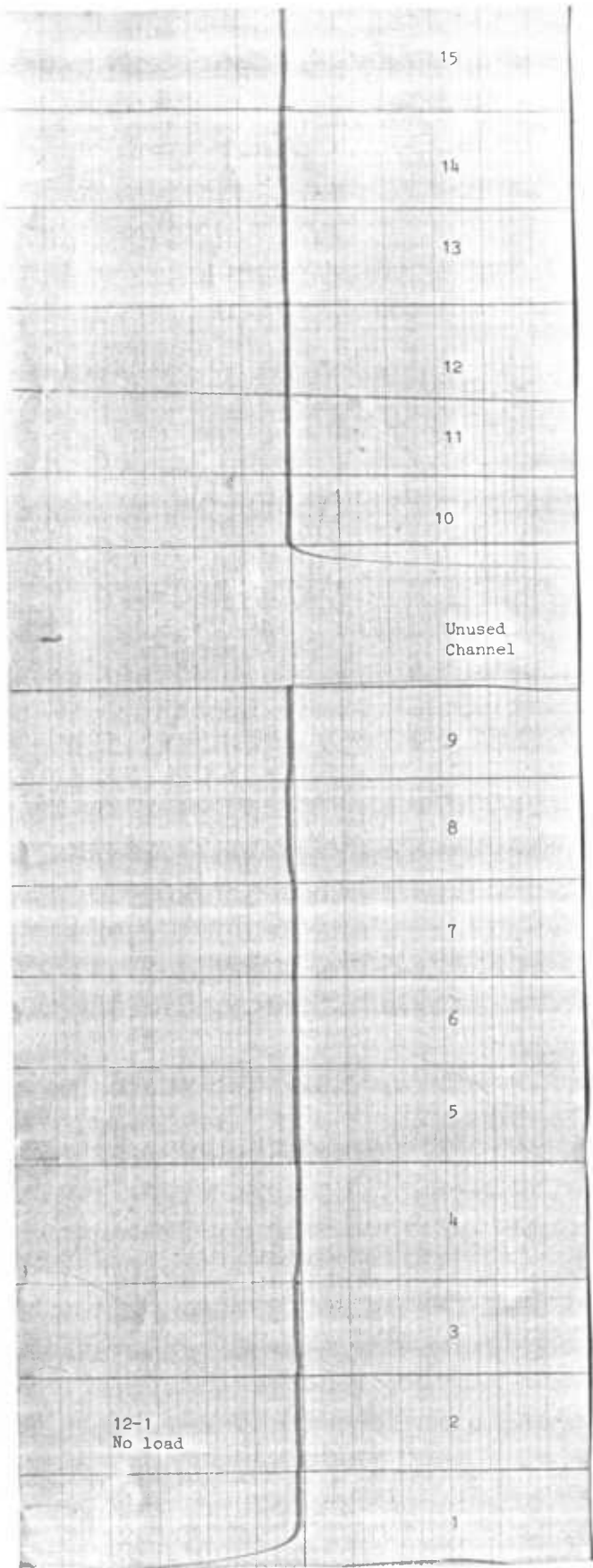
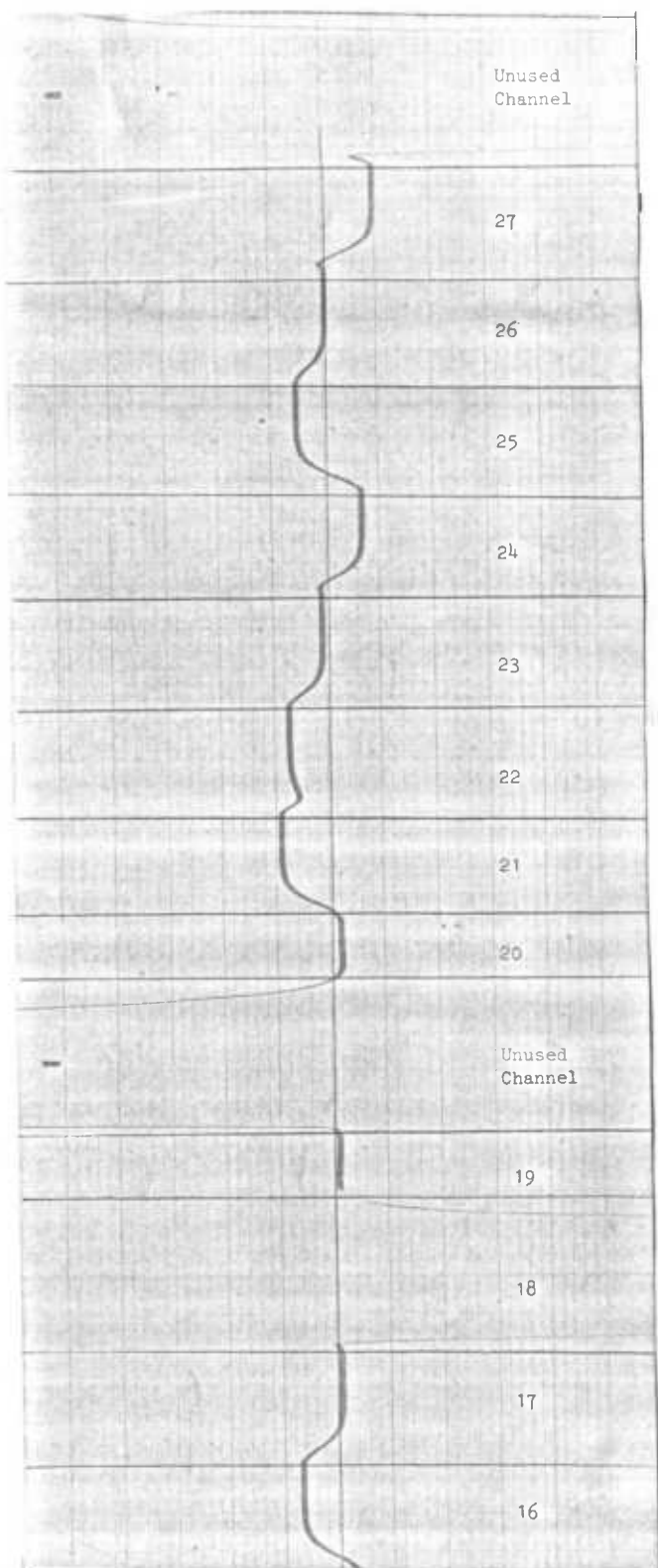
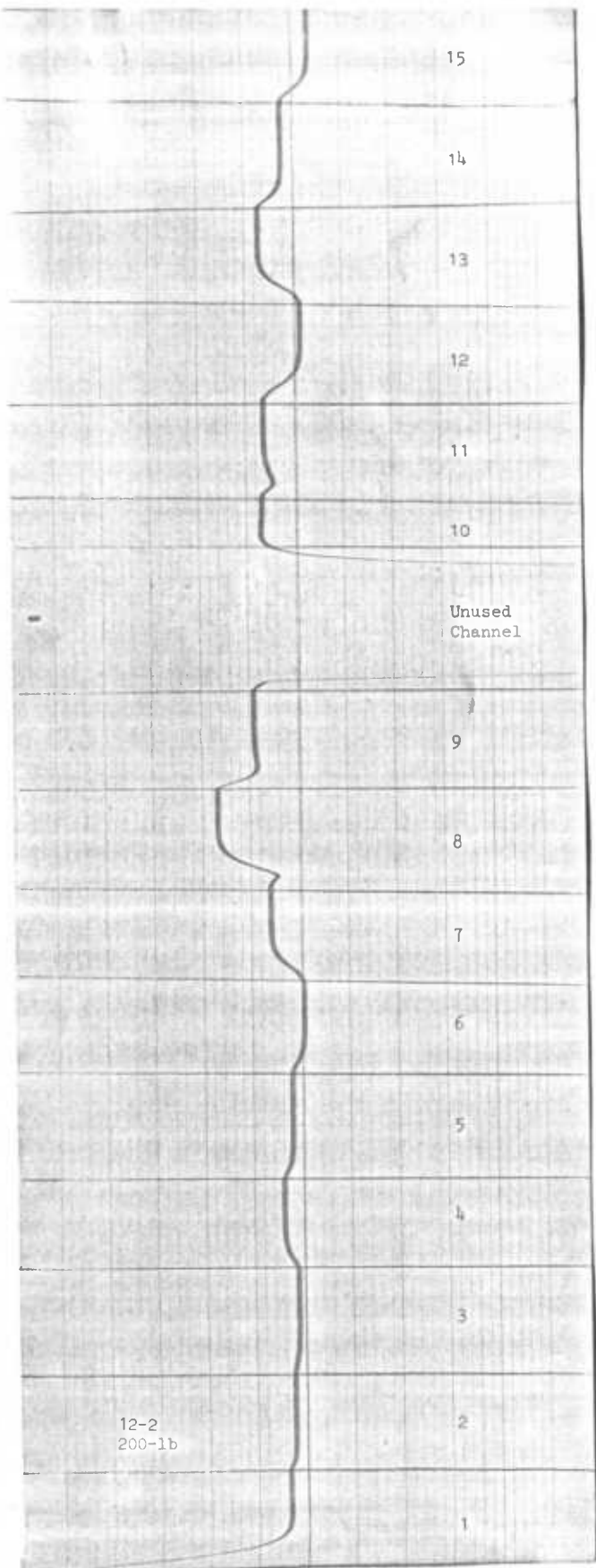
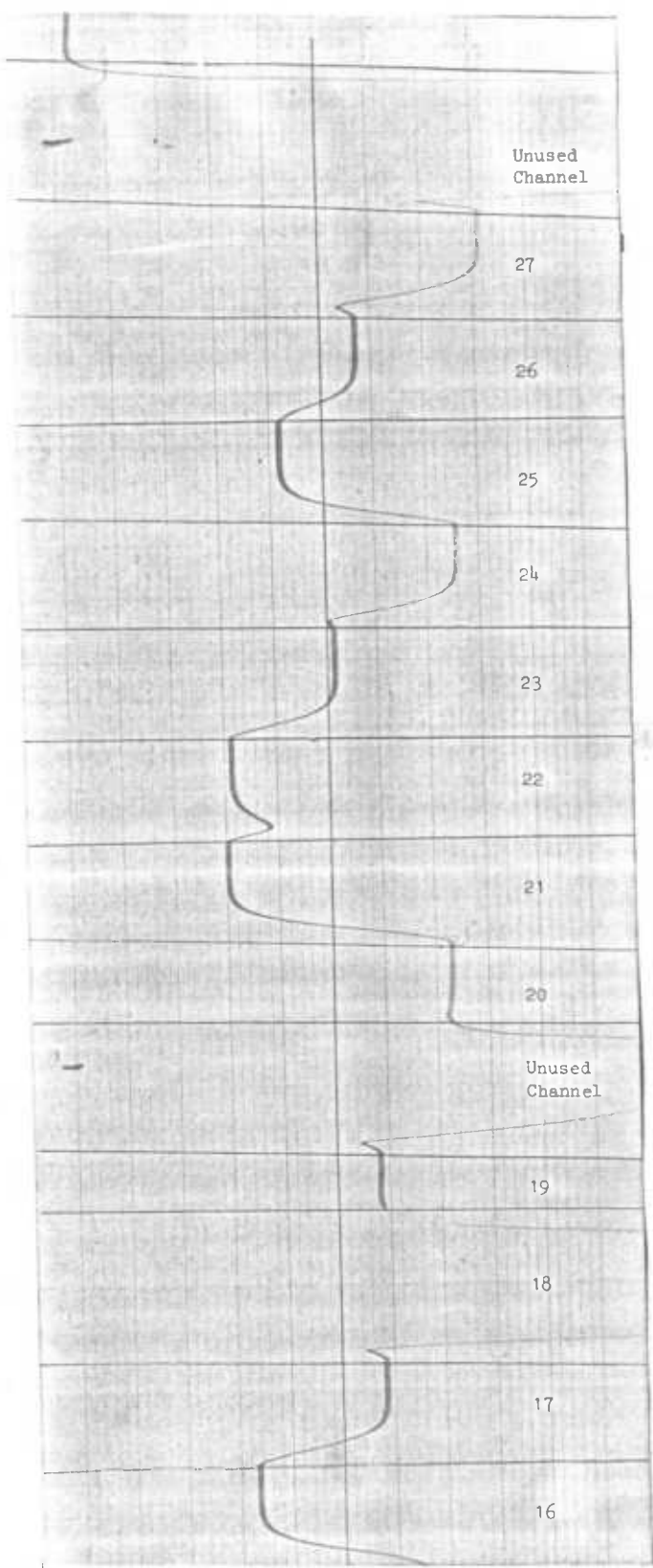
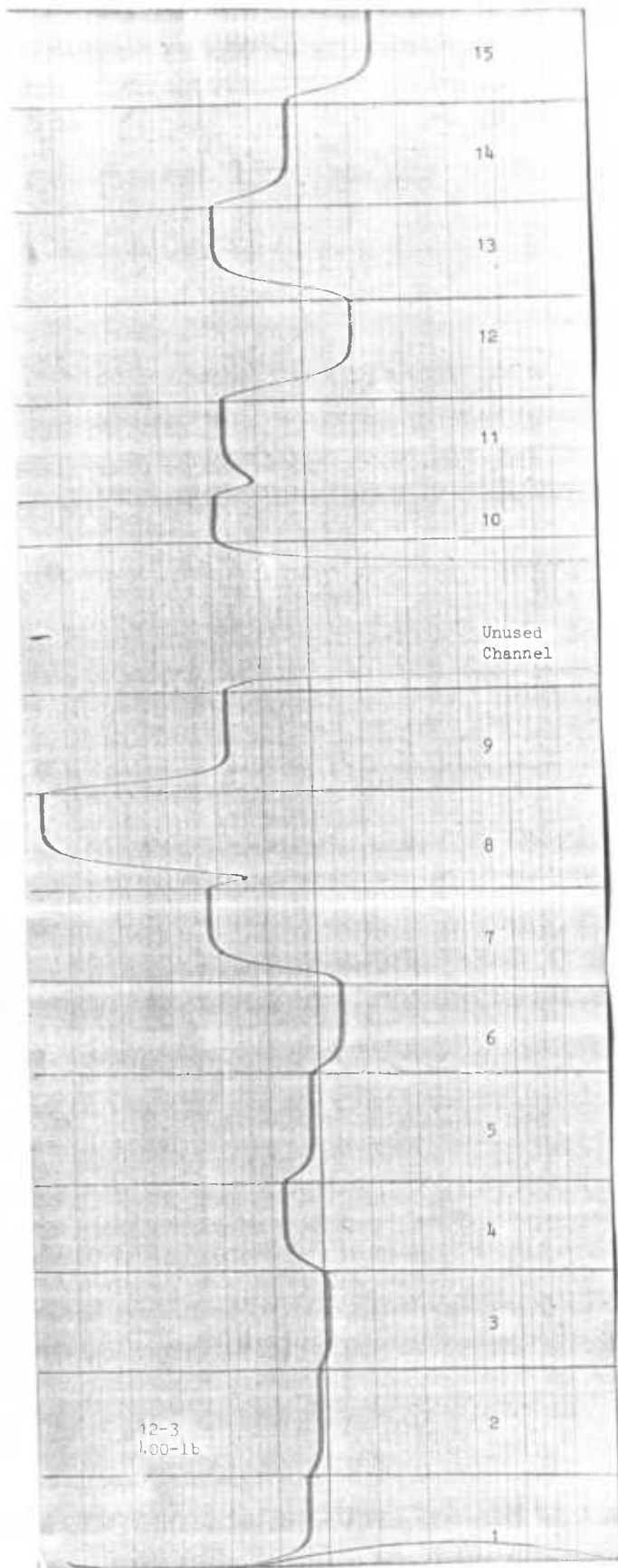
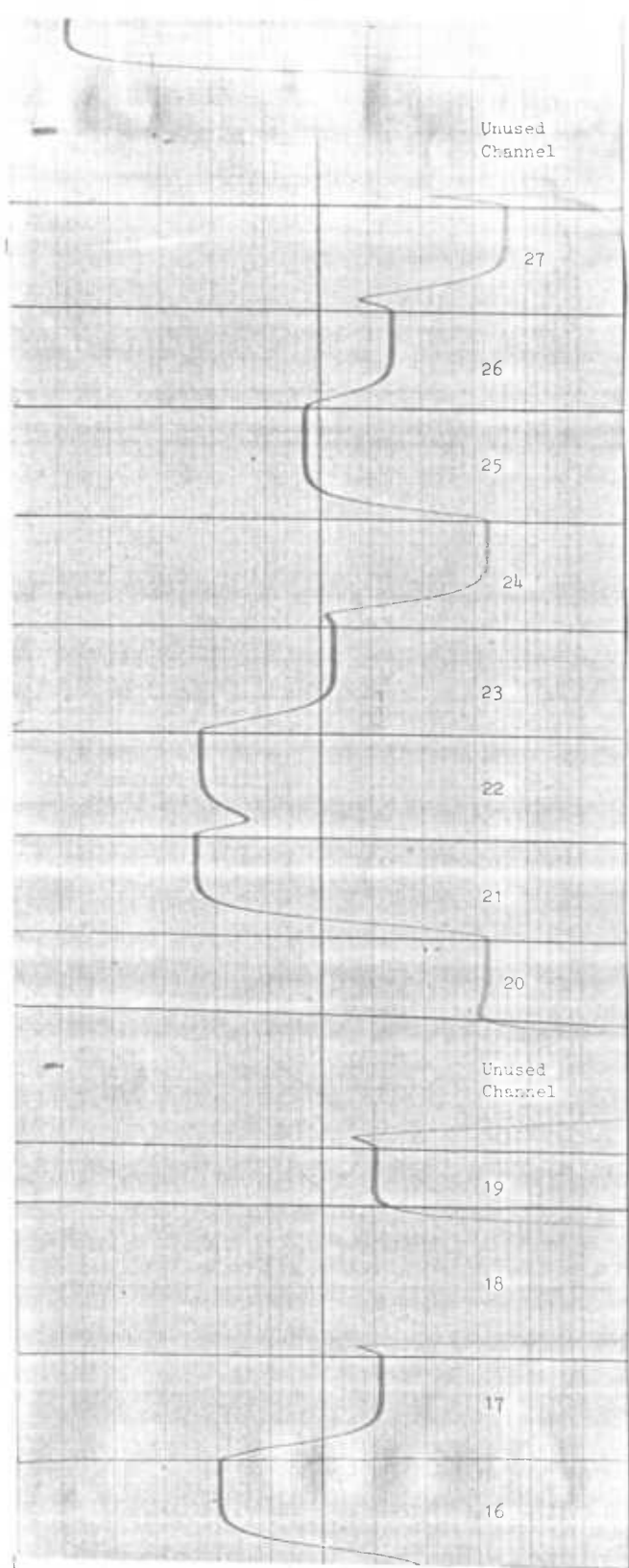
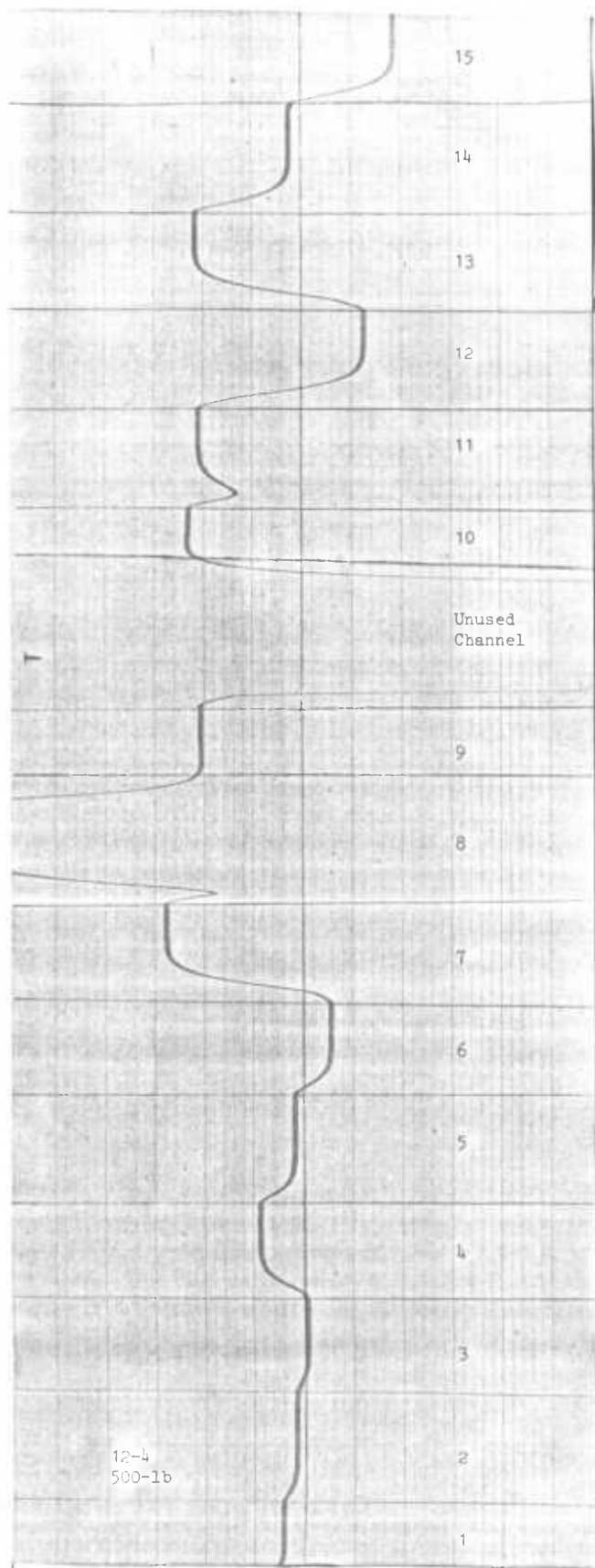


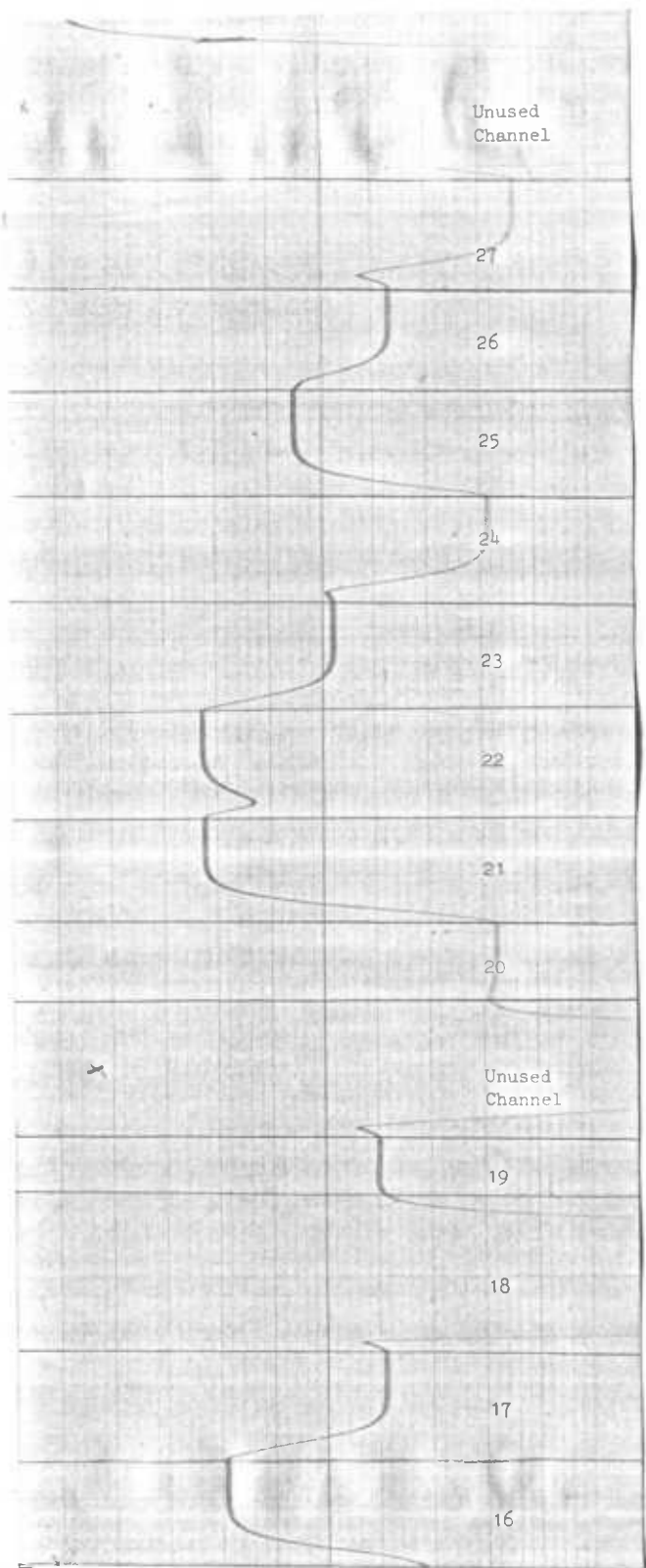
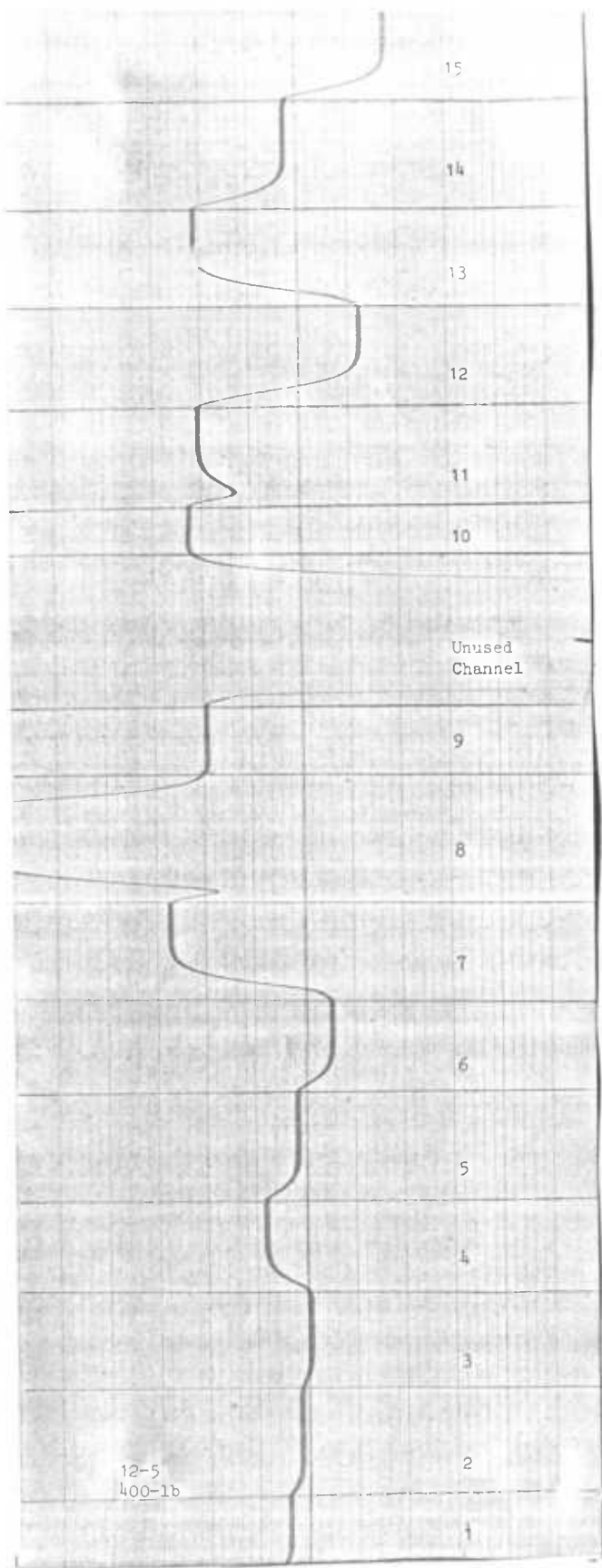
Fig. 2.47. Dial gauge and point load locations.

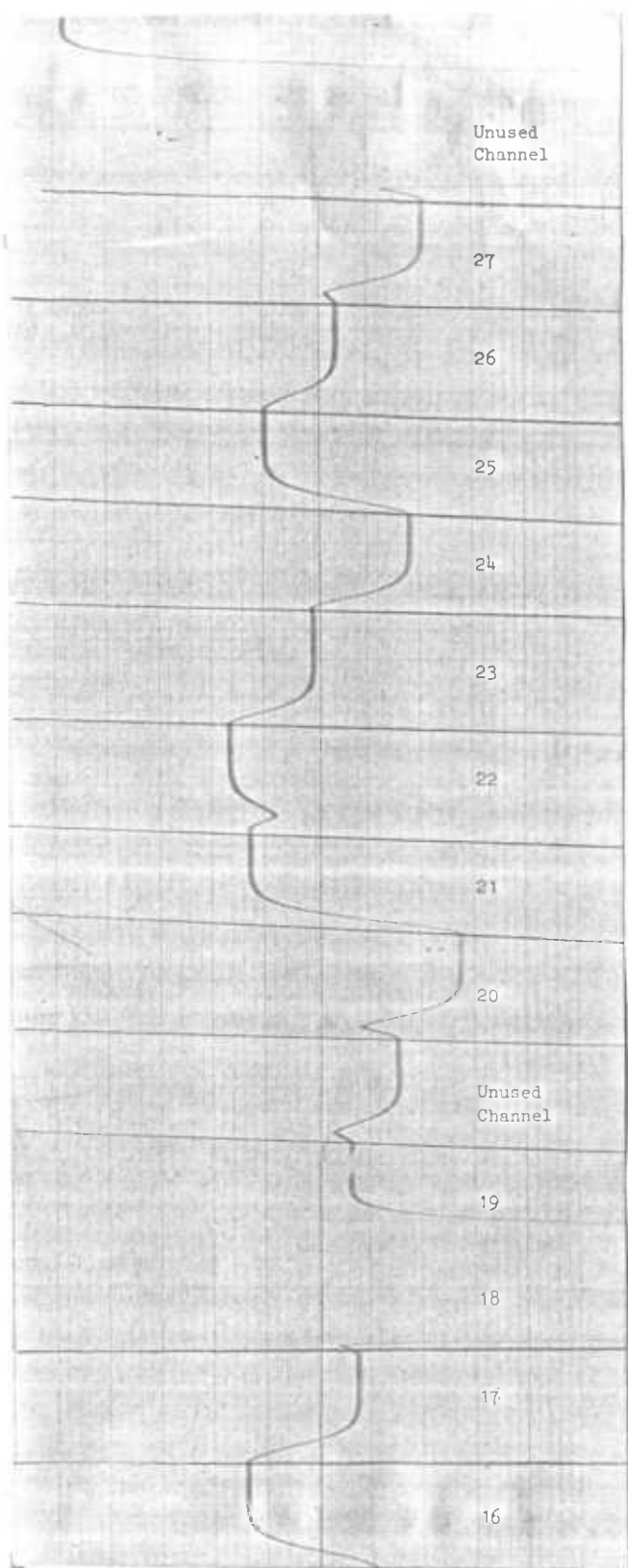
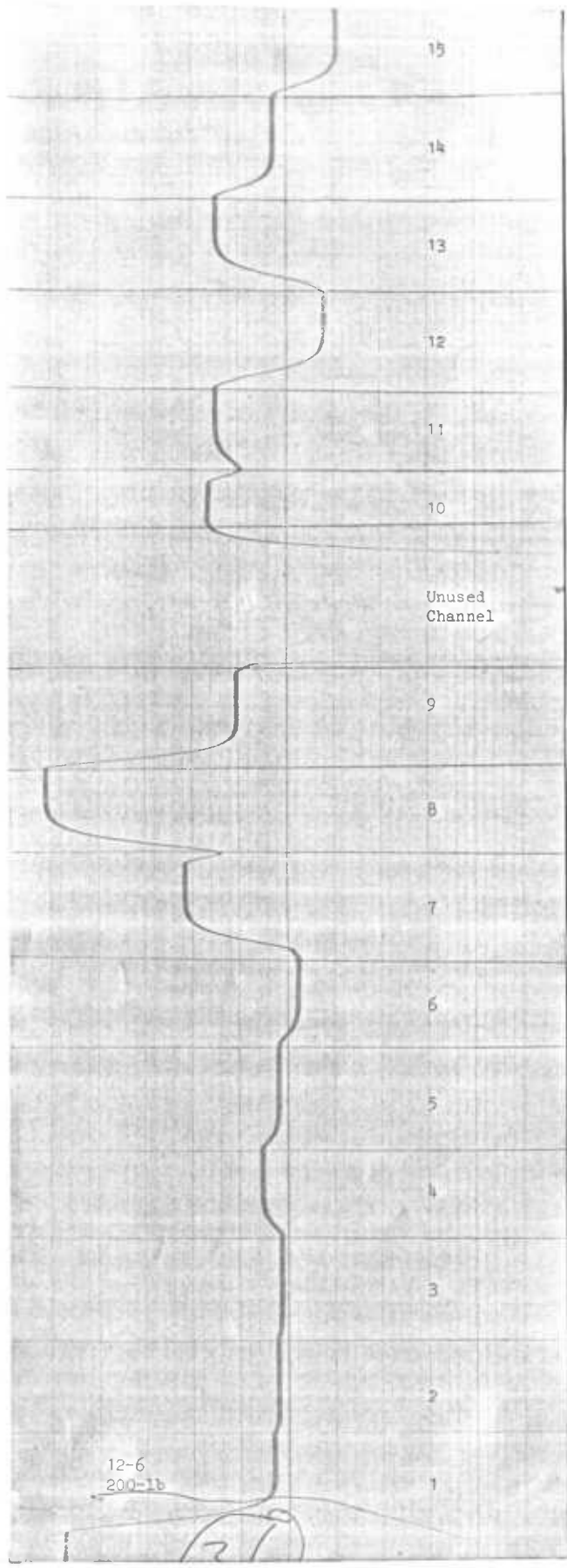












STRESS

9

THE TOTAL NUMBER OF READINGS = 9

INPUT THE STRAINS OF READING NO. 1
97.34, 83.43, 27.81

1 .00009734 .00008343 .00002781 .00015335 .00002742 87.86 45.63

INPUT THE STRAINS OF READING NO. 2
236.29, 139.05, 0.0

2 .00023639 .000139050.00000000 .00038165-.00000621 203.56 74.09

INPUT THE STRAINS OF READING NO. 3
361.53, 889.92, 528.39

3 .00036153 .00088992 .00052839 .00090728 .00034417 556.74 368.77

INPUT THE STRAINS OF READING NO. 4
417.15, 361.53, -55.62

4 .00041715 .00036153-.00005562 .00083517-.00005649 436.76 139.11

INPUT THE STRAINS OF READING NO. 5
417.15, 152.96, -194.67

5 .00041715 .00015296-.00019467 .00078263-.00021252 376.91 44.71

INPUT THE STRAINS OF READING NO. 6
0.0, 0.0, 0.0,

6 0.000000000.000000000.000000000.000000000.00000000 0.00 0.00

INPUT THE STRAINS OF READING NO. 7
-55.62, -83.43, 514.49

7 -.00005562-.00008343 .00051449 .00051466-.00065371 143.59 -246.43

INPUT THE STRAINS OF READING NO. 8
417.15, 55.62, -889.34

8 .00041715 .00005562-.00038934 .00088770-,00041493 392.24 -42.60

INPUT THE STRAINS OF READING NO. 9
305.91, -55.62, -556.20

9 .00030591-.00005562-.00055620 .00083006-.00057977 327.86 -142.76

STOP

>STRESS

9

THE TOTAL NUMBER OF READINGS = 9

INPUT THE STRAINS OF READING NO. 1

139.05, 27.81, -83.43

1 .00013905 .00002781-.00008343 .00025932-.00009246 120.41 2.99

INPUT THE STRAINS OF READING NO. 2

444.96, 97.34, -264.20

2 .00044496 .00009734-.00026420 .00083401-.00029171 388.42 12.64

INPUT THE STRAINS OF READING NO. 3

1237.55, 3031.29, 1001.16

3 .00123755 .00303129 .00100116 .00357964 .00068920 2060.95 1096.07

INPUT THE STRAINS OF READING NO. 4

1070.69, 945.54, -556.20

4 .00107069 .00094554-.00055620 .00257368-.00055745 1268.16 222.94

INPUT THE STRAINS OF READING NO. 5

1015.07, 139.05, -848.21

5 .00101507 .00013905-.00084821 .00206812-.00091400 924.50 -70.98

INPUT THE STRAINS OF READING NO. 6

0.0, 0.0, 0.0,

6 .000000000.000000000.000000000.000000000.00000000 0.00 0.00

INPUT THE STRAINS OF READING NO. 7

-472.77, -1293.17, 1112.4,

7 -.00047277-.00129317 .00111240 .00115413-.00292007 27.02 -1333.02

INPUT THE STRAINS OF READING NO. 8

1084.59, -83.43, -1446.12

8 .00108459-.00008343-.00144612 .00253299-.00153183 1048.66 -308.25

INPUT THE STRAINS OF READING NO. 9

472.77, -500.58, -1752.03

9 .00047277-.00050058-.00175203 .00179107-.00181888 592.25 -612.81

STOP

DSTRESS

9

THE TOTAL NUMBER OF READINGS = 9

INPUT THE STRAINS OF READING NO. 1

166.86, 55.62, -83.43

1 .00016686 .00005562-.00008343 .00031370-.00002122 149.85 14.68

INPUT THE STRAINS OF READING NO. 2

500.58, 111.24, -305.91

2 .00050058 .00011124-.00030591 .00094795-.00039613 440.56 11.91

INPUT THE STRAINS OF READING NO. 3

0.0, 0.0, 0.0

3 .000000000.000000000.000000000.000000000.00000000 0.00 0.00

INPUT THE STRAINS OF READING NO. 4

1307.07, 1195.83, -695.25

4 .00130707 .00119583-.00069525 .00319894-.00069604 1575.62 275.40

INPUT THE STRAINS OF READING NO. 5

1237.55, 139.05, -1042.88

5 .00123755 .00013905-.00104288 .00250452-.00112792 1115.32 -97.25

INPUT THE STRAINS OF READING NO. 6

0.0, 0.0, 0.0

6 .000000000.000000000.000000000.000000000.00000000 0.00 0.00

INPUT THE STRAINS OF READING NO. 7

-556.20, -1807.65, 1362.69

7 -.00055620-.00180765 .00136269 .00143849-.00380234 .65 -1748.83

INPUT THE STRAINS OF READING NO. 8

1307.07, -152.96, -1835.46

8 .00130707-.00015296-.00183546 .00309760-.00194349 1268.16 -414.64

INPUT THE STRAINS OF READING NO. 9

166.86, -862.11, -2044.04

9 .00016686-.00086211-.00204404 .00142509-.00212034 334.68 -848.85

STOP

>STRESS

9

THE TOTAL NUMBER OF READINGS = 9

INPUT THE STRAINS OF READING NO. 1

139.05, 27.81, -83.43

1 .00013905 .00002781-.00008343 .00025932-.00009246 120.41 2.99

INPUT THE STRAINS OF READING NO. 2

472.77, 83.43, -305.91

2 .00047277 .00008343-.00030591 .00089370-.00033750 411.17 .17

INPUT THE STRAINS OF READING NO. 3

1557.36, -83.43, 1112.40

3 .00155736-.00008343 .00111240 .00163918-.00016525 846.20 243.65

INPUT THE STRAINS OF READING NO. 4

1307.07, 1168.02, -695.25

4 .00130707 .00116802-.00069525 .00317159-.00069650 1560.84 269.61

INPUT THE STRAINS OF READING NO. 5

1195.83, 139.05, -1015.07

5 .00119583 .00013905-.00101507 .00243097-.00109609 1082.30 -95.09

INPUT THE STRAINS OF READING NO. 6

0.0, 0.0, 0.0,

6 0.000000000.000000000.000000000.000000000.00000000 0.00 0.00

INPUT THE STRAINS OF READING NO. 7

-584.01, -1835.46, 1279.26

7 -.00058401-.00183546 .00127926 .00135671-.00377618 -37.94 -1751.38

INPUT THE STRAINS OF READING NO. 8

1293.17, -139.05, -1779.84

8 .00129317-.00013905-.00177984 .00304035-.00188623 1249.05 -395.52

INPUT THE STRAINS OF READING NO. 9

305.91, -806.49, -2057.94

9 .00030591-.00080649-.00205794 .00164099-.00214157 446.24 -816.45

STOP

>STRESS

9

THE TOTAL NUMBER OF READINGS = 9

INPUT THE STRAINS OF READING NO. 1
83.43, 55.62, 13.91

1 .00008343 .00005562 .00001391 .00012685 .00001220 70.55 32.28

INPUT THE STRAINS OF READING NO. 2
305.91, 111.24, -125.15

2 .00030591 .00011124-.00012515 .00055620-.00013905 270.30 38.21

INPUT THE STRAINS OF READING NO. 3
1223.64, 2850.53, 597.92

3 .00122364 .00285053 .00059792 .00369023 .00038394 2058.37 954.68

INPUT THE STRAINS OF READING NO. 4
931.64, 862.11, -458.87

4 .00093164 .00086211-.00045887 .00225307-.00045932 1116.00 210.56

INPUT THE STRAINS OF READING NO. 5
862.11, 166.86, -597.92

5 .00086211 .00016686-.00059792 .00167994-.00065097 769.54 -8.56

INPUT THE STRAINS OF READING NO. 6
0.0, 0.0, 0.0

6 0.000000000.000000000.000000000.000000000.000000000 0.00 0.00

INPUT THE STRAINS OF READING NO. 7
-444.96, -1501.74, 723.06

7 -.00044496-.00150174 .00072306 .00080345-.00275015 -126.72 -1312.97

INPUT THE STRAINS OF READING NO. 8
653.54, 0.0, -1028.97

8 .000653540.00000000-.00102897 .00172133-.00106779 707.19 -223.87

INPUT THE STRAINS OF READING NO. 9
556.20, -305.91, -1168.02

9 .00055620-.00030591-.00116802 .00148826-.00123797 547.58 -362.48
STOP

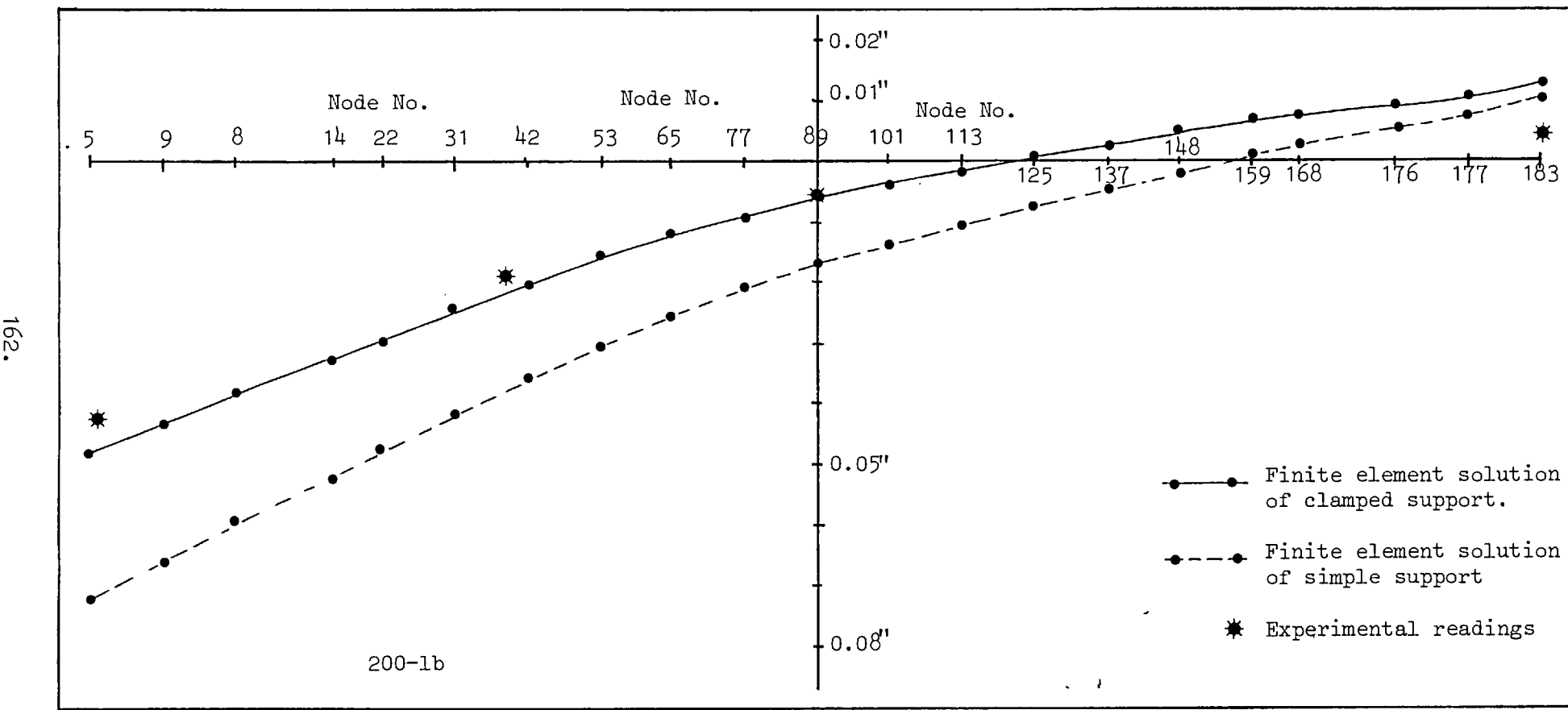


Fig. 2.48. Comparison of deflections due to point load at Node 6 along x-axis.

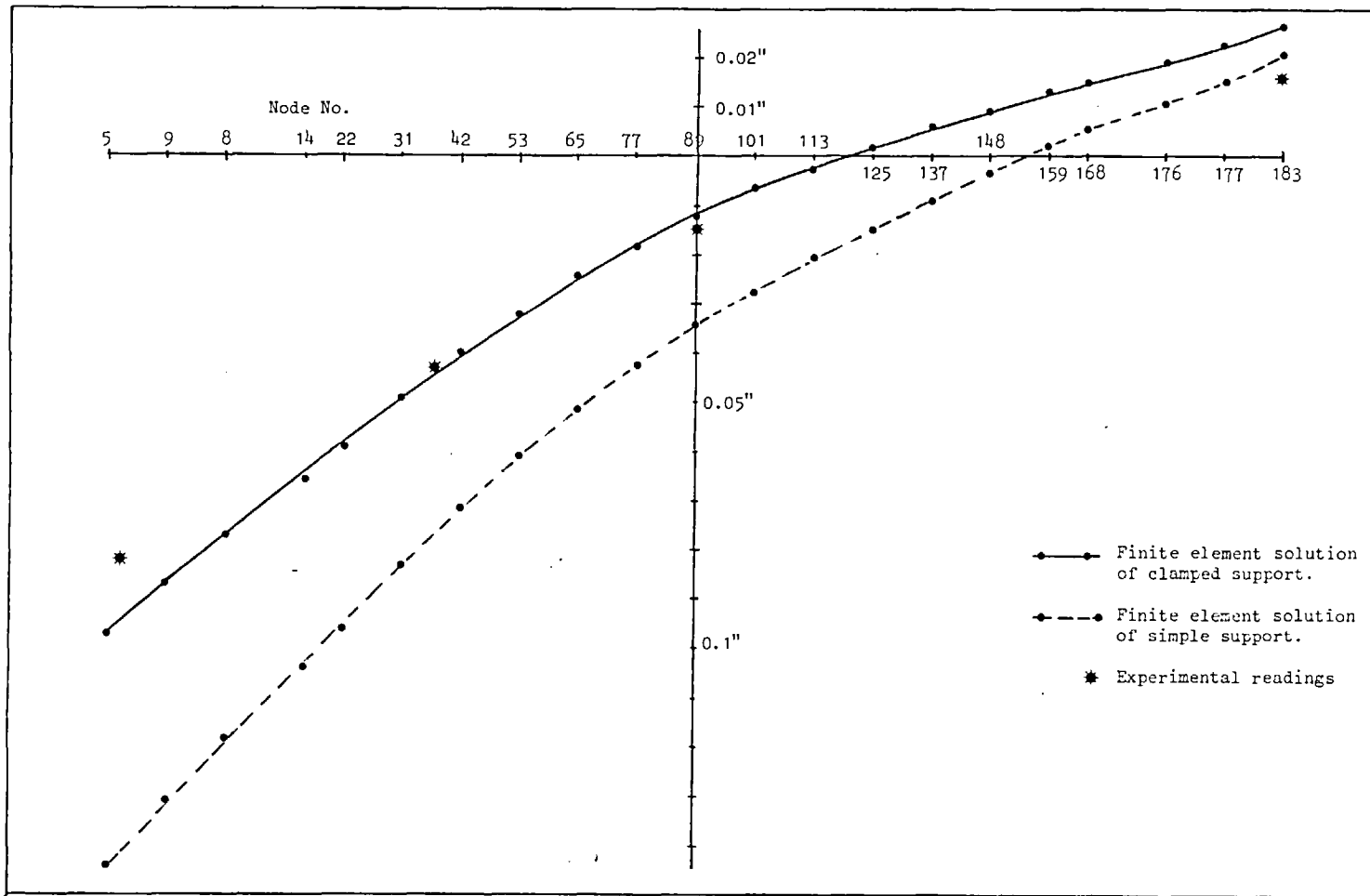


Fig. 2.49. Comparison of deflections due to point load at Node 6 along x-axis.

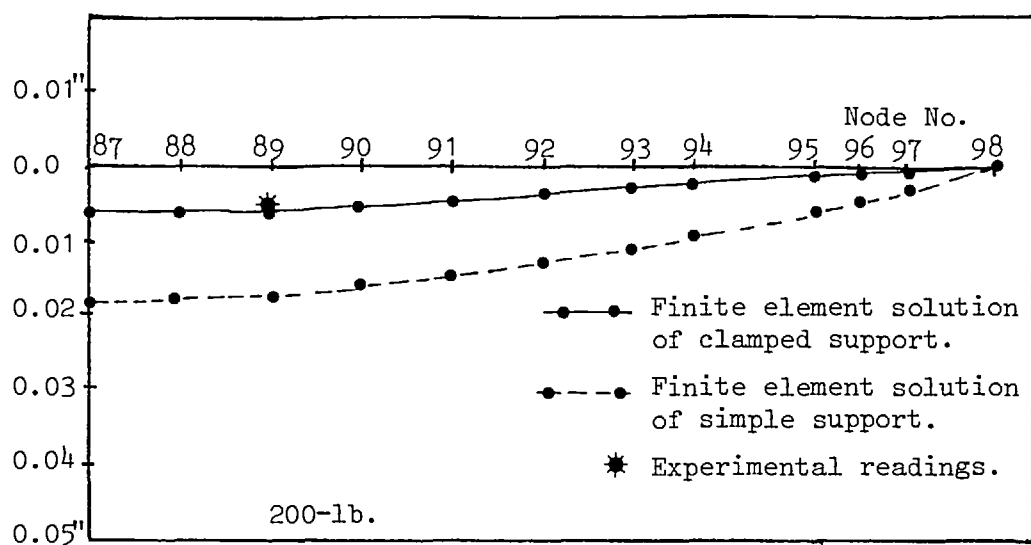


Fig. 2.50a. Comparison of deflections due to point load at Node 6 along y-axis.

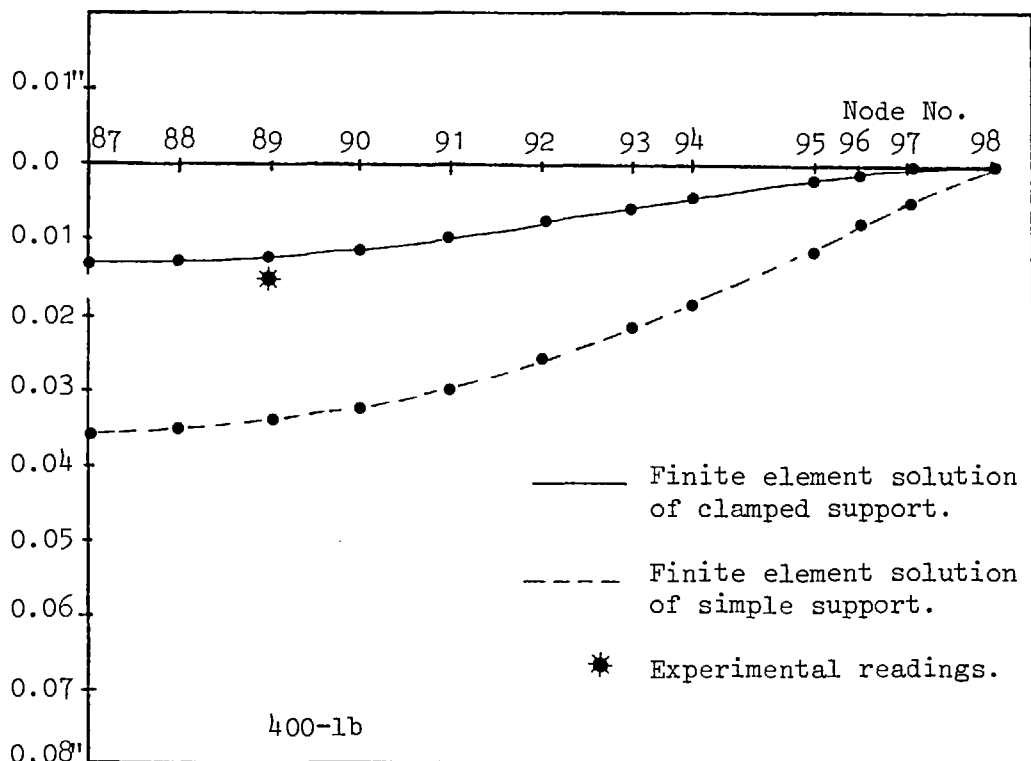


Fig. 2.50b. Comparison of deflections due to point load at Node 6 along y-axis.

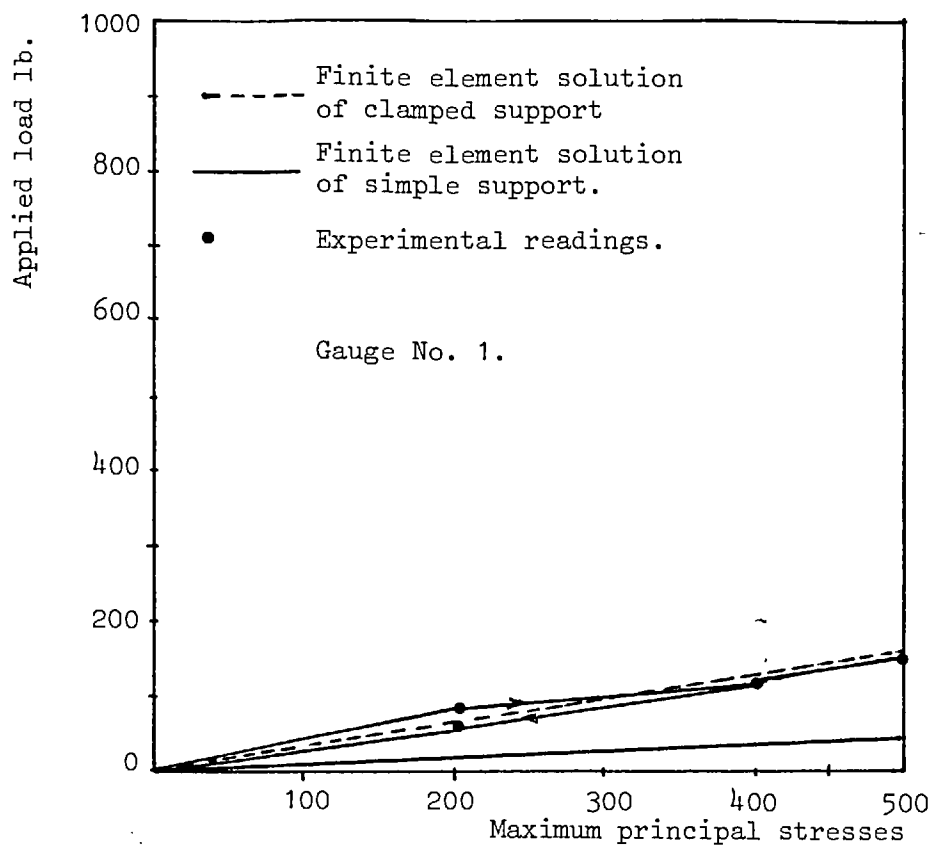


Fig. 2.51. Comparison of principal stresses

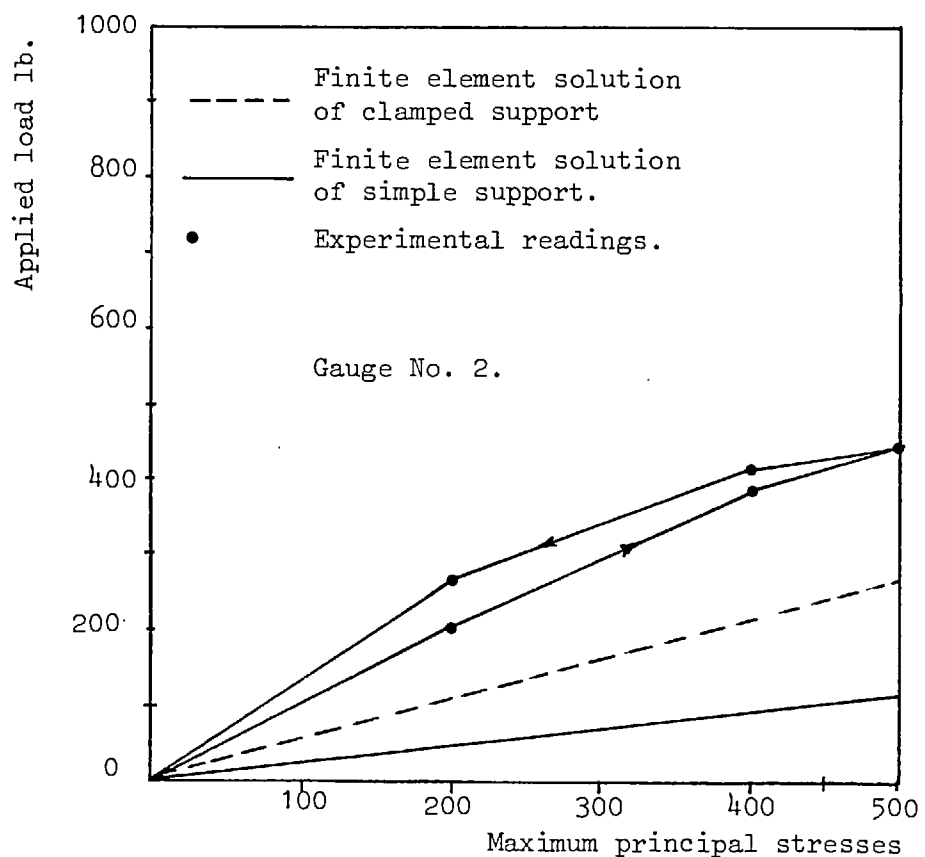


Fig. 2.52. Comparison of principal stresses

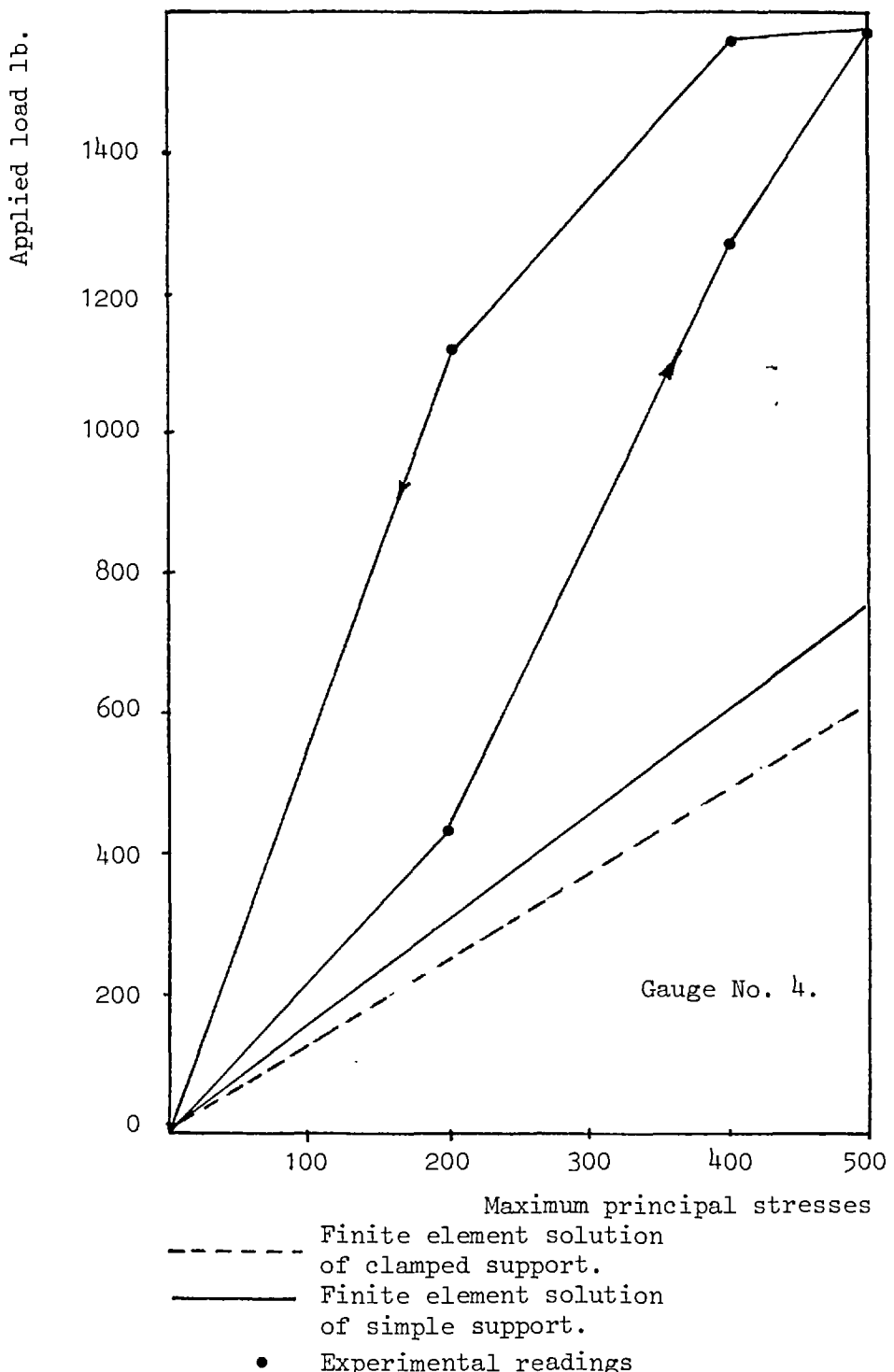


Fig. 2.53. Comparison of principal stresses

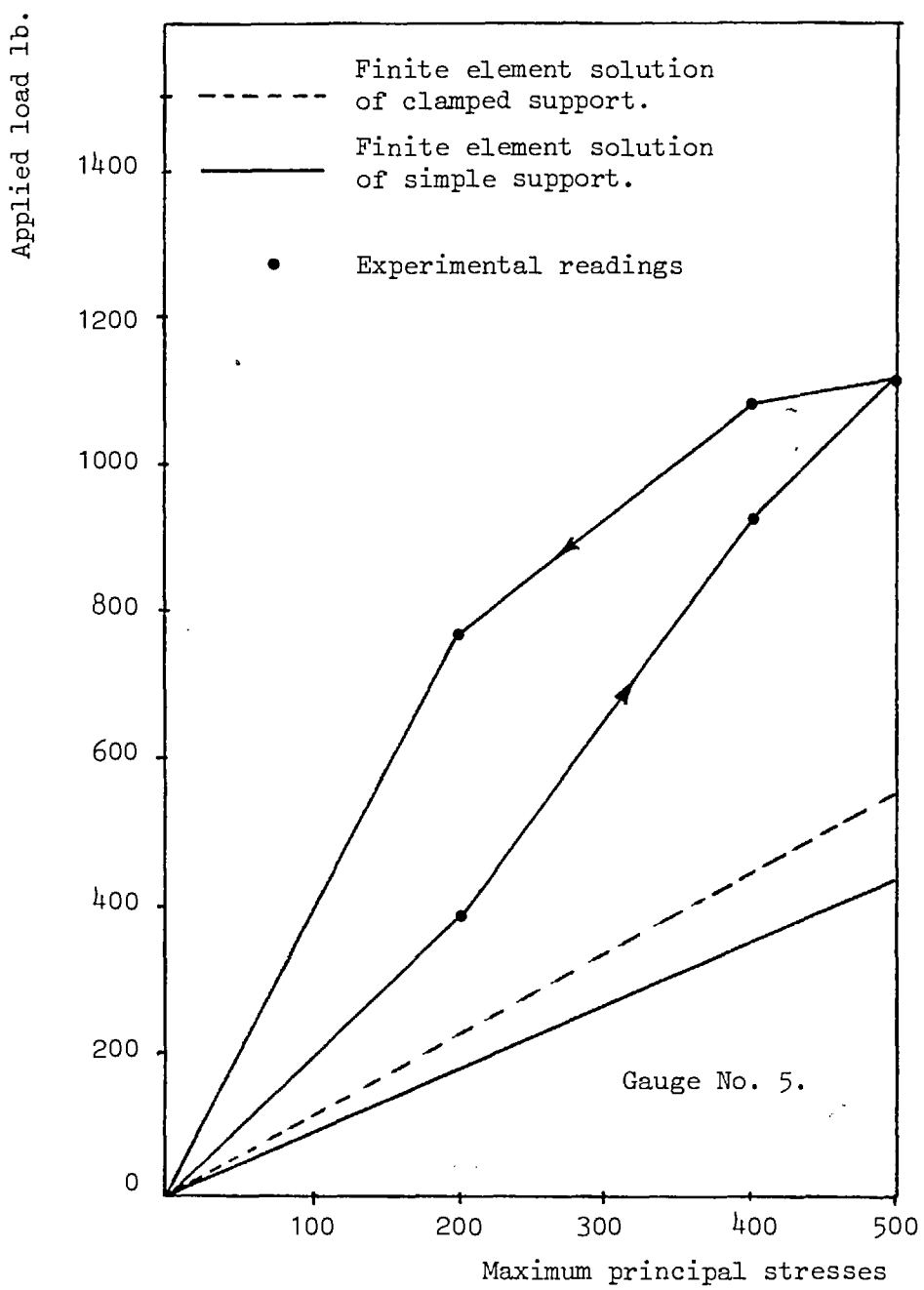


Fig. 2.54. Comparison of principal stresses

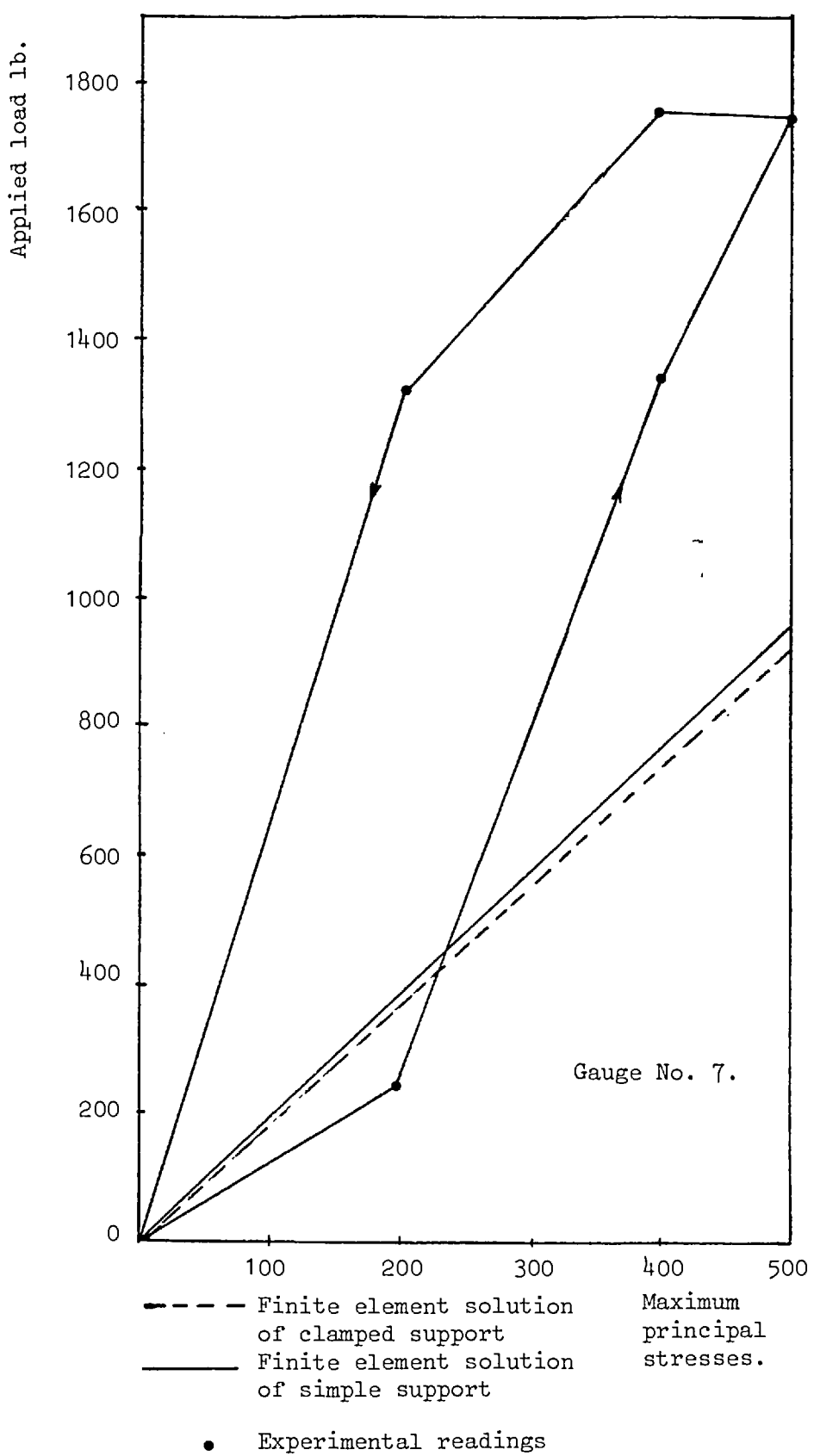


Fig. 2.55. Comparison of principal stresses.

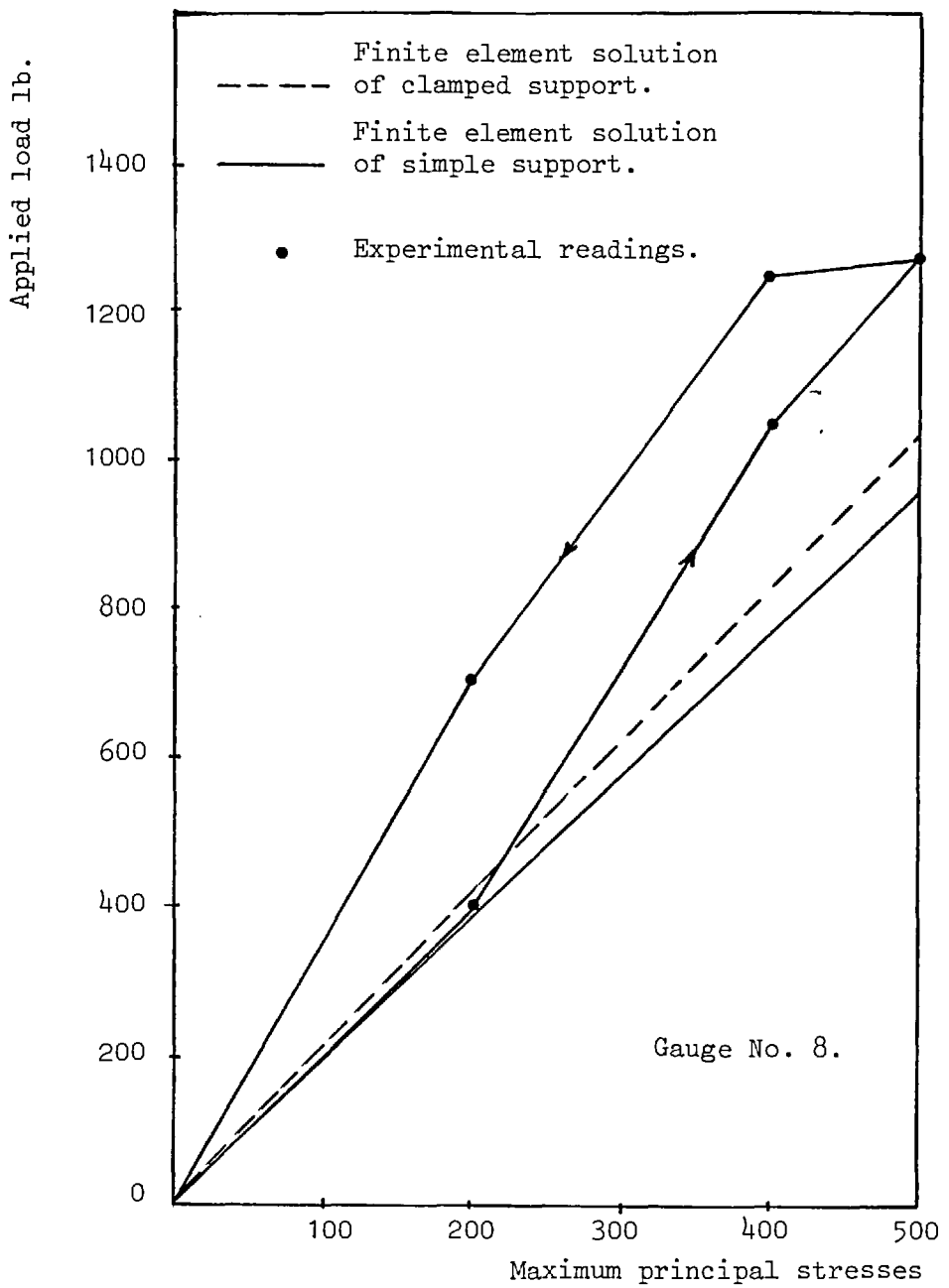


Fig. 2.56. Comparison of principal stresses.

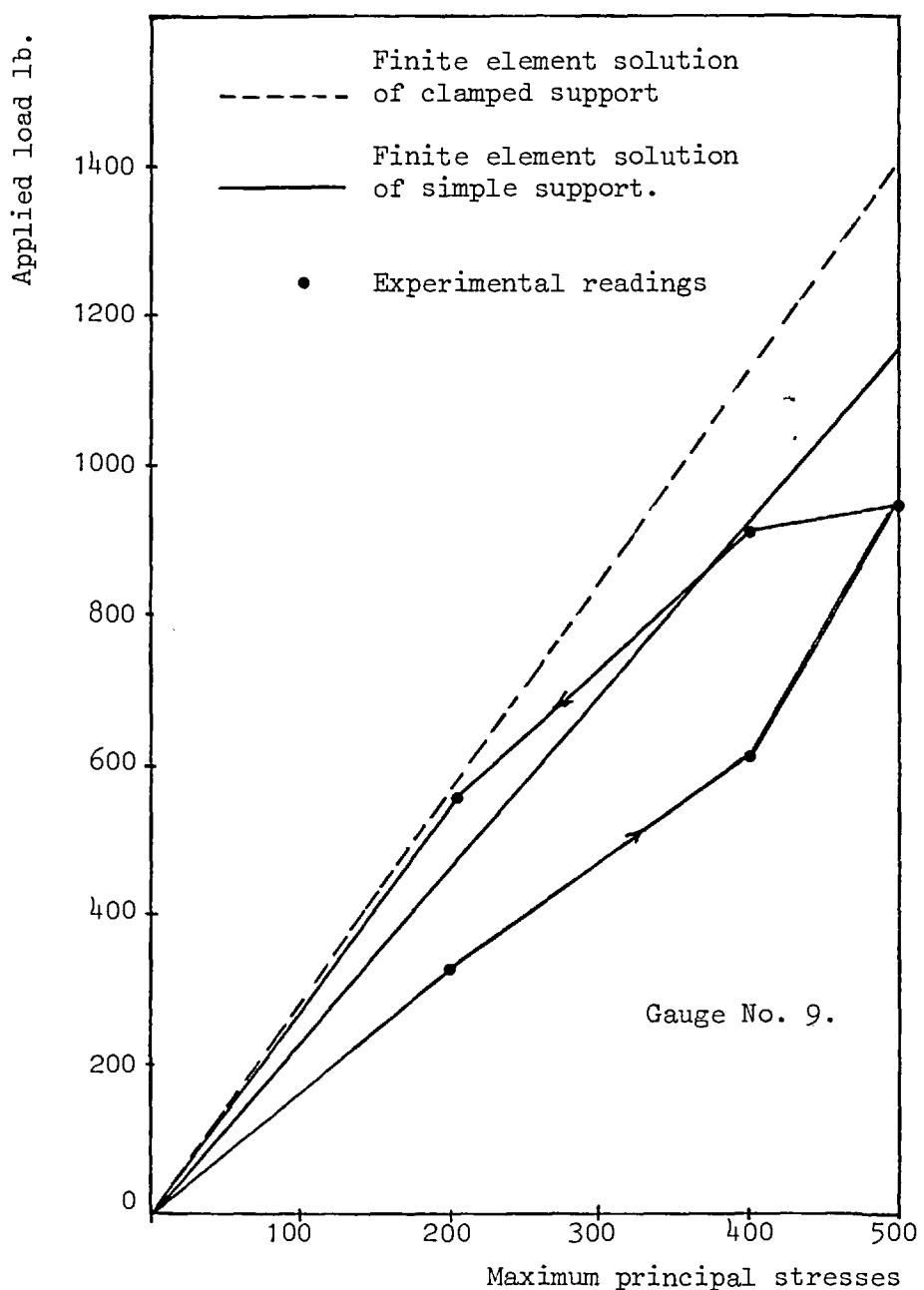


Fig. 2.57. Comparison of principal stresses

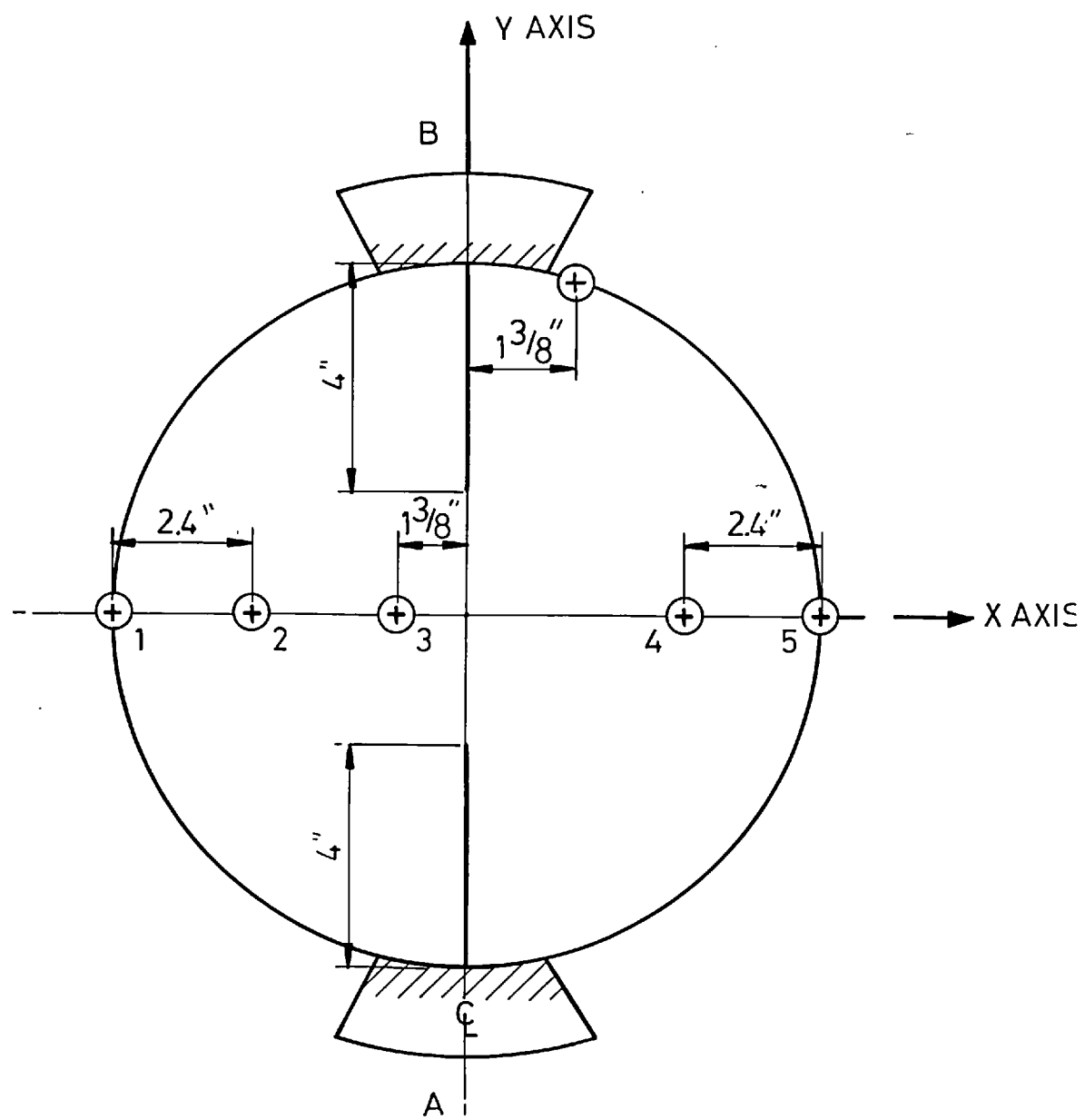


Fig. 2.58. Dial gauge locations.

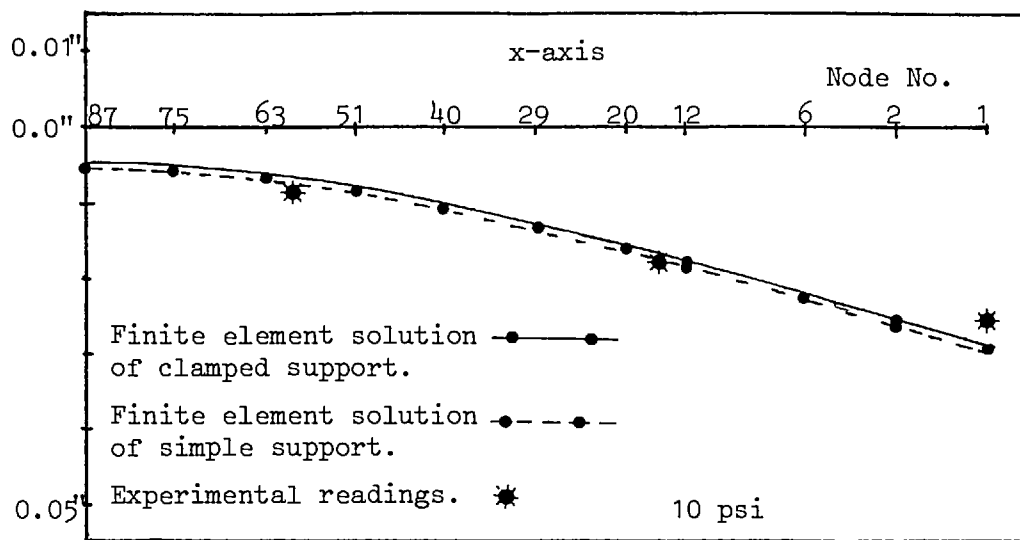


Fig. 2.60. Comparison of deflections due to uniform distributed pressure along x-axis.

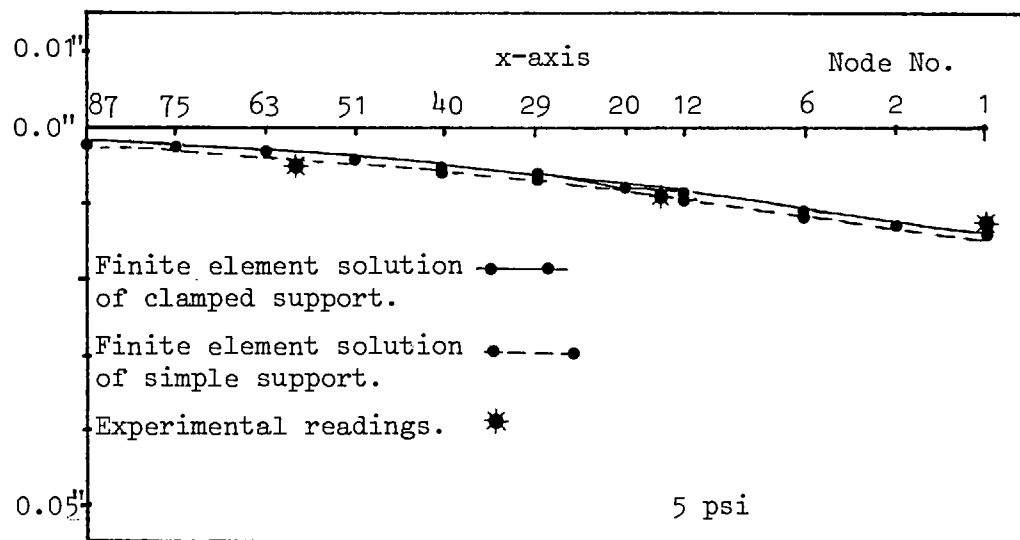
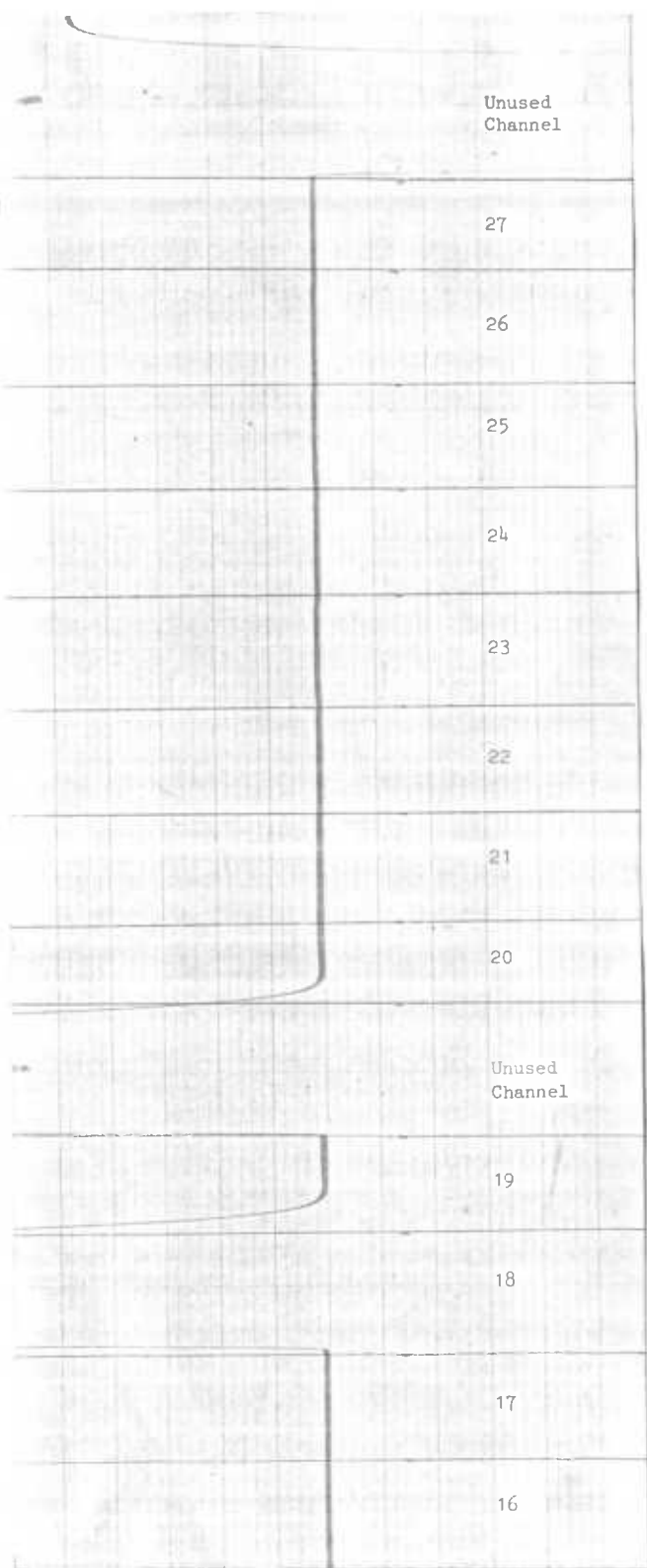
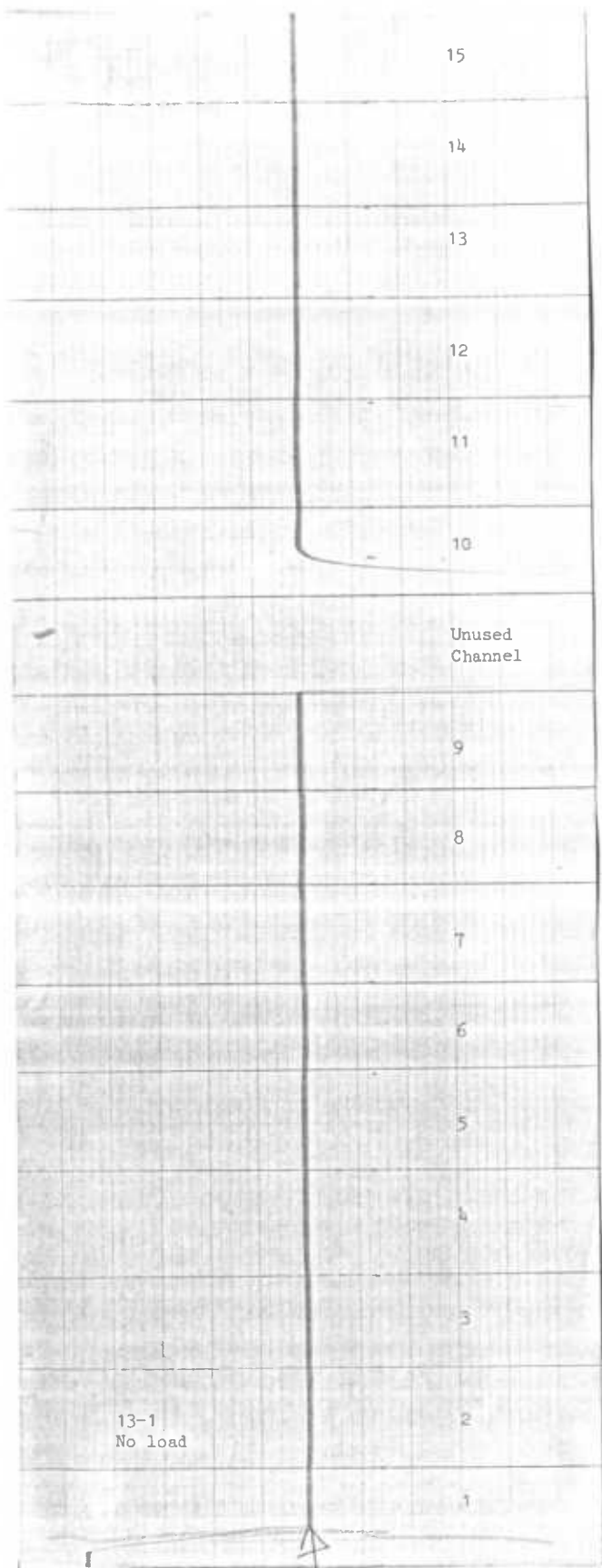
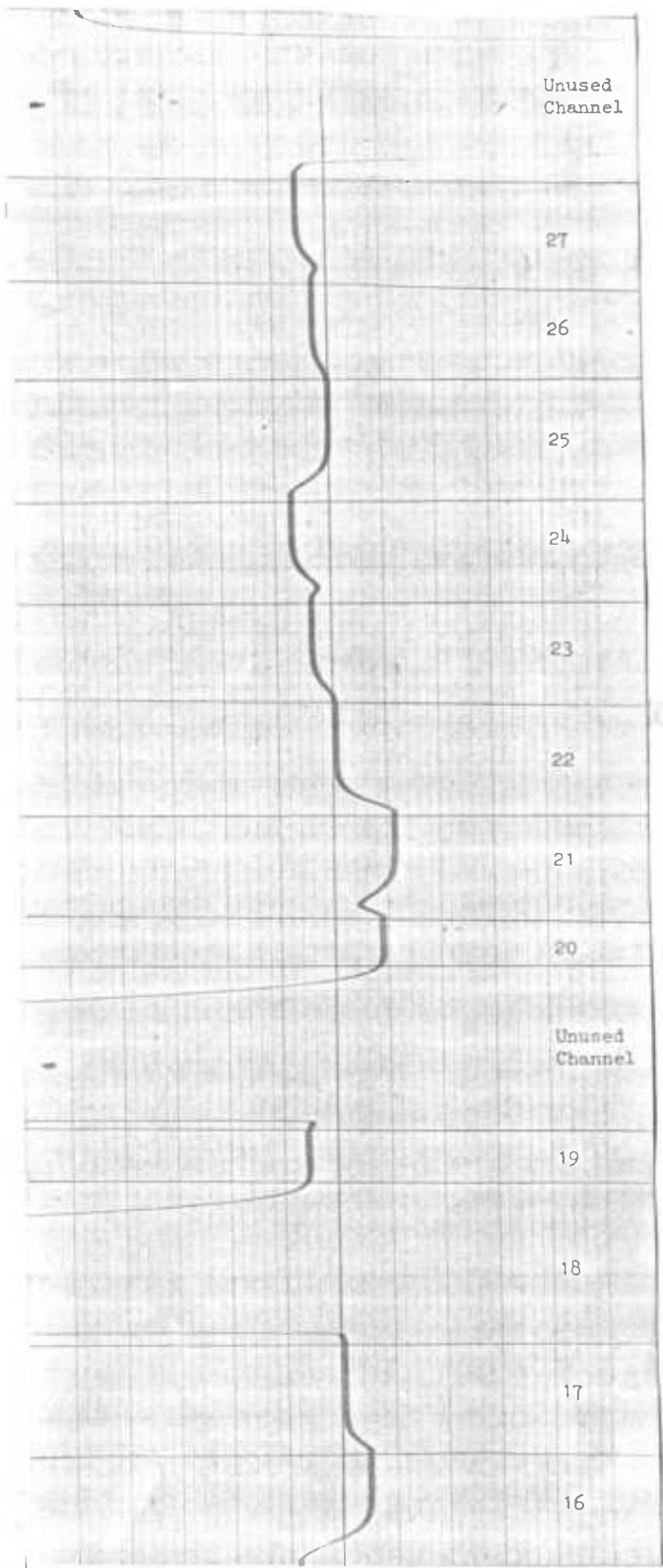
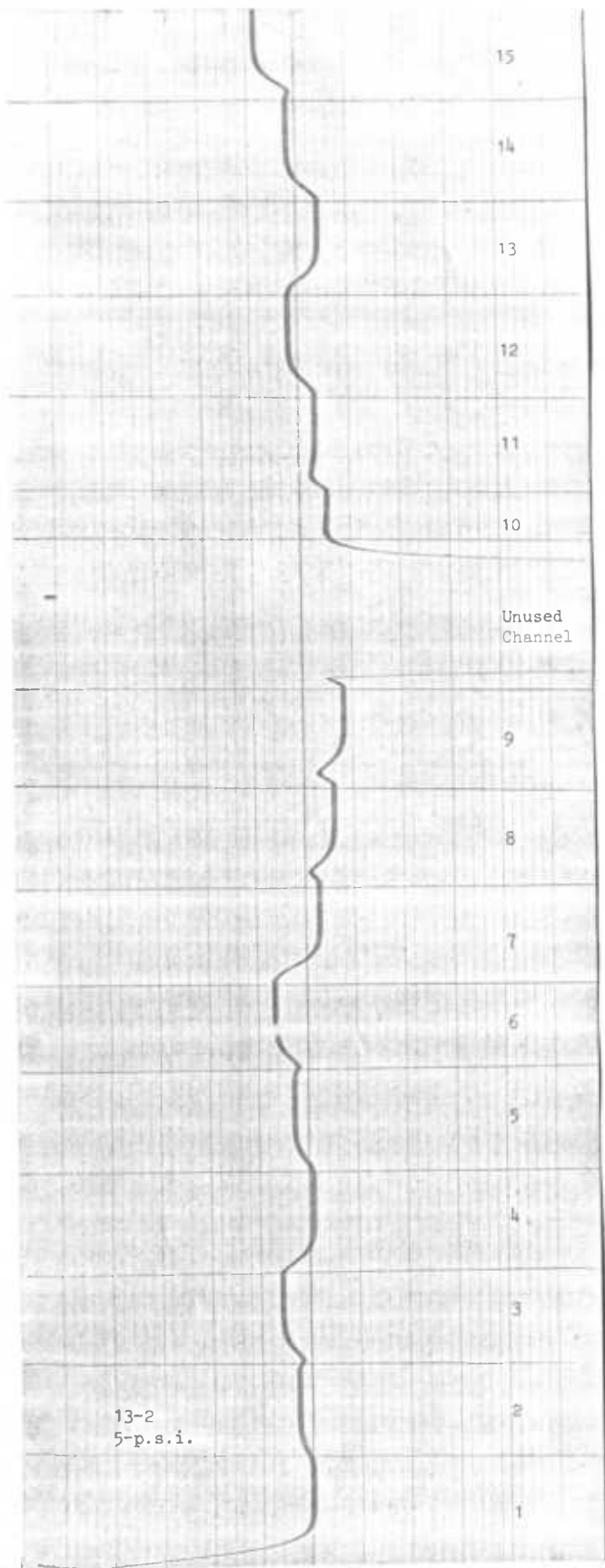
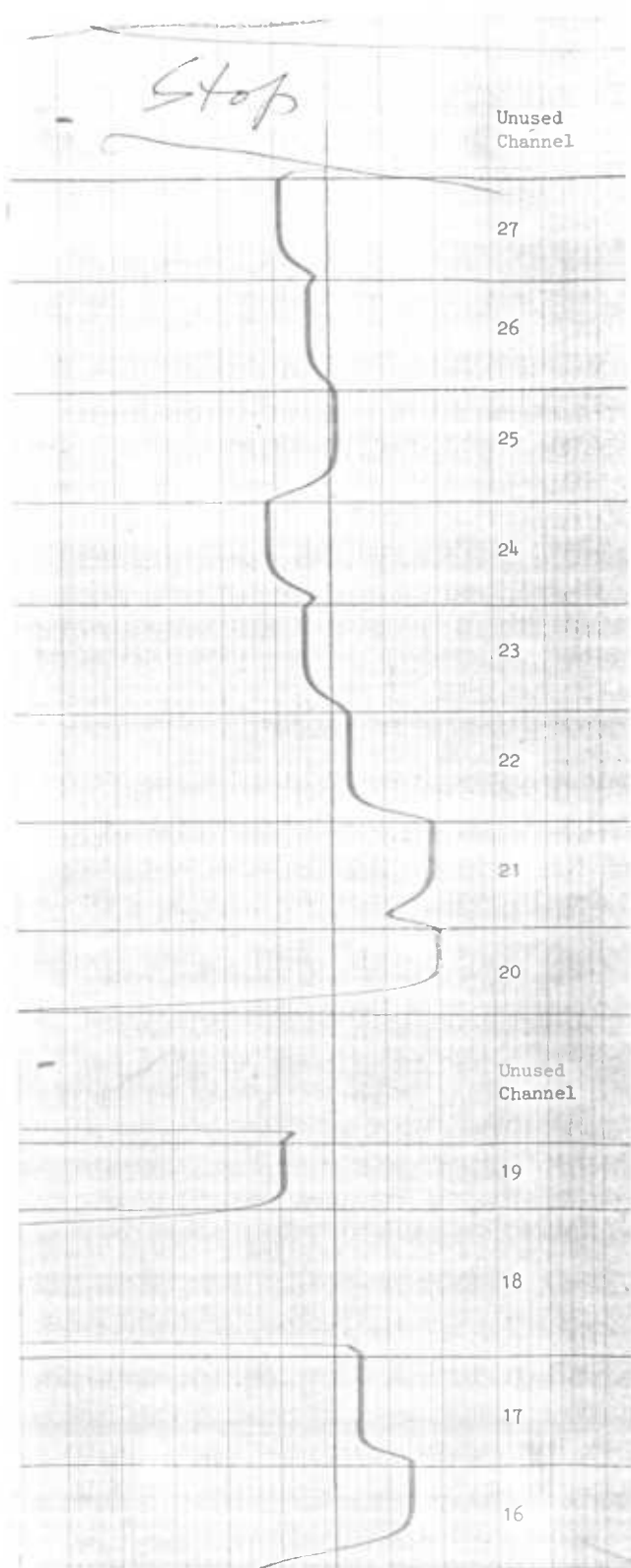
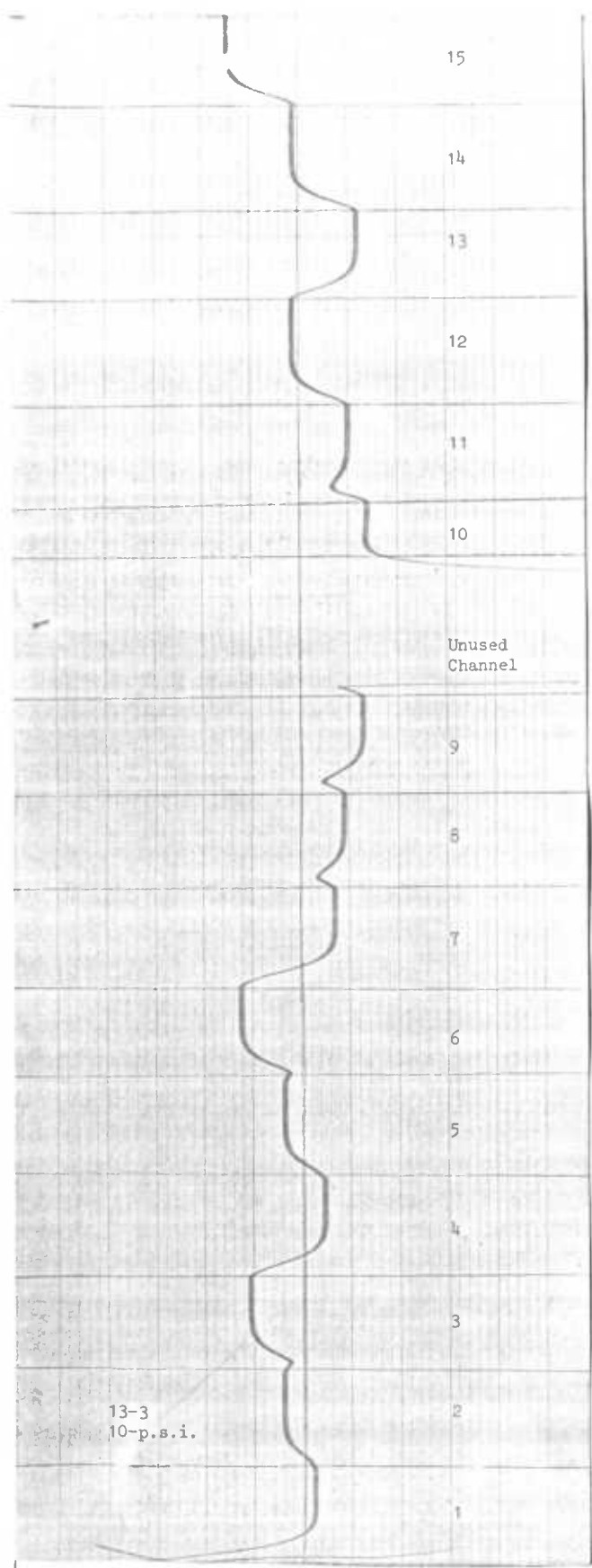
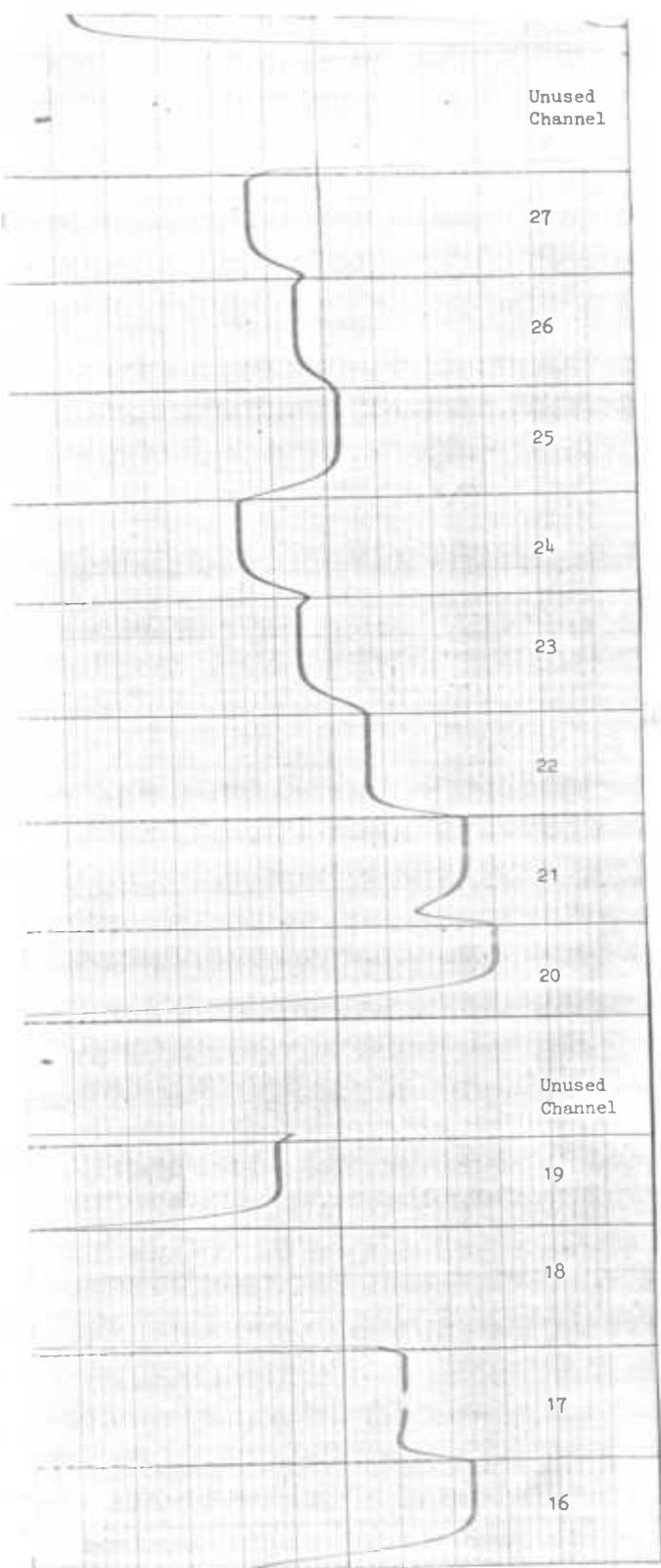
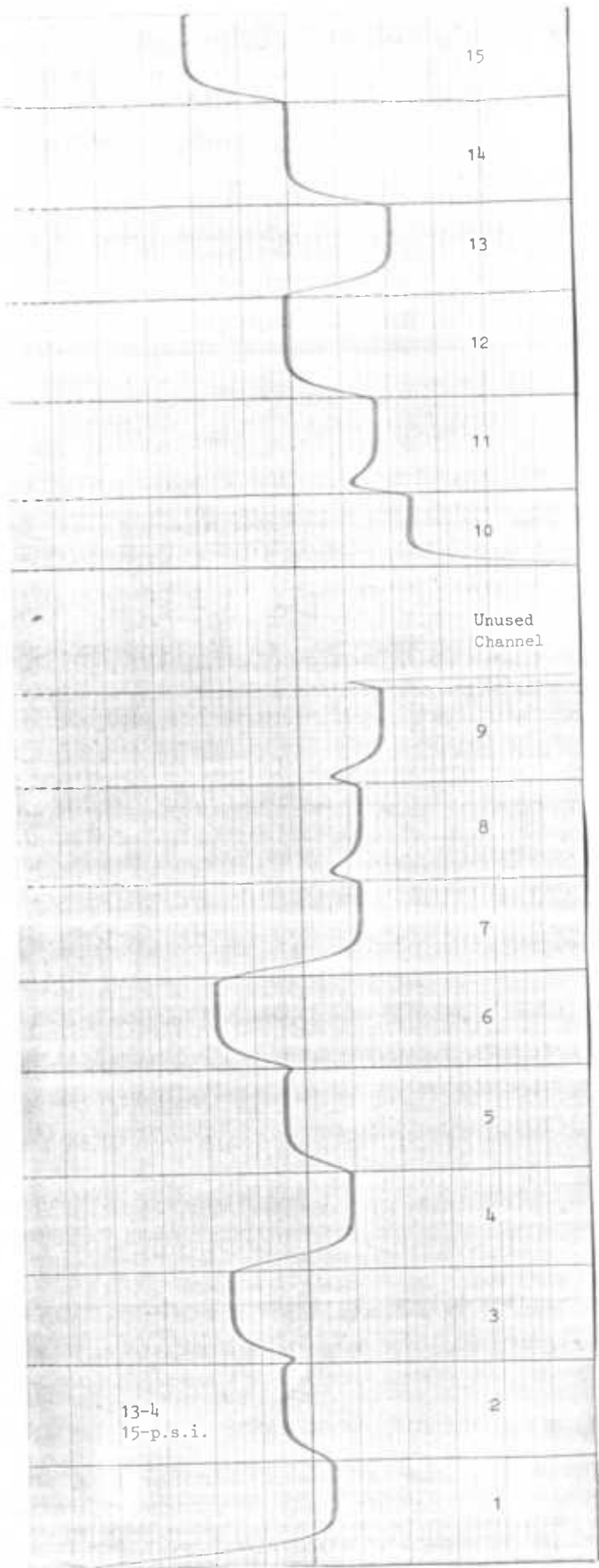


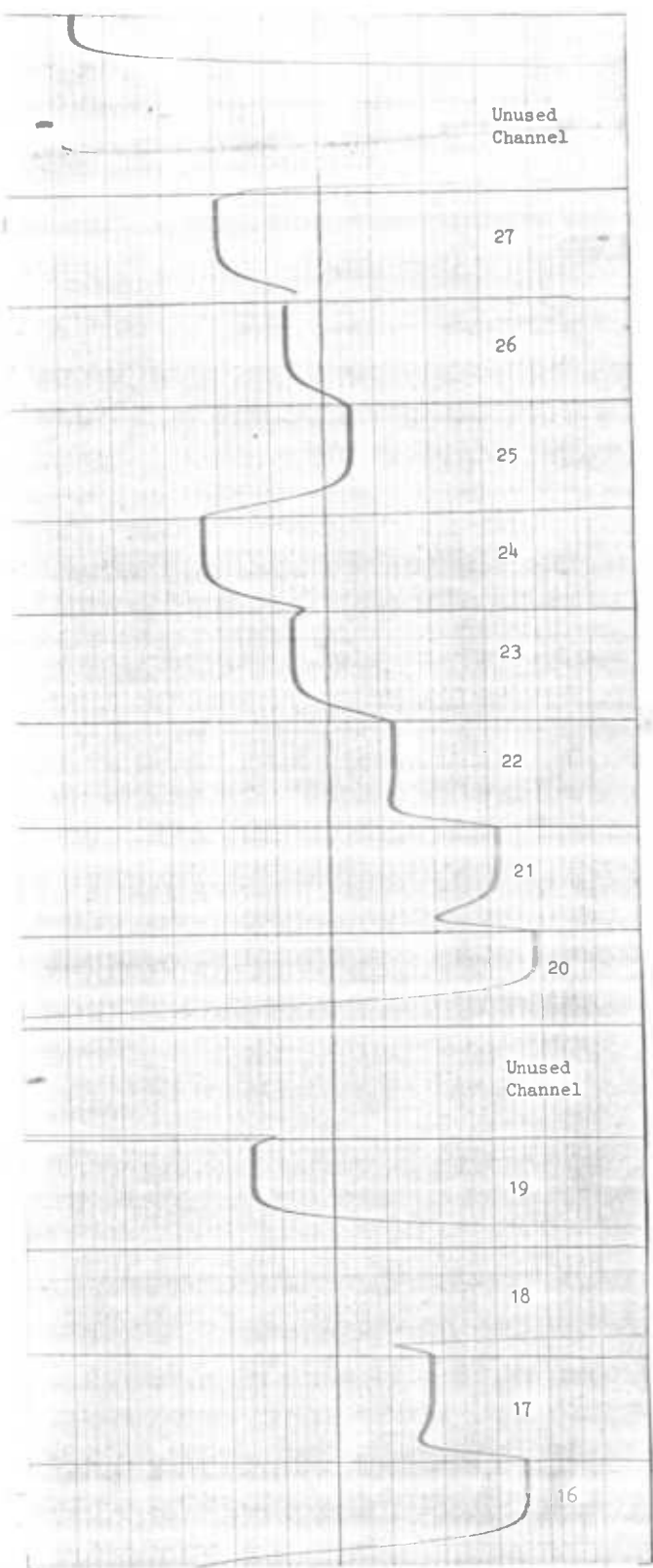
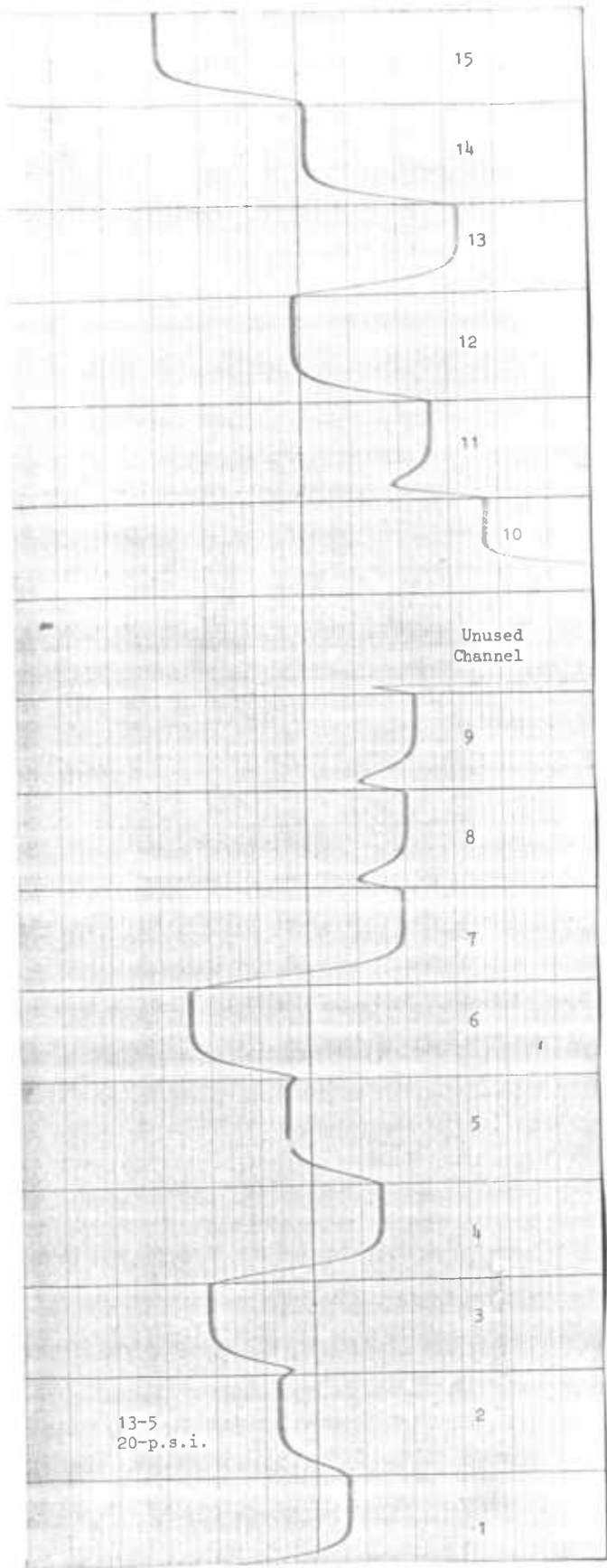
Fig. 2.59. Comparison of deflections due to uniform distributed pressure along x-axis.

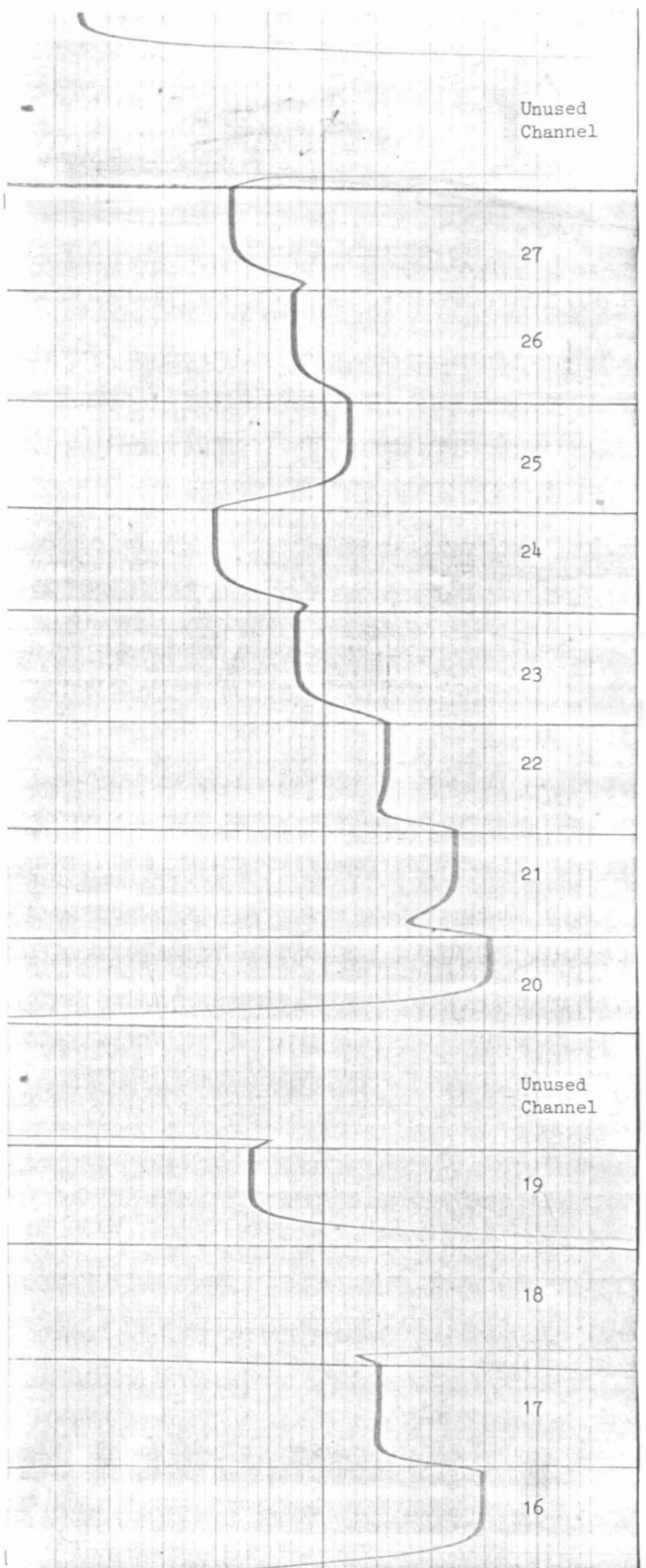
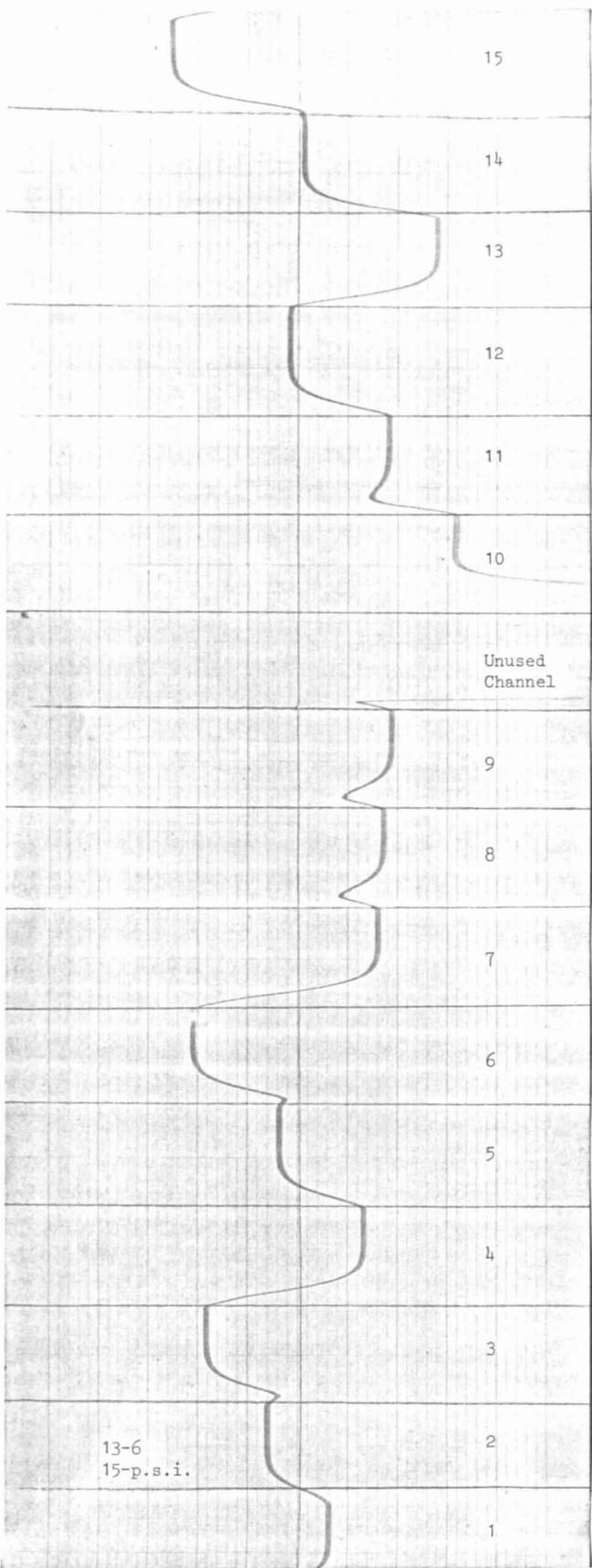


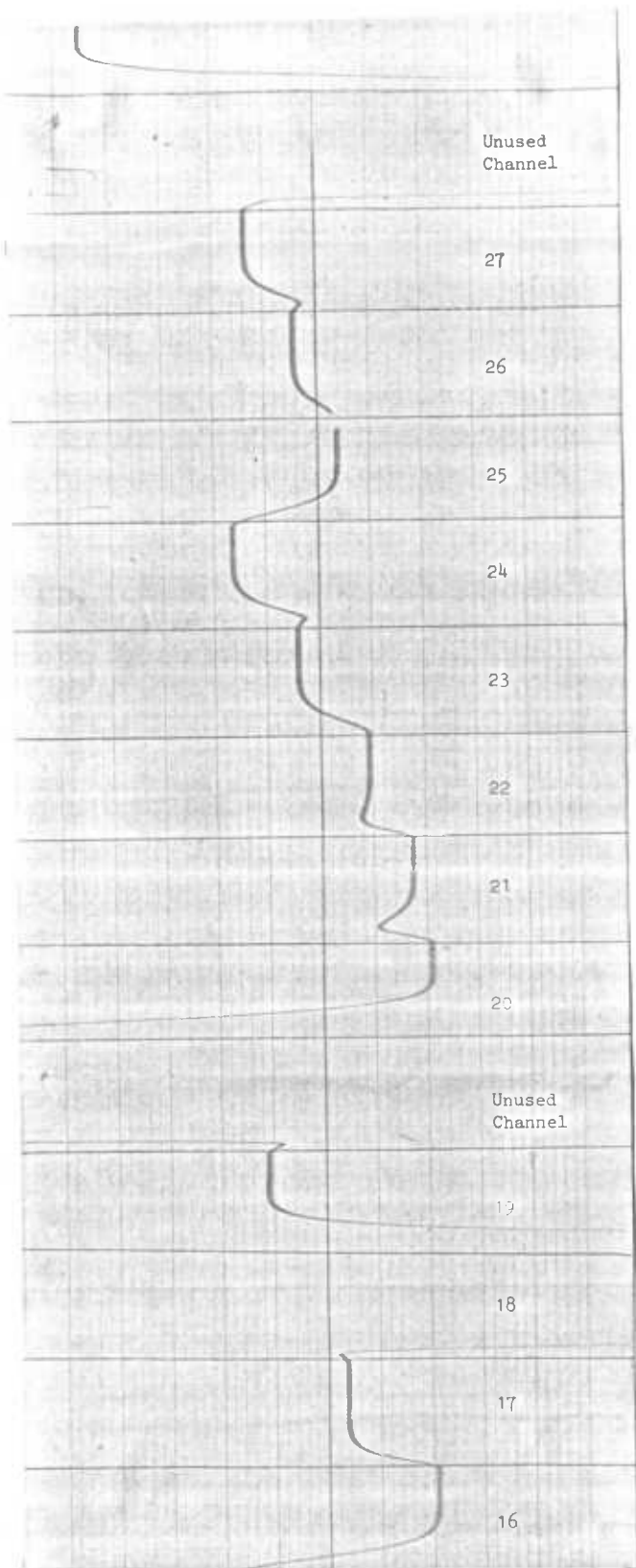
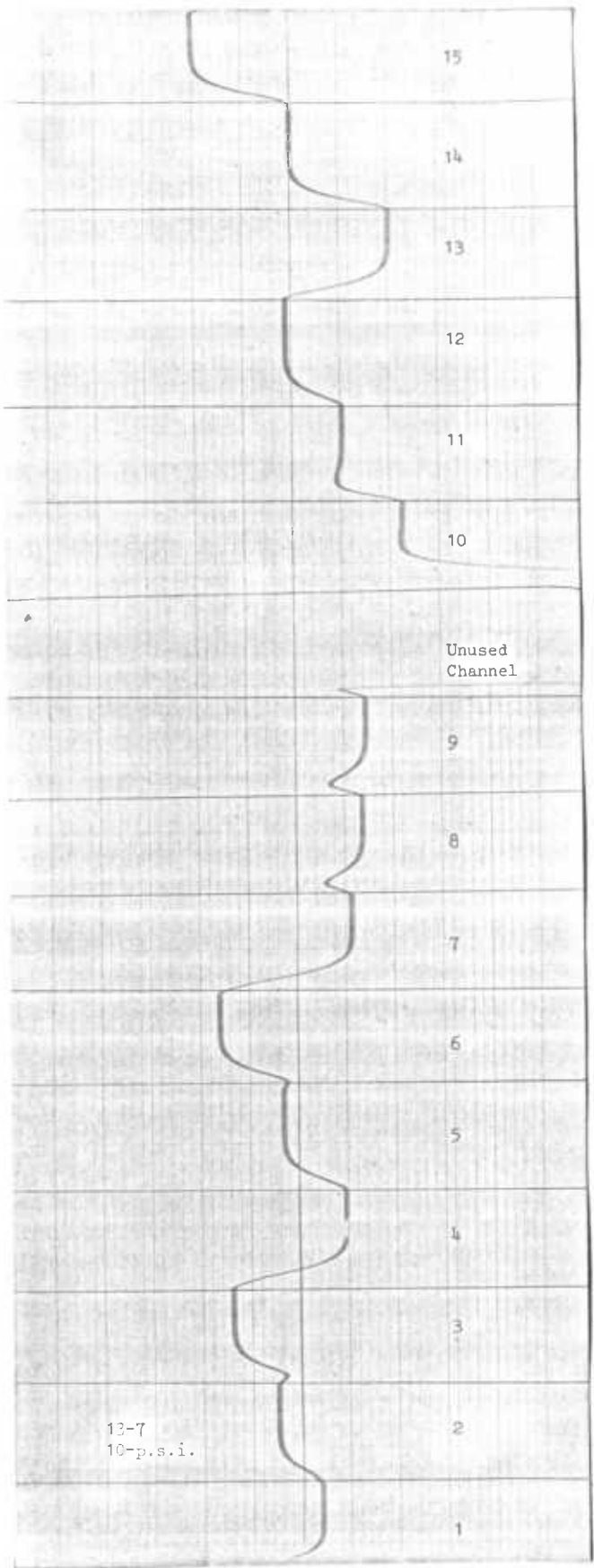


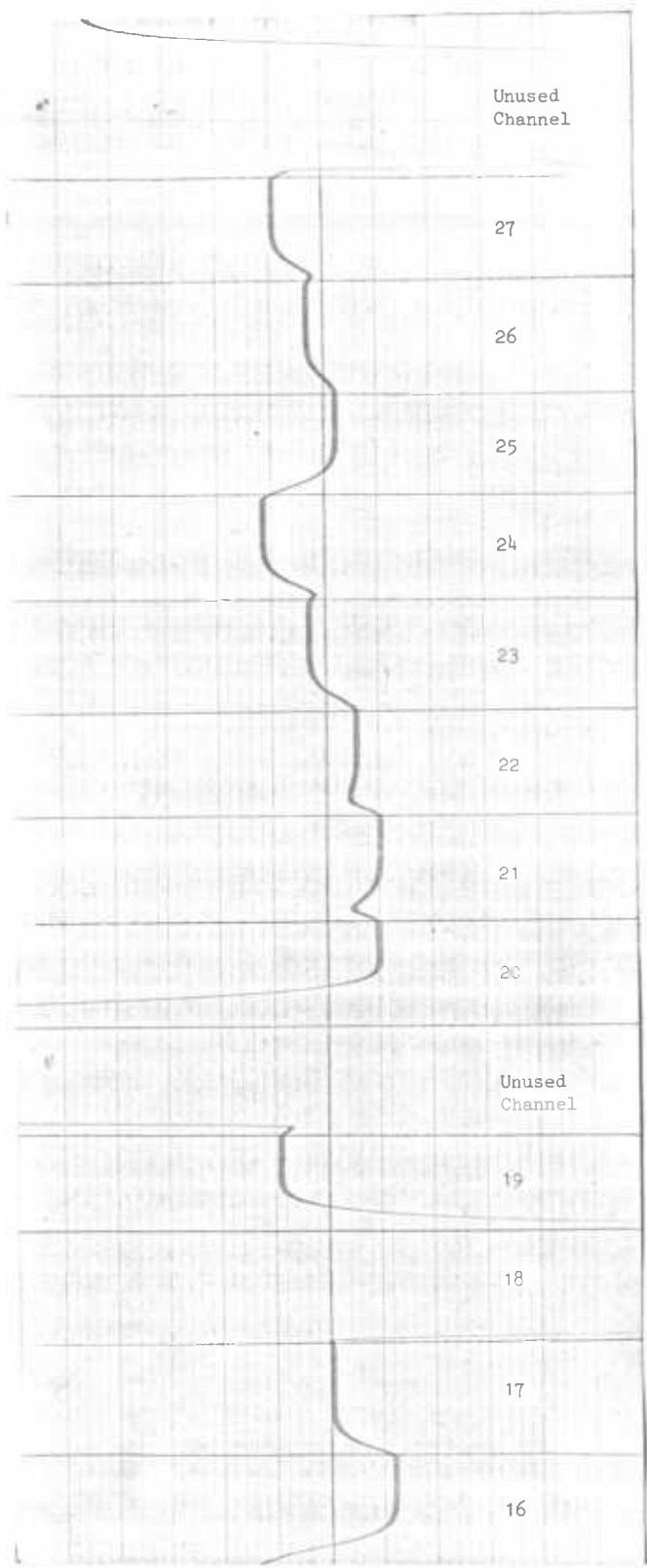
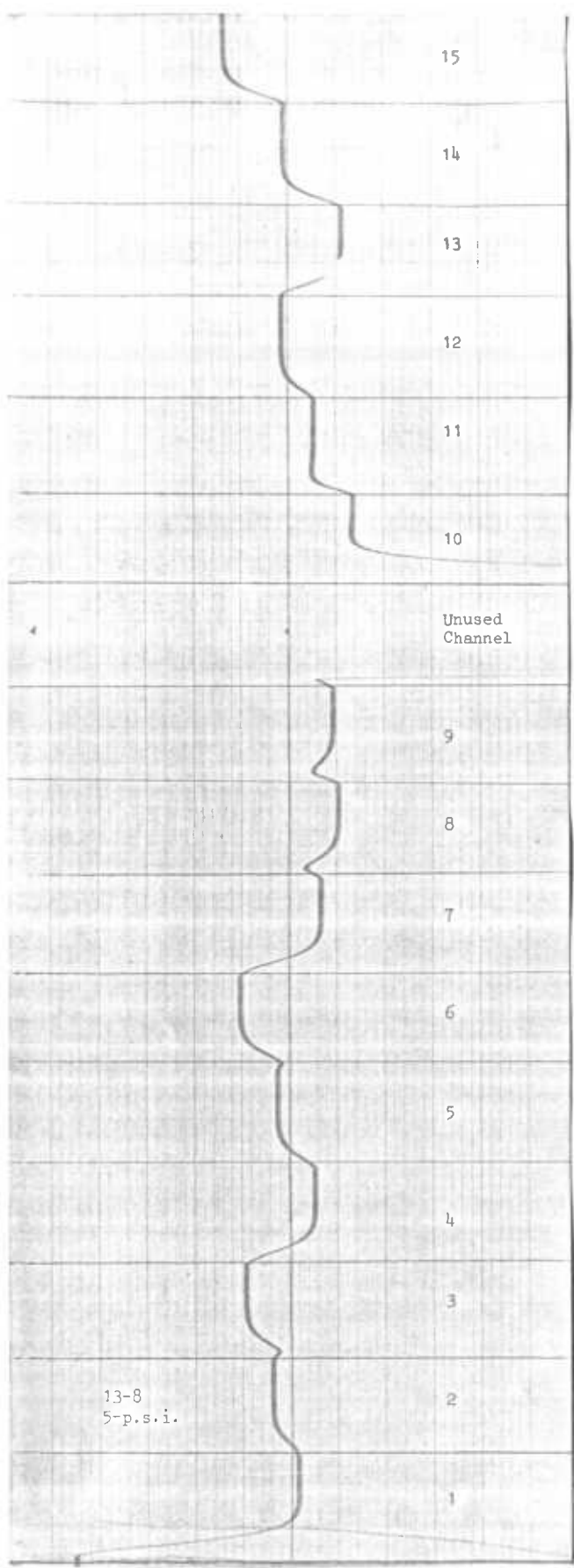












STRESS
9

THE TOTAL NUMBER OF READINGS = 9

INPUT THE STRAINS OF READING NO. 1
0.0, 139.05, 333.72

1 .000000000 .00013905 .00033372 .00034271-.00020366 142.61 -39.73

INPUT THE STRAINS OF READING NO. 2
44.06, 155.74, 389.34

2 .00004406 .00015574 .00038934 .00039468-.00019488 172.28 -24.52

INPUT THE STRAINS OF READING NO. 3
164.02, -372.65, -486.67

3 .00016402-.00037265-.00048667 .00036280-.00057143 78.79 -233.08

INPUT THE STRAINS OF READING NO. 4
-319.82, -211.35, 111.24

4 -.00031982-.00021135 .00011124 .00011512-.00064629 -69.33 -323.50

INPUT THE STRAINS OF READING NO. 5
-250.29, 111.24, 472.77

5 -.00025029 .00011124 .00047277 .00050210-.00064115 139.40 -242.24

INPUT THE STRAINS OF READING NO. 6
0.0, 0.0, 0.0

6 .000000000.000000000.000000000.000000000.000000000 0.00 0.00

INPUT THE STRAINS OF READING NO. 7
319.82, -500.58, -653.54

7 .00031982-.00050058-.00065354 .00060634-.00078710 165.74 -299.42

INPUT THE STRAINS OF READING NO. 8
-27.81, 194.67, 406.03

8 -.00002781 .00019467 .00040603 .00042467-.00025781 175.61 -52.21

INPUT THE STRAINS OF READING NO. 9
-13.90, 155.74, 333.72

9 -.00001390 .00015574 .00033372 .00034707-.00020523 144.63 -39.73

STOP

>STRESS

9

THE TOTAL NUMBER OF READINGS = 9

INPUT THE STRAINS OF READING NO. 1
-111.24, 222.48, 611.82

1 -.00011124 .00022248 .00041132 .00063631-.00052507 234.98 -152.71

INPUT THE STRAINS OF READING NO. 2
-289.22, 211.36, 695.25

2 -.00028922 .00021136 .00069525 .00073674-.00081460 230.14 -287.72

INPUT THE STRAINS OF READING NO. 3
-400.46, -511.70, -736.96

3 -.00040046-.00051170-.00073696-.00016975-.00074241 -241.71 -432.88

INPUT THE STRAINS OF READING NO. 4
-792.59, -586.79, 97.34

4 -.00079259-.00058679 .00009734 .00010404-.00148342 -245.10 -775.02

INPUT THE STRAINS OF READING NO. 5
-681.35, 83.43, 834.80

5 -.00068135 .00008343 .00083430 .00089708-.00149500 178.16 -620.35

INPUT THE STRAINS OF READING NO. 6
0.0, 0.0, 0.0

6 0.000000000.000000000.000000000.000000000.00000000 0.00 0.00

INPUT THE STRAINS OF READING NO. 7
528.39, -1112.40, -1056.78

7 -.00052839-.00111240-.00105678 .00082957-.00141358 158.45 -590.35

INPUT THE STRAINS OF READING NO. 8
-194.67, 250.29, 656.32

8 -.00019467 .00025029 .00065632 .00069453-.00063891 243.13 -202.00

INPUT THE STRAINS OF READING NO. 9
-69.52, 211.36, 500.58

9 -.00006952 .00021136 .00050058 .00052295-.00038111 203.34 -98.45
STOP

>STRESS
9

THE TOTAL NUMBER OF READINGS = 9

INPUT THE STRAINS OF READING NO. 1
-250.29, 389.72, 917.73

1 -.00025029 .00033372 .00091773 .00096512-.00088169 389.10 -277.40

INPUT THE STRAINS OF READING NO. 2
-537.51, 225.27, 1056.78

2 -.00053951 .00022527 .00105678 .00111558-.00142982 308.65 -541.05

INPUT THE STRAINS OF READING NO. 3
-692.47, -706.37, -1001.16

3 -.00069247-.00070637-.00100116-.00039760-.00100124 -416.50 -618.01

INPUT THE STRAINS OF READING NO. 4
-1112.4, -1003.94, 55.62

4 -.00111240-.00100394 .00005562 .00005694-.00217328 -410.33 -1154.81

INPUT THE STRAINS OF READING NO. 5
-1195.83, 0.0, 1195.83

5 -.001195830.00000000 .00119583 .00129286-.00248869 188.93 -1073.36

INPUT THE STRAINS OF READING NO. 6
0.0, 0.0, 0.0

6 0.000000000.000000000.000000000.000000000.00000000 0.00 0.00

INPUT THE STRAINS OF READING NO. 7
681.35, -1696.41, -1418.31

7 .00068135-.00169641-.00141831 .00099012-.00200518 124.60 -875.29

INPUT THE STRAINS OF READING NO. 8
-417.15, 292.01, 923.52

8 -.00041715 .00029201 .00092352 .00098588-.00111047 303.53 -396.08

INPUT THE STRAINS OF READING NO. 9
-180.76, 266.90, 778.68

9 -.00018076 .00026690 .00077868 .00081198-.00072584 288.53 -224.82

STOP

>STRESS

9

THE TOTAL NUMBER OF READINGS = 9

INPUT THE STRAINS OF READING NO. 1

-389.34, 403.25, 1209.74

1 -.00035934 .00040325 .00120974 .00127334-.00125943 427.89 -417.60

INPUT THE STRAINS OF READING NO. 2

-817.61, 239.17, 1362.69

2 -.00081761 .00023917 .00136269 .00144514-.00202358 365.07 -792.85

INPUT THE STRAINS OF READING NO. 3

-1123.52, -1151.33, -1293.16

3 -.00112352-.00115133-.00129314-.00098107-.00129378 -788.99 -893.38

INPUT THE STRAINS OF READING NO. 4

-2071.85, -1518.42, 69.53

4 -.00207185-.00151842 .00006953 .00008995-.00368022 -698.32 -1956.87

INPUT THE STRAINS OF READING NO. 5

-1835.46, -83.43, 1626.89

5 -.00183546-.00008343 .00162689 .00177122-.00369011 201.99 -1621.10

INPUT THE STRAINS OF READING NO. 6

0.0, 0.0, 0.0

6 0.000000000.000000000.000000000.000000000.00000000 0.00 0.00

INPUT THE STRAINS OF READING NO. 7

889.92, -2183.09, -1793.75

7 .00088992-.00218309-.00179375 .00127092-.00256409 161.91 -1118.28

INPUT THE STRAINS OF READING NO. 8

-723.06, 347.63, 1268.14

8 -.00072306 .00034763 .00126814 .00136345-.00173888 378.98 -656.63

INPUT THE STRAINS OF READING NO. 9

-319.81, 378.22, 1126.31

9 -.00031981 .00037822 .00112631 .00118049-.00112208 405.92 -362.72

STOP

>STRESS

9

THE TOTAL NUMBER OF READINGS = 9

INPUT THE STRAINS OF READING NO. 1
-347.63, 361.53, 1028.97

1 - .00034763 .00036153 .00102897 .00108873-.00107483 366.26 -355.98

INPUT THE STRAINS OF READING NO. 2
-761.99, 197.46, 1195.83

2 - .00076199 .00019746 .00119583 .00127173-.00183626 310.00 -727.50

INPUT THE STRAINS OF READING NO. 3
-914.95, -970.57, 1098.49

3 - .00091495-.00097057 .00109849 .00109868-.00293420 -15.75 -1378.69

INPUT THE STRAINS OF READING NO. 4
-1807.65, -1045.65, 97.34

4 - .00180765-.00104565 .00009734 .00014424-.00299754 -530.69 -1579.47

INPUT THE STRAINS OF READING NO. 5
-1585.17, -55.62, 1168.02

5 - .00158517-.00005562 .00116802 .00131002-.00295081 104.45 -1317.89

INPUT THE STRAINS OF READING NO. 6
0.0, 0.0, 0.0

6 0.000000000.000000000.000000000.000000000.000000000 0.00 0.00

INPUT THE STRAINS OF READING NO. 7
764.78, -1752.03, -1390.50

7 - .00076478-.00175203-.00139050 .00105168-.00203893 150.79 -880.91

INPUT THE STRAINS OF READING NO. 8
-681.35, 264.20, 1156.90

8 - .00068135 .00026420 .00115690 .00123643-.00165358 328.12 -636.62

INPUT THE STRAINS OF READING NO. 9
-292.00, 294.79, 973.35

9 - .00029200 .00029479 .00097335 .00101667-.00101388 339.95 -337.88

STOP

>STRESS

9

THE TOTAL NUMBER OF READINGS = 9

INPUT THE STRAINS OF READING NO. 1
-236.39, 264.20, 778.68

1 -.00023639 .00026420 .00077868 .00081860-.00079079 278.90 -258.34

INPUT THE STRAINS OF READING NO. 2
-567.32, 169.65, 889.92

2 -.00056732 .00016965 .00088992 .00095059-.00134826 236.65 -530.74

INPUT THE STRAINS OF READING NO. 3
-650.75, -789.8, -834.30

3 -.00065075-.00078980-,00083430-.00058673-.00085382 -488.10 -577.26

INPUT THE STRAINS OF READING NO. 4
-1279.26, -600.69, 69.53

4 -.00127926-.00060069 .00006953 ,00012502-.00200497 -339.64 -1050.67

INPUT THE STRAINS OF READING NO. 5
-1140.21, 0.0, 1140.21

5 -.001140210.00000000 .00114021 .00123273-.00237294 180.19 -1023.44

INPUT THE STRAINS OF READING NO. 6
0.0, 0.0, 0.0

6 0.000000000.000000000.000000000.000000000.00000000 0.00 0.00

INPUT THE STRAINS OF READING NO. 7
625.73, -1195.83, -1001.16

7 .00062573-.00119583-.00100116 .00087354-.00144364 175.95 -597.57

INPUT THE STRAINS OF READING NO. 8
-528.39, 208.58, 934.42

8 -.00052839 .00020858 .00093442 .00099479-.00131460 267.20 -503.72

INPUT THE STRAINS OF READING NO. 9
-222.48, 239.17, 778.68

9 -.00022248 .00023917 .00077868 .00081252-.00079583 274.62 -262.28

STOP

>STRESS
9

THE TOTAL NUMBER OF READINGS = 9

INPUT THE STRAINS OF READING NO. 1

-83.43, 208.58, 528.39

1 -.00008343 .00020858 .00052839 .00055074-.00042559 209.23 -116.68

INPUT THE STRAINS OF READING NO. 2

-303.13, 141.84, 597.92

2 -.00030313 .00014184 .00059792 .00063346-.00079475 178.74 -298.02

INPUT THE STRAINS OF READING NO. 3

-372.65, -595.13, -542.29

3 -.00037265-.00059513-.00054229-.00035825-.00060953 -315.92 -399.80

INPUT THE STRAINS OF READING NO. 4

-750.87, -308.69, 83.43

4 -.00075087-.00030869 .00008343 .00012207-.00118163 -174.20 -609.40

INPUT THE STRAINS OF READING NO. 5

-639.63, 69.53, 778.68

5 -.00063963 .00006953 .00077868 .00083622-.00140632 163.49 -585.11

INPUT THE STRAINS OF READING NO. 6

0.0, 0.0, 0.0,

6 0.00000000.00000000.00000000.00000000.00000000 0.00 0.00

INPUT THE STRAINS OF READING NO. 7

514.49, -556.20, -584.01

7 .00051449-.00055620-.00058401 .00075615-.00079786 243.95 -274.80

INPUT THE STRAINS OF READING NO. 8

-333.72, 139.05, 656.32

8 -.00033372 .00013905 .00065632 .00069252-.00088719 191.68 -335.65

INPUT THE STRAINS OF READING NO. 9

-126.14, 183.55, 542.30

9 -.00012614 .00018355 .00054230 .00056513-.00050772 200.30 -157.84

STOP

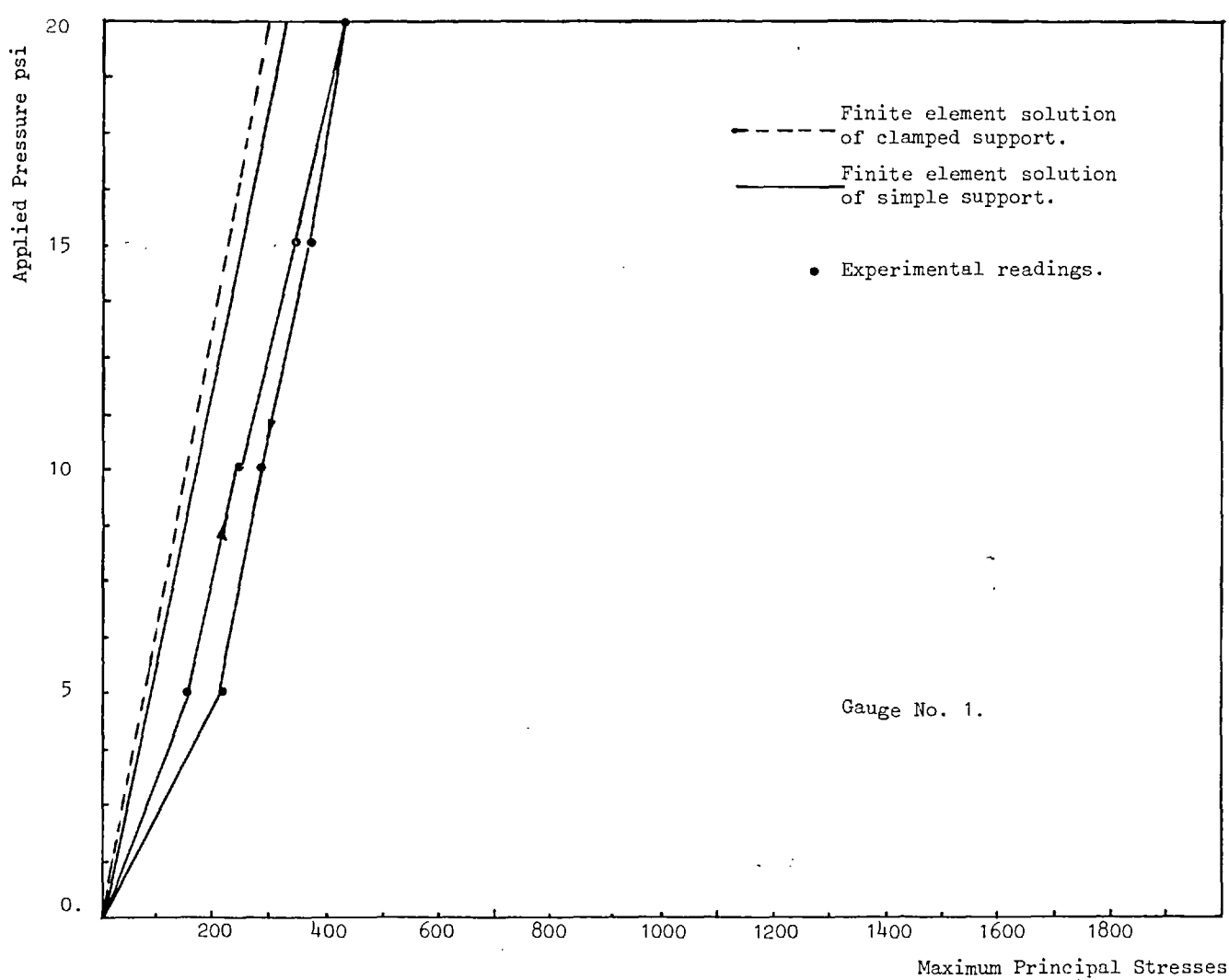


Fig. 2.61. Comparison of principal stresses

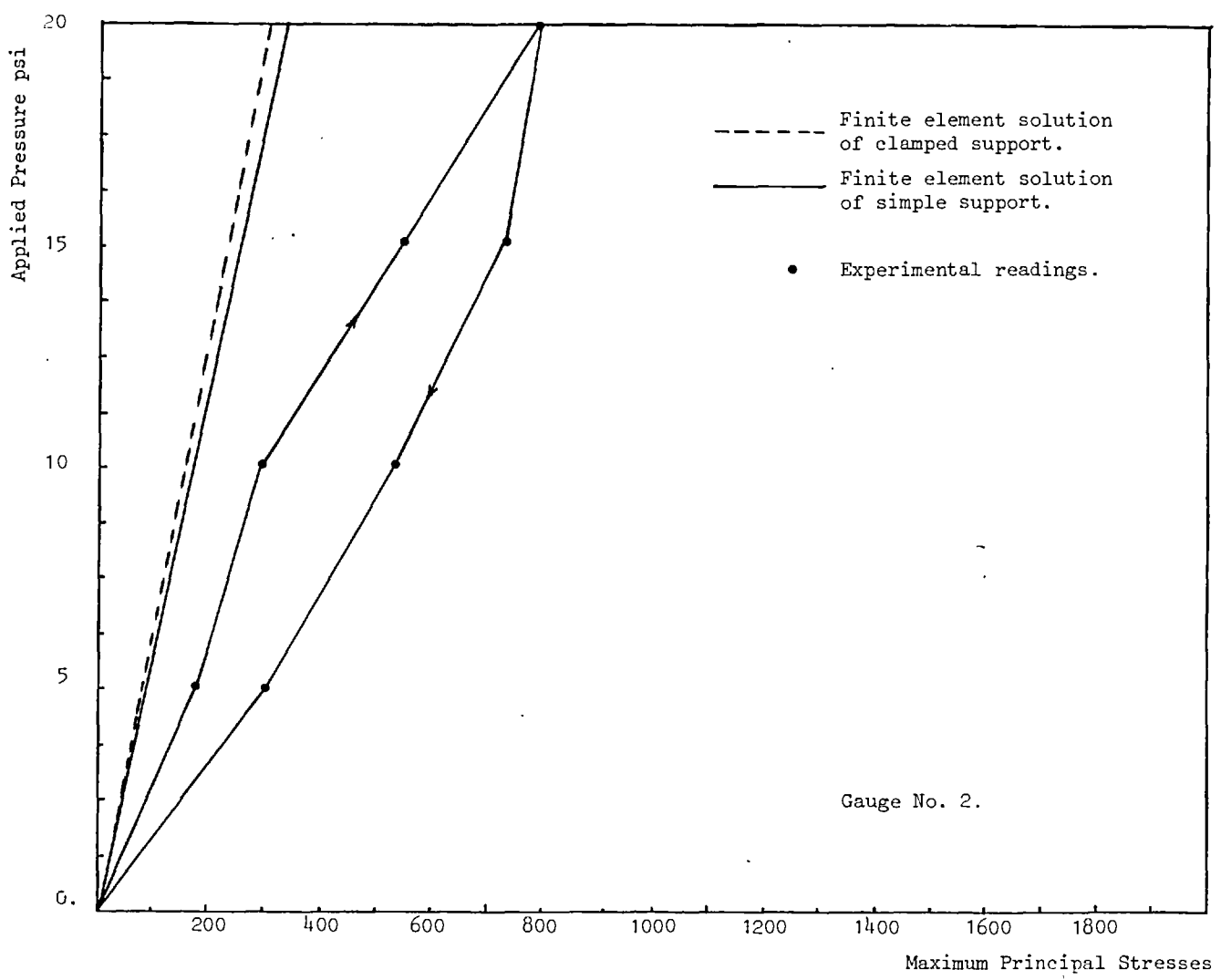


Fig. 2.62. Comparison of principal stresses

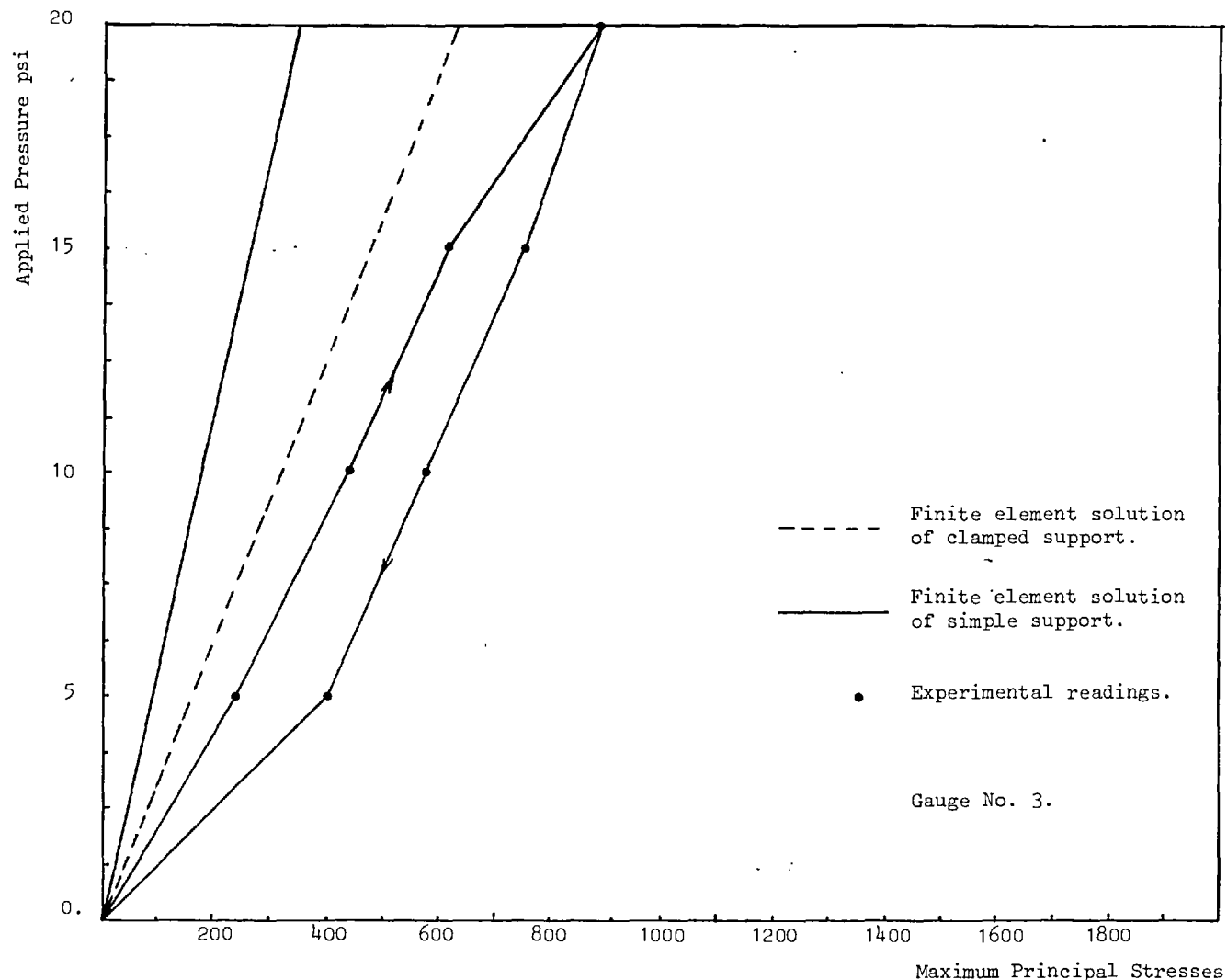


Fig. 2.63. Comparison of principal stresses

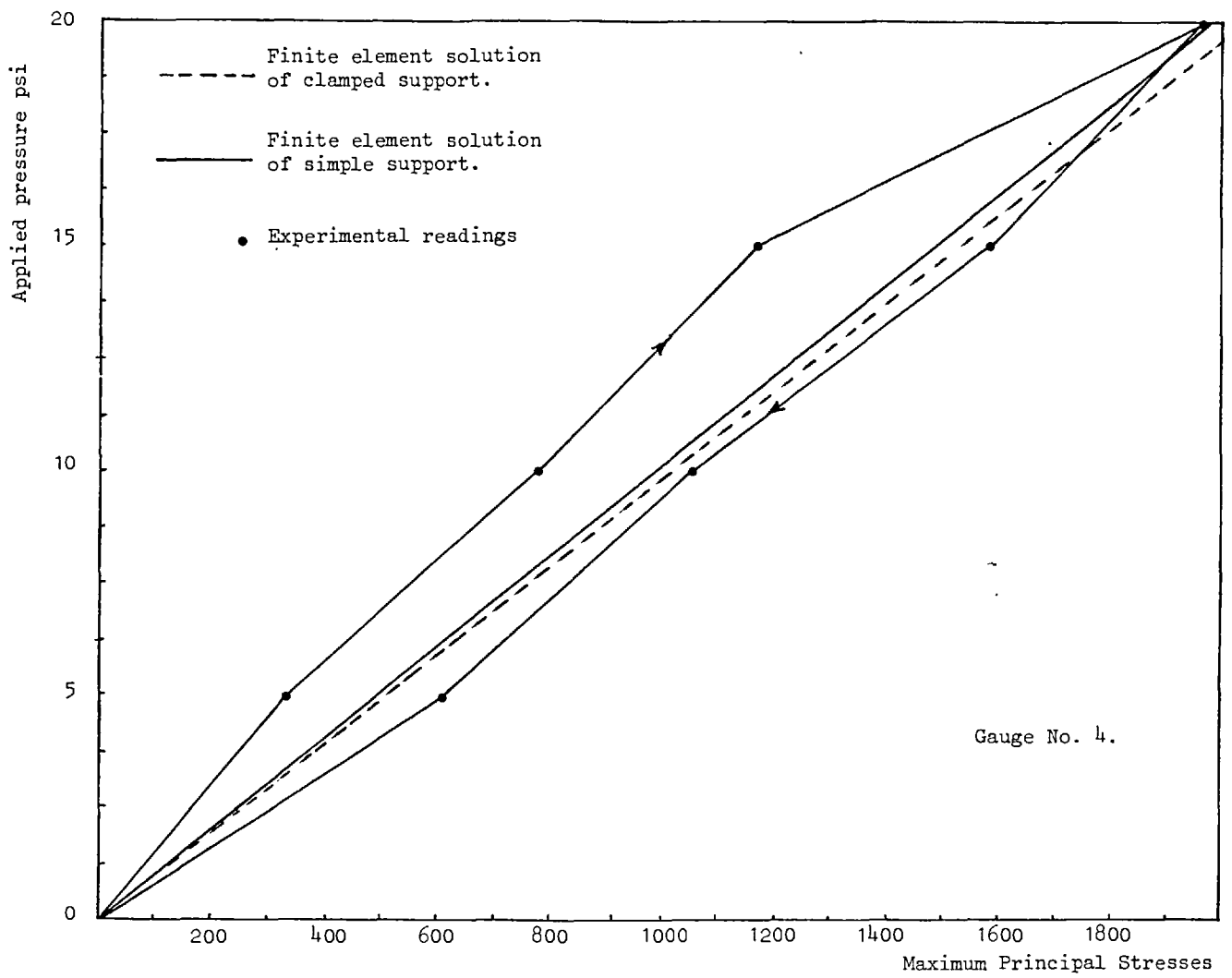


Fig. 2.64. Comparison of principal stresses

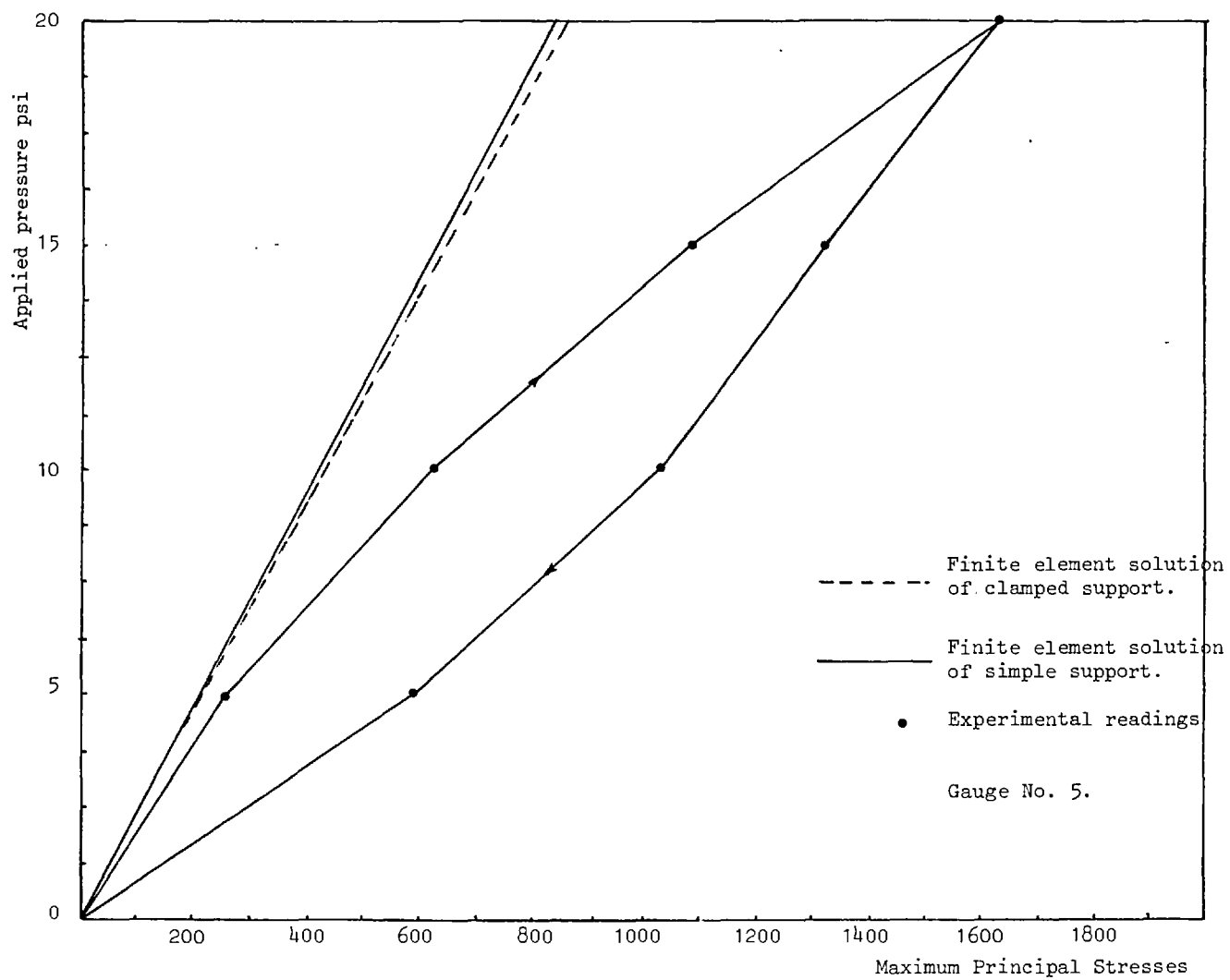


Fig. 2.65. Comparison of principal stresses

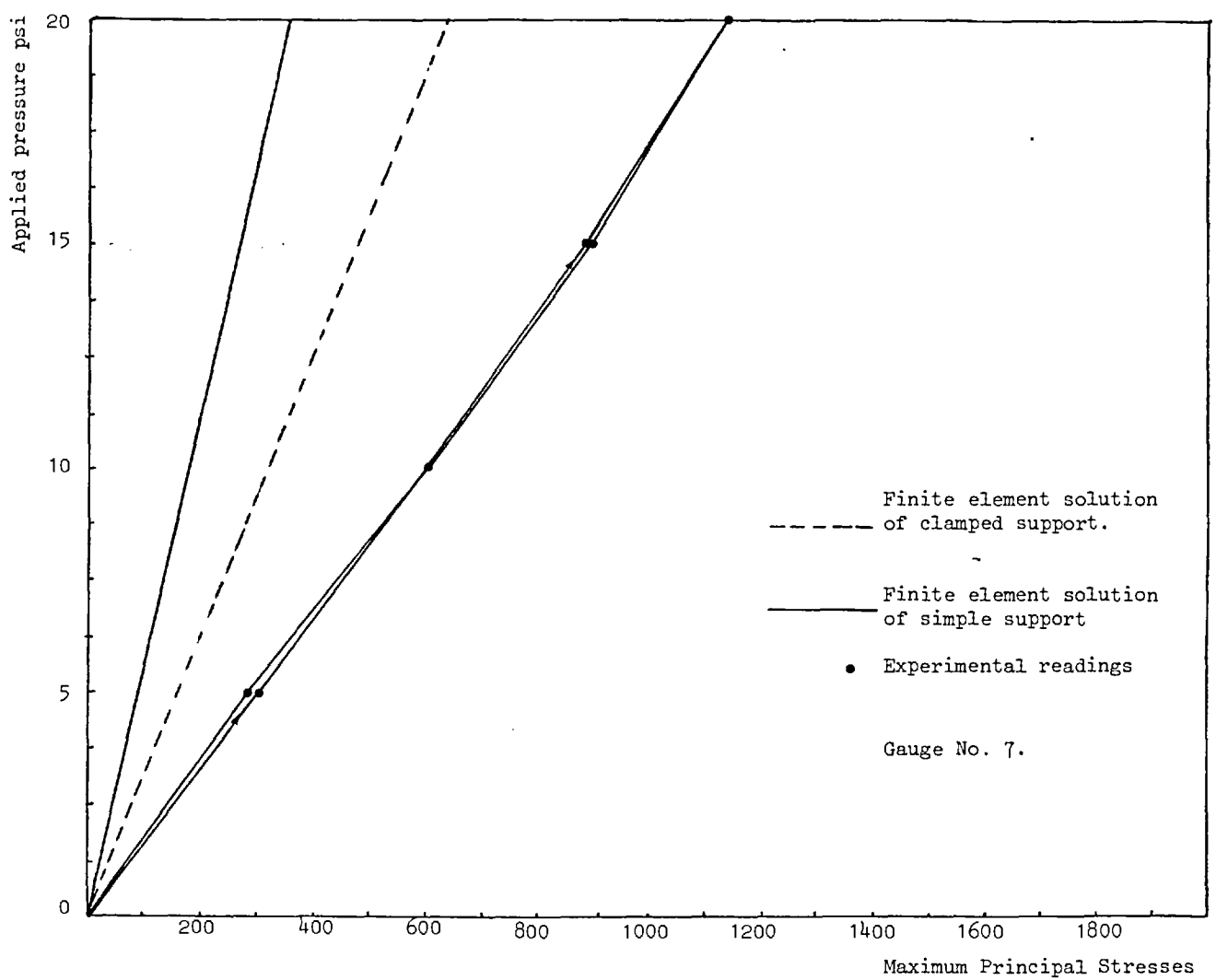


Fig. 2.66. Comparison of principal stresses

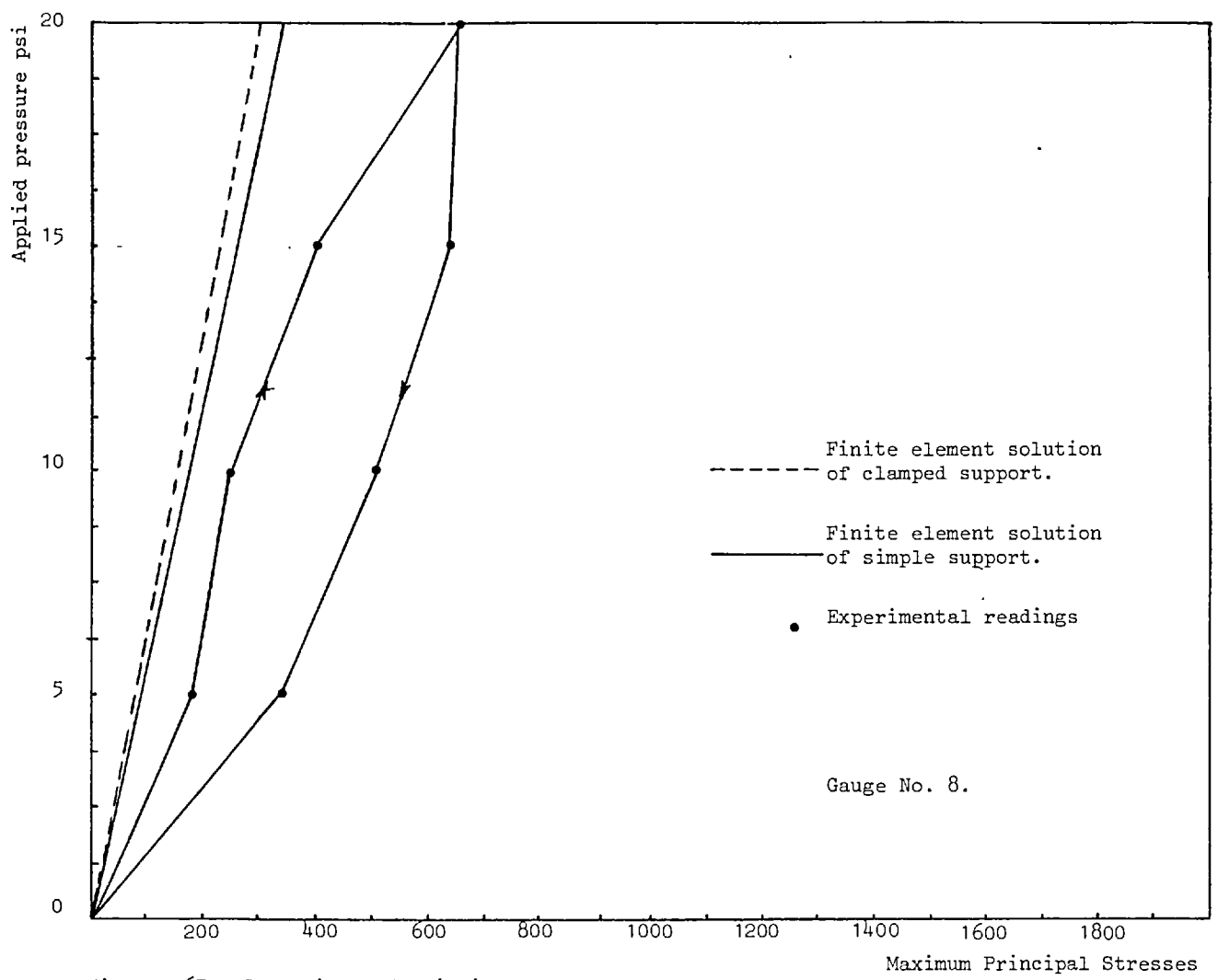


Fig. 2.67. Comparison of principal stresses

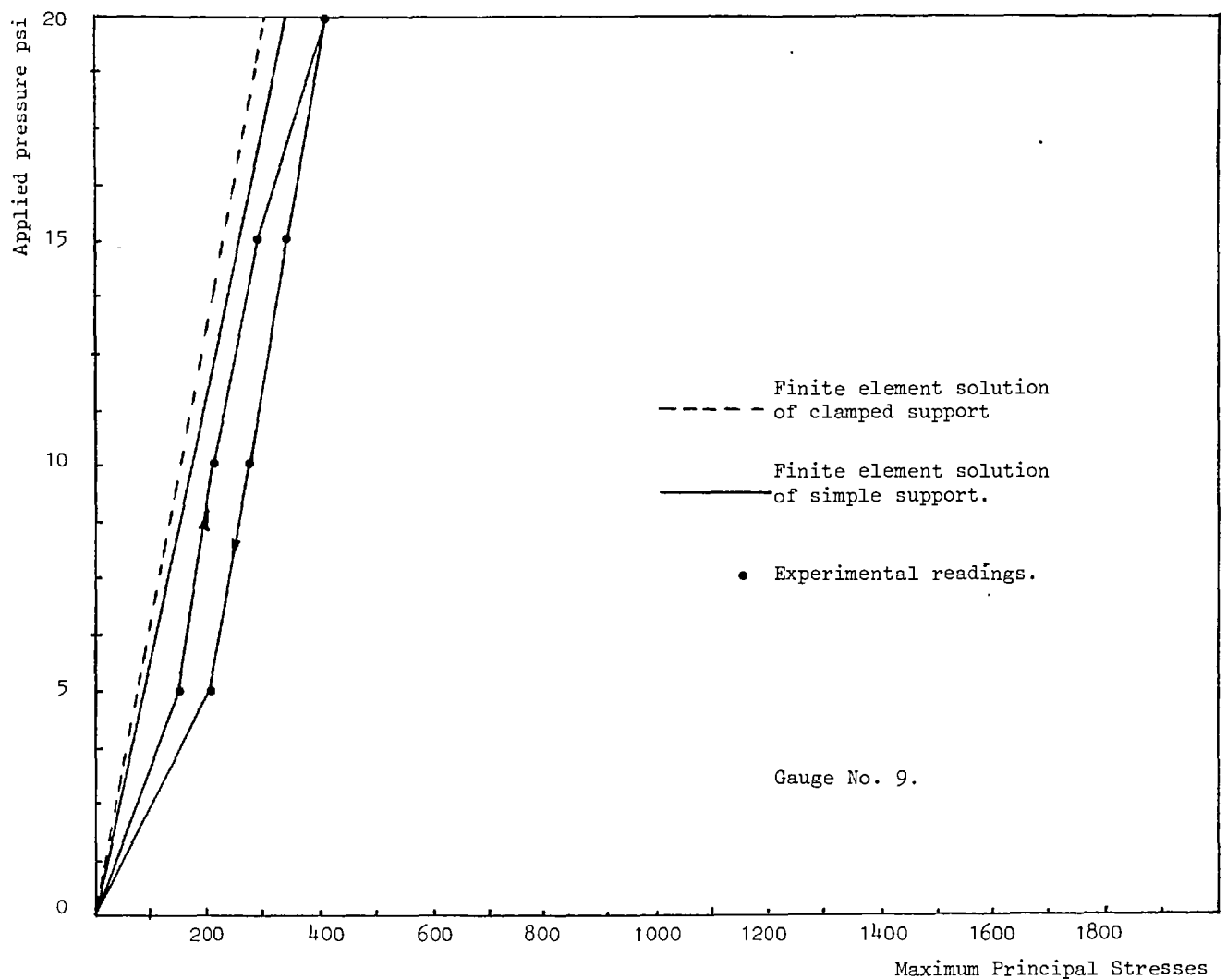


Fig. 2.68. Comparison of principal stresses

CHAPTER THREE

RELEVANT PARTS OF THE THEORY OF

ANISOTROPIC ELASTICITY

CHAPTER THREE

RELEVANT PARTS OF THE THEORY OF ANISOTROPIC ELASTICITY

3.1. Introduction:-

It is proposed to consider a general class of complex materials i.e. composites in which non-woven fibres are deliberately orientated in a matrix in such a way as to increase its structural efficiency. An imaginary general square solid with fibres embedded in a matrix in three directions, coinciding with its axes is shown diagrammatically in Fig. (3.1).

In practice a filamentary composite is normally made up of several plies or laminae. One lamina of a filamentary composite consists of one row of parallel filaments surrounded by the matrix. Considering this case, as illustrated in Fig. (3.2), the laminae are stacked with various orientations of the filament directions between laminae to obtain a laminate which has the desired stiffness or strength properties.

It is evident that each individual ply or lamina of a filamentary composite has three mutually perpendicular planes of symmetry for the material constants. The intersection of the three planes forms the axes of the co-ordinates system as shown. Since the lamina has three perpendicular axes it can be considered to be an orthotropic material on the macroscopic level. Also, the lamina may be considered homogeneous on the macro scale. The set of axes which are parallel and perpendicular to the filament directions are termed the material natural principal axes. These orthotropic properties if

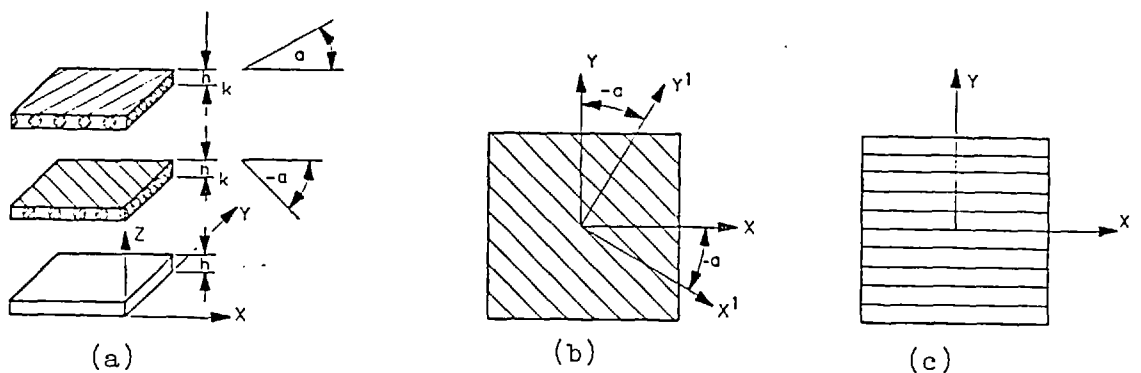


Fig. 3.2. Illustration of an orthotropic material in its laminated and lamina forms.

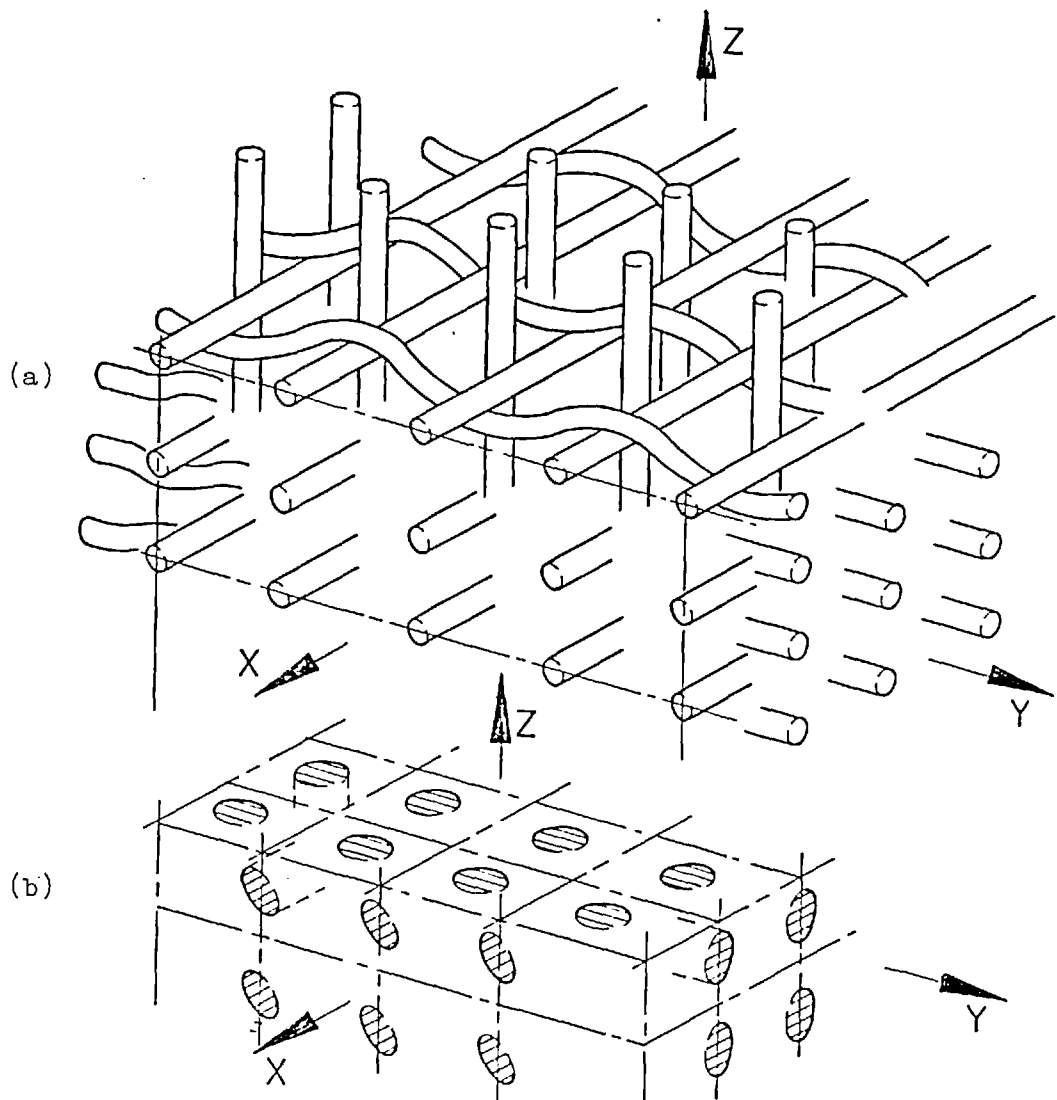


Fig. 3.1. A 3-dimensional solid of fibres embedded in matrix

translated into other convenient axes will produce an anisotropic solid in the new axes. To describe the mechanical constitution of the material a generalised Hooke's Law for the stress strain relationships is required. Ref. (39), (40), (41) & (42).

3.2. The Generalised Hooke's Law for Anisotropy

To obtain the stress strain relationships in an elastic body of this type the generalised Hooke's Law for anisotropic material will be derived first, then simplified so as to apply to orthotropic material. First consider the three-dimensional stress state illustrated in Fig. (3.3), in which it is assumed that the components of strain are linear functions of the components of stress. The equation which expresses the generalised Hooke's Law in rectangular orthogonal cartesian co-ordinates $x_1 x_2 x_3$ (or has xyz) the generalised form

$$\epsilon_{ij} = c_{ijkl} \sigma_{ij} \quad 3.1a$$

in tensor notation, with the repeated suffixes i and j taking values 1 to 3, k and l 1 to 9 and Einstein's summation convention applying. This equation may be expressed in matrix form, using engineering shear strains such as τ_{xy} etc.

thus:-

$$\begin{bmatrix} \epsilon_x \\ \epsilon_y \\ \epsilon_z \\ \gamma_{xy} \\ \gamma_{yz} \\ \gamma_{zx} \\ \gamma_{yx} \\ \gamma_{zy} \\ \gamma_{xz} \end{bmatrix} = \begin{bmatrix} c_{1111} & c_{2233} & c_{1133} & c_{1123} & c_{1131} & c_{1112} & c_{1132} & c_{1113} & c_{1121} \\ c_{2211} & c_{2222} & c_{2233} & c_{2223} & c_{2231} & c_{2212} & c_{2232} & c_{2213} & c_{2221} \\ . & . & . & . & . & . & . & . & . \\ . & . & . & . & . & . & . & . & . \\ . & . & . & . & . & . & . & . & . \\ c_{2111} & c_{2121} & c_{2133} & c_{2123} & c_{2131} & c_{2112} & c_{2132} & c_{2113} & c_{2131} \end{bmatrix} \begin{bmatrix} \sigma_x \\ \sigma_y \\ \sigma_z \\ \tau_{xy} \\ \tau_{yz} \\ \tau_{zx} \\ \tau_{yx} \\ \tau_{zy} \\ \tau_{xz} \end{bmatrix} \quad 3.1b$$

or

$$\{\epsilon\} = [C] \{\sigma\} \quad 3.1c$$

The $[C]$ matrix is the 'compliance' or 'flexibility' matrix which gives the strain stress relations for the material.

The inverse of the flexibility matrix is the stiffness matrix, and it gives the stress-strain relations.

Since there are only six independent stresses and strains, because the stress and strain tensors are symmetric, i.e.

$$\gamma_{xy} = \gamma_{yx}, \quad \tau_{xy} = \tau_{yx}$$

$$\gamma_{yz} = \gamma_{zy}, \quad \tau_{yz} = \tau_{zy}$$

$$\gamma_{zx} = \gamma_{xz}, \quad \tau_{zx} = \tau_{xz}$$

The 81 constants in the flexibility matrix are reduced to 36 elastic constants and Equation (3lc) can be written as:

$$\begin{bmatrix} \{\epsilon\} \\ 6 \times 1 \end{bmatrix} = \begin{bmatrix} [C] \\ 6 \times 6 \end{bmatrix} \begin{bmatrix} \{\sigma\} \\ 6 \times 1 \end{bmatrix} \quad 3.2$$

Where the shear components of $\{\epsilon\}$ are the three engineering shear strains rather than the tensor shear strains and the components of σ are σ_x , σ_y and σ_z (normal stresses) and τ_{xy} , τ_{yx} and τ_{zx} (shear stresses).

The solution of the above equations will give an equivalent form for the equations of the generalised Hooke's Law, namely:

$$\{\sigma\} = [D] \{\epsilon\} \quad 3.3$$

where $[D] = [C]^{-1}$, the stiffness matrix.

Assuming that an elastic potential exists equal to the potential strain energy density (strain energy per unit volume) (Ω) of deformation i.e. Ω is a function of strain then:

$$\Omega = \frac{1}{2} (\sigma_{ij} \epsilon_{ij}) \quad 3.4$$

in tensor notation

$$i,j = 1 \rightarrow 3$$

with the property that

$$\sigma_{ij} = \frac{\partial \Omega}{\partial \epsilon_{ij}} \quad 3.5$$

using Equation (3.2a) we have

$$\sigma_{ij} = \frac{\partial \Omega}{\partial \epsilon_{ij}} = C_{ijkl} \epsilon_{kl} \quad 3.6$$

$$k,l = 1 \rightarrow 3$$

Differentiating this equation with respect to ϵ_{kl} gives

$$\frac{\partial^2 \Omega}{\partial \epsilon_{ij} \partial \epsilon_{kl}} = C_{ijkl} \quad 3.7$$

in the same way we can prove that

$$\frac{\partial^2 \Omega}{\partial \epsilon_{kl} \partial \epsilon_{ij}} = C_{kl ij} \quad 3.8$$

but

$$\frac{\partial^2 \Omega}{\partial \epsilon_{ij} \partial \epsilon_{kl}} = \frac{\partial^2 \Omega}{\partial \epsilon_{kl} \partial \epsilon_{ij}} \quad 3.9$$

hence

$$C_{ij} = C_{kl ij}$$

This symmetrical property of the elements of the elasticity matrix reduces the unknowns to a total of 21 elastic constants. The most general form of this matrix for anisotropic materials may be written as:

$$[C] = \begin{bmatrix} C_{11} & C_{12} & C_{13} & C_{14} & C_{15} & C_{16} \\ C_{12} & C_{22} & C_{23} & C_{24} & C_{25} & C_{26} \\ & & & & & \\ & & & & & \\ & & & & & \\ C_{16} & C_{26} & C_{36} & C_{46} & C_{56} & C_{66} \end{bmatrix} \quad 3.10$$

where all the elements are populated.

3.3. Elastic Symmetry and Orthotropic Case

Considering one layer Fig.(3.1b), if the density of fibre is uniform, then the assumption that the three orthogonal planes of elastic symmetry can pass through any point of the body is a valid assumption.

Considering an element of the body in the form of a rectangular parallelopiped with sides parallel to the planes of elastic symmetry, after a deformation due to the action of the stress σ_z , it will remain a rectangular parallelopiped as shown in Fig. (3.4).

As the three principal directions apply to each point of the body, we can assume that the normal and shear stresses are all uncoupled, i.e. C_{14} , C_{15} , C_{16} , C_{24} , C_{25} , C_{26} , C_{34} and C_{36} are all equal to zero.

By essentially the same reasons the coupling between the shear stresses will also vanish, i.e. C_{45} , C_{46} and C_{56} are all equal to zero. The coupling between normal stresses, however, are expected to remain Tsai Ref. (39).

By directing the axes of the co-ordinates perpendicular to these planes, we obtain the following equations for the generalised Hooke's Law.

$$\epsilon_x = C_{11} \sigma_x + C_{12} \sigma_y + C_{13} \sigma_z \quad 3.11a$$

$$\epsilon_y = C_{12} \sigma_x + C_{22} \sigma_y + C_{23} \sigma_z \quad 3.11b$$

$$\epsilon_z = C_{13} \sigma_x + C_{23} \sigma_y + C_{33} \sigma_z \quad 3.11c$$

$$\gamma_{xy} = C_{44} \tau_{xy} \quad 3.11d$$

$$\gamma_{yz} = C_{55} \tau_{yz} \quad 3.11e$$

$$\gamma_{zx} = C_{66} \tau_{zx} \quad 3.11f$$

and the compliance (flexibility) matrix becomes

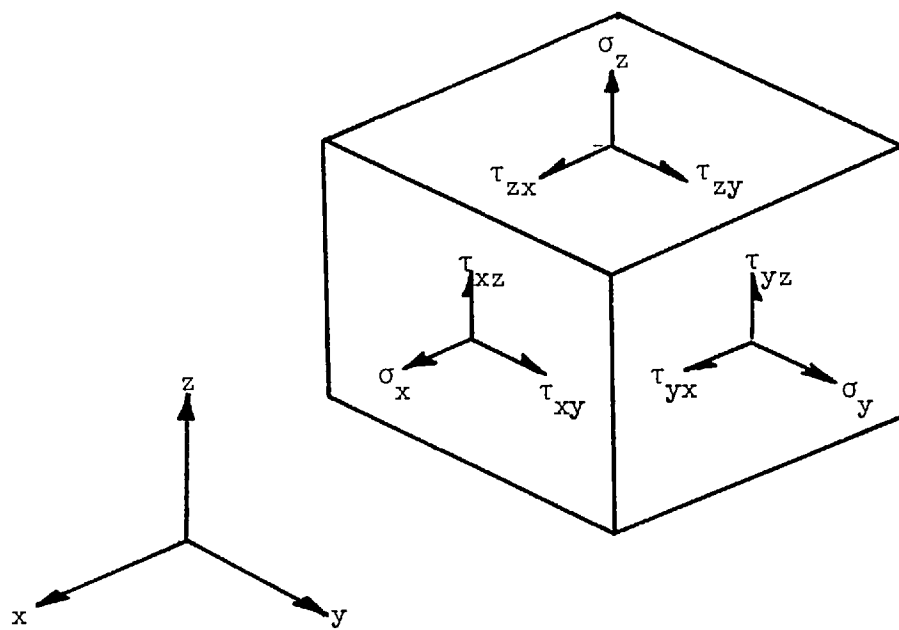


Fig. 3.3. 3-Dimensional state of stress

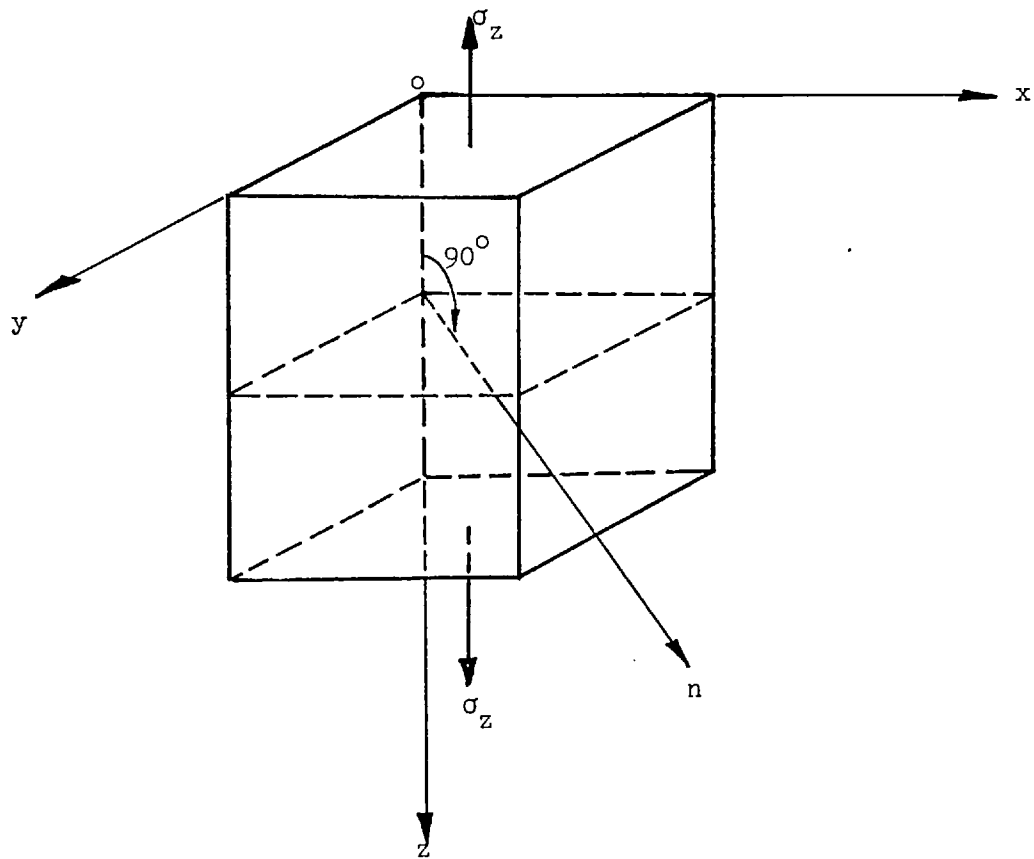


Fig. 3.4. 3-Dimensional element

$$[c] = \begin{bmatrix} c_{11} & c_{12} & c_{13} & 0 & 0 & 0 \\ & c_{22} & c_{23} & 0 & 0 & 0 \\ & & c_{33} & 0 & 0 & 0 \\ \text{Symmetrical} & & & c_{44} & 0 & 0 \\ & & & & c_{55} & 0 \\ & & & & & c_{66} \end{bmatrix} \quad 3.12$$

and nine independent elastic constants remain. They are called the principal constants and can be expressed in terms of "technical constants". Adopting the notation

E_x, E_y, E_z (Young's moduli), G_{xy}, G_{yz}, G_{zx} (Shear moduli)

and $\nu_{12}, \nu_{21}, \nu_{13}, \nu_{31}, \nu_{23}, \nu_{32}$ (Poisson's ratios)

Equation (3.11) may be written in the form:

$$\epsilon_x = \frac{1}{E_x} \sigma_x - \frac{\nu_{21}}{E_y} \sigma_y - \frac{\nu_{31}}{E_z} \sigma_z \quad 3.13a$$

$$\epsilon_y = \frac{\nu_{12}}{E_x} \sigma_x + \frac{1}{E_y} \sigma_y - \frac{\nu_{32}}{E_z} \sigma_z \quad 3.13b$$

$$\epsilon_z = -\frac{\nu_{13}}{E_z} \sigma_x - \frac{\nu_{23}}{E_y} \sigma_y + \frac{1}{E_z} \sigma_z \quad 3.13c$$

$$\gamma_{xy} = \frac{1}{G_{xy}} \tau_{xy} \quad 3.13d$$

$$\gamma_{yz} = \frac{1}{G_{yz}} \tau_{yz} \quad 3.13e$$

$$\gamma_{zx} = \frac{1}{G_{zx}} \tau_{zx} \quad 3.13f$$

where

$$E_x \nu_{21} = E_y \nu_{12} \quad 3.14a$$

$$E_y \nu_{32} = E_z \nu_{23} \quad 3.14b$$

$$E_z \nu_{13} = E_x \nu_{31} \quad 3.14c$$

and

$$C_{11} = \frac{1}{E_x} \quad 3.14d$$

$$C_{12} = -\frac{\nu_{21}}{E_y} \quad 3.14e$$

$$C_{13} = -\frac{\nu_{31}}{E_z} \quad 3.14f$$

$$C_{22} = \frac{1}{E_y} \quad 3.14g$$

$$C_{23} = \frac{\nu_{32}}{E_y} \quad 3.14h$$

$$C_{33} = \frac{1}{E_z} \quad 3.14i$$

$$C_{44} = \frac{1}{G_{xy}} \quad 3.14j$$

$$C_{55} = \frac{1}{G_{yz}} \quad 3.14k$$

$$C_{66} = \frac{1}{G_{zx}} \quad 3.14l$$

The body which has three orthogonal planes of elastic symmetry at each point is called orthogonally-anisotropic, or for brevity, orthotropic. This form of elastic symmetry is very important because it occurs in fibre composites. If such a material is considered in any other co-ordinates it becomes anisotropic and since the properties will be identified together with the finite element locations in eleven local axes the orthotropic properties are all that is required.

3.4. Transformation Rules for an Orthotropic Body

3.4.1. Stress Transformation

Knowing the stresses in three mutually perpendicular planes or directions, which are referred to as the material natural axes (1, 2, 3), the stress which acts on any plane passing through the same point can be determined. Hence

$$(\sigma_x)_n = \sigma_{11} \cos(n,1) + \tau_{12} \cos(n,2) + \tau_{13} \cos(n,3)$$

$$(\sigma_y)_n = \tau_{12} \cos(n,1) + \sigma_{22} \cos(n,2) + \tau_{23} \cos(n,3)$$

$$(\sigma_z)_n = \tau_{13} \cos(n,1) + \tau_{23} \cos(n,2) + \sigma_{33} \cos(n,3)$$

where $(\sigma_x)_n$, $(\sigma_y)_n$ and $(\sigma_z)_n$ are components of stress which act on any plane with the arbitrary normal direction n and $\cos(n,1)$ is the direction cosine between the n -direction and the 1-direction, for example. By projection, using equations above, it is possible to find the normal and tangential components of stress acting on any arbitrary plane.

Considering, for convenience, the reference cartesian system x, y, z , the position of this system with respect to the 1, 2, 3 system is determined by the Table (3.1) of direction cosines, where $l_i = \cos(n_i, 1)$, $m_i = \cos(n_i, 2)$ etc. Equation (3.14).

By projecting $(\sigma_x)_n$, $(\sigma_y)_n$, $(\sigma_z)_n$ in the direction of reference axes (i.e. on to the planes normal to the x, y, z axes), we obtain

$$\begin{aligned} \sigma_x &= \sigma_1 l_1^2 + \sigma_2 m_1^2 + \sigma_3 n_1^2 + 2 \tau_{12} l_1 m_1 + 2 \tau_{13} l_1 n_1 \\ &\quad + 2 \tau_{23} n_1 m_1 \end{aligned} \quad 3.15$$

and

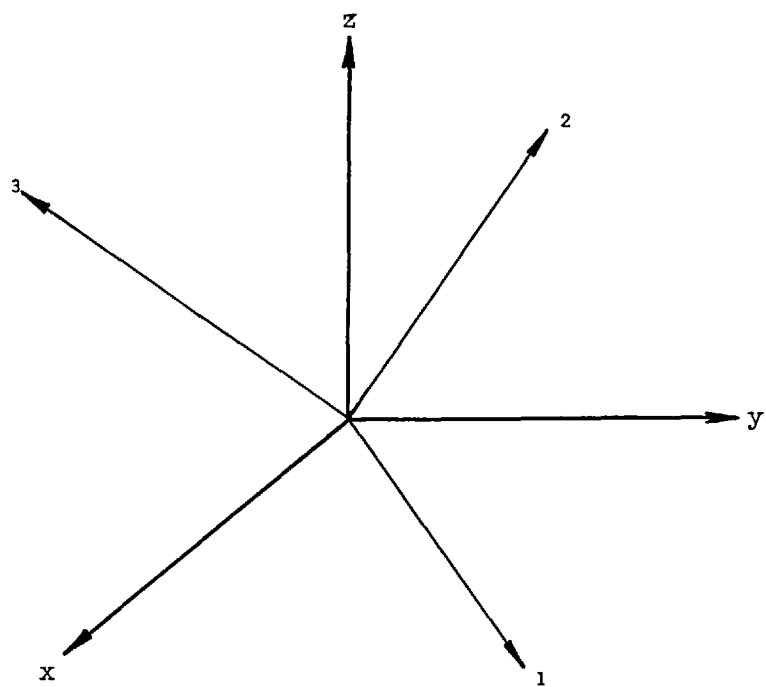
$$\begin{aligned} \tau_{xy} &= \sigma_1 l_1 m_1 + \sigma_2 m_1 n_1 + \sigma_3 n_1 l_1 + \tau_{12} (l_1 m_2 + l_2 m_1) \\ &\quad + \tau_{23} (m_1 n_2 + m_2 n_1) + \tau_{31} (n_1 l_2 + n_2 l_1) \end{aligned} \quad 3.16$$

The expression for σ_y and σ_z are obtained by means of cyclic permutation of the suffixes of l, m and n in Equation (3.15).

Similarly, τ_{yz} and τ_{xz} may be obtained from Equation (3.16).

The general formula for the transformation from 1, 2, 3 to x, y, z systems, in matrix form, will be:-

$$\left[\begin{array}{c} \sigma_x \\ \sigma_y \\ \sigma_z \\ \tau_{xy} \\ \tau_{yz} \\ \tau_{zx} \end{array} \right] = \left[\begin{array}{cccccc} l_1^2 & m_1^2 & n_1^2 & 2l_1 m_1 & 2m_1 n_1 & 2n_1 l_1 \\ l_2^2 & m_2^2 & n_2^2 & 2l_2 m_2 & 2m_2 n_2 & 2n_2 l_2 \\ l_3^2 & m_3^2 & n_3^2 & 2l_3 m_3 & 2m_3 n_3 & 2n_3 l_3 \\ l_1 m_1 & m_1 n_1 & n_1 l_1 & (l_1 m_2 + l_2 m_1) & (m_1 n_2 + m_2 n_1) & (n_1 l_2 + n_2 l_1) \\ l_2 m_2 & m_2 n_2 & n_2 l_2 & (l_2 m_3 + l_3 m_2) & (m_2 n_3 + m_3 n_2) & (n_2 l_3 + n_3 l_2) \\ l_3 m_3 & m_3 n_3 & n_3 l_3 & (l_3 m_1 + l_1 m_3) & (m_3 n_1 + m_1 n_3) & (n_3 l_1 + n_1 l_3) \end{array} \right] \left[\begin{array}{c} \sigma_1 \\ \sigma_2 \\ \sigma_3 \\ \tau_{12} \\ \tau_{23} \\ \tau_{31} \end{array} \right]$$



	x	y	z
1	l_1	m_1	n_1
2	l_2	m_2	n_2
3	l_3	m_3	n_3

Table: 3.1. Direction cosines between two sets of coordinates

or

$$\{\sigma\} = \begin{bmatrix} R_{11} & R_{12} \\ R_{21} & R_{22} \end{bmatrix} \{\bar{\sigma}\} \quad 3.17a$$

$$\{\sigma\} = [\bar{R}] \{\bar{\sigma}\} \quad 3.17b$$

3.4.2. Strain Transformation

Let \bar{C}_{ij} be the coefficients of strain for the system 1, 2, 3 of the elements. It is required to determine the coefficients for the new global system x, y, z which will be denoted by C_{ij} . For this new system the equations of the generalised Hooke's law are:

$$\{\epsilon\} = [C] \{\sigma\} \quad 3.18$$

The elastic potential, which is considered as a function of the components of stress, is determined by Equation (3.4), and its expression is:

$$\Omega = \frac{1}{2} [\bar{C}] \{\sigma\}^T \{\sigma\}, \quad 3.19$$

whilst the elastic potential for the natural axes of the original element is given by the expression:

$$\Omega = \frac{1}{2} [\bar{C}] \{\bar{\sigma}\}^T \{\bar{\sigma}\} \quad 3.20$$

Equating the two expressions for the elastic potential we obtain the following:

$$\frac{1}{2} [\bar{C}] \{\sigma\}^T \{\bar{\sigma}\} = \frac{1}{2} [C] \{\sigma\}^T \{\sigma\}. \quad 3.21$$

since

$$\{\bar{\sigma}\} = [\bar{C}] \{\bar{\epsilon}\}$$

and

$$\{\sigma\} = [C] \{\varepsilon\}$$

Equation (3.21) gives:

$$\{\bar{\varepsilon}\}^T \{\bar{\sigma}\} = \{\varepsilon\}^T \{\sigma\}$$

Using Equation (3.17b) we get:

$$\begin{aligned} \{\bar{\varepsilon}\}^T \{\bar{\sigma}\} &= \{\varepsilon\}^T [R] \{\bar{\sigma}\} \\ \{\varepsilon\} &= [R^T]^{-1} \{\bar{\varepsilon}\} \\ \{\varepsilon\} &= [R_\varepsilon] \{\bar{\varepsilon}\} \end{aligned} \quad 3.22$$

This gives the strain transformation rule. The matrices

$[R]$ & $[R_\varepsilon]$ each have the property that the inverse of one equals the transpose of the other, i.e.

$$[R]^T [R_\varepsilon] = [I]$$

and

$$[R_\varepsilon] = \begin{bmatrix} R_{11} & \frac{1}{2}R_{12} \\ - & - & - & - \\ 2R_{21} & R_{22} \end{bmatrix} \quad 3.23$$

3.4.3. Constants of Elasticity

The stress-strain relations may be written in either coordinate system as:-

$$\{\sigma\} = [D] \{\varepsilon\} \quad 3.24$$

in one and

$$\{\bar{\sigma}\} = [\bar{D}] \{\bar{\varepsilon}\} \quad 3.25$$

in the other

Suppose $\underline{[D]}$ is the elasticity matrix related to the material natural axes, and $\underline{[D]}$ is required.

We are dealing with orthotropic materials where the elastic properties are known in the principal directions 1, 2, 3 but these properties are needed in global coordinates x, y, z to generate the element stiffness matrix as will be discussed.

Transformation of $\underline{[D]}$ is also needed for the isoparametric shell element of Chapter Four.

The transformation is derived from the arguments that during any loading process the resulting strain energy density must be the same regardless of the coordinate system in which it is computed, thus from Equations (3.19) to (3.22):

$$\Omega = \frac{1}{2} \{\epsilon\}^T \{\sigma\} = \frac{1}{2} \{\bar{\epsilon}\}^T \{\bar{\sigma}\} \quad 3.26$$

Substituting from Equations (3.24) and (3.25) leads to:

$$\begin{aligned} \{\epsilon\}^T \{\sigma\} &= \{\epsilon\}^T [\underline{R}_\epsilon]^T [\underline{\bar{D}}] \{\bar{\epsilon}\} \\ \{\epsilon\}^T \left[\{\sigma\} - [\underline{R}_\epsilon]^T [\underline{\bar{D}}] [\underline{R}_\epsilon] \{\bar{\epsilon}\} \right] &= 0 \end{aligned} \quad 3.27$$

As the latter relation must be true for any $\{\epsilon\}$, the coefficients of $\{\epsilon\}$ must vanish. Thus we obtain:

$$\{\sigma\} = [\underline{D}] \{\epsilon\}$$

where the coefficients of D are as follows:

$$[\underline{D}] = [\underline{R}_\epsilon]^T [\underline{\bar{D}}] [\underline{R}_\epsilon] \quad 3.28$$

CHAPTER FOUR

FINITE ELEMENT MODEL AND SOLUTION

CHAPTER FOUR
VARIABLE NUMBER NODE THICK ANISOTROPIC
SHELL ELEMENT

4.1. INTRODUCTION

In this chapter a general formulation for a quadratic, isoparametric, anisotropic element of a thick shell is developed which permits the analysis of any arbitrarily layered curved shell or solid structure.

The use of general shell theory to derive doubly curved elements involves geometric complexities that make shell theory difficult. These difficulties are avoided with gained economy by appropriately specialising a three-dimensional solid element which has suitable doubly curved surfaces.

To achieve this, an isoparametric element is chosen, Ref. (45) with the same interpolation functions to define the element shape as those used to define displacements within the element.

4.2. Geometrical Representation of Various Elements in Natural
and Global Coordinates.

In this work, all elements will be geometrically represented according to its global nodal coordinates. On the other hand each one of them should be represented according to the orthotropic properties of its material. Therefore, it is necessary to define the natural axes of each material with respect to the global axes to obtain a general representation.

Consider the linear interpolation function

$$f_1 = \alpha_1 + \alpha_2\xi + \alpha_3\eta + \alpha_4\zeta + \alpha_5\xi\eta + \alpha_6\eta\zeta + \alpha_7\xi\zeta + \alpha_8\xi\eta\zeta \quad 4.1$$

To represent a linear 8-node hexahedron Fig. (4.1), where ξ, η, ζ are the isoparametric (natural) coordinates of the elements, then the boundary conditions are as follows:-

$$\xi, \eta, \zeta = 0 \text{ (at the centroid of the element)} \quad 4.2$$

and $\xi, \eta, \zeta = \pm 1$ (at the surface). See Appendix (5).

A more warped element with doubly curved surfaces Fig. (4.2) could be adequately represented by the quadratic interpolation function

$$f_2 = f_1 + \alpha_9\xi^2 + \alpha_{10}\eta^2 + \alpha_{11}\zeta^2 + \alpha_{12}\xi^2\eta + \alpha_{13}\xi^2\zeta + \alpha_{14}\eta^2\xi + \alpha_{15}\eta^2\zeta + \alpha_{16}\zeta^2\xi + \alpha_{17}\zeta^2\eta + \alpha_{18}\xi^2\eta\zeta + \alpha_{19}\eta^2\xi\zeta + \alpha_{20}\zeta^2\xi\eta \quad 4.3$$

The global coordinates of any nodal point (x, y, z) would then be

$$x = \sum_{i=1}^{20} N_i x_i \quad 4.4$$

$$y = \sum_{i=1}^{20} N_i y_i$$

$$z = \sum_{i=1}^{20} N_i z_i$$

Where (N_i) the mapping or shape functions are

$$N_i = \frac{1}{8}(1+\xi\xi_i)(1+\eta\eta_i)(1+\zeta\zeta_i)(\xi\xi_i+\eta\eta_i+\zeta\zeta_i-2) \quad 4.5a$$

for $i = 1$ to 8

$$N_i = \frac{1}{4}(1-\xi^2)(1+\eta\eta_i)(1+\zeta\zeta_i) \quad 4.5b$$

for $i = 9, 11, 13, 15$

$$N_i = \frac{1}{4}(1-\eta^2)(1+\xi\xi_i)(1+\zeta\zeta_i) \quad 4.5c$$

for $i = 10, 12, 14, 16$

$$N_i = \frac{1}{4}(1-\zeta^2)(1+\xi\xi_i)(1+\eta\eta_i) \quad 4.5d$$

for $i = 17, 18, 19, 20$

This mapping is an interpolation scheme that yields the global xyz coordinates of any point in the element when the corresponding natural $\xi\eta\zeta$ coordinates are given.

The natural coordinate axes $\xi\eta\zeta$ are in general not orthogonal. They are orthogonal, of course, when the surfaces are planes and the element is the basic rectangular parallelepiped.

Fig. (4.3a).

4.3. Displacement Fields

The displacements within the element are defined by the same interpolation (shape) functions as are used to define the element shape. Thus

$$u = \sum_{i=1}^{20} N_i u_i \quad 4.6$$

$$v = \sum_{i=1}^{20} N_i v_i$$

$$w = \sum_{i=1}^{20} N_i w_i$$

In which u , v and w are measured along the global coordinate axes x , y and z and the u_i , v_i , w_i are measured along the natural coordinate directions $\xi\eta\zeta$

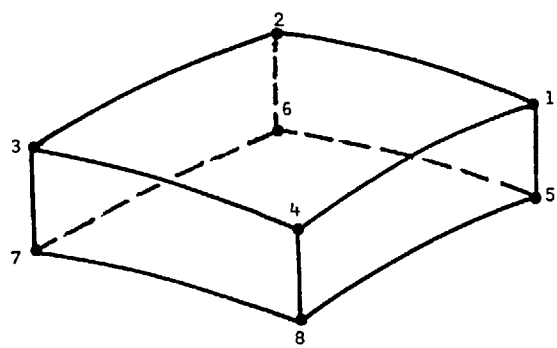


Fig. 4.1. 8-Node first order hexahedron

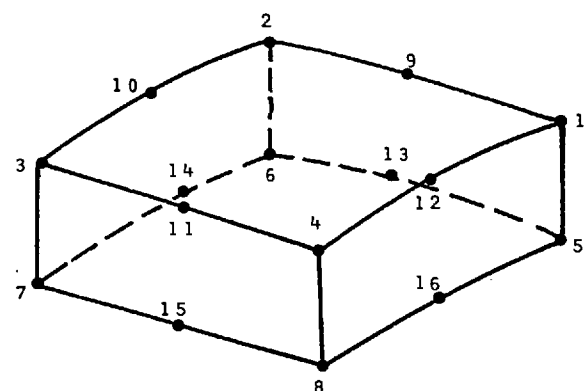
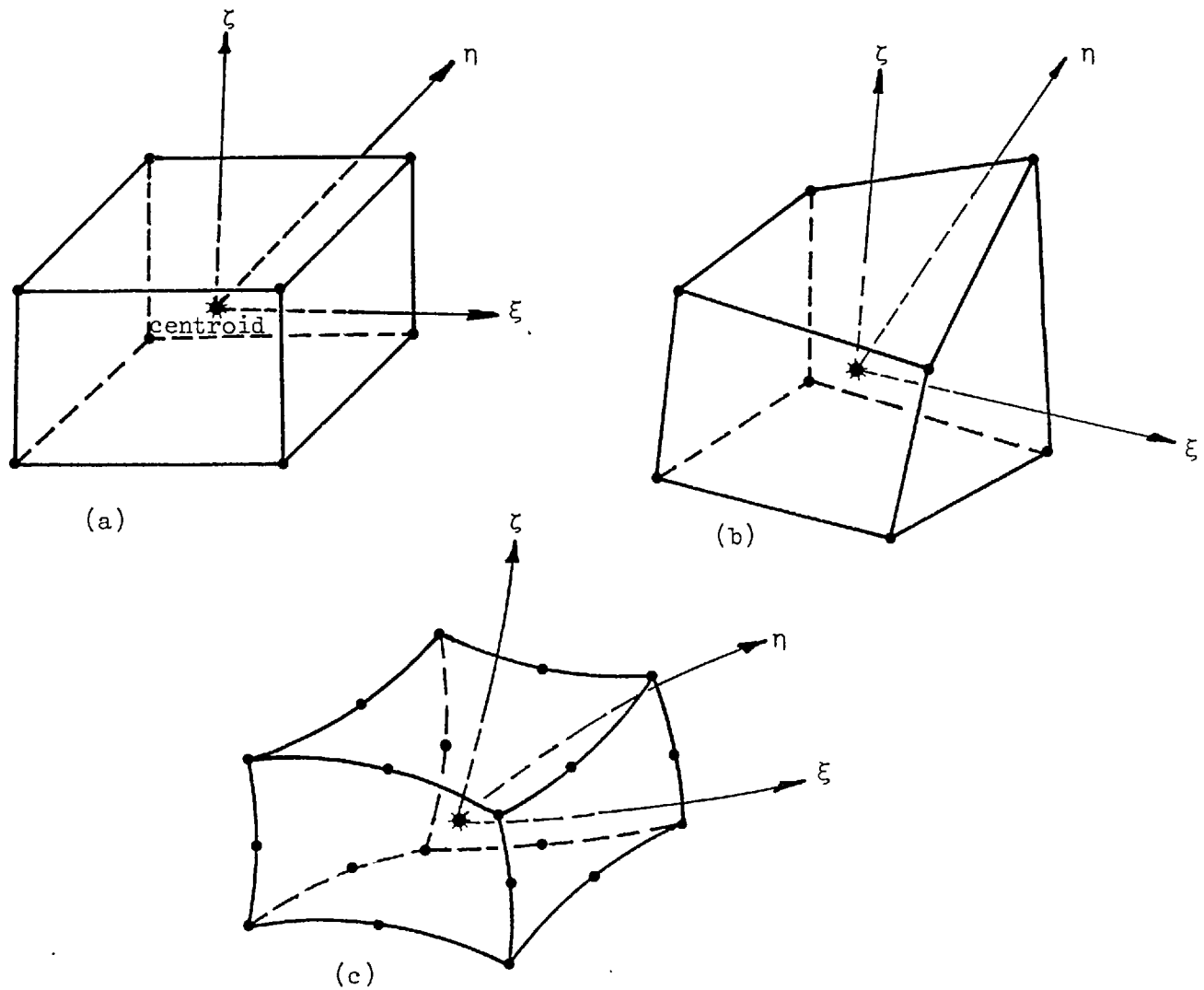


Fig. 4.2. 16-Node Element



Figs. 4.3a., 4.3b & 4.3c General elements (natural coordinates).

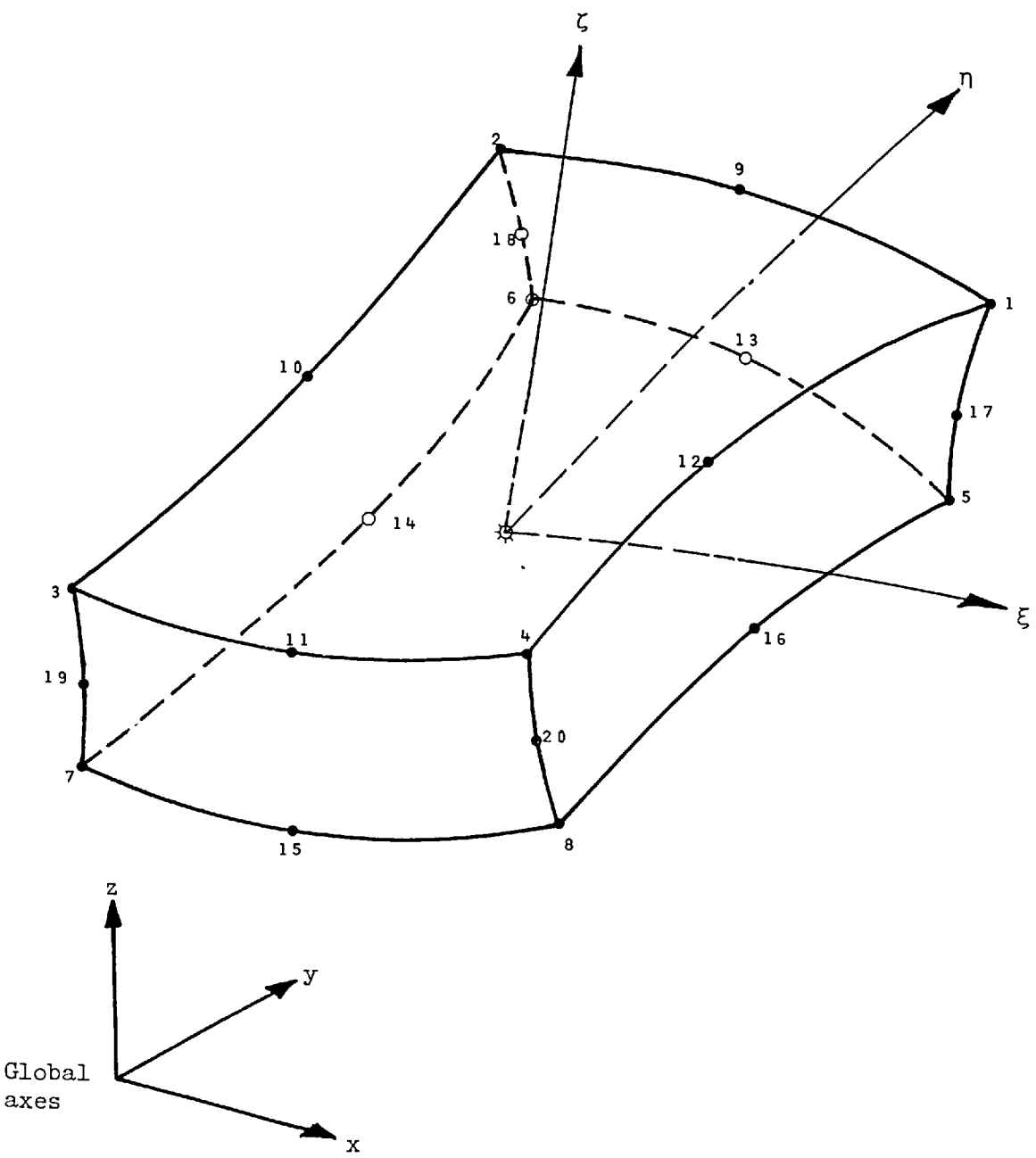


Fig. 4.4. Twenty node quadratic hexahedron

The relationships between derivatives in the two coordinate systems are established by the chain rule of differentiation as follows, for example (where, e.g., $x_{,\xi}$ means $\frac{\partial x}{\partial \xi}$)

$$\begin{Bmatrix} (),_{,\xi} \\ (),_{,\eta} \\ (),_{,\zeta} \end{Bmatrix} = \begin{bmatrix} x_{,\xi} & y_{,\xi} & z_{,\xi} \\ x_{,\eta} & y_{,\eta} & z_{,\eta} \\ x_{,\zeta} & y_{,\zeta} & z_{,\zeta} \end{bmatrix} \begin{Bmatrix} (),_{,x} \\ (),_{,y} \\ (),_{,z} \end{Bmatrix} = [J] \begin{Bmatrix} (),_{,x} \\ (),_{,y} \\ (),_{,z} \end{Bmatrix} \quad 4.7$$

Where $[J]$ is the summed Jacobian matrix, defined by the following:-

$$[J] = \sum_{i=1}^{20} \left\{ \begin{array}{c} \frac{\partial N_i}{\partial \xi} \\ \frac{\partial N_i}{\partial \eta} \\ \frac{\partial N_i}{\partial \zeta} \end{array} \right\} \begin{bmatrix} x_i & y_i & z_i \end{bmatrix} \quad 4.8$$

The differential volume of the whole element transforms to

$$d(\text{volume}) = \left| \det [J] \right| d\xi d\eta d\zeta \quad 4.9$$

in which $\left| \det [J] \right|$ = the absolute value of the determinant of the summed Jacobian matrix.

Since $[J]$ is a variable, numerical integration is unavoidable. Three dimensional gaussian quadrature is used.

The nodal variables are translations (without derivatives) and the coordinate transformations have the same form as those of the displacements.

To ensure convergence

$$\sum_{i=1}^{20} N_i = 1 \quad 4.10$$

4.4. Strain Displacement Relationships

For the three dimensional solid the field of total strain is expressed as:

$$\{\epsilon\} = \begin{Bmatrix} \epsilon_x \\ \epsilon_y \\ \epsilon_z \\ \gamma_{xy} \\ \gamma_{yz} \\ \gamma_{zx} \end{Bmatrix} = \begin{Bmatrix} \frac{\partial u}{\partial x} \\ \frac{\partial v}{\partial x} \\ \frac{\partial w}{\partial z} \\ \frac{\partial u}{\partial y} + \frac{\partial v}{\partial x} \\ \frac{\partial v}{\partial z} + \frac{\partial w}{\partial y} \\ \frac{\partial w}{\partial x} + \frac{\partial u}{\partial z} \end{Bmatrix} \quad 4.11$$

Substituting Equation (4.6) into (4.11) gives:

$$\frac{\partial u}{\partial x} = \sum_{i=1}^{20} \frac{\partial N_i}{\partial x} u_i$$

$$\frac{\partial v}{\partial y} = \sum_{i=1}^{20} \frac{\partial N_i}{\partial y} v_i$$

$$\frac{\partial w}{\partial z} = \sum_{i=1}^{20} \frac{\partial N_i}{\partial z} w_i$$

4.12

$$\frac{\partial u}{\partial y} + \frac{\partial v}{\partial x} = \sum_{i=1}^{20} \frac{\partial N_i}{\partial y} u_i + \sum_{i=1}^{20} \frac{\partial N_i}{\partial x} v_i$$

$$\frac{\partial v}{\partial z} + \frac{\partial w}{\partial y} = \sum_{i=1}^{20} \frac{\partial N_i}{\partial z} v_i + \sum_{i=1}^{20} \frac{\partial N_i}{\partial y} w_i$$

$$\frac{\partial w}{\partial x} + \frac{\partial u}{\partial z} = \sum_{i=1}^{20} \frac{\partial N_i}{\partial x} w_i + \sum_{i=1}^{20} \frac{\partial N_i}{\partial z} u_i$$

Thus

$$\{\varepsilon\} = \sum_{i=1}^{20} \left\{ \begin{array}{ccc} \frac{\partial N_i}{\partial x} & 0 & 0 \\ 0 & \frac{\partial N_i}{\partial y} & 0 \\ 0 & 0 & \frac{\partial N_i}{\partial z} \\ \frac{\partial N_i}{\partial y} & \frac{\partial N_i}{\partial x} & 0 \\ 0 & \frac{\partial N_i}{\partial z} & \frac{\partial N_i}{\partial y} \\ \frac{\partial N_i}{\partial z} & 0 & \frac{\partial N_i}{\partial x} \end{array} \right\} \begin{bmatrix} u_i \\ v_i \\ w_i \end{bmatrix} \quad 4.13$$

or

$$\{\varepsilon\} = \sum_{i=1}^{20} [B]_i \{\delta\}_i \quad 4.14$$

The interpolation functions N_i are defined in terms of the natural curvilinear coordinates ξ, η, ζ , so that a change in the derivatives of $[B]_i$ is required to relate global to natural derivatives thus:-

$$\begin{bmatrix} \frac{\partial}{\partial x} \\ \frac{\partial}{\partial y} \\ \frac{\partial}{\partial z} \end{bmatrix} = [J]^{-1} \begin{bmatrix} \frac{\partial}{\partial \xi} \\ \frac{\partial}{\partial \eta} \\ \frac{\partial}{\partial \zeta} \end{bmatrix} \quad 4.15$$

Where $[J]$ is as defined in Equation (4.8).

Hence

$$\{\varepsilon\} = \sum_{i=1}^{20} [J]^{-1} [B^*]_i \{\delta\} \quad 4.16$$

Where $[B^*]$ is given by the Equation.

$$[\underline{\underline{B^*}}] = \begin{bmatrix} \frac{\partial N_i}{\partial \xi} & 0 & 0 \\ 0 & \frac{\partial N_i}{\partial \eta} & 0 \\ 0 & 0 & \frac{\partial N_i}{\partial \zeta} \\ \frac{\partial N_i}{\partial \eta} & \frac{\partial N_i}{\partial \xi} & 0 \\ 0 & \frac{\partial N_i}{\partial \zeta} & \frac{\partial N_i}{\partial \eta} \\ \frac{\partial N_i}{\partial \zeta} & 0 & \frac{\partial N_i}{\partial \xi} \end{bmatrix}$$

Equation (4.16) can be written as:

$$\{\varepsilon\} = [\underline{\underline{B}}] \{\delta\} \quad 4.17$$

Which is the required strain-displacement relationship

4.5. Stress-Strain Relations

For an orthotropic material whose natural axes are 1-2-3, the stress strain relations are: Ref. (46).

$$\left\{ \begin{array}{l} \sigma_{11} \\ \sigma_{22} \\ \sigma_{33} \\ \tau_{12} \\ \tau_{23} \\ \tau_{31} \end{array} \right\} = \left[\begin{array}{cccccc} D_{11} & D_{12} & D_{13} & 0 & 0 & 0 \\ & D_{22} & D_{23} & 0 & 0 & 0 \\ & & D_{33} & 0 & 0 & 0 \\ & & & G_{12} & 0 & 0 \\ & & & & G_{23} & 0 \\ & & & & & G_{31} \end{array} \right] \left\{ \begin{array}{l} \varepsilon_{11} \\ \varepsilon_{22} \\ \varepsilon_{33} \\ \gamma_{12} \\ \gamma_{23} \\ \gamma_{31} \end{array} \right\}$$

Symmetrical

or

$$\{\sigma'\} = [\underline{\underline{D'}}] \{\varepsilon'\} \quad 4.18$$

4.6. Derivation of the Stiffness Matrix

The stiffness matrix of the element is

$$[k] = \int_{-1}^1 \int_{-1}^1 \int_{-1}^1 [B]^T [D] [B] \left| \det[J] \right| d\xi d\eta d\zeta \quad 4.19$$

The Jacobian matrix and its determinant are computed directly from Equation (4.8), whilst the integration of the above Equation is carried out numerically.

Gauss quadrature with respect to ξ , η and ζ completes the integration according to the required degree using two, three or four integration points, which are controlled in the present program.

For thick shells the through thickness interpolations, in ζ can be evaluated less accurately than those in-plane (i.e. in the ξ and η plane), for which the number of points may be 4.

Integration can be achieved by integrating first with respect to one coordinate and then with respect to the other two. Thus, integration is as follows:

$$\begin{aligned} I &= \int_{-1}^1 \int_{-1}^1 \int_{-1}^1 f(\xi, \eta, \zeta) d\xi d\eta d\zeta \\ &= \sum_{i=1}^n \sum_{j=1}^n \sum_{k=1}^n w_i w_j w_k f(\xi_i, \eta_j, \zeta_k) \end{aligned}$$

where n = the number of integration points and w = their associated 'weights'.

It is possible to use the same number of points in each direction, but it is not essential to do so, for the reasons explained above.

Where

$$D_{11} = E_1/c_3$$

$$D_{12} = (c_1/c_2) D_{11}$$

$$D_{13} = c_4 D_{11}$$

$$D_{22} = E_2/c_1 + (c_2/c_1) D_{12}$$

$$D_{23} = v_{32} E_2/c_1 + (c_2/c_1) D_{13}$$

$$D_{33} = E_3 + v_{31} D_{13} + v_{32} D_{23}$$

where

$$c_1 = 1 - v_{32}^2 (E_2/E_3)$$

$$c_2 = v_{21} + v_{31} v_{32} (E_2/E_3)$$

$$c_3 = 1 - (E_1/E_3) \left[v_{31}^2 + ((E_3/E_2) (c_2^2/c_1)) \right]$$

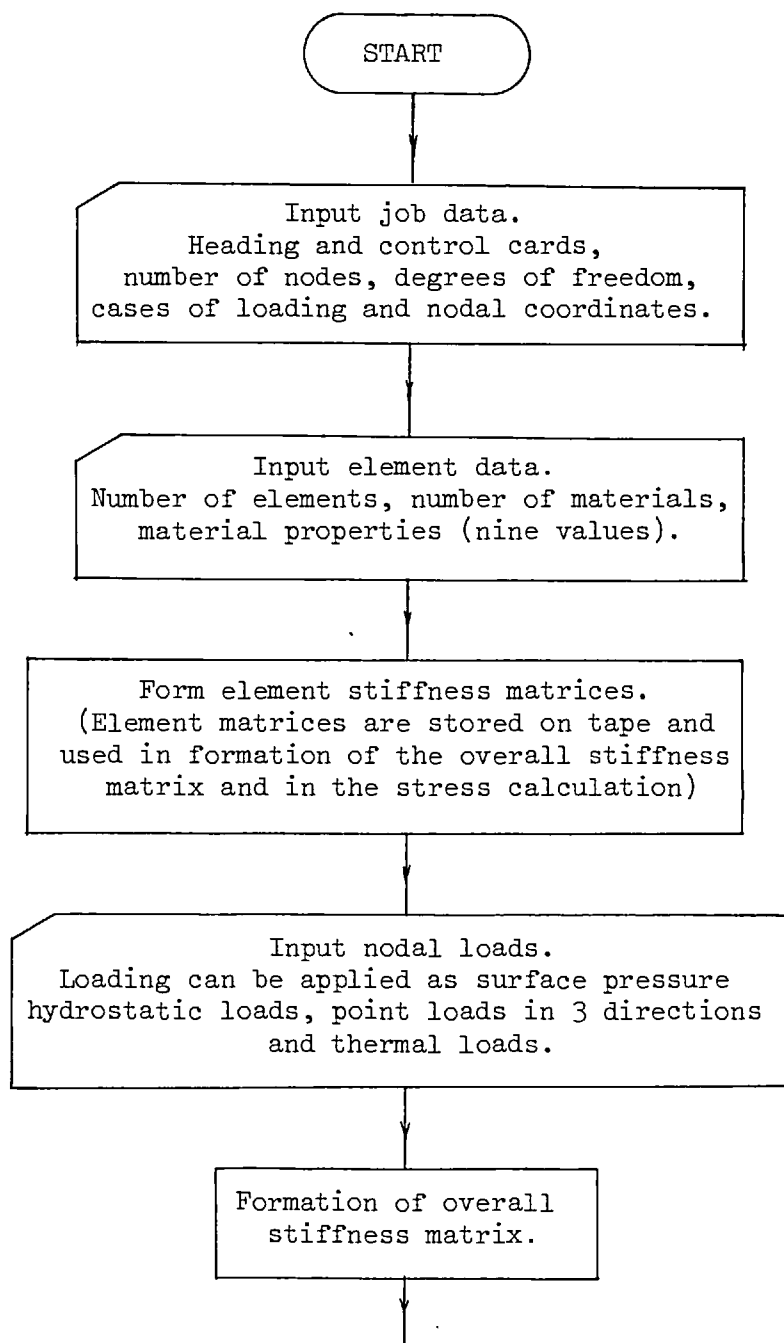
$$c_4 = v_{31} + v_{32} (c_2/c_1)$$

in which E_1 , E_2 , E_3 are Young's moduli of the material in the directions of its natural axes 123, v_{12} , v_{23} , v_{13} are the Poisson's ratios and G_{12} , G_{23} and G_{31} are the moduli of Rigidity Constants.

If the directions of symmetry of the material do not coincide with the global reference directions the matrix $[D]$ has to be transformed, as discussed in Chapter 3.

4.7. Flow chart of solid finite element computer programme

The equations in Chapter 3 and the work done in this chapter were written in a computer programme (BFSOLID). The following is a flow chart and the listing in FORTRAN IV is given in APPENDIX 2E.



Solve equations.
Equations are solved using
standard semi-banded width technique.

Output results which includes

- Deflections
- Six global stresses at the eight corners of each element.
- Average stresses at each node.
- The first ten nodes with maximum stresses.

END

CHAPTER FIVE

IDEALIZATION OF FINITE ELEMENTS FOR STRUCTURAL
DESIGN, NUMERICAL AND EXPERIMENTAL RESULTS

CHAPTER FIVE

IDEALIZATION OF FINITE ELEMENTS FOR STRUCTURAL DESIGN,

NUMERICAL AND EXPERIMENTAL RESULTS

5.1. Introduction

The finite element program (BFSOLID) was used to solve the challenging problems of large water valves more accurately, especially when the blade dimensions were such as to exclude the work done in Chapter Two, i.e. outside the assumption of thin plate theory, such as when the thickness-diameter ratio is more than 1/8. An example of an ordinary cast iron blade is discussed in 5.2.

The program, or any equivalent isotropic solid finite element program, proved to be the only accurate method for structural analysis and design when the large diameter and high pressure necessitated the blade to take the form of a thick plate supported on a lattice which could take different complicated configurations as shown in Figs. (5.1a) and (5.1b). Ref. (50).

For anisotropic material of the fibre composite type, the various elastic constants have to be inserted into the computer program according to Equations (3.14a) to (3.14l). For isotropic material the same equations are used but with only three elastic constants E, v and G to which all others are equal as explained later in 5.2.

229.

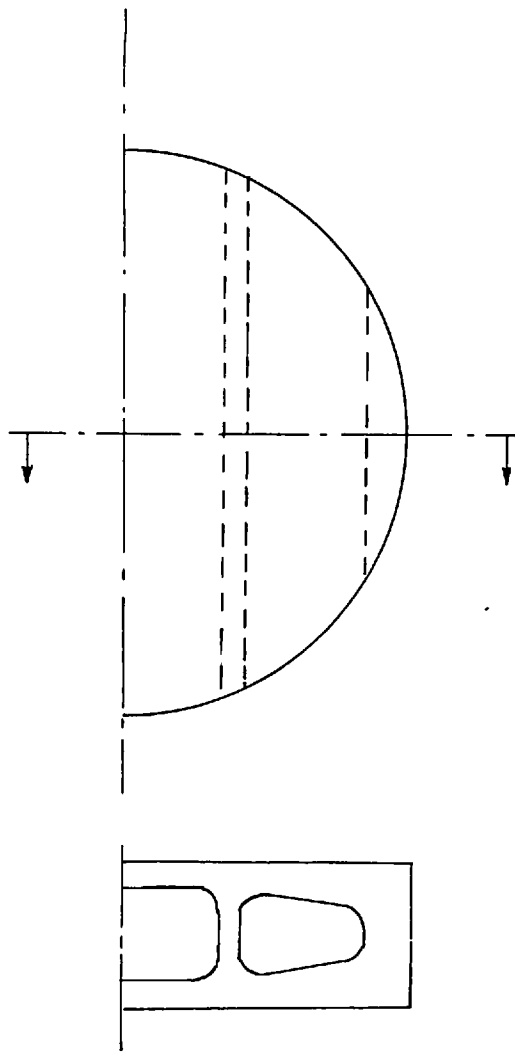


Fig. 5.1a. Blades of throughflow valves

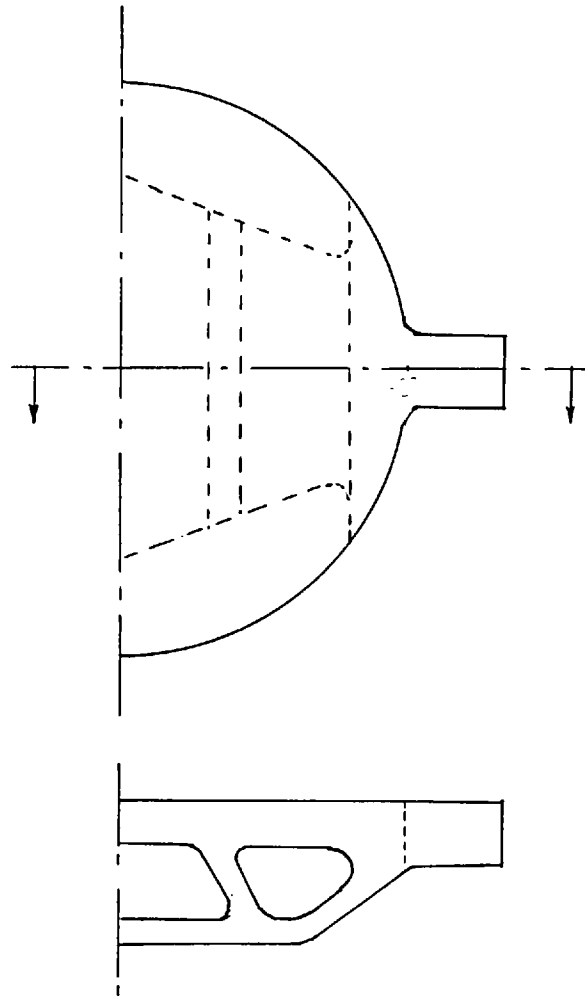


Fig. 5.1b. Blades of throughflow valves

The analysis of fibre composite material is a vast subject of a complex nature and theories have been developed whereby, knowing the properties of the fibres the matrix and their volume fractions in a composite, one can estimate the elastic constants and strength properties of unidirectional laminates, unidirectional laminates with orientated fibres, balanced laminates and multilayer, multidirectional composites.

The ability to predict the elastic properties of various types of laminates and composites has been verified experimentally. A great deal of theoretical and experimental work on predicting strength properties and failure modes in composite materials subjected to various types of loading has also been done. Refs. (42), (43), (51), (52), (53), (54), (55), (56) and (57), give a good impression of the underlying difficulties of the subject.

Various factors of manufacturing technology, as well as temperature, chemical and environmental effects that influence the strength and modes of failure have also been covered extensively in Refs. (58), (59), (60), (61) and (62).

To develop a practical approach to analyse stresses and strains in the elastic region where the environmental problems of temperature, chemical and time dependent factors are covered by complying with standards, Ref. (63), only partial experimental verification of the elastic properties of such composites has been obtained up to the present time. A great deal of work is still in progress to overcome this problem where, by specifying the fibre

content and alignment of known types it is possible to predict the elastic constants of the end product as though it were an anisotropic continuum.

An attempt to give a practical approach for stress analysts and designers is discussed in 5.3.

The program was also used to analyse a 60" butterfly valve made up of three materials, namely; woven roving g.r.p., chopped strand mat g.r.p. and stainless steel shaft inserts. This is described in 5.4.

5.2. Cast Iron Blade of an Ordinary Butterfly Valve.

A 72" diameter, 6" thick blade of a butterfly valve, shown in Fig. (5.2), made of cast iron GR17 which is fitted in a body made of the same material, is to be checked for a design requirement of a maximum deflection of 0.125" for sealing under a test pressure of 75 psi. Using Appendix 3:

$$v = 0.26$$

$$C_1 = 0.386$$

$$q = 75 \text{ psi}$$

$$a = 71.2''/2$$

$$t = 6''$$

$$w = \frac{0.386 \times 75 \times 71.2^4 \times 12(1-0.26^2)}{16 \times 18 \times 10^6 \times 6^3}$$
$$= 0.134''$$

Deflection due to the reaction couple

$$W = \frac{MR}{2D} \left(\frac{\pi}{2} - 1\right) \quad M = R \times \frac{t}{3}$$

$$2R = 298614 \text{ lb.}$$

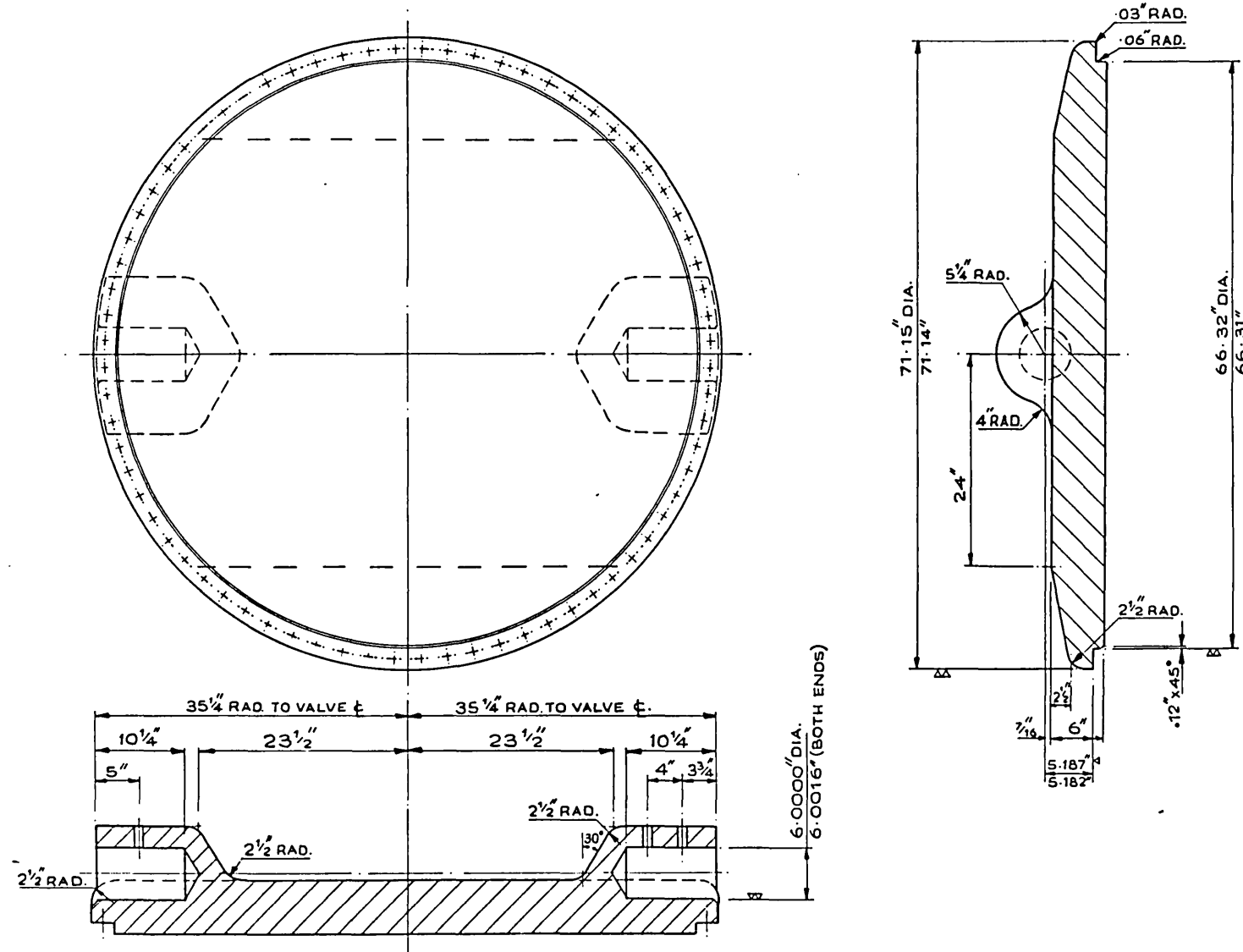


Fig. 5.2. 72" dia. Cast iron butterfly valve - blade

$$W = \frac{298614 \times 71.2 \times 12(1-v^2)(\frac{\pi}{2} - 1)}{2 \times 2 \times 18 \times 10^6 \times 6^3}$$

Total $W = 0.134 + 0.008 = 0.142"$

Idealizing the blade into 34 21-node elements with a total of 94 nodes as shown in Figs. (5.3a), (5.3b) and (5.3c) and giving $E_{11} = E_{22} = E_{33} = 18 \times 10^6$ psi and $v_{12} = v_{13} = v_{31} = 0.26$ and $G_{12} = G_{13} = G_{23} = \frac{E}{2(1+v)} = 7.14 \times 10^6$ psi the maximum deflection occurring at node 92 or 89 was - .10387".

The valve was pressurised up to 75 psi and the deflections measured at locations shown on Fig. (5.4a) relative to the body. The total deflection was 0.095" as shown in Figs. (5.4b) and (5.4c) which also shows the deflected shape in the two perpendicular planes of interest.

5.3. Test Samples of Composite Materials.

5.3.1. Introduction

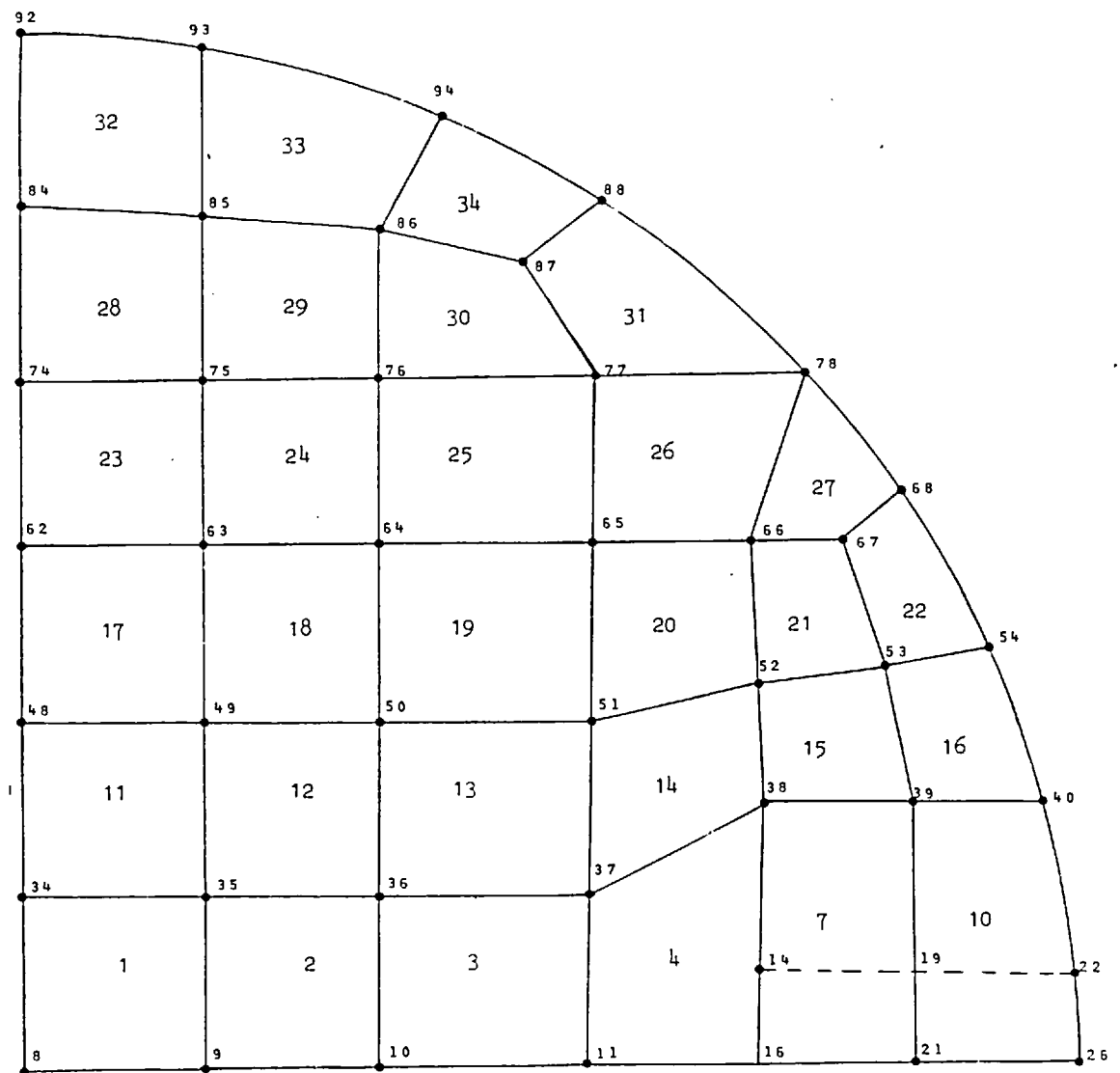
G.R.P. can be taken as a good example of fibre composite material which is widely used in an increasing number of manufacturing industries. One major use is for manufacturing pipes and pipe fittings which can combat the corrosive effect of sea water. Ref. (64).

A great deal of literature on G.R.P. is available. Ref. (61), (62), (65) and (66) are given as samples of this literature.

Many G.R.P. manufacturers are now prepared to give reliable basic mechanical properties as shown in Table (5.1). Ref. (67).

In these tables the flexural (elastic) modulus of a composite consisting of continuous, aligned fibres in a softer matrix is given by simple elasticity theory using

$$E_c = E_c V_f + E_m (1-V_f)$$



Upper face

Fig. 5.3a.

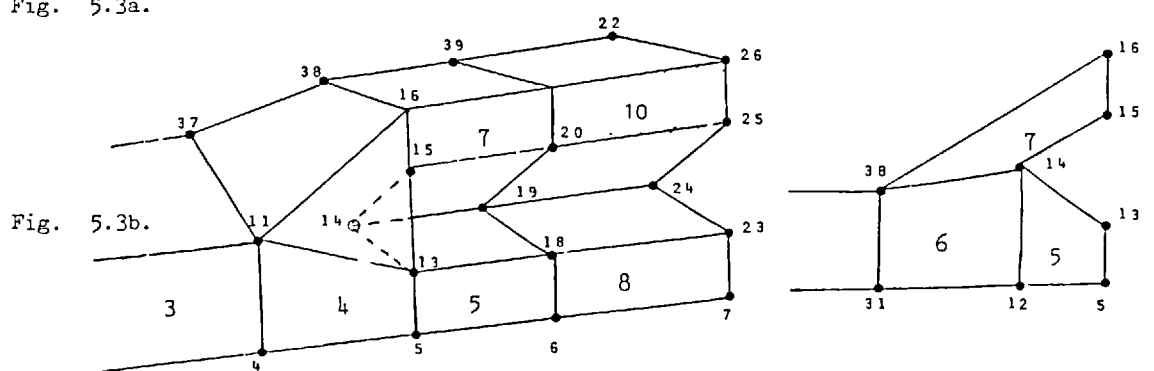


Fig. 5.3b.

Figs. 5.3a & 5.3b. Finite element mesh of the cast iron blade

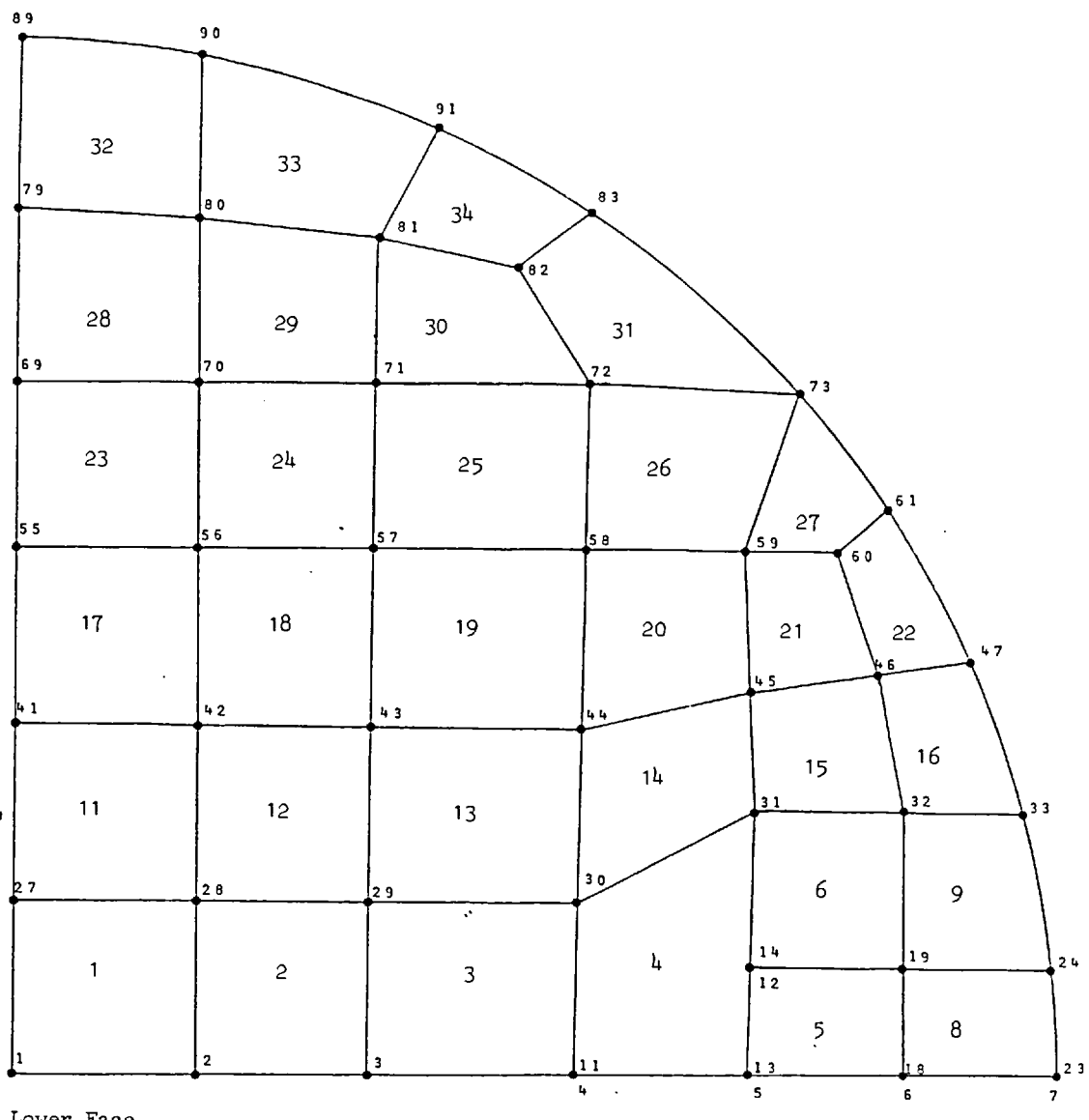


Fig. 5.3c. Finite element mesh of the cast iron blade.

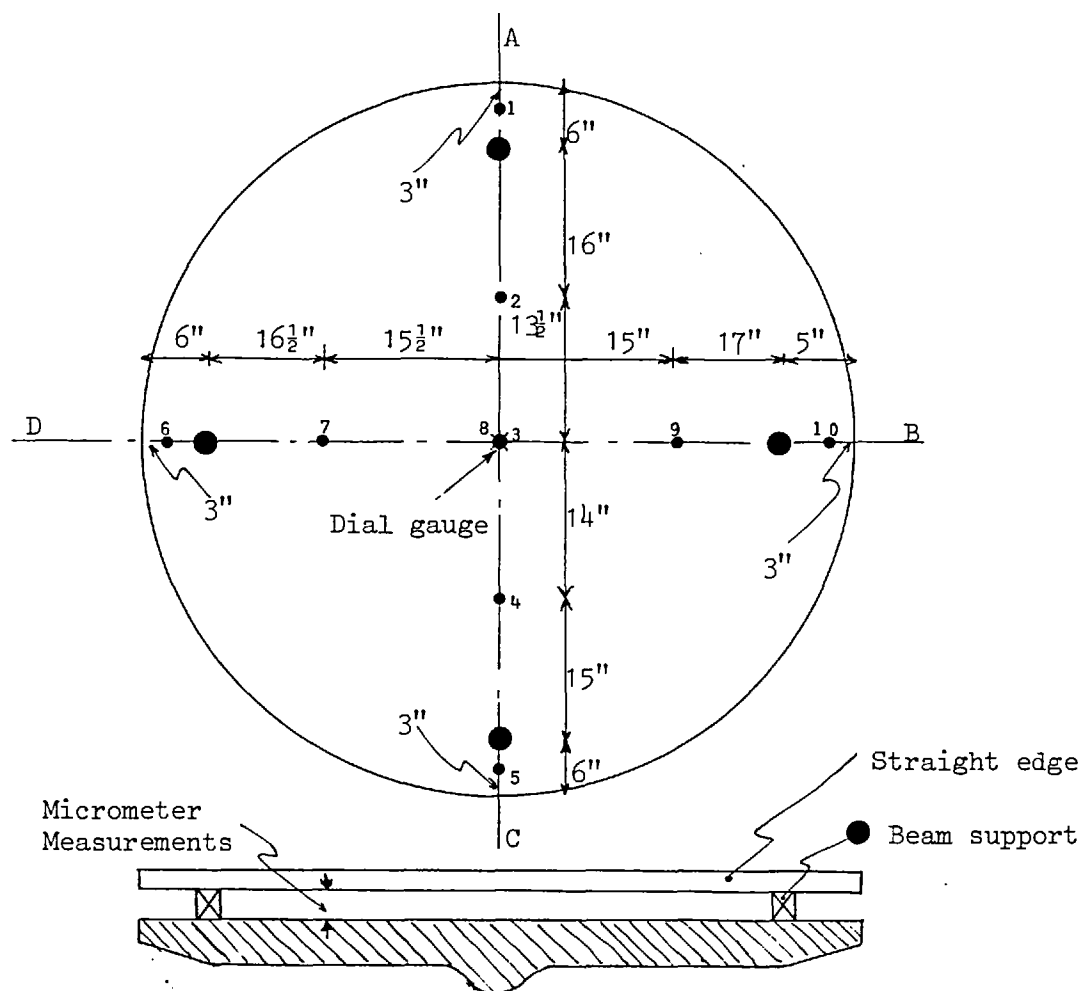


Fig. 5.4a. Deflection test of cast iron blade.

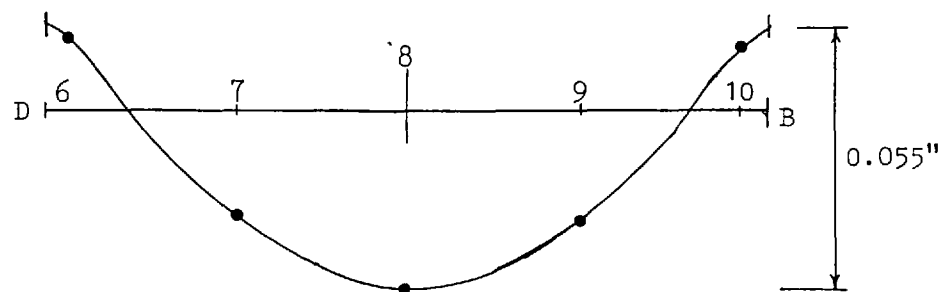


Fig. 5.4b. Deflection at centre relative to bearings.

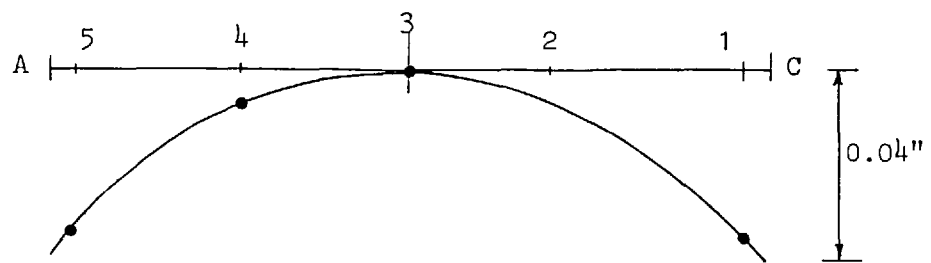


Fig. 5.4c. Deflection at wings relative to centre.

Material	Fibre Content by Weight %	Density Mg/m ²	Tensile Strength GN/m ²	Tensile Modulus GN/m ²	Compressive Strength MN/m ²	Flexural Strength MN/m ²	Flexural Modulus GN/m ²
<u>Uni-directional glass</u> Wound epoxide Uni-directional polyester	60-90 50-75	1.7-2.2 1.6-2.0	530-1730 410-1180	28-62 21-41	310-480 210-480	690-1860 690-1240	34-48 27-41
<u>Bi-directional glass</u> Satin weave polyester Woven roving polyester	50-70 45-60	1.6-1.9 1.5-1.8	250-400 230-340	14-25 13-17	210-280 98-140	207-450 200-270	17-23 10-17
<u>Random glass mat</u> Preform polyester Hand & spray up polyester	25-50 25-40	1.4-1.6 1.4-1.5	70-170 63-40	6-12 6-12	130-160 130-170	70-240 140-250	5-8
<u>Moulding compounds</u> DMC polyester SMC polyester Glass filled nylon	10-40 20-35 20-40	1.8-2.0 1.8-1.85 1.3-1.5	34-70 50-90 120-200	12-14 9 6-14	140-180 240-310 110-170	40-140 140-210 9-14	

$$1 \text{ GN/m}^2 = .14508 \times 10^6 \text{ psi}$$

Table: 5.1. Material properties as given by manufacturers. Ref. (67).

where the subscripts c, f and m refer to composite, fibre and matrix and V_f is the fibre volume fraction. This expression is strictly true only for the case where both fibre and matrix are isotropic and it assumes that the two components are constrained to deform together. This elementary "Rule of mixtures" is in fact a lower bound.

Such moduli will generally be exceeded by an amount depending upon the difference in Poisson's ratio of the two constituents, as a result of the lateral elastic constraint which the two phases exert on one another. The equivalent theoretical expression for the shear modulus can be written as follows:-

$$\frac{G_c}{G_m} = \left[\frac{\left(\frac{G_f}{G_m} + 1 \right) + \left(\frac{G_f}{G_m} - 1 \right) V_f}{\left(\frac{G_f}{G_m} + 1 \right) - \left(\frac{G_f}{G_m} - 1 \right) V_f} \right]$$

Which shows that the ratio $\frac{G_c}{G_m}$ is a function of V_f depending on the value of stiffness ratio, $\frac{G_f}{G_m}$, after Tsai, Adams and Doner Ref. (68).

As discussed in Chapter 3, an aligned composite is highly anisotropic. A lot of work is based on the assumption that the material is transversely isotropic. However, if the material is being used in plate form, as is frequently the case with laminates, the assumption of a plane stress state reduces the number of elastic constants to four, E_{11} , E_{22} , v_{12}/E_{11} or v_{21}/E_{22} and G_{12} , which can be easily established by a simple testing procedure for the first three carried out on a test coupon supplied by the

manufacturer. This would be an improvement on the manufacturer's information and is covered in the present work.

To test the solid finite element experimentally an attempt to establish as many elastic constants as possible to satisfy Equations (3.14a) to (3.14l) was made. In many texts, Ref. (69), $E_{33} \approx E_{22}$ where E_{22} is $< E_{11}$. From the tests v_{13} and v_{23} can be easily obtained and, using Equation (3.14b) and Equation (3.14c), most of the remaining elastic constants can be estimated.

The shear modulus proved a more critical factor to assume without the difficult and expensive experimental measurement which would otherwise be necessary. One of the most serious limitations of fibre composite materials is that the shear strength parallel with the fibres can be as low as that of the matrix or the fibre resin interface, either of which may be an order of magnitude (or more) lower than the maximum tensile strength of the composite. Consequently the composite may fail at low loads if the stress system is such as to cause a high shear stress on these planes of weakness. A bar loaded in flexure will fail in shear at the neutral plane before it breaks by tensile failure of the outer fibres if the ultimate shear stress, τ_{\max} is reached before the outer fibre failure stress σ_{\max} . Thus a short composite beam was used as a test sample to ensure that no shear failure occurred in the elastic region and the shear modulus assumption is a lower bound one. This assumes the material to be homogeneous and isotropic in all directions which, although not true, if observed with the guidelines laid down in BS.4994 would produce a structurally sound product.

From this simple beginning a sample of each distinctive layer or solid can be specified and the general behaviour of the complete structure can be predicted as discussed below.

5.3.2. Preparation of test specimens, testing equipment and procedure

(i) The Samples

A number of deep short beams, samples (D1, D2, D3, D4) made of three distinctive layers are cut from a block which is layered up from three distinctive layers, as shown in Figs. (5.5a), (5.5b), (5.6a) and (5.6b).

The block is made during the laying of the layers by installing plastic insulation sheets after the completion of each layer, as shown in Fig. (5.7), the layers being made from woven roving and uni-directional glass polyester material as shown in Fig. (5.8). Each layer is then cut into specimens and carefully marked to show the principal natural axis of the material as shown in Figs. (5.9), (5.10), (5.11) and (5.12).

(ii) Test procedure

Two longitudinal and two transverse strain gauges of two rosette strain gauges type FRA-6-11 made by T.S.K. Ltd. gauge resistance $120 \pm 0.5\Omega$, gauge length 6mm were stuck at the top and bottom surfaces. The adhesive used was CN adhesive made by T.M.L. Ltd. of T.S.K. Ltd.

The two longitudinal strain gauges were arranged as a 'half-bridge' and fed with 3.V through a Brueiland and Kjaer strain gauge amplifier, type 1525. The output was fed back to the amplifier which indicated the total strain (microstrain).

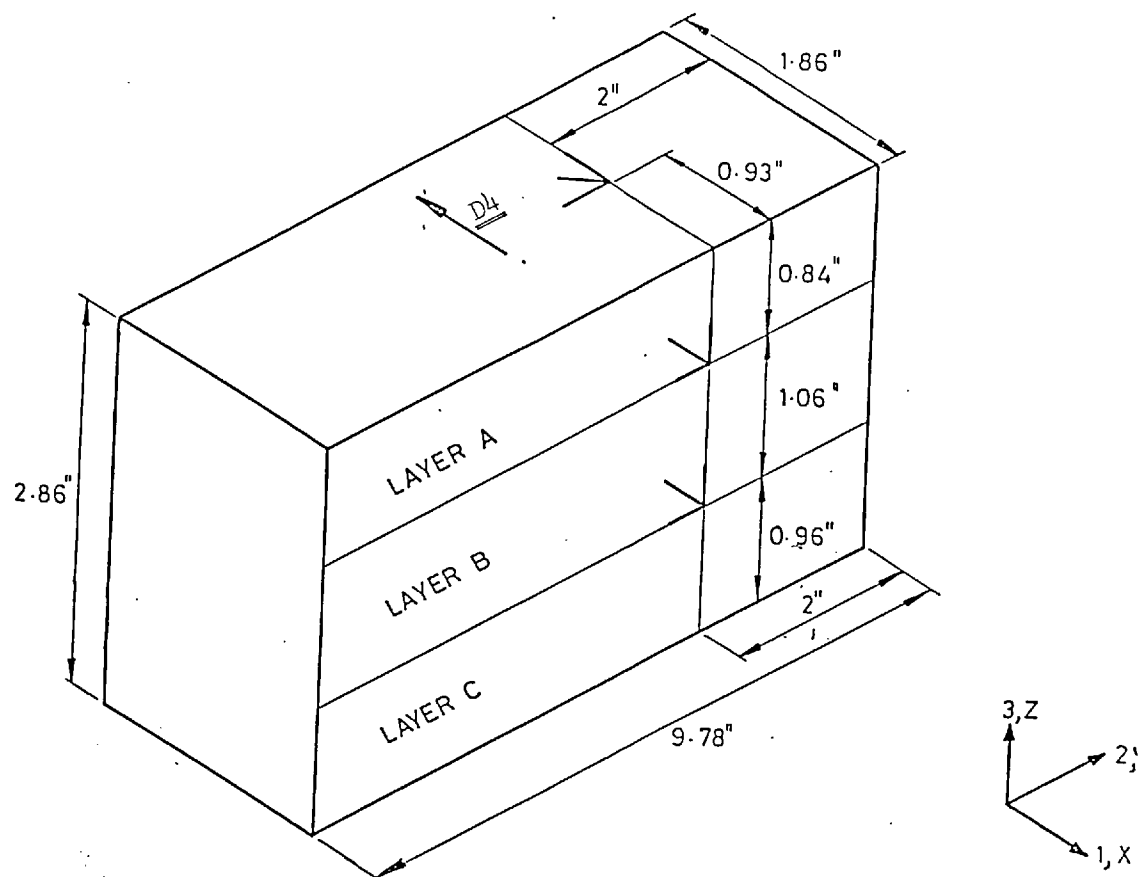


Fig. 5.5a. Actual dimensions of composite deep beam No. D1.

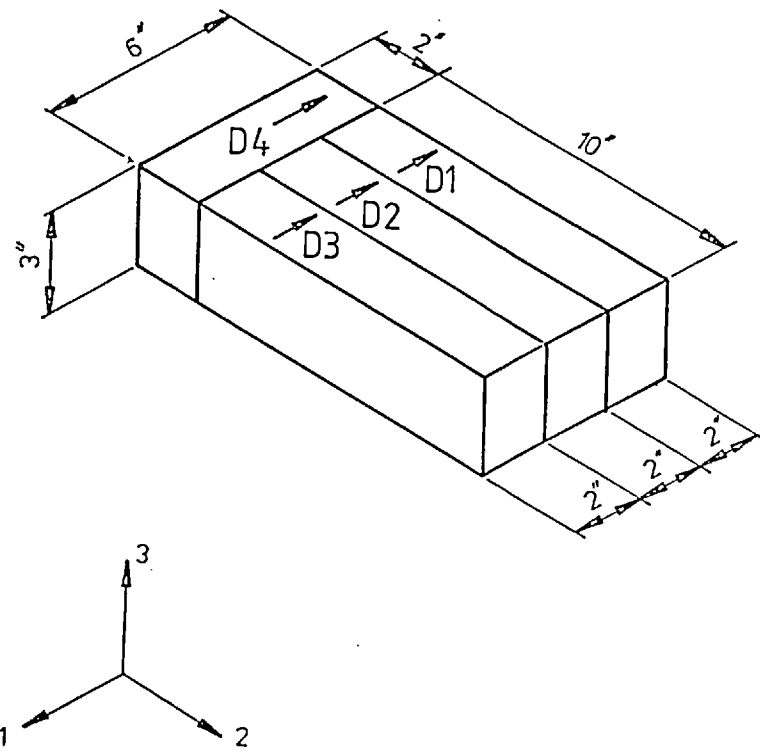


Fig. 5.5b. Composite deep beam specimen



Fig. 5.6a. Composite deep beam specimen



Fig. 5.6b. Composite deep beam specimen

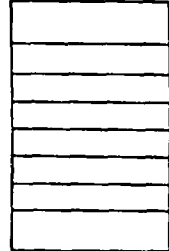
243

TOTAL 18

FINISH 3 W.R.O

2 W.R.O
2 W.R.O
2 W.R.O
2 W.R.O
2 W.R.O
2 W.R.O
2 W.R.O

START 3 W.R.O



7

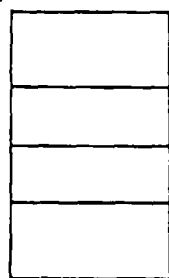
7th U.D. ROV
6th U.D. ROV
5th U.D. ROV
4th U.D. ROV
3rd U.D. ROV
2nd U.D. ROV
1st U.D. ROV

TOTAL 22

FINISH 6 W.R.O

5 W.R.O
5 W.R.O
1st U.D. ROV

START 6 W.R.O



3

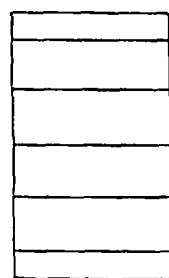
3rd U.D. ROV
2nd U.D. ROV
1st U.D. ROV

TOTAL 20

FINISH 2 W.R.O

4 W.R.O
4 W.R.O
4 W.R.O
4 W.R.O

START 2 W.R.O



5

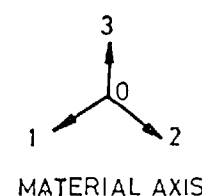
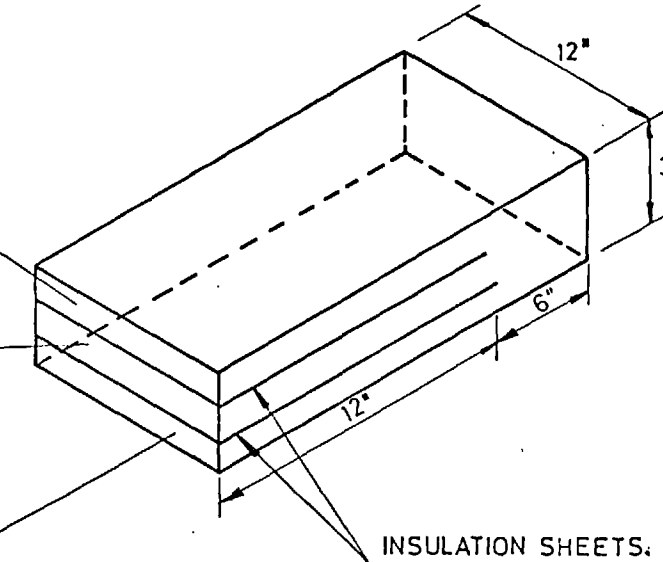
5th U.D. ROV
4th U.D. ROV
3rd U.D. ROV
2nd U.D. ROV
1st U.D. ROV

LAYER A

LAYER B

LAYER C

Fig. 5.7. Layout of multi G.R.P. layer samples



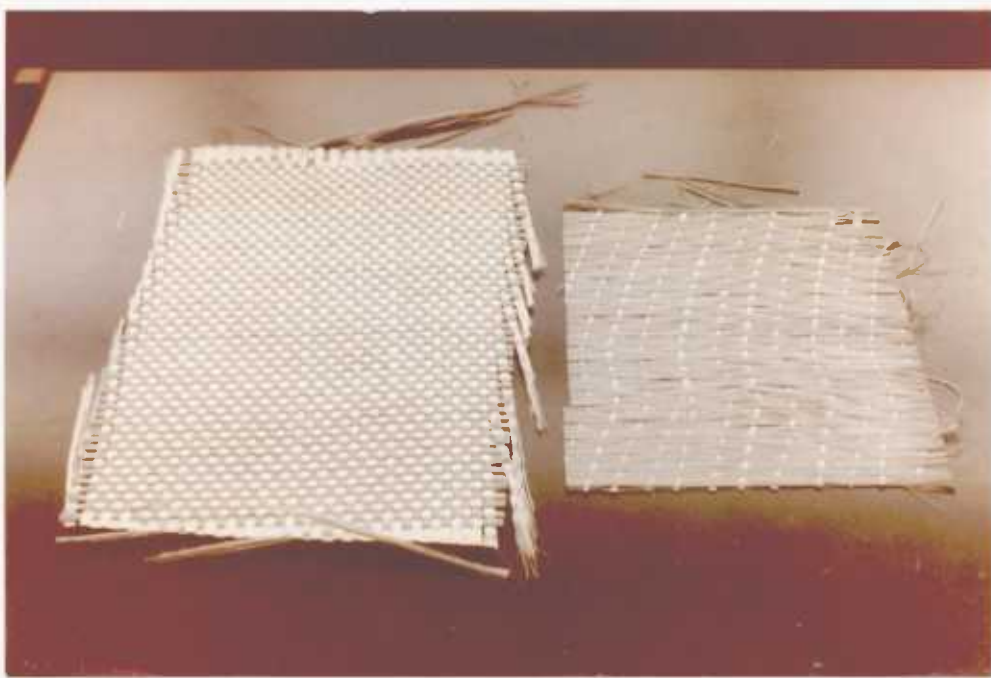


Fig. 5.8. Woven roving and unidirectional glass layers.



Fig. 5.9. Individual layer specimens

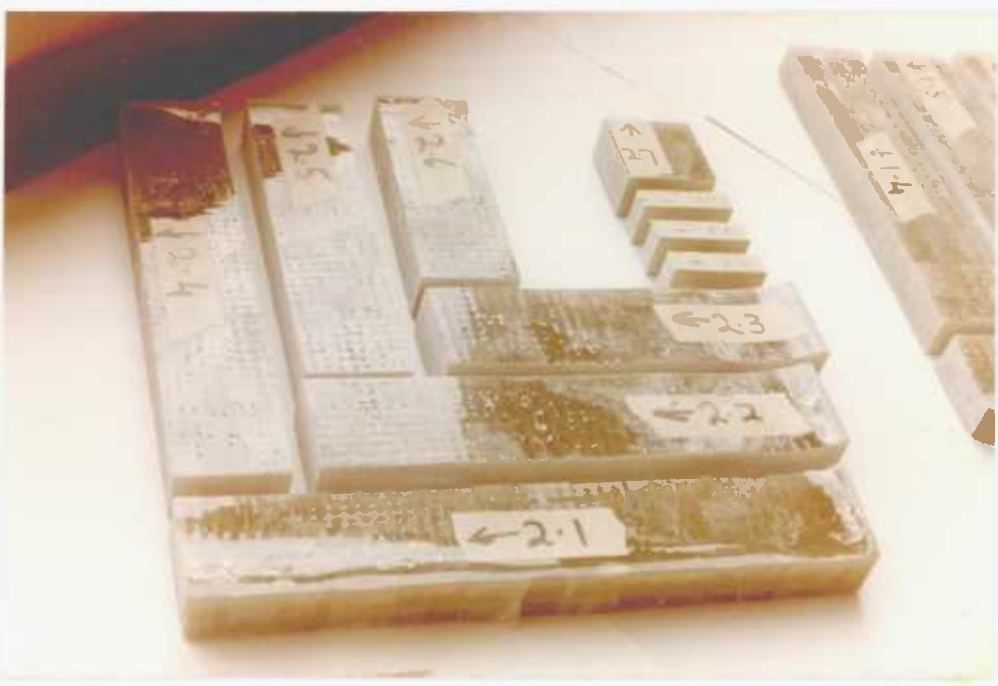


Fig. 5.10. Individual layer specimens.



Fig. 5.11. Individual layer specimens.

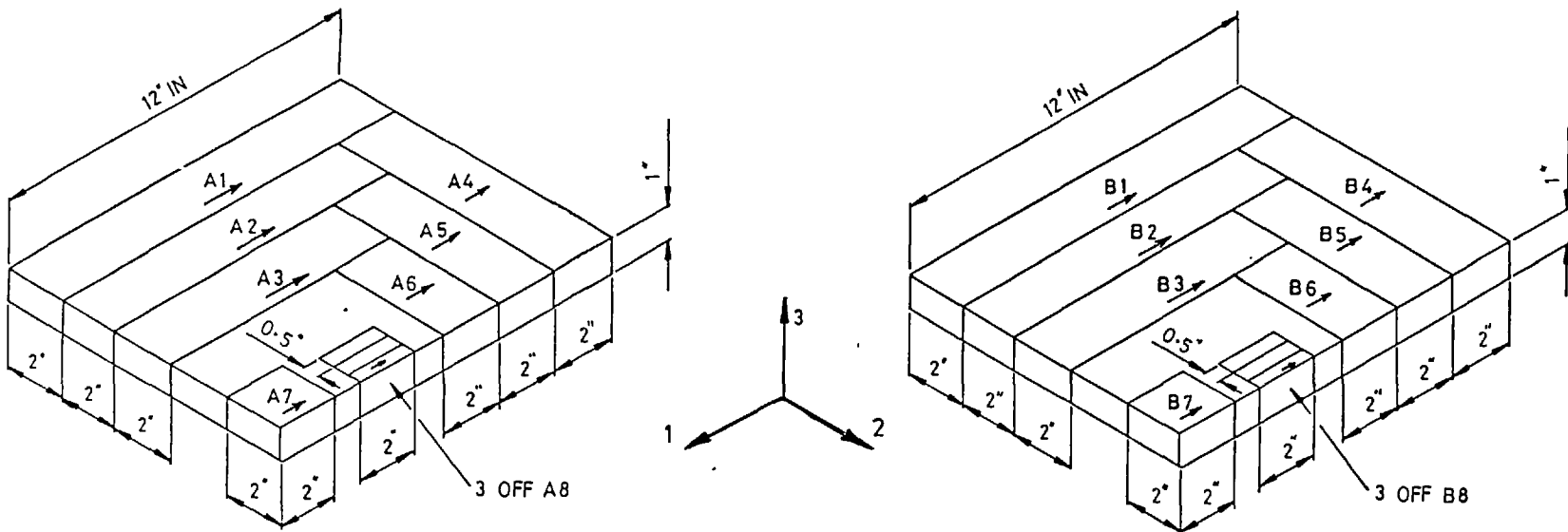
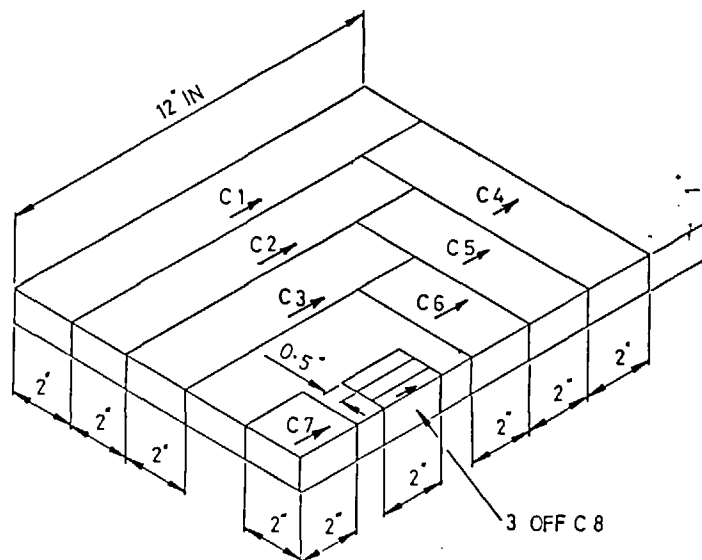


Fig. 5.12. Individual layer specimens.



The transverse strain gauges were arranged in the same manner using another amplifier of the same type. Four point bend testing of the G.R.P. beams was carried out to establish the elastic moduli by applying the load through a load cell as shown in Figs. (5.13) and (5.14). Figs. (5.15) and (5.16) are a sample of the results for layer A. Figs. (5.17) and (5.18) are a sample of the results for layer B. Figs. (5.19) and (5.20) relate to layer C. The two strains were plotted against the central deflections and Figs. (5.21) and (5.22) are a sample of the results for layer A. Figs. (5.23) and (5.24) relate to layer B and Figs. (5.25) and (5.26) to layer C.

Two more strain gauges, one longitudinal and one vertical, of the same type of rosette were stuck to the sides of the test specimens at approximately one third of the beam depth using the same adhesive. Two dummy gauges of the same type were stuck on another specimen and arranged with the active ones into two half-bridges using two amplifiers of the same type as before. This is shown in Figs. (5.27), (5.28), (5.29) and (5.30). The two readings were plotted against one another. Figs. (5.31) and (5.32) are examples of the results for layer A. Figs. (5.33) and (5.34) relate to layer B and Figs. (5.35) and (5.36) to layer C. Figs. (5.37) shows a minimum group of samples, i.e. two per layer and the apparatus used is shown in Fig. (5.38).

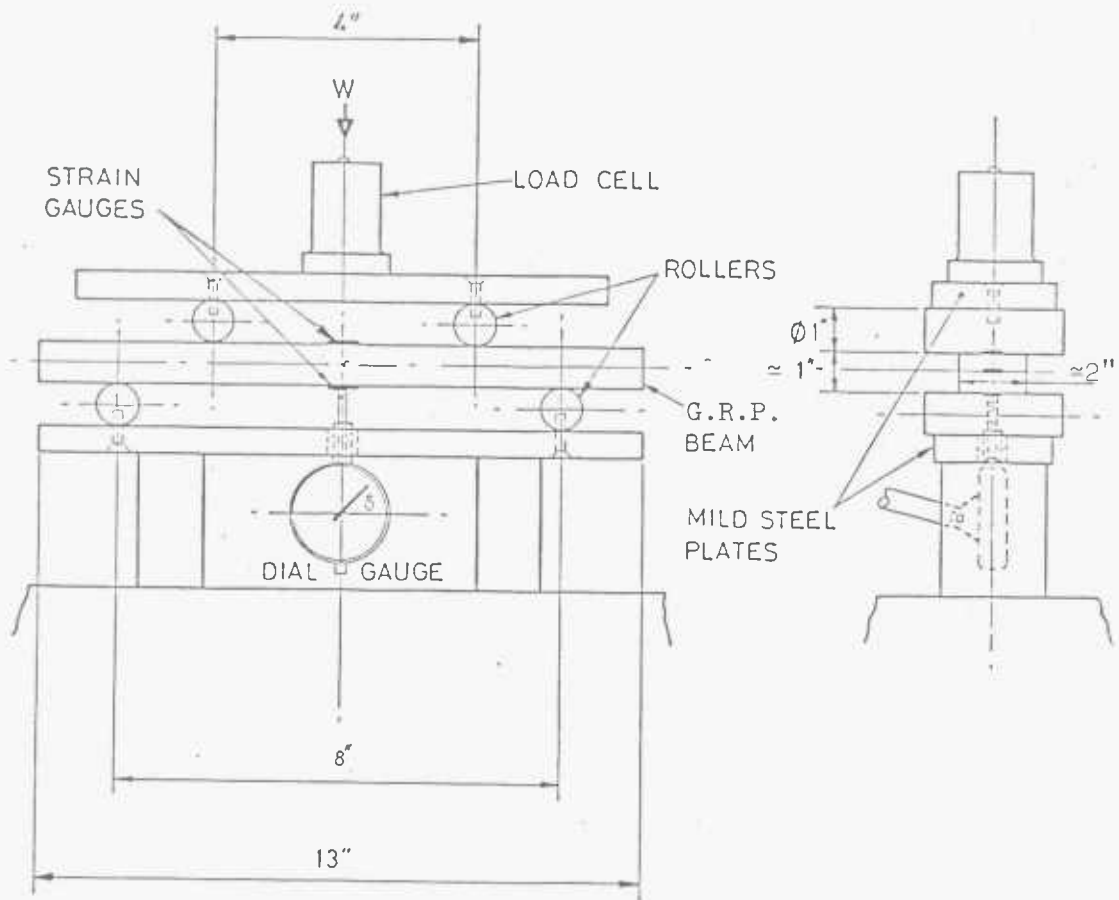


Fig. 5.13. 4-Point testing of G.R.P. beam specimens.

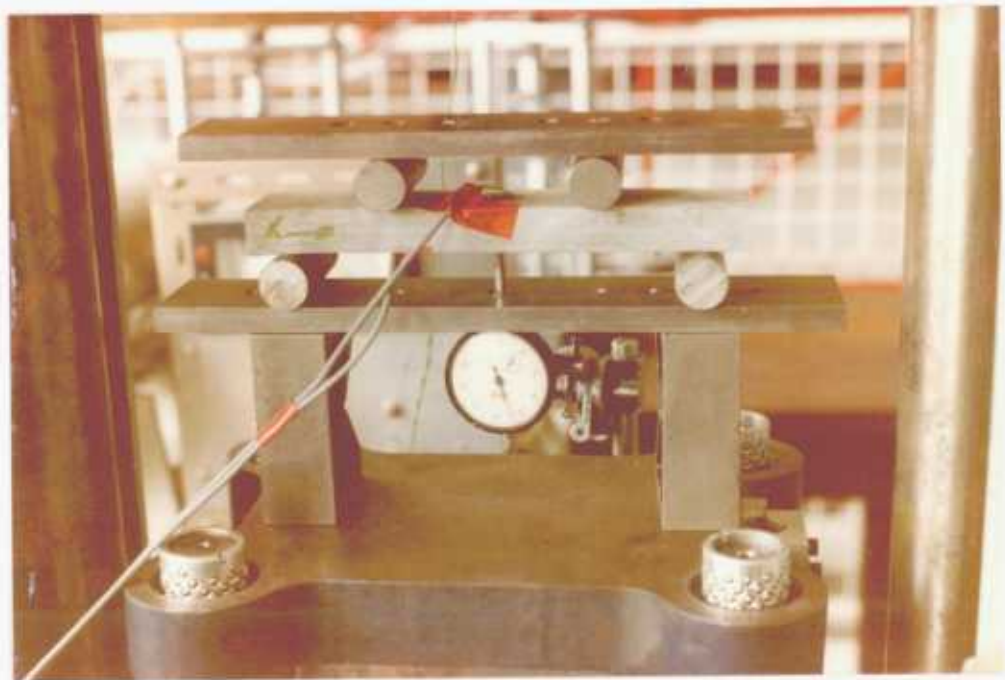


Fig. 5.14. 4-Point testing of G.R.P. beam specimens.

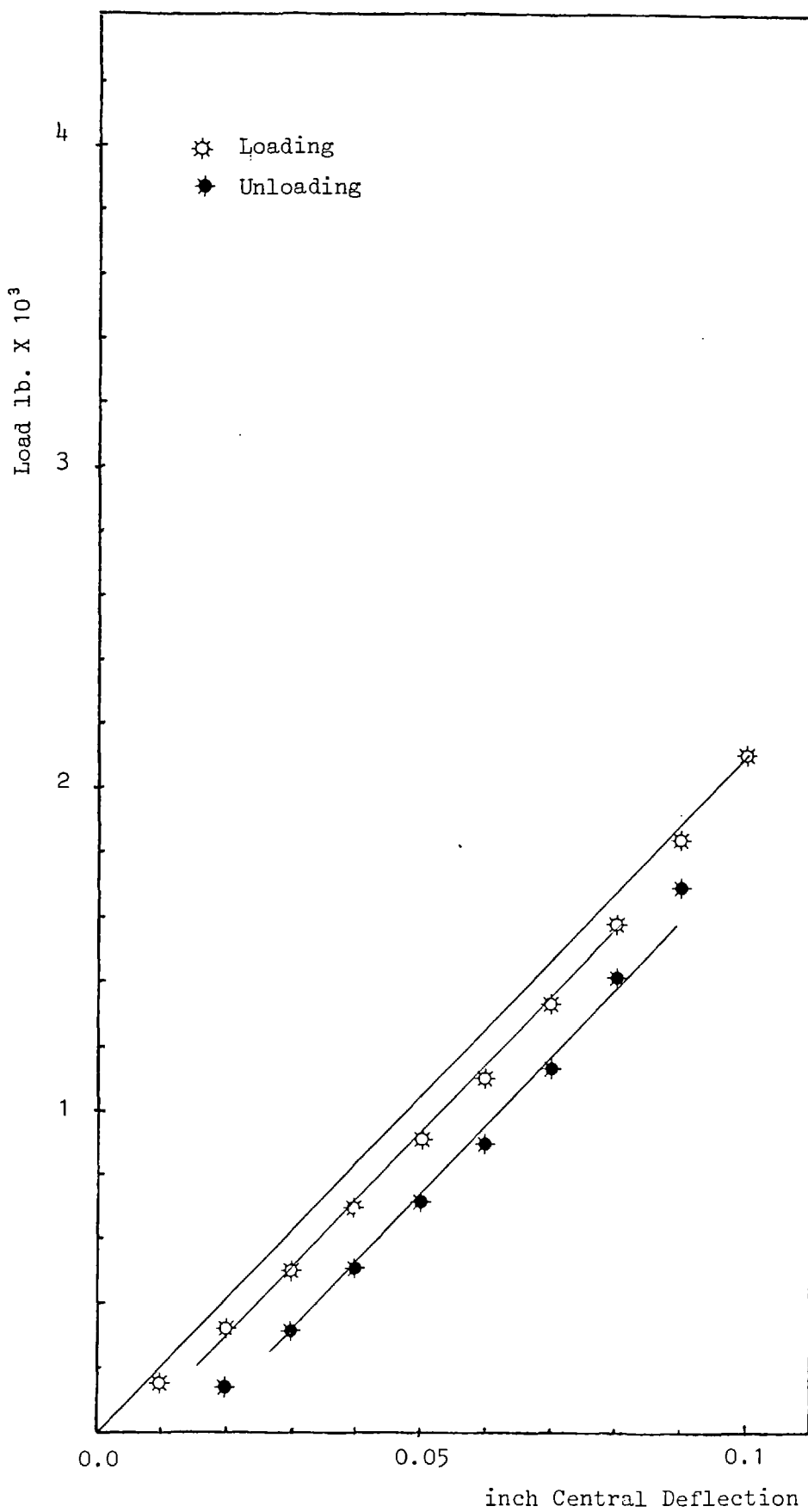


Fig. 5.15. Load vs. deflection in direction 1 - Layer A

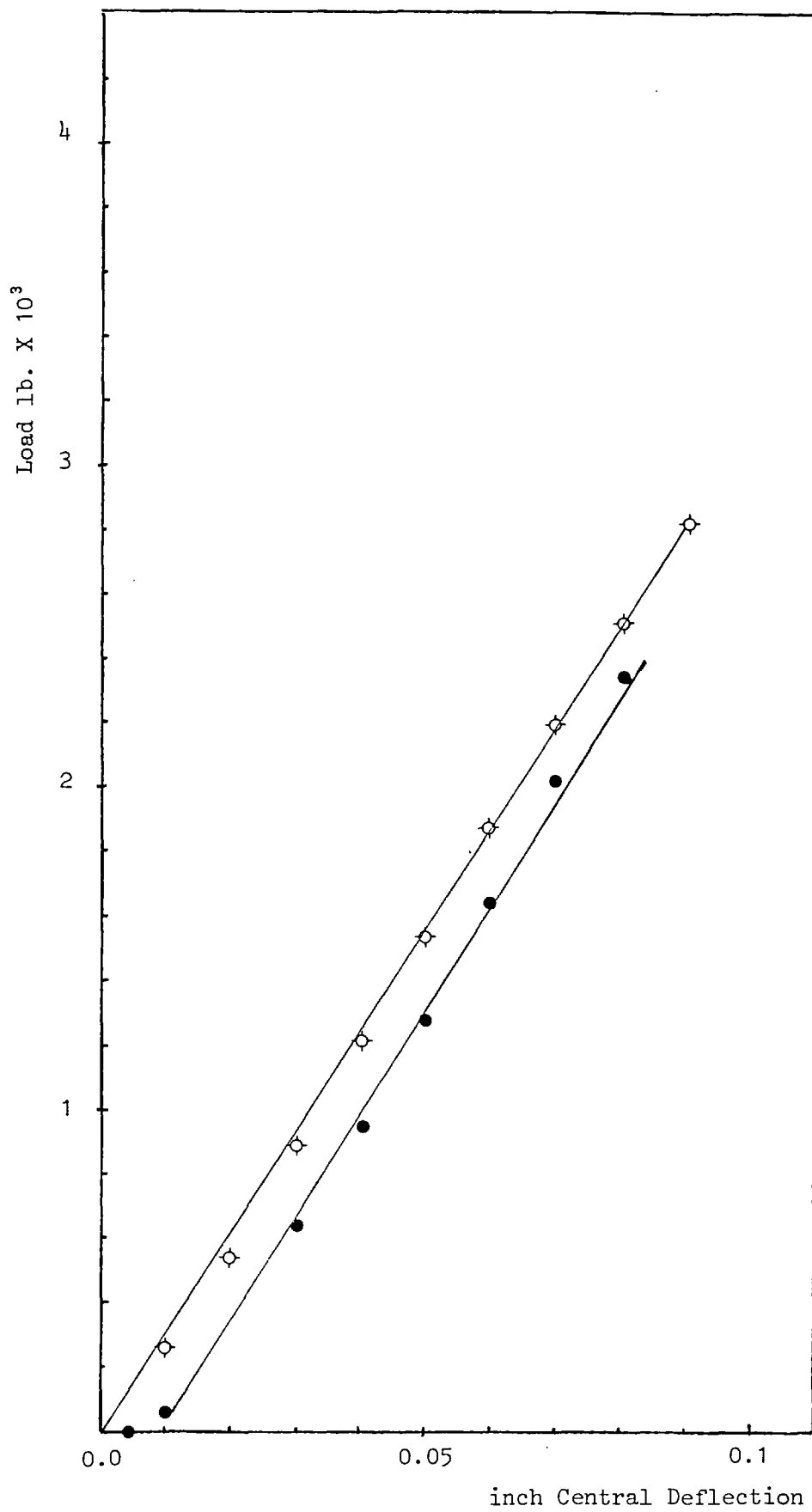


Fig. 5.16. Load vs. deflection in direction 2 - Layer A

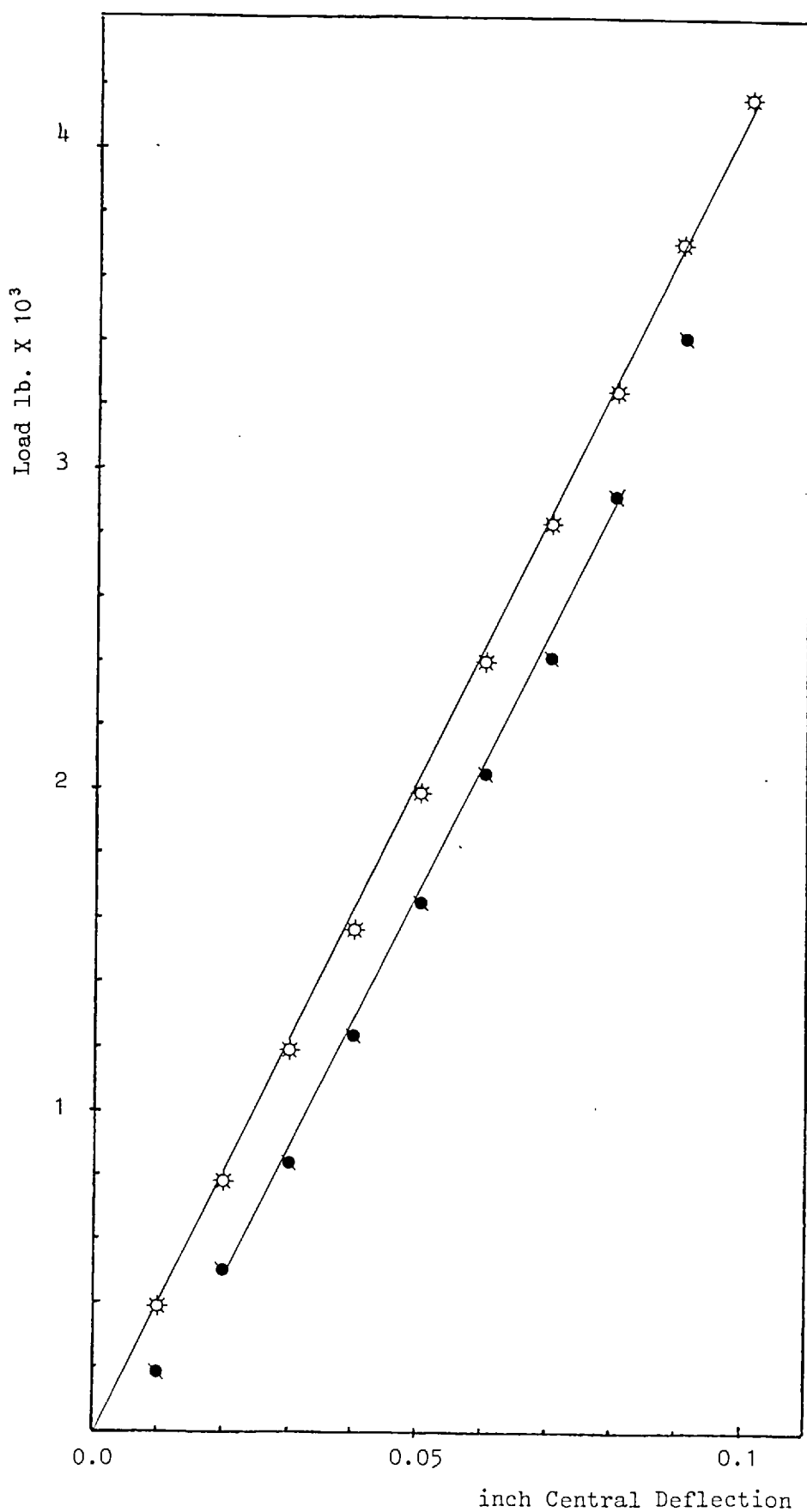


Fig. 5.17. Load vs. deflection in direction 1 - Layer B

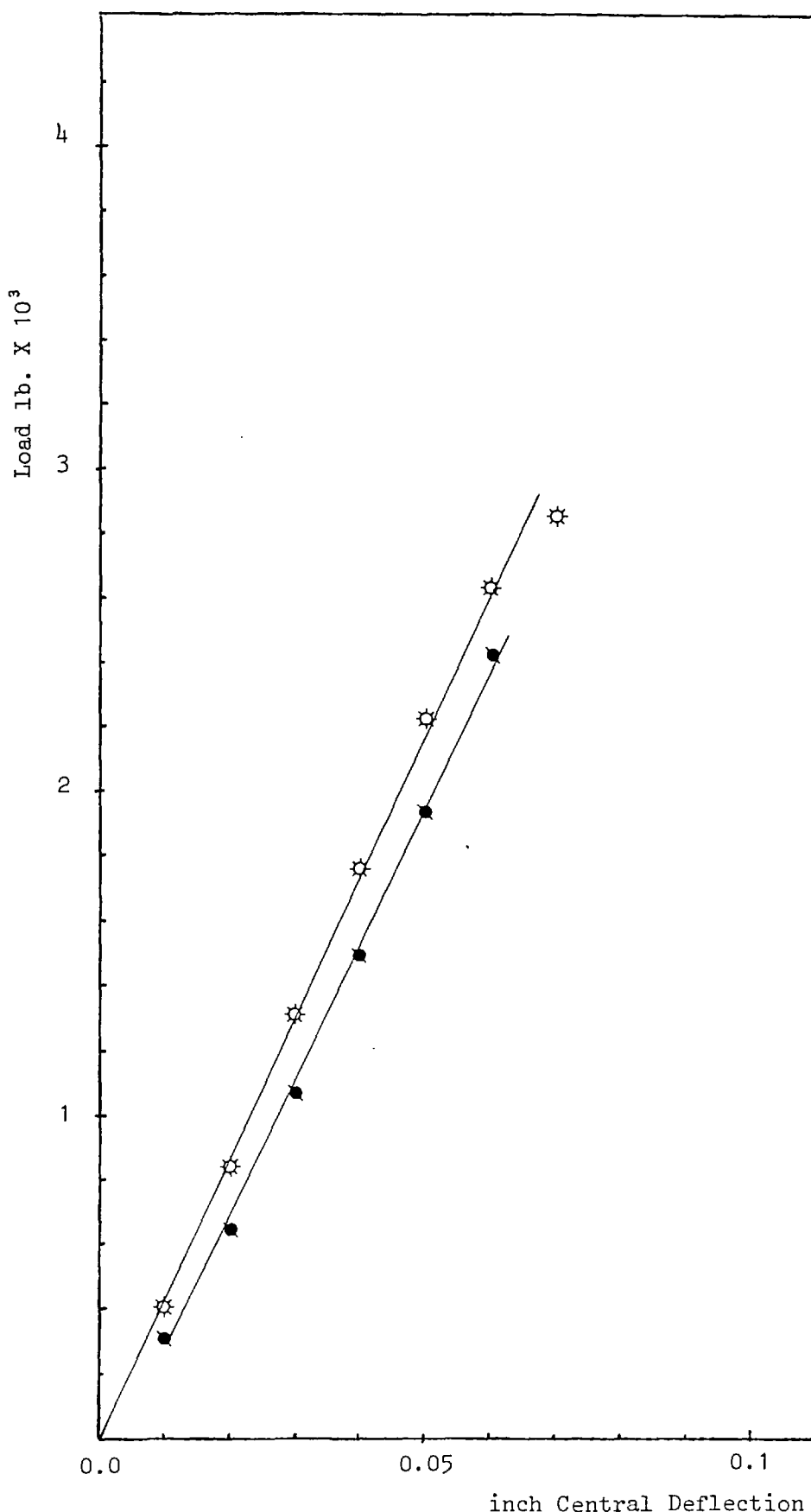


Fig. 5.18. Load vs. deflection in direction 2 - Layer B

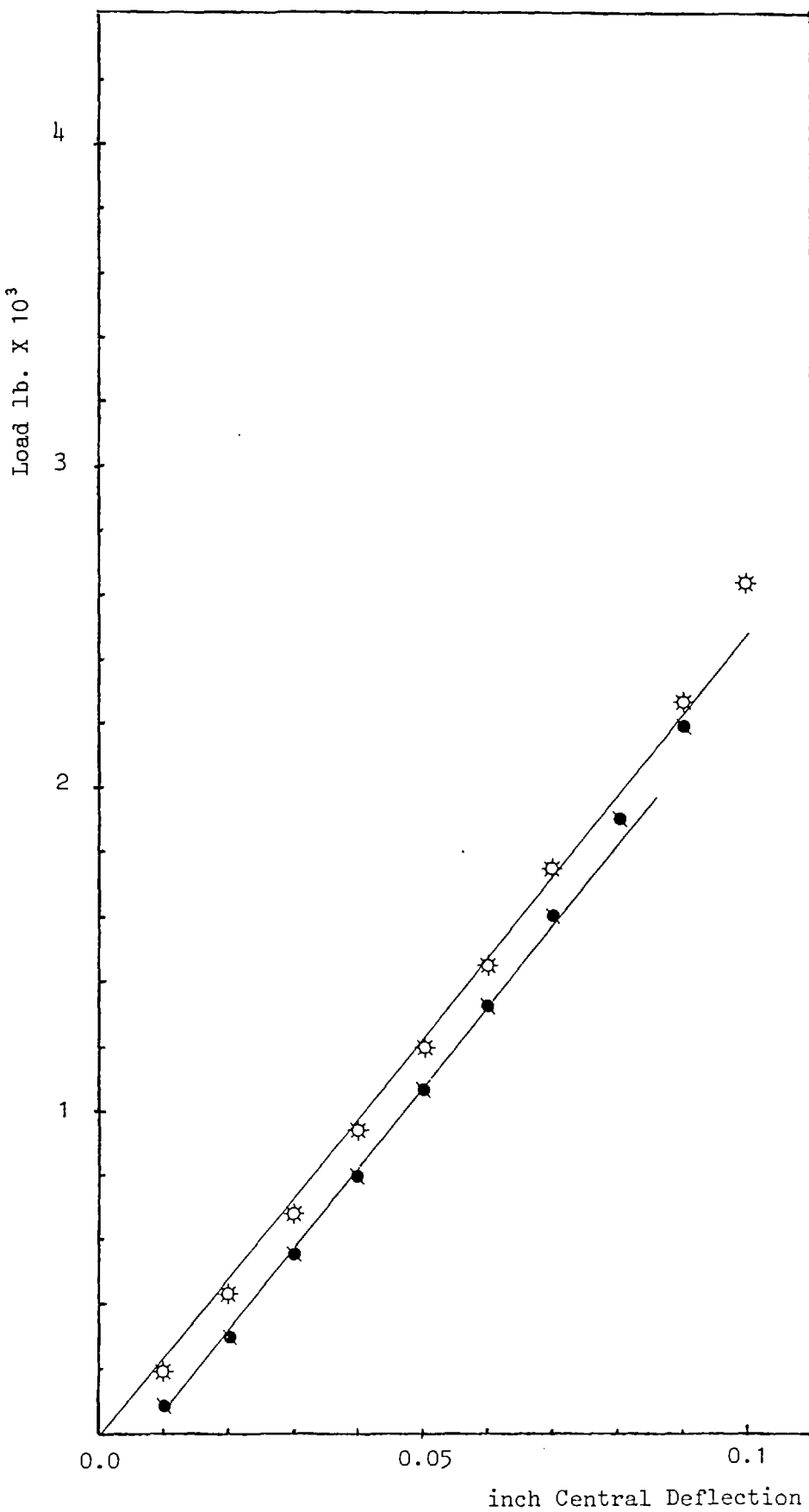


Fig. 5.19. Load vs. deflection in direction 1 - Layer C

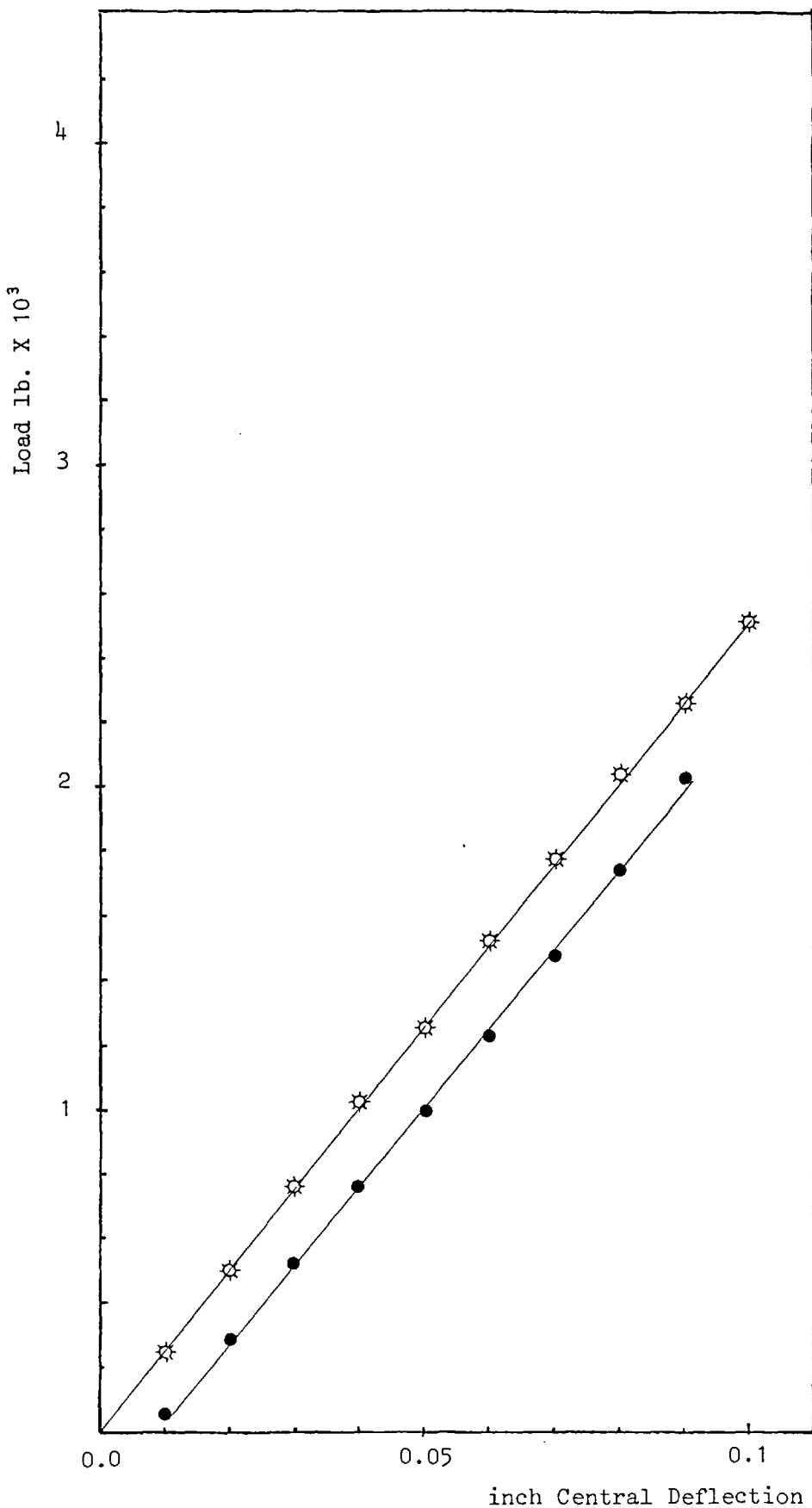


Fig. 5.20. Load vs. deflection in direction 2 - Layer C

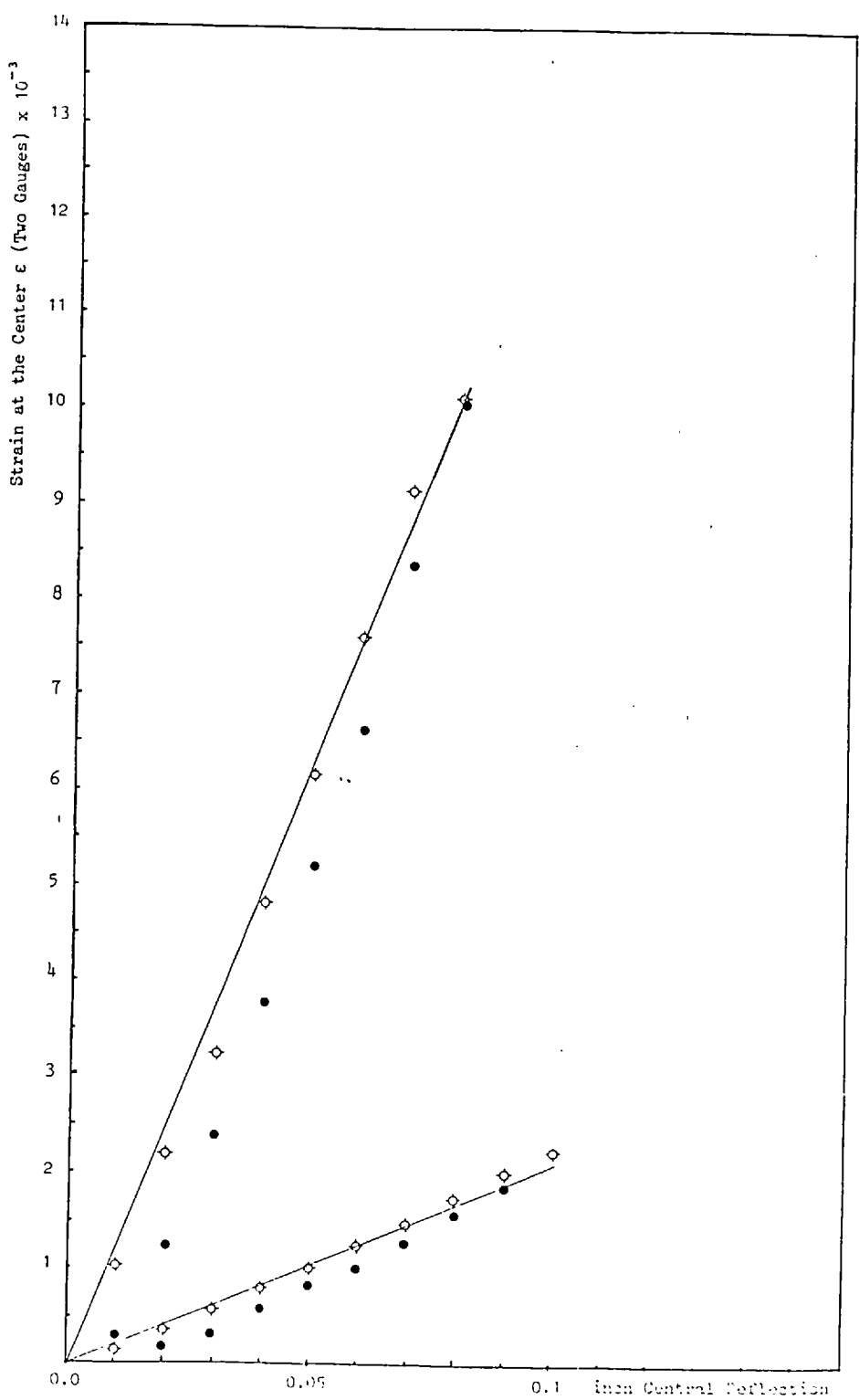


Fig. 5.21. Longitudinal & transverse strain vs. deflection direction 1 - Layer A.

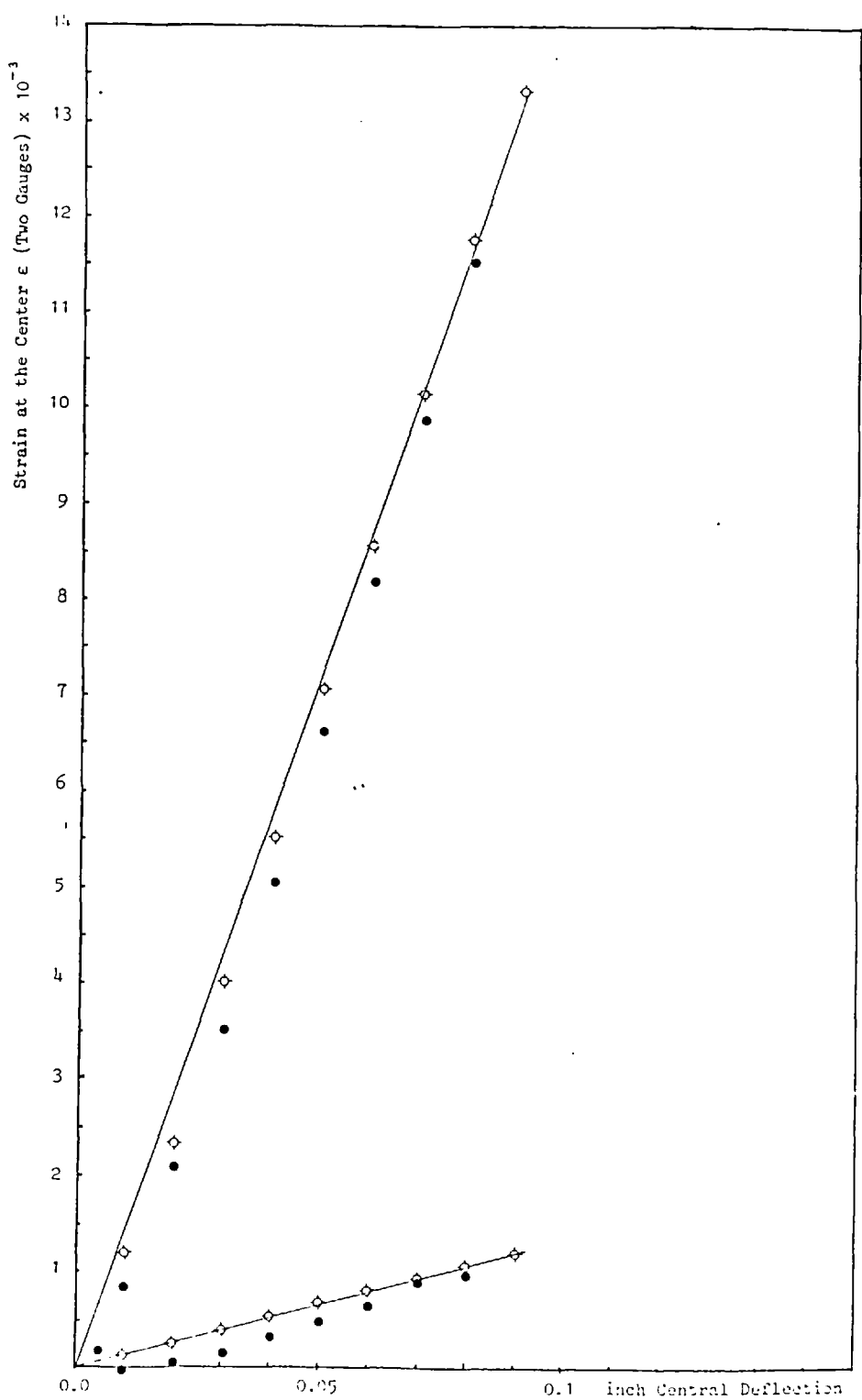


Fig. 5.22. Longitudinal & transverse strain vs. deflection direction 2 - Layer A.

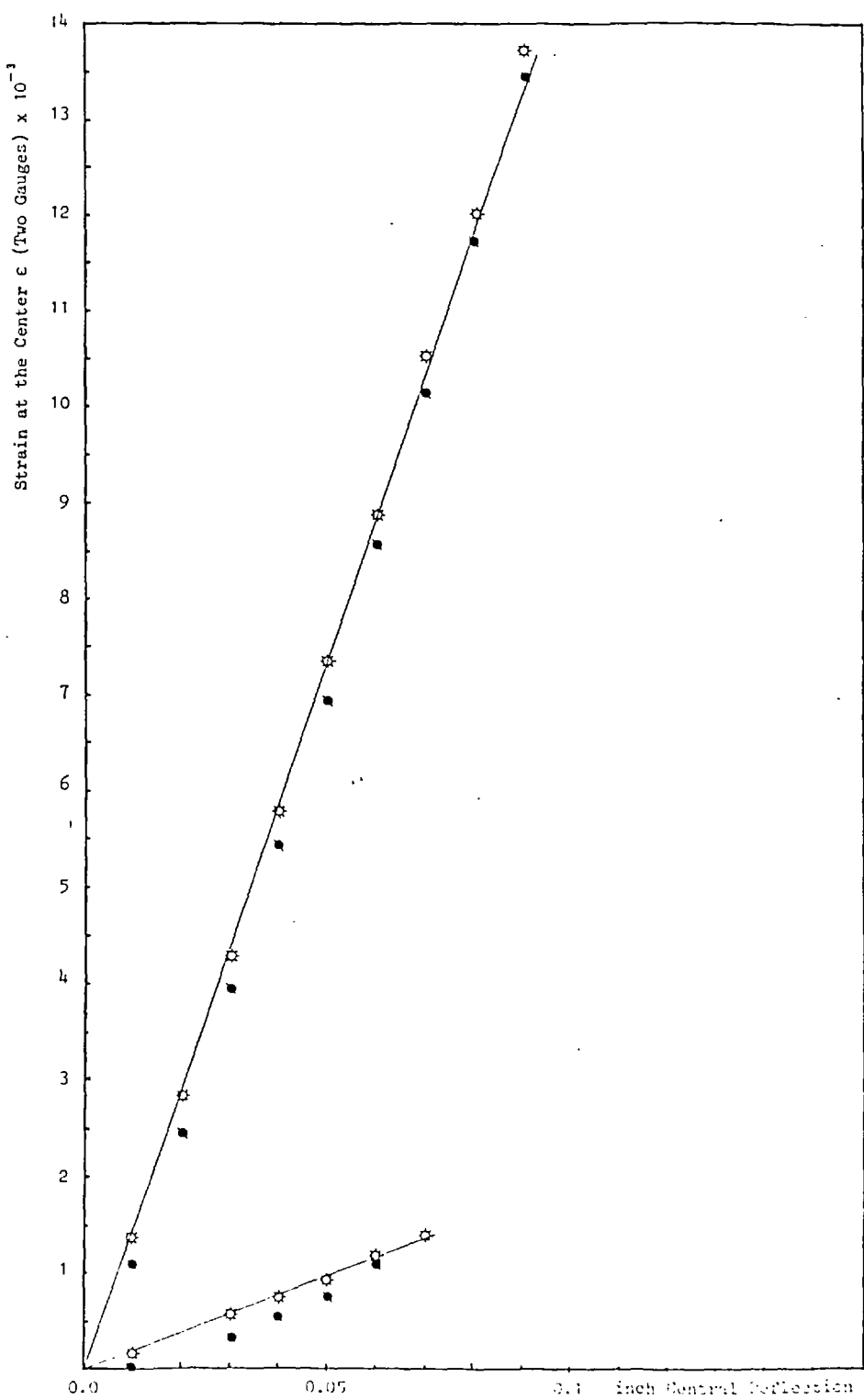


Fig. 5.23. Longitudinal & transverse strain vs. deflection direction 1 - Layer B.

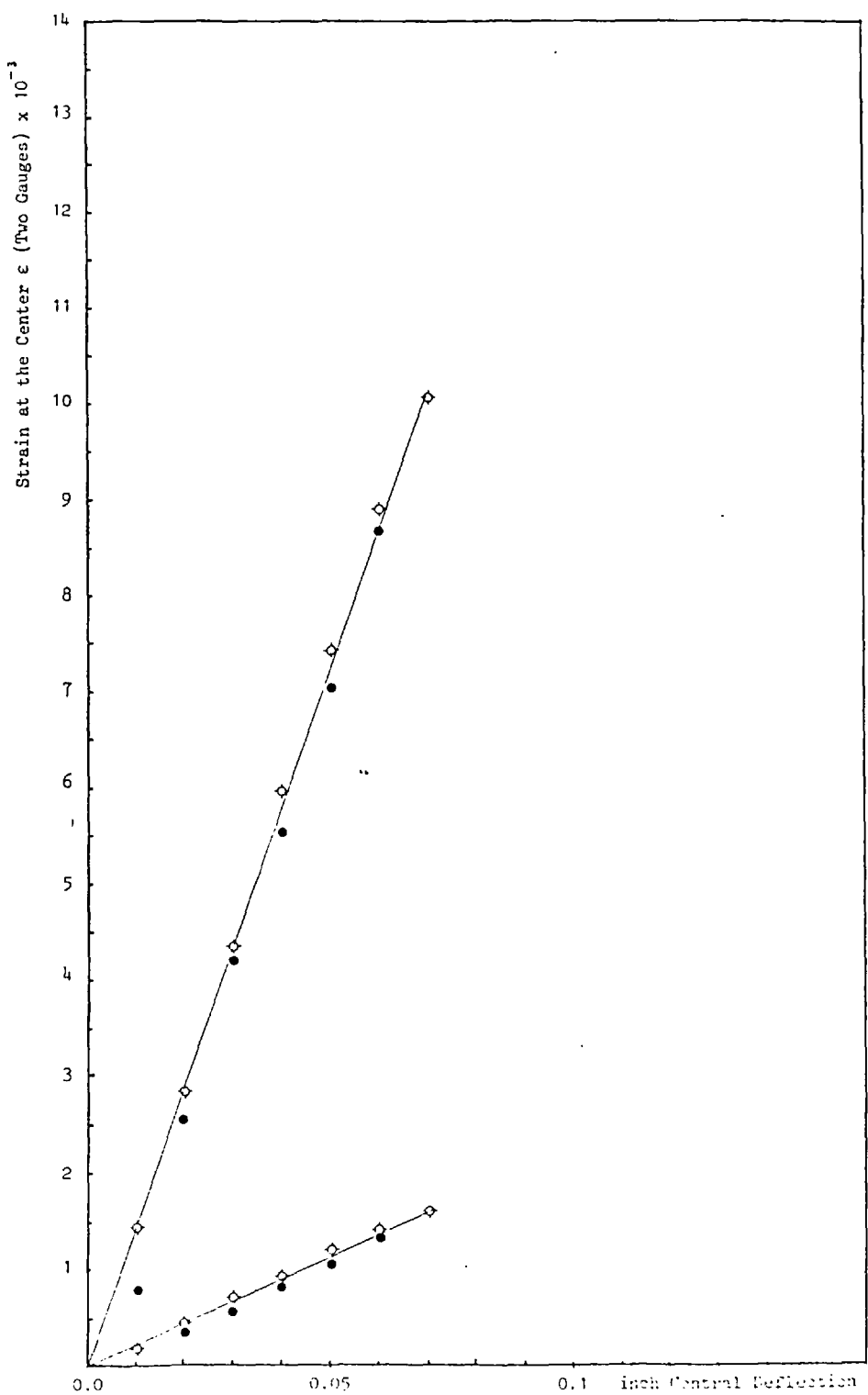


Fig. 5.24. Longitudinal & transverse strain vs. deflection
direction 2 - Layer B

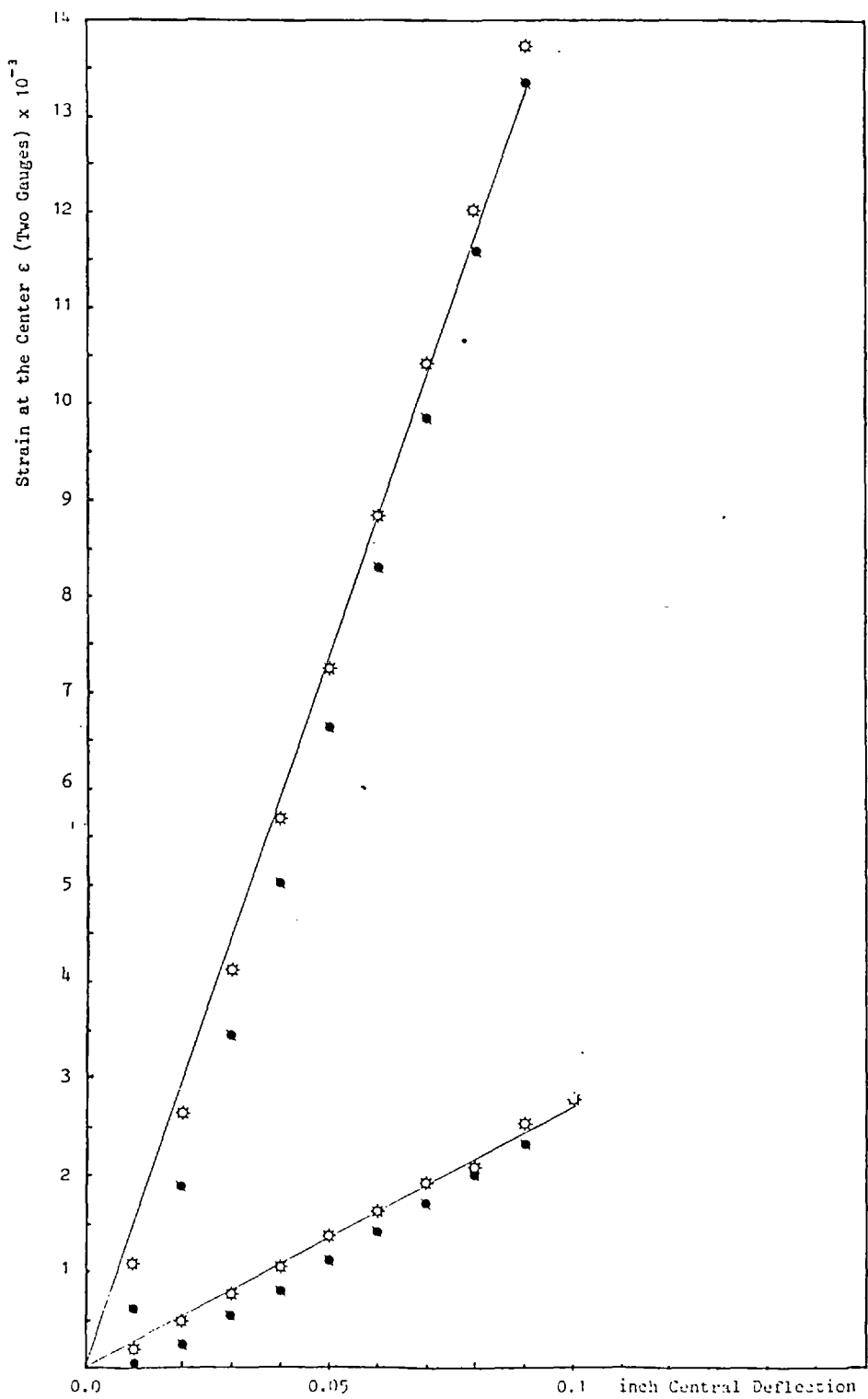


Fig. 5.25. Longitudinal & transverse strain vs. deflection
direction 1 - Layer C.

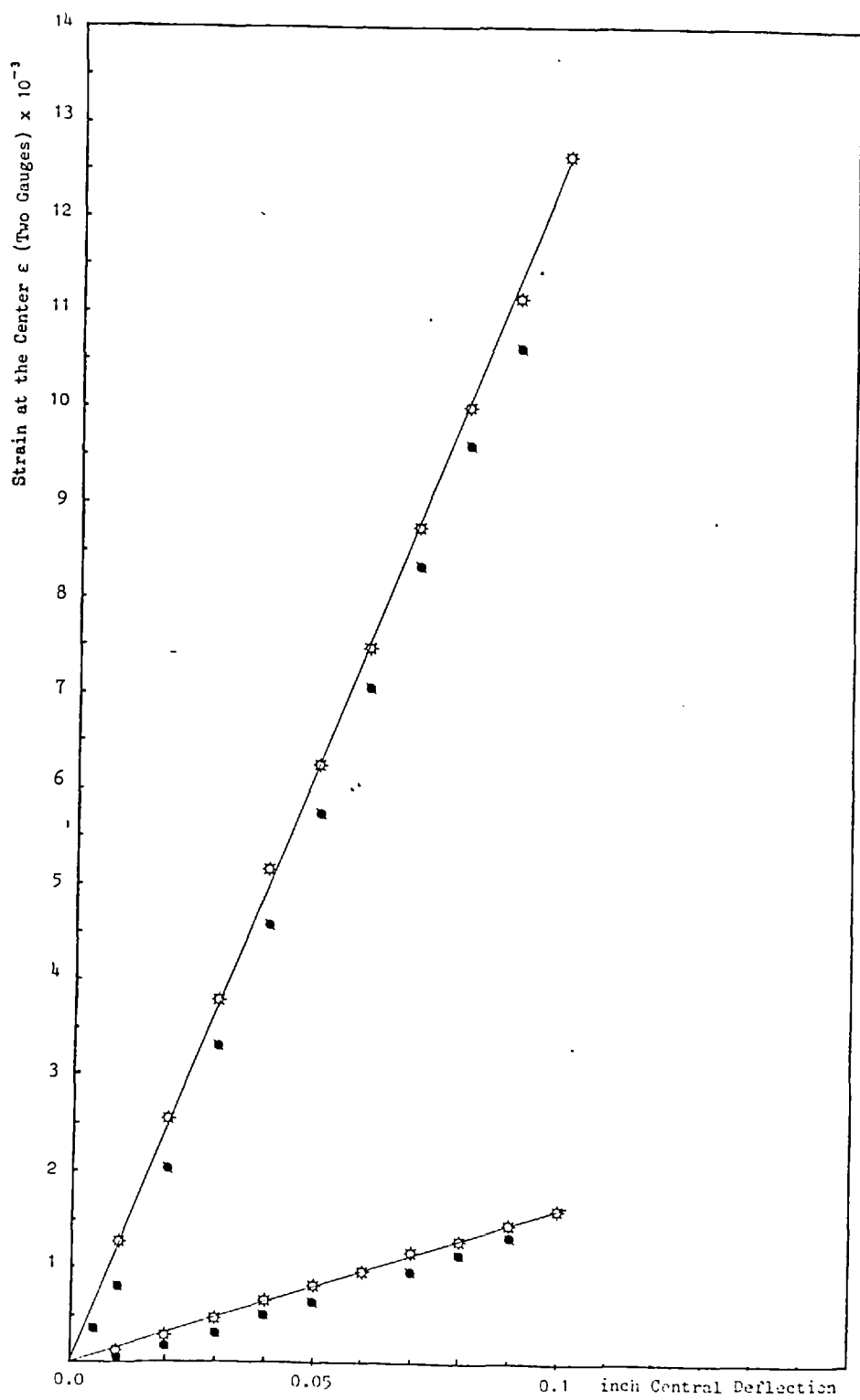


Fig. 5.26. Longitudinal & transverse strain vs. deflection direction 2 - Layer C.

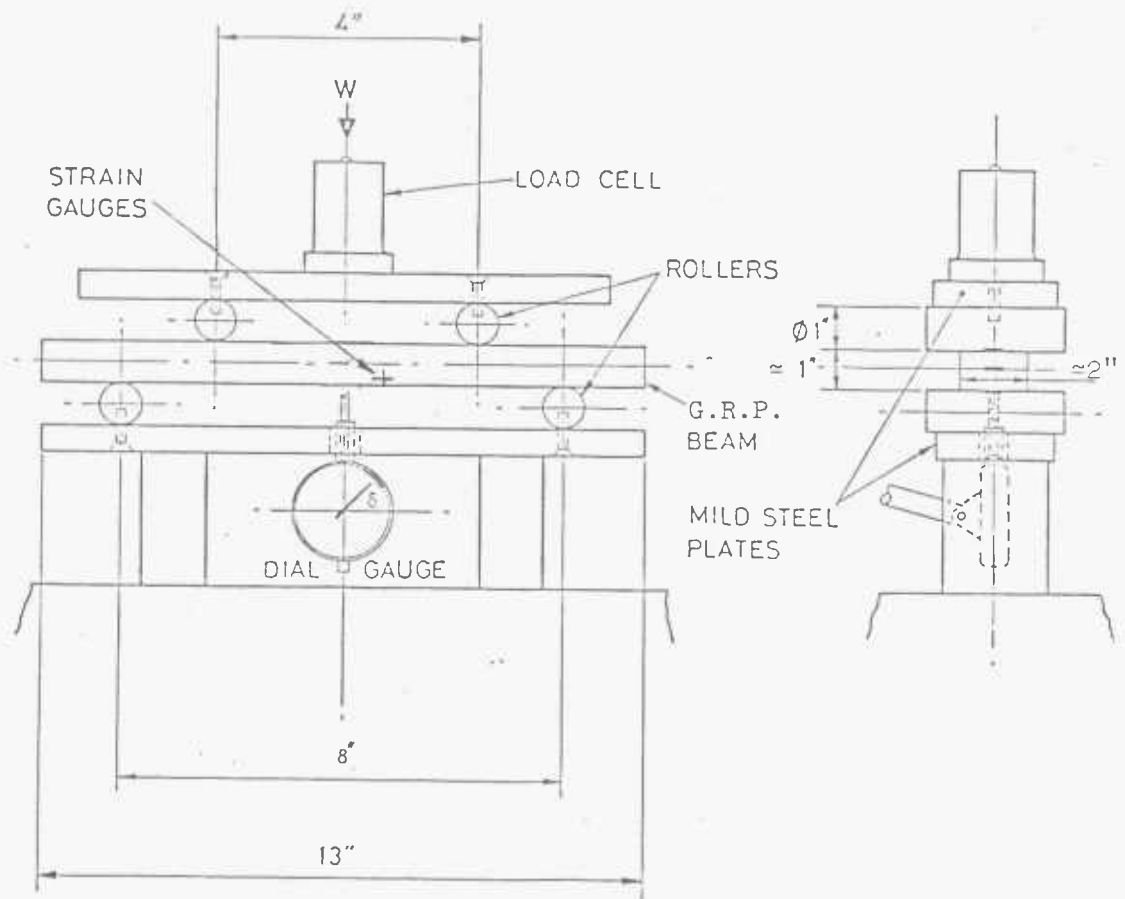


Fig. 5.27. 4-Point bend testing of G.R.P. beam for v_{13} & v_{23}

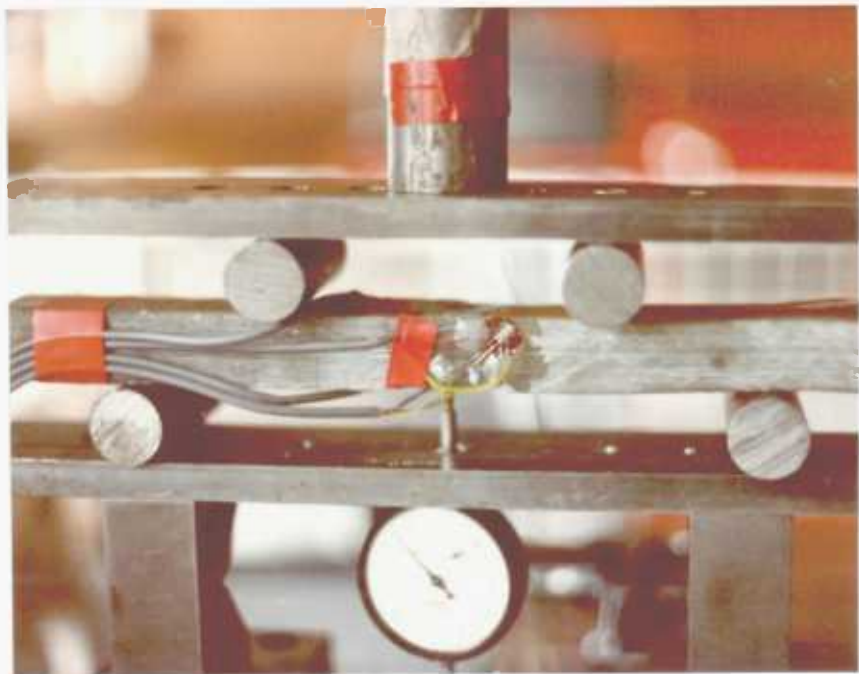


Fig. 5.28. 4-Point bend testing of G.R.P. beam for v_{13} & v_{23}

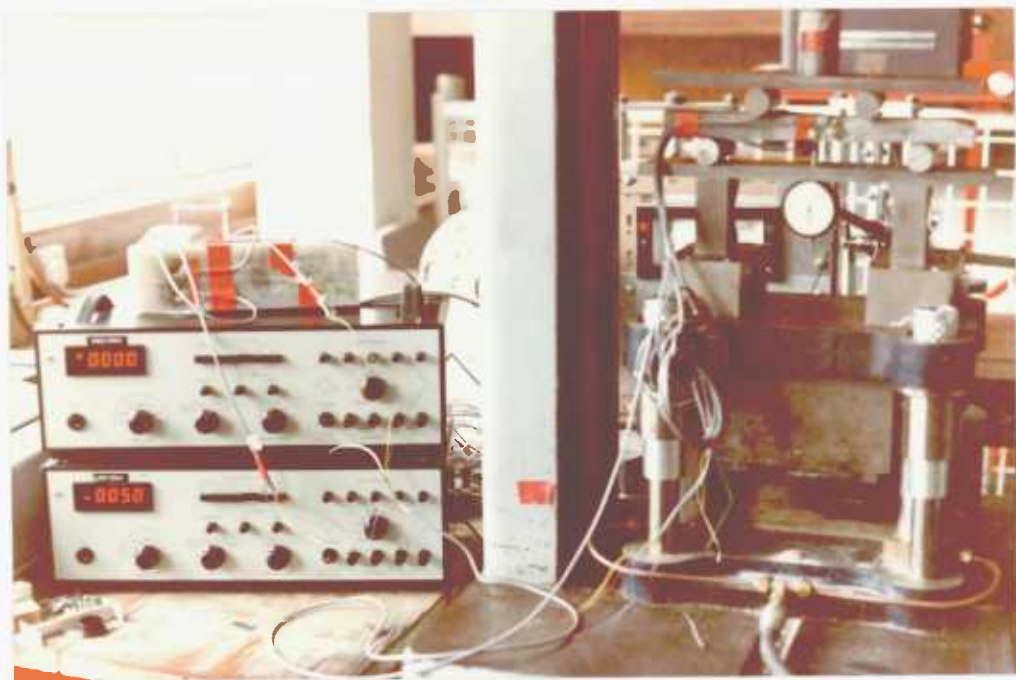


Fig. 5.29. 4-Point bend testing of G.R.P. beam for v_{13} & v_{23}

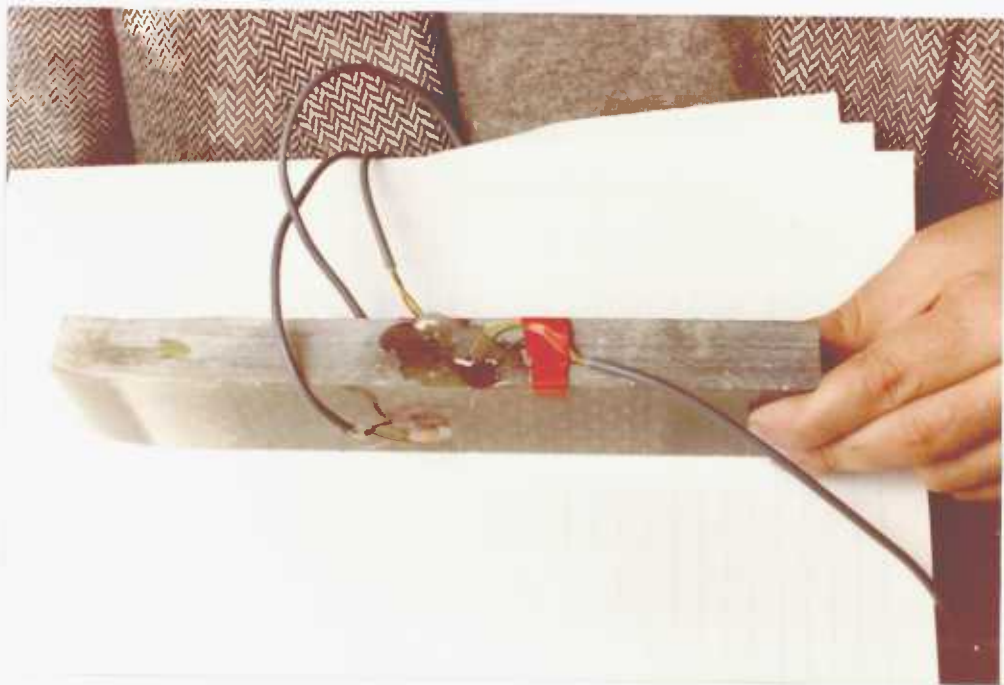


Fig. 5.30. Actual size of specimen.

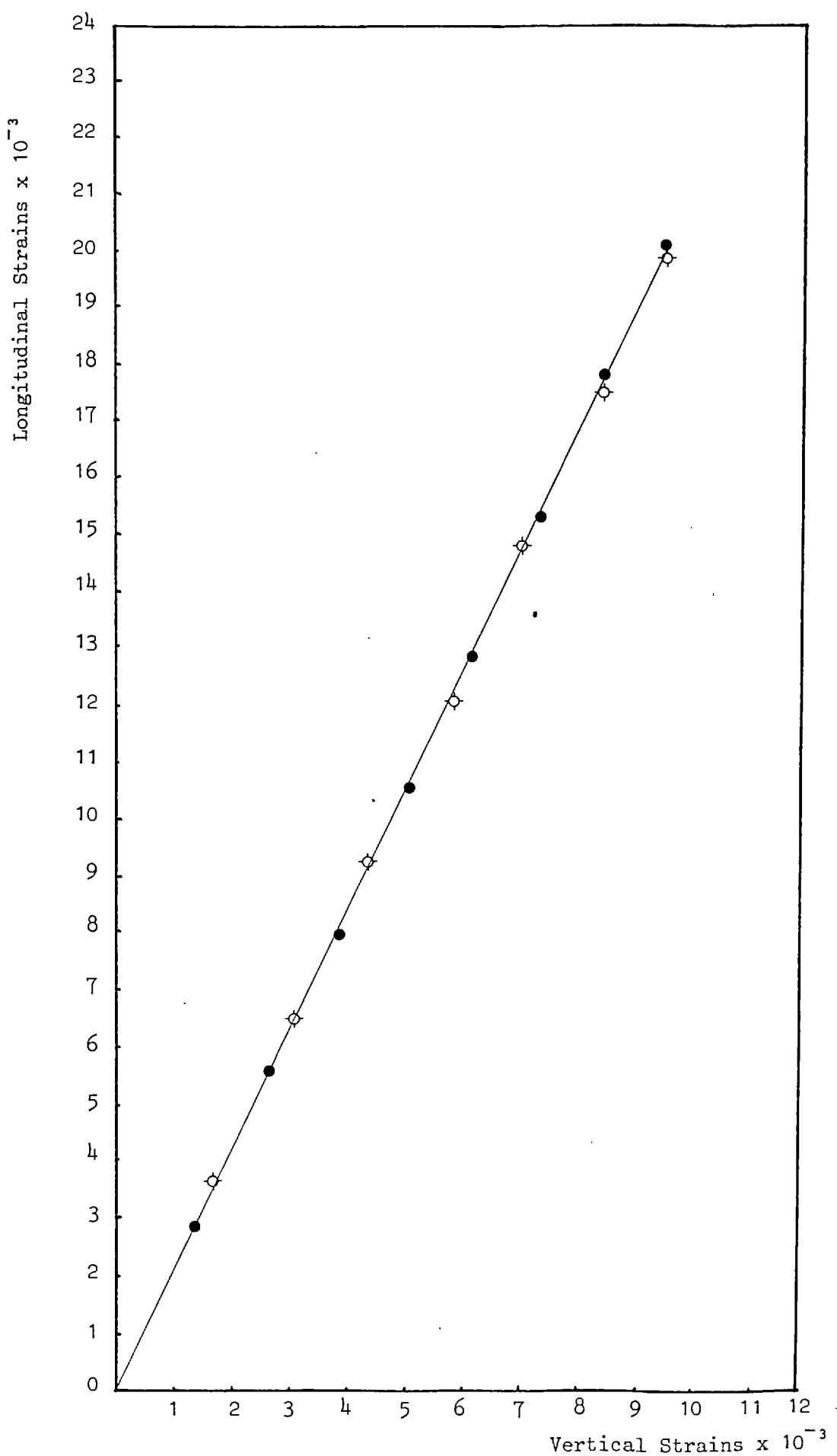


Fig. 5.31. Longitudinal vs. vertical strains in direction 1 - Layer A
263.

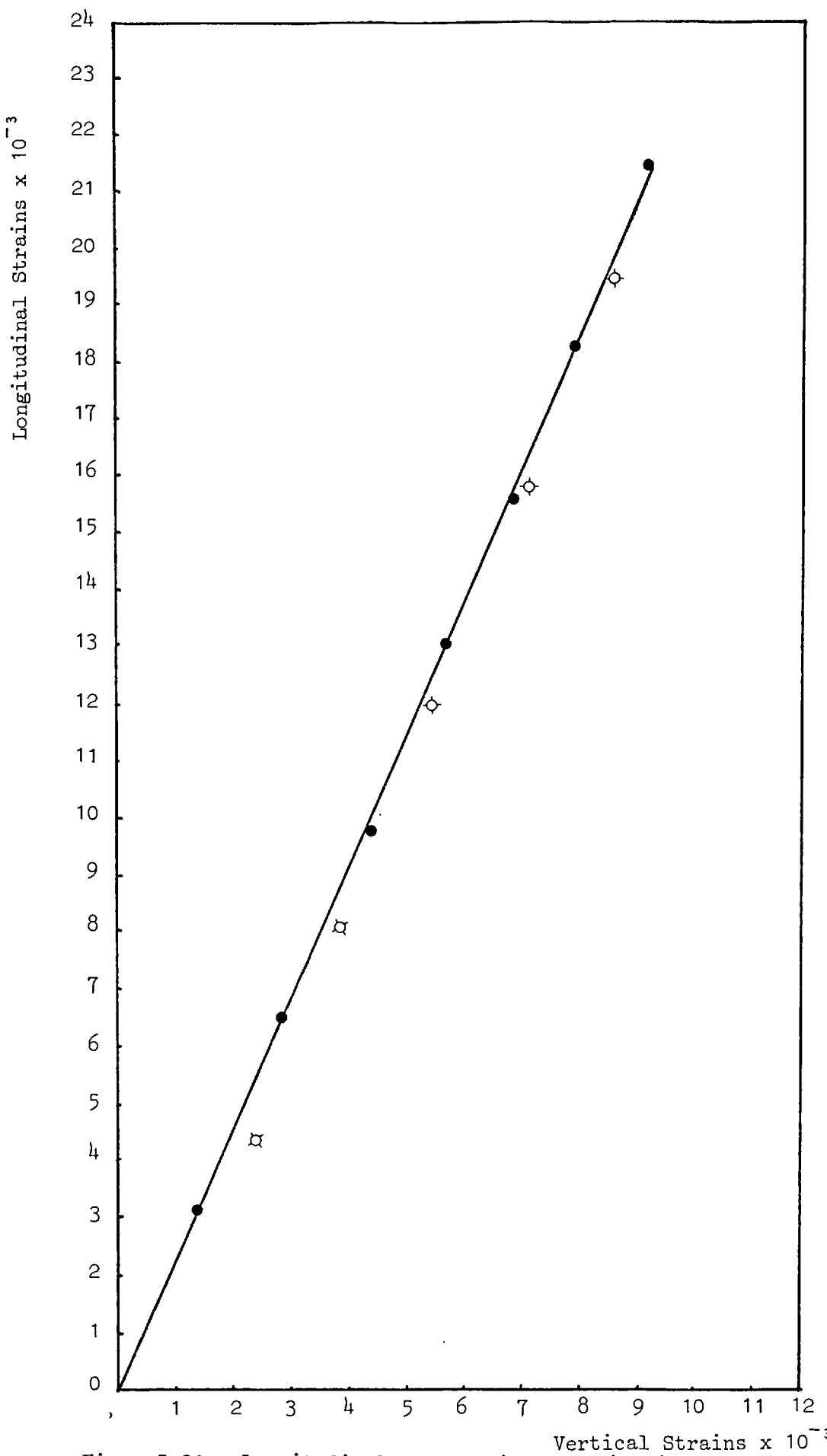


Fig. 5.32. Longitudinal vs. vertical strains in direction 2 - Layer A

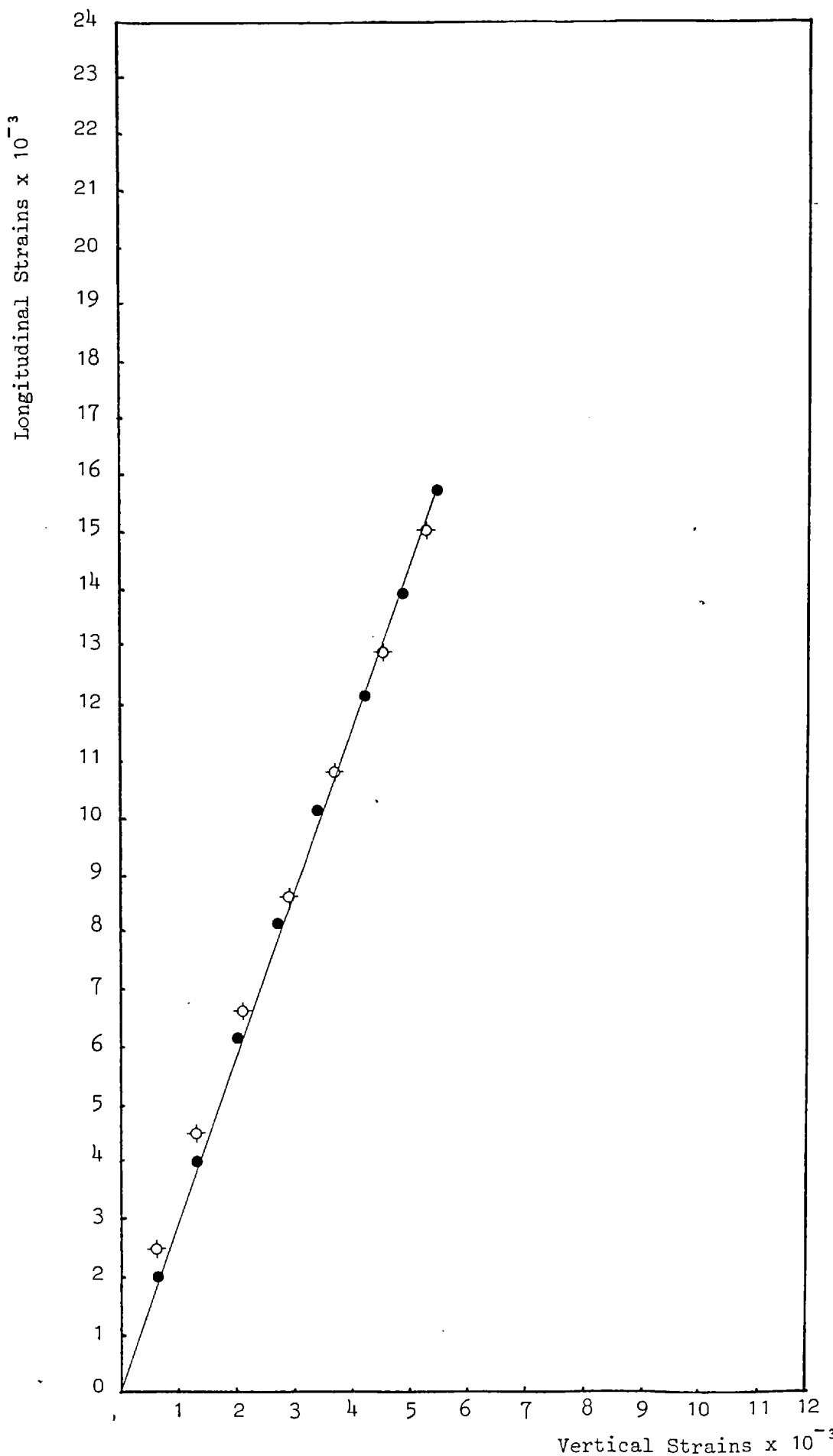


Fig. 5.33. Longitudinal vs. vertical strains in direction 1 - Layer B

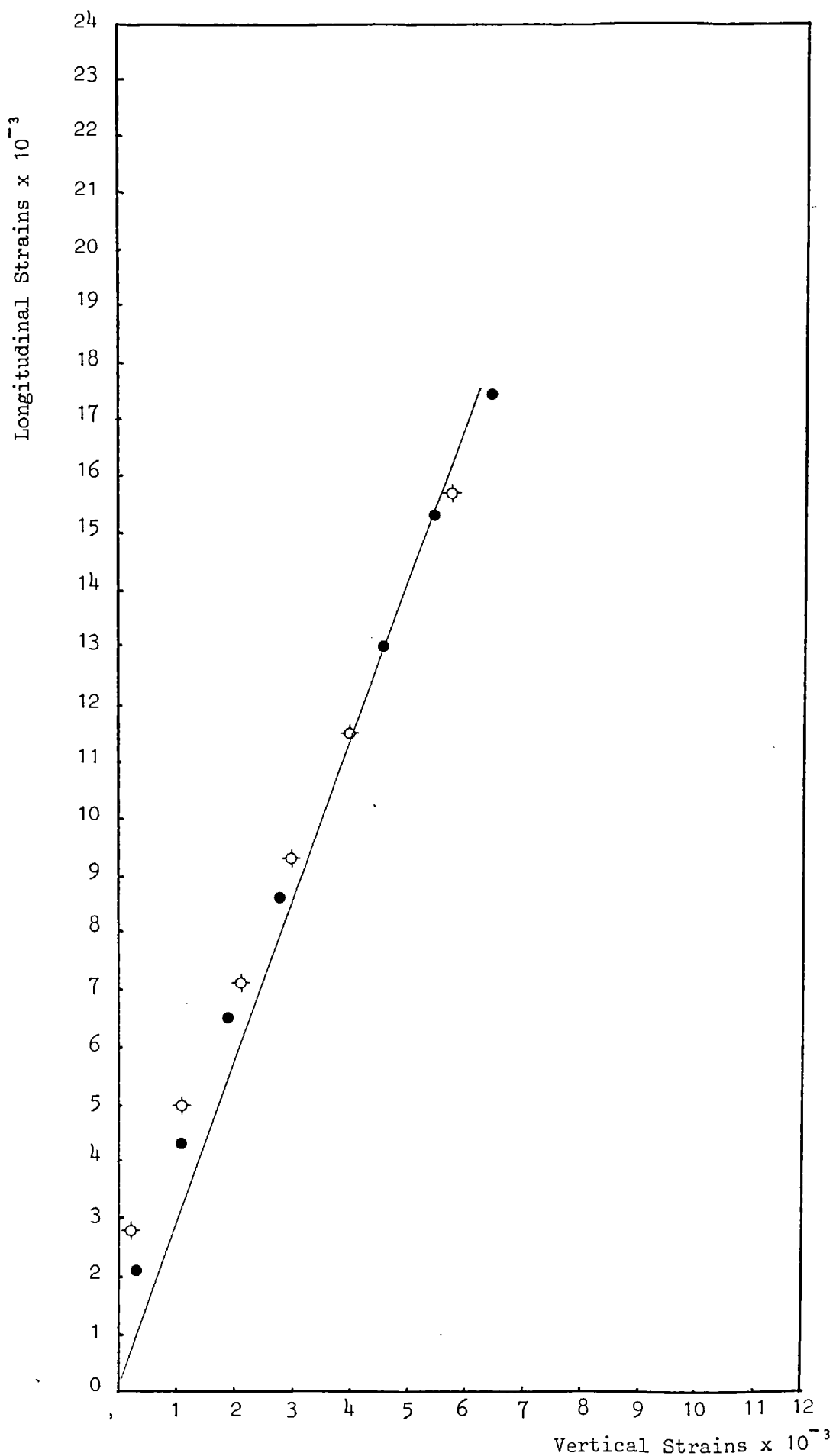


Fig. 5.34. Longitudinal vs. vertical strains in direction 2 - Layer B

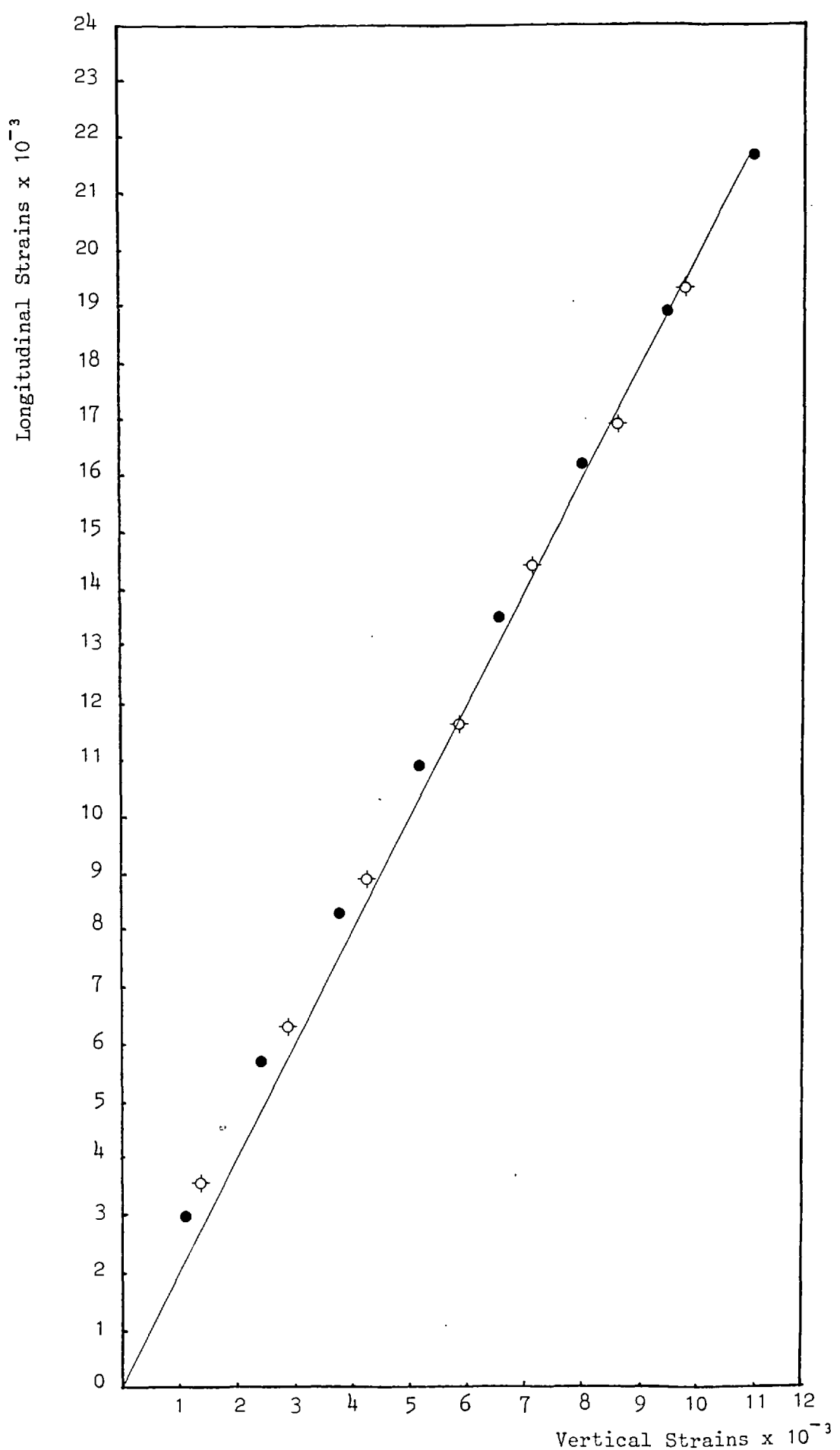


Fig. 5.35. Longitudinal vs. vertical strains in direction 1 - Layer C

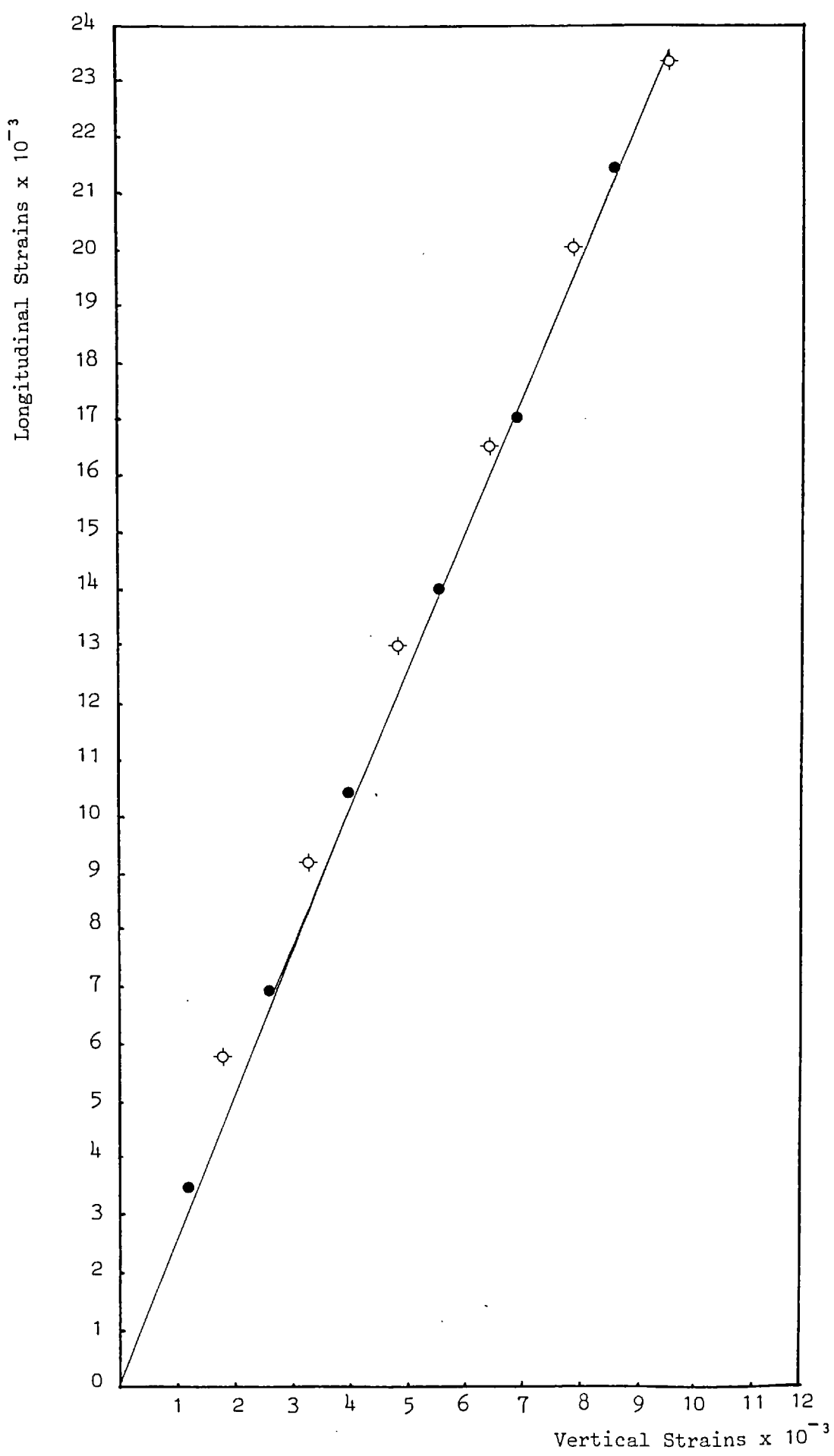


Fig. 5.36. Longitudinal vs. vertical strains in direction 2 - Layer C



Fig. 5.37. Minimum set of specimens

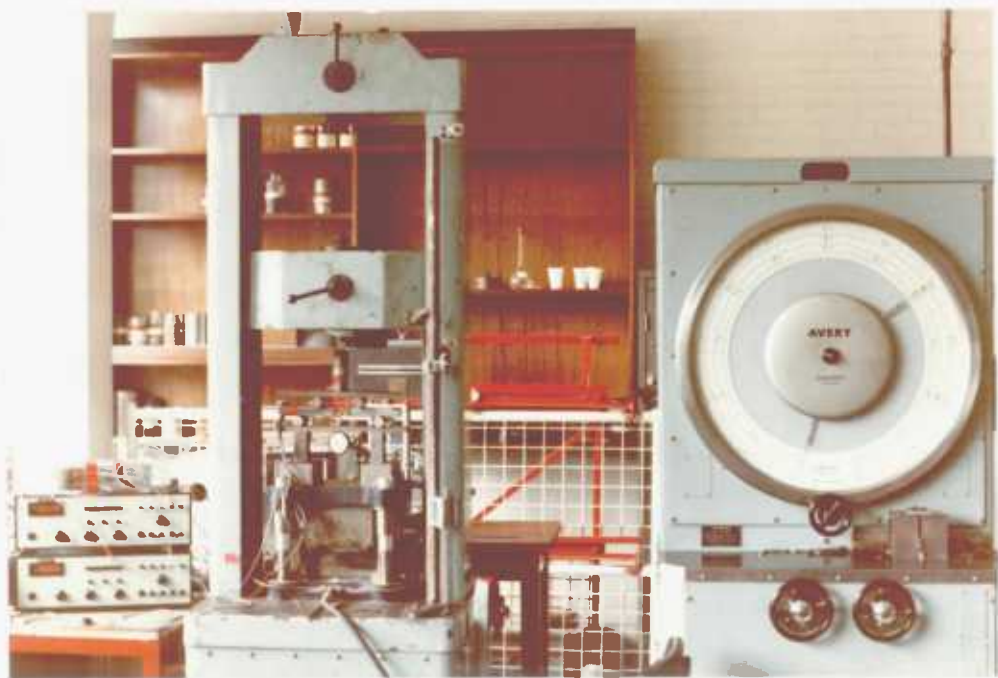


Fig. 5.38. Apparatus used for 4-point bend testing of beams.

5.3.3. Elastic constants of the specimens

Using Equation (2.104) with $\ell_1 = 4"$ and $\ell_2 = 2"$ as shown in Figs. (5.13) and (5.27) and Equation (2.105) gives:-

$$E = \frac{W}{\delta} \times \frac{22}{3} \times \frac{12}{b d^3} \text{ lb. in.}$$

and measuring all specimens accurately to $\pm 0.001"$, E_{33} was assumed to be lower than E_{11} and E_{22} and taken to be 1×10^6 psi as suggested by a reliable manufacturer. G_{12} was assumed to be 2×10^5 psi and G_{13} and G_{23} were assumed to be the same proportions as the relevant elastic moduli.

(i) For Layer A

From Fig. (5.15) $E_{11} = 1.274 \times 10^6$ psi $\pm 7\frac{1}{2}\%$

From Fig. (5.16) $E_{22} = 1.565 \times 10^6$ psi $\pm 7\frac{1}{2}\%$

From Fig. (5.22) $v_{12} = .163 \pm 5\%$

From Fig. (5.23) $v_{21} = 0.99 \pm 4\%$

From Fig. (5.31) $v_{13} = .48 \pm 2\%$

From Fig. (5.32) $v_{23} = .438 \pm 2\%$

E_{33} was assumed to be 1×10^6 psi,

G_{12} was assumed to be 2×10^5 psi,

G_{13} was assumed to be 1.3×10^5 psi,

G_{23} was assumed to be 1.6×10^5 psi.

(ii) For Layer B

From Fig. (5.17) $E_{11} = 1.62 \times 10^{-6}$ psi $\pm 7\frac{1}{2}\%$

From Fig. (5.18) $E_{22} = 1.8 \times 10^{-6}$ psi $\pm 7\frac{1}{2}\%$

From Fig. (5.23) $v_{12} = .159 \pm 3\%$

From Fig. (5.24) $v_{21} = .128 \pm 2\%$

From Fig. (5.33) $v_{13} = .325 \pm 2\%$

From Fig. (5.34) $v_{23} = .29 \pm 2\%$

E_{33} was assumed to be 1×10^6 psi,
 G_{12} was assumed to be 2×10^5 psi,
 G_{13} was assumed to be 1.11×10^5 psi,
 G_{23} was assumed to be 1.68×10^5 psi.

(iii) For Layer C

From Fig. (5.19) $E_{11} = 1.62 \times 10^6$ psi $\pm 6\%$

From Fig. (5.20) $E_{22} = 1.66 \times 10^6$ psi $\pm 6\%$

From Fig. (5.25) $v_{12} = .128 \pm 1\%$

From Fig. (5.26) $v_{21} = .128 \pm 1\%$

From Fig. (5.35) $v_{13} = .49 \pm 1\%$

From Fig. (5.36) $v_{23} = .40 \pm 2\%$

E_{33} was assumed to be 1×10^6 psi,

G_{12} was assumed to be 2×10^5 psi,

G_{13} was assumed to be 1.2×10^5 psi,

G_{23} was assumed to be 1.95×10^5 psi.

5.3.4. Finite Element Idealization of G.R.P. Test Beam

A finite element mesh as shown in Fig. (5.39) was arranged to suit the different average thicknesses of all three layers, to suit the supporting arrangement of the test, the location of the strain gauges on the test beam and to allow the application of a load off the centre so as to cause a complicated case of torsional bending as well as pure bending. The mesh consisted of 144 elements and 260 nodes. The properties of each element were read individually as E_{11} , E_{22} , E_{33} , v_{12} , v_{13} , v_{23} , G_{12} , G_{13} , and G_{23} . v_{21} was used to check the accuracy of the experimental results.

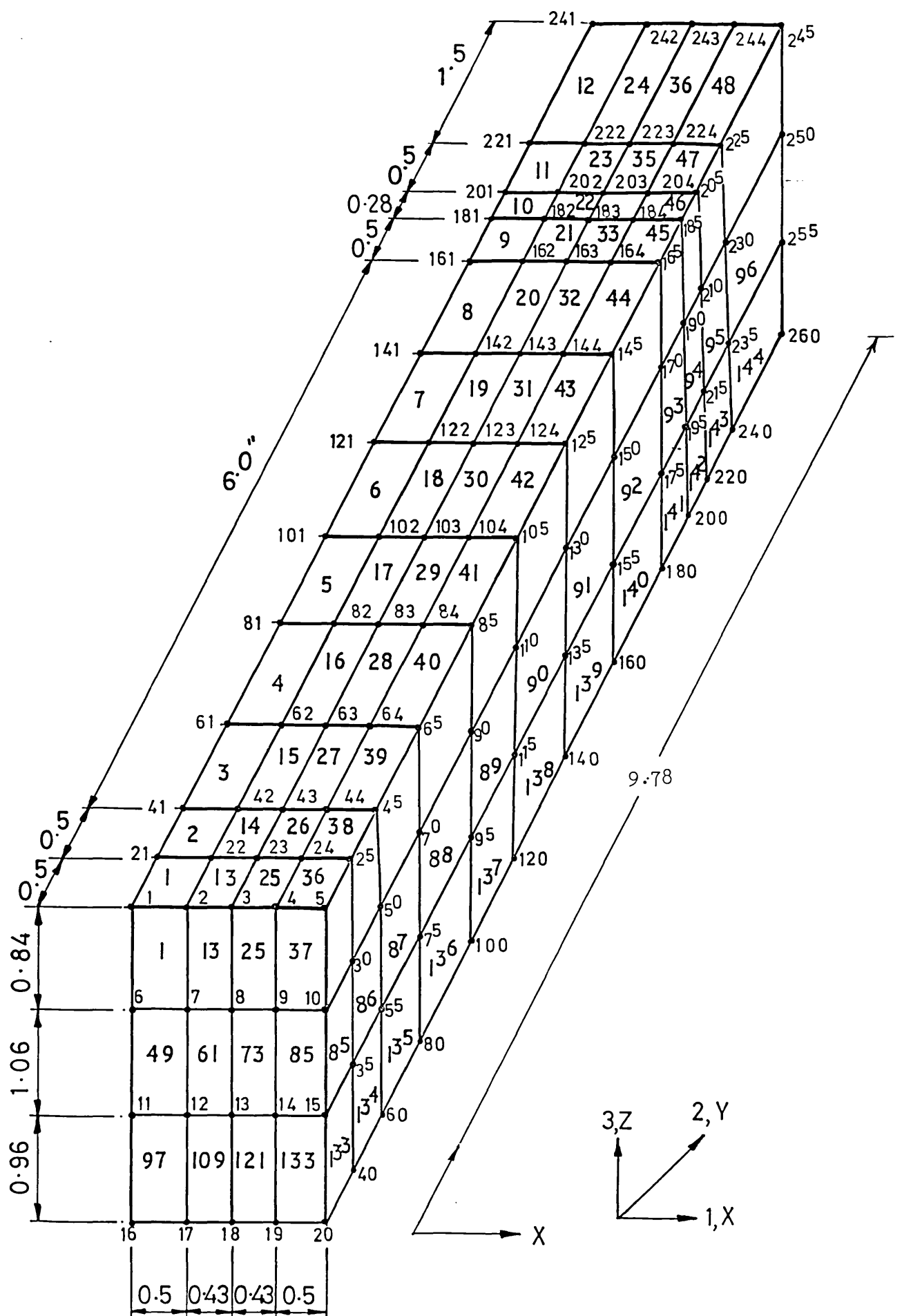


Fig. 5.39. Finite element idealization of G.R.P. test beam.

The program would give values for v_{21} , v_{31} , v_{32} using Equations (3.14a) (3.14b) and (3.14c). In calculating stresses the average of the values from all elements adjacent to the node is used. If the node is at the interface of two layers, the average of the elements in one layer is calculated separately from those elements meeting at the node from another layer.

5.3.5. Experimental Work on G.R.P. Test Beam

(i) Test specimen

The test on the multilayered beam from the end Block D, No. D4 is described in this section. Its measured dimensions were 2.86" x 1.86" x 9.78", considering the average thickness of Layer A to be 0.84", Layer B - 1.06" and Layer C - 0.98".

Six rosette strain gauges type FRA-6-11 made by T.S.K. Ltd. Gauge resistance $120 \pm 0.5\Omega$, gauge length 6mm were stuck 0.5" away from the support as shown in Figs. (5.40a), (5.40b) and (5.41) and their location on the finite element mesh is shown in Fig. (5.44). The gauges were located near the support and a cantilever arrangement was adopted to give higher and more readable strains from the equipment available.

The upper surface of the specimen had to be filed smooth to stick rosette No. 1 which reduced the thickness of Layer A by 0.14" for a length of 0.78".

The specimen was clamped to a heavy table as shown in Figs. (5.41), (5.42) and (5.43). The loads were applied through a free hook into a shallow dent in the upper surface of the

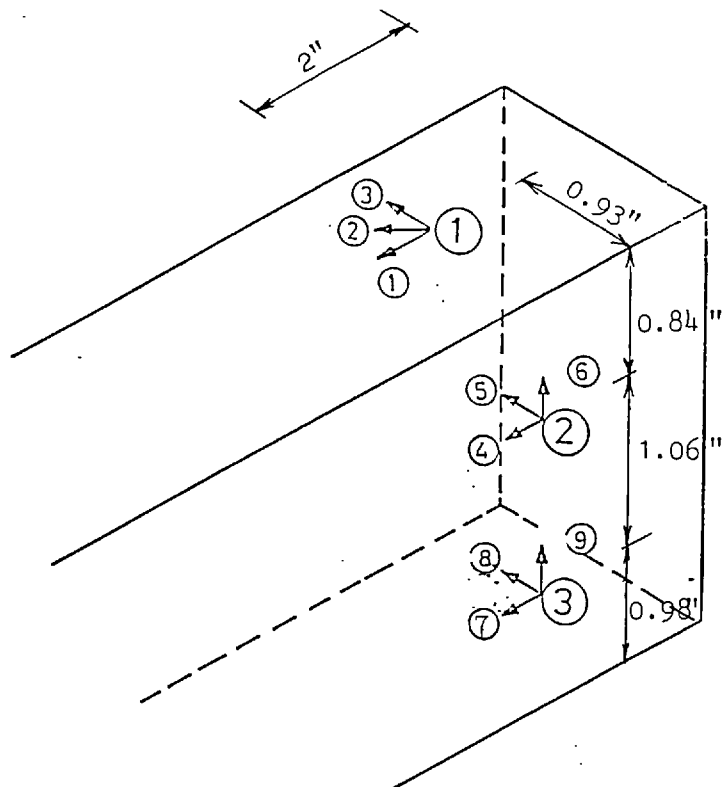


Fig. 5.40a. Location and numbers of strain gauges.

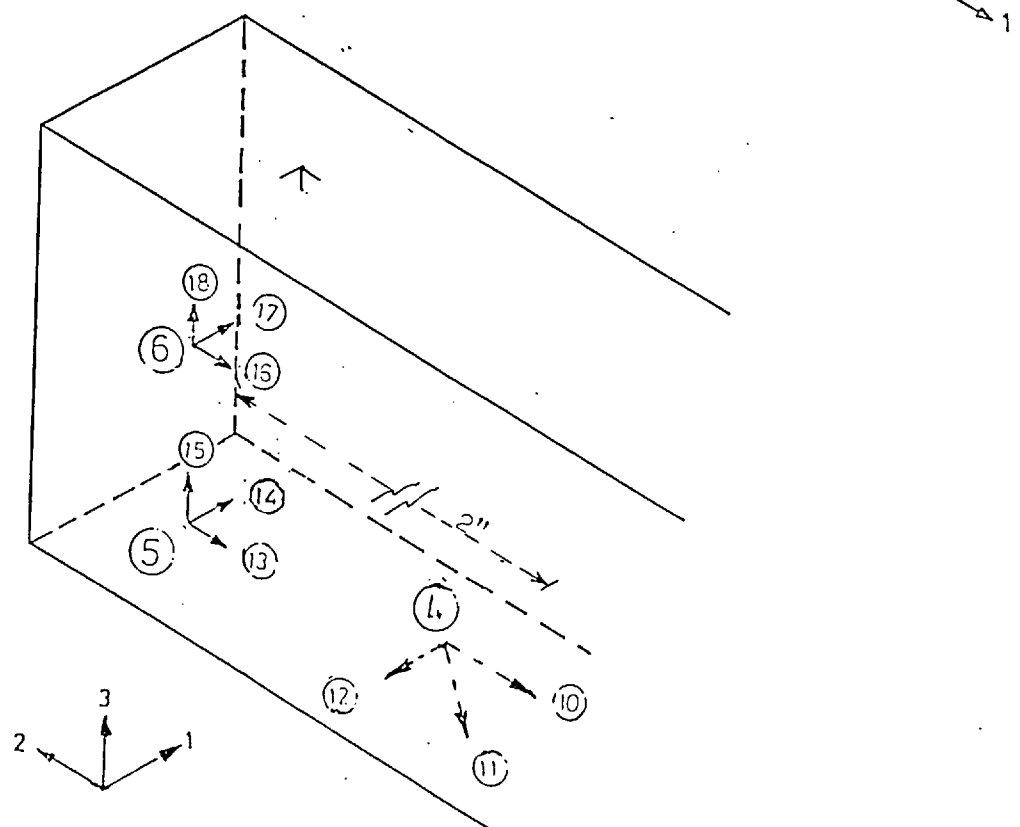


Fig. 5.40b. Location and numbers of strain gauges.

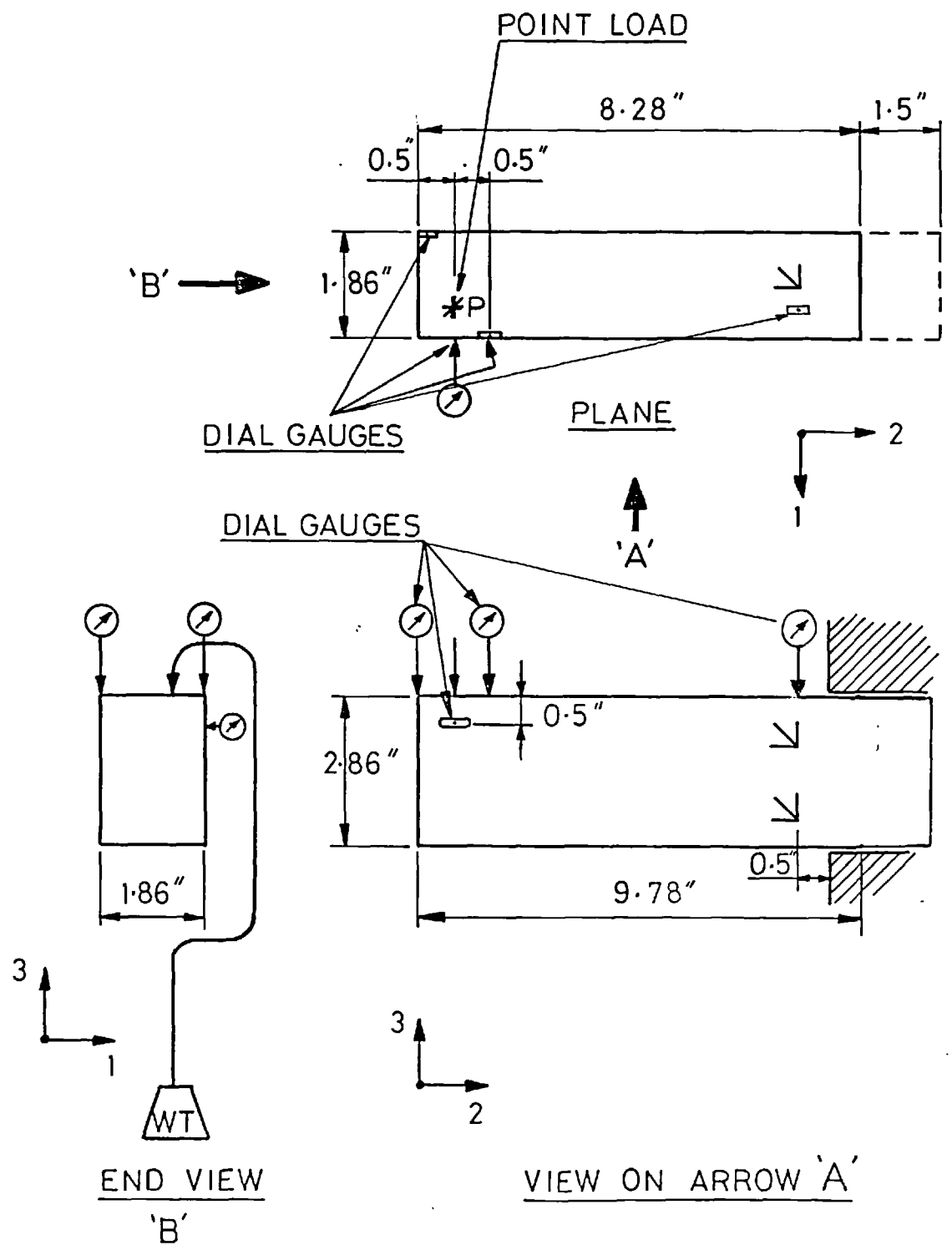


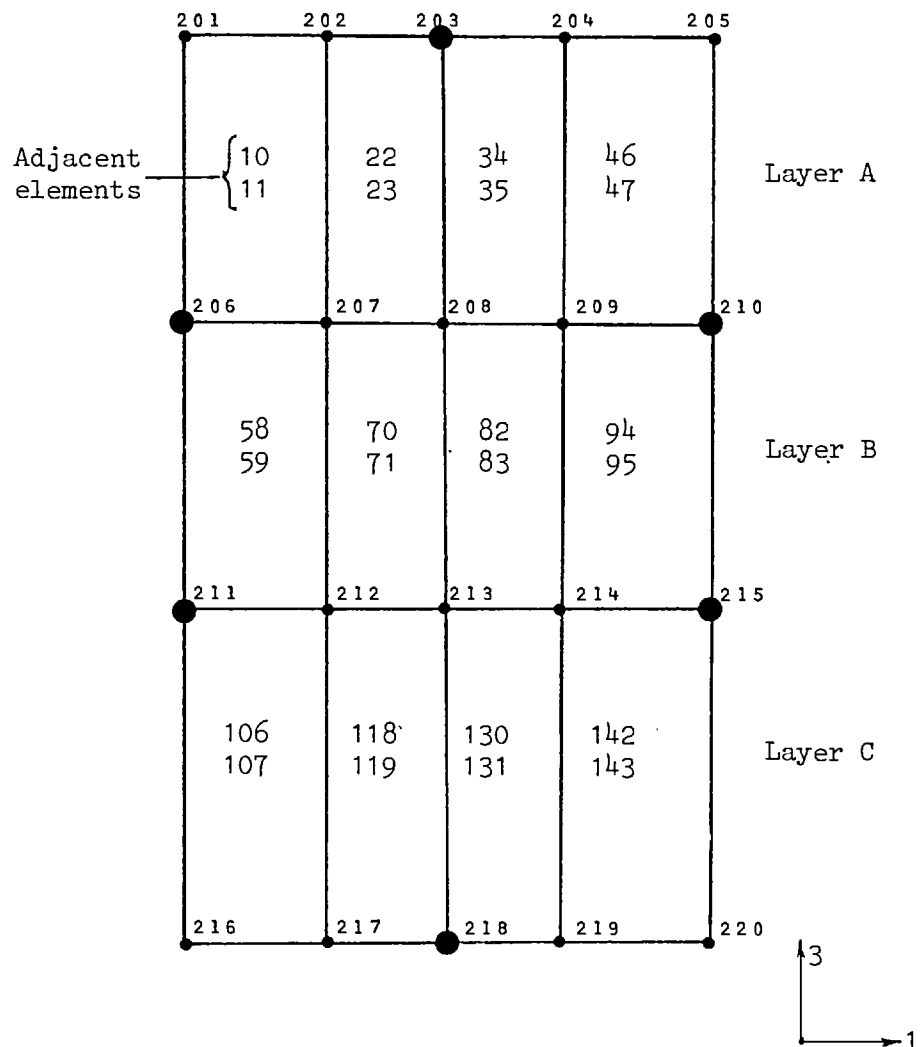
Fig. 5.41. Experiment arrangement of G.R.P. test beam.



Fig. 5.42. Experiment arrangement of G.R.P. test beam.



Fig. 5.43. Experiment arrangement of G.R.P. test beam.



● Strain gauges

Fig. 5.44. Gauge locations on the finite element mesh.

specimen 0.5" from both edges equivalent to Node 24 on the finite element mesh, so as to introduce combined torsion and bending.

(ii) Testing procedure

(a) Stresses

The 18 gauges from the six rosettes were arranged with 18 dummy gauges from six similar gauges stuck on other specimens of the same material so that each active gauge and the corresponding dummy gauge were connected to a channel of a Brueiland and Kjaer switching unit type 1542 from which they were arranged in a half bridge and fed with 3.0V through a Brueiland and Kjaer strain gauge amplifier type 1526. The output was fed back to the amplifier which indicated the total strains in microstrains on a L.E.D. display. The highest strain recorded was 630 microstrains with the accuracy of the equipment of ± 30 microstrains.

The stresses were calculated using the first terms of Equations (3.13a), (3.13b) and (3.13c).

The equivalent stresses to those occurring at the corner of the relevant elements in the relevant layer were plotted on Figs. (5.45), (5.46), (5.47), (5.48), (5.49), (5.50), (5.51), (5.52), (5.53), (5.54), (5.55) and (5.56) against the results from the finite element solution. As can be seen the results were very satisfactory.

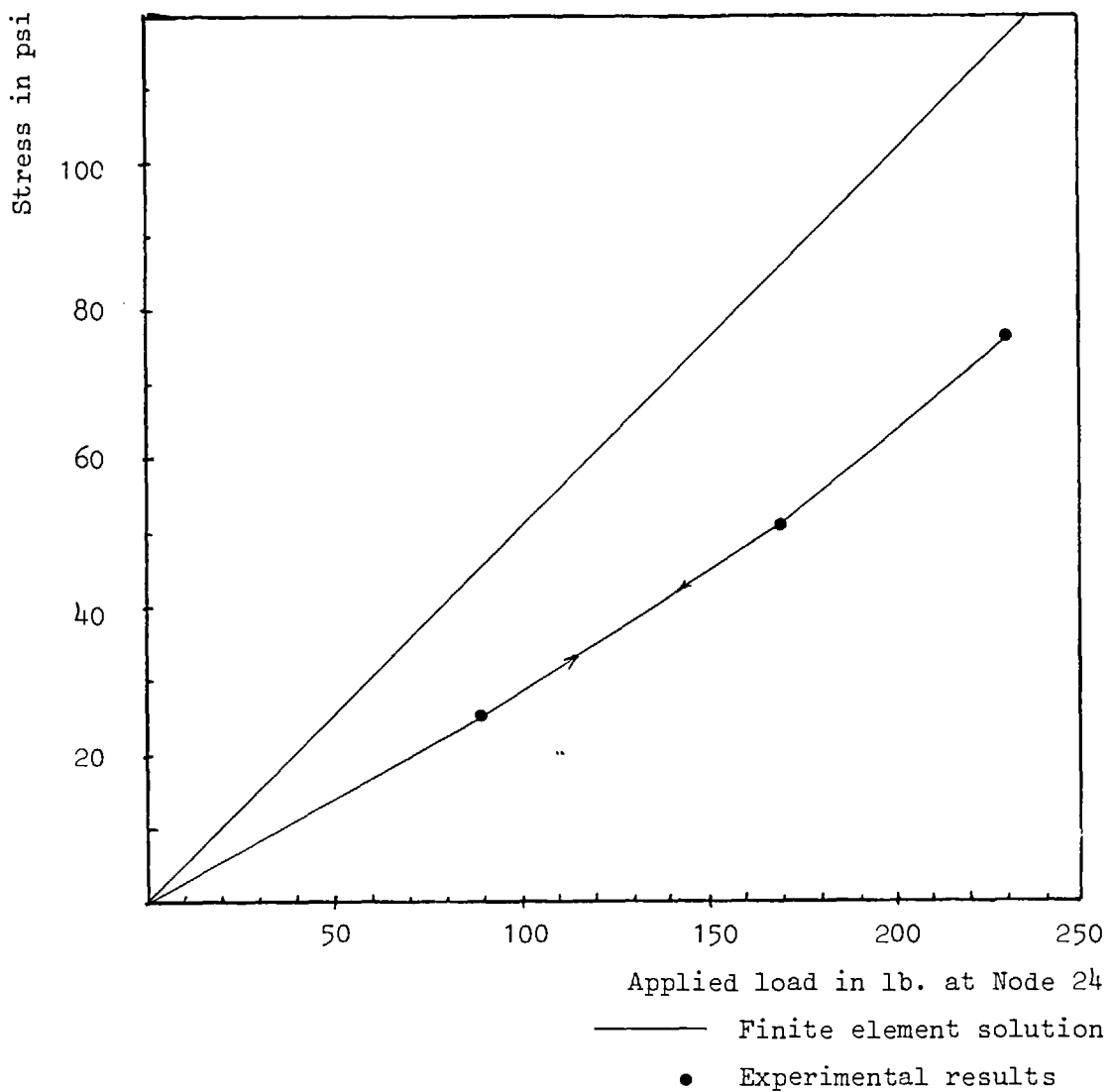


Fig. 5.45. Comparison of stresses in direction 1 at Node 203

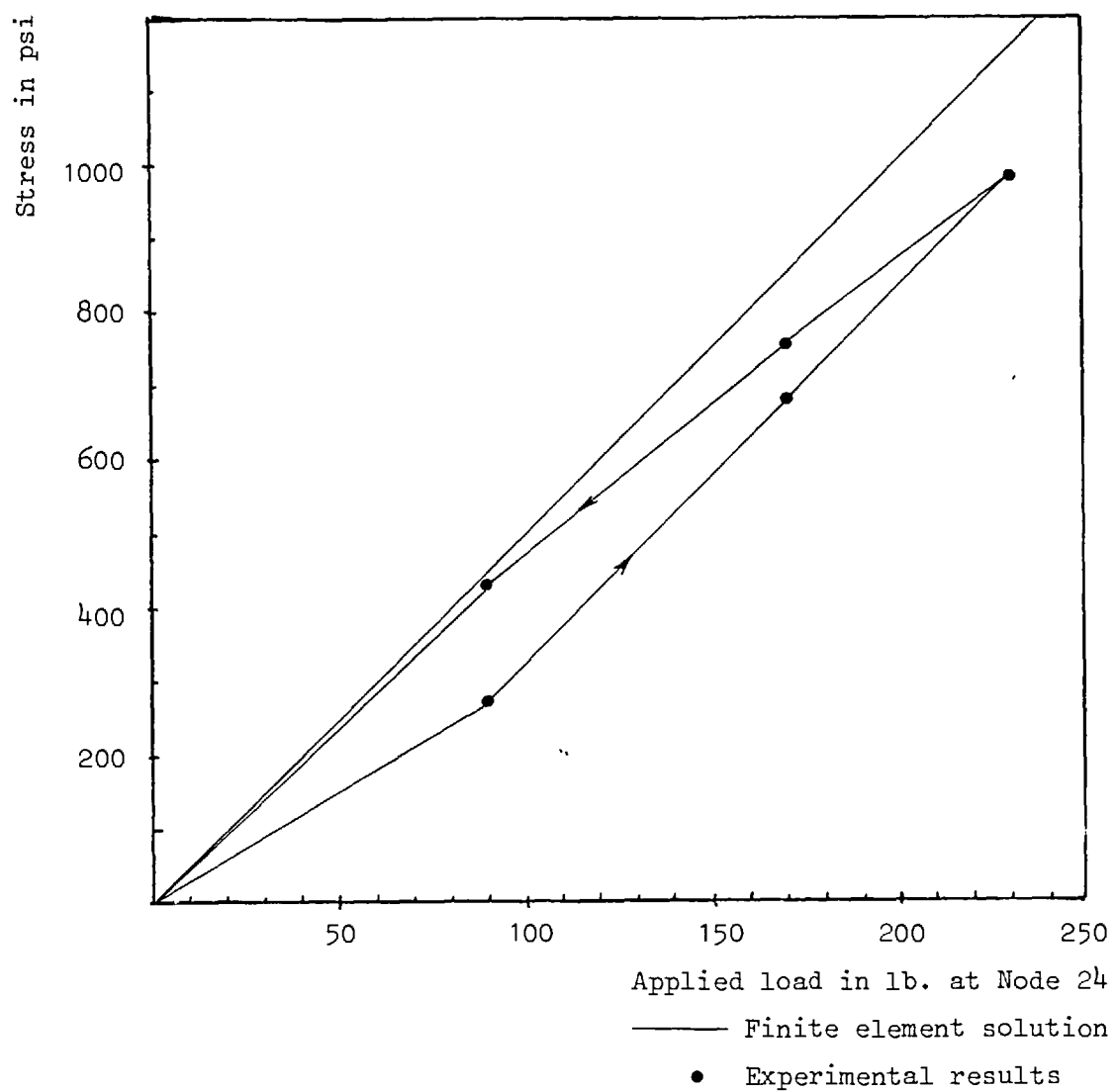


Fig. 5.46. Comparison of stresses in direction 2 at Node 203

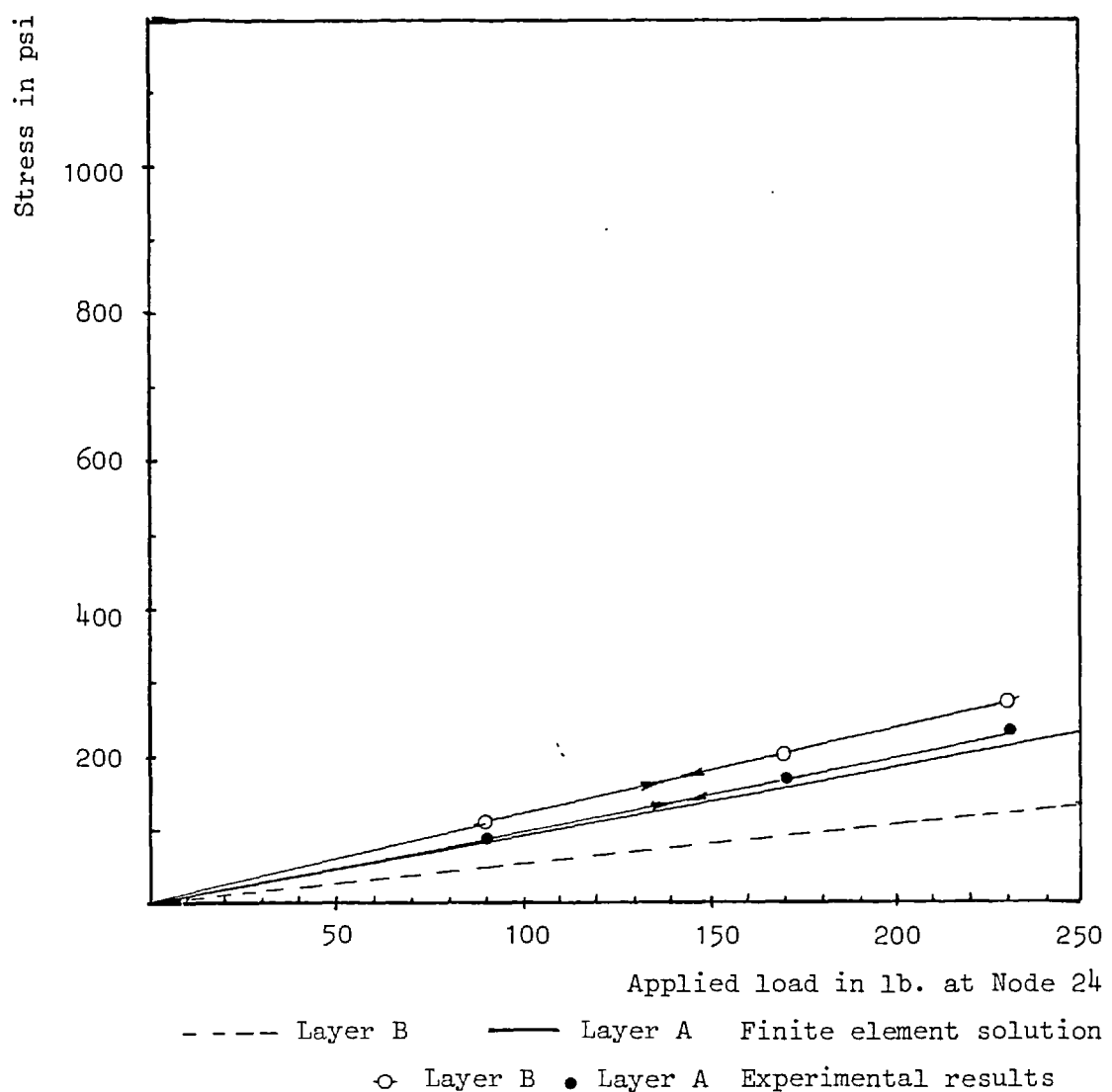


Fig. 5.47. Comparison of stresses in direction 2 at Node 210

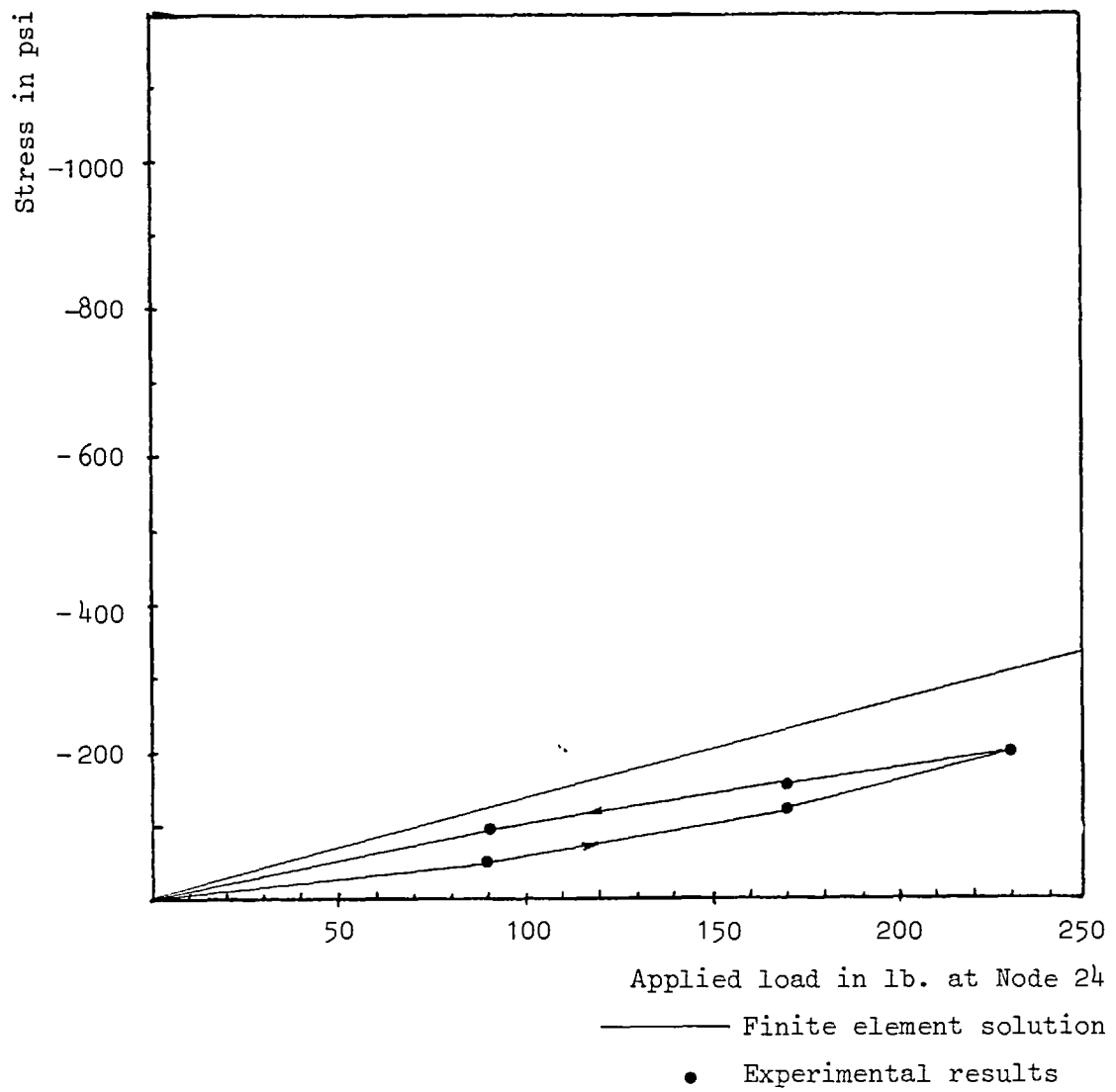


Fig. 5.48. Comparison of stresses in direction 3 at Node 210

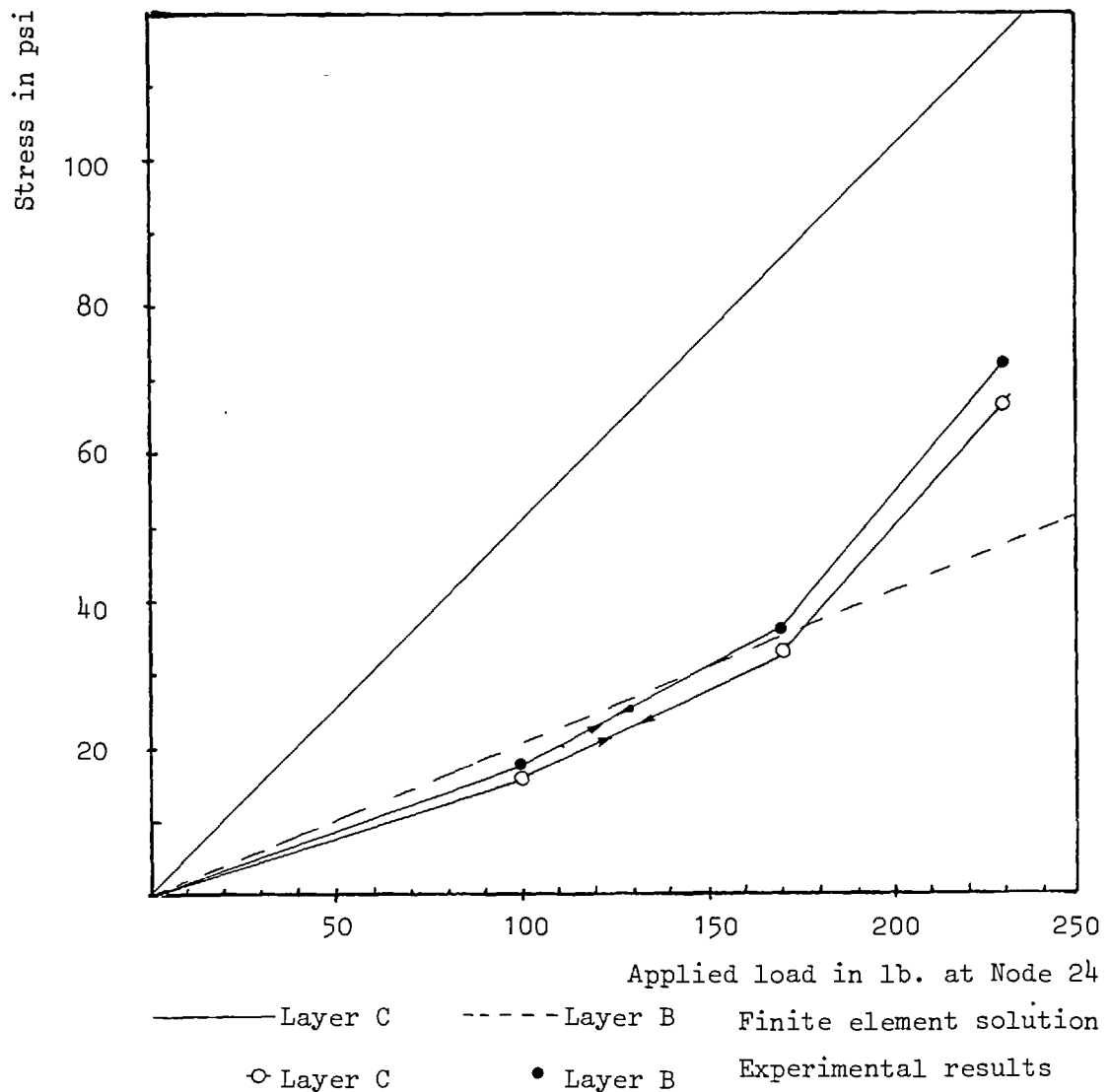


Fig. 5.49. Comparison of stresses in direction 2 at Node 215

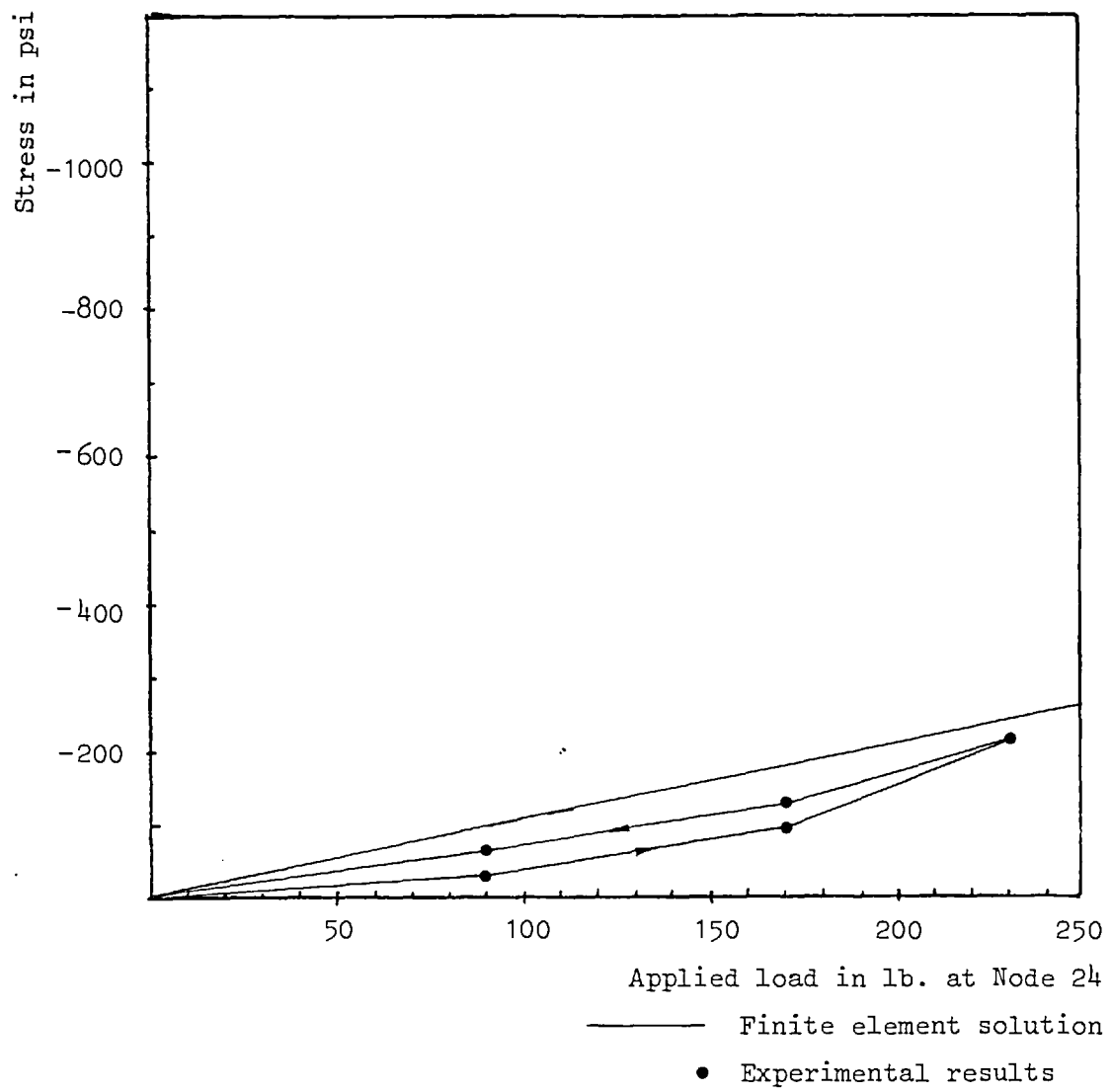


Fig. 5.50. Comparison of stresses in direction 3 at Node 215

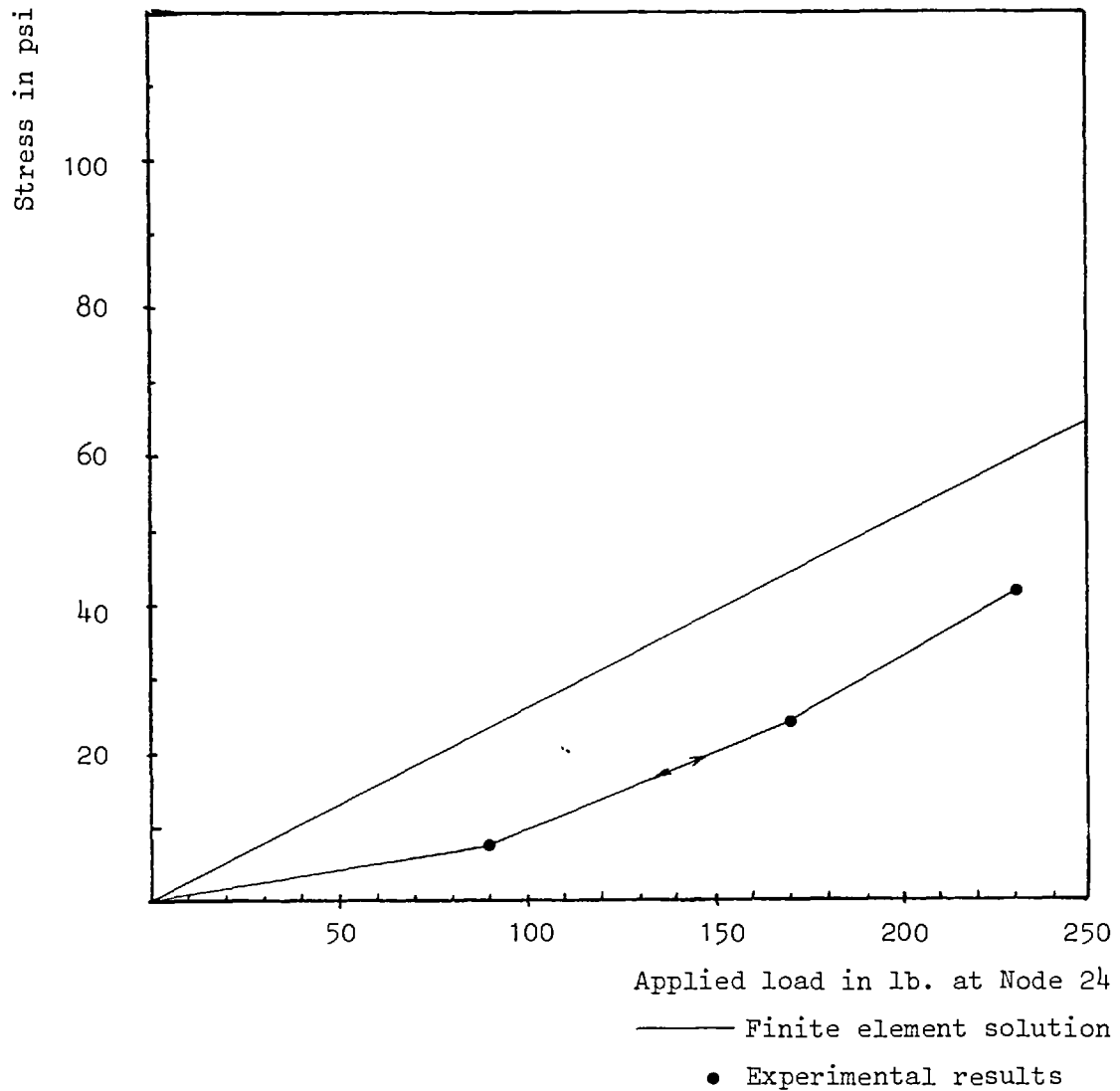


Fig. 5.51. Comparison of stresses in direction 1 at Node 218

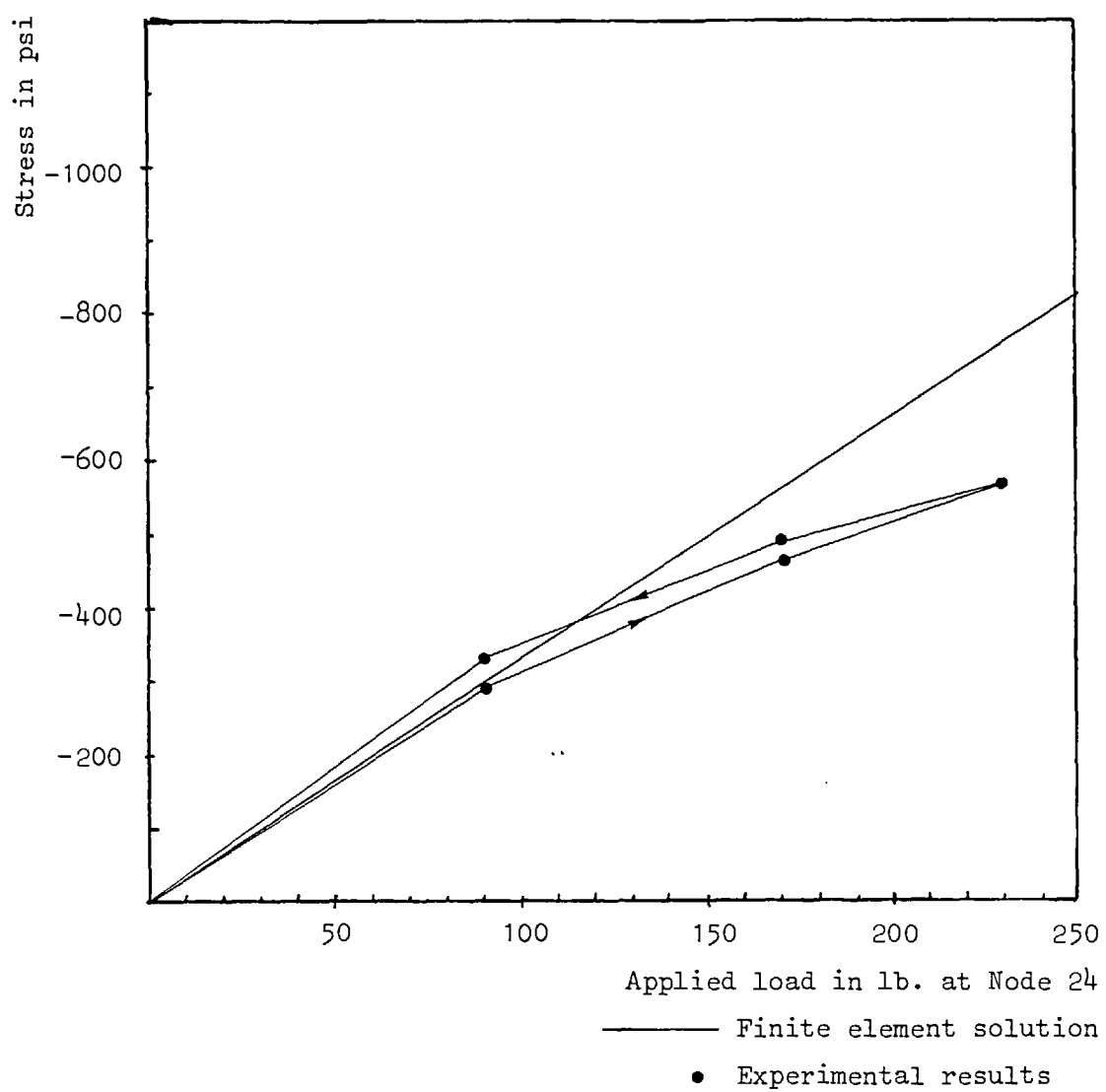


Fig. 5.52. Comparison of stresses in direction 2 at Node 218

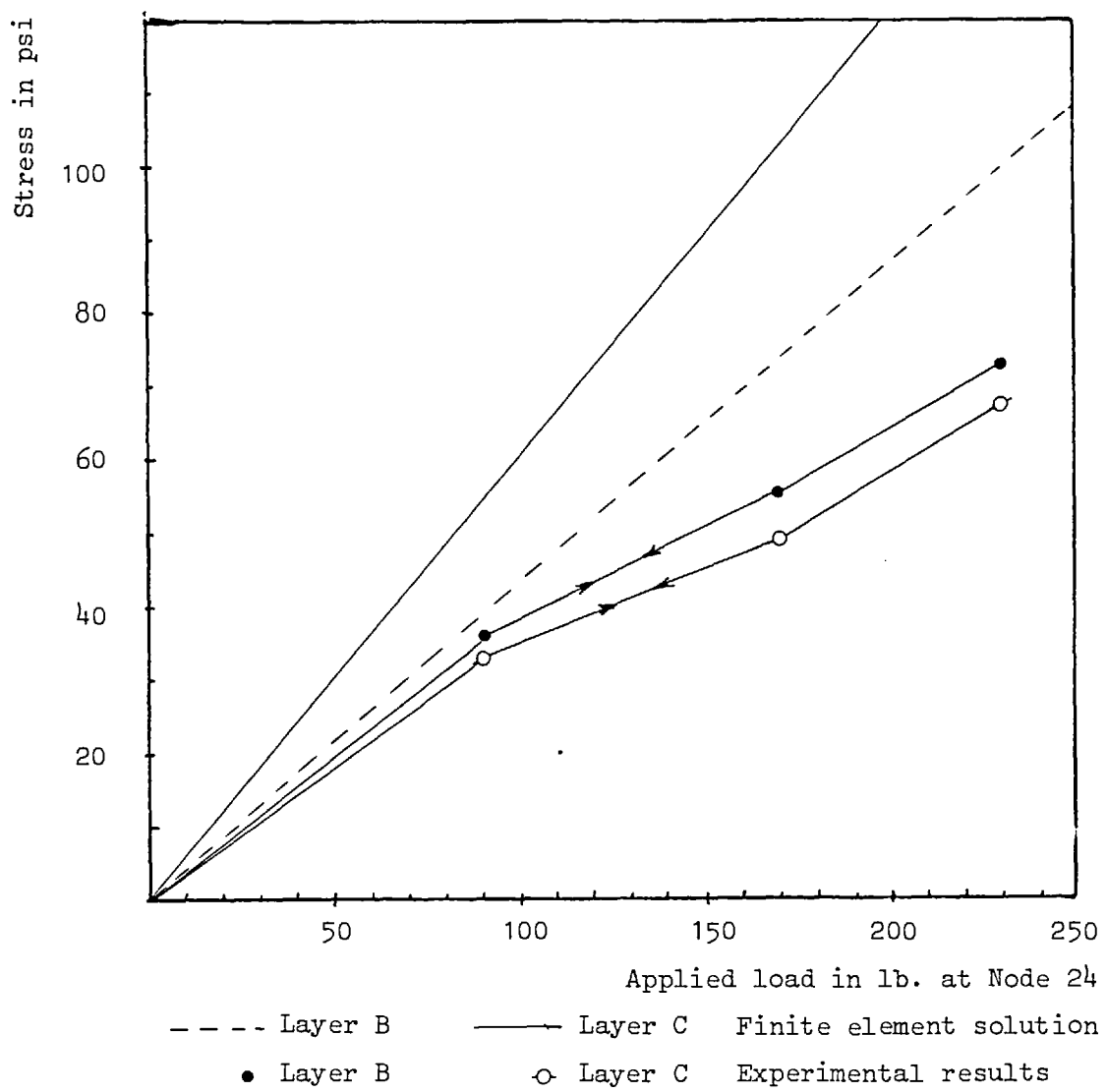


Fig. 5.53. Comparison of stresses in direction 2 at Node 211

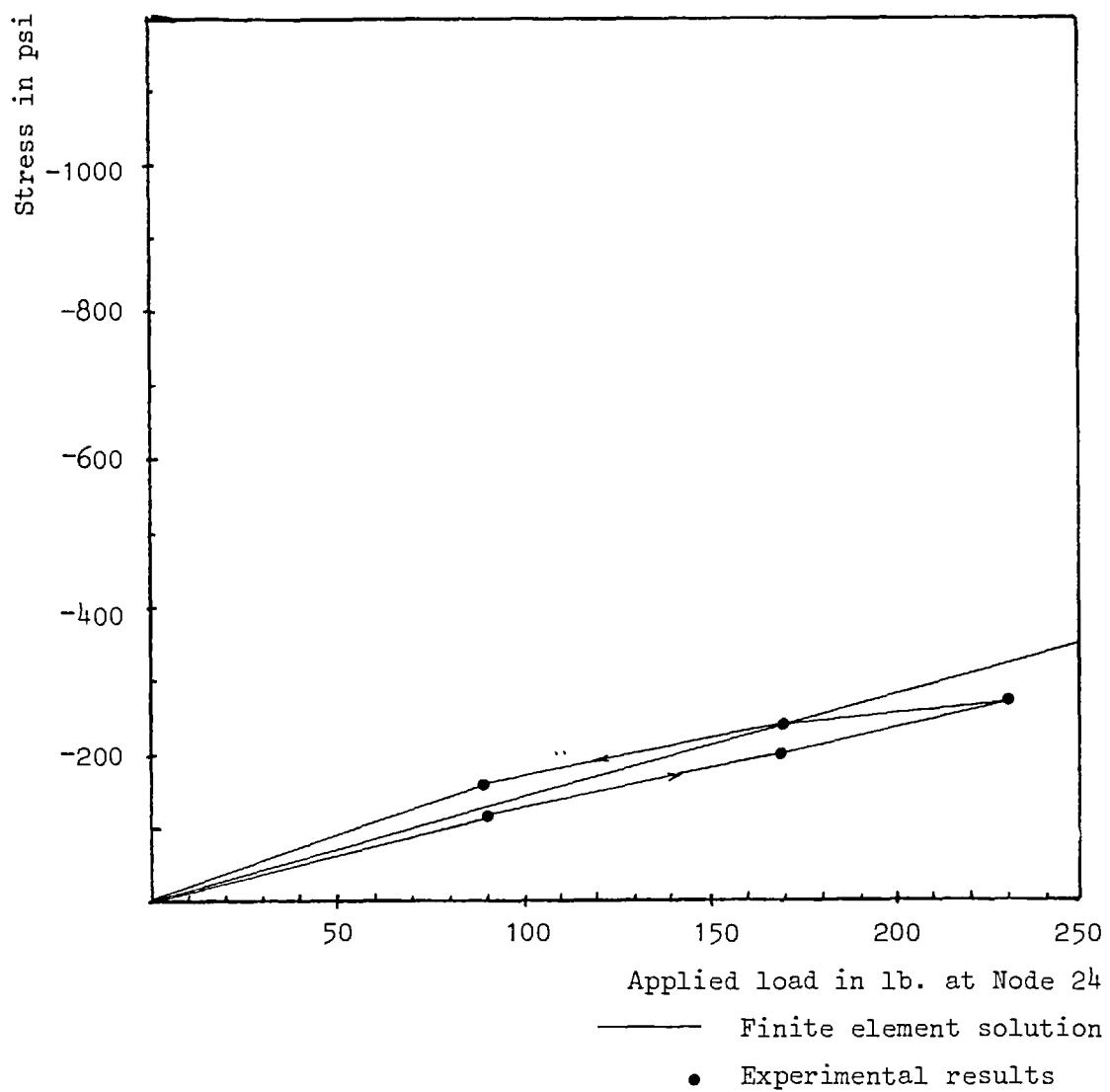


Fig. 5.54. Comparison of stresses in direction 3 at Node 211

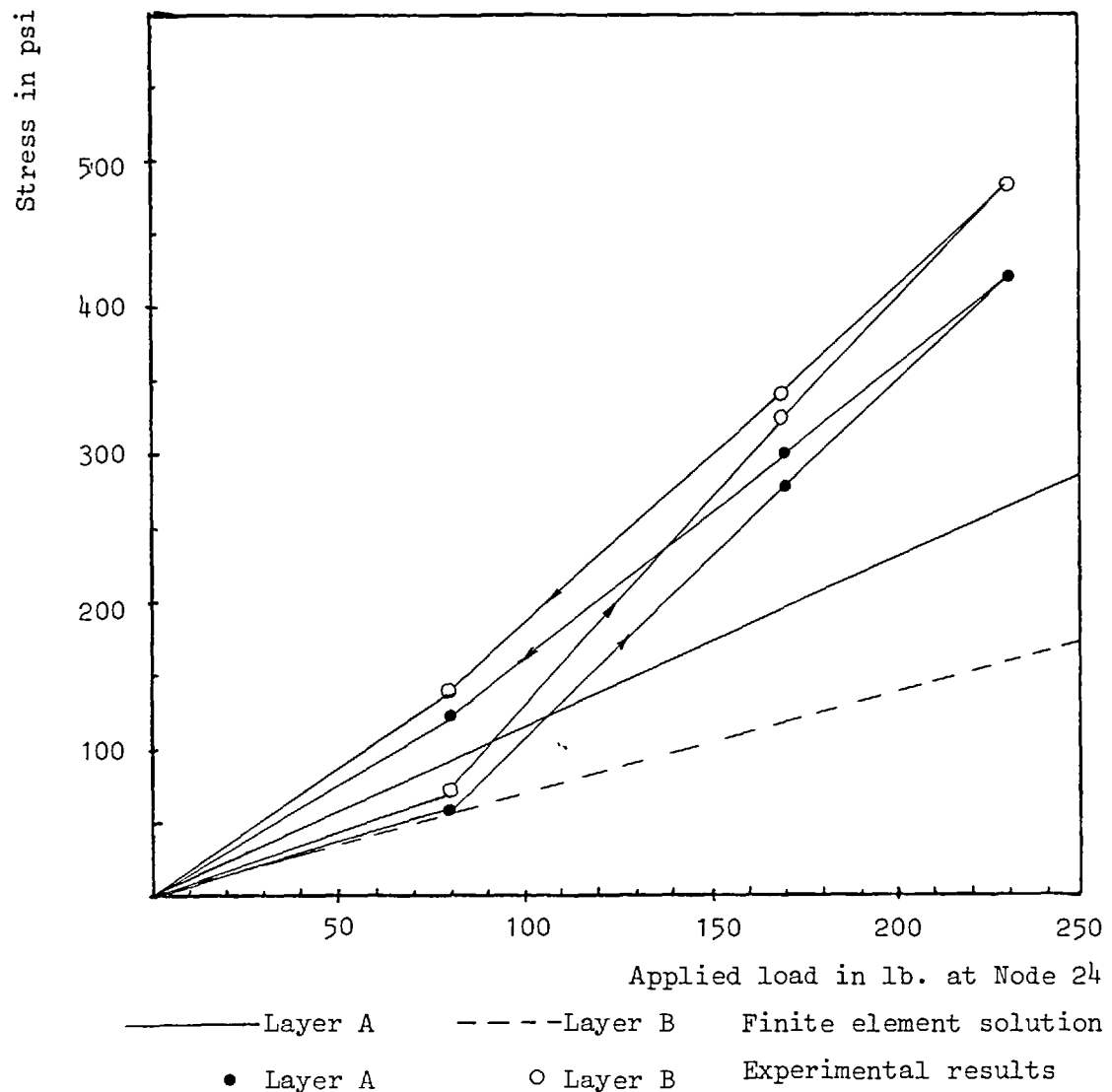


Fig. 5.55. Comparison of stresses in direction 2 at Node 206

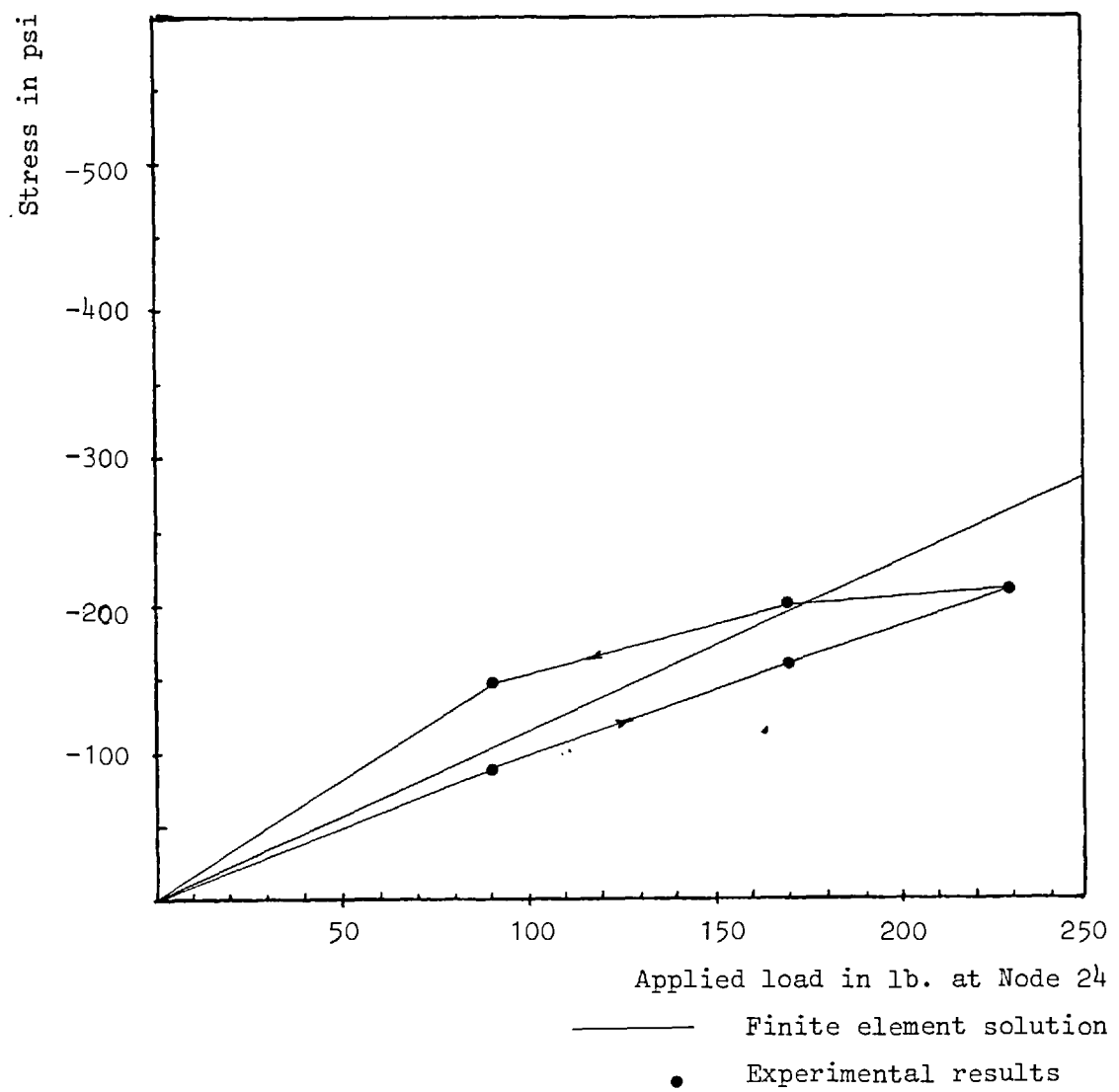


Fig. 5.56. Comparison of stresses in direction 3 at Node 206

(b) Deflections

Three dial gauges were set up to measure the deflections.

Two vertical directions at the equivalent locations of Node 1 and 45 on the finite element mesh and one horizontal at the equivalent location of Node 30, as shown in Figs. (5.41), (5.42) and (5.43).

As the clamping length was short a fourth gauge was located 0.5" away from the support to indicate any rigid body rotation.

The deflections measured were plotted against the finite element predicted deflections in Figs. (5.57), (5.58) and (5.59). The relative deflections in the three directions corresponded closely to the theoretical predictions although the absolute magnitudes were somewhat different. It should be remembered that the deflections were small and difficult to measure accurately.

5.4. G.R.P. Blade of an Ordinary Butterfly Valve

A 60" nominal diameter G.R.P. butterfly valve as shown in Figs. (5.60), (5.61), (5.62) and (5.63), made of isophthalic polyester resin reinforced by woven-roving glass fibres as the main material and chopped strand mat as another material around the shaft hubs. The blade is retained and driven within the body of the valve, which is made from woven-rovings and chopped strand reinforced polyester resin of the same type, by stainless steel stub shafts located in the disc by stainless steel inserts.

The dimensions shown in Fig. (5.60) were calculated so as to satisfy the maximum allowable deflection for sealing the valve using the work done in Chapter 2.

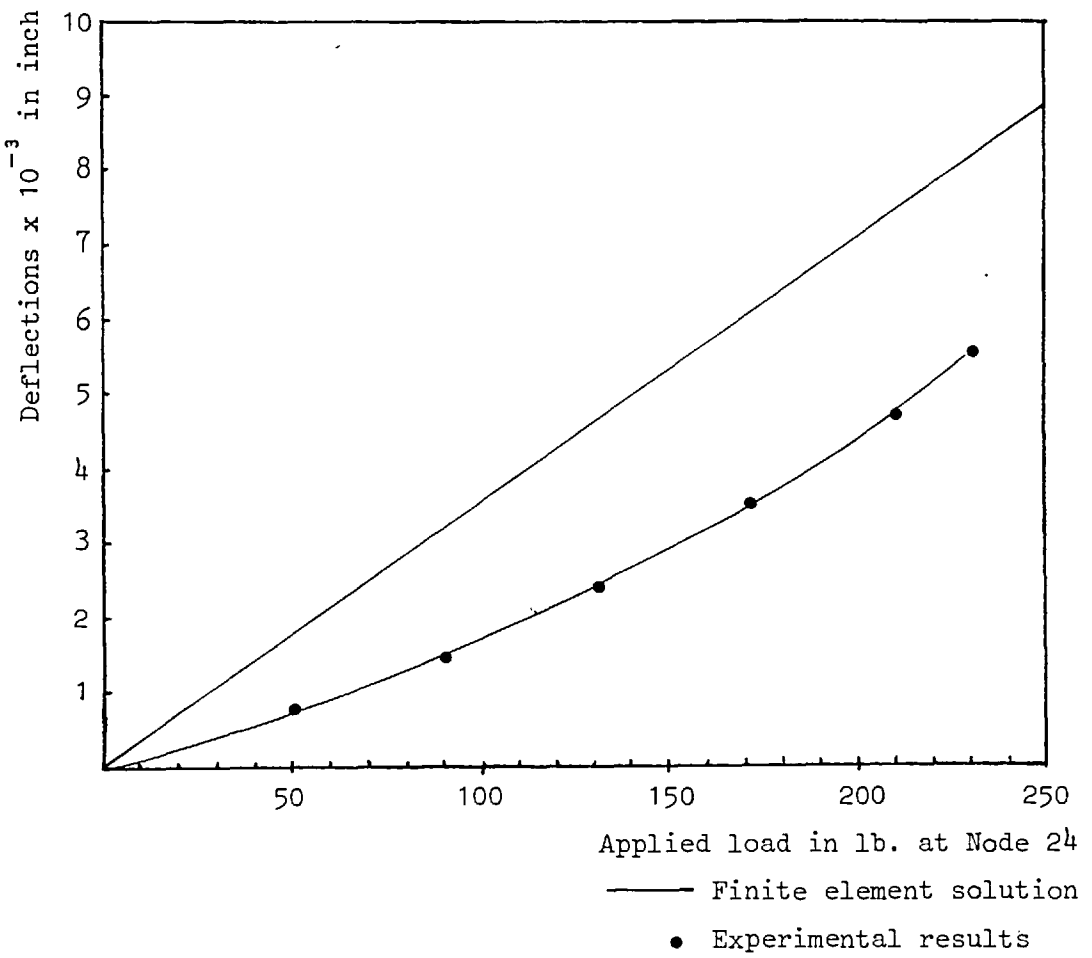


Fig. 5.57. Load vs. deflections in direction 3 at Node 1

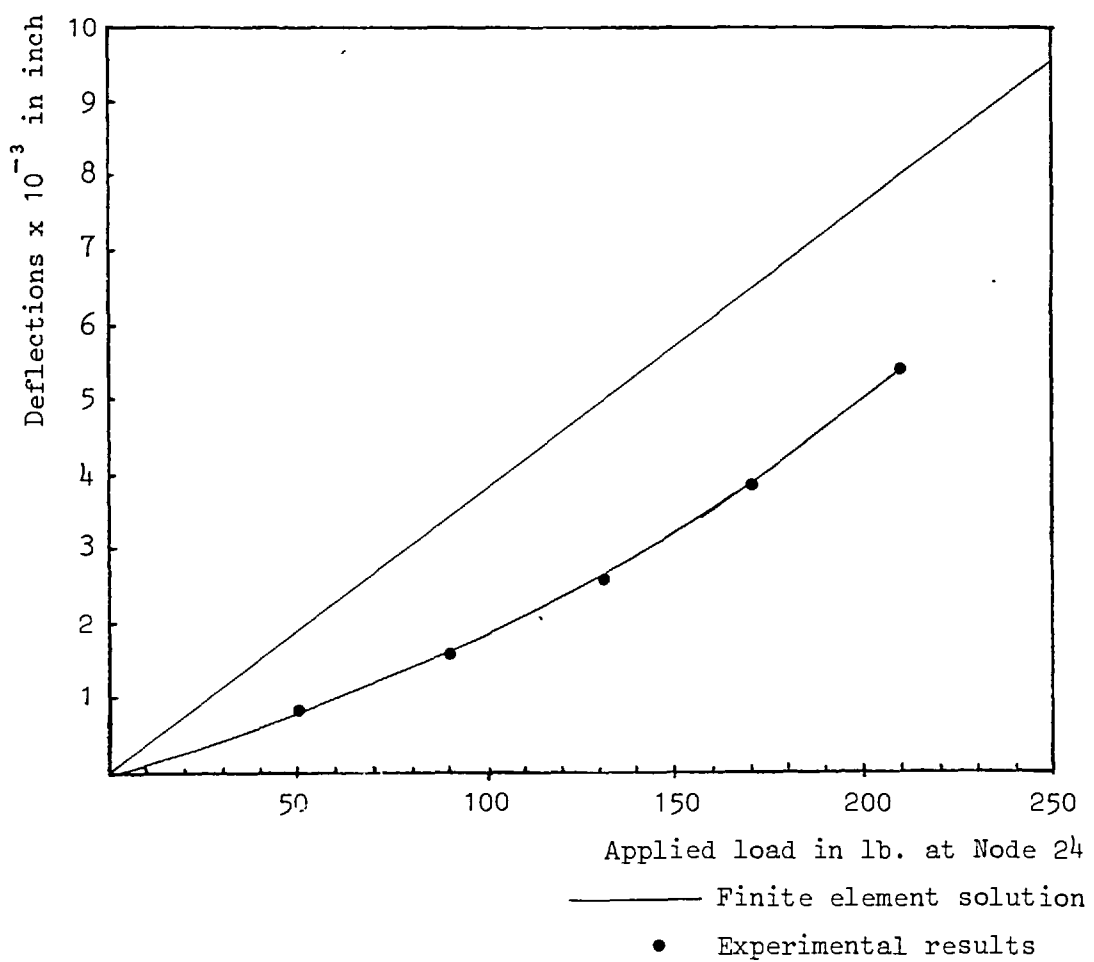


Fig. 5.58. Load vs. deflections in direction 3 at Node 45.

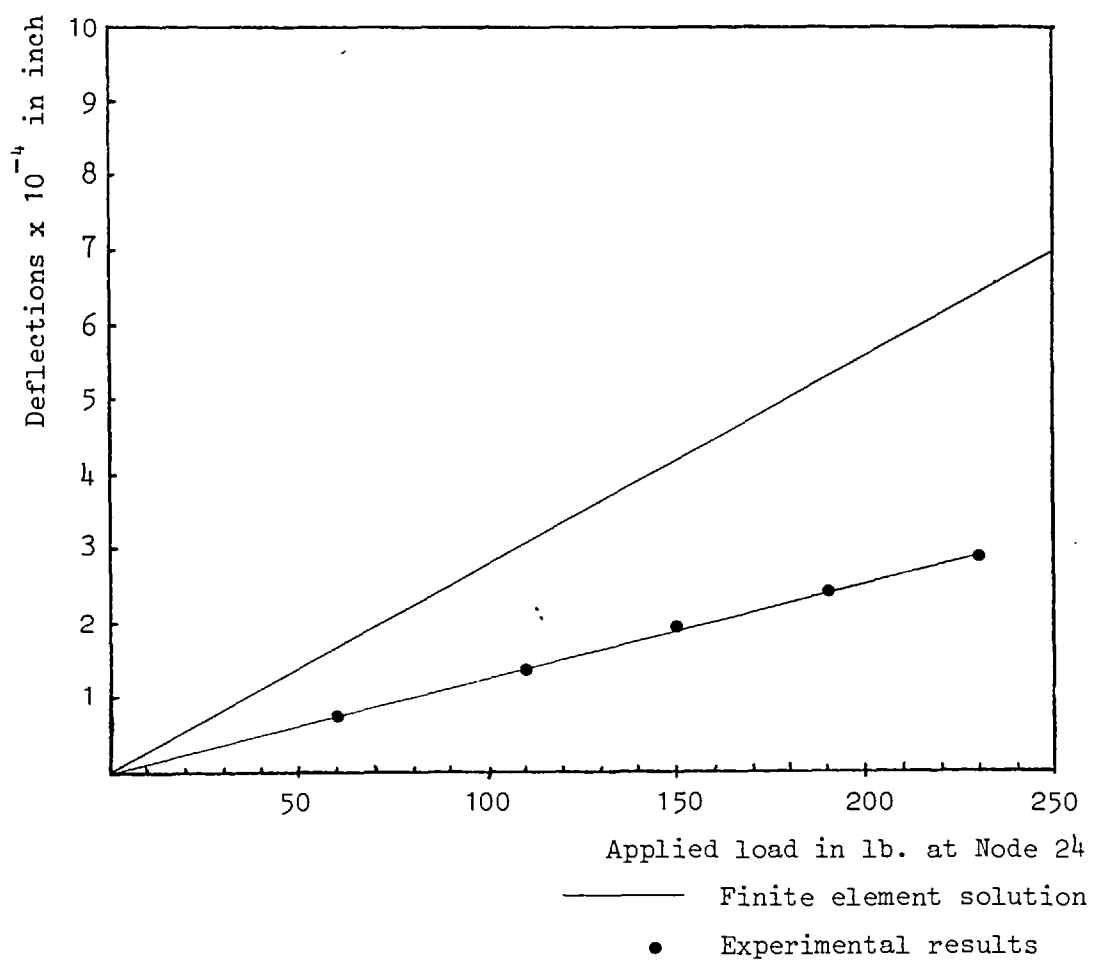


Fig. 5.59. Load vs. deflections in direction 1 at Node 30

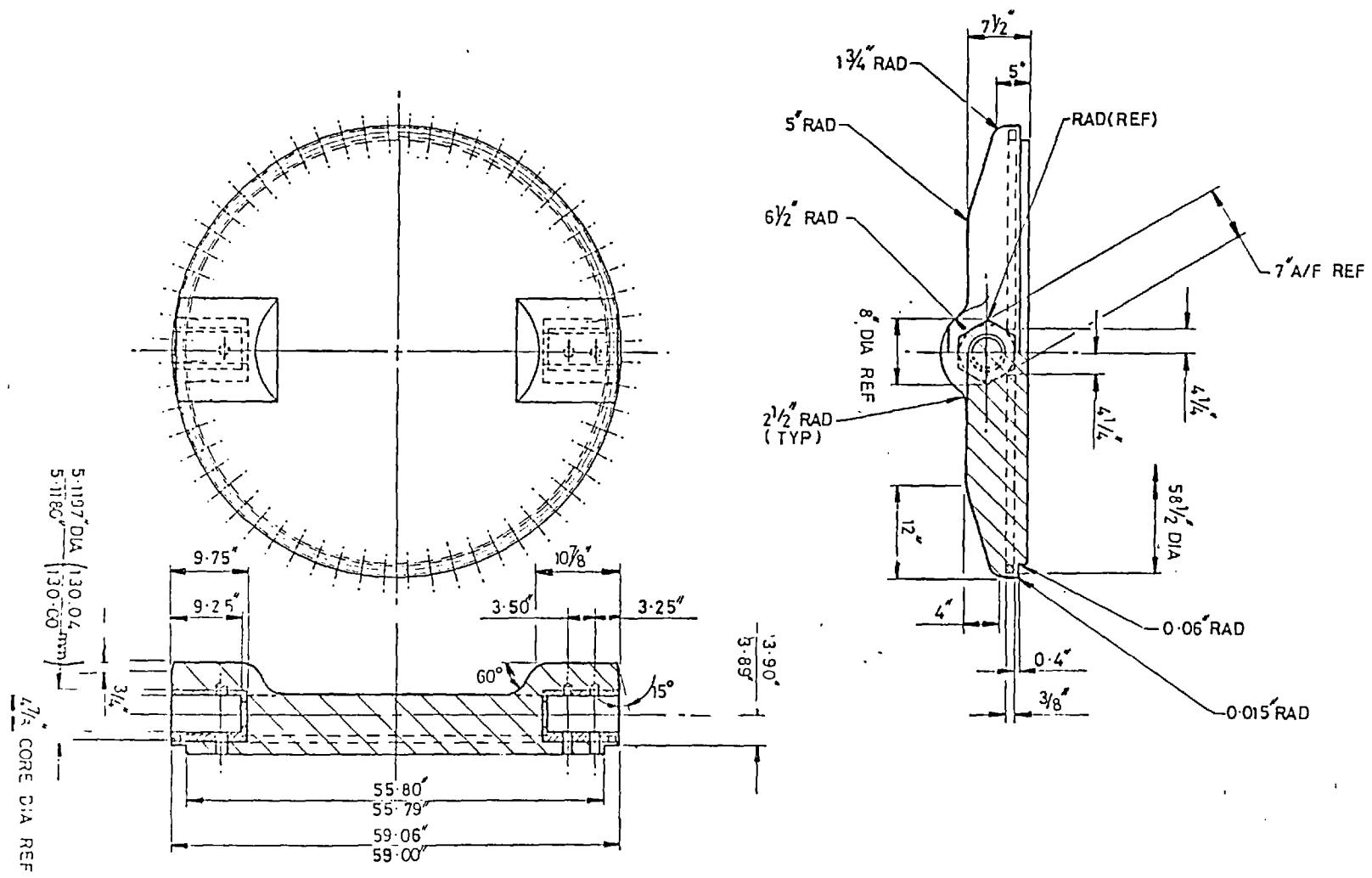


Fig. 5.60. G.R.P. butterfly blade



Fig. 5.61. G.R.P. butterfly blade.



Fig. 5.62. G.R.P. butterfly blade



Fig. 5.63. G.R.P. butterfly blade.

A finite element analysis using (BFSOLID) was carried out. The blade was idealized into 44 elements, 9 of which were given the stainless steel mechanical properties, 11 were given the chopped strand woven glass reinforced plastic mechanical properties as a homogenous material as shown in Figs. (5.64a) and (5.64b). The deflections predicted were very satisfactory.

For the allowable design stresses the factor of safety was calculated in accordance with BS.4994, Ref. (63) as follows:-

Factor relating to method of manufacturing $k_1 = 1.6$

Factor relating to long term behaviour $k_2 = 1.2$

Factor relating to temperature $k_3 = 1.1$

Factor relating to cyclic loading $k_4 = 1.1$

Factor relating to curing procedure $k_5 = 1.3$

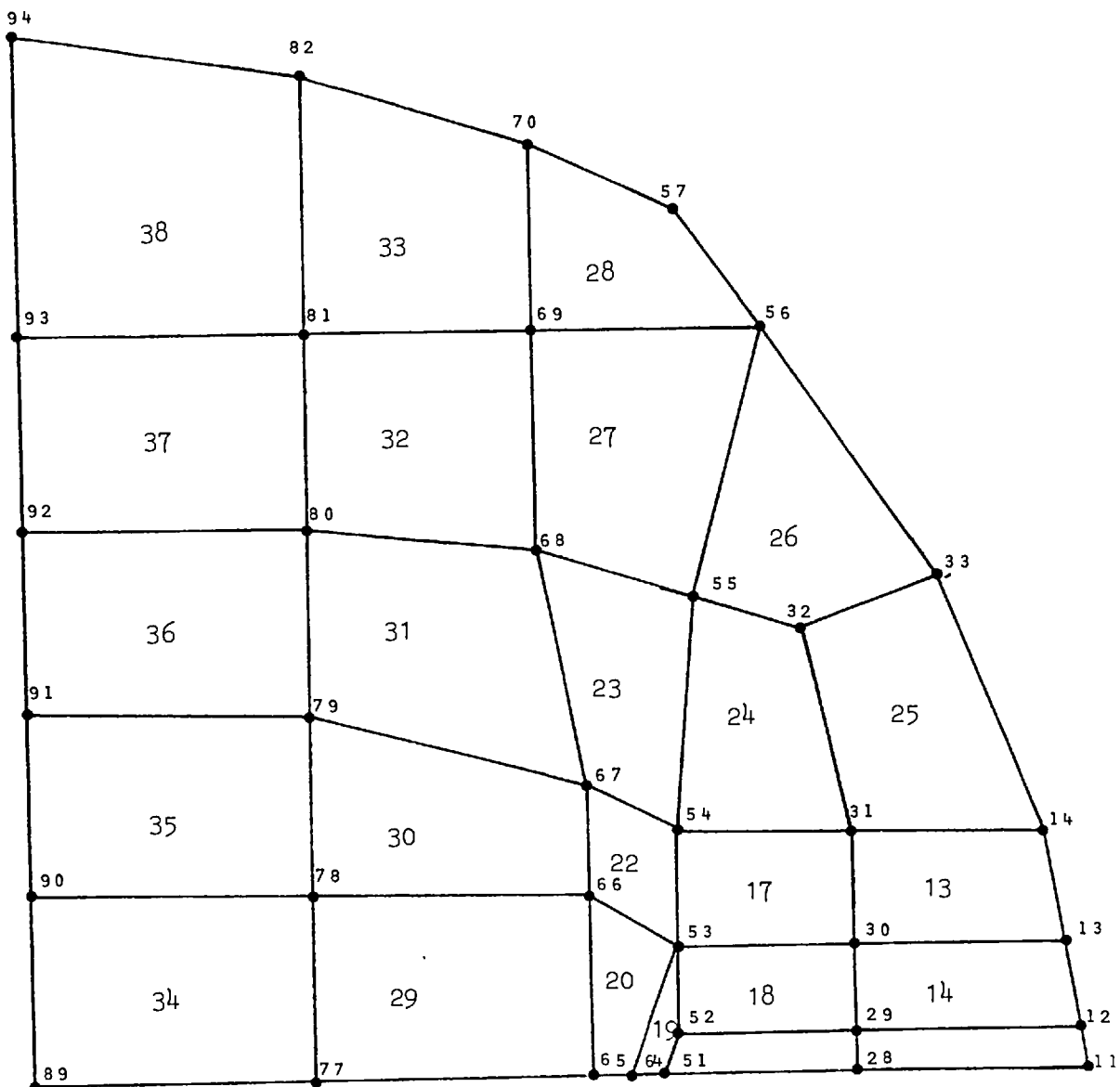
Overall design factor:-

$$k = 3 \times k_1 \times k_2 \times k_3 \times k_4 \times k_5 = 9.06$$

Adopted factor = 10.

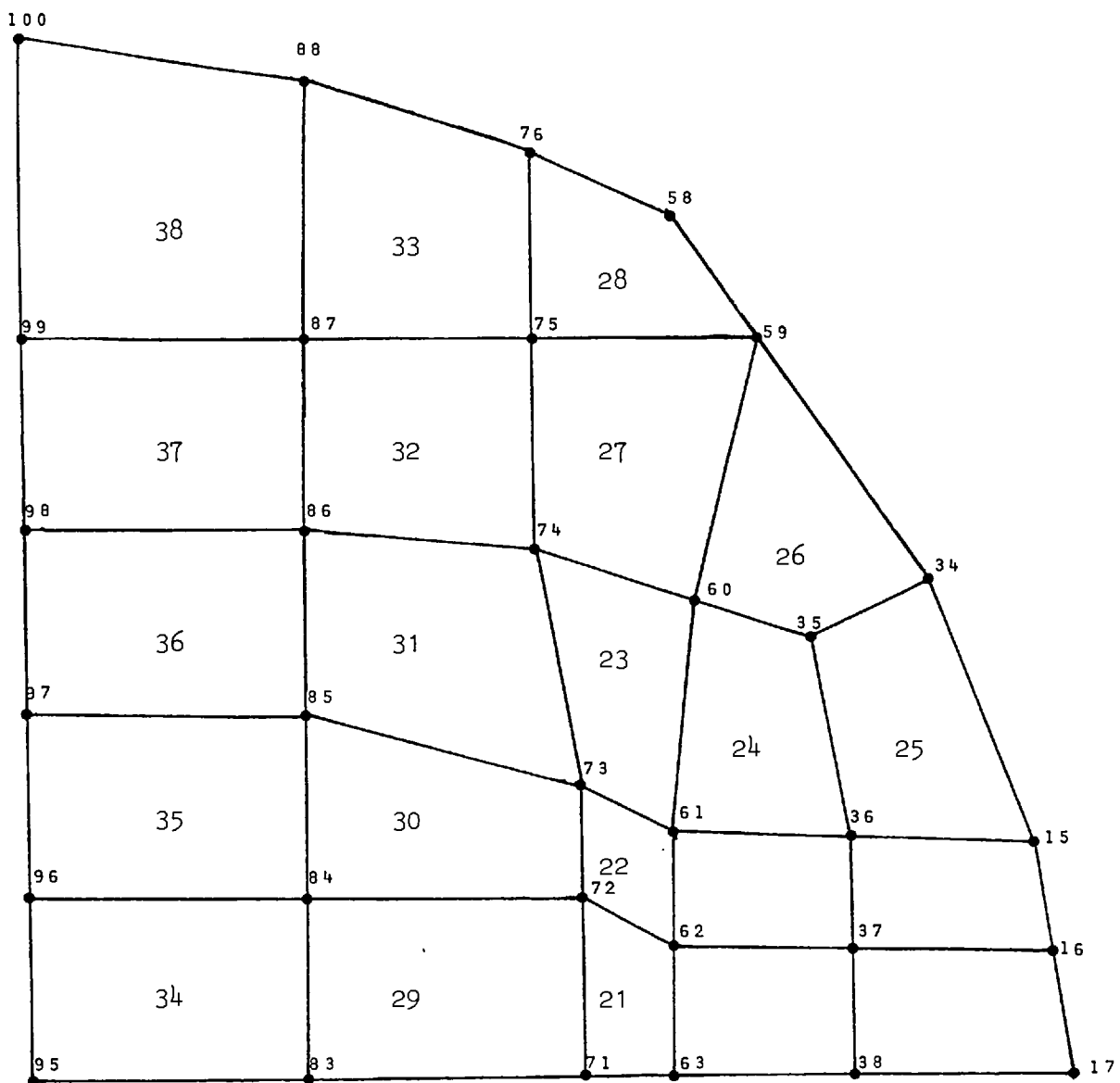
All the stresses predicted by the finite element analysis were lower than the allowable stresses.

An experimental programme for determining the stresses is planned in the near future. The location and direction of the strain gauges has been chosen to suit the finite element analysis, as shown in Figs. (5.65a) and (5.65b). The deflections will also be checked. The testing arrangement is shown in Fig. (5.66). A fair comment on the test results will be given in Ref. (70), by the eventual users of the valve, two of which will be put into actual service by the C.E.G.B. before the end of 1980.



Lower Face.

Fig. 5.64a. Finite element idealization of G.R.P. blade



Upper Face.

Fig. 5.64b. Finite element idealization of G.R.P. blade

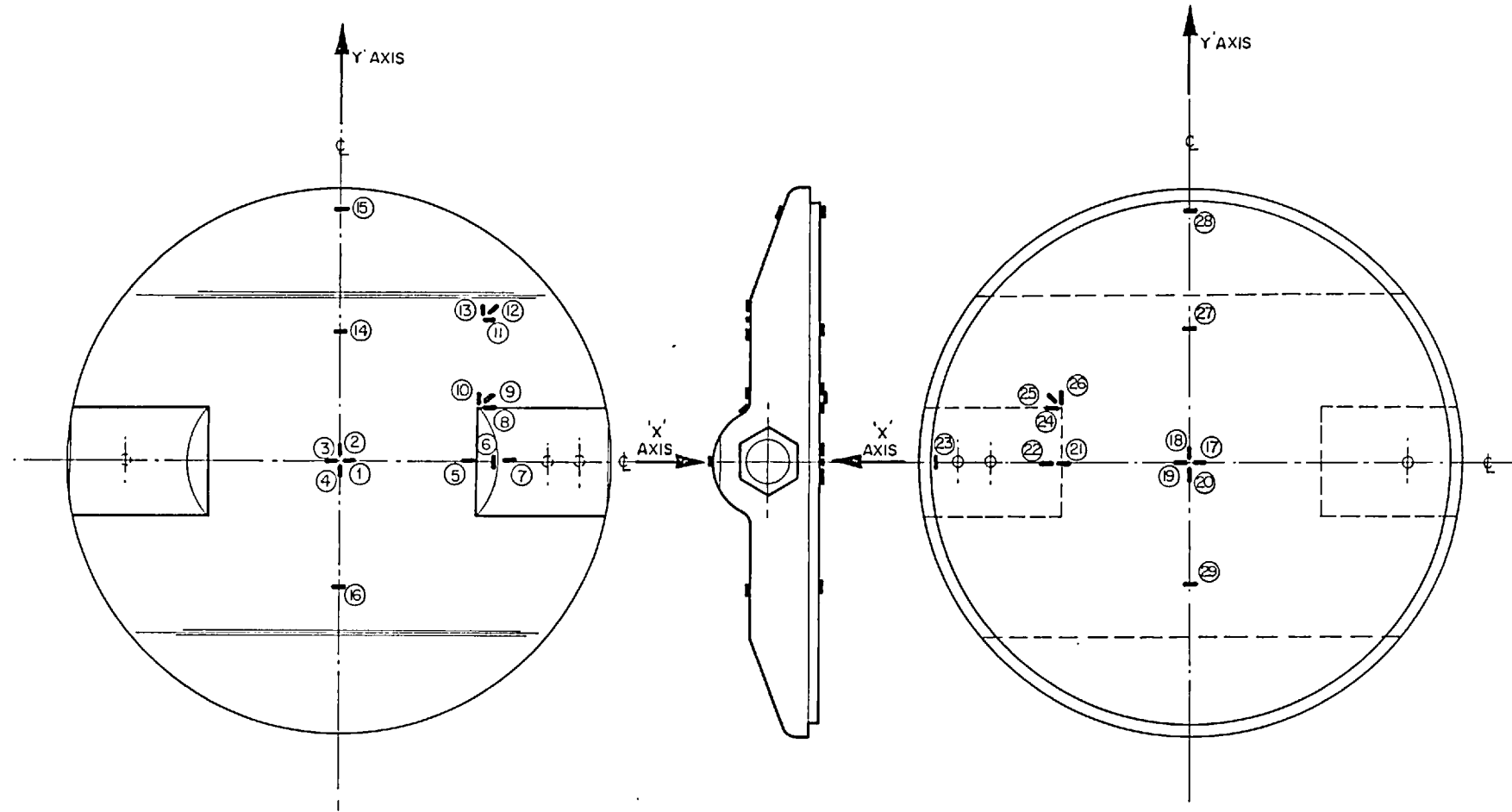


Fig. 5.65a. Strain gauge locations on G.R.P. blade.

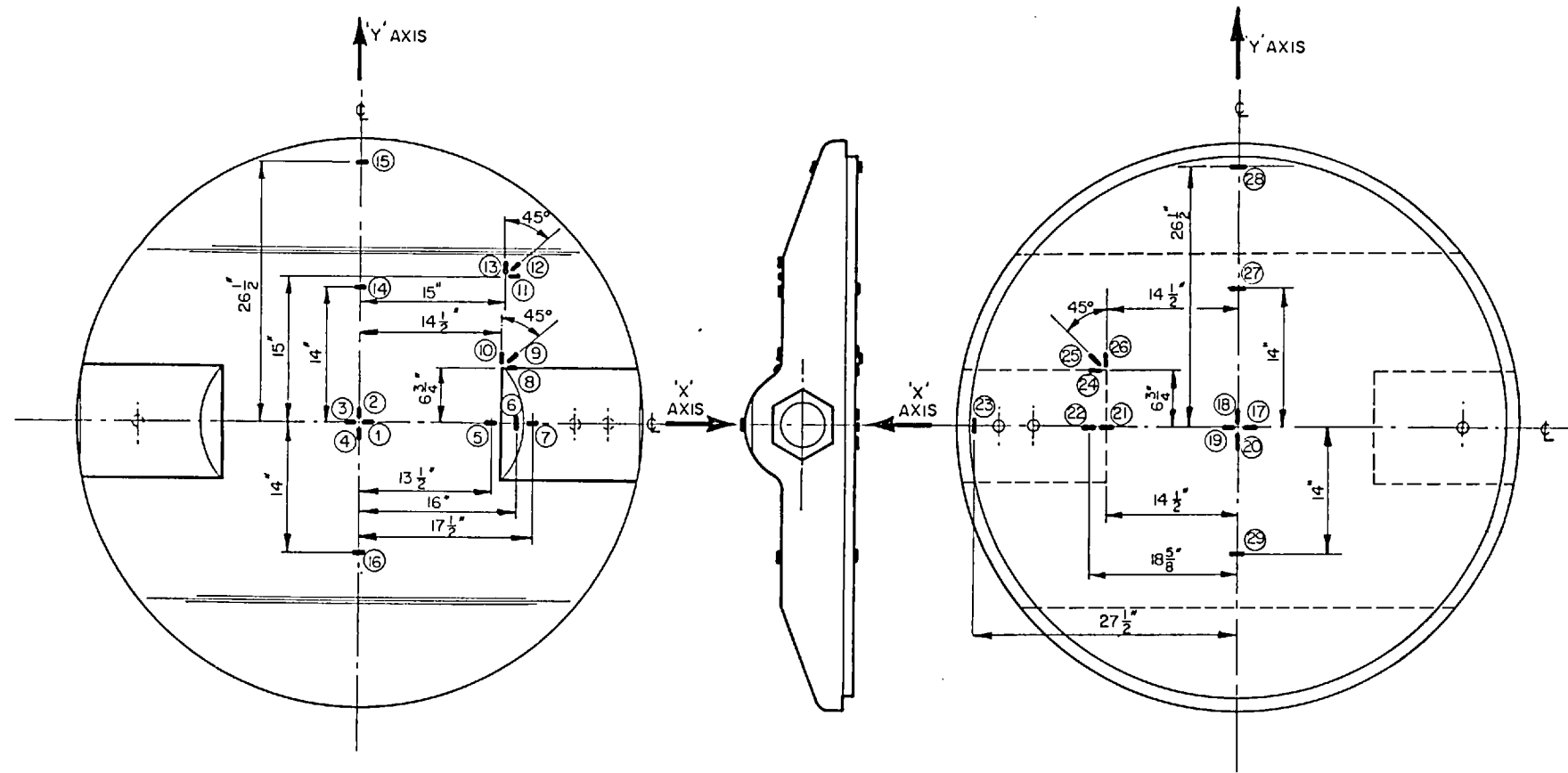


Fig. 5.65b. Strain gauge locations on G.R.P. blade.

303.

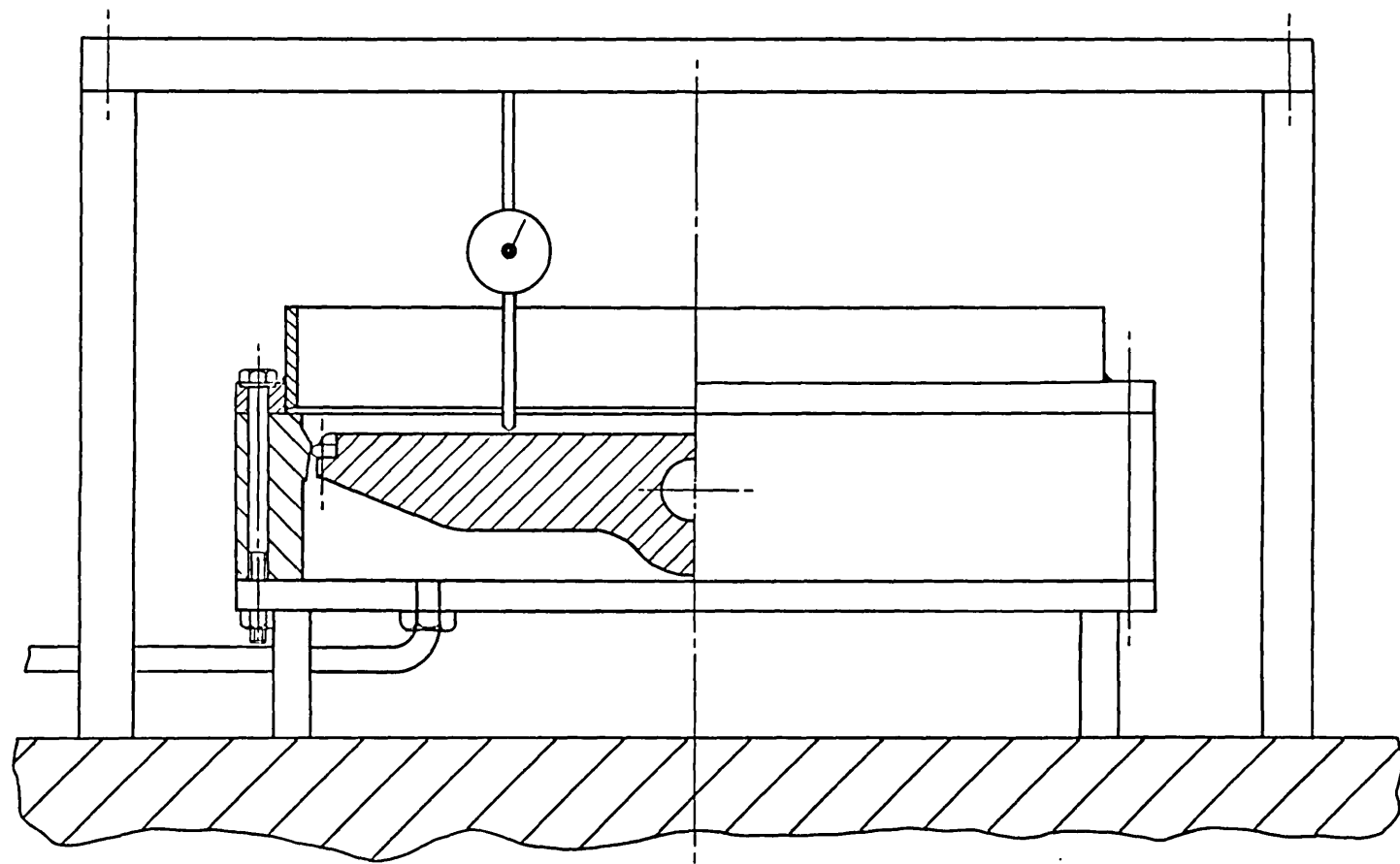


Fig. 5.66. Testing arrangement for deflections in G.R.P. blade.

CHAPTER SIX

CONCLUSIONS AND RECOMMENDATIONS FOR FUTURE WORK

CHAPTER SIX

CONCLUSIONS AND RECOMMENDATIONS FOR FURTHER WORK

6.1. The Analysis of Ordinary Blades

6.1.1. Conclusions

Prior to this research there has been no really serious attempt to study the structural problems of ordinary butterfly valve blades. The work described in Chapter 2 is considered by the author to be a major contribution to the advancement of knowledge in relation to the design and operation of valves of this type.

The use of the finite element method as a technique for obtaining design coefficients represents a major break through, since the majority of practical cases have no mathematical solutions. This is because there are a great number of combinations of complex loading and support conditions which are required in practice.

The very important problem of predicting the behaviour of blades can be solved by adopting this method. The tapering configuration must then be expressed as a function of the radius or alternatively as a fraction of the thickness of the theoretically embracing flat blade. This would lead to savings of material and also better meet the hydraulic requirements.

The finite element solution requires a large computer to carry the mathematics involved in inverting the stiffness matrices. On the other hand storing a large number of tables on the floppy discs of very small desk top computers is a much cheaper and more

practical proposition, which justifies the approach and the use of coefficients which has been emphasised throughout this thesis. This work should contribute to possible relaxation of the standard minimum required thicknesses at present demanded by the various authorities and, with improved quality control, to the testing procedures.

Since the deflections could be predicted with greater accuracy by the methods described in this thesis, a significant saving in the cost of seals and the use of different materials for resilient seals should be possible.

The effect of the length of the arc of the periphery occupied by the shaft is clear from reading through the tables of Appendix 3. This knowledge can be used to optimize the cost of blades and their operating equipments and actuators.

Finally, this work could lead to a complete set of structural models to cover all possibilities of behaviour for the ordinary butterfly valve blade, on which some confidence can be placed in terms of the extensive experimental comparisons which have been made.

6.1.2. Further work

The major area of further work should be in the field of simulating real valves to the different structural models presented. In real valves the clearance between the shaft and the body is a parameter whose importance has not been sufficiently appreciated and identified in the past. A study of the effect of this clearance (generally specified in "thous per in." of shaft diameter) on the structural behaviour of the blade should be made.

In this study the following factors should be considered:-

- (i) The length of the supported part of the shaft.
- (ii) The type of bearings used.
- (iii) The type of shaft used and the effect of the clearance between shaft and blade, bearing in mind the method of attachment.

In the present day, with the introduction of microprocessors and minicomputers for the control of machine tools (as can be seen from Ref. (71)) it is no longer difficult or expensive to attain near-perfect clearances.

Another factor which has not been covered in this study is the effect of the eccentricity of the shaft centre line from the middle surface of the blade. This is not important for thin blades. As the blade and shaft humps increase in size, eventually they clearly indicate when the blade should be considered as being a thick plate problem.

A criterion for the effect of the eccentricity has to be developed and the only clear method is the use of solid finite elements.

Finally it must be remembered by any structural analyst working on the subject that a close relationship exists between any structural changes and the flow characteristics of the valve, particularly in relation to the ever-increasingly important problem of noise and the requirements of the operating equipment.

6.2. Fibre Composite Blades

6.2.1. Approach for optimal design

An approach towards the design of fibre composite blades can be seen from the work done in Section 5.3. There, it was shown that it is possible to assess the stresses fairly accurately by using the measured values of the various moduli. The butterfly valve blade is an ideal structure to be made from fibre composite materials since it is governed by a failure criterion based on very low deflections (conditioned by the requirement for sealing). This means that high strains need not be considered as a criterion for failure and yielding of the structure is therefore not a factor to be considered.

The major cost in fibre composites is directly related to the fibre content, especially when the fibres or woven-roving layers have to be hand laid. Therefore, their distribution through the thickness of the blade should be optimised according to the particular requirements of the loading and geometrical arrangement of the blade. In this way, a blade which has the minimum deflection and adequate strength can be optimally designed so as to have minimum cost.

The main concern in fibre composite structures is the fear of failure due to shear or lap stress at interfaces and it is inadequate to assume that the material is homogeneous in order to estimate strains at these surfaces. This is true even for thin blades and it is always necessary to make a three-dimensional analysis, even if a homogeneous equivalent material is assumed for the purpose of obtaining a lower bound for the strains as, in a three dimensional analysis, the inter-laminar stresses or lap shear

will be revealed.

Young's moduli and Poisson's ratios can easily and cheaply be obtained experimentally in a layer as has been demonstrated in this work and, although the through-thickness properties are more difficult to obtain experimentally, they can be estimated conservatively by using the properties of the resin matrix which are provided by the manufacturers.

The method of selecting samples for a multi-layered fibre composite demonstrated in this thesis, from which the various moduli and Poisson's ratios were estimated, coupled with their use in predicting the stresses and deflections of a structure (a cantilever) subjected to a complex loading situation, indicate the feasibility of the optimal designing of a blade using these methods. Also, with the use of the finite element program, the optimal combination of metallic and fibre composite materials can be achieved, provided that the interfacial conditions are adequately defined. In particular, the bond should be examined independently.

6.2.2. Further work

Two full-size fibre composite butterfly valves have been made and are being tested for use in service at the Fawley Power Station, by the Central Electricity Generating Board (C.E.G.B.). These valves have been designed, as regards their structural integrity, by the author and their behaviour in long-term use will be a final justification for the procedures described in this thesis. Further research is required in the more accurate determination of through-thickness properties and shear moduli of the various fibre composite

layers used in such structures. In addition to this, much development is needed in the manufacturing techniques required for the laying-up of structures of this type. Laying-up manually is both costly and inaccurate and any methods which could be devised for automatic laying-up are highly desirable and should be actively pursued. Such investigations are at present being carried out under the supervision of the author and this will facilitate accurate determination of through-thickness and shear moduli at a minimum cost.

Some work of this type has been done in aero-space industries, mainly from the point of view of optimising strength-weight ratios. However, the present objectives are different, being mainly concerned with minimising corrosion, cost and maximising reliability. Therefore it would be very desirable to survey the literature already available from the aero-space industries, with these different objectives in mind.

REFERENCES

CHAPTER ONE

1. GRIFFITHS, J.M. "Proceedings of the International Valve Conference". Brighton, 1978.
2. British Valve Manufacturers Association Handbook, 1972.
3. "A guide to the Selection of Automatic Control Valves"; Engineering Equipment Users Association Handbook, No. 32. 1969.
4. British Standards Institution BS.5155, 1979.
5. Central Electricity Generating Board, C.E.G.B. Std. 568502.
6. American Water Works Association, AWWA. C.504-74.
7. British Standards Institution, BS.4504, BS.1560, BS.3290.
8. Boving Valves, Boving & Co. Ltd., 1978.
9. ROSATO, D.V., Editor, Polymer Engineering and Technology Series, John Wiley & Sons, N.Y.
10. GRESZCZUK, L.B., "Consideration of Failure Modes in the Design of Composite Structures", McDonnell Douglas Astronautics Co., 1975.
11. MAJMUDAR, A.A., "Proceedings of the International Valve Conference", Brighton, 1978.
12. PEARSON, G.A., "Valve Design", Mechanical Engineering Publications Ltd., London, 1972.
13. ADDISON, H. "A Treatise on Applied Hydraulics". Chapman & Hall Ltd., London.

14. CREAGER, W.P., JUSTIN, J.D., "Hydroelectric Handbook", John Wiley & Sons Ltd.,
15. DAVIES, C.V., "Handbook of Applied Hydraulics" McGraw-Hill, New York, 1942.
16. "a-Choosing Valves, Water Works and Pumping Practices", Glenfield and Kennedy Ltd., Kilmarnock, 1955.
17. "b, c-Choosing Valves, Water Works and Pumping Practices", Glenfield and Kennedy Ltd., Kilmarnock, 1955.
18. KURKJIAN, G.A., "Follow these simple rules to get long life from your large Butterfly Valves". Henry Pratt Co., Power V.118, No. 7, July, 1974.
19. FREEMAN, M.L., SPROUT, D.H., "Butterfly Valves-Correct Installation and Alignment", Masoneilan Ltd., London, Paper Technology, V. 15, No. 2, April, 1974.
20. "A Bibliography on Butterfly Valves", The British Hydromechanics Research Association, BIB24, April, 1966.
21. BOGER, H.W., "Low-torque Butterfly Valve Design", Masoneilan International, Inc., Instrument Technology, V. 17, No. 9, Sept., 1970.
22. HAMPHILL, J.E., "Development of a Low-torque Butterfly Control Valve", Advances in Instrumentation, V. 24, Part 1, Proceedings of 24th Annual ISA Conference, Houston, Oc-. 1969.
23. SHALNEV, K.K., ZHESTKOV, A.A., "Mechanism of Cavitation Vibrations in Butterfly Valves", Proceedings of 5th Conference on Fluid Mechanics, Budapest, 1975.
24. JAMES, B.W., TULLIS, P.J., "Cavitation in Butterfly Valves", ASCE Journal of the Hydraulics Division, V. 99, No. H.79, Sept., 1973.

25. BELAND, R., "New Standard Metric Valves", Proceedings of the International Valve Conference, Brithton, 1978.
26. CARLETON, R.L., "Noise Created by Control Valves in Compressible Service", Masoneilan Int., Inc., ISA Translations, V. 17, No. 1, 1978.
27. MILLEVILLE, B.J., "What every Engineer needs to know about Valve Sealing", Rockwell Int., Pittsburgh, Pennsylvania, Specification Engineering, V. 34, No. 5, Nov. 1975.
28. EXEKOYE, L.I., "Simplified Method for Calculating the Natural Frequency of Valve Superstructures", Westinghouse Nuclear Energy Systems, Pittsburgh, Pennsylvania, ASME, Paper No. 78-PVP-4, June, 1978.
29. WAYNE, B., "Pressure Sensitive and Temperature Responsive Butterfly Valve for Cryogenic Service", SAME, Paper No. 78, Nov., 1978.

CHAPTER TWO

- 30 CLEBSCH, A. "Theorie der Elastizität fester Körper". B.G. Teubner, Leipzig, 1962.
31. SZILARD, R. "Theory and Analysis of Plates" Prentice-Hall Inc., Englewood Cliffs, New Jersey.
32. TIMOSHENKO, S.P. and WOINOWSKY-KRIEGER, S., "Theory of Plates and Shells", McGraw-Hill Book Company Inc., 1959.
33. FLÜGGE, W., Editor, "Handbook of Engineering Mechanics", McGraw-Hill Book Company Inc., 1962.
34. BARES, R., "Tables for the Analysis of Plates, Slabs and Diaphragms Based on the Elastic Theory", Bauverlag GmbH., Wiesbaden, Germany 1969.
35. TURNER, C.E., "Introduction to Plate and Shell Theory", Longmans, Green & Co. Ltd., 1965.

36. The Billings Microsystem Model BC-12FD, Stemmos Ltd., London.
37. ZIENKIEWICZ, O.C., "The Finite Element Method in Engineering Science", 2nd Edition, McGraw-Hill, London, 1971.
38. "Shell", Finite Element Programme for the Analysis of Plates and Shells, Stemmos Ltd., London.

CHAPTER THREE

39. TSAI, S.W. "Mechanics of Composite Materials", Part II, Technical Report AFML-TR-66-149, November, 1966.
40. LEKHNITSKI, S.G., "Theory of Elasticity of an Anisotropic Elastic Body, Holden-Day, Inc., 1963.
41. ALEXANDER, J.M., "Strength of Material" To be published.
42. ASHTON, J.E., HALPIN, J.C. and PETIT, P.H. "Primer and Composite Materials Analysis", Technomic Publishing Co., Inc., 1969.
43. SCHWARTZ, R.T. and SCHWARTZ, H.S., Editors, "Fundamental Aspects of Fiber Reinforced Plastics Composites.
44. WILLIAMS, J.G., "Stress Analysis of Polymers" Longman Group Ltd., 1973.

CHAPTER FOUR

45. IRONS, B.M., "Quadrature Rules for Brick Based Finite Elements", Int. J. Num. Meth. Eng., 3, 1971.
46. BREBBIA, C.A., and CONNOR, J.J., "Fundamentals of Finite Element Techniques", Butterworths, 1973.

47. COOK, R.D., "Concepts and Applications of Finite Element Analysis", John Wiley & Sons, 1974.
48. ROBINSON, J., "Integrated Theory of Finite Element Methods", John Wiley & Sons, 1973.
49. FENNER, R.T., "Finite Element Methods for Engineers", The MacMillan Press Ltd., 1975.

CHAPTER FIVE

50. BRAMHAM, H.T., "Throughflow Type Butterfly Valve Development", Proceedings of the International Valve Conference, Brighton, 1978.
51. TSAI, S.W., WU, E.M., "A General Theory of Strength for Anisotropic Materials". J. Composite Materials, V. 5, Jan., 1971.
52. AZZI, V.D., TSAI, S.W., "Elastic Moduli of Laminated Anisotropic Composites", Experimental Mechanics, V. 5, June, 1965.
53. TSAI, S.W., PAGANO, N.J., "Invariant Properties of Composite Materials", Composite Materials Workshop, Edited by Tsai, S.W., Halpin, J.C., Pagano, N.J., Technomic Publishing Company, Stamford, Connecticut, 1968.
54. ARGYRIS, J.H., "Three-Dimensional Anisotropic and Inhomogeneous Elastic Media Matrix Analysis for Small and Large Displacements", Sonderabdruck Aus, Ingenieur-Archiv, 3⁴ Band, 1 Heft, S.33-55, Springer-Verlag, Berlin, 1965.
55. HUANG, Chi-Lung, KIRMSER, P.G., "A Criterion of Strength for Orthotropic Materials", Fibre Sci. Technol., V. 8, No. 2, April, 1975.

56. OWEN, D.R., PRAKASH, A., ZIENKIEWICZ, O.C., "Finite Element Analysis of Non-linear Composite Materials by use of Overlay Systems", Computers and Structures, V. 4, 1974.
57. TSAI, S.W., "Strength Characteristics of Composite Materials", NASA Report CR-224, 1965.
58. ISHAI, O., MOEHLERPAH, A.E., PREIS, A., "Yield and Failure of Glass-Epoxy Composites", J. Engineering Mechanics Div., Proc. ASCE., Oct., 1970.
59. AGARWAL, B.D., NARANG, J.N., "Strength and Failure Mechanism of Anisotropic Composites", Fibre Sci. Technol. V. 10, No. 1, Jan., 1977.
60. ECKOLD, G.C., LEADBETTER, D., SODEN, P.D., GRIGGS, P.R., "Lamination Theory in the Prediction of Failure Envelopes for Filament Wound Materials subjected to Biaxial Loading", Composites, Oct. 1978.
61. Symposium on "Reinforced Plastics in Anti-Corrosion Applications", National Engineering Laboratory, East Kilbride, Glasgow, Sept., 1979.
62. Symposium on "Reinforced Plastic Constructed Equipment in Chemical Process Industry", The North Western Branches of the Institution of Chemical and Mechanical Engineering, Manchester, March, 1980.
63. British Standards Institution, BS.4994, 1973.
64. BRYAN-BROWN, M.H., "Operational Experience of G.R.P. Structures in Power Stations". (Ref. (62) above).
65. CHEREMISINOFF, N.P., CHEREMISINOFF, P.N., "Fibre Glass Reinforced Plastics Deskbook", Ann Arbor Science Publishers Inc., Michigan, 1978.

66. PENN, W.S., "G.R.P. Technology Handbook to the Polyester/Glass Fibre Plastics Industry", MacLaren & Sons Ltd., London, 1966.
67. TODS of Weymouth, "Fibre Reinforced Composites", Dorset, 1980.
68. TSAI, S.W., ADAMS, D.F., DONER, D.R., NASA Report CR-620, Nov., 1966.
69. Langley, M., Editor "Carbon Fibres in Engineering" McGraw-Hill Book Company (U.K.) Ltd., England, 1973.
70. BRYAN-BROWN, D.M., WALTER, O.M., WIGATT, R.C., "Advances in the use of G.R.P. for the Power Industry" to be submitted for Reinforced Plastic Congress 80, Brighton, November, 1980.
71. 21st International Machine Tool Design and Research Conference to be held 8-12th Sept., 1980, University of Swansea, (Private communication Prof. J.M. Alexander).

APPENDICES

APPENDIX 1

Coefficients tables for the calculation of deflections
and forces in circular plates simply supported on two
points at opposite ends of a diameter.

$$W = C_1 \frac{qa^2}{D}$$

$$M_r = C_2 q a^2$$

$$M_t = C_3 q a^2$$

$$M_{rt} = C_4 q a^2$$

$$Q_r = C_5 q a^2$$

$$Q_t = C_6 q a^2$$

in the tables coefficients C_1 to C_6 are listed under W ,
 MR , MT , MRT , QR and QT respectively.

POISSON,S RATIO= .050
THETA = 0/DEGREES

ROH	DEFLECTION	MR	MT	MRT	QR	Q T
0	.240636	.518494	-.137244	0	-.500000	0
.10	.238005	.515724	-.140559	0	-.566236	0
.20	.230138	.507373	-.150683	0	-.636612	0
.30	.217112	.493347	-.168190	0	-.716176	0
.40	.199062	.473405	-.194177	0	-.812223	0
.50	.176173	.447085	-.230481	0	-.936732	0
.60	.148692	.413204	-.279912	0	-1.111037	0
.70	.116937	.368472	-.346271	0	-1.374608	0
.80	.081329	.304038	-.433535	0	-1.806730	0
.90	.042488	.197918	-.543121	0	-2.523087	0
1.00	.001465	-.000000	-.667316	0	-3.778689	0

POISSON,S RATIO= .050
THETA = 15.00/DEGREES

ROH	DEFLECTION	MR	MT	MRT	QR	Q T
0	.240636	.474568	-.093318	.163934	-.500000	0
.10	.238237	.471019	-.095384	.165258	-.557116	.033361
.20	.231074	.460221	-.101534	.169322	-.616196	.070334
.30	.219252	.441683	-.111584	.176415	-.679135	.115518
.40	.202954	.414454	-.125075	.187017	-.747452	.175223
.50	.182446	.376948	-.141011	.201734	-.821256	.265489
.60	.158100	.326841	-.157492	.221055	-.896650	.389576
.70	.130410	.261438	-.171401	.244611	-.960062	.594511
.80	.100029	.179374	-.173564	.269430	-.977198	.931025
.90	.067770	.085270	-.175291	.286253	-.873285	1.494918
1.00	.034564	-.000000	-.162795	.272458	-.500002	2.447247

POISSON,S RATIO= .050
THETA = 30.00/DEGREES

ROH	DEFLECTION	MR	MT	MRT	QR	Q T
0	.240636	.354560	.026690	.283943	-.500000	0
.10	.238870	.349796	.027117	.284674	-.532452	.057356
.20	.233618	.335401	.028609	.286697	-.562737	.118113
.30	.225027	.311116	.031800	.289432	-.587850	.185563
.40	.213341	.276708	.037698	.291705	-.602998	.262420
.50	.198908	.232375	.047524	.291472	-.600538	.349382
.60	.182178	.179440	.062365	.235579	-.569038	.441775
.70	.163684	.121348	.082606	.269921	-.493069	.522621
.80	.144014	.064724	.107219	.240756	-.354801	.549752
.90	.123740	.019934	.133238	.198537	-.133063	.433458
1.00	.103312	-.000000	.156045	.156524	.155740	.000001

POISSON,S RATIO= .050
THETA = 45.00/DEGREES

ROH	DEFLECTION	MR	MT	MRT	QR	Q T
0	.240636	.190625	.190625	.327869	-.500000	0
.10	.239732	.186325	.192317	.326290	-.499344	.065567
.20	.237064	.173727	.197298	.321309	-.494763	.130938
.30	.232759	.153797	.205216	.312251	-.482439	.195141
.40	.227020	.128311	.215289	.298241	-.459107	.255752
.50	.220104	.099960	.226087	.278639	-.423156	.308658
.60	.212300	.072224	.235389	.253702	-.376717	.349061
.70	.203886	.048719	.240273	.225274	-.329085	.375268
.80	.195098	.031672	.237643	.196913	-.301781	.397730
.90	.186107	.019076	.225436	.172219	-.335605	.457003
1.00	.177042	-.000000	.204815	.149180	-.500002	.555737

POISSON'S RATIO = .050
THETA = 60.00/DEGREES

ROH	DEFLECTION	MR	MT	MRT	QR	QT
0	.240636	.026691	.354559	.283943	-.500000	0
.10	.240592	.025243	.355107	.280514	-.466892	.056221
.20	.240476	.021302	.356464	.270398	-.432009	.109041
.30	.240326	.015386	.357847	.254157	-.394302	.155146
.40	.240195	.010360	.358136	.232834	-.353961	.191591
.50	.240140	.005896	.356550	.207954	-.312372	.216285
.60	.240203	.002913	.352535	.181297	-.270967	.228242
.70	.240412	.000736	.346850	.154421	-.228011	.226587
.80	.240789	-.001944	.341444	.128197	-.171943	.206425
.90	.241357	-.004781	.338842	.103125	-.069266	.148717
1.00	.242136	.000000	.333652	.081989	.155739	.000002

POISSON'S RATIO = .050
THETA = 75.00/DEGREES

ROH	DEFLECTION	MR	MT	MRT	QR	QT
0	.240636	-.093318	.474568	.163935	-.500000	0
.10	.241221	-.091188	.472785	.161097	-.443539	.032226
.20	.242953	-.084948	.467486	.152980	-.389042	.061234
.30	.245769	-.075073	.458836	.140674	-.338426	.084504
.40	.249564	-.062389	.447160	.125679	-.293441	.100673
.50	.254207	-.048001	.432892	.109564	-.255589	.109645
.60	.259548	-.033065	.416353	.093708	-.226633	.112455
.70	.265429	-.018500	.397346	.079203	-.210854	.111396
.80	.271696	-.005171	.374795	.066881	-.221022	.111321
.90	.273216	-.004311	.347073	.057144	-.291112	.123705
1.00	.284856	.000000	.314229	.048853	-.500001	.175702

POISSON'S RATIO = .050
THETA = 90.00/DEGREES

ROH	DEFLECTION	MR	MT	MRT	QR	QT
0	.240636	-.137244	.518494	.000001	-.500000	0
.10	.241451	-.133498	.515549	.000001	-.435075	.000000
.20	.243856	-.122784	.507037	.000001	-.373897	.000000
.30	.247742	-.106539	.493831	.000000	-.319521	.000000
.40	.252940	-.086790	.477136	.000000	-.273860	.000000
.50	.259246	-.065812	.458269	.000000	-.237449	.000000
.60	.266442	-.045910	.438611	.000000	-.208955	.000000
.70	.274322	-.029328	.419797	.000000	-.183233	.000000
.80	.282710	-.017849	.403957	.000000	-.145782	.000001
.90	.291484	-.010912	.393398	.000000	-.060253	.000001
1.00	.300562	.000000	.388422	.000000	.155738	.000003

POISSON'S RATIO = .100
THETA = 0/DEGREES

ROH	DEFLECTION	MR	MT	MRT	QR	QT
0	.245898	.516331	-.128831	0	-.500000	0
.10	.243227	.513503	-.132319	0	-.565168	0
.20	.235240	.504984	-.142969	0	-.634409	0
.30	.222012	.490657	-.161372	0	-.712659	0
.40	.203669	.470295	-.188661	0	-.807187	0
.50	.180389	.443426	-.226738	0	-.929688	0
.60	.152407	.408882	-.278555	0	-.1.101181	0
.70	.120021	.363472	-.348225	0	-.1.360502	0
.80	.083625	.293684	-.440461	0	-.1.779750	0
.90	.043799	.193474	-.558339	0	-.2.490456	0
1.00	.001524	-.000000	-.697715	0	-.3.725806	0

POISSON'S RATIO= .100
THETA = 15.00/DEGREES

ROH	DEFLECTION	MR	MT	MRT	QR	Q T
0	.245898	.473113	-.085613	.161290	-.500000	0
.10	.243468	.469540	-.087371	.162598	-.556195	.032823
.20	.230212	.458673	-.094606	.166615	-.614321	.069206
.30	.224234	.440038	-.105560	.173634	-.676246	.113556
.40	.207711	.412719	-.120622	.184142	-.743461	.172377
.50	.185906	.375191	-.138577	.198779	-.816674	.256287
.60	.162181	.325223	-.157731	.218111	-.890252	.383292
.70	.134025	.260225	-.175058	.241979	-.952641	.584912
.80	.103078	.178871	-.186338	.267893	-.969502	.916008
.90	.070147	.085525	-.187367	.287654	-.867265	1.470847
1.00	.036160	-.000000	-.177695	.280829	-.500002	2.407776

POISSON'S RATIO= .100
THETA = 30.00/DEGREES

ROH	DEFLECTION	MR	MT	MRT	QR	Q T
0	.245898	.355040	.032460	.279363	-.500000	0
.10	.244125	.350312	.032673	.280116	-.531929	.056431
.20	.233855	.336029	.033524	.282224	-.561725	.116208
.30	.230233	.311946	.035643	.285138	-.586433	.182570
.40	.218504	.277848	.040045	.287757	-.601337	.250187
.50	.204018	.233933	.047994	.288150	-.598917	.343747
.60	.187225	.181480	.060695	.283314	-.567324	.434649
.70	.168666	.123802	.078782	.269294	-.493181	.514191
.80	.148935	.066726	.101665	.242357	-.357143	.540885
.90	.128618	.021813	.127009	.202493	-.144885	.426467
1.00	.108189	-.000000	.150941	.161332	.145163	.000001

POISSON'S RATIO= .100
THETA = 45.00/DEGREES

ROH	DEFLECTION	MR	MT	MRT	QR	Q T
0	.245898	.193750	.193750	.322581	-.500000	0
.10	.245021	.189498	.195270	.321169	-.499355	.064510
.20	.242434	.177031	.199752	.316457	-.494847	.126826
.30	.238267	.157284	.206897	.307978	-.482722	.191993
.40	.232726	.131970	.216014	.294823	-.459767	.251627
.50	.226072	.103683	.225809	.276354	-.424395	.303630
.60	.218593	.075775	.234220	.252774	-.378706	.343431
.70	.210593	.051739	.238495	.225790	-.331842	.369215
.80	.202299	.033751	.235537	.198770	-.304978	.391315
.90	.193898	.019956	.223012	.175250	-.338257	.449632
1.00	.185524	-.000000	.201209	.153763	-.500002	.645160

POISSON'S RATIO= .100
THETA = 60.00/DEGREES

ROH	DEFLECTION	MR	MT	MRT	QR	Q T
0	.245898	.032460	.355040	.279363	-.500000	0
.10	.245314	.030998	.355535	.276093	-.467426	.055314
.20	.245973	.026979	.356752	.266444	-.433105	.107282
.30	.246133	.021399	.357954	.250941	-.396007	.152644
.40	.246433	.015568	.358139	.230562	-.356316	.188501
.50	.246936	.010621	.356388	.206742	-.315398	.212796
.60	.247691	.006978	.352331	.181164	-.274661	.224561
.70	.243730	.004008	.346620	.155298	-.232398	.222932
.80	.250079	.000471	.341158	.129959	-.177235	.263096
.90	.251769	-.003317	.338586	.105558	-.076213	.146318
1.00	.253830	-.000000	.340188	.084508	.145163	.000002

POISSON'S RATIO = .100
THETA = 75.00/DEGREES

ROH	DEFLECTION	MR	MT	MRT	QR	QT
0	.245898	-.085613	.473113	.161291	-.500000	0
.10	.240507	-.083599	.471413	.158572	-.444450	.031706
.20	.248554	-.077703	.466354	.150795	-.390832	.060246
.30	.251793	-.068384	.458075	.138991	-.341032	.083141
.40	.250183	-.056439	.446858	.124587	-.296773	.099050
.50	.261594	-.042936	.433080	.109077	-.259531	.107876
.60	.267874	-.028398	.417002	.093777	-.231042	.110642
.70	.274870	-.015526	.398375	.079735	-.215518	.109606
.80	.282425	-.003372	.376051	.067762	-.225521	.109526
.90	.290390	.004957	.348166	.058288	-.294481	.121709
1.00	.298679	-.000000	.313984	.050354	-.500001	.172868

POISSON'S RATIO = .100
THETA = 90.00/DEGREES

ROH	DEFLECTION	MR	MT	MRT	QR	QT
0	.245898	-.128831	.516331	.000001	-.500000	0
.10	.246806	-.125247	.513528	.000001	-.436123	.000000
.20	.249492	-.114999	.505416	.000000	-.375931	.000000
.30	.253845	-.099473	.492802	.000000	-.322432	.000000
.40	.253698	-.080626	.476792	.000000	-.277507	.000000
.50	.256845	-.060657	.458599	.000000	-.241683	.000000
.60	.275069	-.041796	.439502	.000000	-.213649	.000000
.70	.284163	-.026216	.421045	.000000	-.188342	.000000
.80	.293951	-.015646	.405315	.000000	-.151495	.000001
.90	.304310	-.009592	.394773	.000000	-.067346	.000001
1.00	.315164	.000000	.390457	.000000	.145161	.000003

POISSON'S RATIO = .150
THETA = 0/DEGREES

ROH	DEFLECTION	MR	MT	MRT	QR	QT
0	.252373	.514335	-.120585	0	-.500000	0
.10	.249652	.511451	-.124245	0	-.564133	0
.20	.241511	.502760	-.135413	0	-.632275	0
.30	.228024	.488143	-.154699	0	-.709323	0
.40	.209309	.467367	-.183269	0	-.802311	0
.50	.185536	.439957	-.223090	0	-.922867	0
.60	.156925	.404761	-.277249	0	-.1091639	0
.70	.123754	.358681	-.350164	0	-.1346843	0
.80	.086390	.293535	-.447258	0	-.1759437	0
.90	.045364	.189191	-.573215	0	-.2458862	0
1.00	.001590	-.000000	-.727348	0	-.3674603	0

POISSON'S RATIO = .150
THETA = 15.00/DEGREES

ROH	DEFLECTION	MR	MT	MRT	QR	QT
0	.252373	.471804	-.078054	.158730	-.500000	0
.10	.249902	.468245	-.080501	.160022	-.555303	.032302
.20	.242524	.457269	-.087811	.163995	-.612507	.068101
.30	.230339	.438535	-.099851	.170941	-.673448	.111754
.40	.213522	.411123	-.116260	.181359	-.739596	.169661
.50	.192328	.373565	-.136197	.195917	-.811057	.252219
.60	.167114	.323720	-.157970	.215262	-.884058	.377208
.70	.138359	.259101	-.178645	.239431	-.945456	.575628
.80	.106693	.178420	-.193956	.266405	-.962049	.901468
.90	.072917	.085790	-.199201	.289011	-.861435	1.447451
1.00	.037954	-.000000	-.192320	.288933	-.500002	2.369557

POISSON'S RATIO = .150
THETA = 30.00/DEGREES

ROH	DEFLECTION	MR	MT	MRT	QR	Q T
0	.252373	.355605	.038145	.274929	-.500000	0
.10	.250587	.356910	.038143	.275707	-.531422	.055536
.20	.245278	.336732	.038370	.277893	-.560745	.114363
.30	.236592	.312841	.039437	.280981	-.585661	.179572
.40	.224774	.279035	.042369	.283935	-.599728	.254089
.50	.210176	.235515	.048473	.284934	-.597346	.338291
.60	.193250	.183518	.059069	.281121	-.566846	.427756
.70	.174543	.126228	.075033	.268687	-.493239	.506030
.80	.154660	.069751	.096195	.243907	-.359410	.532299
.90	.134203	.023650	.120837	.206323	-.150521	.419697
1.00	.113670	-.000000	.145800	.165988	.134922	.000001

POISSON'S RATIO = .150
THETA = 45.00/DEGREES

ROH	DEFLECTION	MR	MT	MRT	QR	Q T
0	.252373	.196875	.196875	.317460	-.500000	0
.10	.251521	.192667	.198226	.316092	-.499365	.063486
.20	.243009	.180326	.202216	.311759	-.494929	.126781
.30	.244969	.160751	.208596	.303841	-.482396	.188946
.40	.239610	.135596	.216767	.291512	-.460406	.247633
.50	.233199	.107362	.225566	.274141	-.425535	.296859
.60	.226036	.079277	.233097	.251876	-.380631	.337980
.70	.218416	.054715	.236726	.226290	-.334511	.363355
.80	.210593	.035800	.233405	.200568	-.308073	.385103
.90	.202758	.020827	.220523	.178185	-.340824	.442495
1.00	.195050	-.000000	.197520	.158201	-.500002	.634920

POISSON'S RATIO = .150
THETA = 60.00/DEGREES

ROH	DEFLECTION	MR	MT	MRT	QR	Q T
0	.252373	.038145	.355605	.274929	-.500000	0
.10	.252452	.036663	.356046	.271813	-.467943	.054436
.20	.252705	.032571	.357119	.262616	-.434167	.105579
.30	.253174	.026828	.358130	.247827	-.397658	.150221
.40	.253918	.020694	.358134	.228362	-.358597	.185509
.50	.254999	.015271	.356256	.205570	-.318329	.209419
.60	.256469	.010976	.352126	.181034	-.278238	.220997
.70	.258367	.067227	.346352	.156147	-.236645	.219394
.80	.260723	.002845	.340789	.131666	-.182358	.199872
.90	.263574	-.001880	.338195	.107913	-.032940	.143996
1.00	.266958	-.000000	.340509	.086946	.134922	.000002

POISSON'S RATIO = .150
THETA = 75.00/DEGREES

ROH	DEFLECTION	MR	MT	MRT	QR	Q T
0	.252373	-.078053	.471803	.158731	-.500000	0
.10	.253132	-.076153	.470101	.156128	-.445332	.031293
.20	.255389	-.070594	.465344	.148679	-.392564	.059290
.30	.259078	-.061817	.457411	.137362	-.343556	.081821
.40	.264100	-.050594	.446617	.123530	-.299999	.097477
.50	.270323	-.037958	.433287	.100606	-.263348	.106164
.60	.277598	-.024997	.417623	.093844	-.235312	.108835
.70	.285770	-.012597	.399325	.080250	-.220033	.107860
.80	.294685	-.001595	.377175	.068615	-.229878	.167787
.90	.304196	.005602	.343083	.050395	-.297743	.119777
1.00	.314196	-.000000	.313549	.051807	-.500001	.170124

POISSON'S RATIO = .150
THETA = 90.00/DEGREES

ROH	DEFLECTION	MR	MT	MRT	QR	QT
0	.252373	-.120565	.514333	.000001	-.500000	0
.10	.253381	-.117159	.511667	.000001	-.437137	.000000
.20	.256367	-.107356	.503935	.000000	-.377900	.000000
.30	.261219	-.092541	.491878	.000000	-.325250	.000000
.40	.267770	-.074575	.476511	.000000	-.261039	.000000
.50	.275814	-.055591	.458944	.000000	-.245704	.000000
.60	.285132	-.037743	.440357	.000000	-.218134	.000000
.70	.295515	-.023152	.422206	.000000	-.193289	.000000
.80	.306786	-.013478	.406539	.000000	-.157027	.000001
.90	.318825	-.008294	.395962	.000000	-.074214	.000001
1.00	.331555	.000000	.392229	.000000	.134921	.000003

POISSON'S RATIO = .200
THETA = 0/DEGREES

ROH	DEFLECTION	MR	MT	MRT	QR	QT
0	.260214	.512500	-.112500	0	-.500000	0
.10	.257429	.509559	-.116328	0	-.563131	0
.20	.249098	.501699	-.128007	0	-.630208	0
.30	.235289	.485796	-.148163	0	-.706043	0
.40	.216114	.464613	-.177994	0	-.797588	0
.50	.191732	.436670	-.219531	0	-.916260	0
.60	.162349	.406831	-.275991	0	-1.082395	0
.70	.128221	.354690	-.352388	0	-1.333611	0
.80	.089683	.288583	-.453933	0	-1.739758	0
.90	.047219	.185060	-.587766	0	-2.428255	0
1.00	.001666	-.000000	-.756250	0	-3.625000	0

POISSON'S RATIO = .200
THETA = 15.00/DEGREES

ROH	DEFLECTION	MR	MT	MRT	QR	QT
0	.260214	.470633	-.070633	.156250	-.500000	0
.10	.257692	.467009	-.073266	.157527	-.554339	.031798
.20	.250158	.456002	-.081142	.161456	-.610749	.067037
.30	.237711	.437168	-.094153	.168332	-.670738	.110007
.40	.220520	.409659	-.111983	.178663	-.735853	.167010
.50	.198837	.372063	-.133866	.193145	-.806197	.248278
.60	.173010	.322326	-.158210	.212501	-.878057	.371315
.70	.143508	.258062	-.182166	.236963	-.938496	.566634
.80	.110953	.178018	-.201426	.264963	-.354830	.887383
.90	.076137	.086066	-.210805	.290325	-.855788	1.424844
1.00	.039983	-.000000	-.206683	.296785	-.500002	2.332533

POISSON'S RATIO = .200
THETA = 30.00/DEGREES

ROH	DEFLECTION	MR	MT	MRT	QR	QT
0	.260214	.356250	.043750	.270633	-.500000	0
.10	.258408	.351586	.043548	.271434	-.530931	.054668
.20	.253039	.337507	.043151	.273698	-.559796	.112576
.30	.244252	.313796	.043183	.276953	-.583732	.176865
.40	.232295	.286267	.044672	.280232	-.598170	.250119
.50	.217521	.237122	.048962	.281818	-.595825	.333005
.60	.200387	.185555	.057487	.278996	-.565802	.421066
.70	.181445	.128628	.071356	.268098	-.493394	.498123
.80	.161313	.072199	.090806	.245409	-.361607	.523982
.90	.140611	.025449	.114710	.210034	-.155982	.413140
1.00	.119864	-.000000	.140625	.170499	.125002	.000001

POISSON'S RATIO = .200
THETA = 45.00/DEGREES

ROH	DEFLECTION	MR	MT	MRT	QR	Q T
0	.200214	.200000	.200000	.312500	-.500000	0
.10	.253385	.195835	.201184	.311231	-.499375	.662494
.20	.256942	.183611	.204689	.307208	-.495008	.124866
.30	.253019	.164199	.210314	.299832	-.483262	.185994
.40	.247830	.139192	.217547	.288305	-.461024	.243764
.50	.241646	.116999	.225354	.271997	-.426758	.294198
.60	.234776	.082732	.231993	.251006	-.382496	.332699
.70	.227524	.057647	.234967	.226774	-.337097	.357677
.80	.220155	.037820	.231251	.202309	-.311072	.379086
.90	.212869	.021689	.217973	.181028	-.343311	.435581
1.00	.205813	-.000000	.193750	.162500	-.500002	.624999

POISSON'S RATIO = .200
THETA = 60.00/DEGREES

ROH	DEFLECTION	MR	MT	MRT	QR	Q T
0	.260214	.043750	.356250	.270633	-.500000	0
.10	.261070	.042248	.356636	.267667	-.468444	.053585
.20	.260809	.038083	.357559	.258907	-.435196	.103930
.30	.261608	.032175	.358371	.244810	-.399257	.147873
.40	.262820	.025742	.358181	.226231	-.360606	.182610
.50	.264508	.019849	.356152	.204434	-.321107	.206146
.60	.266731	.014913	.351919	.180909	-.281703	.217544
.70	.269531	.010394	.346045	.156970	-.240760	.215966
.80	.272944	.005181	.340342	.133319	-.187321	.196749
.90	.277013	-.000470	.337677	.110195	-.089457	.141746
1.00	.281787	-.000000	.340625	.089309	.125001	.000002

POISSON'S RATIO = .200
THETA = 75.00/DEGREES

ROH	DEFLECTION	MR	MT	MRT	QR	Q T
0	.260214	-.070633	.470633	.156250	-.500000	0
.10	.261070	-.068844	.469082	.153760	-.446106	.030715
.20	.263617	-.063612	.464453	.146629	-.394243	.058363
.30	.267792	-.055367	.456838	.135783	-.346000	.080543
.40	.273492	-.044850	.440435	.122507	-.303124	.095954
.50	.280588	-.033062	.433512	.108149	-.267645	.104505
.60	.288931	-.021058	.418216	.093909	-.239447	.107184
.70	.298364	-.009709	.400199	.080749	-.224408	.106175
.80	.308734	.000162	.378174	.069442	-.234699	.106103
.90	.319891	.006245	.349831	.060468	-.300903	.117906
1.00	.331720	-.000000	.312932	.053215	-.500001	.167466

POISSON'S RATIO = .200
THETA = 90.00/DEGREES

ROH	DEFLECTION	MR	MT	MRT	QR	Q T
0	.260214	-.112500	.512500	.000001	-.500000	0
.10	.261331	-.109228	.509959	.000001	-.438119	.000000
.20	.264641	-.099878	.502586	.000000	-.379808	.000000
.30	.270034	-.085737	.491054	.000000	-.327981	.000000
.40	.277340	-.068630	.476289	.000000	-.284450	.000000
.50	.286352	-.050610	.459302	.000000	-.249756	.000000
.60	.296849	-.033767	.441177	.000000	-.222597	.000000
.70	.308620	-.020134	.423285	.000000	-.198082	.000000
.80	.321487	-.011343	.407635	.000000	-.162386	.000001
.90	.335326	-.007019	.396975	.000000	-.080867	.000001
1.00	.350065	.000000	.393750	.000000	.125000	.000003

POISSON'S RATIO= .250
THETA = 0/DEGREES

ROH	DEFLECTION	MR	MT	MRT	QR	QT
0	.269626	.510817	-.104567	0	-.500000	0
.10	.266764	.507821	-.108562	0	-.562100	0
.20	.258200	.498734	-.120745	0	-.628205	0
.30	.243996	.483609	-.141758	0	-.702873	0
.40	.224259	.462024	-.172832	0	-.793010	0
.50	.199137	.433556	-.216058	0	-.809856	0
.60	.168817	.397184	-.274780	0	-1.073435	0
.70	.133534	.349690	-.353398	0	-1.328786	0
.80	.093587	.283317	-.460490	0	-1.726685	0
.90	.049409	.181074	-.602006	0	-2.398589	0
1.00	.001752	-.000000	-.784455	0	-3.576923	0

POISSON'S RATIO= .250
THETA = 15.00/DEGREES

ROH	DEFLECTION	MR	MT	MRT	QR	QT
0	.269626	.469594	-.063344	.153846	-.500000	0
.10	.267040	.465945	-.066161	.155109	-.553602	.031308
.20	.259312	.454867	-.074534	.158995	-.609045	.066006
.30	.246540	.435931	-.088559	.165803	-.668112	.108315
.40	.228888	.408320	-.107787	.176050	-.732224	.164440
.50	.206600	.370679	-.131583	.190458	-.801486	.244459
.60	.180018	.321037	-.158449	.209825	-.872241	.365602
.70	.149602	.257104	-.185625	.234570	-.931750	.557916
.80	.115963	.177663	-.208754	.263566	-.947832	.873731
.90	.079886	.086351	-.222190	.291599	-.850314	1.402923
1.00	.042295	-.000000	-.220797	.304395	-.500002	2.296647

POISSON'S RATIO= .250
THETA = 30.00/DEGREES

ROH	DEFLECTION	MR	MT	MRT	QR	QT
0	.269626	.356971	.049279	.266469	-.500000	0
.10	.267792	.352337	.048875	.267292	-.530455	.053827
.20	.262338	.338350	.047869	.269631	-.558876	.110844
.30	.253411	.314809	.046884	.273050	-.582443	.174144
.40	.241261	.281542	.046953	.276643	-.596600	.246271
.50	.226241	.238751	.049460	.278797	-.594351	.327882
.60	.208815	.187591	.055946	.276937	-.564789	.414588
.70	.189543	.131003	.067746	.267528	-.493495	.490459
.80	.169056	.074607	.085495	.246865	-.363736	.515921
.90	.147994	.027211	.108650	.213630	-.161275	.406784
1.00	.126915	-.000000	.135417	.174871	.115336	.000001

POISSON'S RATIO= .250
THETA = 45.00/DEGREES

ROH	DEFLECTION	MR	MT	MRT	QR	QT
0	.269626	.203125	.203125	.307692	-.500000	0
.10	.268818	.199000	.204144	.306521	-.499385	.061532
.20	.266438	.186887	.207170	.302798	-.495085	.122880
.30	.262625	.167627	.212049	.295947	-.483519	.183132
.40	.257594	.142757	.218353	.285197	-.461624	.240014
.50	.251626	.114596	.225173	.269919	-.427885	.289664
.60	.245036	.086143	.230915	.250162	-.384304	.327580
.70	.238140	.060538	.233217	.227244	-.339603	.352175
.80	.231213	.039813	.229074	.203997	-.313979	.373254
.90	.224468	.022543	.215363	.183783	-.345722	.428880
1.00	.213058	-.000000	.189904	.166567	-.500002	.515384

POISSON'S RATIO= .250
THETA = 60.00/DEGREES

ROH	DEFLECTION	MR	MT	MRT	QR	QT
0	.269626	.649279	.356971	.266476	-.500000	0
.10	.263841	.047757	.357301	.263648	-.468929	.052761
.20	.270501	.043517	.358071	.255313	-.436193	.102331
.30	.271654	.037446	.358676	.241886	-.400857	.145598
.40	.273364	.030715	.358276	.224165	-.362948	.179801
.50	.275702	.024358	.356076	.203333	-.323918	.202975
.60	.278727	.018789	.351711	.180788	-.285061	.214197
.70	.282490	.013513	.345704	.157757	-.244748	.212643
.80	.287031	.007479	.339820	.134921	-.192131	.193722
.90	.292400	.000916	.337038	.112407	-.095773	.139565
1.00	.298654	.000000	.340545	.091599	.115386	.000002

POISSON'S RATIO= .250
THETA = 75.00/DEGREES

ROH	DEFLECTION	MR	MT	MRT	QR	QT
0	.269626	-.063344	.469594	.153847	-.500000	0
.10	.270588	-.061664	.468110	.151465	-.447014	.030242
.20	.273453	-.056754	.463673	.144642	-.395870	.057465
.30	.278156	-.049027	.456354	.134254	-.348369	.079303
.40	.284597	-.039202	.446368	.121514	-.306153	.094478
.50	.292644	-.028244	.433754	.107787	-.270629	.102897
.60	.302149	-.017179	.418784	.093971	-.243456	.105535
.70	.312954	-.006861	.401001	.081233	-.228648	.104541
.80	.324302	.001899	.379054	.070243	-.238190	.104471
.90	.337842	.006887	.350419	.061508	-.303966	.116092
1.00	.351651	-.000000	.312142	.054580	-.500001	.164890

POISSON'S RATIO= .250
THETA = 90.00/DEGREES

ROH	DEFLECTION	MR	MT	MRT	QR	QT
0	.269626	-.104567	.510817	.000001	-.500000	0
.10	.271862	-.101445	.508397	.000001	-.439071	.000000
.20	.274529	-.092528	.501362	.000000	-.381657	.000000
.30	.280515	-.079055	.490325	.000000	-.330627	.000000
.40	.288648	-.062788	.476123	.000000	-.287776	.000000
.50	.298720	-.045711	.459673	.000000	-.253606	.000000
.60	.310506	-.029845	.441965	.000000	-.226865	.000000
.70	.323792	-.017160	.424286	.000000	-.202727	.000000
.80	.338397	-.009238	.408608	.000000	-.167580	.000001
.90	.354195	-.005764	.397818	.000000	-.087315	.000001
1.00	.371116	.000000	.395032	.000000	.115385	.000003

POISSON'S RATIO= .300
THETA = 0/DEGREES

ROH	DEFLECTION	MR	MT	MRT	QR	QT
0	.280884	.509280	-.096780	0	-.500000	0
.10	.277928	.506230	-.100939	0	-.561218	0
.20	.269080	.497037	-.113619	0	-.626263	0
.30	.254398	.481575	-.135477	0	-.699799	0
.40	.233980	.459593	-.167777	0	-.788570	0
.50	.207962	.430608	-.212667	0	-.983646	0
.60	.176514	.393510	-.273613	0	-1.064746	0
.70	.139844	.345471	-.355895	0	-1.308350	0
.80	.098212	.279230	-.466936	0	-1.702190	0
.90	.051994	.177227	-.615951	0	-2.369823	0
1.00	.001851	-.000000	-.811995	0	-3.530303	0

POISSON'S RATIO = .300
THETA = 15.00/DEGREES

ROH	DEFLECTION	MR	MT	MRT	QR	QT
0	.280884	.408682	-.056182	.151515	-.500000	0
.10	.278219	.405008	-.053179	.152764	-.552789	.030634
.20	.270254	.453857	-.068161	.156669	-.607393	.065006
.30	.257082	.434818	-.083066	.163351	-.665564	.106674
.40	.238865	.407102	-.103669	.173516	-.728745	.101949
.50	.215840	.369409	-.129345	.187852	-.796918	.240755
.60	.188339	.319847	-.158690	.207231	-.865601	.360063
.70	.156812	.256223	-.189022	.232250	-.925208	.549463
.80	.121862	.177353	-.215948	.262211	-.941047	.860492
.90	.084265	.086646	-.233365	.292835	-.845006	1.381667
1.00	.044948	-.000000	-.234672	.311774	-.500002	2.261850

POISSON'S RATIO = .300
THETA = 30.00/DEGREES

ROH	DEFLECTION	MR	MT	MRT	QR	QT
0	.280884	.357765	.054735	.262432	-.500000	0
.10	.279013	.353158	.054132	.263275	-.529394	.053011
.20	.273447	.339259	.052528	.265688	-.557984	.109165
.30	.264335	.315877	.050542	.269264	-.581194	.171505
.40	.251928	.282858	.049214	.273163	-.595195	.242539
.50	.236583	.240402	.049967	.275869	-.592922	.322914
.60	.218770	.189626	.054443	.274940	-.563808	.408307
.70	.199060	.133354	.064201	.266975	-.493594	.483028
.80	.178098	.076976	.080258	.248277	-.355801	.568104
.90	.156548	.028937	.102630	.217117	-.166407	.400620
1.00	.135003	-.000000	.130177	.179110	.106062	.000001

POISSON'S RATIO = .300
THETA = 45.00/DEGREES

ROH	DEFLECTION	MR	MT	MRT	QR	QT
0	.280884	.206250	.206250	.303030	-.500000	0
.10	.280095	.202163	.207107	.301953	-.499394	.060606
.20	.277775	.190155	.209660	.298520	-.495159	.121019
.30	.274063	.171038	.213800	.292180	-.483769	.180357
.40	.269182	.146294	.219184	.282183	-.462205	.236377
.50	.263419	.118155	.225020	.267905	-.428977	.265275
.60	.257100	.089510	.229863	.249344	-.386057	.322617
.70	.250552	.063390	.231475	.227699	-.342033	.346839
.80	.244064	.041779	.226877	.205634	-.316797	.367599
.90	.237860	.023390	.212698	.186455	-.348059	.422382
1.00	.232100	-.000000	.185985	.170707	-.500002	.606060

POISSON'S RATIO = .300
THETA = 60.00/DEGREES

ROH	DEFLECTION	MR	MT	MRT	QR	QT
0	.280884	.054735	.357765	.262432	-.500000	0
.10	.281175	.053192	.358037	.259751	-.469400	.051962
.20	.282064	.048877	.358651	.251827	-.437150	.100780
.30	.283600	.042643	.359040	.239051	-.402310	.143392
.40	.285851	.035617	.358417	.222162	-.365024	.177077
.50	.288892	.028801	.356025	.202265	-.326586	.199900
.60	.292739	.022609	.351502	.186671	-.288318	.210951
.70	.297596	.016586	.345327	.158540	-.248016	.209421
.80	.303359	.009741	.339227	.136475	-.196796	.190787
.90	.310136	.002277	.336282	.114551	-.101837	.137450
1.00	.317993	-.000000	.340278	.093820	.106062	.000002

POISSON'S RATIO = .300
THETA = 75.00/DEGREES

ROH	DEFLECTION	MR	MT	MRT	QR	QT
0	.280834	-.056182	.468682	.151516	-.500000	0
.10	.281964	-.054037	.467259	.149240	-.447817	.29784
.20	.285180	-.050012	.463001	.142715	-.397448	.056535
.30	.290463	-.042793	.455953	.132770	-.356607	.678192
.40	.297729	-.033645	.446235	.120552	-.309090	.193147
.50	.306828	-.023501	.434012	.107278	-.274105	.101338
.60	.317616	-.013357	.419326	.094032	-.247343	.103936
.70	.329933	-.004050	.401735	.081702	-.232759	.12957
.80	.343619	-.003618	.379821	.071020	-.242156	.102888
.90	.358519	-.007527	.350854	.062516	-.306936	.114333
1.00	.374499	-.000000	.311187	.055903	-.500001	.162391

POISSON'S RATIO = .300
THETA = 90.00/DEGREES

ROH	DEFLECTION	MR	MT	MRT	QR	QT
0	.284884	-.096780	.509280	.000001	-.500000	0
.10	.282252	-.093804	.506974	.000000	-.439994	.000000
.20	.286316	-.085309	.500260	.000000	-.383450	.000000
.30	.292961	-.072489	.489688	.000000	-.333193	.000000
.40	.302014	-.057043	.476012	.000000	-.290992	.000000
.50	.313262	-.040888	.460057	.000000	-.257339	.000000
.60	.326477	-.025981	.442721	.000000	-.231004	.000000
.70	.341439	-.014227	.425212	.000000	-.207231	.000000
.80	.357365	-.007163	.409465	.000000	-.172617	.000001
.90	.375924	-.004530	.398501	.000000	-.093568	.000001
1.00	.395249	-.000000	.396086	.000000	.106061	.000003

POISSON'S RATIO = .350
THETA = 0/DEGREES

ROH	DEFLECTION	MR	MT	MRT	QR	QT
0	.294357	.507882	-.089132	0	-.500000	0
.10	.291287	.534778	-.093453	0	-.560305	0
.20	.282035	.495423	-.106623	0	-.624370	0
.30	.266834	.479686	-.129317	0	-.696817	0
.40	.245594	.457314	-.162824	0	-.784263	0
.50	.218495	.427817	-.209353	0	-.897621	0
.60	.185689	.390104	-.272488	0	-.1056317	0
.70	.147352	.341425	-.357779	0	-.1296285	0
.80	.103704	.274814	-.473275	0	-.1684247	0
.90	.055055	.173513	-.629613	0	-.2341915	0
1.00	.001967	-.000000	-.838899	0	-.3485075	0

POISSON'S RATIO = .350
THETA = 15.00/DEGREES

ROH	DEFLECTION	MR	MT	MRT	QR	QT
0	.294357	.467890	-.049140	.149254	-.500000	0
.10	.291596	.464190	-.052315	.150489	-.552001	.030374
.20	.283341	.452967	-.061838	.154294	-.605790	.064036
.30	.269682	.433822	-.077669	.160972	-.663093	.105082
.40	.250776	.405998	-.099626	.171057	-.725232	.159532
.50	.226854	.368246	-.127151	.185325	-.792487	.237161
.60	.193238	.318753	-.158930	.204713	-.861129	.354689
.70	.165367	.255416	-.192363	.230000	-.918862	.541262
.80	.128834	.177086	-.223013	.260897	-.934464	.847649
.90	.089409	.086950	-.244339	.294033	-.839857	1.361045
1.00	.043021	-.000000	-.248320	.318933	-.500002	2.228091

POISSON'S RATIO = .350
THETA = 30.00/DEGREES

ROH	DEFLECTION	MR	MT	MRT	QR	QT
0	.294357	.358629	.060121	.258515	-.500000	0
.10	.292438	.354047	.059323	.259379	-.529546	.052220
.20	.286729	.346230	.057130	.261062	-.557119	.157535
.30	.277379	.316999	.054159	.265532	-.579982	.168946
.40	.264641	.284212	.051457	.269787	-.593774	.238919
.50	.243880	.242073	.050482	.273027	-.591535	.318095
.60	.230570	.191660	.052979	.273003	-.562855	.402213
.70	.210295	.135683	.060718	.266439	-.493690	.475819
.80	.188718	.079307	.075091	.249646	-.367804	.500520
.90	.166532	.030630	.096656	.220501	-.171386	.394641
1.00	.144368	-.000000	.124907	.183223	-.097017	.000001

POISSON'S RATIO = .350
THETA = 45.00/DEGREES

ROH	DEFLECTION	MR	MT	MRT	QR	QT
0	.294357	.209375	.209375	.298507	-.500000	0
.10	.293586	.205324	.210071	.297521	-.499403	.059696
.20	.291321	.193415	.212157	.294371	-.495232	.119212
.30	.287704	.174433	.215568	.288525	-.484011	.177666
.40	.282966	.149803	.220039	.279259	-.462769	.232359
.50	.277402	.121678	.224896	.265950	-.430038	.281017
.60	.271348	.092837	.228834	.248551	-.387758	.317802
.70	.265146	.066204	.229741	.228140	-.344391	.341662
.80	.259100	.043720	.224659	.207223	-.319532	.362112
.90	.253445	.024228	.209978	.189047	-.350327	.416078
1.00	.248351	-.000000	.181996	.174627	-.500001	.597014

POISSON'S RATIO = .350
THETA = 60.00/DEGREES

ROH	DEFLECTION	MR	MT	MRT	QR	QT
0	.294357	.060122	.358628	.258515	-.500000	0
.10	.294732	.058558	.358842	.255971	-.469857	.051186
.20	.295873	.054167	.359295	.248446	-.438098	.09276
.30	.297831	.047769	.359462	.236300	-.403768	.141252
.40	.300680	.040452	.358603	.220219	-.367039	.174434
.50	.304497	.033182	.356000	.201229	-.329175	.196916
.60	.309355	.026375	.351292	.180557	-.291477	.207803
.70	.315312	.019615	.344919	.159290	-.252368	.206296
.80	.322423	.011969	.338566	.137982	-.201321	.187940
.90	.330750	.003615	.335416	.116632	-.107839	.135399
1.00	.340372	.000000	.339832	.095974	.097016	.000002

POISSON'S RATIO = .350
THETA = 75.00/DEGREES

ROH	DEFLECTION	MR	MT	MRT	QR	QT
0	.294357	-.049140	.467890	.149254	-.500000	0
.10	.295569	-.047670	.466524	.147081	-.448596	.029340
.20	.299180	-.043381	.462430	.140846	-.398979	.055750
.30	.305128	-.036661	.455632	.131331	-.352896	.076936
.40	.313308	-.028176	.446212	.119619	-.311939	.091658
.50	.323587	-.018830	.434286	.106862	-.277476	.099826
.60	.335812	-.009590	.419845	.094091	-.251114	.102385
.70	.349821	-.001277	.402402	.082157	-.236748	.101421
.80	.365449	.005319	.380478	.071774	-.246005	.101352
.90	.382536	.008166	.351142	.063495	-.309818	.112627
1.00	.400936	-.000000	.310073	.057186	-.500001	.159968

POISSON'S RATIO = .350
THETA = 90.00/DEGREES

ROH	DEFLECTION	MR	MT	MRT	QR	Q T
.0	.294357	-.009132	.507882	.000000	-.503000	0
.10	.295875	-.186299	.505684	.000000	-.440890	.000000
.20	.303386	-.078217	.493272	.000000	-.385189	.000000
.30	.307775	-.066034	.489138	.000000	-.335683	.000000
.40	.317864	-.051391	.475953	.000000	-.294111	.000000
.50	.330436	-.036140	.460452	.000000	-.260961	.000000
.60	.345257	-.022173	.443447	.000000	-.235018	.000000
.70	.362102	-.011335	.426066	.000000	-.211600	.000000
.80	.380781	-.005117	.410211	.000000	-.177543	.000001
.90	.401160	-.003314	.399030	.000000	-.099634	.000001
1.00	.423170	.000000	.396922	.000000	.097015	.000003

POISSON'S RATIO = .400
THETA = 0/DEGREES

ROH	DEFLECTION	MR	MT	MRT	QR	Q T
.0	.310546	.506618	-.081618	0	-.500000	0
.10	.307338	.503460	-.086098	0	-.559418	0
.20	.297728	.493944	-.099753	0	-.622549	0
.30	.281766	.477936	-.123270	0	-.693923	0
.40	.259529	.455178	-.157969	0	-.780083	0
.50	.231124	.425178	-.206114	0	-.891774	0
.60	.196676	.386856	-.271404	0	-.1048136	0
.70	.156332	.337545	-.359651	0	-.1284575	0
.80	.110262	.270560	-.479513	0	-.1666831	0
.90	.058703	.169925	-.643004	0	-.2314828	0
1.00	.002103	-.000000	-.865196	0	-.3441176	0

POISSON'S RATIO = .400
THETA = 15.00/DEGREES

ROH	DEFLECTION	MR	MT	MRT	QR	Q T
.0	.310546	.457213	-.042213	.147059	-.500000	0
.10	.307667	.463488	-.045564	.148281	-.551237	.029927
.20	.299058	.452191	-.055619	.152047	-.604234	.063094
.30	.284806	.432940	-.072364	.158663	-.660695	.103536
.40	.265062	.405004	-.095654	.168671	-.721979	.157186
.50	.240048	.367186	-.124999	.182871	-.788185	.233674
.60	.210076	.317750	-.159171	.202270	-.855818	.349473
.70	.175577	.254680	-.195648	.227815	-.912702	.533393
.80	.137130	.176859	-.229954	.259621	-.928075	.835184
.90	.095498	.087262	-.255123	.295196	-.834859	1.341030
1.00	.051619	-.000000	-.261750	.325881	-.500002	2.195325

POISSON'S RATIO = .400
THETA = 30.00/DEGREES

ROH	DEFLECTION	MR	MT	MRT	QR	Q T
.0	.310546	.359559	.065441	.254713	-.500000	0
.10	.308566	.355001	.064450	.255597	-.529112	.051452
.20	.302675	.341261	.061677	.258149	-.556279	.105954
.30	.293023	.318171	.057736	.262028	-.578806	.166461
.40	.279869	.285605	.053681	.266510	-.592395	.235406
.50	.263579	.243764	.051004	.270270	-.590189	.313417
.60	.244640	.193693	.051550	.271122	-.561931	.396298
.70	.223649	.137991	.057295	.265918	-.493782	.468822
.80	.201291	.081603	.069991	.250976	-.369748	.493160
.90	.178291	.032290	.090727	.223785	-.176218	.388837
1.00	.155325	-.000000	.119608	.187214	.088237	.000001

POISSON'S RATIO = .400
THETA = 45.00/DEGREES

ROH	DEFLECTION	MR	MT	MRT	QR	QT
0	.310546	.212500	.212500	.294118	-.500000	0
.10	.309792	.208483	.213036	.293229	-.499412	.358818
.20	.307578	.196668	.214661	.290343	-.495362	.117459
.30	.304052	.177811	.217350	.284978	-.484246	.175053
.40	.299451	.153287	.220916	.276421	-.463317	.229425
.50	.294080	.125157	.224799	.264053	-.431066	.276834
.60	.288290	.096125	.227829	.247780	-.389408	.313128
.70	.282438	.068983	.228015	.228568	-.346679	.336638
.80	.276845	.045637	.222421	.208764	-.322186	.356787
.90	.271760	.025060	.207207	.191563	-.352528	.409959
1.00	.267362	-.000000	.177941	.178431	-.500001	.588234

POISSON'S RATIO = .400
THETA = 60.00/DEGREES

ROH	DEFLECTION	MR	MT	MRT	QR	QT
0	.310546	.065441	.359559	.254714	-.500000	0
.10	.311015	.063856	.359713	.252302	-.476300	.050433
.20	.312438	.059390	.360002	.245164	-.439000	.097815
.30	.314872	.052829	.359938	.233631	-.405183	.139175
.40	.318390	.045221	.358831	.218333	-.368994	.171869
.50	.323079	.037503	.355998	.202224	-.331687	.194026
.60	.329015	.030088	.351080	.186446	-.294544	.204747
.70	.336264	.022602	.344479	.160018	-.256010	.203262
.80	.344885	.014165	.337840	.139445	-.205714	.185176
.90	.354949	.004932	.334444	.118651	-.113606	.133408
1.00	.366546	-.000000	.339216	.098065	-.088236	.000002

POISSON'S RATIO = .400
THETA = 75.00/DEGREES

ROH	DEFLECTION	MR	MT	MRT	QR	QT
0	.310546	-.042213	.467213	.147059	-.500000	0
.10	.311908	-.040845	.465900	.144985	-.449351	.028908
.20	.315971	-.036858	.461957	.139032	-.400464	.054938
.30	.322669	-.030625	.455388	.129934	-.355059	.075805
.40	.331898	-.022791	.446237	.118713	-.314705	.090310
.50	.343521	-.014227	.434575	.106458	-.280749	.098358
.60	.357383	-.005874	.420342	.094148	-.254774	.100879
.70	.373315	-.001463	.403007	.082599	-.240619	.099929
.80	.391149	-.007004	.381032	.072505	-.249740	.099862
.90	.410715	-.008804	.351290	.064444	-.312615	.110970
1.00	.431854	-.000000	.308808	.058432	-.500001	.157615

POISSON'S RATIO = .400
THETA = 90.00/DEGREES

ROH	DEFLECTION	MR	MT	MRT	QR	QT
0	.310546	-.081618	.506618	.000000	-.500000	0
.10	.312235	-.078924	.504521	.000000	-.441759	.000000
.20	.317259	-.071244	.498394	.000000	-.386878	.000000
.30	.325439	-.059686	.488671	.000000	-.338099	.000000
.40	.336773	-.045828	.475944	.000000	-.297139	.000000
.50	.350858	-.031463	.460859	.000000	-.264476	.000000
.60	.367512	-.018419	.444144	.000000	-.238915	.000000
.70	.386504	-.008480	.426852	.000000	-.215842	.000000
.80	.407634	-.003098	.410850	.000000	-.182246	.000001
.90	.430764	-.002117	.399412	.000000	-.105521	.000001
1.00	.455825	-.000000	.397549	.000000	.088235	.000003

POISSON'S RATIO = .450
THETA = 0/DEGREES

ROH	DEFLECTION	MR	MT	MRT	QR	QT
0	.330142	.505480	-.074230	0	-.500000	0
.10	.326764	.502270	-.078869	0	-.558557	0
.20	.316646	.492595	-.093902	0	-.620773	0
.30	.299626	.476319	-.117332	0	-.691112	0
.40	.276378	.453180	-.153208	0	-.776024	0
.50	.246381	.422683	-.202946	0	-.886096	0
.60	.209940	.383760	-.270359	0	-1.040192	0
.70	.167162	.333824	-.361511	0	-1.273265	0
.80	.118160	.266463	-.485653	0	-1.649321	0
.90	.063088	.166458	-.656137	0	-2.288526	0
1.00	.002264	-.000000	-.890912	0	-3.398551	0

POISSON'S RATIO = .450
THETA = 15.00/DEGREES

ROH	DEFLECTION	MR	MT	MRT	QR	QT
0	.330142	.466647	-.035397	.144927	-.500000	0
.10	.327118	.462895	-.038920	.146137	-.550494	.029493
.20	.318076	.451525	-.049502	.149866	-.602724	.052179
.30	.303097	.432165	-.067146	.156421	-.656366	.102036
.40	.282326	.404115	-.091750	.166355	-.718762	.154908
.50	.255978	.366225	-.122886	.180489	-.784009	.230287
.60	.224353	.316833	-.159412	.199898	-.850662	.344408
.70	.187869	.254011	-.198881	.225694	-.906721	.525573
.80	.147093	.176672	-.236778	.258382	-.921671	.823080
.90	.102783	.087582	-.265723	.296326	-.830006	1.321594
1.00	.055884	-.000000	-.274972	.332628	-.500002	2.163508

POISSON'S RATIO = .450
THETA = 30.00/DEGREES

ROH	DEFLECTION	MR	MT	MRT	QR	QT
0	.330142	.360553	.070697	.251022	-.500000	0
.10	.328085	.356018	.069517	.251925	-.528690	.050706
.20	.321964	.342349	.066173	.254544	-.555463	.104418
.30	.311934	.319392	.061276	.258567	-.577664	.164049
.40	.298253	.287032	.055888	.263328	-.591056	.231994
.50	.281299	.245475	.051534	.267592	-.588882	.308875
.60	.261568	.195725	.050155	.269296	-.561033	.390554
.70	.239674	.140277	.053928	.265413	-.493872	.462027
.80	.216330	.083865	.064956	.252266	-.371636	.486012
.90	.192299	.033919	.084840	.226973	-.180911	.383202
1.00	.168309	-.000000	.114281	.191091	.079712	.000001

POISSON'S RATIO = .450
THETA = 45.00/DEGREES

ROH	DEFLECTION	MR	MT	MRT	QR	QT
0	.330142	.215625	.215625	.289855	-.500000	0
.10	.329402	.211640	.216046	.289043	-.499420	.057965
.20	.327237	.199913	.217173	.286432	-.495370	.115757
.30	.323798	.181173	.219147	.281534	-.484475	.172516
.40	.319329	.156745	.221815	.273666	-.463849	.226100
.50	.314152	.128622	.224727	.262211	-.432065	.272871
.60	.308630	.099375	.226845	.247033	-.391011	.308590
.70	.303139	.071727	.226297	.228984	-.348951	.331759
.80	.298019	.047531	.220165	.210261	-.324763	.351616
.90	.293538	.025884	.204386	.194006	-.354665	.404017
1.00	.289883	-.000000	.173822	.182126	-.500001	.579709

POISSON'S RATIO = .450
THETA = 60.00 DEGREES

ROH	DEFLECTION	MR	MT	MRT	QR	QT
0	.330142	.670698	.360552	.251022	-.500000	0
.10	.330717	.669091	.360646	.248738	-.476730	.049702
.20	.332465	.664548	.360767	.241977	-.433092	.096399
.30	.335441	.657824	.360466	.231038	-.406557	.137158
.40	.339726	.649928	.359100	.216502	-.370893	.169378
.50	.345411	.641767	.356019	.199248	-.334126	.191208
.60	.352581	.633752	.350867	.180338	-.297521	.201780
.70	.361306	.625548	.344029	.160725	-.259546	.200316
.80	.371652	.616330	.337051	.140866	-.209979	.182492
.90	.383649	.606227	.333370	.126012	-.119206	.131474
1.00	.397549	-.000000	.338436	.100095	.079711	.000002

POISSON'S RATIO = .450
THETA = 75.00 DEGREES

ROH	DEFLECTION	MR	MT	MRT	QR	QT
0	.330142	-.035397	.466647	.144928	-.500000	0
.10	.331678	-.034128	.465382	.142951	-.450085	.028489
.20	.336265	-.030437	.461573	.137271	-.401907	.054134
.30	.343834	-.024682	.455217	.128577	-.357160	.074706
.40	.354279	-.017485	.446309	.117833	-.317390	.089001
.50	.367460	-.009690	.434878	.106065	-.283926	.096932
.60	.383215	-.002208	.420816	.094204	-.258328	.099417
.70	.401372	-.004168	.403552	.083028	-.244378	.098461
.80	.421754	-.008672	.381487	.073215	-.253367	.098415
.90	.444179	-.009440	.351305	.065366	-.315330	.109362
1.00	.468472	-.000000	.307399	.059642	-.500001	.155331

POISSON'S RATIO = .450
THETA = 90.00 DEGREES

ROH	DEFLECTION	MR	MT	MRT	QR	QT
0	.330142	-.074230	.505480	.000000	-.500000	0
.10	.332029	-.071673	.503480	.000000	-.442603	.000000
.20	.337650	-.064387	.497621	.000000	-.388517	.000000
.30	.346881	-.053439	.488284	.000000	-.340446	.000000
.40	.359533	-.040351	.475981	.000000	-.304079	.000000
.50	.375375	-.026853	.461277	.000000	-.267889	.000000
.60	.394158	-.014715	.444814	.000000	-.242699	.000000
.70	.415638	-.005663	.427573	.000000	-.219950	.000000
.80	.439606	-.001104	.411387	.000000	-.186851	.000001
.90	.465917	-.000938	.399654	.000000	-.111238	.000001
1.00	.494439	.000000	.397977	.000000	.079710	.000003

POISSON'S RATIO = .500
THETA = 0 DEGREES

ROH	DEFLECTION	MR	MT	MRT	QR	QT
0	.354117	.504464	-.066964	0	-.500000	0
.10	.350532	.501202	-.071759	0	-.557720	0
.20	.339787	.491370	-.086365	0	-.619048	0
.30	.321917	.474830	-.111499	0	-.688362	0
.40	.296973	.451315	-.148536	0	-.772080	0
.50	.265022	.420326	-.199847	0	-.880580	0
.60	.226134	.380810	-.269350	0	-.1032475	0
.70	.180371	.330255	-.363360	0	-.1262159	0
.80	.127782	.262514	-.491700	0	-.1633493	0
.90	.068423	.163108	-.669022	0	-.2262976	0
1.00	.002458	-.000000	-.916071	0	-.3357143	0

POISSON'S RATIO = .500
THETA = 15.00/DEGREES

ROH	DEFLECTION	MR	MT	MRT	QR	Q T
0	.354117	.466186	-.028686	.142857	-.500000	0
.10	.351916	.462408	-.032380	.144055	-.543773	.029072
.20	.341338	.450963	-.043480	.147746	-.601256	.061231
.30	.325461	.431494	-.062012	.154243	-.656104	.100578
.40	.303424	.403327	-.087911	.164104	-.715637	.152635
.50	.275430	.365358	-.120811	.178175	-.779952	.226997
.60	.241768	.316000	-.159653	.197593	-.845652	.339488
.70	.202841	.253407	-.202063	.223634	-.900911	.518055
.80	.159205	.176522	-.243488	.257178	-.915644	.811321
.90	.111611	.087911	-.276148	.297423	-.825291	1.302714
1.00	.061015	-.000000	-.287995	.339183	-.500002	2.132601

POISSON'S RATIO = .500
THETA = 30.00/DEGREES

ROH	DEFLECTION	MR	MT	MRT	QR	Q T
0	.354117	.361687	.075893	.247436	-.500000	0
.10	.351964	.357093	.074525	.248357	-.528280	.049982
.20	.345555	.343491	.070618	.251041	-.554671	.102927
.30	.335045	.320659	.064780	.255205	-.576555	.161705
.40	.320703	.288495	.058078	.260237	-.589755	.228680
.50	.302911	.247203	.052072	.264991	-.587612	.304462
.60	.282181	.197756	.048792	.267523	-.560161	.384975
.70	.259149	.142544	.050615	.264922	-.493960	.455427
.80	.234559	.086095	.059983	.253520	-.373469	.479059
.90	.209221	.035519	.078994	.230071	-.185469	.377728
1.00	.183925	-.000000	.108929	.194856	.071430	.000001

POISSON'S RATIO = .500
THETA = 45.00/DEGREES

ROH	DEFLECTION	MR	MT	MRT	QR	Q T
0	.354117	.218750	.218750	.285714	-.500000	0
.10	.353393	.214795	.218976	.284986	-.499429	.057137
.20	.351273	.203151	.219692	.282633	-.495436	.114103
.30	.347917	.184521	.220958	.278188	-.484697	.170051
.40	.343580	.160180	.222735	.270989	-.464365	.222870
.50	.338598	.132045	.224679	.260421	-.433036	.268973
.60	.333353	.102590	.225882	.246306	-.392568	.304182
.70	.328244	.074438	.224586	.229389	-.351060	.327019
.80	.323633	.049404	.217892	.211715	-.327206	.346593
.90	.319807	.026702	.201519	.196379	-.356742	.398246
1.00	.316964	-.000000	.169643	.185714	-.500001	.571428

POISSON'S RATIO = .500
THETA = 60.00/DEGREES

ROH	DEFLECTION	MR	MT	MRT	QR	Q T
0	.354117	.075893	.361607	.247436	-.500000	0
.10	.354818	.074264	.361639	.245277	-.471149	.048992
.20	.356944	.069644	.361590	.238881	-.440751	.095022
.30	.360553	.062758	.361045	.228520	-.407892	.135199
.40	.365734	.054576	.359407	.214723	-.372737	.166958
.50	.372582	.045975	.356061	.198299	-.336496	.188477
.60	.381190	.037369	.350654	.180234	-.300414	.198897
.70	.391637	.028456	.343511	.161412	-.262981	.197454
.80	.403996	.018466	.336203	.142246	-.214122	.179885
.90	.418352	.007502	.332199	.122517	-.124646	.129596
1.00	.434825	-.000000	.337500	.102068	.071430	.000002

POISSON'S RATIO = .500
THETA = 75.00/DEGREES

ROH	DEFLECTION	MR	MT	MRT	QR	Q T
0	.354117	-.028686	.466186	.142857	-.500000	0
.10	.355860	-.027515	.464966	.140974	-.450739	.028082
.20	.361066	-.024113	.461288	.135559	-.403308	.053361
.30	.369666	-.018827	.455116	.127260	-.359200	.073639
.40	.381547	-.012257	.446426	.116979	-.319999	.087730
.50	.396566	-.005216	.435194	.105684	-.287013	.095547
.60	.414555	.001410	.421270	.094258	-.261780	.097997
.70	.435334	.006843	.404039	.083444	-.248030	.097074
.80	.458714	.010324	.381846	.073905	-.256890	.097009
.90	.484501	.010075	.351191	.066262	-.317969	.107800
1.00	.512437	-.000000	.305851	.060817	-.500001	.153112

POISSON'S RATIO = .500
THETA = 90.00/DEGREES

ROH	DEFLECTION	MR	MT	MRT	QR	Q T
0	.354117	-.066964	.594464	.000000	-.500000	0
.10	.356241	-.064541	.502555	.000000	-.443423	.000000
.20	.362569	-.057641	.496949	.000000	-.390110	.000000
.30	.372973	-.047289	.487973	.000000	-.342725	.000000
.40	.387257	-.034955	.476064	.000000	-.302935	.000000
.50	.405179	-.022307	.461705	.000000	-.271205	.000000
.60	.426477	-.011059	.445458	.000000	-.246375	.000000
.70	.450894	-.002880	.428231	.000000	-.223960	.000000
.80	.478211	.000864	.411827	.000000	-.191324	.000001
.90	.503269	.000225	.399760	.000000	-.116792	.000001
1.00	.540995	.000000	.398214	.000000	.071429	.000003

APPENDIX 2

Listing of computer programmes. All programmes are in FORTRAN IV computer language.

APPENDIX 2A.

Computer programme for the creation of tables of coefficients for the deflections and forces in circular plates simply supported on two points at opposite ends of a diameter.

APPENDIX 2B.

Computer programme for the deflections and forces in circular plates simply supported on two points at opposite ends of a diameter.

APPENDIX 2C

Computer programme for the creation of tables of coefficients for the deflections and bending moment forces in circular plates simply supported on two lengths of arcs at opposite ends of a diameter.

APPENDIX 2D

Computer programme to obtain principal stresses from micro-strains rosette strain gauge readings at a point on the surface of structures.

APPENDIX 2E

Finite element programme. BFSOLID listing.

```

PROGRAM SLAB(INPUT,OUTPUT,TAPE5=INPUT,TAPE6=OUTPUT)
PI = 3.141591
N0 = 6.0
AA = 4.0+ ALOG(2.0)
PR = 0.0
30 PR = PR + 0.05
    PR3=(3.+PR)
    PR2=(1.+PR)/PR3
    PRR =(1.+PR)/N0*(1.-PR)
    RR = 1./PRR
    WRITE(6,4) RR
    4 FORMAT(1H0)
    11 FORMAT(1H0)
    THETA = 0.0
    20 RO = -1.0
    ATHETA = THETA * PI / 180.0
    WRITE(6,4) RO,THETA
    40 FORMAT(//16X,2POISSON,S=RATIO=F9.3/10X*THETA =F9.2*/DEGREES*)
    WRITE(6,6)
    60 FORMAT(//12X,+ROH*8X*DEFLECTION*9X*MR*14X*MTR*14X*MRT*14X*GR*14X*Q
    1T*)
    10 RO = RO + 0.1
    R2 = RO + RO
    P21=(1.-R2)
    R22=1.+R2
    W1 = (1.0-R2)/64.0*(1.(5.+PR)/A(5.+PR)-R2)
    W1 = AA/(1.0-PR) - PI*PI + PRR / 12.0 - 1.0
    R41=(PR3*(1.-R2))/16.
    SUM = 0.0
    SUM1 = SUM2 = SUM3 = SUM4 = SUM5 = 0.0
    DO 1 I=2,10,2
    AI = I
    SUN = 1.0/(AI*(AI-1.))+.2.0-PRR/(AI*AI*(AI-1.)) - R2/(AI*(AI+1.))
    SUN = SUN + R0**AI * COS(AI*ATHETA)
    SUN1=(RR1+(2./AI))*R21*R0***(I-2)*COS(AI*ATHETA)
    SUN2=(RR1*R21+(2./AI)*R22)+R0***(I-2)*COS(AI*ATHETA)
    SUN3=(RR1*R21+2./AI)*R0***(I-2)*SIN(AI*ATHETA)
    SUN4=R0***(I-1)*COS(AI*ATHETA)
    SUN5=R0***(I-1)*SIN(AI*ATHETA)
    SUM = SUM + SUN
    SUM2 = SUN2 + SUN
    SUM3 = SUM3 + SUN3
    SUM4 = SUM4 + SUN4
    SUM5 = SUM5 + SUN5
    1 SUM1 = SUM1 + SUN1
    W2 = C.50 + (AI - SUM1) / (3.0 + PR)
    W = W1 + W2
    R12=0.5*PR2*SUM1
    T41=(PR3-(1.+3.+PR)*R2)/16.
    TM2=0.5*PR2*SUM2
    RM=RM1+RM2
    TH=TM1-TH0
    RTM=0.5*PR2*SUM3
    QR=-.5-(2./PR3)*SUM4
    QT=(2./PR3)*SUM5
    WRITE(6,5) RO,W,RH,T0,RTM,QR,Q1
    IF(R0.LT.1.0) GO TO 10
    THETA = THETA + 15.0
    IF(THETA.LE.90) GO TO 20
    IF(PR.LT.0.50) GO TO 30
    50 FORMAT(//10X,F5.2,6(6X,F10.6))
    STOP
    END

```

APPENDIX 2A.

BLADE.FORTRAN: PROGRAML

```

PROGRAM PLATE
WRITE(5,10)
10 FORMAT(3X,5HINPUT YOUNG'S MODULUS, POISSON'S RATIO, ROH ,THE
*TA,/,3X,3H THICKNESS, RADIIAS ,PRESSURE ,//)
READ(5,20) E,V,RO,TH,T,R,P
20 FORMAT(7F10.0)
PI = 4.*ATAN(1.0)
AA = ALOG(2.0)*4.
PR3=3.+V
PR2=(1.+V)/PR3
PR=(1.+V)/(1.-V)
RR=1./PR
THITA=TH*PI/180.
R2=RO *RO
R21=1.-R2
R22=1.+R2
W1=(1.-R2)/64.*((5.+V)/(1.+V)-R2)
WI=AA/(1.-V)-PI*PI*PR/12.-1.
RM1=(PR3*R21)/16.
SUM=0.
SUM1=0.
SUM2=0.
SUM3=0.
SUM4=0.
SUM5=0.
DO 1 I=2,100,2
AI=I
SU=1./(AI*(AI-1.))+2.*PR/(AI*AI*(AI-1.))-R2/(AI*(AI+1.))
SU=SU*RO**I*COS(AI*THITA)
SU1=(RR+(2./AI))*R21*RO**((I-2)*COS(AI*THITA))
SU2=(RR*R21+(2./AI)*R22)*R0**((I-2)*COS(AI*THITA))
SU3=(RR*R21 +2./AI)*R0**((I-2)*SIN(AI*THITA))
SU4=R0**((I-1)*COS(AI*THITA))
SU5=R0**((I-1)*SIN(AI*THITA))
SUM=SUM+SU
SUM1=SUM1+SU1
SUM2=SUM2+SU2
SUM3=SUM3+SU3
SUM4=SUM4+SU4
SUM5=SUM5+SU5
1 CONTINUE
W2=.5*(WI-SUM)/(3.+V)
W=W1+W2
RM2=.5*PR2*SUM1
TM1=(PR3-(1.+3.*V)*R2)/16.
TM2=.5*PR2*SUM2
RM=RM1+RM2
TM=TM1-TM2
RTM=.5*PR2*SUM3
QR=-.5-(2./PR3)*SUM4
GT=(2./PR3)*SUM5
D=E*T**3/(1.-V*V)
D=D/12.
R4=R**4
DEF=W*R4*P/D
C
      WRITE(3,70) RO,TH,DEF
70 FORMAT(10X,22HTHE DEFLECTION AT ROH=,F5.3,3X,9H: THETA =,F7.2,
*3X,9HDEGREES =,//20X,F12.5/)
END

```

APPENDIX 2B.

T.A. FORTRAN COMPILER (VERSION 5.3 - 13/09/78) ON THE 6200 UNDER NOS/BE 1.2 ON

F.

```
PROGRAM SEAB(INPUT,OUTPUT,TAPE5 = INPUT,TAPE6 = OUTPUT)
PI = 3.141591
N0 = 6
AALFA=2.
70 AALFA=AALFA+.5
PR = 0.0
30 PR = PR + 0.05
PR3=(3.+PR)
PR2=(1.+PR)/PR3
PRR = (1. + PR) / (1. - PR)
PRP=1./PRR
WRITE(N0,11)
11 FORMAT(1HQ)
THETA = 0.0
20 RO = -1
ALFA =AALFA*PI/180.
ATHETA = THETA * PI / 180.0
WRITE(6,40) PR,THETA,AALFA
40 FORMAT(//10X,*POISSON,S RATIO=*F9.3/10X*THETA =*F9.2*/DEGREES*/10
*X*ALFA =*F9.2*/DEGREES*)
WRITE(6,60)
60 FORMAT(//12X,*ROH*8X*DEFLECTION*9X*MR*14X*MT*14X*MRT*)
10 RO = RO + 0.1
R2 = RO * RO
R21=(1.-R2)
R22=1.+R2
W1 = (1.-R2)/64.0 * ((5.+PR)/(1.+PR) - R2)
RM1=(PR3*(1.-R2))/16.
SUI1=SUI2=SUI3=SUI4=SUI5=0.
DO 1 I=2,10,2
AI = I
AI1= 1./AI
AI2=AI1*AI1
AI3=1./(AI-1)
AI4=1./(AI+1.)
SUL1=SIN(AI*ALFA)*AI1*(AI1*AI3+2.*PRR*AI2*AI3-AI1*AI4)*COS(AI*ALF
*A)
SUL2=SIN(AI*ALFA)*AI1*(AI1*AI3+2.*PRR*AI2*AI3-RO**2*AI1*AI4)*RO
***I*COSTAI*ATHETA)
SUL3=SIN(AI*ALFA)*AI1*(2.*AI1+PRP)*R21*RC***(I-2)*COS(AI*ATHETA)
SUL3=SUL3*.5*PR2/ALFA
SUL4=SIN(AI*ALFA)*AI1*(PRP*R21+R22*2.*AI1)*RO***(I-2)*COS(AI*ATHETA
*)
SUL4=SUL4*.5*PR2/ALFA
SUL5=SIN(AI*ALFA)*AI1*(PRP*R21+2.*AI1)*RC***(I-2)*SIN(AI*ATHETA)
SUI1=SUI1+SUL1
SUI2=SUT2+SUL2
SUI3=SUI3+SUL3
SUI4=SUI4+SUL4
1 SUI5=SUI5+SUL5
SUL=(SUI1-SUI2)*.5/(ALFA*PR3)
W=W1+SUL
RM=RM1+SUI3
TM1=(PR3-(1.+3.*PR)*R2)/16.
TM=TM1-SUI4
RTM=SUI5*.5*PR2/ALFA
WRITE(6,50) RO,N,RM,TM,RTM
IF (RO.LT.1.0) GO TO 10
THETA = THETA + 15.0
IF (THETA.LE.90.) GO TO 20
IF (PR.LT.0.50) GO TO 30
IF (AALFA.LE.9.) GO TO 70
50 FORMAT(10X,F5.2,4(6X,F10.6))
STOP
END
```

APPENDIX 2C.

PRESSURE //)
STRESS.FORTRAN:PROGRAML

```
PROGRAM STRES
E=4.4E05
V=.378
E1=E/(1.-V*V)
READ(3,1) NN
1 FORMAT(I5)
WRITE(5,2) NN
2 FORMAT(//,5X,30HTHE TOTAL NUMBER OF READINGS =,I5,/)
DO 11 N=1,NN
WRITE(5,50) N
50 FORMAT(10X,32HINPUT THE STRAINS OF READING NO.,I5,/)
READ(3,4) EX,EY,EXY
EX=EX*1.0E-06
EY=EY*1.0E-06
EXY=EXY*1.0E-06
X=.5*(EX+EY)
Y=.5*(EX-EY)
Z=X-EXY
R=SQRT(Y*Y + Z*Z)
EE1=X+R
EE2=X-R
S1=E1*(EE1+V*EE2)
S2=E1*(EE2+V*EE1)
WRITE(5,10) N,EX,EY,EXY,EE1,EE2,S1,S2
10 FORMAT(2X,I3,3X,5F10.8,3X,2F10.2,/)
11 CONTINUE
4 FORMAT(3F10.0)
STOP
END
```

APPENDIX 2D.


```

233 FORMAT (A12,3HNO V E R A L L T I M E L O G, //)
  1 F8.2 /
  2 F8.2 /
  3 F8.2 /
  4 F8.2 /
  5 F8.2 /
  6 F8.2 /
  7 F8.2 /
  8 F8.2 /
  9 F8.2 /
100 FORMAT (// 4AH ** ERROR. (AT LEAST ONE LOAD CASE IS REQUIRED).)
101 FORMAT (// 3SH ** ERROR. ANALYSIS CODE (NDYN =,13,9H) IS BAD.)
102 FORMAT (// 3SH ** WARNING. ESTIMATE OF STORAGE FOR A DYNAMIC,
103          32H ANALYSIS EXCEEDS AVAILABLE CORE, // 1X)
1041 FORMAT (14I5)
      END
      SUBROUTINE INDATA (ID,X,Y,Z,T,NUMNP,NEQ)
      DIMENSION X(1),Y(1),Z(1),IJ(NUMLP),T(1)
      COMMON /EXTPR/ MOLEK,N1D
      COMMON /IPRC/ (4)
      DATA IMRCLM,/1MA,1HD,1HC/
      IP1 = IPRC(1)
      NAD = ATAN(1.0)/ 45.0
      WRITE (6,2001)
      2001 FORMAT (1X,I1,I1,I1,I1,I1,I1,I1,I1,I1,I1,I1,I1,I1,I1,I1)
      10 P1=10 IT,N,JPR,(ID(I,I,I),I=1,6),X(N),Y(N),Z(N),KN,T(N)
      11 P1=10 IT,N,JPR,(I(I,I,I),I=1,6),X(N)+Y(N)+Z(N),KN,T(N)
      IF (N.EQ.1) IT=1
      IF (IT.EQ.1) JPR=1
      IF (IT.EQ.1) GO TO 15
      OJ1 = Z(1)*RAD
      Z(1) = X(1)*COS(DUM)
      X(1) = X(1)*SIN(DUM)
      15 C1=1
      IF (NOLD.EQ.0) GO TO 50
      D1=20
      IF (C1.EQ.1) D1=10
      IF (C1.EQ.1) ID(NOLD,I)=ID(NOLD,I)
      20 C1=1
      IF (C1.EQ.0) GO TO 50
      N1=ID(NOLD)/KN
      N1=N1+1
      IF (N1.EQ.LT.1) GO TO 50
      X1H=1.0
      OX=(X(1)-X(NOLD))/XNRM
      OY=(Y(1)-Y(NOLD))/XNRM
      OZ=(Z(1)-Z(NOLD))/XNRM
      DT=(T(1)-T(NOLD))/XNRM
      K=JOLD
      DO 30 J=1,NUMN
      K=K+1
      X(J)=X(K)+DX
      Y(J)=Y(K)+DY
      Z(J)=Z(K)+DZ
      T(J)=T(K)+DT
      OJ=1
      I1(I,J)=ID(K,I)
      IF (I1(I,J).EQ.1) ID(K,I)=ID(KK,I)+KN
      30 CONTINUE
      C1=1
      51 NOLD=N
      IF (N.NE.NUMNP) GO TO 10
      IF (IPRC(1).IPRC(12).EQ.1) IPRC(1)=IPRC(1) GO TO 52
      WRITE (6,2013)
      WRITE (6,2013) (N,(ID(N,I),I=1,E),X(N),Y(N),Z(N),T(N),N=1,NUMNP)
      52 C1=1
      N1=1
      D1=6, N=1,NUMNP
      DO 61 I=1,6
      I1(I,I)=ID(N,I)
      IF (I1(I,I).NE.1) 57,58,59
      57 I1(I,I)=JFQ
      G1 TO E1
      58 I1(I,I)=C
      G0 T0
      59 I1(I,I)= -ID(N,I)
      60 C1=1
      IF (IPRC(1).IPRC(1).EQ.1) 62, IP2, E2, IPRC(4) GO TO 62
      IP1=14, I1,I2,I3,I4 (N,(ID(N,I),I=1,E),I=1,NUMNP)
      62 C1=1
      IF (I1(I,J).EQ.1) GO TO 72
      WRITE (6,101) ((IDEN,I),I=1,9),N=1,NUIMP)
      72 C1=1
      1000 FORMAT (2(A1,I1),5I5,3F14.1,15,F13.3)
      1001 FORMAT (//23H NODAL POINT INPUT DATA)
      2001 FORMAT (//23H NODAL COORDINATES / 7H NUMBER 2X 1X 4X 1HY 4X 1HZ 3X
      *   2HXX 3X 2HYY 3X 2HZZ12X 1HX 1HY 1HZ 1CX 1HT)
      2002 FORMAT (1X,A1,I1,A1,I3,5I5,2F13.3,F13.3)
      2003 FORMAT (//21H GENERATED NODAL DATA)
      2004 FORMAT (//17H EQUATION NUMBERS/
      1 35H N X Y Z XX YY ZZ / (7I5))
      2005 FORMAT (I5,6I5,4F13.3)
      END
      SUBROUTINE THICKS(MTYPE)
      CALL SOT
      RETURN
      END
      SUBROUTINE SOT
      DIMENSION MAXN(10),SIGN(10)
      DIMENSION INDO(18),AJ13(7,10,5),SIG(7,5)
      COMMON /ELPAR/ IPAR(14),NUIMP,NULN,HELTYP,N1,N2,N3,N4,N5,HTOT,NEQ
      COMMON /EM/ NS,ND,L1(63),3(43,53),J(63,4)
      COMMON /JUNK/ LT,LH,L,SEG(43),N8,17,N8,N9,N11,N12,N13,N14,
      N12,N11,N11
      COMMON /EXTRA/ MOLEK,N1D,N13V,NTU
      COMMON /J1/ J1
      J1=1,10
      MAXN(1)=J1
      SIGN(1)=J1
      32 CONTINUE
      OJ=1
      J1=1,700
      OJ=88
      J1=1,6
      808 ASIGN(I,J)=0.0
      807 S1=1
      IF (IPRC(1).EQ.0) GO TO 500
      WRITE (6,1003)
      IF (NS.(1).GT.0) GO TO 510
      WRITE (6,1003) (NPAR(K),K=1,10)
      WRITE (6,1003)
      CALL EXIT
      13 IF (NPAR(1).GT.0) GO TO 20
      WRITE (6,1003) (NPAR(K),K=1,10)
      WRITE (6,1003)
      CALL EXIT
      21 IF (NPAR(4).EQ.0) NPAR(4)=1
      IF (NPAR(7).EQ.3 .AND. NPAR(7).LE.21) GO TO 30
      WRITE (6,1003) (NPAR(K),K=1,10)
      WRITE (6,1003)
      CALL EXIT
      30 IF (NPAR(1).EQ.1) NPAR(3)=2
      IF (NPAR(1).GE.2 .AND. NPAR(1).LE.4) GO TO 40
      WRITE (6,1003) (NPAR(K),K=1,10)
      WRITE (6,1003)
      CALL EXIT
      40 IF (NPAR(1).EQ.0) NPAR(1)=2
      IF (NPAR(1).GE.2 .AND. NPAR(1).LE.4) GO TO 50
      WRITE (6,1003) (NPAR(K),K=1,10)
      WRITE (6,1003)
      CALL EXIT
      50 N6 = N5 + NUMNP
      N7 = N6 + NPAR(3)
      N8 = N7 + NPAR(3)
      N9 = N8 + NPAR(3)
      N10 = N9 + NPAR(3) * 13
      N11 = N10 + NPAR(5) * 9
      N12 = N11 + NPAR(6)
      N13 = N12 + NPAR(6)
      N14 = N13 + NPAR(6) * 7
      N15 = N14 + NPAR(8) * 8
      N16 = N15 + NPAR(3)
      N17 = N16 + NPAR(7) * 139
      IF (N17.GT.HTOT) CALL ERROR(N17-HTOT)
      CALL OVFRLAY(4HTSMC,7,0,6,6H,ECALL)

```

```

501 CONTINUE (0,247,1)
      WRITE(*,*) NUME
      DO 835 I=1,NUME
      CALL STRESS(1,I,N1),A(3),NEQ,0,INCON)
      IF(I>1) GO TO 835
      IF(N1>2) L0 TO 800
      821 T=76.34/52
      U11L=0.153/(A(11),A(3),NEQ,1,INCON)
      L03=IS/0
      X+1=7
      S1=1.1,N=1,LOC
      T1=(1.04)(1)
      S13=(1.1)=S1(SIAS)+1.0
      X1=21,K=6
      X2=21,K=5
      IF(N1-1) 836,1 MITE (0,3001) MM,L,N,(SIG(I),I=K1,K2)
      IF(N1-1) 837,1 MITE (0,4331) MM,L,N,(SIG(I),I=K1,K2)
      D1=d/2 K=K1,K2
      IF(K-1) 838,1 MITE (IAS,I)=SIG(IAS,I)+SIG(IK)
      832 CONTINUE
      IF(N1-1) 839,1 MITE (N1,I)=MM,L,N,(SIG(I),I=K1,K2)
      693 CONTINUE
      N=5000
      733 CONTINUE
      803 CONTINUE
      DO 813 I=1,NUMNP
      S1=1.1,N=1,6
      IF(S1(I)=1.1) GO TO 835
      A1G1,I,N)=SIG(I,N)/SN3(I)
      403 CONTINUE
      WRITE(*,*) 404 FORMAT(3DH AVERAGE STRESS AT NODC,,,
     2,44, NODE,CNSH,DX,6HSIG-XX,9X,6HSIG-YY,9X,6HSIG-ZZ,
     3,44, 0.45 SIG-XY,9X,6HSIG-YZ,9X,6HSIG-ZX,,/IX)
      R13=S1(C,1)
      R14=S1(B,B39)I,ISNS,(ASIG(I,N),N=1,6)
      909 F14=N(I,J,G,J,0E15.6)
      806 CONTINUE
      11 PRIN1(132) PRINCIPAL STRESSES AT EACH NODE,/,6H "NODC,19X,
     12 PRIN1-1,8X,7PRIN-2,0X,7PRIN-3,0X,9HM4X SHEAR)
      D0 121 I=1,NUMNP
      S1=A1G1,I,1
      S1=A1G1,I,2
      S1=A1G1,I,3
      S1=A1G1,I,4
      S1=A1G1,I,5
      S1=A1G1,I,6
      S1=A1G1,I,7
      S1=A1G1,I,8
      S1=A1G1,I,9
      S1=A1G1,I,10
      S1=A1G1,I,11
      S1=A1G1,I,12
      S1=A1G1,I,13
      S1=A1G1,I,14
      S1=A1G1,I,15
      S1=A1G1,I,16
      S1=A1G1,I,17
      S1=A1G1,I,18
      S1=A1G1,I,19
      S1=A1G1,I,20
      S1=A1G1,I,21
      S1=A1G1,I,22
      S1=A1G1,I,23
      S1=A1G1,I,24
      S1=A1G1,I,25
      S1=A1G1,I,26
      S1=A1G1,I,27
      S1=A1G1,I,28
      S1=A1G1,I,29
      S1=A1G1,I,30
      S1=A1G1,I,31
      S1=A1G1,I,32
      S1=A1G1,I,33
      S1=A1G1,I,34
      S1=A1G1,I,35
      S1=A1G1,I,36
      S1=A1G1,I,37
      S1=A1G1,I,38
      S1=A1G1,I,39
      S1=A1G1,I,40
      S1=A1G1,I,41
      S1=A1G1,I,42
      S1=A1G1,I,43
      S1=A1G1,I,44
      S1=A1G1,I,45
      S1=A1G1,I,46
      S1=A1G1,I,47
      S1=A1G1,I,48
      S1=A1G1,I,49
      S1=A1G1,I,50
      S1=A1G1,I,51
      S1=A1G1,I,52
      S1=A1G1,I,53
      S1=A1G1,I,54
      S1=A1G1,I,55
      S1=A1G1,I,56
      S1=A1G1,I,57
      S1=A1G1,I,58
      S1=A1G1,I,59
      S1=A1G1,I,60
      S1=A1G1,I,61
      S1=A1G1,I,62
      S1=A1G1,I,63
      S1=A1G1,I,64
      S1=A1G1,I,65
      S1=A1G1,I,66
      S1=A1G1,I,67
      S1=A1G1,I,68
      S1=A1G1,I,69
      S1=A1G1,I,70
      S1=A1G1,I,71
      S1=A1G1,I,72
      S1=A1G1,I,73
      S1=A1G1,I,74
      S1=A1G1,I,75
      S1=A1G1,I,76
      S1=A1G1,I,77
      S1=A1G1,I,78
      S1=A1G1,I,79
      S1=A1G1,I,80
      S1=A1G1,I,81
      S1=A1G1,I,82
      S1=A1G1,I,83
      S1=A1G1,I,84
      S1=A1G1,I,85
      S1=A1G1,I,86
      S1=A1G1,I,87
      S1=A1G1,I,88
      S1=A1G1,I,89
      S1=A1G1,I,90
      S1=A1G1,I,91
      S1=A1G1,I,92
      S1=A1G1,I,93
      S1=A1G1,I,94
      S1=A1G1,I,95
      S1=A1G1,I,96
      S1=A1G1,I,97
      S1=A1G1,I,98
      S1=A1G1,I,99
      S1=A1G1,I,100
      S1=A1G1,I,101
      S1=A1G1,I,102
      S1=A1G1,I,103
      S1=A1G1,I,104
      S1=A1G1,I,105
      S1=A1G1,I,106
      S1=A1G1,I,107
      S1=A1G1,I,108
      S1=A1G1,I,109
      S1=A1G1,I,110
      S1=A1G1,I,111
      S1=A1G1,I,112
      S1=A1G1,I,113
      S1=A1G1,I,114
      S1=A1G1,I,115
      S1=A1G1,I,116
      S1=A1G1,I,117
      S1=A1G1,I,118
      S1=A1G1,I,119
      S1=A1G1,I,120
      S1=A1G1,I,121
      S1=A1G1,I,122
      S1=A1G1,I,123
      S1=A1G1,I,124
      S1=A1G1,I,125
      S1=A1G1,I,126
      S1=A1G1,I,127
      S1=A1G1,I,128
      S1=A1G1,I,129
      S1=A1G1,I,130
      S1=A1G1,I,131
      S1=A1G1,I,132
      S1=A1G1,I,133
      S1=A1G1,I,134
      S1=A1G1,I,135
      S1=A1G1,I,136
      S1=A1G1,I,137
      S1=A1G1,I,138
      S1=A1G1,I,139
      S1=A1G1,I,140
      S1=A1G1,I,141
      S1=A1G1,I,142
      S1=A1G1,I,143
      S1=A1G1,I,144
      S1=A1G1,I,145
      S1=A1G1,I,146
      S1=A1G1,I,147
      S1=A1G1,I,148
      S1=A1G1,I,149
      S1=A1G1,I,150
      S1=A1G1,I,151
      S1=A1G1,I,152
      S1=A1G1,I,153
      S1=A1G1,I,154
      S1=A1G1,I,155
      S1=A1G1,I,156
      S1=A1G1,I,157
      S1=A1G1,I,158
      S1=A1G1,I,159
      S1=A1G1,I,160
      S1=A1G1,I,161
      S1=A1G1,I,162
      S1=A1G1,I,163
      S1=A1G1,I,164
      S1=A1G1,I,165
      S1=A1G1,I,166
      S1=A1G1,I,167
      S1=A1G1,I,168
      S1=A1G1,I,169
      S1=A1G1,I,170
      S1=A1G1,I,171
      S1=A1G1,I,172
      S1=A1G1,I,173
      S1=A1G1,I,174
      S1=A1G1,I,175
      S1=A1G1,I,176
      S1=A1G1,I,177
      S1=A1G1,I,178
      S1=A1G1,I,179
      S1=A1G1,I,180
      S1=A1G1,I,181
      S1=A1G1,I,182
      S1=A1G1,I,183
      S1=A1G1,I,184
      S1=A1G1,I,185
      S1=A1G1,I,186
      S1=A1G1,I,187
      S1=A1G1,I,188
      S1=A1G1,I,189
      S1=A1G1,I,190
      S1=A1G1,I,191
      S1=A1G1,I,192
      S1=A1G1,I,193
      S1=A1G1,I,194
      S1=A1G1,I,195
      S1=A1G1,I,196
      S1=A1G1,I,197
      S1=A1G1,I,198
      S1=A1G1,I,199
      S1=A1G1,I,200
      301 IF(X>=0.1**2+B9**2+C
      X<=(-F**3+3*F**2-4.0*C**G1)/2.0
      X>=0.1*X1-X2*(X2)
      X>=0.1*X1-X3*(X3)
      X>=0.1*X1-X2*(X2)
      IF(X>=0.1*X1) X01=X02
      X>=0.1*X1-X2*(X2)
      X>=0.1*X1-X3*(X3)
      P13=IF((X1+X2+X3)/3.0,PM=AD3(X3)
      P14=AD3(X3,1.0)
      PM=AD3(X3)
      S11=11.1=PM
      D112=K=1,9
      513=K=6+1
      D113=J=H,I,11
      IF(SIGH(I),D1,SIGH(I)) GO TO 13
      H=MAX(I)
      I=1
      MAX(I)=MAX(H,I)
      SIGH(I)=SIGH(I)
      MAX(I)=H
      SIGH(I)=SIGH(I)
      13 CONTINUE
      21 CONTINUE
      21 CONTINUE
      305 FORMAT(9,16H OUTPUT FIRST TEN MAXIMUM PRINCIPAL STRESSES (IN DECE
      14 INCHES DRAFTED // 63H WOKE NO MAX PR
      21101 PRINCIPAL STRESS //)
      D114,I=1,16
      SIGH(I)=SIGH(I),SIGH(I)
      44 CONTINUE
      3005 FORMAT(15X,15,25X,E12.4)
      3006 RETURN
      1000 F23HAT (53H121 - N D O E S O L I J E L E M E N T I N P U T,
      1001 1 SCH D A T A //3AH3C C H T R O L I N F O R M A T I O N , / 1 X)
      1002 F23HAT (32H NO 1/C SOLID ELEMENTS SPECIFIED , / 1 X)
      1003 F23HAT (32H NO MATERIALS REQUESTED , / 1 X)
      1004 F23HAT (43H MAXIMUM NUMBER OF NODES MUST BE GE.3 . AND. LE.21, / 1 X)
      1005 F23HAT (15H INTEGRATION ORDER MUST BE 2 . AND. LE.4, / 1 X)
      2001 F23HAT (54H 3 - N D O E S O L I J E L E M E N T S T R E S ,
      134 E 3 //
      23H ELEMENT LOAD LOCATION , IX,6HSIG-XX,9X,6HSIG-YY,9X,6HSIG-ZZ,
      3 F23HAT (13,1L,I,9,6E15.6)
      4131 FORMAT ( 14X,19,6E15.6)
      5033 FORMAT ( / )
      E12) SUBROUTINE INL(I,D,TR,THASS,NUHNP,HEQ,LL)
      D1 IF NODN ID(NUHNP,6),D(HEQ,LL),TR(6,LL),THASS(HEQB)
      D1 NDN / JUNK / R(6),TAA(6)
      D1 NDN / EXTRX / MODEX,HTA
      NT=3
      RE1NDO NT
      KSHF=0
      D1 IT(5,2002)
      IF(HD0TX.EQ.1) GO TO 50
      D0 750 I=1,HEQ3
      D1 I=3(I)=
      C1,75,K=1,LL
      C1,75,K=1,LL
      D1 J=6,N=1,HUMNP
      D0 110 I=1,6
      TXM(I)=0
      C0 110 J=1,LL
      101 T2(I,I,J)=0
      D1 I=1,N=1) GO TO 300
      150 IF(N,NE,NH) GO TO 400
      D2 2JC I=1,6
      IF(LI,J,J,180,190
      181 T1(111)=R(I)
      D0 100 J=1,J,J
      191 T2(I,L,T2(I,I))
      200 C1 CONTINUE
      301 RE1D(21,145)I,N,L,R
      D1 N,L,R) GO TO 150
      D1 T1=0.2011,N,L,R
      G1 T1=0
      400 IF(10NEX.EQ.1) GO TO 900
      D0 H13,J=1,6
      D1 J=1,J(J,J,KSHF
      D1 J=1,J,D1,I8,J,500
      500 D1 J=1,J,K=1,LL
      D1 J=1,K=1,LL
      D1 MASS(111)=THASS(J)
      610 IF(L1,NH,EQ.1) GO TO 800
      D1 T1=0.1,N,L,Q
      700 J(I,J)=3.0
      800 C1 NUF
      D1 C1 NUF
      IF(HD0EX.EQ.1) RETURN

```

```

      501 IF(J-JJ) 5,1,5,6,3,4
      502 KKE=I+KK,I-(I-1)*J/2+J
      503 GO TO 504
      504 KKE=I+KK,J-(J-1)*J/2+I
      505 C(I,I,J)=A(I,I,KK)*SS(KK)
      506 C(I,I,J)=B(I,I,J)
      507 CONTINUE
      508 IF (I>4,0,I,1) GO TO 700
      509 JJJ=I,I=1,NQD
      510 I=I+1,I-NSHIFT
      511 IF(I>1,1,NE20,AND.II.LE.NEBO) GO TO 660
      512 C(I,I,J)=B(I,I,J)
      513 N(I,I,J)=LRC,IS(I),I=1,LRC
      514 N(I,I,J)=HJM7+1
      515 CONTINUE
      516 A(I,I,J)=1,NEQD
      517 A(I,I,J)=ANORM+A(L,1)
      518 IF ((A(L,1)).NE.0.) NOEG=NOEG + 1
      519 IF ((A(L,1)).LE.0.) A(L,1)=E+20
      520 IF ((A(L,1)).EQ.0.) VVV=VVV + 1
      521 C(I,I,J)=B(I,I,J)
      522 IF(I>1,1,NE20,I,1) GO TO 716
      523 A(I,I,J)=A(I,I,J)+A0* TMASS(I)
      524 A(I,I,J)=(A(I,I,J),I=1,NQD),J=1,MJAND
      525 GO TO 723
      526 WRITE (91, (TMASS(I),I=1,NE20),J=1,MJAND), ((B(I,L),I=1,NE20),L=1,LL)
      527 WRITE (91, (TMASS(I),I=1,NE20),J=1,MJAND)
      528 IF ((I>1,1,NE20,I,1) VVV=VVV + 1
      529 C(I,I,J)=B(I,I,J)
      530 A(I,I,J)=ANORM+A(L,1)
      531 IF ((A(L,1)).NE.0.) NOEG=NOEG + 1
      532 IF ((A(L,1)).LE.0.) A(L,1)=E+20
      533 IF ((A(L,1)).EQ.0.) VVV=VVV + 1
      534 CONTINUE
      535 IF(I>1,1,NE20,I,1) GO TO 726
      536 C(I,I,J)=X(I,I,J)
      537 A(I,I,J)=A(I,I,J)+A0* TMASS(I)
      538 WRITE (91, (A(I,I,J),I=K,NE20),J=1,MJAND)
      539 GO TO 729
      540 WRITE (91, (TMASS(I),I=K,NE20),J=1,MJAND)
      541 IF ((I>1,1,NE20,I,1) VVV=VVV + 1
      542 C(I,I,J)=B(I,I,J)
      543 A(I,I,J)=ANORM+NE20
      544 IF ((I>1,1,NE20,I,1) GO TO 730
      545 WRITE (91,101)
      546 STOP
      547 A(I,I,J)=(ANORM/NOEG)*1.E-8
      548 RETURN
      549 FORMAT (+F10.0)
      550 FORMAT (I15,F13.0)
      551 FORMAT (15HSTRUCTURE WITH NO DEGREES OF FREEDOM. CHECK DATA )
      552 FORMAT (15H MULTPLIERS,15H LCAD CASE,12X,1HA,9X,1HB,9X,1HD,9X,1IX)
      553 FORMAT (15H10 TIME - STEP SOLUTION ,15H0N TIME IN FORMATTION //,
      554 32HNUMBER OF TIME VARYING FUNCTIONS =, I5
      555 32HSECOND MOTION INDICATOR =, I5 //)
      556 4X, 35HACCELERATION INPUT, //, I5
      557 4X, 35HNUMBER OF A21 MOTION TIMES =, I5
      558 4X, 26HQU, ALL FUNCTIONS ACTIVE, /
      559 4X, 16HNUMBER OF SOLUTION TIME STEPS =, I5 //,
      560 4X, 25HINPUT (PRTIN) TIME INTERVAL =, I5 //,
      561 4X, 35HSOLUTION TIME INCREMENT =, E14.4 //
      562 4X, 35HPROPORTIONAL DAMPING, /, E14.4 //
      563 4X, 35HNONPROPORTIONAL DAMPING, /, E14.4 //
      564 4X, 35HTIMELESS-PROPORTIONAL DAMPING, /, E14.4 // IX)
      565 FORMAT (12FH*** ERROR ZERO TIME STEP, / IX)
      566 SUBROUTINE PRINTD (I,J,B,NE20,NU1P,LL,NBLOCK,NEQ,NT,NQ)
      567 NT=1,I=1,I-NU1P,6,I-3(NE20,LL),D(6,LL)
      568 RE/I3=8
      569 READ (8) ID
      570 NE=I
      571 N=NE,I=NBLOCK
      572 IF ((I>1,1,NE20,I,1) GO TO 55
      573 IF ((I>1,1,NE20,I,1) GO TO 55
      574 REWIND 8

```



```

14  DO 15 J=1,N
15  WRITE (6,3001) NDIS,NUMMAT,MAXTP,NORTHO,NOLS,MAXV00,HOPSET,INTRS,
1   CALL INP21      INTL              (NUIMAT,MAXTP,NORTHO,NOLS,HOPSET,WT3SV,NUINP,X,
1                                     Y,Z,DEH,RHU,HTP,LE,DOA,NFACE,LT,PHA,LGK,MAXPTS)
1   READ(I,J)        NREAD = J
1   IF(MAXNOJ.GT.3) NREAD = 21
1   WRITE(6,3011) (I,I=1,3)
1   IF(4*XNOJ.GT.3) I=I+3
1   NEL = [I,3C10] (I,I=3,21)
1   NEL = [5,1000] INEL,NDIS,NXYZ,NMAT,MAXES,IOP,TZ,KG,NRSINT,NTINT
1   NEL = [5,1100] (I,I=1,9),I=ED1,I=1,NREAD)
1   WRITE(I,3012) I=ED1,I=1,NREAD
1   IF(NEL.GT.0) GO TO 51
1   NEL = [5,1200] INEL
1   NEL = [5,1400] CALL EXIT
51  READ(I,3013) INEL,NDIS,NXYZ,NMAT,MAXES,IOP,TZ,KG,NRSINT,NTINT
1   I=ED1,I=1,NREAD)
1   I=ED1,I=1,NDIS = MAXNOJ
1   IF(NDIS.GT.0) MAXNOJ GO TO 5051
1   WRITE(6,3014) INEL,NDIS,NXYZ,NMAT,MAXES,IOP,TZ,KG,NRSINT,NTINT
1   I=REUSE([5,15],I=1,4)
1   I=REUSE([5,15],I=1,4),NDIS,IAXNOO
1   CALL EXIT
5051 IF(NDIS.GT.81) GO TO 52
1   NEL = [5,16] NDIS
1   CALL EXIT
52  IF(NXYZ.EQ.0) NXYZ = NDIS
1   IF(NXYZ.EQ.0,NDIS) GO TO 5052
1   WRITE(I,3016) NXYZ,NDIS
1   WRITE(I,3017)
1   K1EX = 1
1   K2EX = 1
5052 IF(IXYZ.EQ.0) GO TO 53
1   WRITE(I,3024) NXYZ
1   WRITE(I,3025)
1   K1EX = 1
53  IF(NMAT.GE.1 .AND. NMAT.LE.NUMMAT) GO TO 54
1   WRITE(I,3025) INEL,NDIS,NXYZ,NMAT,MAXES,IOP,TZ,KG,NRSINT,NTINT
1   I=REUSE([5,15],I=1,4)
1   I=REUSE([5,15],I=1,4)
1   I=REUSE([5,15],I=1,4)
1   K1EX = 1
54  IF(MAXES.LE.4*CRH0) GO TO 55
1   WRITE(I,3025) INEL,NDIS,NXYZ,NMAT,MAXES,IOP,TZ,KG,NRSINT,NTINT
1   I=REUSE([5,15],I=1,4)
1   I=REUSE([5,15],I=1,4)
1   I=REUSE([5,15],I=1,4)
1   K1EX = 1
55  IF(T4.GE.1 .AND. T4.LE.HOPSET) GO TO 56
1   WRITE(I,3025) INEL,NDIS,NXYZ,NMAT,MAXES,IOP,TZ,KG,NRSINT,NTINT
1   I=REUSE([5,15],I=1,4)
1   I=REUSE([5,15],I=1,4)
1   I=REUSE([5,15],I=1,4)
1   K1EX = 1
56  D1 = 57,I=1,4
1   IF(L5(I).EQ.1) NEL,LS(I),LE,NDIS,GO TO 57
1   WRITE(I,3012) INEL,NDIS,NXYZ,NMAT,MAXES,IOP,TZ,KG,NRSINT,NTINT
1   I=ED1,I=1,J=1,LS(I)
1   WRITE(I,3022) LS(I)
1   WRITE(I,3025)
1   K1EX = 1
57  D1 = 58,I=1,2
1   IF(K2(I).EQ.1) NPSINT = INTRS
1   IF(UTINT.GT.0,LI,UTINT = INTT
1   D2 = 58,I=1,4
1   IF(L5(I).GT.0,EQ.1) INEL,NDIS,NXYZ,NMAT,MAXES,IOP,TZ,KG,NRSINT,NTINT
1   I=ED1,I=1,J=1,LS(I)
1   LS(I) = 1,NDIS(I)
1   CALL EXIT
58  D1 = 59,I=1,4
1   IF(M1.EQ.0) GO TO 60
1   D2 = 59,I=1,4
1   IF(UTD1(I).LT.0) GO TO 59
1   D1 = 59,I=1,4
1   NDIS(I) = I
1   IF(HD1(I).LE.NUMNP) GO TO 59

```



```

      152H) 1/1X) AVERAGE TEMPERATURE ((F10,2,5H) F1P,
      1 1MH ELEMENT (,I5,29H) OUT OF RANGE FOR MATERIAL (,I3,
      2 2MH , 1X)
      4,34 FTR1AT T12A,31H PROCED IN DATA CHECK ONLY MODE. / IX)
      E1J
      SUBROUTINE INP21 (INUMAT,MAXTP,NORTH0,NOLS,NOPGET,HT1SV,HU1NP,X,
      Y,Z,DEH,RHO,HTP,EE,DCA,NFACE,L1,PH4,LOC,MAXPTS)
      COMMON /JUNK/ D4M(6),XLFI(4),YLF(4),ZLF(4),PLF(4),
      COMMON /EXTRA/ H03X,M1B
      COMMON /X/ X(11)*Y(11)*Z(11),PH1(1),HTP(1),EE((MAXTP,13,1),
      DCA(3,3,1),PHAC(1,1),L1,PH4(1,1),LOC(8,1),
      UTENSION MAXPI(11),
      HEC(6)
      DO 10 I=1,10
      CALL C1T1H
      K10=19.19811 M,NTP(I),DEN(I),RHO(I),HED(N),N=1,6
      IF(K10.GE.1.0) RHO(I)=DEN(I)/386.4
      IF(HTP(I).LT.0.0) HTP(I)=1
      ZE1=(0.3*Z(2) M,HTP(1),DEN(I),RHO(I),HED(N),N=1,6)
      ZE1=0.002
      CALL C1T1H
      2 IF(HTP(1).LE.MAXTP) GO TO 4
      ZE1=(0.4*0.2) MAXTP
      CALL C1T1H
      4 NT=HTP(1)
      DO 5 I=1,NT
      DO 51 I=1,13) (EE(K,1,M),F,VG,VP,GG,GP,EG,EP,(EE(K,L,M),L=11,13)
      DO 52 I=1,13) (EE(K,1,M),F,EG+25*EGP,
      DO 53 I=1,13) (EE(K,1,M),F,EGP/(F*EGP+0.25*EG*0.3375)
      DO 54 I=1,13) (EE(K,1,M),F,VG+25*VG,
      DO 55 I=1,13) (EE(K,2,M)/EE(K,3,M)
      DO 56 I=1,13) (EE(K,3,M)+EG*VG*GP)
      DO 57 I=1,13) (EE(K,4,M))
      DO 58 I=1,13) (EE(K,5,M))
      DO 59 I=1,13) (EE(K,6,M))
      DO 60 I=1,13) (EE(K,7,M))
      DO 61 I=1,13) (EE(K,8,M))
      DO 62 I=1,13) (EE(K,9,M))
      DO 63 I=1,13) (EE(K,10,M))
      DO 64 I=1,13) (EE(K,11,M))
      DO 65 I=1,13) (EE(K,12,M))
      DO 66 I=1,13) (EE(K,13,M))
      6 C1T1H
      IF(LT(1).LT.1) GO TO 10
      DO 3 I=2,NT
      IF(LT(I).LT.1) GT+EE(J-1,1,M)) GO TO 8
      WRITE (6,4033)
      CALL EXIT
      8 C1T1H
      IF(LT(1).EQ.0) GO TO 12
      DO 21 I=1,10
      WRITE (NT,I) M,HTP(M),DEN(M),RHO(M)
      NT=HTP(M)
      WRITE (NT,I) ((EE(K,L,M),L=1,13),K=1,NT)
      11 C1T1H
      12 IF(WP1TH0.EQ.0) GO TO 21
      WRITE (6,3044)
      DO 22 J=1,10
      WRITE (5,133) N,NI,NJ,NK
      WRITE (5,3119) N,NI,NJ,NK
      * WRITE (NT,I) N,NI,NJ,NK
      * WRITE (NT,I) N,NI,NJ,NK
      IF(N,E,1,M) GO TO 13
      WRITE (6,4034)
      CALL EXIT
      13 IF(NI,NJ,0 .AND. NI.LE.NUHNP) GO TO 5015
      L=NI
      5014 WRITE (6,4035) L
      CALL EXIT
      5015 IF(NI,NJ,0 .AND. NJ.LE.NUHNP) GO TO 5016
      L=NJ
      5016 IF(NI,NJ,0 .AND. NK.LE.NUHNP) GO TO 5014
      L=NK
      5017 C1T1H
      CALL C1TP2 (DCA(1,1,M),X(MI),Y(MI),Z(MI),X(MJ),Y(MJ),Z(MJ),IERR)
      IF(E,1,3) GO TO 16
      CALL C1T1H
      16 CALL C1TP2 (X(MI),Y(MI),Z(MI),X(MK),Y(MK),Z(MK),IERR)
      IF(E,1,3) GO TO 17
      CALL C1T1H
      17 CALL C1TP2 (DCA(1,1,M),V3,DCA(1,3,M),ICPR)
      IF((E,1,3) .OR. (E,1,3)) GO TO 18
      CALL C1T1H
      18 IF((E,1,3) .OR. (E,1,3)) GO TO 20
      WRITE (6,4008)
      CALL C1T1H
      20 IF((E,1,3) .OR. (E,1,3)) GO TO 31
      WRITE (6,3030)
      DO 34 I=1,10
      WRITE (6,317) N,NFACE(M),LT(M)
      IF(I,E,1,M) GO TO 22
      WRITE (6,4010)
      CALL EXIT
      22 IF(NFACE(M).GE.1 .AND. NFACE(M).LE.6) GO TO 23
      WRITE (6,4011)
      CALL EXIT
      23 IF(LT(1).EQ.0) LT(M)=1
      IF(LT(1).GE.1 .AND. LT(M).LE.2) GO TO 24
      WRITE (6,4012)
      CALL EXIT
      24 IF(LT(1).EQ.2) GO TO 26
      READ (5,105) (PHA(I,M),I=1,4)
      DO 25 I=2,4
      25 IF(PHA(I,1).EQ.0) PHA(I,M)=PHA(1,M)
      WRITE (5,3105) (PHA(I,M),I=1,4)
      DO 26 READ (5,105) (PHA(I,M),I=1,7)
      WRITE (6,3105) (PHA(I,M),I=1,7)
      31 C1T1H
      IF(N1SV.EQ.1) GO TO 5031
      DO 513 I=1,NOLS
      WRITE (NT,I) NFACE(M),LT(M),(PHA(I,N),I=1,7)
      5030 C1T1H
      31 C1T1H
      31 IF((E,1,3) .EQ. 0) GC TO 49
      WRITE (2,3111) (1,1,1,8)
      J=4,I=1,NOPSET
      READ (5,1136) (LOC(I,J),I=1,8)
      WRITE (6,3111) R,(LOC(I,J),I=1,8)
      L=5
      J=5,I=1,8
      IF(LC(J,1).EQ.0) GO TO 36
      IF(LC(J,1).NE.1 .AND. LOC(J,M).LE.27) GO TO 35
      WRITE (6,4013) J
      NOLX=1
      36 C1T1H
      36 IF(LLGT,0) GO TO 37
      L=1
      LOC(1,1)=21
      37 NACPTSM)=L
      40 C1T1H
      40 IF(NT31V.EQ.1)
      * WRITE (NT31,(LOC(I,J),I=1,8),J=1,NOPGET)
      49 WRITE (6,3112)
      * DO 50 (6,1313) XLF,YLF,ZLF,TLF,PLF
      * WRITE (6,3113) XLF,YLF,ZLF,TLF,PLF
      * WRITE (6,1313) XLF,YLF,ZLF,TLF,PLF
      RETURN
      1001 FORMAT (2I5,2F10.5,6A6)
      1002 FORMAT (8F10.0/3F10.0)
      1003 FORMAT (4I5)
      1004 FORMAT (3I5)
      1005 FORMAT (7E19.0)
      1006 FORMAT (6I5)
      1007 FORMAT (4F10.0)
      3331 FORMAT (/48F MATERIAL PROPERTY TABLES )
      3002 FORMAT (/23HMATERIAL NUMBER = (I13,10),/
      1 1MH NUMBER OF /
      2 2MH TEMPERATURE POINTS = (I13,10),/
      3 2MH WEIGHT DENSITY = (F12.4,10),/
      4 2MH MASS/DENSITY = (F12.4,10),/
      5 2MH IDENTIFICATION = (,E8,1H),/
      6 IX,1CHTEMPERATURE,3X,3HE11,3X,3HE22,3X,3HE33,4X,3HV12,4X,3HV13,
      7 4X,3HV23,8X,3HV12,MX,3HV13,8X,3HV23,3X,7HALPHA-1,3X,7HALPHA-2,
      8 3X,7HALPHA-3,1X)
      3003 FORMAT (F12.2,F12.1,F7.3,F11.1,F2.0,3)
      3004 FORMAT (/9HMATERIAL AXIAL ORIENTATION,

```

```

1 IX,3HT A3 L F//2
2 33.1 SET NODE NODE NODE / 1X)
3 38.1 NUMBER HI NJ NKI / 1X)
3005 FORMAT (4(17))
3105 FORMAT (//5LHDISTRIBUTED SURFACE LOAD )
3207 FORMAT (//7X,27HLOAD SET NUMBER
1 11HT A R L E 3//1X)
1 74,27HLAD TYPE CODE = 16 /
1 74,27HLAD 16 // 1X)
3309 FORMAT (12H DISTRIBUTED 11X,4HP(1),11X,4HP(2),11X,4HP(3),11X,
1 4HP(4), / 1X,8HREGGORE, F15.3)
3009 FORMAT (12H HYDROSTATIC,11X,2HUA,11X,11X,4HX(S),11X,4HY(S),11X,
1 4HZ(S),11X,11X(H),11X,4HY(H),11X,4HZ(N), /
1 4X,8HPRESSURE, F15.3)
3105 FORMAT (//5SH STRESS OUTPUT REQUEST TABLE,
1 8H// SET, 8(2X,5HPOINT), / 8H NUMBER ,8(4X,1H(I,I,1H)), / 1X)
3111 FORMAT (//34H E L E M E N T L O A D C A S E ,3X,
1 21H U L T I P L I E R S ,// 31X,6HCASE A,4X,6HCASE B,4X,6HCASE C,
1 21X,3HCASE D, / 1X)
3113 FORMAT (12H X-DIRECTION GRAVITY = ,4F14.2,
1 12H Y-DIRECTION GRAVITY = ,4F14.2,
1 12H Z-DIRECTION GRAVITY = ,4F14.2,
1 12H THE-SAME LOADING = ,4F14.2 // 1X)
4001 FORMAT (12H,1E15.5*** MATERIAL CARD OUT OF ORDER., / 1X)
4002 FORMAT (52H,1E15.5*** NUMBER OF TEMPERATURE CARDS EXCEEDS USER,
1 12H,1E15.5*** 12H)
4113 FORMAT (12H,1E15.5*** TEMPERATURES MUST BE INPUT IN ASCENDING,
1 12H ORDER., / 1X)
4104 FORMAT (12H,1E15.5*** AXIS DEFINITION CARD OUT OF ORDER., / 1X)
4105 FORMAT (12H,1E15.5*** UNDEFINED MODE NUMBER, / 1X)
4106 FORMAT (12H,1E15.5*** VECTORS IJ HAS ZERO LENGTH., / 1X)
4107 FORMAT (12H,1E15.5*** VECTORS IK HAS ZERO LENGTH., / 1X)
4108 FORMAT (12H,1E15.5*** VECTORS JK HAS ZERO LENGTH., / 1X)
4109 FORMAT (12H,1E15.5*** VECTORS ARE PARALLEL., / 1X)
4110 FORMAT (12H,1E15.5*** XY AND FZ VECTORS ARE PARALLEL., / 1X)
4111 FORMAT (12H,1E15.5*** SET NUMBER MUST BE IN ASCENDING ORDER., / 1X)
4112 FORMAT (12H,1E15.5*** INVALID SURFACE FACE NUMBER., / 1X)
4113 FORMAT (12H,1E15.5*** INVALID LOAD TYPE., / 1X)
4114 FORMAT (12H,1E15.5*** INVALID OUTPUT POINT NUMBER = , 16 / 1X)

E13
SUBROUTINE CROS2 (A,B,C,IERR)
DIMENSION A(3),B(3),C(3)
X = A(1) * B(2) - A(2) * B(1)
Y = A(3) * B(2) - A(2) * B(3)
Z = A(1) * B(3) - A(3) * B(1)
XLN = SQRT(X*X+Y*Y+Z*Z)
IF (XLN.LE.1.E-18) RETURN
XLN = 1. / XLN
C(1) = Z * XLN
C(2) = Y * XLN
C(3) = X * XLN
C(1) = 0
C(2) = 0
C(3) = 0
RETURN
E14
SUBROUTINE VECTR2 (V,XI,YI,ZI,XJ,YJ,ZJ,IERR)
DIMENSION V(3)
IERR = 1
X = XJ - XI
Y = YJ - YI
Z = ZJ - ZI
L1 = SQRT(X*X+Y*Y+Z*Z)
IF (XLN.LE.1.E-18) RETURN
XLN = 1. / XLN
V(1) = Z * XLN
V(2) = Y * XLN
V(3) = X * XLN
RETURN
E15
SUBROUTINE OSSAH (D,E,TEMP,CCA,KAXCS,KMAT,NFL,DUM,ALPHA)
DIMENSION D(6,6),E(12),TLM(6,6),DCA(3,3),IPPM(3),DUM(6,6),
1 ALPHA(6)
DATA IP24 / 2,3,1 /
D(2,2) = 1,1,3
ALPHA(1,1) = E(1+5)
ALPHA(1,1) = E(1+5)
IF (E(1,1).GT.1.E-08) GO TO 15
DUM(1,1) = 0
FORMAT (12H,1E15.5)
3005 FORMAT (23HCFRPORT** MODULUS E(2I1,16H) FOR MATERIAL (,I2,
1 14H) IN ELEMENT (,I5,10H) IS ZERO., / 1X)
1 14H)
5 ITEMP(I,I) = 1.0/E(I)
21 CONTINUE
120(I,2) = -E(4)* TEMP(2,2)
120(I,3) = -E(5)* TEMP(3,2)
120(I,1) = -E(6)* TEMP(1,3)
120(I,2) = -E(7)* TEMP(2,3)
120(I,3) = -E(8)* TEMP(3,3)
120(I,1) = -E(9)* TEMP(1,2)
120(I,2) = -E(10)* TEMP(2,1)
120(I,3) = -E(11)* TEMP(3,1)
120(I,1) = -E(12)* TEMP(1,1)
120(I,2) = -E(13)* TEMP(2,2)
120(I,3) = -E(14)* TEMP(3,2)
120(I,1) = -E(15)* TEMP(1,3)
120(I,2) = -E(16)* TEMP(2,3)
120(I,3) = -E(17)* TEMP(3,3)
DO 30 J=1,3
X = 1.0/TEMP(1,J)
30 TEMP(1,J) = - TEMP(1,J)* X
DO 40 J=1,3
IF (N,E,J,1) GO TO 40
TEMP(I,J) = TEMP(I,J) + TEMP(I,J)* TEMP(N,J)
50 CONTINUE
TEMP(I,1) = X
6) CONTINUE
DO 70 I=1,6
DO 70 J=1,6
DO 80 I=1,3
DO 80 J=1,3
C(I,J) = TEMP(I,J)
D(1,1) = E(1)
D(2,1) = E(2)
D(3,1) = E(3)
IF (KAXCS(I,I)) RETURN
DO 100 I=1,3
DO 100 J=1,3
I2 = IR4(I,I)
DO 90 J=1,3
I2 = IR4(J,J)
DO 110 I=1,3
DO 110 J=1,3
I2 = IR4(I,J)
I2 = I2 + D(1,K)*TEMP(K,J)
110 D(1,I+J,J) = X
130 CONTINUE
DO 120 I=1,6
DO 120 J=1,6
X = 1.0/TEMP(K,I)*DU((K,J)
120 D(1,I,J) = X
130 CONTINUE
DO 140 I=1,6
DO 140 J=1,6
X = 1.0*TEMP(K,I)*DU((K,J)
140 D(1,I,J) = X
150 CONTINUE
DO 160 I=1,6
DO 160 J=1,6
X = 1.0/TEMP(K,I)*DU((K,J)
160 D(1,I,J) = X
170 CONTINUE
DO 180 I=1,3
DO 180 J=1,3
X = 1.0*TEMP(K,I)*E(1+9)
180 D(1,I,J) = X*2.0
200 ALPHA(1,1) = X
RETURN
E16
SUBROUTINE ST8P21 (E,B,S,XX,NOD9,H,P,GIGDT,DELT,FT,UL,XM,NEL,ND,
1 DIMENSION C(6,1),B(5,1),S(5,1),XX(3,1),NOD9(1,4(1),P13,1),
1 SIG(1,1),TEL(1,1),T(1,1),DL(1,1),M(1,1),U(1,1),ST(1,1),
2 AV(63)W(3,3),PERM(3,3),KDX(3),LUX(3)
2 COMMON /GAUSS/ XG(4,4),RUT(4,4)
25KLD3DCN
DATA IPERM / 1,4,6, 4,2,5, 6,5,3 /
VOL = 1.0
CUL = 1,1
DO 20 I=4,6
J = I-1
DO 21 K=1,J
DUM = DUM + ABS(E(K,I))
21 DO 22 I=2,3
IF (DUM.GT.1.E-08) IS = 0
IF (IS.GT.0) GO TO 24
DO 22 I=2,3
DUM = DUM + ABS(E(I,I)) - E(I-1,I-1))

```



```

P(5,11) = 1.25*RR*SH
P(5,12) = -0.25*RR*SS*TP
P(5,13) = -0.25*RR*SP*TH
P(5,14) = -0.25*RR*SP*TT
P(5,15) = -0.25*RR*SP*TH
P(5,16) = -0.25*RR*SP*TT
P(5,17) = -0.25*RR*SP*TH
P(5,18) = -0.25*RR*SP*TT
P(5,19) = -0.25*RR*SP*TH
P(5,20) = -0.25*RR*SP*TT
P(5,21) = -0.25*RR*SP*TH
P(5,22) = -0.25*RR*SP*TT
P(6,11) = -0.25*RR*SP*TH
P(6,12) = -0.25*RR*SP*TT
P(6,13) = -0.25*RR*SP*TH
P(6,14) = -0.25*RR*SP*TT
P(6,15) = -0.25*RR*SP*TH
P(6,16) = -0.25*RR*SP*TT
P(6,17) = -0.25*RR*SP*TH
P(6,18) = -0.25*RR*SP*TT
P(6,19) = -0.25*RR*SP*TH
P(6,20) = -0.25*RR*SP*TT
P(6,21) = -0.25*RR*SP*TH
P(6,22) = -0.25*RR*SP*TT
G(1,1) = 1.25*RR*SP*TT
G(1,2) = -0.25*RR*SP*TH
G(1,3) = -0.25*RR*SP*TT
G(1,4) = -0.25*RR*SP*TH
G(1,5) = -0.25*RR*SP*TT
G(1,6) = -0.25*RR*SP*TH
G(1,7) = -0.25*RR*SP*TT
G(1,8) = -0.25*RR*SP*TH
G(1,9) = -0.25*RR*SP*TT
G(1,10) = -0.25*RR*SP*TH
G(1,11) = -0.25*RR*SP*TT
G(1,12) = -0.25*RR*SP*TH
G(1,13) = -0.25*RR*SP*TT
G(1,14) = -0.25*RR*SP*TH
G(1,15) = -0.25*RR*SP*TT
G(1,16) = -0.25*RR*SP*TH
G(1,17) = -0.25*RR*SP*TT
G(1,18) = -0.25*RR*SP*TH
G(1,19) = -0.25*RR*SP*TT
G(1,20) = -0.25*RR*SP*TH
G(1,21) = -0.25*RR*SP*TT
G(1,22) = -0.25*RR*SP*TH
H(1,11) = 1.25*RR*SP*TT
H(1,12) = -0.25*RR*SP*TH
H(1,13) = -0.25*RR*SP*TT
H(1,14) = -0.25*RR*SP*TH
H(1,15) = -0.25*RR*SP*TT
H(1,16) = -0.25*RR*SP*TH
H(1,17) = -0.25*RR*SP*TT
H(1,18) = -0.25*RR*SP*TH
H(1,19) = -0.25*RR*SP*TT
H(1,20) = -0.25*RR*SP*TH
H(1,21) = -0.25*RR*SP*TT
H(1,22) = -0.25*RR*SP*TH
I:=I+-1
I:=I+-1
H(I1)=H(I1) + 0.125*H(21)
H(I2)=H(I2) + 0.125*H(21)
D) J2, J=1,3
P(J,11)=P(J,11) + 0.125*P(J,21)
P(J,12)=P(J,12) + 0.125*P(J,21)
G) J=31
33 I:=I+-1
I:=I+-1
H(I1)=H(I1) + 0.125*H(21)
H(I2)=H(I2) + 0.125*H(21)
D) J3, J=1,3
P(J,11)=P(J,11) + 0.125*P(J,21)
P(J,12)=P(J,12) + 0.125*P(J,21)
G) J=31
35 D) J6, I=1,3
H(I1)=H(I1) + 0.125*H(21)
D) J6, J=1,3
36 P(J,11)=P(J,11) - 0.125*P(J,21)
H(I1)=H(I1) + 0.125*H(21)
D) J6, J=1,3
IF (0.4,E,2,8) GO TO 51
D) J3, J=9,NN
H(I1)=H(I1) + 0.125*H(21)
D) J3, J=1,3
38 P(J,11)=P(J,11) - 0.125*P(J,21)
H(I1)=H(I1) + 0.125*H(21)
D) J3, J=1,3
P(J,11)=P(J,21)
IF (IELX.LT.IELD) RETURN
D) J3, I=1,3
D) J3, J=1,3
G) J=IELX
D) H=JUN + P(I1,K)*AX(I,J,K)
100 X(I1,J1)=0.0
D) I1,I2=1,11
D) J1,J2=1,3
1  X(I1,J1)*X(I2,J2)*X(J3,J1)
2  + X(J1,J1)*X(I2,J2)*X(J3,J2)
3  + X(J1,J3)*X(I2,J2)*X(J3,J1)
4  + X(J1,J2)*X(I2,J3)*X(J3,J1)
5  + X(I1,J1)*X(J2,J3)*X(J3,J2)
IF (0.7,G,1,9) GO TO 11
WRITE (6,300) RELR,S,T
STOP
11 IF ((IELX.LT.IELD) GO TO 42
2001 FORMAT (43HERROR*** NEGATIVE OR ZERO JACOBIAN DETERMINANT,
23H COMPUTED FOR ELEMENT (,I1,I2),
12X, 3HR , F10.5 /
12X, 3HS , F10.5 /
12X, 3HT , F10.5 / 1X)
END
C$DISPLAY (IGHE,1,10)
PROGRAM SOLEQ
COMMON A(1)
L1(1)=1.PAP/ NP(14),NUMNP,10AND,1ELTYP,N1,N2,N3,N4,N5,MTOT,NEC
C(1)=0.9/SOL / NBLOCK,NEQB,LL,NF
DIMENSION TT(4)
CALL SECOND (TT(1))
NS3=(M3*10LL)/NEQ3
NS30=(M3*10LL)/NEQ30
IF (NS3.LT.NS3) NS30=NS3
N=N3*103
M=134N + NEQB -1
CALL SECUD (A(11),A(13),A(14),NEG,10AND,LL,NBLOCK,NEQB,NS3,M,
1 CALL SECOND (TT(2))
N2=N1+NUMNP*6
N3=N2*10LL
CALL PRINIO (A(11),A(12),A(13),NEQB,NUMNP,LL,NCLOCK,NEG,2,1)
CALL SECOND (TT(3))
N3=N2*10LL
N3=N3*NEQ3*LL
L1=103*103/NEQ +12
CALL SECUD (A(11),A(12),A(13),NEQB,LL,NEQ,NEQ3*LL)
CALL SECUD (TT(4))
D) J3, K=1,3
51 TT(3)=TT(K+1)-TT(K)
WRITE (6,200) TT(1),L=1,3
2001 FORMAT (/// 4PH S L A T C S O L U T I O N T I M E L O G,
//2X,21HEQUATION SOLUTION =, F8.2 /
3 5X,21H(G)PLACEMENT OUTPUT =, F8.2 /
3 5X,21H(G)PRESS RECOVERY =, F3.2 /)
D) T1P3)

```



```

      0 J 2 3; L=1,NV
      0 J 3 2; L=1,NEQ
      0 K=3(*NEDO)
  820 X=X - 1
      X=X + NEBT + NEQ
      X=X
      1 IF=0
      1 IF=(J-2,1) NOIF=NEQ - (NOLOCK*NEQ - NEQ)
      1 J=2 L=1,NV
      1 J=2 K=1 NOIF
  850 ((K+1)=((K+K)/A(K))
      X=K + NEQ
  855 X=K + NEBT
      IF(MA,EQ,1) G0 TO 915
      IL=1
      1 L=1,NEQ
      1 J=1,NEQ
      1 J=1,XA(N)
      1 F=(J-IL) 860,870,870
  870 Z=1
      K=1
      0 J=1 L=1,NV
      X=K
      0 J=1 KK=KL,KU,INC
      0 ((K)=B(KJ) - A(KK)*B(KH)
  890 XJ=XJ - 1
      K=K + NEBT
      K=K + NEBT
      CONTINUE
      N=NEQ
      0 J=1 I=2,NEQ
      X=I + INC
      X=IXA(N)
      1 F=(KJ-XL) 910,920,920
  920 X=U
      0 J=1 L=1,NV
      X=K
      0 J=1 KK=KL,KU,INC
      0 ((K)=B(KJ) - A(KK)*B(K)
  940 X=K + NEBT
  950 X=U - 1
  915 K=X
      X=K
      1 J=1 L=1,NV
      0 J=0 K=1,NEQB
      X=K
      1 ((K)=B(KH+K)
  960 X=K + NEBT
      PRINT(ML)(A(K),K=1,NHV)
  980 FORMAT(// 46H STOP ** ZERO DIAGONAL ENCOUNTERED DURING, /
           18H EQUATION SOLUTION, /
           2 13X,16H EQUATION NUMBER = 16 )
 1010 FORMAT(// 59H WARNING ** NEGATIVE DIAGONAL ENCOUNTERED DURING,
           18H EQUATION SOLUTION, /
           2 13X,16H EQUATION NUMBER = 16, 5X, 7HVALUE =, E20.8 )
 2 RETURN
END

```

APPENDIX 3

Part of coefficients tables for the calculation of deflections and bending moments forces in circular plates simply supported on two short lengths of arcs at opposite ends of a diameter.

$$W = C_1 \frac{qa^2}{D}$$

$$M_r = C_2 q a^2$$

$$M_t = C_3 q a^2$$

$$M_{rt} = C_4 q a^2$$

in the tables coefficients C_1 to C_4 are listed under W, MR, MT and MRT respectively.

POISSON'S RATIO= .050
 THETA = 0/DEGREES
 ALFA = 2.50/DEGREES

ROH	DEFLECTION	MR	MT	MRT
.10	.237805	.518078	-136828	
.20	.235176	.515308	-141130	
.30	.227316	.506929	-150213	
.40	.214302	.492847	-167642	
.50	.195268	.472821	-193494	
.60	.173402	.446365	-229567	
.70	.145952	.412278	-273615	
.80	.114238	.367240	-344301	
.90	.078684	.302509	-431513	
1.00	.039914	.196454	-533534	
	-0.001022	-0.000000	-660799	

POISSON'S RATIO= .050
 THETA = 15.00/DEGREES
 ALFA = 2.50/DEGREES

ROH	DEFLECTION	MR	MT	MRT
.10	.237805	.474268	-0.092958	.153726
.20	.235498	.470656	-0.095017	.165040
.30	.224250	.459852	-0.101149	.169073
.40	.215439	.441306	-0.111170	.176106
.50	.200154	.414078	-0.124629	.186603
.60	.173664	.376601	-0.140548	.201151
.70	.153338	.326585	-0.157069	.220235
.80	.127673	.251374	-0.171140	.243306
.90	.097316	.179605	-0.178721	.267684
1.00	.065080	.035733	-0.176189	.283956
	-0.031891	-0.000000	-0.164723	.270025

POISSON'S RATIO= .050
 THETA = 30.00/DEGREES
 ALFA = 2.50/DEGREES

ROH	DEFLECTION	MR	MT	MRT
.10	.237805	.354352	.026898	.283582
.20	.236040	.349596	.027318	.294305
.30	.231792	.335229	.028789	.286303
.40	.222205	.310996	.031935	.289099
.50	.213526	.276674	.037751	.291235
.60	.196100	.232462	.047441	.291942
.70	.173375	.179677	.062081	.285155
.80	.151834	.121725	.082058	.269719
.90	.141214	.066157	.106376	.240973
1.00	.120934	.003250	.132122	.199329
	.100496	-0.000000	.154734	.157646

POISSON'S RATIO= .050
 THETA = 45.00/DEGREES
 ALFA = 2.50/DEGREES

ROH	DEFLECTION	MR	MT	MRT
.10	.237805	.190625	.190625	.327453
.20	.236901	.136337	.192305	.325877
.30	.234233	.173774	.197250	.320904
.40	.229927	.153895	.205112	.311871
.50	.224136	.128462	.215117	.237908
.60	.217268	.10143	.235856	.278378
.70	.203458	.072387	.235142	.253518
.80	.201037	.048784	.240098	.225123
.90	.192242	.031576	.237674	.196675
1.00	.183244	.018859	.225828	.171747
	.174175	-0.000000	.205680	.148533

POISSON'S RATIO= .050
 THETA = 60.00/DEGREES
 ALFA = 2.50/DEGREES

ROH	DEFLECTION	MR	MT	MRT
.10	.237805	.066839	.354351	.283583
.20	.237761	.035450	.354893	.280166
.30	.237641	.0121521	.332235	.270086
.40	.237485	.0016109	.357502	.253900
.50	.237347	.0010573	.357941	.232644
.60	.237281	.0006035	.356235	.207831
.70	.237331	.0003178	.352275	.181237
.80	.237527	.00010907	.346541	.154428
.90	.237887	.0001716	.340978	.128305
1.00	.233437	.00000000	.339044	.103391
	.233195	-0.000000	.333353	.082362

POISSON'S RATIO = .300
 THETA = 0/DEGREES
 ALFA = 2.50/DEGREES

ROH	DEFLECTION	MR	MT	MRT
.0	.277258	.508806	-.096398	00000000
.10	.274305	.505839	-.100543	00000000
.20	.265464	.436625	-.113195	00000000
.30	.251797	.481123	-.134972	00000000
.40	.231451	.459076	-.167146	00000000
.50	.204411	.429983	-.211821	00000000
.60	.175302	.392721	-.272396	00000000
.70	.135383	.344454	-.354033	00000000
.80	.994823	.277993	-.463978	00000000
.90	.643694	.176060	-.511241	00000000
1.00	-.001328	-.000000	-.304534	00000000

POISSON'S RATIO = .300
 THETA = 15.00/DEGREES
 ALFA = 2.50/DEGREES

ROH	DEFLECTION	MR	MT	MRT
.0	.277258	.468349	-.055849	.151323
.10	.274595	.454673	-.058840	.152564
.20	.265637	.453517	-.067802	.156381
.30	.255478	.434474	-.082670	.163071
.40	.235277	.406760	-.103247	.173146
.50	.212275	.369092	-.128895	.187336
.60	.184801	.319604	-.158256	.216479
.70	.153305	.256134	-.183710	.231138
.80	.113388	.177501	-.216011	.260589
.90	.080822	.086935	-.234201	.290587
1.00	.041530	-.000000	-.236873	.308939

POISSON'S RATIO = .300
 THETA = 30.00/DEGREES
 ALFA = 2.50/DEGREES

ROH	DEFLECTION	MR	MT	MRT
.0	.277258	.357573	.054927	.262099
.10	.275388	.352973	.054320	.262935
.20	.263828	.330938	.052639	.255325
.30	.261721	.315765	.050676	.268867
.40	.248321	.282812	.049231	.272729
.50	.232985	.240458	.049916	.275417
.60	.215130	.189807	.054209	.274530
.70	.195475	.133652	.063798	.256730
.80	.174513	.077324	.079439	.248389
.90	.152958	.029195	.091456	.217799
1.00	.131400	-.000000	.123677	.130394

POISSON'S RATIO = .300
 THETA = 45.00/DEGREES
 ALFA = 2.50/DEGREES

ROH	DEFLECTION	MR	MT	MRT
.0	.277258	.206250	.0626250	.302646
.10	.276469	.262173	.027096	.301579
.20	.274148	.196195	.0209513	.298144
.30	.270436	.171121	.0213710	.291823
.40	.265553	.146422	.0213031	.281863
.50	.259786	.118313	.0224408	.267643
.60	.253461	.039655	.0229622	.249149
.70	.246904	.063461	.0231729	.227538
.80	.240406	.041722	.0226859	.205411
.90	.234192	.023233	.0213055	.186015
1.00	.228426	-.000000	.186974	.169966

POISSON'S RATIO = .300
 THETA = 60.00/DEGREES
 ALFA = 2.50/DEGREES

ROH	DEFLECTION	MR	MT	MRT
.0	.277258	.054927	.357573	.262099
.10	.277547	.053387	.357839	.259429
.20	.271432	.043079	.357439	.251534
.30	.271951	.042847	.358810	.238804
.40	.282232	.0335813	.358174	.221972
.50	.285230	.028976	.355775	.202134
.60	.289111	.022761	.351241	.180596
.70	.293395	.015736	.345019	.158527
.80	.293642	.009927	.338769	.136554
.90	.306394	.032435	.335469	.114788
1.00	.314222	-.000000	.338791	.094247

POISSON,S RATIO=.300
 THETA = 75.00/DEGREES
 ALFA = 2.50/DEGREES

ROH	DEFLECTION	MR	MT	MRT
.0	.277258	-.055849	.468349	.151323
.10	.273335	-.054283	.465930	.149157
.20	.281544	-.049712	.462684	.142558
.30	.286822	-.042532	.455657	.132648
.40	.294067	-.033432	.445065	.120466
.50	.303148	-.023342	.433774	.107222
.60	.313915	-.013259	.419134	.093397
.70	.325209	-.004033	.401623	.081672
.80	.333472	-.003527	.379903	.070967
.90	.354756	-.007345	.351333	.062402
1.00	.371712	-.000000	.312404	.0555704

POISSON,S RATIO=.300
 THETA = 90.00/DEGREES
 ALFA = 2.50/DEGREES

ROH	DEFLECTION	MR	MT	MRT
.0	.277258	-.096336	.598896	.00000001
.10	.273623	-.093434	.566599	.00000000
.20	.282679	-.084977	.499900	.00000000
.30	.283311	-.072212	.489373	.00000000
.40	.293347	-.056326	.475735	.00000000
.50	.309575	-.040726	.459814	.00000000
.60	.322767	-.025856	.442494	.00000000
.70	.337704	-.014104	.424953	.00000000
.80	.354233	-.006995	.409062	.00000000
.90	.372132	-.004315	.397735	.00000000
1.00	.391421	-.000000	.394601	.00000000

POISSON,S RATIO=.350
 THETA = 0/DEGREES
 ALFA = 2.50/DEGREES

ROH	DEFLECTION	MR	MT	MRT
.0	.290494	.507504	.088754	.00000000
.10	.287427	.504393	.093083	.00000000
.20	.273244	.495918	.106196	.00000000
.30	.262998	.479243	.128818	.00000000
.40	.241781	.456308	.162203	.00000000
.50	.214712	.427210	.208203	.00000000
.60	.181946	.389340	.271239	.00000000
.70	.143665	.346447	.355037	.00000000
.80	.100093	.273629	.470331	.00000000
.90	.051540	.172400	.624945	.00000000
1.00	-.001419	-.000000	.331271	00000000

POISSON,S RATIO=.350
 THETA = 15.00/DEGREES
 ALFA = 2.50/DEGREES

ROH	DEFLECTION	MR	MT	MRT
.0	.290494	.457552	.349812	.149164
.10	.287735	.453865	.351981	.153292
.20	.273488	.452633	.361481	.154070
.30	.265342	.433484	.377287	.162698
.40	.246955	.405663	.399298	.170696
.50	.223056	.367934	.426703	.184820
.60	.194468	.318512	.458494	.203979
.70	.161632	.255323	.492050	.228912
.80	.125134	.277218	.523159	.259300
.90	.095742	.287200	.245165	.291794
1.00	.044382	-.000000	.250577	.316084

POISSON,S RATIO=.350
 THETA = 30.00/DEGREES
 ALFA = 2.50/DEGREES

ROH	DEFLECTION	MR	MT	MRT
.0	.290494	.358445	.260317	.258187
.10	.283576	.353865	.259508	.259943
.20	.282871	.340071	.257299	.261505
.30	.273528	.316882	.254293	.265201
.40	.261799	.284165	.251525	.269360
.50	.245047	.242124	.250436	.272581
.60	.226746	.193831	.252753	.272594
.70	.205476	.135967	.260235	.266136
.80	.184900	.179640	.274277	.249746
.90	.162737	.030877	.295472	.221163
1.00	.140529	-.000000	.123372	.184536

POISSON,S RATIO=.350
THETA = 45.00/DEGREES
ALFA = 2.50/DEGREES

ROH	DEFLECTION	MR	MT	MRT
0	.290494	.209375	.209375	.238129
.10	.289723	.205334	.210961	.297144
.20	.287457	.193454	.212117	.234030
.30	.283840	.174513	.215486	.288172
.40	.273100	.149928	.219399	.273941
.50	.273531	.121832	.224637	.265638
.60	.267471	.032979	.228594	.244353
.70	.261260	.056276	.222541	.227978
.80	.255203	.043670	.214631	.207002
.90	.249538	.024082	.210320	.138613
1.00	.244437	.000000	.193008	.173869

POISSON,S RATIO=.350
THETA = 60.00/DEGREES
ALFA = 2.50/DEGREES

ROH	DEFLECTION	MR	MT	MRT
0	.290494	.260311	.353432	.258137
.10	.291867	.258753	.368647	.255553
.20	.292004	.254365	.359186	.248156
.30	.293955	.247970	.359235	.236055
.40	.296793	.240644	.358362	.220029
.50	.303596	.233354	.355751	.201097
.60	.305437	.225524	.351031	.180479
.70	.311375	.219761	.344611	.159273
.80	.313463	.212148	.338109	.138756
.90	.326764	.203822	.334600	.116863
1.00	.335354	.000000	.338312	.096411

POISSON,S RATIO=.350
THETA = 75.00/DEGREES
ALFA = 2.50/DEGREES

ROH	DEFLECTION	MR	MT	MRT
0	.290494	.348812	.467562	.49055
.10	.291793	.47355	.466200	.146981
.20	.295307	.43036	.462118	.140691
.30	.301243	.36403	.455338	.131209
.40	.309406	.27965	.445942	.119532
.50	.319666	.18672	.434047	.106885
.60	.331369	.09494	.419650	.094055
.70	.345853	.091255	.402290	.082126
.80	.361457	.05237	.381552	.071721
.90	.371520	.07996	.351616	.063382
1.00	.396900	.000000	.311318	.056984

POISSON,S RATIO=.350
THETA = 90.00/DEGREES
ALFA = 2.50/DEGREES

ROH	DEFLECTION	MR	MT	MRT
0	.290494	.88754	.507504	.000000
.10	.292209	.85934	.505314	.000000
.20	.296512	.77889	.498925	.000000
.30	.303887	.65760	.438825	.000000
.40	.313958	.51175	.475677	.000000
.50	.326508	.35979	.463208	.000000
.60	.341305	.22849	.443219	.000000
.70	.359123	.11215	.425807	.000000
.80	.376773	.04956	.409810	.000000
.90	.397119	.003111	.398262	.000000
1.00	.419692	.000000	.395413	.000000

POISSON,S RATIO=.400
THETA = 0/DEGREES
ALFA = 2.50/DEGREES

ROH	DEFLECTION	MR	MT	MRT
0	.306406	.506244	.391244	.000000
.10	.303293	.53081	.485714	.000000
.20	.293600	.433545	.499333	.000000
.30	.277654	.477502	.412277	.000000
.40	.255442	.454684	.457357	.000000
.50	.227060	.424588	.405293	.000000
.60	.192655	.386118	.270219	.000000
.70	.152379	.336605	.357828	.000000
.80	.105388	.269428	.476582	.000000
.90	.054934	.158865	.638209	.000000
1.00	.001525	.000000	.357461	.000000

POISSON,S RATIO= .400
THETA = 15.00/DEGREES
ALFA = 2.50/DEGREES

ROH	DEFLECTION	MR	MT	MRT
0	.306406	.466896	.541890	.146872
.10	.303526	.463163	.545234	.148987
.20	.294928	.451802	.555272	.151827
.30	.231690	.432607	.571696	.158394
.40	.261965	.414674	.592440	.168318
.50	.235376	.366880	.424593	.182378
.60	.205036	.317511	.453733	.221553
.70	.171573	.254582	.495326	.226751
.80	.133164	.176977	.29984	.258550
.90	.091569	.187556	.255937	.292956
1.00	.047719	.000000	.264056	.322971

POISSON,S RATIO= .400
THETA = 30.00/DEGREES
ALFA = 2.50/DEGREES

ROH	DEFLECTION	MR	MT	MRT
0	.306406	.359372	.656228	.254390
.10	.304427	.354322	.64632	.255266
.20	.298540	.341103	.61845	.257797
.30	.288896	.318055	.657871	.261643
.40	.275751	.285555	.653752	.266889
.50	.253471	.243810	.651964	.269829
.60	.240541	.193854	.651335	.278715
.70	.213556	.138260	.656821	.285558
.80	.197199	.081921	.69182	.251051
.90	.174193	.032527	.89532	.224427
1.00	.151212	.000000	.118040	.138557

POISSON,S RATIO= .400
THETA = 45.00/DEGREES
ALFA = 2.50/DEGREES

ROH	DEFLECTION	MR	MT	MRT
0	.306406	.212500	.212500	.293744
.10	.303651	.208492	.213028	.292848
.20	.303437	.196735	.214623	.289977
.30	.299917	.177338	.217265	.284629
.40	.295317	.153407	.223773	.276105
.50	.289932	.125315	.224593	.263791
.60	.284135	.096264	.227589	.247581
.70	.273274	.069356	.227811	.228405
.80	.272669	.045594	.222386	.208546
.90	.267573	.024924	.217552	.191134
1.00	.263167	.000000	.178975	.177657

POISSON,S RATIO= .400
THETA = 60.00/DEGREES
ALFA = 2.50/DEGREES

ROH	DEFLECTION	MR	MT	MRT
0	.306406	.656228	.359372	.254390
.10	.306872	.64046	.359521	.251988
.20	.308292	.59585	.363795	.244877
.30	.310717	.553026	.359714	.233387
.40	.314224	.45410	.368592	.213143
.50	.318898	.37673	.355750	.200990
.60	.324816	.30235	.350819	.180366
.70	.332044	.22744	.344171	.159998
.80	.341641	.14337	.337384	.139514
.90	.350676	.05128	.333625	.118377
1.00	.362239	.000000	.337662	.048512

POISSON,S RATIO= .400
THETA = 75.00/DEGREES
ALFA = 2.50/DEGREES

ROH	DEFLECTION	MR	MT	MRT
0	.306406	.41890	.465890	.146873
.10	.307765	.445530	.465531	.144808
.20	.311820	.36566	.461648	.138878
.30	.313505	.330370	.455036	.129813
.40	.327717	.22581	.445969	.118626
.50	.333319	.14076	.443335	.106408
.60	.353156	.05775	.420143	.094112
.70	.363063	.01487	.402889	.082508
.80	.386870	.06929	.381098	.072454
.90	.406410	.08845	.361759	.064333
1.00	.427527	.000000	.310080	.058225

POISSON'S RATIO = .250
 THETA = 15.00/DEGREES
 ALFA = 7.50/DEGREES

ROH	DEFLECTION	MP	MT	MPT
0	.253739	.466561	.050311	.152095
.10	.251173	.462895	.063072	.153280
.20	.243507	.451773	.071341	.156918
.30	.230837	.432792	.085044	.163250
.40	.213331	.405199	.103956	.172686
.50	.191232	.367779	.127613	.186770
.60	.164880	.318795	.154526	.203040
.70	.134728	.256241	.182835	.224614
.80	.101368	.178916	.209075	.249203
.90	.065555	.089325	.228917	.272040
1.00	.028182	-0.000000	.238448	.280914

POISSON'S RATIO = .250
 THETA = 30.00/DEGREES
 ALFA = 7.50/DEGREES

ROH	DEFLECTION	MP	MT	MPT
0	.253739	.355221	.051030	.263436
.10	.251917	.350652	.050581	.264188
.20	.246497	.336330	.049419	.266322
.30	.237624	.313745	.048099	.269431
.40	.225541	.281134	.047544	.272695
.50	.210595	.239726	.048989	.274692
.60	.193235	.189258	.053830	.273264
.70	.174006	.133748	.063335	.265246
.80	.153521	.077830	.078235	.247686
.90	.132409	.029621	.098312	.219258
1.00	.111227	-0.000000	.122255	.185155

POISSON'S RATIO = .250
 THETA = 45.00/DEGREES
 ALFA = 7.50/DEGREES

ROH	DEFLECTION	MP	MT	MPT
0	.253739	.203125	.203125	.304190
.10	.252931	.199024	.204049	.303033
.20	.250550	.187252	.206792	.299375
.30	.246730	.168389	.211218	.292697
.40	.241652	.143041	.216958	.282292
.50	.235681	.116052	.223240	.267556
.60	.229037	.087495	.228719	.248428
.70	.222053	.061224	.231439	.225857
.80	.215057	.039341	.228787	.202131
.90	.208231	.021155	.218226	.180158
1.00	.201762	-0.000000	.197871	.160787

POISSON'S RATIO = .250
 THETA = 60.00/DEGREES
 ALFA = 7.50/DEGREES

ROH	DEFLECTION	MP	MT	MPT
0	.253739	.051031	.355219	.263436
.10	.253942	.049536	.355499	.268703
.20	.254557	.045355	.356140	.252647
.30	.255660	.039309	.356689	.239647
.40	.257284	.032502	.356074	.222451
.50	.259511	.025951	.353321	.202162
.60	.262404	.020153	.349333	.190120
.70	.266012	.014848	.342995	.157644
.80	.270376	.009121	.336874	.135582
.90	.275540	.002828	.330205	.114354
1.00	.281552	-0.000000	.328404	.094983

POISSON'S RATIO = .250
 THETA = 75.00/DEGREES
 ALFA = 7.50/DEGREES

ROH	DEFLECTION	MP	MT	MPT
0	.253739	-0.260311	.456561	.152095
.10	.254681	-0.058708	.465116	.149801
.20	.257487	-0.054924	.460799	.143213
.30	.262994	-0.046650	.453670	.133147
.40	.268406	-0.037266	.443872	.120740
.50	.276238	-0.026799	.431616	.107215
.60	.285526	-0.016290	.417056	.093668
.70	.296240	-0.005683	.400020	.080976
.80	.307393	-0.001113	.379663	.069799
.90	.320749	-0.005301	.354284	.050663
1.00	.334399	-0.000000	.321826	.053011

POISSON'S RATIO = .250
 THETA = 30.00/DEGREES
 ALFA = 7.50/DEGREES

ROH	DEFLECTION	MP	MT	MPT
0	.253739	-101065	.507315	.0000001
.10	.254952	-.098079	.504979	.0000000
.20	.258551	-.089005	.498178	.0000000
.30	.264428	-.076533	.497471	.0000000
.40	.272418	-.060817	.473630	.0000000
.50	.292319	-.044246	.457501	.0000000
.60	.293913	-.028727	.439955	.0000000
.70	.306988	-.016076	.422024	.0000000
.80	.321365	-.007769	.405163	.0000000
.90	.336910	-.003893	.391427	.0000000
1.00	.353541	-.000000	.383016	.0000000

POISSON'S RATIO = .300
 THETA = 30.00/DEGREES
 ALFA = 7.50/DEGREES

ROH	DEFLECTION	MP	MT	MPT
0	.264010	.505831	-.093331	0
.10	.261079	.502721	-.097395	0
.20	.252305	.493344	-.109730	0
.30	.237752	.477534	-.130951	0
.40	.217523	.454975	-.162147	0
.50	.191763	.425063	-.205155	0
.60	.150660	.396547	-.262863	0
.70	.124448	.336578	-.339569	0
.80	.083426	.268502	-.441194	0
.90	.038021	.167188	-.574964	0
1.00	-.011069	-.000000	-.747855	0

POISSON'S RATIO = .300
 THETA = 15.00/DEGREES
 ALFA = 7.50/DEGREES

ROH	DEFLECTION	MP	MT	MPT
0	.254010	.465694	-.053194	.149790
.10	.261366	.462004	-.056136	.150964
.20	.253465	.450013	-.064954	.154567
.30	.240402	.431732	-.079596	.160848
.40	.222339	.404037	-.099877	.170226
.50	.199513	.366554	-.125297	.183274
.60	.172256	.317629	-.154749	.200505
.70	.141010	.255324	-.186151	.222510
.80	.106359	.178477	-.216118	.248080
.90	.069046	.039426	-.239989	.273351
1.00	.029955	-.001000	-.252752	.287724

POISSON'S RATIO = .300
 THETA = 30.00/DEGREES
 ALFA = 7.50/DEGREES

ROH	DEFLECTION	MP	MT	MPT
0	.264010	.356040	.056460	.259444
.10	.262151	.351498	.055814	.260219
.20	.255662	.337907	.054062	.262431
.30	.247556	.314819	.051756	.265704
.40	.235230	.282432	.043827	.259276
.50	.219364	.240876	.049548	.271812
.60	.202223	.191201	.052410	.271219
.70	.182559	.135956	.059981	.264627
.80	.161602	.080057	.073041	.248932
.90	.140001	.031259	.092197	.222569
1.00	.118345	-.000000	.116596	.139643

POISSON'S RATIO = .300
 THETA = 45.00/DEGREES
 ALFA = 7.50/DEGREES

ROH	DEFLECTION	MP	MT	MPT
0	.264010	.206250	.206250	.299581
.10	.263231	.202254	.207015	.290517
.20	.260999	.190508	.209293	.295145
.30	.257190	.171776	.212992	.288968
.40	.252281	.147440	.217822	.279300
.50	.246484	.119569	.223118	.265540
.60	.240109	.090832	.227677	.247582
.70	.233484	.064082	.229674	.226294
.80	.226906	.041367	.226511	.203786
.90	.220515	.022195	.215502	.182877
1.00	.214791	-.000000	.194146	.164685

POISSON'S RATIO = .300
 THETA = 60.00/DEGREES
 ALFA = 7.50/DEGREES

ROH	DEFLECTION	MP	MT	MPT
0	.264010	.056460	.356040	.269445
.10	.264288	.054344	.356263	.256854
.20	.265140	.050685	.356747	.249193
.30	.266512	.044474	.356980	.236829
.40	.268773	.037374	.356235	.220448
.50	.271697	.030370	.353780	.201080
.60	.275452	.023961	.349173	.179927
.70	.280095	.017888	.342618	.158785
.80	.285670	.011319	.335200	.137001
.90	.292228	.004096	.329424	.116454
1.00	.299826	.000000	.327843	.097285

POISSON'S RATIO = .300
 THETA = 75.00/DEGREES
 ALFA = 7.50/DEGREES

ROH	DEFLECTION	MP	MT	MPT
0	.264010	.053194	.465694	.149791
.10	.265168	.051695	.464309	.147599
.20	.268222	.047320	.460161	.141302
.30	.273409	.040446	.453291	.131663
.40	.280533	.031727	.443805	.119774
.50	.289467	.022064	.431855	.106777
.60	.300067	.012461	.417572	.093720
.70	.312180	.003843	.400704	.081441
.80	.325658	.002906	.380357	.070584
.90	.340359	.006042	.354674	.061586
1.00	.356168	.000000	.321105	.054296

POISSON'S RATIO = .300
 THETA = 90.00/DEGREES
 ALFA = 7.50/DEGREES

ROH	DEFLECTION	MP	MT	MPT
0	.264010	.093331	.505831	.000000
.10	.265353	.090470	.503635	.000000
.20	.269345	.082327	.497111	.000000
.30	.275876	.069994	.486853	.000000
.40	.284777	.055088	.473522	.000000
.50	.295843	.039430	.457874	.000000
.60	.308853	.024870	.440697	.000000
.70	.323592	.013167	.422945	.000000
.80	.339873	.005755	.406033	.000000
.90	.357562	.002754	.392096	.000000
1.00	.376575	.000000	.333778	.000000

POISSON'S RATIO = .350
 THETA = 0/DEGREES
 ALFA = 7.50/DEGREES

ROH	DEFLECTION	MP	MT	MPT
0	.276339	.504484	.085734	0
.10	.273295	.501324	.089052	0
.20	.264182	.491791	.102793	0
.30	.249058	.475724	.124857	0
.40	.228018	.452902	.157277	0
.50	.201193	.422426	.201949	0
.60	.168752	.383369	.261881	0
.70	.137902	.332972	.341621	0
.80	.108790	.264544	.447647	0
.90	.040123	.163937	.588378	0
1.00	-.011928	-.000000	-.773237	0

POISSON'S RATIO = .350
 THETA = 15.00/DEGREES
 ALFA = 7.50/DEGREES

ROH	DEFLECTION	MP	MT	MPT
0	.276339	.464947	.046197	.147555
.10	.273500	.461232	.049317	.148717
.20	.266413	.449971	.058676	.152287
.30	.251870	.430790	.074243	.15517
.40	.233127	.402988	.095872	.167838
.50	.209417	.365444	.123124	.180853
.60	.181061	.316558	.164974	.198244
.70	.149491	.264483	.189412	.220468
.80	.112273	.173095	.223036	.246989
.90	.073161	.089541	.250863	.274523
1.00	.032029	.000000	.256814	.294330

POISSON'S RATIO = .350
 THETA = 30.00/DEGREES
 ALFA = 7.50/DEGREES

ROH	DEFLECTION	NP	MT	MOT
0	.276339	.356930	.051820	.255572
.10	.274432	.352411	.060982	.258369
.20	.268761	.339706	.058648	.258656
.30	.269471	.315946	.055371	.262088
.40	.266811	.283770	.052091	.265958
.50	.231133	.242498	.050113	.269019
.60	.212911	.193144	.051025	.269292
.70	.192678	.138171	.056496	.264026
.80	.171108	.082252	.067916	.250141
.90	.148869	.032848	.086131	.225782
1.00	.126585	-0.000000	.111116	.193998

POISSON'S RATIO = .350
 THETA = 45.00/DEGREES
 ALFA = 7.50/DEGREES

ROH	DEFLECTION	NP	MT	MOT
0	.276339	.203775	.209375	.295109
.10	.275567	.205412	.209982	.294135
.20	.273300	.193756	.211892	.291042
.30	.269577	.175146	.214782	.285350
.40	.264920	.150913	.218708	.276396
.50	.259319	.123051	.223024	.263584
.60	.253206	.094129	.226658	.246769
.70	.246923	.066002	.227858	.226718
.80	.240780	.043367	.224216	.205392
.90	.235032	.023025	.212726	.185516
1.00	.229868	-0.000000	.190344	.168467

POISSON'S RATIO = .350
 THETA = 60.00/DEGREES
 ALFA = 7.50/DEGREES

ROH	DEFLECTION	NP	MT	MOT
0	.276339	.061821	.356929	.255572
.10	.276700	.060282	.357094	.253114
.20	.277801	.055945	.357419	.245843
.30	.279602	.040570	.357427	.234094
.40	.282445	.042180	.356440	.218505
.50	.285138	.034727	.353763	.200330
.60	.290845	.027706	.348961	.179850
.70	.296627	.120886	.342209	.159104
.80	.303536	.013485	.334637	.138555
.90	.311628	.005343	.328533	.118491
1.00	.320969	-0.000000	.327111	.099519

POISSON'S RATIO = .350
 THETA = 75.00/DEGREES
 ALFA = 7.50/DEGREES

ROH	DEFLECTION	NP	MT	MOT
0	.276339	-.046197	.464947	.147556
.10	.277527	-.044800	.463616	.145463
.20	.281072	-.041727	.459624	.139448
.30	.286912	-.034341	.452991	.132234
.40	.294947	-.026276	.443799	.118937
.50	.305050	-.017400	.432130	.106352
.60	.317074	-.008687	.418065	.093770
.70	.330865	-.001041	.401724	.081892
.80	.346269	-.004673	.380944	.071345
.90	.363140	-.006778	.354918	.062578
1.00	.381356	-0.000000	.320219	.055543

POISSON'S RATIO = .350
 THETA = 90.00/DEGREES
 ALFA = 7.50/DEGREES

ROH	DEFLECTION	NP	MT	MOT
0	.276339	-.095734	.504834	.090000
.10	.277330	-.093022	.502362	.090000
.20	.282265	-.075273	.496158	.090000
.30	.286532	-.063666	.496322	.090000
.40	.299459	-.049451	.473465	.090000
.50	.311838	-.034689	.458260	.090000
.60	.326440	-.021069	.441408	.090000
.70	.343045	-.010297	.423794	.090000
.80	.361462	-.003767	.406720	.090000
.90	.381549	-.001632	.392611	.090000
1.00	.403225	-0.000000	.384371	.090000

POISSON'S RATIO = .400
 THETA = 0/DEGREES
 ALFA = 7.50/DEGREES

ROH	DEFLECTION	MP	MT	MPT
0	.291188	.503269	-.079269	0
.10	.289007	.500058	-.032649	0
.20	.278483	.490373	-.005979	0
.30	.262667	.474250	-.118876	0
.40	.240543	.450769	-.152503	0
.50	.212530	.412236	-.138815	0
.60	.178473	.380345	-.260935	0
.70	.138649	.329722	-.343657	0
.80	.093274	.260734	-.453994	0
.90	.042648	.160799	-.601530	0
1.00	-.012716	-.000000	-.798154	0

POISSON'S RATIO = .400
 THETA = 15.00/DEGREES
 ALFA = 7.50/DEGREES

ROH	DEFLECTION	MP	MT	MPT
0	.291188	.454314	-.039314	145385
.10	.288333	.460574	-.042609	146536
.20	.279797	.449243	-.052501	150975
.30	.255668	.429958	-.068980	156255
.40	.246098	.402047	-.091937	16521
.50	.221311	.364431	-.120992	178502
.60	.191619	.315578	-.155199	195951
.70	.157442	.253713	-.192619	218487
.80	.119342	.177737	-.229835	245931
.90	.078046	.089671	-.261550	275858
1.00	.034444	-.000000	-.280647	300743

POISSON'S RATIO = .400
 THETA = 30.00/DEGREES
 ALFA = 7.50/DEGREES

ROH	DEFLECTION	MP	MT	MPT
0	.291188	.357885	.067115	251814
.10	.289221	.353388	.066086	25232
.20	.283371	.339844	.063189	254993
.30	.273784	.317123	.058948	258579
.40	.260712	.285145	.054335	262738
.50	.244513	.244142	.050686	266308
.60	.225658	.196090	.049673	257423
.70	.204725	.140355	.053147	263443
.80	.182377	.084415	.062357	251315
.90	.159322	.034417	.080113	228899
1.00	.136226	-.000000	.105517	198224

POISSON'S RATIO = .400
 THETA = 45.00/DEGREES
 ALFA = 7.50/DEGREES

ROH	DEFLECTION	MP	MT	MPT
0	.291188	.212500	.212500	290769
.10	.290433	.203568	.212952	289883
.20	.288217	.196997	.214317	287060
.30	.284684	.178500	.216587	281839
.40	.280063	.154362	.219616	273578
.50	.274554	.126499	.222956	261686
.60	.263802	.097388	.225662	245980
.70	.262853	.062586	.226111	227130
.80	.257156	.045342	.221904	206950
.90	.251979	.023945	.209900	188076
1.00	.247504	-.000000	.186471	172137

POISSON'S RATIO = .400
 THETA = 60.00/DEGREES
 ALFA = 7.50/DEGREES

ROH	DEFLECTION	MP	MT	MPT
0	.291188	.067116	.357894	251914
.10	.291642	.065555	.357990	249485
.20	.293023	.061139	.358152	242591
.30	.295384	.056599	.357929	231440
.40	.299301	.046321	.356687	216619
.50	.303356	.030225	.353769	199012
.60	.303131	.031329	.349748	179717
.70	.316191	.023841	.341769	159801
.80	.324596	.015520	.333919	139975
.90	.334406	.006571	.327577	120460
1.00	.345697	-.000000	.328218	.101687

POISSON'S RATIO=.401
THETA = 75.00/DEGREES
ALFA = 7.50/DEGREES

ROH	DEFLECTION	MP	MT	MPT
0	.291188	-.039313	.464313	.145385
.10	.292626	-.039017	.463032	.143389
.20	.296517	-.034239	.459184	.137648
.30	.303100	-.028333	.452768	.128842
.40	.312174	-.020909	.443821	.117923
.50	.323608	-.012805	.432411	.105940
.60	.337253	-.004956	.418537	.093819
.70	.352050	.001726	.401883	.082730
.80	.370541	.006421	.381430	.072084
.90	.389873	.017509	.355025	.063541
1.00	.410811	-.000000	.319176	.056753

POISSON'S RATIO=.400
THETA = 90.00/DEGREES
ALFA = 7.50/DEGREES

ROH	DEFLECTION	MP	MT	MPT
0	.291188	-.078269	.503269	.000000
.10	.292849	-.075693	.501244	.000000
.20	.297791	-.069338	.495315	.000000
.30	.305900	-.057244	.485873	.000000
.40	.317102	-.043902	.473458	.000000
.50	.330873	-.030018	.458657	.000000
.60	.347297	-.017321	.442032	.000000
.70	.366030	-.007464	.424575	.000000
.80	.386878	-.001904	.407441	.000000
.90	.409693	-.000525	.392980	.000000
1.00	.434389	-.000000	.384684	.000000

POISSON'S RATIO=.450
THETA = 0/DEGREES
ALFA = 7.50/DEGREES

ROH	DEFLECTION	MP	MT	MPT
0	.309194	.502180	-.070930	0
.10	.305847	.498919	-.075469	0
.20	.295820	.480083	-.080283	0
.30	.279160	.472507	-.113001	0
.40	.256939	.448872	-.147820	0
.50	.226257	.417585	-.195760	0
.60	.191236	.377465	-.260024	0
.70	.148016	.325921	-.345576	0
.80	.093763	.257068	-.460241	0
.90	.045703	.157769	-.614429	0
1.00	-.013769	-.000000	.822492	0

POISSON'S RATIO=.450
THETA = 15.00/DEGREES
ALFA = 7.50/DEGREES

ROH	DEFLECTION	MP	MT	MPT
0	.309194	.463789	-.032539	.143278
.10	.306197	.460025	-.036009	.144419
.20	.297233	.448622	-.046426	.147926
.30	.287387	.429233	-.063303	.154059
.40	.261804	.401210	-.098068	.163271
.50	.235700	.363516	-.118899	.176220
.60	.214376	.314684	-.155424	.193725
.70	.169241	.253012	-.195777	.216563
.80	.127843	.177432	-.236520	.244904
.90	.093901	.093814	-.272056	.277057
1.00	.037307	-.000000	.294261	.306969

POISSON'S RATIO=.450
THETA = 30.00/DEGREES
ALFA = 7.50/DEGREES

ROH	DEFLECTION	MP	MT	MPT
0	.309194	.358303	.072347	.248164
.10	.307152	.354427	.071131	.249003
.20	.301076	.340949	.067660	.251435
.30	.291115	.318348	.052486	.255171
.40	.277524	.296558	.056562	.260611
.50	.260668	.245805	.051263	.263675
.60	.241029	.197037	.048353	.266607
.70	.219291	.142522	.049863	.262873
.80	.195371	.086543	.057862	.252454
.90	.171781	.035358	.074139	.231925
1.00	.147643	-.000000	.099899	.202328

PCISSON,S RATIO= .450
 THETA = 45.00/DEGREES
 ALFA = 7.50/DEGREES

ROH	DEFLECTION	MP	MT	MPT
0	.309194	.215625	.215625	.286555
.10	.308495	.211722	.215923	.285754
.20	.306288	.200231	.216340	.283192
.30	.302840	.181840	.218405	.278429
.40	.298352	.157796	.220544	.270842
.50	.293133	.129915	.222912	.259843
.60	.287545	.100611	.224687	.245214
.70	.281260	.072435	.224362	.227530
.80	.275728	.047291	.219576	.209464
.90	.272136	.024855	.207026	.190563
1.00	.268395	-0.000000	.182529	.175701

PCISSON,S RATIO= .450
 THETA = 60.00/DEGREES
 ALFA = 7.50/DEGREES

ROH	DEFLECTION	MP	MT	MPT
0	.309194	.072348	.358902	.248164
.10	.309755	.070764	.358948	.245960
.20	.311457	.066269	.358943	.239433
.30	.314355	.059565	.358481	.228864
.40	.318530	.051601	.356973	.214787
.50	.324072	.043266	.353798	.198022
.60	.331067	.035043	.348534	.179688
.70	.339589	.026758	.341298	.160479
.80	.349699	.017726	.333139	.141356
.90	.351470	.007790	.326440	.122389
1.00	.374986	-0.000000	.325169	.103793

PCISSON,S RATIO= .450
 THETA = 75.00/DEGREES
 ALFA = 7.50/DEGREES

ROH	DEFLECTION	MP	MT	MPT
0	.309194	-0.032539	.463789	.143278
.10	.310705	-0.031340	.462554	.141376
.20	.315215	-0.027853	.458835	.125900
.30	.322660	-0.022415	.452617	.127490
.40	.332938	-0.015620	.443899	.117045
.50	.345014	-0.008275	.432705	.105539
.60	.361435	-0.001294	.418987	.093866
.70	.379337	.004459	.402383	.082756
.80	.399453	.008152	.381818	.072801
.90	.421622	.008227	.354909	.064477
1.00	.445695	-0.000000	.317981	.057928

PCISSON,S RATIO= .450
 THETA = 90.00/DEGREES
 ALFA = 7.50/DEGREES

ROH	DEFLECTION	MP	MT	MPT
0	.309194	-0.029330	.502180	.000000
.10	.311052	-0.068487	.520247	.000000
.20	.316585	-0.061518	.494575	.000000
.30	.325675	-0.051022	.485503	.000000
.40	.338141	-0.038439	.477498	.000000
.50	.353753	-0.025414	.459065	.000000
.60	.372285	-0.013624	.442749	.000000
.70	.393484	-0.004668	.425290	.000000
.80	.417145	.000134	.407900	.000000
.90	.443113	.000569	.393208	.000000
1.00	.471297	-0.000000	.384846	.000000

PCISSON,S RATIO= .500
 THETA = 0/DEGREES
 ALFA = 7.50/DEGREES

ROH	DEFLECTION	MP	MT	MPT
0	.331258	.501212	.063712	0
.10	.327706	.497201	.068408	0
.20	.317050	.487915	.082699	0
.30	.299360	.471090	.107230	0
.40	.274665	.447104	.143225	0
.50	.243155	.415369	.192749	0
.60	.204623	.374726	.259146	0
.70	.169456	.322563	.347680	0
.80	.132692	.254529	.466301	0
.90	.094937	.154843	.627088	0
1.00	-0.015035	-0.000000	.846293	0

POISSON, S RATIO= .250
 THETA = 15.00/DEGREES
 ALFA = 9.50/DEGREES

ROH	DEFLECTION	MR	MT	MRT
.0	.245052	.464737	.058487	.151042
.10	.245498	.461362	.0561216	.152132
.20	.235868	.443914	.0569388	.155673
.30	.223260	.430908	.0582935	.161725
.40	.205841	.413326	.0521656	.170692
.50	.185856	.366027	.125753	.183015
.60	.157643	.317408	.1521119	.199093
.70	.127649	.255612	.180697	.218886
.80	.094464	.179458	.208852	.241028
.90	.054812	.090827	.232052	.261018
1.00	.021581	.000000	.247331	.267752

POISSON, S RATIO= .250
 THETA = 30.00/DEGREES
 ALFA = 9.50/DEGREES

ROH	DEFLECTION	MR	MT	MRT
.0	.245052	.354167	.052093	.261612
.10	.244236	.349638	.051668	.262322
.20	.233837	.335994	.050334	.264335
.30	.223996	.313099	.048838	.267621
.40	.217954	.280879	.047320	.270328
.50	.203052	.239553	.046749	.272217
.60	.185733	.191267	.046336	.273909
.70	.166532	.135332	.060800	.263711
.80	.145350	.079716	.074912	.247823
.90	.124911	.031362	.092214	.221945
1.00	.103672	.000000	.114345	.199339

POISSON, S RATIO= .250
 THETA = 45.00/DEGREES
 ALFA = 9.50/DEGREES

ROH	DEFLECTION	MR	MT	MRT
.0	.245052	.233125	.203125	.302084
.10	.245243	.139150	.20393	.300936
.20	.242861	.187457	.205568	.297317
.30	.233037	.138841	.211726	.290740
.40	.233979	.144645	.2161229	.280537
.50	.227958	.116926	.222081	.266120
.60	.221283	.083327	.227377	.247364
.70	.214269	.061696	.2279236	.225050
.80	.207207	.039166	.223493	.221176
.90	.200331	.020446	.219526	.178362
1.00	.193821	.000000	.201931	.157871

POISSON, S RATIO= .250
 THETA = 60.00/DEGREES
 ALFA = 9.50/DEGREES

ROH	DEFLECTION	MR	MT	MRT
.0	.246052	.052083	.354167	.261613
.10	.246248	.050605	.354416	.258940
.20	.246351	.046458	.354930	.251041
.30	.247908	.042427	.355336	.238295
.40	.243481	.033577	.354749	.221411
.50	.251641	.026910	.352466	.201447
.60	.254453	.020980	.347994	.179717
.70	.257969	.015609	.341425	.157534
.80	.262228	.010067	.333686	.135830
.90	.267271	.003831	.326544	.115311
1.00	.273143	.000000	.322067	.096652

POISSON, S RATIO= .250
 THETA = 75.00/DEGREES
 ALFA = 9.50/DEGREES

ROH	DEFLECTION	MR	MT	MRT
.0	.245052	.058487	.464737	.151242
.10	.245982	.056930	.463317	.148800
.20	.243751	.052381	.459069	.142352
.30	.254301	.045217	.452152	.132477
.40	.263535	.036095	.442461	.120270
.50	.263333	.025922	.431320	.116316
.60	.277555	.015735	.415991	.093487
.70	.283954	.016526	.399354	.080833
.80	.299638	.007533	.379823	.063576
.90	.312330	.034568	.356120	.060098
1.00	.325879	.000000	.326550	.052239

POISSON,S RATIO=.250
THETA = 30.00/DEGREES
ALFA = 9.50/DEGREES

ROH	DEFLECTION	MR	MT	MRT
.0	.245052	-.038959	.505220	.0000000
.10	.247256	-.039604	.502292	.0000000
.20	.251808	-.037685	.496261	.0000000
.30	.255620	-.035012	.485750	.0000000
.40	.264534	-.032627	.472120	.0000000
.50	.274322	-.030363	.456190	.0000000
.60	.285300	-.028004	.433767	.0000000
.70	.297466	-.025468	.420724	.0000000
.80	.312939	-.023092	.413284	.0000000
.90	.323384	-.020293	.393066	.0000000
1.00	.344847	-.010000	.376799	.0000000

POISSON,S RATIO=.300
THETA = 0/DEGREES
ALFA = 9.50/DEGREES

ROH	DEFLECTION	MR	MT	MRT
.0	.255837	.533757	.091257	.0000000
.10	.252920	.500614	.095250	.0000000
.20	.244192	.491127	.197398	.0000000
.30	.223716	.475117	.128242	.0000000
.40	.203656	.452227	.158795	.0000000
.50	.183995	.421732	.256581	.0000000
.60	.153097	.382431	.339156	.0000000
.70	.117156	.331478	.425553	.0000000
.80	.076494	.262445	.551936	.0000000
.90	.031562	.161600	.712182	.0000000
1.00	-.016920	-.000000		

POISSON,S RATIO=.300
THETA = 15.00/DEGREES
ALFA = 9.50/DEGREES

ROH	DEFLECTION	MR	MT	MRT
.0	.255837	.493899	.051339	.148753
.10	.253206	.460199	.054308	.149883
.20	.245344	.448935	.063228	.153344
.30	.232346	.429881	.077514	.159354
.40	.214374	.402197	.097651	.168274
.50	.191669	.364837	.122396	.180583
.60	.164559	.316259	.152334	.196750
.70	.133482	.254680	.184268	.216903
.80	.099012	.178946	.212811	.246032
.90	.061877	.130826	.243062	.262358
1.00	.021949	-.010000	.261849	.274243

POISSON,S RATIO=.300
THETA = 30.00/DEGREES
ALFA = 9.50/DEGREES

ROH	DEFLECTION	MR	MT	MRT
.0	.255837	.325004	.057436	.257648
.10	.253985	.352499	.056826	.253247
.20	.248476	.336932	.054986	.263569
.30	.233455	.314176	.052494	.263545
.40	.222716	.282159	.050215	.263538
.50	.211945	.241128	.049338	.263538
.60	.194247	.192095	.051263	.268933
.70	.174614	.137477	.057399	.263259
.80	.153662	.081860	.068844	.248961
.90	.132033	.032632	.086046	.225158
1.00	.110316	-.010000	.103994	.134953

POISSON,S RATIO=.300
THETA = 45.00/DEGREES
ALFA = 9.50/DEGREES

ROH	DEFLECTION	MR	MT	MRT
.0	.255837	.206250	.206250	.237557
.10	.255047	.202308	.205960	.296451
.20	.252724	.130716	.209076	.331166
.30	.243011	.172212	.212514	.287033
.40	.244092	.148122	.217212	.277567
.50	.238274	.126417	.221979	.264134
.60	.231866	.031645	.226342	.246514
.70	.223194	.054554	.226344	.225434
.80	.218562	.041224	.226283	.202829
.90	.212216	.021437	.216756	.181103
1.00	.206348	-.010000	.198302	.161698

APPENDIX 4

Use of the coefficients for bending moments from finite element solution. The finite element solution using a quadratic plate element as shown in Fig. (2.7) produces the bending moments at the centroid of the elements and related to its own local axis.

The local axes of the elements are defined from the coordinates of the nodes of the element and they are dependent on the numbering directions. (The connection matrix as follows):

The x axis passes through the centroid of the element and the middle point of the fourth side of the element as it is numbered in the connection matrix of the elements, i.e. the side connecting node No. 4 with Node No. 1 as in Fig. (2.6).

The y axis is perpendicular to the x axis and passes through the first side of the element, i.e. the side connecting Node No. 1 with Node No. 2 as in Fig. (2.6), as all elements must be as near as possible to a rectangular shape.

M_x , and M_y are positive when causing tension stresses on the top surface of the element as in Fig. (2.1). Thus the coefficients obtained from a finite element solution would produce M_x , M_y and M_{xy} when multiplied by qa^2 . To transform these moments into global polar coordinates the following equations can be used.

$$M_r = M_x \cos^2 \Psi + M_y \sin^2 \Psi + M_{xy} \sin 2\Psi$$

$$M_\theta = M_x \sin^2 \Psi + M_y \cos^2 \Psi - M_{xy} \sin 2\Psi$$

$$M_{r\theta} = -\frac{1}{2} (M_x - M_y) \sin 2\Psi + M_{xy} \cos 2\Psi$$

Where Ψ is the angle between the polar direction and the element local axes x-y. as shown in Fig. (A4.1).

For a given principal moment M_1 & M_2 the following equations can be used:-

$$M_r = M_x \cos^2 \beta + M_y \sin^2 \beta$$

$$M_\theta = M_x \sin^2 \beta + M_y \cos^2 \beta$$

$$M_{r\theta} = \frac{1}{2} (M_x - M_y) \sin^2 \beta$$

Where β is the angle between the polar direction and the principal directions 1-2 as shown in Fig. (A4.1).

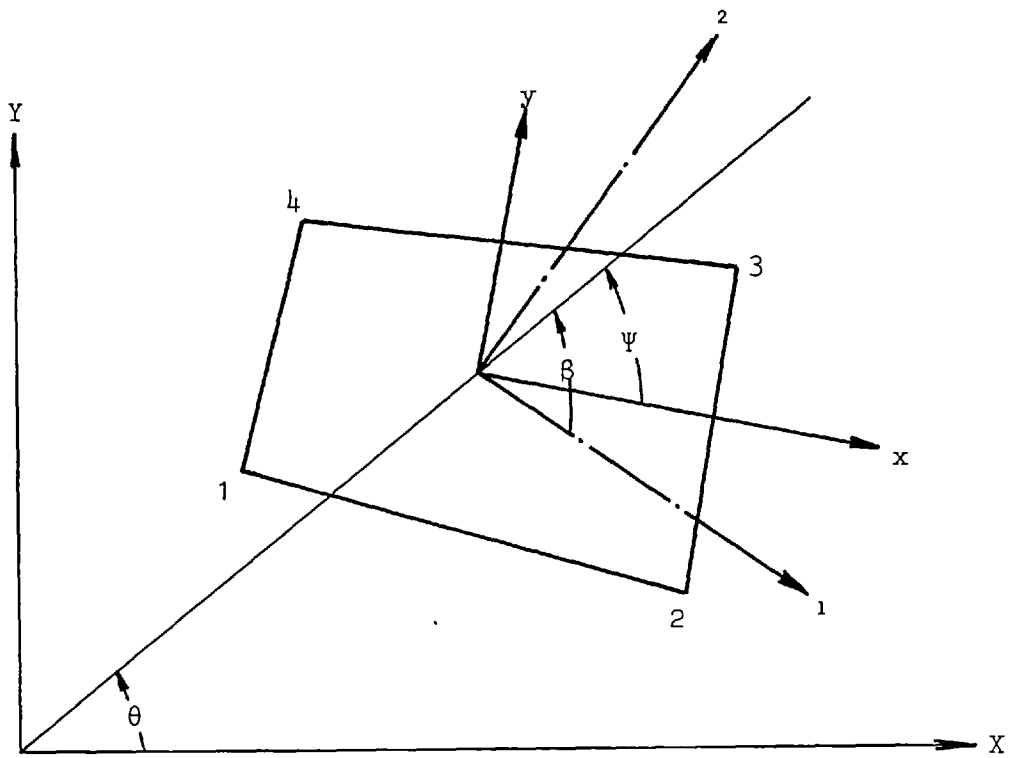


Fig. A4.1. Global, local and principal directions for a thin shell element.

APPENDIX 5

According to the following linear interpolation function

$$f_1 = \alpha_1 + \alpha_2 \xi + \alpha_3 \eta + \alpha_4 \zeta + \alpha_5 \xi\eta + \alpha_6 \eta\zeta + \alpha_7 \xi\zeta + \alpha_8 \xi\eta\zeta \quad (A5.1)$$

we can represent the shape of any three dimensional parallel piped with lengths 2a, 2b and 2c. Fig. (A5.1).

Where the local dimensionless coordinates ξ η ζ referred to the centroid (x_c , y_c , z_c)

$$= (x - x_c)/a$$

$$= (y - y_c)/b$$

$$= (z - z_c)/c$$

Solving for α 's in the following way:-

$$x_1 = \alpha_1 + \alpha_2 + \alpha_3 + \alpha_4 + \alpha_5 + \alpha_6 + \alpha_7 + \alpha_8$$

$$y_1 = \alpha_1 + \alpha_2 + \alpha_3 + \alpha_4 + \alpha_5 + \alpha_6 + \alpha_7 + \alpha_8$$

,

,

,

$$\therefore \begin{pmatrix} x_1 \\ x_2 \\ x_3 \\ x_4 \\ x_5 \\ x_6 \\ x_7 \\ x_8 \end{pmatrix} = \begin{pmatrix} 1 & 1 & 1 & 1 & 1 & 1 & 1 & 1 \\ 1 & -1 & 1 & -1 & 1 & 1 & -1 & -1 \\ 1 & -1 & -1 & 1 & 1 & -1 & -1 & 1 \\ 1 & 1 & -1 & 1 & -1 & -1 & 1 & -1 \\ 1 & 1 & 1 & -1 & 1 & -1 & -1 & -1 \\ 1 & -1 & 1 & -1 & -1 & -1 & 1 & 1 \\ 1 & -1 & -1 & -1 & 1 & 1 & 1 & -1 \\ 1 & 1 & -1 & -1 & -1 & 1 & -1 & 1 \end{pmatrix} \begin{pmatrix} \alpha_1 \\ \alpha_2 \\ \alpha_3 \\ \alpha_4 \\ \alpha_5 \\ \alpha_6 \\ \alpha_7 \\ \alpha_8 \end{pmatrix} \quad (A5.2)$$

Then replacing i 's by nodal coordinates using the substitutions $x = x_1$ at $\xi = \eta = 1$ etc. Equation (A5.1) is produced.

$$x = \sum_{i=1}^{\infty} N_i x_i$$

$$y = \sum_{i=1}^{\infty} N_i y_i$$

$$z = \sum_{i=1}^{\infty} N_i z_i$$

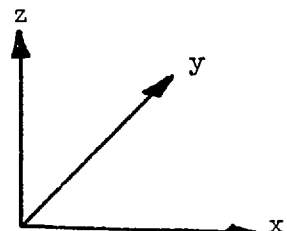
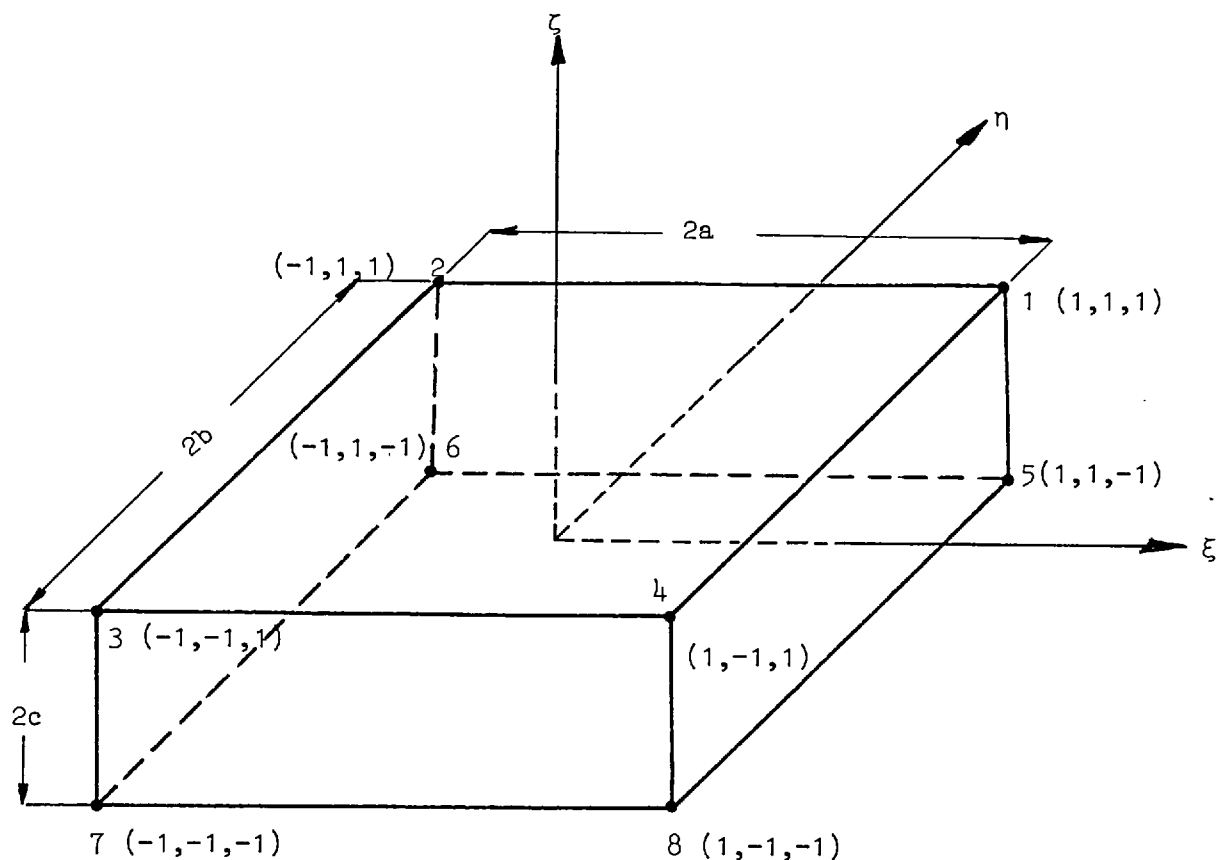


Fig. A5.1.